Aus dem Zentrum für Physiologie und Pathophysiologie der Universität zu Köln
Institut für Neurophysiologie
Geschäftsführender Direktor: Universitätsprofessor Dr. med. J. Hescheler

Funktionelle Charakterisierung des $Ca_v2.3$ E/R-Typ Ca^{2+}-Kanals bei neuronaler Rhythmizität, Hyperexzitabilität und Neurodegeneration

Functional Characterisation of $Ca_v2.3$ E/R-Type Ca^{2+}-Channels in Neuronal Rhythmicity, Hyperexcitability and Neurodegeneration

Kumulative Habilitationsschrift zur Erlangung der *venia legendi*
für das Fach Physiologie
an der Hohen Medizinischen Fakultät
der Universität zu Köln

vorgelegt von
Dr. nat. med. Dr. med. Marco Weiergräber (MD/PhD)
aus Jülich

Köln 2009

Danksagung

Die vorliegende Habilitationsschrift basiert auf eigenen experimentellen Arbeiten in den Jahren 2005 bis 2009 am Institut für Neurophysiologie der Universität zu Köln.

Mein besonderer Dank gilt Herrn Prof. Dr. T. Schneider für sein stetiges Interesse am Fortgang dieser Arbeit, die zahlreichen fruchtbaren und ermutigenden Diskussionen sowie die Schaffung eines optimalen Umfeldes zur Erstellung dieser Arbeit.

Bedanken möchte ich mich weiterhin bei Frau Dipl. biol. Margit Henry, Frau Dipl. biol. Tamara Rotsteyn und Frau Renate Clemens für deren Beiträge sowie das produktive und freundschaftliche Arbeitsklima.

Ein besonderer Dank gilt weiterhin den Kooperationspartnern Prof. Dr. E. Bertram III. (*Department of Neurology*, *University of Virginia*, Charlottesville, USA), Prof. Dr. E. Perez-Reyes (*Department of Pharmacology*, *University of Virginia*, Charlottesville, USA), Prof. Dr. S. Todorovic (*Department of Anesthesiology*, *University of Virginia*, Charlottesville, USA), Dr. J. C. Gomora (*Instituto de Fisiologia Celular*, *Universitad Nacional Autonoma de Mexico*; Mexico), Dr. N. Smyth (*School of Biological Sciences*, *University of Southampton*, UK) und Prof. Dr. R. Köhling (Institut für Physiologie, Universität Rostock).

Mein Dank gilt auch dem Zentrum für Molekulare Medizin Köln (ZMMK), in dessen Rahmen die hier dargelegten Untersuchungen durchgeführt werden konnten.

Herrn Prof. Dr. J. Hescheler danke ich für die Bereitstellung der Räumlichkeiten im Institut für Neurophysiologie der Universität zu Köln.

Ein besonderer Dank gilt meinen Eltern, meinem Bruder und meinen Großeltern für deren Unterstützung.

Die vorliegende Habilitationsschrift fasst die wesentlichen Aussagen meiner Arbeiten zur Rolle des $Ca_v2.3$ Ca^{2+}-Kanals bei der neuronalen Rhythmogenese, Hyperexzitabilität und Neurodegeneration zusammen. Die wichtigsten zu Grunde liegenden eigenen Publikationen finden sich in Kapitel 3. Eine Gesamtübersicht aller Arbeiten ist im Anhang dargelegt.

Anmerkung

In der vorliegenden Schrift werden, soweit sinnvollerweise möglich, Termini technici in der deutschen Fassung verwendet. In einigen Bereichen sind allerdings deutsche Bezeichnungen entweder nicht existent oder zumindest ungebräuchlich; in diesen Fällen finden die englischen, französischen bzw. lateinischen Pendants Verwendung und werden als solche durch kursiven Schriftsatz gekennzeichnet.

Videmus nunc per speculum in aenigmate…

…die Wahrheit verbirgt sich im Rätsel,
bevor sie sich uns von Angesicht zu Angesicht offenbart,
und nur für kurze Augenblicke tritt sie hervor im Irrtum der Welt,
weshalb wir ihre getreulichen Zeichen entziffern müssen,
auch wo sie uns dunkel erscheinen…

Adson von Melk
aus dem Prolog „Der Name der Rose“
(Umberto Eco)

Inhaltsverzeichnis

Abkürzungsverzeichnis

ADJME	*autosomal dominant juvenile myoclonic epilepsy*
ADNFLE	*autosomal dominant nocturnal frontal lobe epilepsy*
ADP	*afterdepolarisation*
ADPEAF	*autosomal dominant partial epilepsy with auditory features*
BFNIS	*benign familial neonatal-infantile seizures*
CA	cornu ammonis
CAE	*childhood absence epilepsy*
CAI	Carboanhydraseinhibitor
CNG	*cyclic nucleotide gated*
CORDX3	*x-linked cone-rod dystrophy type 3*
DAG	Diazylglycerol
DHP	Dihydropyridin
EA2	episodische Ataxie Typ 2
FHM1	familiäre hemiplegische Migräne Typ 1
FS	*febrile seizures*
$GEFS^+$	*generalized epilepsy with febrile seizures plus*
HVA	*high-voltage activated*
HypoPP1	hypokaliämische periodische Paralyse Typ 1
IGE	*ideopathic generalized epilepsy*
IP3	Inositoltrisphosphat
JAE	*juvenile absence epilepsy*
JME	*juvenile myoclonic epilepsy*
LVA	*low-voltage activated*
MH	maligne Hyperthermie
PDS	paroxysmaler Depolarisationsshift
PKC	Proteinkinase C
PLC	Phospholipase C
PNS	Peripheres Nervensystem
PP	Plateau-Potential
SCA6	spinozerebelläre Ataxie Typ 6
SMEI	*severe myoclonic epilepsy of infancy*
TLE	Temporallappenepilepsie
XCSNB2	*x-linked congenital stationary night blindness type 2*
ZNS	Zentrales Nervensystem

Zusammenfassung

Spannungsgesteuerte Ca^{2+}-Kanäle sind Schlüsselelemente in Ätiologie und Pathogenese neuronaler und neuromuskulärer Erkrankungen. Bislang sind eine Reihe sog. Ca^{2+}-Kanalopathien sowohl beim Menschen als auch in Tiermodellen beschrieben, die sich auf Mutationen der L-Typen $Ca_v1.2$ und $Ca_v1.4$, des Non-L-Typ $Ca_v2.1$ sowie des T-Typ $Ca_v3.2$ zurückführen lassen. Im Bereich epileptiformer Krankheitsbilder sind innerhalb der Familie spannungsgesteuerter Ionenkanäle bislang nur Mutationen im $Ca_v2.1$ und $Ca_v3.2$ Ca^{2+}-Kanal bekannt geworden. Dies ist umso bemerkenswerter, als von den zehn porenbildenden ionenleitenden Ca_v-α_1-Untereinheiten neun zentralnervös exprimiert werden. Eigene radiotelemetrische, zellulär-elektrophysiologische, immunologische und molekularbiologische Studien zeigen jedoch deutlich, dass auch der $Ca_v2.3$ E/R-Typ Ca^{2+}-Kanal eine entscheidende Rolle bei der Genese iktiformer/epileptiformer Aktivität spielt. So weisen $Ca_v2.3^{-/-}$ Mäuse eine verminderte Anfallssuszeptibilität gegenüber PTZ und 4-AP induzierten generalisiert tonisch-klonischen sowie NMDA- und Kainat-induzierten hippokampalen Anfällen auf. Bei letzteren zeigt sich darüber hinaus, dass die Anfallsresistenz mit einer Resistenz gegenüber Hyperexzitabilitäts-vermittelter Exzitotoxizität vergesellschaftet ist. Dies legt den Schluss nahe, dass eine pharmakologische Blockade von $Ca_v2.3$ Ca^{2+}-Kanälen auch neuroprotektiv wirksam ist. Mit $Ca_v2.3$ getriggerten Plateau-Potentialen existiert weiterhin ein zellulär-epileptiformes Korrelat für die gewonnenen systemisch-elektrophysiologischen Daten. Interessanterweise fand sich im GHB-Modell der Absencenepilepsie, dass $Ca_v2.3$-Defizienz die Anfallssuszeptibilität gegenüber *spike-wave* Graphoelementen deutlich erhöht. Dies legt nahe, das $Ca_v2.3$ Aktivierung entsprechend seiner mittel- bis hochspannungsaktivierten Charakteristik den tonischen Aktivitätsmodus in retikulär-thalamischen Neuronen favorisiert und damit Absencen-protektive Kapazität in sich trägt. Studien mit dem Inhalationsnarkotikum Isofluran bestätigen die funktionelle Bedeutung der $Ca_v2.3$ Kanalentität im thalamokortikalen System. So inhibiert Isofluran nicht nur $Ca_v2.3$ im Nucleus reticularis thalami, sondern beeinflusst auf diese Weise auch komplex das Isofluran-mediierte kortikale *burst* und *burst-suppression* Muster. Die pharmakologische Interaktion mit $Ca_v2.3$ Ca^{2+}-Kanälen eröffnet somit vielfältige Perspektiven in der Therapie konvulsiver und nicht-konvulsiver Anfälle, aber auch neurodegenerativer Prozesse.

Summary

Voltage-gated Ca^{2+} channels are key elements in the etiology and pathogenesis of neuronal and neuromuscular diseases. Up to now, various Ca^{2+}-channelopathies have been described in both humans and animal models which are related to mutations in $Ca_v1.2$ and $Ca_v1.4$ L-type, $Ca_v2.1$ non-L-type and $Ca_v3.2$ T-type Ca^{2+} channels. Regarding epilepsy, there are mainly two Ca_v-α_1 subunits involved, the $Ca_v2.1$ and $Ca_v3.2$ channels. This is a striking result as nine out of ten pore-forming α_1-subunits are actually expressed within the central nervous system. Own radiotelemetric, cellular-electrophysiological, immunological and molecular-biology studies demonstrate that $Ca_v2.3$ E/R-type Ca^{2+} channels play an essential role in the genesis of ictiform/epileptiform activity. In particular, $Ca_v2.3^{-/-}$ mice exhibt reduced susceptibility to PTZ and 4-AP induced generalized tonic-clonic seizures and NMDA and kainic acid induced hippocampal seizures. Interestingly, kainic acid related limbic seizure resistance in $Ca_v2.3^{-/-}$ mice is clearly accompanied by resistance in hyperexcitability mediated excitotoxicity. These results indicate that pharmacological blockade of $Ca_v2.3$ Ca^{2+} channels can be neuroprotective as well. The recently described $Ca_v2.3$ triggered hippocampal plateau-potentials display an interesting cellular-epileptiform correlate for the above mentioned systemic electrophysiological data. Interestingly, $Ca_v2.3^{-/-}$ mice turned out to be more susceptible to GHB induced petit-mal seizures of the absence type resulting in increased spike-wave discharge activity. These data suggest that $Ca_v2.3$ activation favors the tonic mode of action in reticular thalamic nucleus neurons thus exerting absence-protective effects upon channel activation. Studies using the inhalative narcotic isoflurane further strengthen the role of $Ca_v2.3$ in the thalamocortical system demonstrating that isoflurane is a potent blocker of $Ca_v2.3$ Ca^{2+} channels that modulates isoflurane mediated cortical burst and burst suppression patterns. Consequently, pharmacological interaction with $Ca_v2.3$ Ca^{2+} channels provides new perspectives in the therapy of convulsive and non-convulsive seizures and neurodegenerative diseases.

1. Einleitung

1.1. Kalzium-Kanalopathien - Spannungsgesteuerte Ca^{2+}-Kanäle in Ätiologie, Pathogenese und Pharmakotherapie neurologischer Krankheitsbilder

1.1.1. Spannungsgesteuerte Ca^{2+}-Kanäle – Struktur und Funktion

Spannungsgesteuerte Ca^{2+}-Kanäle gehören zu einer Familie transmembranärer Kanalproteine, die in Reaktion auf eine Membrandepolarisation mit einer Erhöhung ihrer Offenwahrscheinlichkeit reagieren und Ca^{2+}-Ionen selektiv entlang ihres elektrochemischen Gradienten in Zellen einströmen lassen. Entsprechend der globalen Funktion des Ca^{2+}-Ions spielen spannungsgesteuerte Ca^{2+}-Kanäle eine entscheidende Rolle bei der Regulation einer Vielzahl zellulärer Prozesse, wie z.B. der Exzitations-Kontraktionskopplung (Bers, 2002), der Exzitations-Sekretionskopplung (Yang and Berggren, 2005), der Hormon- und Transmitterfreisetzung (Catterall, 1999), sowie der Regulation der Genexpression (Bito et al., 1997;Hofmann et al., 1999). Spannungsgesteuerte Ca^{2+}-Kanalkomplexe sind hochmolekulare Strukturen (> 400 kDa), die aus mindestens drei Untereinheiten (α_1-, $\alpha_2\delta$– und β-Untereinheit) in einer 1:1:1 Stöchiometrie zusammengesetzt sind. Gewebsabhängig kann der Ca^{2+}-Kanalkomplex eine zusätzliche γ-Untereinheit umfassen (**Abb.1**, Catterall et al., 2005).

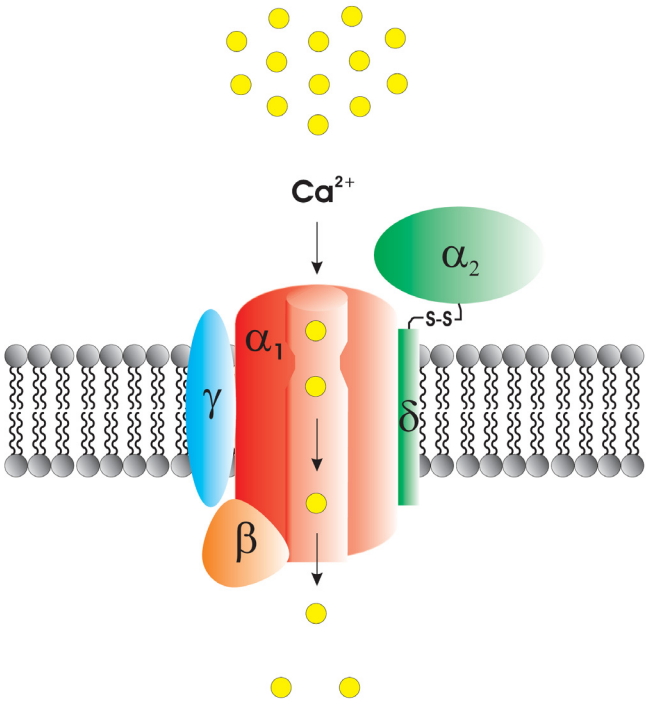

Abb. 1: Heteromere Struktur spannungsgesteuerter Ca^{2+}-Kanäle ($\alpha_1\alpha_2\delta\beta\gamma$), dargestellt am Beispiel des Skelettmuskel Ca^{2+}-Kanals (L-Typ, $Ca_v1.1$). Die zentrale porenbildende, ionenleitende Ca_v-α_1-Untereinheit wird durch eine Reihe von Hilfsuntereinheiten flankiert. Die δ- und γ-Untereinheiten sind membranintegral, β intrazellulär und die an δ kovalent gebundene α_2-Untereinheit extrazellulär lokalisiert (Weiergräber et al., 2008b).

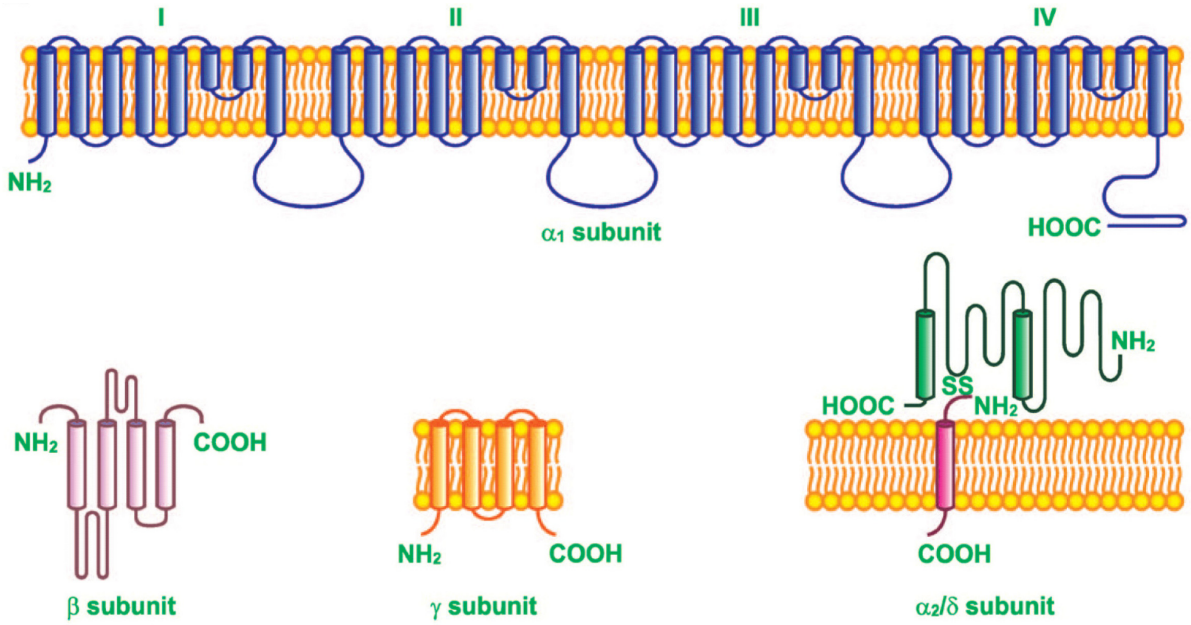

Abb. 2: Schematische Darstellung der porenbildenden, ionenleitenden α_1-Untereinheit und zugehöriger Hilfsuntereinheiten. Die zentrale α_1-Untereinheit umfasst vier Domänen aus jeweils sechs transmembranären α-Helices sowie einer Schleife für die Porenregion zwischen Insertionssegment 5 und 6. Die akzessorischen Untereinheiten ($\alpha_2\delta$,β,γ) wurden in den Proteinkomplexen einiger Kanalkomplexe vorgefunden und durch Homologie-*Screening* komplettiert (modifiziert nach Yang and Berggren, 2005).

Zehn verschiedene porenbildende, ionenleitende Ca_v-α_1-Untereinheiten sind bis heute identifiziert worden, welche strukturelle Homologien mit spannungsgesteuerten Na^+- und K^+-Kanälen aufweisen. Während sich bei den klassischen spannungsgesteuerten K^+-Kanälen vier separate Peptid-Untereinheiten mit jeweils sechs transmembranären α-Helices zu einem Porenkomplex (Quartärstruktur) vereinen, findet sich bei spannungsgesteuerten Na^+- und K^+-Kanälen eine Vier-Domänenstruktur zu jeweils sechs α-Helices, die über intrazelluläre Schleifen (*loops*) kovalent verknüpft sind (**Abb. 2**). Spannungsgesteuerte Na^+- und Ca^{2+}-Kanäle sind offensichtlich das Resultat von Genduplikationen und somit phylogenetisch jünger. Nach klassischen pharmakologischen und elektrophysiologischen Gesichtspunkten lassen sich die Ca_v-α_1-Untereinheiten in hochspannungsaktivierte (*high-voltage activated, HVA*) und niederspannungsaktivierte (*low-voltage activated, LVA*) differenzieren, wobei sich die hochspannungsaktivierten Kanäle weiter in Dihydropyridin (DHP)-sensitive L-Typ („L“ für *long-lasting*) Kanäle Ca_v1.1.-1.4 und DHP-„unempfindlichere“ Non-L-Typ Ca^{2+}-Kanäle Ca_v2.1-2.3 untergliedern lassen. Die niederspannungsaktivierten T-Typ („T“ für *transient/tiny*) Ca^{2+}-Kanäle umfassen Ca_v3.1-3.3 (Ertel et al., 2000;Perez-Reyes, 2003;Catterall et al., 2005) (**Abb. 3**). Diese Kanäle aktivieren bereits bei vergleichsweise negativen Potentialen (V_a = -44 mV

bis -46 mV; τ_a = 1 - 7 ms; Klöckner et al., 1999) und inaktivieren in der Folge sehr schnell (V_h = -72 mV bis -73 mV; τ_h = 11 – 69 ms; Klöckner et al., 1999). Ihre Einzelkanalleitfähigkeit ist niedrig (7,5 - 11 pS; Klöckner et al., 1999;Catterall et al., 2005) und die Deaktivierung langsam. Hochspannungsaktivierte Ca^{2+}-Kanäle dagegen aktivieren erst bei stärkerer Depolarisation ($Ca_v1.1$: V_a = +8 bis +14 mV; τ_a = > 50 ms; Dirksen and Beam, 1995;Freise et al., 2000; $Ca_v1.2$: V_a = -17 mV; τ_a = 1 ms; Hu and Marban, 1998;Koschak et al., 2001), weisen eine vergleichsweise hohe Einzelkanalleitfähigkeit auf ($Ca_v1.1$: 13 - 17 pS; Dirksen et al., 1997;Freise et al., 2000; $Ca_v1.2$: ~25 pS; Tsien and Nilius, 1987) und zeigen eine schnelle Deaktivierung. Der Inaktivierungsprozess verläuft langsam (V_h = -50 bis -60 mV; $\tau_{h,fast}$ = 150 ms; $\tau_{h,slow}$ = 1100 ms; Hu and Marban, 1998), im Gegensatz zu T-Typ Ca^{2+}-Kanälen, die eine schnelle Inaktivierung aufweisen (Perez-Reyes, 2003;Catterall et al., 2005).

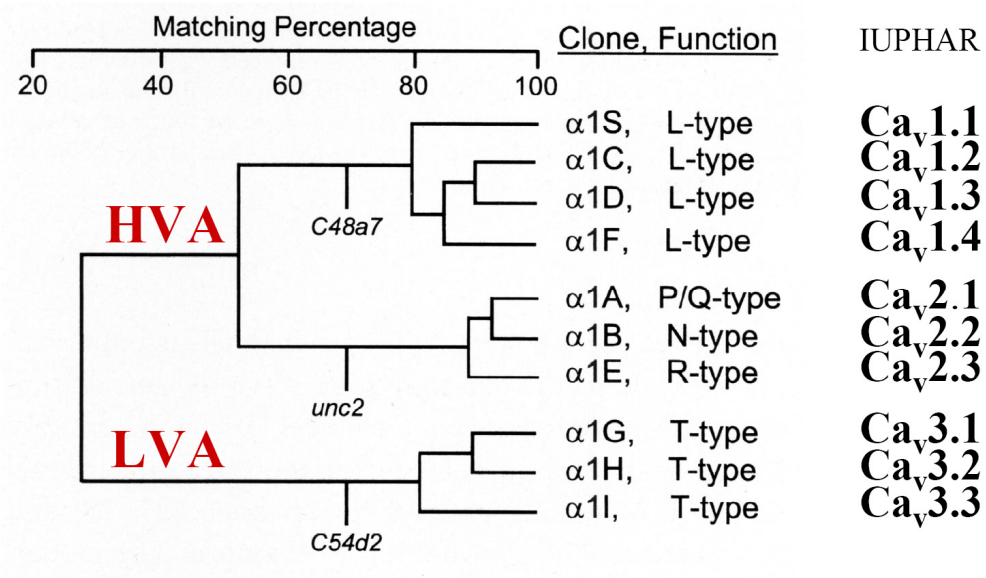

Abb. 3: Klassifikation spannungsabhängiger Ca^{2+}-Kanäle. Die älteren Bezeichnungen für die L-Typ, Non-L-Typ sowie T-Typ Ca^{2+}-Kanäle wurden durch die IUPHAR-Terminologie ersetzt. Die Bestimmung verwandtschaftlicher Beziehungen erfolgte mittels Aminosäuresequenzvergleich. Die Bezeichnungen C48a7, unc2 und C54d2 entsprechen den ursprünglich in C. elegans identifizierten Klonen (modifiziert nach Catterall et al., 2005).

Wie andere Ionenkanalfamilien umfasst auch ein Ca^{2+}-Kanalkomplex nicht nur eine porenbildende α_1-Untereinheit, sondern weitere Hilfsuntereinheiten, die sich aus den bislang klonierten $\alpha_2\delta_{1\text{-}4}$-, $\beta_{1\text{-}4}$-, und $\gamma_{1\text{-}8}$-Untereinheiten rekrutieren und die elektrophysiologischen und pharmakologischen Eigenschaften der zentralen α_1-Untereinheit des Ca^{2+}-Kanalkomplexes sowie deren Plasmamembran-Expression zu modulieren vermögen (Catterall, 2000;Arikkath and Campbell, 2003;Lacinova, 2005) (**Abb. 1, 2**). Die $\alpha_2\delta$-Untereinheit entsteht aus einem

Vorläufer (*precursor*)-Protein, welches nach proteolytischer Prozessierung in zwei separate Peptide (α_2 und δ) gespalten wird, die über eine Disulfidbrücke verknüpft bleiben. Diese $\alpha_2\delta$-Untereinheit kann direkt mit der porenbildenden Ca_v-α_1-Untereinheit interagieren und dient bemerkenswerterweise auch als Zielstruktur einer Reihe neuerer Antiepileptika, wie z.B. Gabapentin oder Pregabalin (Klugbauer et al., 2003;Felix, 2005). Die intrazellulär lokalisierte β-Untereinheit interagiert unmittelbar mit dem I-II-*loop* und scheint von besonderer Wichtigkeit für die Signalvermittlung und die kinetischen Eigenschaften der Ca_v-α_1-Untereinheit zu sein (Walker and De Waard, 1998;Dolphin, 2003) und somit auch ätiopathogenetische Relevanz zu haben (Herzig et al., 2007). Die äußerst wichtige Funktion der β-Untereinheiten wird dadurch unterstrichen, dass *knock-out* Mäuse entsprechend schwere physiologische Beeinträchtigungen aufweisen (Khosravani and Zamponi, 2006).

Subunit	Gene name	Chromosomal location	Accession number
$\alpha_2\delta1$	CACNA2D1	7q21-q22	NM_000722
$\alpha_2\delta2$	CACNA2D2	3p21.3	NM_006030
$\alpha_2\delta3$	CACNA2D3	3p21.1	NM_018398
$\alpha_2\delta4$	CACNA2D4	12p13.33	NM_172364
β1	CACNB1	17q11.2-q22	NM_000723
β2	CACNB2	10p12	NM_000724
β3	CACNB3	12q13	NM_000725
β4	CACNB4	2q22-q23	NM_000726
γ1	CACNG1	17q24	NM_000727
γ2	CACNG2	22q13.1	NM_006078
γ3	CACNG3	16p12-p13.1	NM_006539
γ4	CACNG4	17q24	NM_014405
γ5	CACNG5	17q24	NM_145811
γ6	CACNG6	19q13.4	NM_031897
γ7	CACNG7	19q13.4	NM_031896
γ8	CACNG8	19q13.4	NM_031895

Tab. 1: Zusammenfassende Darstellung der verschiedenen, bislang klonierten akzessorischen Untereinheiten spannungsgesteuerter Ca^{2+}-Kanäle (Kamp et al., 2005).

Ebenso wie die α_1-Untereinheit liegen auch die γ-Untereinheiten als membranintegrale Proteine vor, die als Hilfsuntereinheit modulierende Funktionen übernehmen. So können sie die Ca^{2+}-Kanalaktivität in Myozyten und Neuronen reduzieren, was vermutlich über eine Reduktion der Zahl funktioneller Ca^{2+}-Kanalkomplexe in der Plasmamembran erfolgt (Black, III, 2003;Felix, 2005) oder auch mit einer Reduktion der Offenwahrscheinlichkeit selbst in Verbindung stehen könnte. Des Weiteren bewirken die γ-Untereinheiten eine Verschiebung der

spannungsabhängigen Inaktivierungskurve zu negativeren Potentialen und begünstigen so thermodynamisch die inaktivierte Kanalkonformation (Kang and Campbell, 2003).

L-Typ Ca^{2+}-Kanäle zeigen eine weite Verbreitung im ZNS, Skelettmuskel, Herzen und anderen Geweben und sind klassischerweise durch Dihydropyridine, wie z.B. Nifedipin, Nitrendipin oder Isradipin (IC_{50} = 13 nM; Glossmann and Striessnig, 1988) blockierbar. Ferner sprechen sie auf Phenylalkylamine wie Verapamil, Gallopamil und Devapamil (IC_{50} < 1 μM), aber auch Benzothiazepine wie Diltiazem (IC_{50} < 80 μM; Glossmann and Striessnig, 1988) an. Als experimentell eingesetzter Aktivator fungiert BayK8644 (Dirksen, 2002) (**Tab. 2**). Die Non-L-Typ Ca^{2+}-Kanäle werden vorwiegend im ZNS und PNS exprimiert und sind durch eine Reihe von Schnecken- und Spinnentoxinen inhibierbar. So lässt sich $Ca_v2.1$ durch ω-Agatoxin IVA (aus Agelenopsis aperta, IC_{50} = 1 - 90 nM; Randall and Tsien, 1995) und ω-Conotoxin MVIIC hemmen, $Ca_v2.2$ durch ω-Conotoxin GVIA (aus Conus geographus) sowie ebenfalls ω-Conotoxin MVIIC (Catterall et al., 2005).

Type	α_1 subunit	Tissue expression	Function	Deficiency model	Drugs/Toxins
L	$Ca_V1.1\alpha_1$ (α_1S)	skeletal muscle	excitation-contraction coupling	muscular dysgenic mouse (*mdg/mdg*)	Dihydropyridines (*Nifedipine*)
	$Ca_V1.2\alpha_1$ (α_1C)	cardiac/smooth muscle neurons endocrine cells	*excitation-contraction coupling* *excitation-transcription coupling, LTP* *stimulus-secretion coupling*	$Ca_V1.2\alpha_1^{-/-}$	Phenylalkylamines (*Verapamil*) Benzothiazepines (*Diltiazem*)
	$Ca_V1.3\alpha_1$ (α_1D)	sinoatrial node, AV-node, heart atria neurons endocrine cells sensory cells	*sinoatrial heart rate control, AV conduction* excitation transcription coupling; *modulation of firing patterns, pacemaking* stimulus-secretion coupling *stimulus-secretion coupling (IHCs)*	$Ca_V1.3\alpha_1^{-/-}$	
	$Ca_V1.4\alpha_1$ (α_1F)	retina	*stimulus-secretion coupling*	CSNB2 (human)	
P/Q	$Ca_V2.1\alpha_1$ (α_1A)	neurons endocrine cells	stimulus-secretion coupling	$Ca_V2.1\alpha_1^{-/-}$	ω-Aga-IVA
N	$Ca_V2.2\alpha_1$ (α_1B)	neurons endocrine cells	stimulus-secretion coupling	$Ca_V2.2\alpha_1^{-/-}$	ω-CgTX-GVIA
R	$Ca_V2.3\alpha_1$ (α_1E) + $Ca_V?\alpha_1$	neurons endocrine cells cardiac/smooth muscle	stimulus-secretion coupling, *LTP* *stimulus-secretion coupling*	$Ca_V2.3\alpha_1^{-/-}$	SNX-482
T	$Ca_V3.1\alpha_1$ (α_1G)	neurons sinoatrial node	*burst-firing; automaticity* *sinoatrial heart rate control*	$Ca_V3.1\alpha_1^{-/-}$ $Ca_V3.2\alpha_1^{-/-}$	(Kurtoxin, Mibefradil) (+)-ECN
	$Ca_V3.2\alpha_1$ (α_1H)	DRGs vascular smooth muscle cardiac muscle kidney, liver	*firing patterns, excitability* *vasodilation*		
	$Ca_V3.3\alpha_1$ (α_1I)	neurons	automaticity	-	

Tab. 2: Nomenklatur, Physiologie und Pharmakologie der Ca_v-α_1-Untereinheiten spannungsgesteuerter Ca^{2+}-Kanäle. Die Tabelle zeigt das Expressionsmuster sowie wichtige pharmakologische Details. Man beachte, dass $Ca_v2.3$ Ca^{2+}-Kanäle nur einen SNX-482 sensitiven Teil des ürsprünglich als R-Typ definierten Ca^{2+}-Stromes vermitteln. Die Identität des SNX-482 insensitiven R-Typ Stromes ist weiterhin ungeklärt (modifiziert nach Striessnig and Koschak, 2008).

Mit Ziconotid (SNX-111) wird seit Kurzem ein $Ca_v2.2$ Ca^{2+}-Kanalblocker zur Therapie schwerer chronischer Schmerzzustände eingesetzt, insbesondere bei Patienten, die gegenüber

Opiaten refraktär erscheinen oder mit Unverträglichkeit reagieren. Es handelt sich um ein 25 Aminosäuren umfassendes polybasisches Peptid, welches ein synthetisches Äquivalent zum ω-Cenotoxin M-VII-A der piscivoren Meeresschnecke Conus magnus darstellt (Klotz, 2006) (**Tab. 2**).

Für den lange Zeit als R-(*resistant*) Typ bezeichneten $Ca_v2.3$ Ca^{2+}-Kanal fand sich erst 1998 mit dem Taranteltoxin SNX-482 (aus Hysterocrates gigas) ein vergleichsweise spezifischer Blocker (IC_{50} = 15 - 30 nM; Newcomb et al., 1998). Weiterhin besteht eine hohe Empfindlichkeit gegenüber Ni^{2+}-Ionen (IC_{50} = 27 μM; Catterall et al., 2005), welche der Kanal mit $Ca_v3.2$ teilt (IC_{50} = 12 μM; Lee et al., 1999). Obwohl es mit Mibefradil (IC_{50} = 1,5 μM) und dem Skorpiontoxin Kurtoxin (IC_{50} = 15 nM ($Ca_v3.1$); Chuang et al., 1998;Perez-Reyes, 2003) erste erfolgsversprechende Ansätze für vergleichsweise selektive T-Typ Blocker gab (Lacinova, 2004), erreichen diese bis heute noch nicht das gewünschte pharmakologische Profil und finden daher v.a. in der Forschung Verwendung (**Tab. 2**).

1.1.2. Humane Ca^{2+}-Kanalopathien - eine Übersicht

Innerhalb des letzten Jahrzehnts hat die Zahl der als sog. Ca^{2+}-Kanalopathien definierten Krankheitsentitäten, die v.a. das neuronale und muskuläre System affizieren, deutlich zugenommen. Beim Menschen finden sich hierbei v.a. Mutationen in den L-Typ $Ca_v1.2$ und $Ca_v1.4$ Ca^{2+}-Kanälen sowie in den Non-L-Typ $Ca_v2.1$ und T-Typ $Ca_v3.2$ Untereinheiten. Derartige Mutationen sind mit Alterationen grundlegender elektrophysiologischer Parameter assoziiert und somit von ätiopathologischer Relevanz. Basierend auf ihrer dominanten Expression im ZNS sind Ca^{2+}-Kanäle aber auch für Epilepsien sowie Erkrankungen aus dem neuropsychiatrischen Formenkreis von besonderer Bedeutung. Eine ausführliche Darstellung humaner Ca^{2+}-Kanalopathien findet sich auch in Weiergräber et al. (2008b).

1.1.2.1. Hochspannungsaktivierte L-Typ Kalziumkanäle ($Ca_v1.1$-1.4)

Bislang sind in der Gruppe der L-Typ Ca^{2+}-Kanäle nur Mutationen der $Ca_v1.1$-, $Ca_v1.2$- und $Ca_v1.4$-, nicht aber der $Ca_v1.3$-Untereinheit bekannt. Beim Menschen sind zwei neurologische Krankheitsbilder ätiopathogenetisch mit $Ca_v1.1$ assoziiert: die hypokaliämische periodische Paralyse Typ 1 (HypoPP1) sowie die maligne Hyperthermie (MH) Typ 5 (Ptacek et al., 1994;Fontaine et al., 1994;Monnier et al., 1997). Erst kürzlich wurde mit dem sog. Timothy-Syndrom auch die erste Mutation der $Ca_v1.2$-Untereinheit beim Menschen detektiert. Es han-

delt sich hierbei um eine Multisystem-Erkrankung, die durch maligne kardiale Arrhythmien (u.a. LQT8), komplexe Entwicklungsstörungen, Immundefizienz und neurologische wie neuropsychiatrische Komplikationen gekennzeichnet ist. So zeigen Timothy-Patienten rezidivierende epileptische Anfälle (21 %), autistische Störungen (80 %) sowie mentale Retardierung in 25 % der Fälle (Splawski et al., 2004;Splawski et al., 2005). Die zu Grunde liegenden *missense*-Mutationen haben eine *gain-of-function* Charakteristik. Die größte Zahl bekannter Mutationen (> 73) vereinigt die $Ca_v1.4$ Ca^{2+}-Kanaluntereinheit auf sich. Entsprechend ihrer retinalen Expression führen Mutationen zur X-chromosomal gebundenen angeborenen Form der Nachtblindheit (*x-linked congenital stationary night blindness, X-CSNB2;* Bech-Hansen et al., 1998) sowie zur X-chromosomal gebundenen Stäbchen-Zapfen Dystrophie Typ 3 (*X-linked cone-rod dystrophy type 3, CORDX3;* Jalkanen et al., 2006). Weiterhin bestehen Hinweise auf eine Assoziation zwischen Schizophrenie und dem CACNA1F Genlokus (Wei and Hemmings, 2006).

1.1.2.2. Hochspannungsaktivierte Non-L-Typ Kalziumkanäle ($Ca_v2.1$-2.3)

Der $Ca_v2.1$ Ca^{2+}-Kanal stellt derzeit die wohl bedeutendste α_1-Untereinheit dar, die mit Ca^{2+}-Kanalopathien in Verbindung gebracht werden konnte (McKeown et al., 2006). Eine weite Verbreitung im ZNS und seine Involvierung in die schnelle Neurotransmitterfreisetzung unterstreichen dessen Relevanz. Aber auch in den Dendriten ausgewählter Neurone lässt sich $Ca_v2.1$ nachweisen und spielt hier bei integrativen dendritischen Prozessen eine wichtige Rolle. Die Zahl beschriebener Mausmodelle mit $Ca_v2.1$-Mutationen ist groß, wobei die pathophysiologischen Mechanismen der entsprechenden Phänotypen wie Ataxie, Absencen etc. noch weitgehend unbekannt sind (Pietrobon, 2005). Die wichtigsten Krankheitsbilder sind die episodische Ataxie Typ 2 (EA2), die familiäre hemiplegische Migräne Typ 1 (FHM1), die spinozerebelläre Ataxie Typ 6 (SCA6) sowie idiopathische generalisierte Epilepsieformen (IGE) (Ophoff et al., 1996;Ophoff et al., 1998). Idiopathische generalisierte Formen der Epilepsie umfassen generalisiert tonisch-klonische Anfälle, myoklonische Anfälle wie die juvenile Myoklonusepilepsie (JME), aber auch typische und atypische Absencen (Khosravani and Zamponi, 2006). Die Assoziation der $Ca_v2.1$ Untereinheit mit einzelnen Epilepsieentitäten beim Menschen ist noch weitgehend unklar, während es eine Vielzahl von Mausmodellen mit einem Absencen-ähnlichen Phänotyp gibt (Pietrobon, 2002;Felix, 2002;Pietrobon, 2005;Felix, 2006). Es ist allerdings eine Tatsache, dass man EA2-Patienten mit generalisierten epileptischen Anfällen vorgefunden hat (Jouvenceau et al., 2001;Strupp et al., 2004). Dennoch, die Koinzidenz von EA2 und Absencen-Epilepsien ist eine Rarität. Das gemeinsame Auftreten

von FHM1 und Absencen ist bislang nicht beschrieben, wohl jedoch Koinzidenz mit anderen Anfallsformen. Für den N-Typ $Ca_v2.2$ liegen bislang keine Informationen über Mutationen beim Menschen vor. Für den $Ca_v2.3$ E/R-Typ Ca^{2+}-Kanal gibt es Hinweise, dass Alterationen in der 5'-untranslatierten Region (5'-UTR) sowie Polymorphismen im CACNA1E-Gen mit Typ II-Diabetes assoziiert sind (Holmkvist et al., 2007; Muller et al., 2007). Auf die Rolle des $Ca_v2.3$ Ca^{2+}-Kanals bei Iktogenese/Epileptogenese und Neurodegeneration wird weiter unten im Detail eingegangen.

1.1.2.3. Niederspannungsaktivierte T-Typ Kalziumkanäle ($Ca_v3.1$-3.3)

Bislang konnten in der Gruppe der niederspannungsaktivierten T-Typ Ca^{2+}-Kanäle nur $Ca_v3.2$-Mutationen nachgewiesen werden, nicht jedoch Mutationen in $Ca_v3.1$ und $Ca_v3.3$ (Khosravani et al., 2004;Khosravani and Zamponi, 2006). Dies ist umso erstaunlicher, als $Ca_v3.1$ im Rahmen der Absencen-Epileptogenese in Tiermodellen eine wichtige Stellung einnimmt. So weisen $Ca_v3.1$ defiziente Mäuse eine Resistenz gegenüber der Induktion von *spike-wave* Graphoelementen (Kim et al., 2001) sowie Störungen des *slow-wave* Schlafes und der REM/NREM-Schlafarchitektur auf (Lee et al., 2004). $Ca_v3.2$-Mutationen hingegen können beim Menschen Epilepsien triggern. So werden *missense*-Mutationen in $Ca_v3.2$, die den Ca^{2+}-Einstrom faszilitieren u.a. für die *childhood absence epilepsy* (CAE) aber auch andere idiopathische generalisierte Anfallsformen beim Menschen verantwortlich gemacht (Chen et al., 2003;Khosravani et al., 2004). Viele der beschriebenen Mutationen befinden sich im I-II-*loop* des Kanals. Es ist bemerkenswert, dass nicht nur $Ca_v1.2$-Mutationen beim Timothy-Syndrom, sondern auch $Ca_v3.2$ mit autistischen Störungen in Verbindung gebracht worden ist (Splawski et al., 2006).

1.1.2.4. Akzessorische Ca^{2+}-Kanaluntereinheiten

Während im Tiermodell eine Reihe von Mutationen akzessorischer Untereinheiten gefunden wurden, ist bislang beim Menschen nur eine einzelne Familie mit juveniler Myoklonusepilepsie beschrieben, die eine trunkierte Form der β_4-Untereinheit aufweist (Escayg et al., 2000). Des Weiteren wurde erst kürzlich eine Mutation in der $\alpha_2\delta4$-Untereinheit des Menschen gefunden, die mit einer autosomal-rezessiven Form der Nachtblindheit, basierend auf einer Stäbchendystrophie, einhergeht (Wycisk et al., 2006). Mutationen in der γ-Untereinheit des Menschen sind nicht bekannt.

Untereinheit	Pharmakologie	Verteilung	Humane Kalziumkanalopathien
$Ca_v1.1$	Dihydropyridne, Benzothiazepine, Phenylalkylamine, TaiCatoxin, Calciseptine, Calcicludine, FS-2	Skelettmuskel	Hypokaliämische periodische Paralyse Typ 1 (HypoPP1) Maligne Hyperthermie Typ 5 (MH5)
$Ca_v1.2$		Ubiquitär	Timothy-Syndrom (LQT8, Epilepsien)
$Ca_v1.3$		Ubiquitär	Nicht bekannt
$Ca_v1.4$		Retina	X-*linked congenital stationary night blindness 2* (xCSNB2), X-*linked cone-rod dystrophy type* 3 (CORDX3), *Aland Island eye disease* (AIED)
$Ca_v2.1$	ω-Agatoxin IVA	ZNS	Absencen-Epilepsie, Episodische Ataxia Typ 2 (EA2), spinozerebelläre Ataxie Typ 6 (SCA6) Familiäre hemiplegische Migräne (FHM1) Lambert-Eaton Myastenie-Syndrom (LEMS)
$Ca_v2.2$	ω-Conotoxin GVIA	ZNS/PNS	Lambert-Eaton-Myastenie-Syndrom (LEMS)
$Ca_v2.3$	SNX-482, Ni^{2+}	ZNS/PNS	*Young onset* Typ 2 Diabetes mellitus
$Ca_v3.1$	Mibefradil, Kurtoxin, Ni^{2+}	ZNS/PNS	Nicht bekannt
$Ca_v3.2$		ZNS/Herz	Absencen-Epilepsie (CAE), idiopathisch generalisierte Epilepsien (IGE), autistischer Formenkreis
$Ca_v3.3$		ZNS	Nicht bekannt

ZNS zentrales Nervensystem, PNS peripheres Nervensystem.

Tab. 3: Kanalopathien der Ca_v-α_1-Untereinheiten. Mit einem epileptischen Phänotyp konnten bislang die $Ca_v1.2$, $Ca_v2.1$ und $Ca_v3.2$ Untereinheiten in Verbindung gebracht werden (Weiergräber et al., 2008b).

1.1.3. Alterationen spannungsgesteuerter Ca^{2+}-Kanäle im Tiermodell

Tiermodelle haben in der Vergangenheit viel zum Verständnis pathophysiologischer Prozesse beigetragen und somit die Möglichkeiten rationaler Therapieansätze geschaffen. Bis zum heutigen Zeitpunkt sind für die verschiedenen porenbildenden Ca_v-α_1- sowie akzessorischen Untereinheiten v.a. in Tiermodellen diverse Mutationen bekannt, die mit einem neurologischen Phänotyp assoziiert sind (Felix, 2002;Striessnig et al., 2004;Pietrobon, 2005). Interessanterweise finden sich eine Vielzahl von $Ca_v2.1$-Mutationen im Mausmodell, wie z.B. die *tottering* (tg), *tottering leaner* (tg^{la}), *rolling* Nagoya (tg^{rol}) oder *rocker* (rkr) Maus, wobei sich ähnlich wie beim Menschen eine komplexe neurologische Symptomatik bestehend aus zerebellärer Ataxie, paroxysmaler Dyskinesie und Absencen-Epilepsie darstellt. Anders als beim Menschen sind jedoch bei der Maus auch eine Reihe von Mutationen akzessorischer Ca^{2+}-Kanaluntereinheiten bekannt. Beispiele hierfür sind das *lethargic* (lh) Mausmodell (β_4-Leserastermutation), *stargazer* (stg) Mausmodell (γ_2-Mutation) sowie Mutationen in der $\alpha_2\delta_2$-Untereinheit (*ducky* (du) und *entla* (ent)-Phänotyp) (Felix, 2002;Felix, 2006). $Ca_v2.1$-Mutationen im Bereich funktioneller Domänen rufen bei Nagern regelmäßig eine Funktionseinschränkung des Kanals hervor mit Beeinträchtigung der synaptischen Neurotransmission (McKeown et al., 2006). Es ist wichtig hervorzuheben, dass in keinem der $Ca_v2.1$-Mausmodelle Absencen isoliert auftreten, sondern stets in Kombination mit Ataxie, zerebellärer Atrophie oder Dyskinesien. So bleibt die funktionelle Involvierung des $Ca_v2.1$ Ca^{2+}-Kanals bei Absencen noch immer ein Enigma.

1.1.4. Spannungs- und ligandengesteuerte Ionenkanäle in Ätiologie und Pathogenese von Epilepsien

Epilepsien stellen weltweit eine neurologische Krankheitsentität dar, die von hoher medizinisch-ökonomischer aber auch soziokultureller Relevanz ist. So finden sich manifeste Epilepsien bei ca. 0,5 - 1 % der Bevölkerung, die Lebenszeit-Inzidenz für einen singulären Anfall beträgt ca. 5 % und etwa 10 % der Bevölkerung weist eine erhöhte Anfallssuszeptibilität auf (Jacobs et al., 2001). Ein Teil der Epilepsien ist symptomatischen Charakters, d.h. das Resultat eines sekundären ZNS-gebundenen Prozesses wie z.B. neuronaler Entwicklungsstörungen, Traumata, Ischämien und Neoplasmen (Sun et al., 2002). In vielen Fällen wird eine strukturelle Läsion vermutet, entzieht sich aber dem Nachweis und man spricht dann von sog. kryptogenen Formen. Übrig bleiben die sog. idiopathischen Epilepsien, die einen primär genetischen Hintergrund zu haben scheinen, wobei bis zu 70 % sog. komplexe generalisierte Anfallsformen darstellen, die polygenetischen Charakter aufweisen (Mulley et al., 2005). Zu letzteren kann man heute u.a. die CAE (*childhood absence epilepsy*), JAE (*juvenile absence epilepsy*), JME (*juvenile myoclonic epilepsy*) und $GEFS^+$ (*generalized epilepsy with febrile seizures plus*) rechnen. Die Zahl der monogenen idiopathischen Epilepsien, die v.a. in den letzten 10 - 15 Jahren aufgeklärt wurden und recht einfache Vererbungsmuster aufweisen, ist noch verhältnismäßig klein, zeigt aber deutlich die pathophysiologische Relevanz spannungs- und ligandengesteuerter Ionenkanäle (**Tab. 4**) (Kullmann, 2002;Mulley et al., 2005). Charakteristischerweise reicht bei einem polygenen Vererbungsmodus das Auftreten eines einzelnen Suszeptibilitätsgens nicht aus, sondern es müssen eine Vielzahl von Suszeptibilitätsfaktoren additiv koinzidieren, um zu neuronaler Hyperexzitabilität zu führen und die Anfallsschwelle zu überwinden (Mulley et al., 2005). Etwa 70 % der Epilepsiepatienten sind unter adäquater Pharmakotherapie anfallsfrei, während sich etwa 30 % als pharmakoresistent erweisen und eine große Herausforderung für die weitere Behandlung darstellen (Remy and Beck, 2006).

In der letzten Dekade hat die Zahl der durch *Screening*-Verfahren und Mutationsanalyse entmystifizierten Epilepsieentitäten eine sprunghafte Zunahme erfahren und gezeigt, dass eine Vielzahl von Proteinen funktionelle Relevanz nicht nur für die Genese spontaner epileptiformer Aktivität, sondern auch für die Anfallssuszeptibilität aufweist. Hierzu zählen Neurotransmitterrezeptoren und Transporter, Signaltransduktionskomponenten, vesikuläre *docking*-Proteine und Neuropeptide, Zellzyklus- und Proliferationsregulatoren sowie Transkriptionsfaktoren. Während mittlerweile auch extrazelluläre Matrixproteine zunehmend an Bedeutung gewinnen (Köhling et al., 2006), sind es aber v.a. die spannungs- und ligandengesteuerten Ionenkanäle, die eine Schlüsselstellung in Ätiologie und Pathogenese von Epilepsien ein-

nehmen und einen Großteil der bekannten Kanalopathien darstellen (Rogawski and Loscher, 2004).

Epilepsie-Gen	Epilepsie-Syndrom	Entdeckungsjahr
Monogene ideopathische Epilepsien (Kanalopathien)		
CHRNA4	ADNFLE	1995
KCNQ2	BFNS	1998
KCNQ3	BFNS	1998
SCN1B	$GEFS^+$	1998
SCN1A	$GEFS^+$/(SMEI)	2000/(01)
CHRNB2	ADNFLE	2000
GABRG2	$CAE/FS/GEFS^+$	2001
SCN2A	$GEFS^+$?/BFNIS	2001/02
GABRA1	ADJME	2002
CLCN2	IGE	2003
Monogene ideopathische Epilepsien (keine Kanalopathien)		
LGI1	ADPEAF	2002
EFHC1	JME	2004
Polygene (komplexe) ideopathische Epilepsien (Kanalopathien)		
CACNA1H	CAE, IGE	2003/04
GABRD	IGE, $GEFS^+$	2004

Tab. 4: Monogene und polygene idiopathische Epilepsien – Gene und Suszeptibilitätsloki. Verwendete Abkürzungen: Ionenkanäle: CHRNA4: nikotinerger Azethylcholinrezeptor, α_4-Untereinheit; KCNQ2: K^+-Kanal; KCNQ3: K^+-Kanal; SCN1B: Na^+-Kanal, $ß_1$-Untereinheit; SCN1A: Na^+-Kanal, α_1-Untereinheit; CHRNB2: nikotinerger Azetylcholinrezeptor, $ß_2$-Untereinheit; GABRG2: $GABA_A$-Rezeptor, γ_2-Untereinheit; SCN2A: Na^+-Kanal, α_2-Untereinheit; GABRA1: $GABA_A$-Rezeptor, α_1-Untereinheit; CLCN2: Cl^--Kanal-Gen 2; LGI1: Leuzin-reiches, Glioma-inaktiviertes Gen 1, EFHC1: EF-Hand-Protein C1; CACNA1H: T-Typ Ca^{2+}-Kanal; GABRD: $GABA_A$-Rezeptor, δ-Untereinheit. Syndrome: ADNFLE: *autosomal dominant nocturnal frontal lobe epilepsy*; BFNS: *benign familial neonatal seizures* ; $GEFS^+$: *generalized epilepsy with febrile seizures plus*; SMEI: *severe myoclonic epilepsy of infancy*; CAE: *childhood absence epilepsy*; FS: *febrile seizures*; BFNIS: *benign familial neonatal-infantile seizures*; ADJME: *autosomal dominant juvenile myoclonic epilepsy*; IGE: *ideopathic generalized epilepsy*; ADPEAF: *autosomal dominant partial epilepsy with auditory features*; JME: *juvenile myoclonic epilepsy* (Mulley et al., 2005).

Hier spielen sowohl sog. *gain-of-function* als auch *loss-of-function* Mutationen eine entscheidende Rolle. So sind derzeit u.a. eine Vielzahl von Mutationen in spannungsgesteuerten Na^+-, K^+- und Cl^--Kanälen bekannt, die mit einem epileptischen Phänotyp assoziiert sein können.

Nicht zuletzt durch Forschungsansätze unter Verwendung transgener Tiere (*knock-in* und *knock-out* Studien) konnte ein detaillierter Einblick in die Molekularbiologie, Elektrophysiologie und pathophysiologische Relevanz beteiligter Ionenkanäle gewonnen werden (McKeown et al., 2006;Bidaud et al., 2006).

1.2. Physiologie und Pathophysiologie des spannungsgesteuerten $Ca_v2.3$ E/R-Typ Ca^{2+}-Kanals

1.2.1. Grundlegende Aspekte des $Ca_v2.3$ E/R-Typ Ca^{2+}-Kanals

Der $Ca_v2.3$ Ca^{2+}-Kanal zeigt eine weites Expressionsmuster im Organismus und beeinflusst vielfältige physiologische und pathophysiologische Mechanismen. Ein Großteil unserer heutigen Erkenntnisse beruht auf Studien an $Ca_v2.3$ defizienten Mäusen, die unabhängig voneinander in den Laboratorien von R. Miller (Chicago), T. Tanabe (Tokyo), H.-S. Shin (Seoul) sowie T. Schneider (Köln) generiert wurden. Detaillierte Untersuchungen haben u.a. gezeigt, dass $Ca_v2.3^{-/-}$ Tiere eine veränderte Spermienmotilität aufweisen (Sakata et al., 2002), eine alterierte zerebelläre Funktion (Osanai et al., 2006), modifizierte Schmerzperzeption (Saegusa et al., 2000), erhöhte Empfindlichkeit gegenüber ischämischem Hirnschaden (Toriyama et al., 2002), erhöhtes Angstniveau (Lee et al., 2002) sowie verminderte Glukosetoleranz und Insulinsekretion (Matsuda et al., 2001;Pereverzev et al., 2002). In pankreatischen β-Zellen trägt $Ca_v2.3$ nur zu einem Viertel zum totalen Ca^{2+}-Einstroms bei (Jing et al., 2005), wobei $Ca_v2.3$ v.a. die zweite, langsame Phase der Insulinsekretion unterstützt (Jing et al., 2005), ein Effekt, welcher auch durch SNX-482 inhibierbar ist. Während der $Ca_v1.2$ Ca^{2+}-Kanal dominant die erste Phase der Insulinsekretion steuert, dient $Ca_v2.3$ eher der Rekrutierung neuer Insulinhaltiger Vesikel zum Zwecke deren Freisetzung. Genetische Analysen deuten darauf hin, dass Polymorphismen im $Ca_v2.3$ Gen mit einem erhöhten Risiko zur Entwicklung eines Typ-II Diabetes vergesellschaftet sind (Holmkvist et al., 2007).

Eine Beteiligung des R-Typ Ca^{2+}-Kanals wurde auch an der myoneuralen Synapse (Matsuda et al., 2001) sowie bei hippokampalen Neuronen beschrieben. Untersuchungen an der Moosfaser-CA3 Synapse von $Ca_v2.3^{-/-}$ Mäusen zeigte zweifelsfrei, dass $Ca_v2.3$ Ca^{2+}-Kanäle eine entscheidende Rolle bei der Mossfaser-Langzeitpotentzierung und posttetanischen Potenzierung als Folge kurzer tetanischer Stimuli spielen (Dietrich et al., 2003;Breustedt et al., 2003). Anders als $Ca_v2.1$ P/Q-Typ und $Ca_v2.2$ N-Typ Ca^{2+}-Kanäle, trägt $Ca_v2.3$ nicht unmittelbar an der durch ein einzelnes Aktionspotential vermittelten Transmitterfreisetzung bei, sondern erst nach repetitiver Stimulation (Dietrich et al., 2003). Ursache hierfür scheint u.a. die mehr distal vom synaptischen Freisetzungsareal gelegende $Ca_v2.3$-Lokalisation zu sein (Dietrich et al., 2003). Übereinstimmend mit den obigen Resultaten Resultaten wurde bei $Ca_v2.3$ defizienten Mäusen auch eine Beeinträchtigung des Ortsgedächtnis beschrieben (Kubota et al., 2001), wobei das erhöhte Angstniveau (Kubota et al., 2001;Saegusa et al., 2001;Lee et al., 2002) dieses Ergebnis relativieren mag. Eine Alteration der Langzeitpotenzierung in der CA1 Regi-

on konnte bei $Ca_v2.3$ *knock-out* Mäusen nicht nachgewiesen werden (Kubota et al., 2001). Auch bei neuropathischen Schmerzen spielen $Ca_v2.3$ Ca^{2+}-Kanäle offensichtlich eine Rolle. So führt intraspinale Applikation von SNX-482 zu einer Dosis-abhängigen Inhibition der durch C- und Aδ-Schmerzfasern vermittelten Aktivität (Matthews et al., 2007). Zuletzt zeigte sich auch im kardiovaskulären System (Weiergräber et al., 2005b), im Gastrointestinaltrakt (Grabsch et al., 1999) sowie bei der angiovasospastische Aktivität in der Folge subarachnoidaler Blutungen beim Menschen (Ishiguro et al., 2005;Link et al., 2008) die funktionelle Relevanz des $Ca_v2.3$ Ca^{2+}-Kanals.

Die Generierung $Ca_v2.3$ defizienter Mäuse hat nicht zuletzt auch die Möglichkeit eröffnet, neue Erkenntnisse über die dem R-Typ Ca^{2+}-Strom zu Grunde liegende molekulare Identität zu gewinnen. So versteht man klassischerweise unter einem R-Typ Strom die nach pharmakologischer Blockade von L-Typ, P/Q-Typ und N-Typ Ca^{2+}-Kanälen verbleibende Stromkomponente, die typischerweise $Ca_v2.3$ zugeschrieben wurde. Die $Ca_v2.3$ *knock-out* Mausmodelle haben jedoch gezeigt, dass der Anteil des $Ca_v2.3$ getragenen R-Typ Stroms zwischen 30 % in zerebellären Körnerzellen (Wilson et al., 2000) und 81 % in zentralen Amygdalaneuronen (Lee et al., 2002) beträgt und dieser die SNX-482 empfindliche Komponente darstellt (Tottene et al., 2000). Die Identität der SNX-482 inresistenten R-Typ Stromkomponente hingegen ist weiterhin ein Enigma (**Tab. 1**). Inwiefern die Nomenklatur als R-Typ Strom adäquat ist, bleibt fraglich. In den eigenen Publikationen sowie in dieser Arbeit wird daher vom E/R-Typ Ca^{2+}-Kanal gesprochen.

1.2.2. Spannungsgesteuerte Ca^{2+}-Kanäle in der Ätiopathogenese hippokampaler Epilepsien

1.2.2.1. Die hippokampale Epilepsie – eine konvulsive Anfallsform im Überblick

Epidemiologische Studien haben gezeigt, dass etwa 40 % aller Epilepsiepatienten unter einer Temporallappenepilepsie (TLE) leiden, weitere ca. 40 % an generalisierten konvulsiven Anfallsformen und etwa 10 % an einer Epilepsie vom Absencen-Typ. Temporallappenepilepsien lassen sich in laterale und mediale (mesiale) Formen differenzieren und sind für die Entstehung typischer komplex-partieller Anfälle beim Menschen verantwortlich. Häufig mit olfaktorischen, gustatorischen, visuellen oder psychischen Auren, wie mentale Diplopie, vergesellschaftet, schließen sich typische automatistische Handlungsabläufe im orofazialen Bereich sowie der oberen Extremität an, in deren Verlauf es regelmäßig zu einer Bewusstseinsein-

schränkung kommt. Der Hippokampus ist eine sehr vulnerable, Ischämie- und Anoxie-suszeptible Struktur. Bei Patienten mit langer TLE-Anamnese findet sich oft eine ein- oder beidseitige Hippokampussklerose. Bei Therapieresistenz und hippokampalem Status epilepticus kommt als ultima ratio die Hippokampektomie als epilepsiechirurgischer Eingriff in Frage (Buzsaki, 2006).

1.2.2.2. Hippokampale neuronale Verschaltung

Der Hippokampus stellt morphologisch und funktionell eine der bestuntersuchten Strukturen des menschlichen Zentralnervensystems dar. Zusammen mit weiteren Strukturen, wie dem Subiculum, Präsubiculum, Parasubiculum und entorhinalen Kortex bildet er die hippokampale Formation. Diese ist funktionell integriert in eine Reihe komplexer Systeme, wie z.B. den Papez-Neuronenkreis oder das basolaterale limbische System. Der Hippokampus spielt eine Schlüsselrolle bei deklarativen (expliziten) und nicht-deklarativen (impliziten) Lernprozessen, Kontextlernen und Kontextverhalten, Konsolidierung von Engrammen zur Langzeitgedächtnisformation sowie Gefühlsentstehung und Emotionalität, wie Freude und Angst. Unter pathophysiologischen Gesichtspunkten erscheint interessant, dass der Hippokampus eine hohe Anfallssuszeptibilität und die niedrigste Anfallsschwelle aller Hirnregionen überhaupt aufweist (Green, 1964).

Die **Abb. 4** zeigt die Verschaltung des Hippokampus mit seiner Eingliederung in das System der assoziativen Kortizes, des parahippokampalen, perirhinalen und entorhinalen Kortex. Vom entorhinalen Kortex erfolgt eine Projektion über den Tractus perforans zu den Körnerzellen des Gyrus dentatus, von hier weiter über die Moosfasern zu CA3-Neuronen mit Kontaktierung im Stratum lucidum. Schaffer-Kollateralen der CA3-Neurone projizieren weiter auf CA1-Neurone, die über das Subiculum u.a. zum entorhinalen Kortex zurückführen. Diese simplifizierte Betrachtungsweise darf nicht darüber hinwegtäuschen, dass der Hippokampus morphologisch und funktionell äußerst komplex ist. So hat sich z.B. gezeigt, dass die Informationspropagationswege unmittelbar von der Frequenz des entorhinalen Inputs abhängen. So führen im sog. trisynaptischen Modell Stimulationsfrequenzen von 5 – 20 Hz primär zu sequentieller Propagation von Information, während niedrigere oder höhere Stimulationsfrequenzen zu einer monosynaptischen Aktivierung von CA3- oder CA1-Neuronen führen (Yeckel and Berger, 1998). Des Weiteren sind hier auch unterschiedliche Formen synaptischer Plastizität anzutreffen.

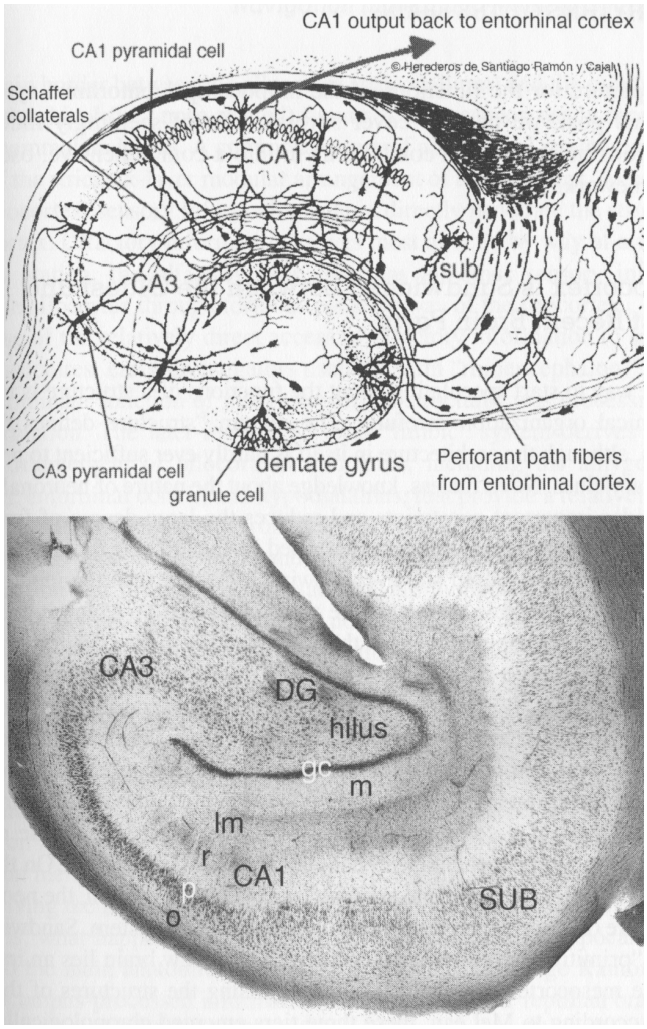

Abb. 4: Darstellung der hippokampalen Verschaltung. Oben: Tractus perforans Fasern aus dem entorhinalen Kortex (II, III) projizieren in Richtung des Gyrus dentatus, der CA3- und CA1-Neurone. Körnerzellen des Gyrus dentatus kontaktieren über Moosfasern CA3-Neurone, die ihrerseits über Schaffer-Kollaterale CA1-Neurone ansprechen. CA1-Pyramidenzellen innervieren über die Fimbriae subkortikale Zielstrukturen, zum großen Teil verlassen CA1-Axone über das Subiculum den Hippokampus und kontaktieren die tiefen Schichten des entorhinalen Kortex. Unten: Schnitt durch den menschlichen Hippokampus (o: Stratum oriens; p: Stratum pyramidale; r: Stratum radiatum; lm: Stratum lacunosum-moleculare; m: stratum moleculare des Gyrus dentatus; gc: Körnerzellen (*granule cells*); DG: Gyrus dentatus; SUB: Subiculum) (Buzsaki, 2006).

1.2.2.3. Zellulär-elektrophysiologische Korrelate epileptiformer Aktivität

Das grundlegende Aktivitätsprofil eines „epileptischen" Neurons wird als paroxysmaler Depolarisationsshift (PDS) bezeichnet. Eine durch verschiedene liganden- und spannungsgesteuerte Ionenkanäle getriggerte Depolarisation führt zu überschiessender neuronaler Aktivität, die sich auf angrenzende, aber auch entfernt liegende Areale ausbreiten kann, ein Vorgang, der als Anfallspropagation bezeichnet wird. Zwei wichtige Spannungsentitäten mit iktogener Potenz sind die sog. Nachdepolarisationen (*afterdepolarisation*, ADPs) und Plateau-Potentiale (PP). Beide vermögen auf der Grundlage einer persistierenden Depolarisation variabler Dauer durch Aktivierung schneller Na^+-Kanäle sog. *burst*-Aktivität, d.h. superpositionierte Na^+-*spikes* zu induzieren. Paroxysmale Depolarisationsshifts vermitteln u.a. einen Ca^{2+}-Einstrom und können eine strukturelle und funktionelle Remodellierung juveniler und maturer neuronaler Schaltkreise sowie eine Alteration synaptischer Transmission zur Folge haben. Experimentell lassen sie sich durch verschiedenartige Manipulationen induzieren: hierzu gehören u.a. eine Inhibition der GABA- oder eine Verstärkung der Glutamat-Neurotransmission (Segal

and Furshpan, 1990;Segal, 1991;Segal, 1994). Neben diesen synaptischen Mechanismen der PDS-Genese sind es aber v.a. somatodendritische Ionenströme, welche die Morphologie und Frequenz von paroxysmalen Depolarisationshifts maßgeblich prägen (Straub et al., 1990;Momiyama et al., 1995;Schiller, 2002). Die ionalen Mechanismen paroxysmaler Depolarisationsshifts sind ein wichtiges Forschungsgebiet zur Identifizierung neuer pharmakologischer Zielstrukturen und kausaler Therapieansätze.

1.2.2.4. Plateau-Potentiale im Hippokampus – molekulare und ionale Grundlagen

Bevorzugtes Untersuchungsobjekt für Plateau-Potentiale sind Pyramidalzellen in der CA1-Region des Hippokampus. In CA1-Neuronen lassen sich Plateau-Potentiale durch Stimulation muskarinerger M_1-, M_3-Rezeptoren, z.B. mittels Pilokarpin oder Carbachol (20 µM) stimulieren (**Abb. 5**). Dies hat eine leichte Membrandepolarisation (von -66 mV auf -60 mV) sowie eine Extinktion der Nachhyperpolarisation (*afterhyperpolarization*, AHP) zur Folge. In Abhängigkeit von der Höhe des applizierten Testpulses bilden sich langsame Nachdepolarisationen (sADP) oder Plateau-Potentiale aus. Die Bedeutung der cholinergen Stimulierbarkeit iktogener Plateau-Potentiale wird dadurch offenbar, dass cholinerge Hyperexzitabilität bei der Genese limbischer Epilepsien wirksam ist (Vosu and Wise, 1975;Cassel et al., 1987;Kawasaki et al., 1996) und die systemische Administration zentralgängiger Cholinergika, z.B. des Pilokarpins, als Model der Temporallappenepilepsie fungiert (Lothman et al., 1991). Beobachtungen einer verminderten hippokampalen Anfallssuszeptibilität nach Pilokarpin-Gabe in M_1-Rezeptor defizienten Mäusen belegen dies deutlich (Hamilton et al., 1997). Umso schwerer wiegt die Frage, welche ionalen Grundlagen Plateau-Potentiale und Nachdepolarisationen tatsächlich haben. Schon früh konnten Fraser und MacVicar (1996) zeigen, dass zyklisch-Nukleotid gesteuerte (CNG) Kanäle wesentlich zu den z.T. Sekunden andauernden Plateau-Potentialen im Hippokampus beitragen. Die im Hippokampus exprimierten Subtypen CNGA1, CNGA2 und CNGA4 unterliegen hierbei einer indirekten muskarinergen Kontrolle. So führt M_1- und M_3-Rezeptoraktivierung zu einem durch hochspannungsaktivierte Ca^{2+}-Kanäle vermittelten Ca^{2+}-Einstrom, der mittels Aktivierung einer löslichen Guanylatzyklase (sGC) und konsekutivem cGMP-Anstieg eine Öffnung der CNG-Kanäle mediiert (Fraser and MacVicar, 1996;Kuzmiski and MacVicar, 2001;Kuzmiski et al., 2005) (**Abb. 6, 7**). Plateau-Potentiale sind also ein sekundäres Phänomen und werden durch einen transienten Ca^{2+}-Einstrom getriggert. Somit entpuppt sich das regelgerechte Feintuning des Ca^{2+}-Einstroms als kritische Komponente der Plateau-Potentialgenese und damit der Genese zellulär-

proepileptiformer Aktivität im ZNS. Wie im Folgenden dargelegt, ist der $Ca_v2.3$ E/R-Typ Ca^{2+}-Kanal eine solche wichtige Komponente bei der Feinregulation des Ca^{2+}-Einstroms.

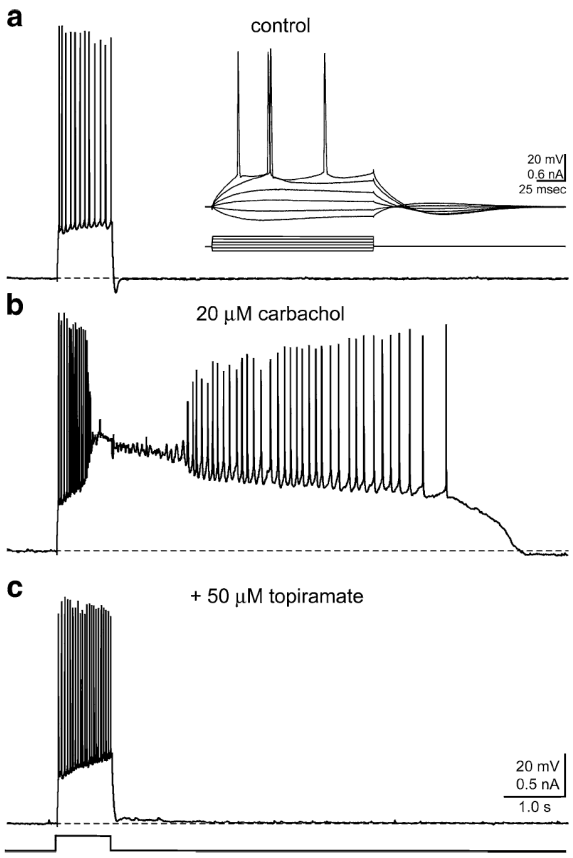

Abb. 5: Provokation von Plateau-Potentialen in hippokampalen CA1-Neuronen durch Administration von Carbachol. A) Charakteristisches Antwortverhalten hippokampaler CA1-Neurone auf verschiedene hyper- und depolarisierende Stromreize in artifizieller zerebrospinaler Flüssigkeit (ACSF). **B**) Nach Applikation von Carbachol (20 μM) kommt es zur Ausbildung eines mehrere Sekunden andauernden Plateau-Potentials. Die anschließende Applikation von Topiramat (50 μM, **C**) führt zu einer kompletten Inhibition der Plateau-Potentiale (Kuzmiski et al., 2005).

Interessanterweise zeigten Kuzmiski et al. (2005), dass Topiramat, ein Breitspektrum-Antiepileptikum, welches zur Therapie partieller Anfälle, primärer generalisiert tonisch-klonischer Anfälle und des Lennox-Gastaut Syndroms eingesetzt wird (LaRoche and Helmers, 2004), Plateau-Potentiale im therapeutisch relevanten Konzentrationsbereich (50 μM) vollständig zu inhibieren vermag (**Abb. 5, 6**). Wie sich in einer Reihe pharmakologisch-elektrophysiologischer Studien zeigte, beruht dieser Topiramat-Effekt in CA1-Neuronen weder auf einer Inhibition der CNG-Kanäle, noch auf einem Antagonismus an muskarinergen oder ionotropen NMDA-, Kainat- oder AMPA-Rezeptoren. Auch das GABAerge System und Ca^{2+}-abhängige K^+-Ströme zeigten sich von therapeutischen Topiramat-Dosen unbeeinflusst, obwohl es sich bei Ca^{2+}-abhängigen K^+-Kanälen an anderer Stelle, wie z.B. in olfaktorischen kortikalen Neuronen, um eine wirksame Zielstruktur dieses Antiepileptikums handelt (Russo et al., 2004). In einer Serie von Experimenten konnten Kuzmiski et al. (2005) zunächst zeigen, dass Topiramat pharmakologisch „isolierte", originäre Ca^{2+}-*spikes* nicht zu modifizieren vermag. Erst nach muskarinerger Stimulation kommt es zu einer deutlich alterierten Ca^{2+}-

spike-Morphologie und ein signifikanter Anteil des Ca^{2+}-Einstroms kann nun durch Topiramat gehemmt werden (**Abb. 8, 9**). Eine Erklärung hierfür liegt in der komplexen, gegenläufig gerichteten muskarinergen Regulation spannungsgesteuerter Ca^{2+}-Kanäle.

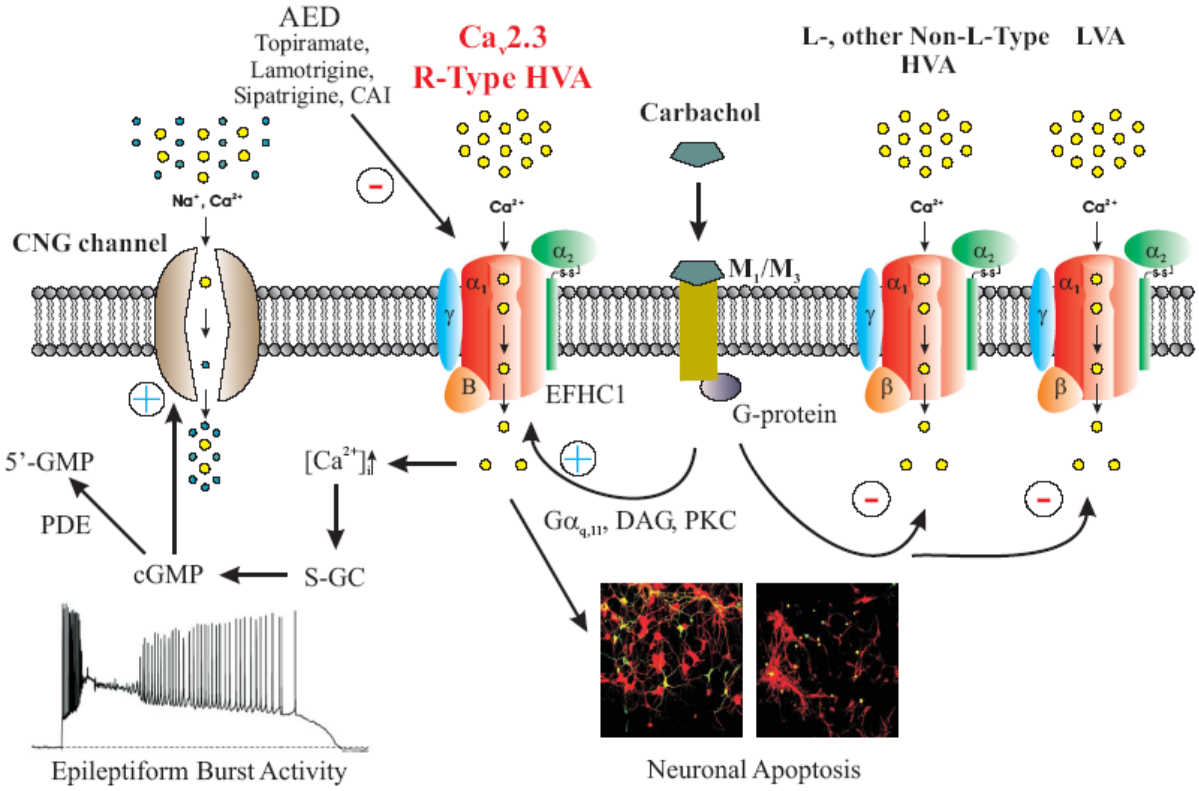

Abb. 6: Neue funktionelle Aspekte des Ca_v2.3 E/R-Typ Ca^{2+}-Kanals in hippokampalen CA1-Neuronen. Muskarinerge Stimulation der CA1-Neurone führt zu Inhibition von L-, Non-L- und T-Typ Ca^{2+}-Kanälen, während Ca_v2.3 selektiv augmentiert wird. Der resultierende Ca^{2+}-Einstrom bewirkt über einen cGMP-abhängigen Mechanismus die Aktivierung von CNG-Kanälen, welche konsekutiv zur Ausbildung von Plateau-Potentialen und epileptiformem *bursting* führen. Ca_v2.3 hat weiterhin Auswirkungen auf die neuronale Apoptose. So bindet der II-III-*loop* des Kanals z.B. das Chaperon HSP70 und ist an der Vermittlung der PKC-Effekte beteiligt. Mutationen in EFHC1, einem C-terminalen Interaktionspartner von Ca_v2.3 führen zu verminderter neuronaler Apoptose während der frühkindlichen Hirnentwicklung mit Ausbildung juveniler Myoklonusepilepsie (JME) (Suzuki et al., 2004). Schließlich haben pharmakologische Studien gezeigt, dass eine Reihe von Antiepileptika (Topiramat, Lamotrigin, Sipatrigin etc.) Ca_v2.3 potent zu inhibieren vermögen. Abk.: AED: antiepileptic drug; CAI: Carboanhydraseinhibitor; EFHC1: EF-Hand Protein C1; S-GC: lösliche Guanylatzyklase; PDE: Phosphodiesterase.

Während muskarinerge Stimulation eine Reduktion von L-, P/Q- und N-Typ vermittelten Ca^{2+}-Strömen bewirkt (Gahwiler and Brown, 1987;Toselli et al., 1989;Toselli and Lux, 1989;Shapiro et al., 1999;Shapiro et al., 2001), führt selbige zu einer Aktivierung des hoch-

spannungsaktivierten $Ca_v2.3$ E/R-Typ Ca^{2+}-Kanals in CA1-Neuronen (Kuzmiski et al., 2005;Tai et al., 2006). Interessanterweise unterliegt der $Ca_v2.3$ Ca^{2+}-Kanal hierbei einer dualen, bidirektionalen muskarinergen Modulation, die im Detail beschrieben (Meza et al., 1999;Melliti et al., 2000;Bannister et al., 2004) und schematisch in **Abb. 6** dargestellt ist. Unter stimulativen Bedingungen führt die Aktivierung von M_1- und M_3-Rezeptoren in CA1-Neuronen (Levey et al., 1995) zur Freisetzung von aktiviertem $G\alpha_{q/11}$. Nach PLC-Stimulierung kommt es zur Bildung von IP_3 und DAG. Das so gebildete Diazylglycerol aktiviert in der Folge Mitglieder einer Ca^{2+}-unabhängigen Gruppe II Proteinkinase C (PKC)-Fraktion (δ,ε,η,θ), mit hoher Wahrscheinlichkeit PKCδ. Die Proteinkinase Cδ weist eine starke Expression in hippokampalen CA1 Neuronen auf (McNamara et al., 1999;Tang et al., 2004) und wird nach muskarinerger Stimulation aktiviert und zur Plasmamembran transloziert (Brown et al., 2005). In Gegenwart von PKC-Inhibitoren kann jedoch auch ein inhibitorischer Prozess überwiegen, in dessen Verlauf die Stimulation von M_2- und M_4-Rezeptoren zur Aktivierung von Pertussistoxin-sensitiven G-Proteinen führt, deren $G_{\beta\gamma}$-Untereinheiten $Ca_v2.3$ zu inhibieren vermögen (Meza et al., 1999;Bannister et al., 2004). Dieser Mechanismus kann somit für die in Gegenwart von PKC-Inhibitoren auftretende Hemmung von E/R-Typ Strömen nach muskarinerger Stimulation von CA1-Neuronen verantwortlich gemacht werden.

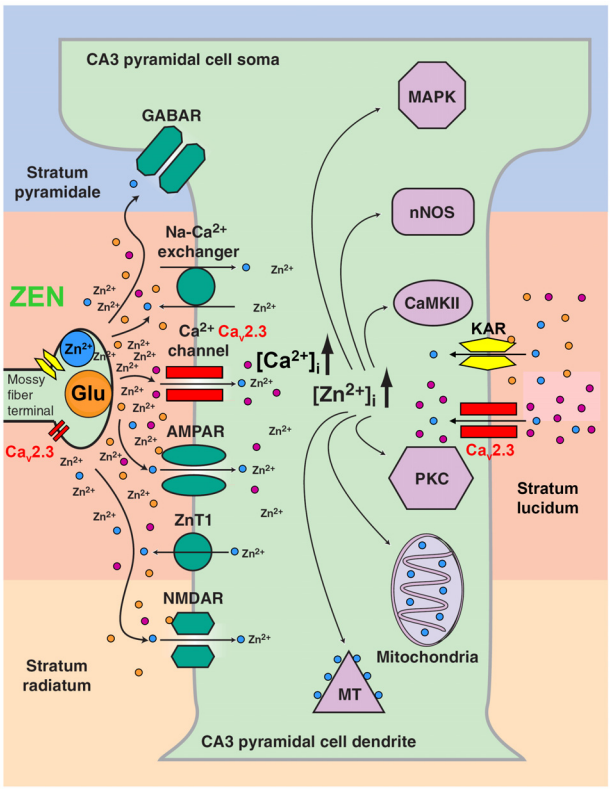

Abb. 7: Funktionelle Integration des $Ca_v2.3$ Ca^{2+}-Kanals, Glutamat-Rezeptoren und Schwermetallkationen (Zn^{2+}) in der CA3-Region. Sowohl $Ca_v2.3$ als auch Kainat-Rezeptoren sind prä- wie postsynaptisch exprimiert und neben physiologischen Prozessen, wie präsynaptischer Langzeitpotenzierung auch an der postsynaptischen Integration beteiligt. Ca^{2+}-mediierte Kosekretion von Glutamat und Zn^{2+} vermag nicht nur diese Prozesse, sondern auch exzitotoxische und neurodegenerative Vorgänge über komplexe intrazelluläre Signaltransduktionskaskaden zu steuern (modifiziert nach Li et al., 2003).

Pharmakologisch oder mittels elektrischer Stimulation induzierte epileptische Aktivität vermag die Expression von M_1- und M_3-Rezeptoren zu verstärken sowie die Effizienz muskaringer Kopplung zu den beteiligten G-Proteinen zu erhöhen. Hier liegt ein weiterer möglicher Mechanismus zur Potenzierung der $Ca_v2.3$ Aktivität während epileptiformen Geschehens (Mingo et al., 1998;Potier et al., 2005).

Isolierte man E/R-Typ Ca^{2+}-*spikes* unter Verwendung von TTX, Nifedipin (DHP), ω-Conotoxin MVIIC, ω-Conotoxin GVIA und ω-Agatoxin IVA, so ließ sich auch hier der residuale, resistente Ca^{2+}-Stromanteil mit 50 μM Topiramat signifikant hemmen (**Abb. 9**). Auch Ni^{2+} (50 μM) führte zu einer vollständigen Extinktion von Plateau-Potentialen nach Carbachol-Gabe (20 μM).

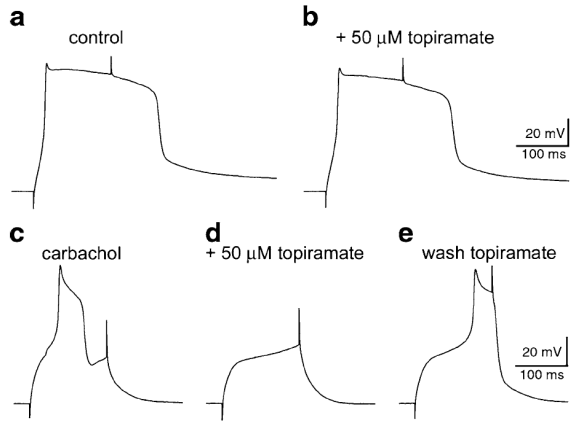

Abb. 8: Topiramat-Wirkung auf Ca^{2+}-*spikes* hippokampaler CA1-Neurone. A) Kontroll-*spike* in Gegenwart von Cs^+ und TTX. **B**) Unter Kontrollbedingungen hat Topiramat (50 μM) keinen Effekt. Erst nach Stimulation durch Carbachol (20 μM) zeigt sich eine deutliche Änderung der Ca^{2+}-*spike*-Morphologie (**C**). Sie ist auf die muskarinerge Inhibition der L-, P/Q- und N-Typ Ca^{2+}-Kanäle sowie die Stimulation des $Ca_v2.3$ E/R-Typs zurückzuführen. Erst jetzt bewirkt Topiramat-Applikation eine signifikante Reduktion der Ca^{2+}-*spike* Amplitude (**D**). Der Effekt ist reversibel (**E**) (Kuzmiski et al., 2005).

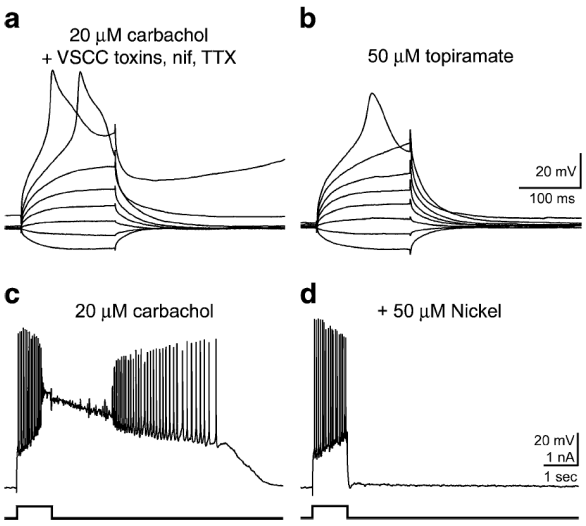

Abb. 9: Isolation von E/R-Typ Ca^{2+}-*spikes* in hippokampalen CA1 Neuronen. Topiramat (50 μM) ist in der Lage, den $Ca_v2.3$ vermittelten Ca^{2+}-*spike* (**A**) signifikant zu inhibieren (**B**). Ni^{2+}-Ionen (50 μM) vermögen $Ca_v2.3$ Kanäle zu hemmen und führen in Konsequenz zu einer kompletten Eliminierung Carbachol-induzierter Plateau-Potentiale (**C, D**) (Kuzmiski et al., 2005).

In extrazellulären Ableitungen aus der CA1-Region zeigt sich nach Carbacholgabe (40 μM) eine deutliche Zunahme der Theta-Aktivität im EEG, die ebenfalls durch Ni^{2+} (100 μM) nahezu vollständig inhibierbar ist (**Abb. 10**). Elektrophysiologische Untersuchungen an rekombinanten $Ca_v2.3$ Ca^{2+}-Kanälen (koexprimiert mit β_{1b} und $\alpha_2\delta1$) im heterologen Expressionssystem (tsA-201 Zellen) erbrachten einen IC_{50}-Wert von 50.9 μM Topiramat und eine Verschiebung der spannungsabhängigen Inaktivierungskurve zu negativeren Potentialen (gemessen bei 100 μM Topiramat), was für eine Verschiebung in Richtung der inaktivierter Kanalkonformation spricht. Erste Hinweise eines Topiramat-Effektes auf $Ca_v2.3$ lieferte zuvor bereits McNaughton et al. (2004). In einer Folgepublikation konnten Tai et al. (2006) detailliert zeigen, dass muskarinerge Stimulation in CA1-Neuronen tatsächlich $Ca_v2.3$ getragene Ca^{2+}-*spikes* augmentiert. Auch hier erfolgte die pharmakologische Isolierung der einzelnen Stromkomponenten über Cd^{2+} (30 μM) und Ni^{2+}-Ionen (50 μM). Prinzipiell ist auch der $Ca_v3.2$ T-Typ Ca^{2+}-Kanal Ni^{2+}-empfindlich (IC_{50} = 12 μM) und käme somit als mögliche Topiramat-Zielstruktur in Frage. Wie Untersuchungen von Tai et al. (2006) gezeigt haben, lassen sich allerdings T-Typ Ca^{2+}-Ströme, anders als E/R-Typ Ströme, über muskarinerge Aktivierung via Carbachol nicht stimulieren. Ein Versuch, den $Ca_v2.3$ vermittelten Ca^{2+}-Strom durch SNX-482 zu hemmen, wurde nicht unternommen. Hierbei ist anzumerken, dass 80 % der Blocker-resistenten Ca^{2+}-Stromkomponente in CA1-Neuronen auf $Ca_v2.3$ beruht und auch Ni^{2+}-sensitiv ist (Sochivko et al., 2002).

Plateau-Potentiale können mehrere hundert Millisekunden bis Sekunden andauern, bevor es zur Termination kommt, und zu einer deutlichen Erhöhung des intrazellulären Ca^{2+}-Spiegels führen ($[Ca^{2+}]_i$ > 200 nM) (Andrew and Dudek, 1984). Bei den für die Termination verantwortlichen Mechanismen handelt es sich u.a. um eine Ca^{2+}-vermittelte K^+-getragene Hyperpolarisation (Hlubek and Cobbett, 2000;Roper et al., 2003). Auch eine Ca^{2+}-abhängige Verlagerung von Ca^{2+}-abhängiger Faszilitierung zu Ca^{2+}-abhängiger Inaktivierung erscheint wahrscheinlich. Der interne Ca^{2+}-Spiegel, der u.a. durch $Ca_v2.3$ mit getragen wird (Dietrich et al., 2003), ist somit bedeutsam, da er nicht nur die K^+-getragene Nachhyperpolarisation mediiert, sondern auch in direktem Zusammenhang mit der somatisch und dendritischen *burst*-Aktivität steht.

Da muskarinerge Rezeptoren und cholinerge Mechanismen eine wichtige Rolle in der Epileptogenese spielen wird deutlich, dass $Ca_v2.3$ auch hier eine entscheidende Funktion zukommt. So hemmt der M_1-Rezeptorantagonist Pirenzepin elektrisches *kindling* bei Ratten (Eskazan et al., 1999). Des Weiteren haben elektrisch und pharmakologisch induzierte Anfälle gezeigt, dass es zu lang anhaltender Hochregulation der M_1- und M_3-Rezeptoren im Hippokampus

kommen kann, die u.a. mit einer gesteigerten Effizienz G-Protein gekoppelter Signaltransduktion assoziiert ist (Mingo et al., 1998;Potier et al., 2005).

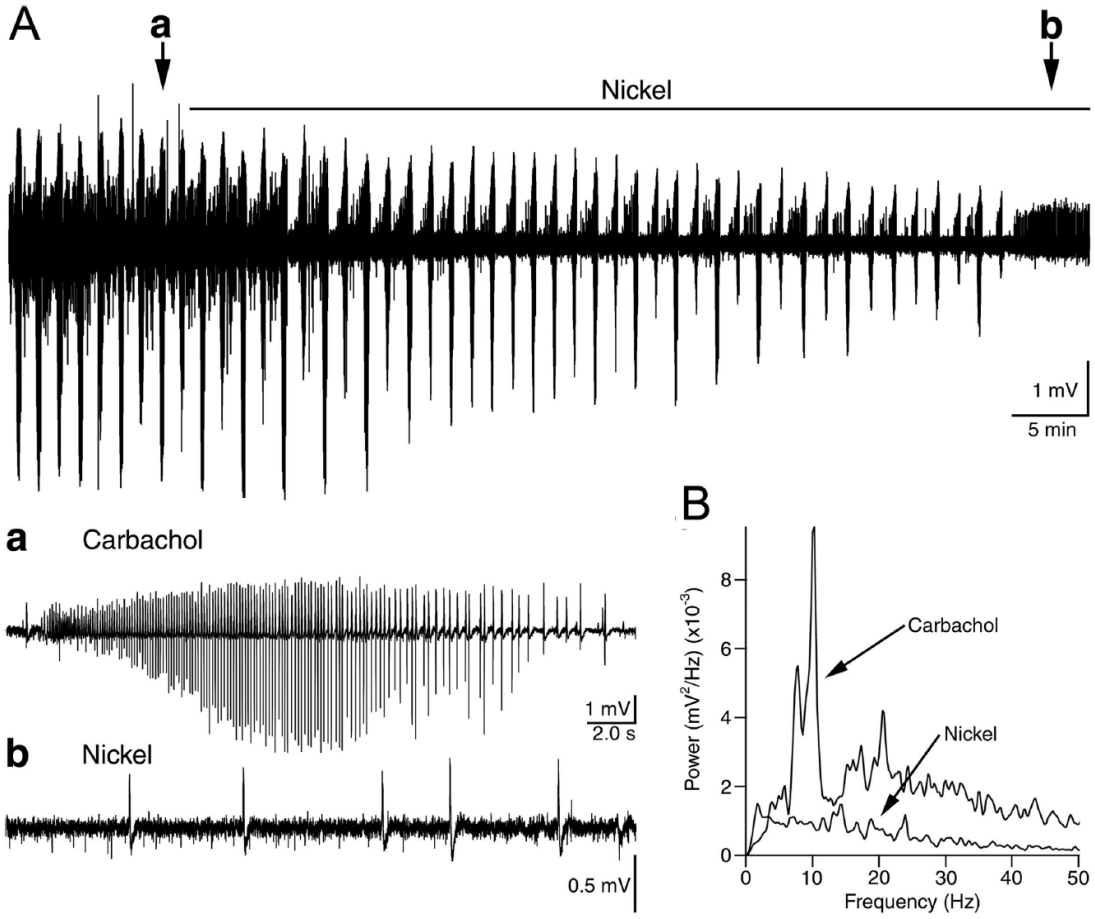

Abb. 10: Carbachol induzierte Theta-*burst* Aktivität. A) Extrazelluläre Aufzeichnung aus der CA1-Region unter Carbachol (40 μM) und anschließender Applikation von Ni^{2+} (100 μM). **a, b**) Ausschnittsvergrößerung der Pfeilregionen in **A**. **B)** Die *Power*-Spektrumanalyse der EEG-Frequenzbänder zeigt eine deutliche Zunahme der Theta-Frequenz nach Carbachol-Applikation sowie deren Inhibition durch Ni^{2+}-Ionen (Tai et al., 2006).

Die hier beschriebenen Phänomene wurden an Sprague-Dawley-Ratten erforscht. Ob die ionale Grundlage der Plateau-Potentiale in anderen Spezies, v.a. beim Menschen, vergleichbare Entitäten umfasst, ist zur Zeit offen und auch der direkte Nachweis der Bedeutung von $Ca_v2.3$ beim Triggern von Plateau-Potentialen anhand von $Ca_v2.3$ defizienten Mäusen steht noch aus. Weniger eindeutig stellt sich die Situation für das Phänomen der Nachdepolarisationen dar. Mittels *nucleated patch*-Technik führten Metz et al. (2005) diese auf die Aktivität des $Ca_v2.3$ Ca^{2+}-Kanals zurück. Die residuale, resistente Stromkomponente ließ sich jedoch nicht mittels SNX-482 hemmen, so dass sie als SNX-482 resistente E/R-Typ Stromkomponente interpre-

tiert wurde. Demgegenüber favorisieren Yue et al. (2005) einen persistierenden Na^+-Einstrom als ursächliche Komponente für das Auftreten von Nachdepolarisationen. Grundsätzlich muss man hierbei die andersartigen experimentellen Kautelen berücksichtigen.

1.2.2.5. $Ca_v2.3$ getriggerte Plateau-Potentiale in hippokampalen CA1-Neuronen – ein Einzelfall oder funktionelles Organisationsprinzip?

Die $Ca_v2.3$ Ca^{2+}-Kanalentität ist trotz markanter Fortschritte in den letzten Jahren immer noch eine der am wenigsten charakterisierten Untereinheiten innerhalb der Gruppe spannungsgesteuerter Ca^{2+}-Kanäle. Im Gegensatz zu anderen Vertretern dieser Familie sind sie resistent gegenüber klassischen Cono- und Agatoxinen (Catterall et al., 2005). Erst 1998 wurde aus dem Venom der Tarantel Hysterocrates gigas das Peptidtoxin SNX-482 isoliert, dass sich als vergleichsweise spezifischer $Ca_v2.3$ Blocker erwiesen hat (IC_{50} = 15 – 30 nM, Newcomb et al., 1998). Besonders die Generierung $Ca_v2.3$ defizienter Mäuse hat einen tieferen Einblick in die Bedeutung des $Ca_v2.3$ Ca^{2+}-Kanals ermöglicht. Neben der Modulation von Angst- und Schmerzverhalten (Saegusa et al., 2000;Lee et al., 2002) sowie der Myelinogenese (Chen et al., 2000), ist $Ca_v2.3$ im ZNS auf zellulärer, präsynaptischer Ebene an der Neurotransmitterfreisetzung und synaptischen Plastizität beteiligt (**Abb. 11, 12;** Dietrich et al., 2003;Breustedt et al., 2003;Bloodgood and Sabatini, 2007).

Auf zellulärer Ebene zeigt $Ca_v2.3$ eine dominante Expression präsynaptisch, z.B. in den Moosfasern des Hippokampus (Day et al., 1996) sowie im Globus pallidus (Hanson and Smith, 2002), aber auch in geringem Grade an der myoneuralen Synapse (Day et al., 1997). Anders als $Ca_v2.1$ und $Ca_v2.2$ befindet sich nur ein kleiner Teil der präsynaptisch lokalisierten $Ca_v2.3$ Ca^{2+}-Kanäle in der sog. aktiven Zone der Vesikel-Fusionsmachinerie, während der weitaus größte Teil der Kanäle weiter distal lokalisiert ist (Wu et al., 1999) und für synaptische Plastizität wie z.B. die Langzeitpotenzierung (LTP) von Bedeutung ist (Dietrich et al., 2003) (**Abb. 12**). Interessanterweise hat sich gezeigt, dass auf präsynaptischer Ebene der Moosfasern neben $Ca_v2.3$ eine ganze Reihe von anderen präsynaptischen Rezeptoren zu finden sind, die für Prozesse der Langzeitpotenzierung aber auch Langzeitdepression wichtig sind. So hemmen z.B. präsynaptisch-lokalisierte Adenosin (A_1)-Rezeptoren die Glutamat-Freisetzung, ebenso wie metabotrope Glutamat-Rezeptoren, während präsynaptisch lokalisierte Kainat-Rezeptoren die Glutamatfreisetzung fördern (Nicoll and Schmitz, 2005). Dies könnte für die bei $Ca_v2.3^{-/-}$ Mäusen beobachtete Kainat-Resistenz eine entscheidende Rolle spielen (Weiergräber et al., 2007).

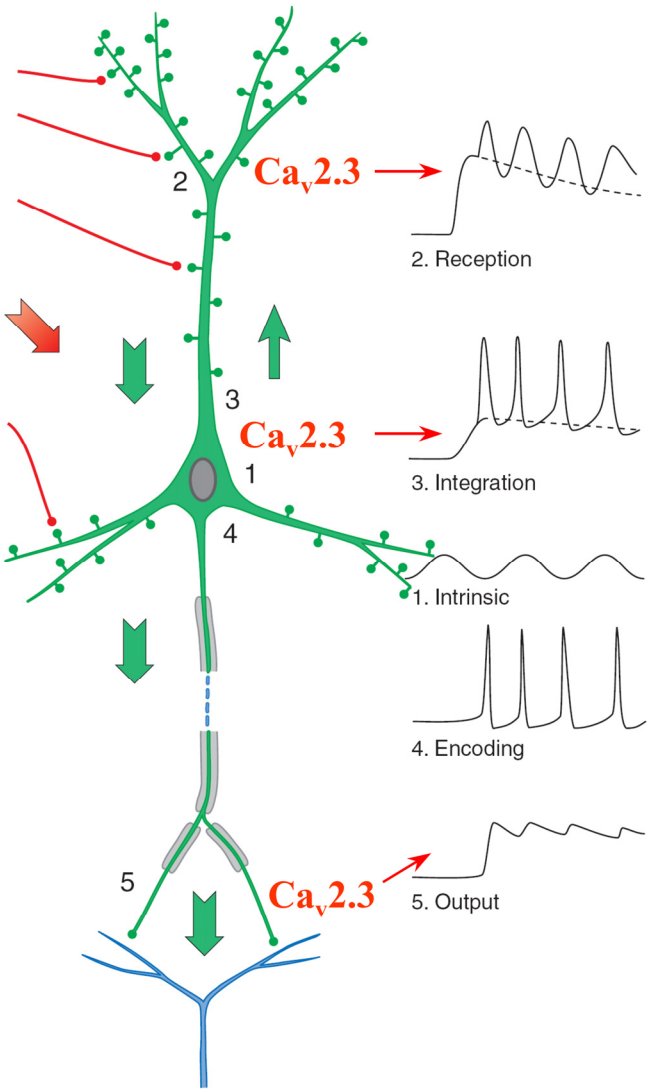

Abb. 11: Strukturelle und funktionelle Topologie eines repräsentativen Neurons. Nervenzellen verfügen über vier Hauptregionen (Dendritenbaum, Soma, Axon und Synapsen) und fünf Funktionsstrukturen. Elektrotonische Ausbreitung ist für die funktionelle Koordination der Regionen von großer Wichtigkeit. Der $Ca_v2.3$ Ca^{2+}-Kanal findet sich sowohl präsynaptisch, wo er für Neurotransmitterfreisetzung und synaptische Plastizität von Bedeutung ist, als auch in somatisch-dendritischen Arealen, und somit in der rezeptiv-integrativen Zone. Hier ist er an oszillatorischen Vorgängen sowie epileptiformen *burst*-Prozessen beteiligt (Byrne and Roberts, 2004).

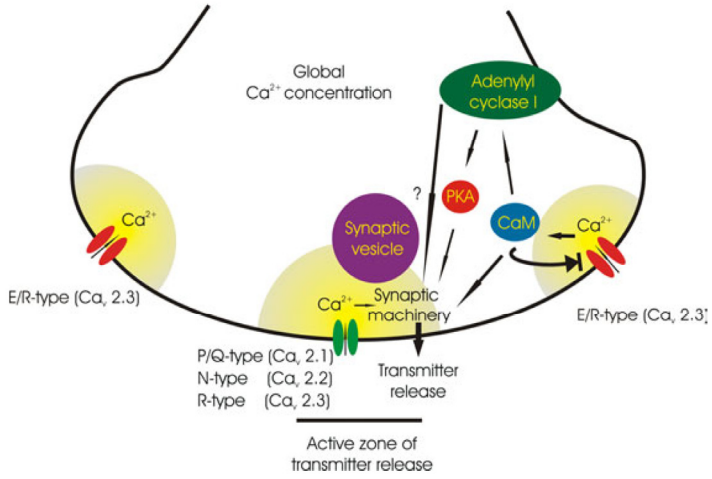

Abb. 12: Modell präsynaptischer Langzeitpotenzierung an einer Moosfaser-Synapse. Verschiedene α_1-Untereinheiten befinden sich in der aktiven Zone der Transmitterfreisetzung. Ein Großteil der $Ca_v2.3$ Ca^{2+}-Kanäle ist hingegen distal dieser Zone lokalisiert (Kamp et al., 2005).

In anderen ZNS-Regionen und Kernstrukturen zeigt sich hingegen eine prominente Expression im Bereich der Somata und des Dendritenbaumes (**Abb. 11**). Diese Verteilung ist Zelltyp-spezifisch, hochorganisiert und unterscheidet sich von dem eher homogenen somatischen und dendritischen Distributionsmuster anderer Ca^{2+}-Kanäle (Westenbroek et al., 1995). Es ist nicht verwunderlich, dass $Ca_v2.3$ für die Generierung komplexer Aktionspotentiale entlang der Dendriten und Somata von besonderer Bedeutung ist, die letztlich auch die Genese epileptiformer/iktiformer Aktivität zu triggern vermögen (Tank et al., 1988). Präsynaptische und somatisch/dendritische Lokalisation sind somit distinkt und bedingen verschiedene funktionelle Relevanz.

Die intrazelluläre Ca^{2+}-Konzentration spielt eine zentrale Rolle bei der Genese epileptiformer Prozesse und wird durch eine Vielzahl von liganden- und spannungsgesteuerten Ionenkanälen sowohl zeitlich als auch räumlich hochorganisiert reguliert. Das u.a. durch spannungsgesteuerte Ca^{2+}-Kanäle in die Neuronen einströmende Ca^{2+} kann eine Vielzahl zellulärer Prozesse, wie Signaltransduktionskaskaden, Neurotransmitterfreisetzung, Gentranskription und natürlich auch die Regulation von Ionenkanalaktivität nach sich ziehen. Die sog. Ca^{2+}-Hypothese der Epileptogenese legt dar, dass Änderungen der internen Ca^{2+}-Konzentration eine kritische Rolle in der Epilepsieentstehung einnehmen (Albowitz et al., 1997;DeLorenzo et al., 1998;Sun et al., 2002). Nach Dietrich et al. (2003) tragen $Ca_v2.3$ Ca^{2+}-Kanäle wesentlich zur „Hintergrund"-Ca^{2+}-Konzentration von ca. 0,5 µM bei (Brenowitz and Regehr, 2003). Folglich kommt es während epileptiformer Aktivität zu einer Abnahme der extrazellulären und einer Zunahme der intrazellulären Ca^{2+}-Konzentration (Hamon and Heinemann, 1986). Hochspannungsaktivierte Ca^{2+}-Kanäle stellen wichtige Komponenten bei einer Erhöhung des intrazellulären Ca^{2+} während epileptiformer Aktivität dar und tragen damit sowohl zur Anfallsinitiation wie Propagation bei (Albowitz et al., 1997;Pisani et al., 2004). So zeigt sich im Hippokampus, dass die interne Ca^{2+}-Konzentration während der Epileptogenese steigt und eine Blockade spannungsgesteuerter Ca^{2+}-Kanäle eine Depression dieser epileptiformen Aktivität zur Folge hat (Straub et al., 1990;Beck et al., 1998). Ähnliches ist auch von der prokonvulsiven Wirksamkeit des Kainats im Hippokampus bekannt, wobei die Effekte auch hier stark von der internen Ca^{2+}-Konzentration abhängen ebenso wie das vergesellschaftete Phänomen der Exzitoxizität (Sullivan, 2005). Somit ist es nicht verwunderlich, dass eine Vielzahl von Antiepileptika, wie z.B. Lamotrigin, auch neuroprotektive Effekte aufweisen, indem sie u.a. als Ca^{2+}-Kanalblocker inhibitorisch in die potentiell exzitotoxische Kaskade eingreifen.

Obwohl bis zum heutigen Zeitpunkt weder im Tiermodell noch beim Menschen Mutationen des $Ca_v2.3$ Ca^{2+}-Kanals bekannt sind, gibt es deutliche Belege dafür, dass dieser Ionenkanal

eine wichtige Funktion beim Triggern epileptiformer Aktivität und damit bei der Anfallssuszeptibilität spielen könnte. Wie sich bisher gezeigt hat, kann dies auf Ebene elektrischer Phänomene, aber auch auf Ebene neuronaler Degenerationsvorgänge erfolgen. Im Jahre 2004 berichteten Suzuki et al. über das Auftreten von *Missense*-Mutationen in EFHC1, einem EF-Hand Protein, welches selektiv mit dem C-Terminus von $Ca_v2.3$ interagiert und über die Regulation des Ca^{2+}-Influx neuronale Apoptose zu vermitteln vermag. Diese Beobachtung wurde unterstützt durch die Tatsache, dass 30 nM SNX-482 Apoptose in einer Kultur hippokampaler Mauszellen zu inhibieren vermag. Interessanterweise findet sich bei Patienten mit derartigen EFHC1-Mutationen eine juvenile Myoklonusepilepsie (JME). Mutationen in EFHC1 beeinträchtigen die Interaktion mit $Ca_v2.3$ Ca^{2+}-Kanälen und verhindern auf diese Weise eine normale, entwicklungsphysiologisch relevante neuronale Apoptose während der frühkindlichen Hirnentwicklung. Dies führt zu erhöhter neuronaler Zelldichte und zur Etablierung modifizierter neuronaler Verschaltung und hyperexzitabler Schaltkreise (Suzuki et al., 2004). Während epileptogene Prozesse häufig mit primären und sekundären Formen neuronaler Degeneration vergesellschaftet sind, stellt dies einen völlig anderen Mechanismus der Epileptogenese bei der JME dar. Erhöhte neuronale Dichte als iktogener Faktor ist ein bemerkenswerter Befund (Andres et al., 2005). Apoptose beinhaltet eine komplexe genetische Reprogrammierung der Zelle sowie die Induktion biochemischer sowie morphologischer Veränderungen, die schließlich im geregelten Zelltod und der Elimination der Zelle resultieren. Unterschiedliche Stimuli, u.a. auch Ca^{2+}-Influx durch spannungsgesteuerte Ca^{2+}-Kanäle, sind hierbei von Bedeutung. Feststeht, dass $Ca_v2.3$ defiziente Mäuse im Spontan-EEG unauffällig sind und eine geringere Anfallssuszeptibilität als Kontrolltiere aufweisen (Weiergräber et al., 2006a;Weiergräber et al., 2007). Die funktionelle Relevanz des $Ca_v2.3$ Ca^{2+}-Kanals im Rahmen neuronaler Apoptose ist äußerst komplex und zeigt sich eindrucksvoll bei der Kainat-vermittelten hippokampalen Exzitotoxizität (Weiergraber et al., 2007).

Spannungsgesteuerte Ca^{2+}-Kanäle haben die Eigenschaft, elektrische Phänomene zu provozieren, die epileptiforme Aktivität zu triggern vermögen. Hierzu gehören neben der Tatsache, zu einer Erhöhung der intrazellulären Ca^{2+}-Konzentration beizutragen, auch komplexe elektrophysiologische Vorgänge wie z.B. die oben bereits beschriebenen Nachdepolarisationen oder Plateau-Potentiale. Es handelt sich hierbei um weit verbreitete elektrische Phänomene im ZNS und betreffen eine Vielzahl von Zelltypen, z.B. spinale und Hirnstamm-Motorneurone, spinale Interneurone, Hinterhornneurone, Neurone des Nucleus subthalamicus, des Nucleus suprachiasmaticus, cholinerge Neurone im Striatum, hippokampale Pyramidenzellen, subikuläre und entorhinale kortikale Zellen (Pierson et al., 2005;Weiergräber et al., 2006b).

Während die Bedeutung spannungsgesteuerter Ca^{2+}-Kanäle, v.a. des $Ca_v2.3$ E/R-Typs, bei der Genese von Nachdepolarisationen kontrovers diskutiert wird (Metz et al., 2005;Yue et al., 2005), hat sich gezeigt, dass $Ca_v2.3$ Ca^{2+}-Kanäle für die Initiation von Plateau-Potentialen von besonderer Bedeutung sind (Kuzmiski et al., 2005;Pierson et al., 2005;Tai et al., 2006). Lange Zeit herrschte die Meinung vor, dass Plateau-Potentiale in diversen ZNS-Neuronen primär durch L-Typ Ca^{2+}-Kanäle getriggert werden (Hounsgaard and Kiehn, 1989;Zhang and Harris-Warrick, 1995;Mills and Pitman, 1997;Morisset and Nagy, 1999;Voisin and Nagy, 2001;Simon et al., 2003).

Aus der Gruppe der L-Typ Ca^{2+}-Kanäle exprimieren ZNS-Neurone $Ca_v1.2$ und $Ca_v1.3$, die i.d.R. eine distinktes Expressionsmuster aufweisen und sich auch in Hinblick auf ihre subzelluläre Distribution, Funktion und Beteiligung an Ca^{2+}-abhängigen Signaltransduktionskaskaden unterscheiden. So findet sich $Ca_v1.3$ primär dendritisch, während $Ca_v1.2$ ein hohes Expressionsniveau im somatischen Bereich aufweist. Studien im Neokortex und Hippokampus der Ratte wiesen nach, dass 75 % des L-Typ Ca^{2+}-Stromes auf $Ca_v1.2$ und nur 20 % auf $Ca_v1.3$ beruhen (Hell et al., 1993).

Simon et al. (2003) zeigten, dass in lumbalen spinalen Motorneuronen dendritische Plateau-Potentiale durch L-Typ Ca^{2+}-Kanalaktivität vermittelt werden. Li and Bennett (2003) führten ursächlich eine TTX-sensitive persistierende Na^{+}-Stromkomponente sowie ebenfalls einen L-Typ Ca^{2+}-Strom an. Sowohl Cd^{2+} (400 μM) als auch Nimodipin (10 - 20 μM) waren in der Lage, das TTX-resistente Plateau zu hemmen. In Übereinstimmung mit Kuzmiski et al. (2005) sowie Tai et al. (2006) konnten auch Li and Bennett (2003) einen signifikanten Beitrag der $Ca_v2.1$ und $Ca_v2.2$ Ca^{2+}-Kanäle zur Plateau-Potentialgenese ausschließen. Interessanterweise handelt es sich bei dem verantwortlich gemachten „L"-Typ Ca^{2+}-Strom um eine nieder- bis mittelspannungsaktivierte (Aktivierungsschwelle -55 bis -40 mV), niedrig-DHP-sensitive Ca^{2+}-Stromkomponente, dessen elektrophysiologischen wie pharmakologischen Eigenschaften deutliche Ähnlichkeiten mit denen der $Ca_v2.3$ Untereinheit aufweisen (Li and Bennett, 2003). Neurologische, aber auch kardiovaskuläre Studien haben gezeigt, dass $Ca_v1.3$ ein potentieller Kandidat für eine niederspannungsaktivierte Ca^{2+}-Stromkomponente sein könnte (Xu and Lipscombe, 2001;Koschak et al., 2001;Michna et al., 2003). Derartige Eigenschaften wurden allerdings in der Vergangenheit auch $Ca_v2.3$ zugeschrieben (Soong et al., 1993) und eine Reihe der im Folgenden dargelegten Untersuchungen bestätigen dies. So haben Studien an rekombinanten $Ca_v2.3$ Kanälen gezeigt, dass die in der Literatur zur Hemmung von Plateau-Potentialen verwendeten DHP-Konzentrationen die IC_{50}-Werte verschiedener $Ca_v2.3$-Spleißvarianten z.T. deutlich überschreiten. So finden sich Konzentrationen von 10 μM Ni-

modipin (Li and Bennett, 2003), 15 μM Nifedipin (Hounsgaard and Kiehn, 1989), 10 μM Nifedipin (Voisin and Nagy, 2001) oder 50 μM Nifedipin (Mills and Pitman, 1997). Obwohl in vitro *slice*-Experimente häufig erhöhte Dihydropyridin-Spiegel erfordern, muss berücksichtigt werden, dass rekombinante L-Typ Ca^{2+}-Kanäle bereits bei Konzentrationen < 1 μM komplett inhibierbar sind (McCarthy and TanPiengco, 1992;Fanelli et al., 1994). Auch die von Li and Bennett (2003) verwendete Cd^{2+}-Konzentration (400 μM) liegt deutlich über dem IC_{50} und stellt damit ebenso wie die vergleichsweise hohen Dihydropyridin-Konzentrationen kein diagnostisches Maß zur Selektionierung von L-Typ-Strömen dar. So konnten wir für die $Ca_v2.3$d- und $Ca_v2.3$e-Spleißvarianten unter Verwendung von Isradipin IC_{50}-Werte von 9,1 μM und 14,6 μM (**Abb. 13**, Lu et al., 2004) ermitteln. Durch Koexpression mit $\alpha_2\delta$ und β_{1b} in COS-7 Zellen erhöhte sich die Empfindlichkeit beträchtlich auf Inhibitionswerte von 51 ± 7 % bei 1 μM Nicardipin (Stephens et al., 1997). In Oozyten-Expressionsstudien hingegen misslang der Nachweis eines inhibitorischen Effektes von Nifedipin oder Nicardipin auf $Ca_v2.3$ (Soong et al., 1993;Williams et al., 1994;Wakamori et al., 1994), was nahe legt, dass das Expressionssystem, die Spleißvarianten- und Untereinheitenverteilung eine zentrale Rolle bei der Dihydropyridin-Empfindlichkeit einnehmen. Dennoch muss die diagnostische Potenz der in einer Reihe von Studien verwendeten Dihydropyridin-Konzentrationen für L-Typ Ca^{2+}-Kanäle angezweifelt werden.

In der Folge konnte auch in hypothalamischen, suprachiasmatischen Neuronen gezeigt werden, dass niedrige Dosen eines Dihydropyridins (2 μM Isradipin) keine Reduktion von Plateau-Potentialen nach sich ziehen (Pierson et al., 2005). Da auch ω-Conotoxin GVIA (1 μM) und ω-Agatoxin IVA (200 nM) nur eine marginale Reduktion der Plateau-Potentialdauer hervorriefen, folgerten Pierson et al. (2005), dass E/R-Typ Ca^{2+}-Ströme, die ca. 50 % des Ca^{2+}-Einstroms in diesen Zellen vermitteln (Cloues and Sather, 2003), maßgeblich an der Plateau-Potentialgenese beteiligt sind.

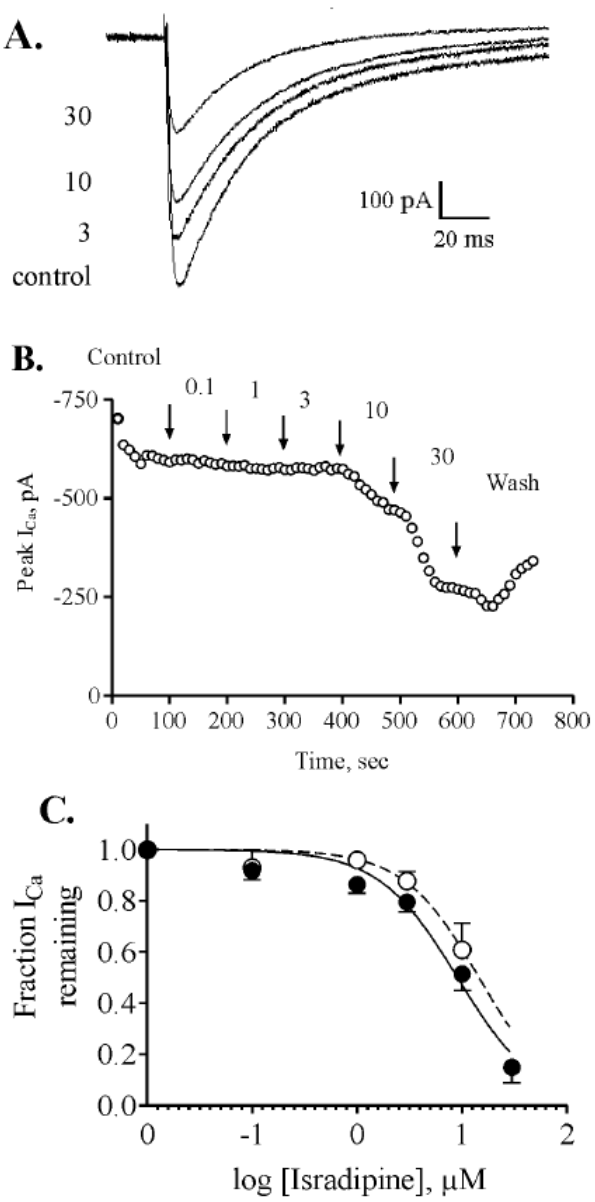

Abb. 13: Dihydropyridin-Empfindlichkeit rekombinanter $Ca_v2.3$ Ca^{2+}-Kanäle. **A**) Superpositionierte Stromspuren in Gegenwart unterschiedlicher Isradipin-Konzentrationen. **B**) Zeitlicher Verlauf der Spitzen-Einwärtsströme bei unterschiedlichen Isradipin-Konzentrationen. Ein Auswaschen gegen Versuchsende ist partiell möglich. **C**) Dosis-Wirkungskurve der $Ca_v2.3d$-(●) und der $Ca_v2.3e$- (○) Isoformen erbrachten IC_{50}-Werte von 9,1 μM und 14,6 μM. Der Hill-Koeffizient wurde mit 1,2 bestimmt (Lu et al., 2004).

Eine umfassende Betrachtungsweise spannungsgesteuerter Ca^{2+}-Kanäle bei hippokampaler Epilepsie schließt auch sekundäre Effekte mit ein. So kann epileptiforme, hippokampale Aktivität sekundär zu erhöhter Ca^{2+}-Leitfähigkeit in CA1-Neuronen führen (Vreugdenhil and Wadman, 1994). Hendriksen et al. (1997) konnten zeigen, dass durch tetanische Stimulation von Schaffer-Kollateralen induzierte epileptische Aktivität im Hippokampus, initial mit einer Transkripterhöhung der $Ca_v1.3$-, $Ca_v2.1$- und v.a. der $Ca_v2.3$-Untereinheit in verschiedenen hippokampalen Strukturen vergesellschaftet ist. Ähnliche Resultate wurden für das hippokampale Modell der *seizure-prone gerbils* gefunden (Kang et al., 2004). Zusammenfassend zeigt sich, dass $Ca_v2.3$ für die Genese von Plateau-Potentialen und epileptiformer Aktivität in einem weiten Feld neuronaler Zelltypen von essentieller bedeutung ist.

1.2.3. Spannungsgesteuerte Ca^{2+}-Kanäle und ihre Bedeutung bei nicht-konvulsiven Anfallsleiden vom Absencen-Typ

Nicht-konvulsive Anfallsformen umfassen v.a. den generalisierten *Petit-Mal* Formenkreis. Typische Absencen sind durch die plötzliche Initiation und Termination von Bewusstseinsverlust sowie das bilateral-synchrone Auftreten von *spike-wave*-Graphoelemente, die eine Spezies-spezifische Frequenzabhängigkeit aufweisen, charakterisiert (Manning et al., 2003). In Ätiologie und Pathogenese der Absencen spielen Komponenten des thalamokortikalen Neuronenkreises, insbesondere der ventrobasale Thalamus sowie der Nucleus reticularis thalami (NRT) eine Schlüsselrolle (Steriade, 2005).

Im Bereich des Thalamus sind v.a. thalamische Relayneurone aus dem ventroposterioren Thalamus involviert, die mit ihren Axonen in die kortikalen Schichten III (Lamina pyramidalis) und IV (Lamina granularis interna) projizieren, vornehmlich im Bereich des somatosensorischen Kortex (Gyrus postcentralis). Pyramidalzellen in den Schichten III und IV projizieren ihrerseits direkt oder über GABAerge inhibitorische Interneurone auf Pyramidenzellen der Schichten V (Lamina ganglionaris mit Betzschen Riesenzellen) und VI (Lamina multiformis). Von hieraus (vornehmlich Schicht V) erfolgt eine Reprojektion zurück auf die ventroposteriore Kerngruppe des Thalamus. In diesen Neuronenkreislauf ist als zentrale Komponente der Nucleus reticularis thalami parallel geschaltet. Diese Kernstruktur umgibt den übrigen Thalamus schüsselförmig von lateral und besteht ausschließlich aus GABAergen inhibitorischen Interneuronen. Der Nucleus reticularis thalami (RTN) erhält kollaterale glutamaterge Projektionen der kortikothalamischen Fasern und kollaterale glutamaterge Projektionen der thalamokortikalen Bahnen. Des Weiteren bestehen Verknüpfungen der GABAergen, retikulären Neurone untereinander, die wesentlich für die Funktion des thalamokortikalen Systems sind (Danober et al., 1998). Die inhibitorische Projektion erfolgt über inhibitorische Synapsen, die GABAerg sind: sog. Gray-Typ-II-Synapsen, während die thalamokortikalen-kortikothalamischen Projektionen primär exzitatorisch sind und Glutamat als Transmitter verwenden (Vermittlung über sog. Gray-Typ-I-Synapsen) (**Abb.14**).

Es existiert daneben eine Vielzahl von extrathalamokortikalen Projektionen (Danober et al., 1998). Ein Großteil entstammt der Formatio reticularis (FR). Es handelt sich um ein System schwer voneinander abgrenzbarer, ineinander übergehender Kerne, welches u.a. das ARAS (aufsteigendes retikuläres aktivierendes System), das Atemzentrum und Kreislaufzentrum umfasst. Die ARAS-Aktivierung führt zur Desynchronisation im thalamokortikalen System und Aufwachvorgängen, da die somatosensorische Informationsprozessierung durch den Thalamus gesteigert wird. Teilweise werden zur Formatio reticularis weitere Strukturen des Hirn-

stamms/Tegmentums gezählt, wie der cholinerge laterodorsale tegmentale Kern (LDT) und der pedunculopontine tegmentale Kern (PPTg).

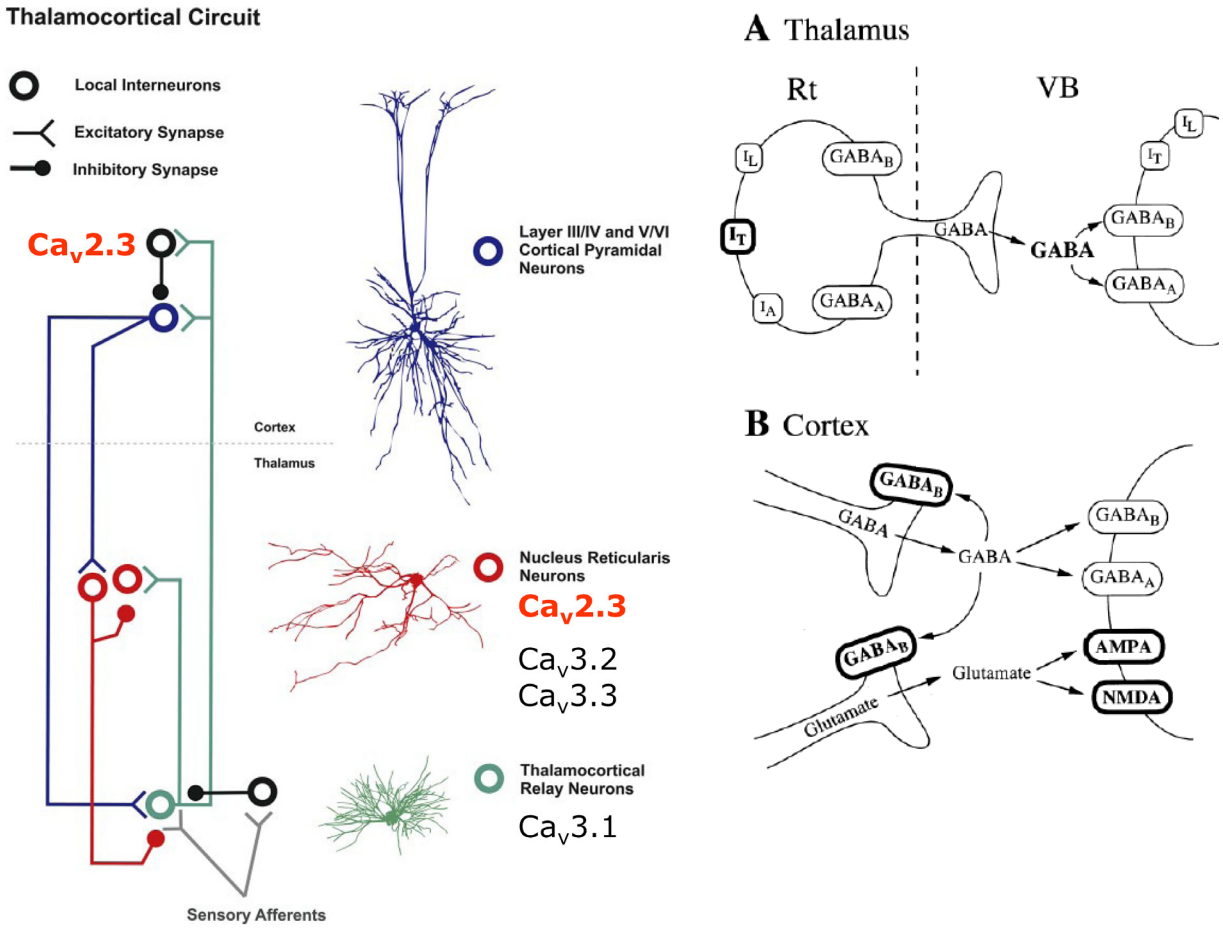

Abb. 14: Schematische Darstellung des thalamokortikalen-kortikothalamischen Neuronenkreises. Links: Sowohl das thalamokortikale wie kortikothalamische Fasersystem entsenden exzitatorische Kollaterale zu NRT-Zellen. Daneben gibt es auch Verknüpfungen der NRT-Interneurone untereinander im Sinne einer lateralen Inhibition. Dargestellt ist weiterhin die Expression des $Ca_v2.3$ E/R-Typ Ca^{2+}-Kanals sowie der $Ca_v3.1$-3.3. T-Typ Kanäle. Abk.: Rt: retikulärer Thalamus, VB: ventrobasaler Thalamus, Cx: Kortex, Hi: Hippokampus, CC: Corpus callosum (modifiziert nach Khosravani and Zamponi, 2006). Rechts: Darstellung der wichtigsten spannungsabhängigen und ligandengesteuerten Ionenströme im thalamokortikalen-kortikothalamischen Neuronenkreis. Neben den hier bereits erwähnten L- und T-Typ Kalziumströmen spielen im Gesamtkonzert der Ionenkanäle auch die GABA(A)- und GABA(B)-Rezeptoren eine bedeutende Rolle. Auch NMDA- und Non-NMDA-(AMPA)-Rezeptoren sowie die erst kürzlich klonierten HCN-(*hyperpolarization and cyclic-nucleotide gated*) Kanäle (nicht eingetragen) sind von essentieller Bedeutung. Abk.: I_T: T-Typ-Ionenstrom, I_L: L-Typ- Ionenstrom, I_A: Anionenstrom (Danober et al., 1998).

Weiterhin gehören hierzu die Raphekerne, die relativ gut abgrenzbar sind, in das limbische System und die ARAS-Region projizieren und eine serotoninerge Kerngruppe darstellen. Darüber hinaus spielen der noradrenerge Nucleus coeruleus (Projektion in das limbische System) und der primär cholinerge Nucleus basalis Meynert (Beziehung zum limbischen System und Neokortex, wichtige Funktion bei Lernprozessen) eine Rolle (**Abb. 15**).

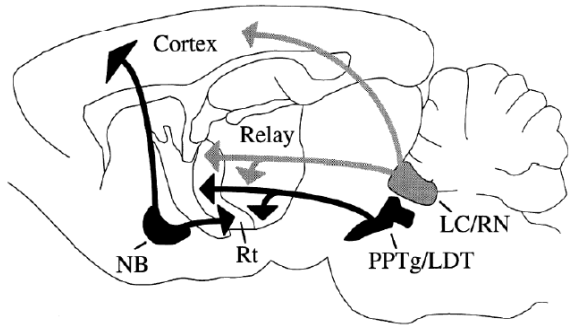

Abb. 15: Projektionen extrathalamokortikaler Kernstrukturen auf den thalamokortikalen Neuronenkreis. Abk.: NB: Nucleus basalis Meynert, Rt: Nucleus reticularis thalami, PPTg/LDT: pedunkulopontiner/laterodorsaler tegmentaler Kern, LC/RN: Locus coeruleus/Raphekern (Danober et al., 1998).

Auch der Hippokampus und das Zerebellum können thalamokortikale Rhythmizität modulieren und sind an der Entstehung eines Absencen-Phänotyps beteiligt (Lakaye et al., 2002). Unter pathophysiologischen Gesichtspunkten stellen aberrante kortikothalamische Rhythmen die Grundlage für die Entstehung von *spike-wave* Graphoelementen dar. Funktionelle Grundlage hierfür ist die herausragende Eigenschaft thalamischer Relayneurone, zwischen zwei verschiedenen Aktivitätsmodi, dem sog. *tonic*-Modus sowie dem *burst*-Modus, in Abhängigkeit von der zentralnervösen Aktivierung (v.a. durch die Formatio reticularis) zu alternieren. Während im tonischen Modus eine dauerhafte Transmission externer, v.a. sensorisch-sensibler Information zum Kortex erfolgt, hyperpolarisieren bei abnehmender Vigilanz thalamische Schaltneurone, gehen in rhythmische *burst*-Aktivität über und schließen auf diese Weise das thalamische „Tor“ und somit den Informationstransfer zum Kortex. Für den *burst*-Modus ist der exklusiv aus GABAergen Interneuronen bestehenden Nucleus reticularis thalami von entscheidender Bedeutung, der auch inhibitorische Projektionen auf die thalamischen Relayzellen aufweist.

Interessanterweise existieren eine Vielzahl von Absencen-Mausmodellen mit singulären Mutationen in spannungsgesteuerten Ca^{2+}-Kanälen, welche die zentrale Rolle dieser Ionenkanäle bei der Absencen-Epileptogenese unterstreichen. Im Mausmodell sind eine Reihe von Mutationen bekannt (*tottering*, *tottering leaner*, *rolling Nagoya*, *rocker*, *lethargic, ducky*, *entla* und *stargazer*), die entweder mit der $Ca_v2.1$ oder akzessorischen Untereinheiten (β_4, $\alpha_2\delta$) in Verbindung stehen und mit zerebellärer Ataxie und Absencen-Epilepsie vergesellschaftet sind. Es ist interessant festzustellen, dass bislang nur $Ca_v2.1$ (bei der Maus) und $Ca_v3.2$ (beim Men-

schen) nachweislich bei der Absencen-Genese von Bedeutung sind. Beim Menschen tritt eine Absencen-ähnliche Symptomatik primär als Begleiterscheinung, z.B. der EA2 oder FHM1 auf. Bei einer geringen Zahl von Patienten mit *childhood absence epilepsy* (CAE) wurden Nukleotid-Polymorphismen (*single nucleotide polymorphisms*, SNPs) im Gen CACNA1H ($Ca_v3.2$) nachgewiesen, die sich in Proben einer gesunden Kontrollgruppe nicht finden lassen (Chen et al., 2003;Vitko et al., 2005). Der $Ca_v3.2$ T-Typ Ca^{2+}-Kanal zeigt deutliche Expression im Bereich des Kortex und des Nucleus reticularis thalami, und spielt damit offensichtlich eine wichtige Rolle bei der Etablierung thalamischer Synchronizität (Suzuki and Rogawski, 1989;Steriade et al., 1993).

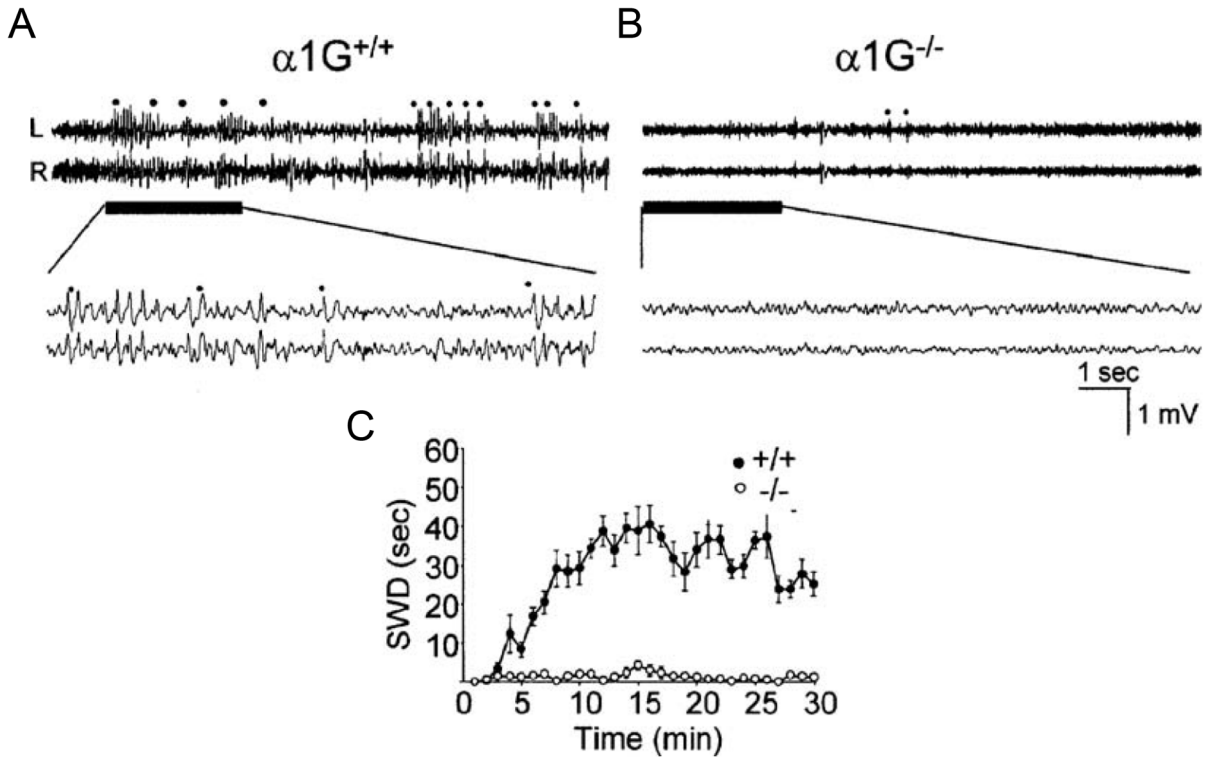

Abb. 16: Auswirkungen des $Ca_v3.1$ (α_1G) T-Typ Ca^{2+}-Kanals auf die thalamokortikale Rhythmizität. In Kontrolltieren (**A**) führt die Administration von Baclofen (20 mg/kg) zur Induktion von *spike-wave* Graphoelementen, die für Absencen typisch sind. Die Ablation von $Ca_v3.1$ hingegen (**B, C**) hat eine massive Abnahme der *spike-wave* Aktivität zur Folge. Grund hierfür ist die Abnahme des niederspannungsaktivierten Ca^{2+}-Einstroms und daraus resultierend ein vermindertes *rebound burst firing* in thalamokortikalen und retikulär-thalamischen Zellen (Shin, 2006).

Den Einfluss niederspannungsaktivierter T-Typ Ca^{2+}-Kanäle auf normgerechte thalamische Rhythmizität wie auch pathologische Hyperoszillation zeigt u.a. die Wirksamkeit der Suximide bei CAE (Coulter et al., 1989;Gomora et al., 2001). Die bei $Ca_v3.2$ beschriebenen SNPs

vermögen die eletrophysiologischen Eigenschaften des T-Typ Ca^{2+}-Kanals zu modifizieren und stellen möglicherweise physiologisch relevante Mutationen dar (Vitko et al., 2005).
Es ist erwähnenswert, dass auch andere Ca^{2+}-Kanäle auf thalamische Rhythmizität Einfluß nehmen. So weisen $Ca_v3.1$ defiziente Mäuse fehlende *burst*-Aktivität thalamokortikaler Zellen und damit verbunden eine erhöhte Anfallsresistenz gegenüber Absencen auf (Kim et al., 2001). Weiterhin zeigte sich, dass $Ca_v3.1^{-/-}$ Tiere eine veränderte REM/NREM Schlaf-Architektur sowie eine verminderte Delta-Wellenaktivität im NREM-Schlaf aufweisen (Lee et al., 2004). Diese Daten sind umso eindrucksvoller, als $Ca_v3.1$ eine Schlüsselrolle bei der *burst*-Aktivität thalamischer Neurone einnimmt und somit auch für pathologische Hyperoszillationen von Bedeutung sein könnte. Dagegen weisen $Ca_v2.1$ defiziente Mäuse spontane *spike-wave* Graphoelemente mit motorischem Arrest auf (Jun et al., 1999). Interessanterweise kommt es in thalamokortikalen Relayzellen $Ca_v2.1$ defizienter Tiere zu einer erhöhten T-Typ Expression (Zhang et al., 2002). Doppel-*knock-out* Experimente mit $Ca_v2.1^{-/-}$ x $Ca_v3.1^{-/-}$-Mäusen haben dementsprechend gezeigt, dass die so gewonnenen Tiere spontan keine *spike-wave* Graphoelemente mehr aufweisen, so dass das Fehlen des $Ca_v3.1$ vermittelten Ca^{2+}-Einstroms in thalamischen Relayneuronen einen Absencen-protektiven Effekt zu haben scheint (Song et al., 2004). Welche Bedeutung kommt hier dem $Ca_v2.3$ E/R-Typ Ca^{2+}-Kanal zu? Zunächst weisen sowohl GABAerge Interneurone im Kortex als auch im NRT als funktionell bedeutsame Strukturen im thalamokortikalen System eine deutliche Expression von $Ca_v2.3$ auf (De Borman et al., 1999;Talley et al., 2000;van de Bovenkamp-Janssen et al., 2004). Auch extrathalamokortikale Strukturen, die auf dieses System projizieren, sind $Ca_v2.3$ positiv. Eine Reihe von Studien zur funktionellen Relevanz von $Ca_v2.3$ in der Absencen-Epileptogenese wurden an den sog. GAERS (*Genetic Absence Epilepsy Rats from Strasbourg*) sowie den WAG/Rij (*Wistar Albino Glaxo*) Ratten durchgeführt. In GAERS wurde eine Zunahme des T-Typ Ca^{2+}-Stromes im NRT berichtet (Tsakiridou et al., 1995) sowie später auch eine alterierte Expression von $Ca_v3.1$ und $Ca_v3.2$ im adulten ventroposterioren Thalamus und NRT (Talley et al., 2000). Interessanterweise fanden de Borman et al. (1999) und Lakaye et al. (2002) auch eine signifikante Reduktion der $Ca_v2.3$ Transkripte im Kleinhirn und der Medulla von GAERS Ratten, zwei extrathalamokortikalen Strukturen, die auf den thalamokortikalen Neuronenkreis projizieren und dessen oszillatorische Aktivität zu modulieren vermögen (Filakovszky et al., 1999;Deransart et al., 2001). In WAG/Rij-Ratten zeigte sich weiter, dass die Entwicklung von *spike-wave* Graphoelementen mit einer Zunahme der $Ca_v2.1$ Expression im NRT koinzidiert, aber auch mit einer fehlenden Zunahme der $Ca_v2.3$ Expression. Obwohl bislang noch keine detaillierten Informationen und Modelle zur Bedeutung von

$Ca_v2.3$ bei Absencen des Menschen vorlagen, spricht vieles für eine funktionelle Relevanz, die im Rahmen der vorliegenden Arbeit aufgeklärt wurde.

1.3. Spannungsgesteuerte Ca^{2+}-Kanäle als Zielstrukturen in der Therapie konvulsiver und nicht-konvulsiver Anfallsleiden

Welche Bedeutung spannungsgesteuerte Ca^{2+}-Kanäle in Ätiologie und Pathogenese von Epilepsien spielen, zeigt sich u.a. darin, dass sie eine wichtige Zielstruktur für eine Vielzahl etablierter wie auch neuerer Antiepileptika darstellen, indem sie neuronale *burst*-Aktivität und intrinsische Oszillationen zu inhibieren vermögen. Pharmakologische Studien haben gezeigt, dass eine Vielzahl von Antiepileptika hoch- und niederspannungsaktivierte Ca^{2+}-Kanäle zu hemmen vermögen. Eine Reihe klassischer Antiepileptika wird auch in der Therapie anderer neurologischer Krankheitsbilder, wie endogener Depressionen, Migräne und neuropathischen Schmerzen eingesetzt (Rogawski and Loscher, 2004;Remy and Beck, 2006).

Hochspannungsaktivierte Ca^{2+}-Kanäle stellen eine wichtige Zielstruktur für Antiepileptika dar, da eine Blockade dieser Ionenkanäle die Neurotransmitterfreisetzung zu inhibieren vermag (Turner, 1998). So hemmen die Antiepileptika Levetiracetam und Felbamat hochspannungsaktivierte Ca^{2+}-Kanäle, wobei Levetiracetam eine deutliche Präferenz für N-Typ Ca^{2+}-Kanäle aufweist (Stefani et al., 1997;Lukyanetz et al., 2002). Neuere Forschungsergebnisse zeigen, dass auch $Ca_v2.3$ eine wichtige Rolle als pharmakologische Zielstruktur spielt. In diesem Zusammenhang ist das Lamotrigin (LTG) zu nennen, welches als Breitspektrum-Antiepileptikum für die Therapie typischer Absencen-Epilepsien, tonisch-klonischer Anfälle, u.a. auch des Lennox-Gasteau-Syndroms sowie partieller Epilepsien herangezogen wird (Matsuo, 1999;McCabe, 2000). Als Wirkmechanismus des Lamotrigins wurde eine Inhibition spannungsgesteuerter Na^+- und Ca^{2+}-Kanäle angeführt (Xie and Hagan, 1998). Innerhalb der Familie spannungsgesteuerter Ca^{2+}-Kanäle werden sowohl Non-L-Typ Ca^{2+}-Kanäle wie $Ca_v2.1$ und $Ca_v2.2$ (Wang et al., 1996;Stefani et al., 1996), aber auch $Ca_v3.1$-3.3 T-Typ und $Ca_v2.3$ E/R-Typ Ca^{2+}-Kanäle inhibiert (Hainsworth et al., 2003). Im Bereich therapeutisch relevanter Konzentrationen (4 – 40 μM) zeigt Lamotrigin (10 μM) eine Hemmung rekombinant exprimierter $Ca_v2.3$ E/R-Typ Ca^{2+}-Kanäle (koexprimiert mit der β_3 Untereinheit) von 30 %. $Ca_v3.1$ und $Ca_v3.3$ weisen dagegen nur geringe Sensitivitäten gegenüber Lamotrigin auf (Hainsworth et al., 2003). Die antikonvulsive Wirksamkeit des Lamotrigin muss u.a. in Zusammenhang mit einer Hemmung des intrazellulären Ca^{2+}-Konzentrationsanstiegs gesehen werden, was zu einer Verminderung der neuronalen Vulnerabilität führt und somit neuroprotektiv wirkt (Pisani et al., 2004). Strukturell verwandte Substanzen, wie Sipatrigin zeigen ebenfalls inhibitorische Effekte auf $Ca_v2.3$ mit IC_{50} Werten von 10 μM (therapeutisch relevante Konzentrationen: 20 – 100 μM). Auch hier ist es nicht überraschend, dass diese Verbindungen neuroprotektive Wirkungen aufweisen (Hainsworth et al., 2000;Caputi et al., 2001)

und auch in unterschiedlichen Tiermodellen wie den *genetically epilepsy-prone rats* und den *DBA/2 audiogenic mice* antikonvulsive Effekte zeigen (Reddy et al., 1998;Hainsworth et al., 2003). Auch Carboanhydrasehemmer, wie z.B. Ethoxyzolamid, Acetazolamid und Dichlorphenamid haben inhibitorische Effekte auf $Ca_v2.3$ E/R-Typ Ca^{2+}-Kanäle. Obwohl Carboanhydrasehemmer ein weites klinisches Anwendungsgebiet haben (Sun and Alkon, 2002;Supuran et al., 2003), zeigen epidemiologische Studien deutlich deren Wirksamkeit in der Absencen-Therapie (Sun and Alkon, 2002) sowie beim Schutz vor provozierten Anfällen im Erwachsenenalter. So führt Ethoxyzolamid (10 μM) zu einer Reduktion des E/R-Typ Ca^{2+}-Stromes um 66 ± 4 %, während Dichlorphenamid (10 μM), dass auch zur Behandlung generalisierter Epilepsien verwendet wird, eine $Ca_v2.3$ vermittelte Stromreduktion um 24 ± 6 % zur Folge hat (McNaughton et al., 2004). Erst kürzlich zeigte sich, dass auch Topiramat (TPM), welches strukturelle Gemeinsamkeit mit Carboanhydrasehemmern aufweist, ein potenter $Ca_v2.3$ E/R-Typ Blocker ist, welcher im therapeutisch relevanten Konzentrationsbereich (10 μM) den $Ca_v2.3$ getragenen Ca^{2+}-Strom um 68 ± 7 % reduziert (McNaughton et al., 2004;Kuzmiski et al., 2005). Darüber hinaus hemmt Topiramat aber auch L-Typ Ca^{2+}-Kanäle (Zhang et al., 2000). Kuzmiski et al. (2005) konnten weiter zeigen, dass Topiramat fähig ist, die Entstehung von Plateau-Potentialen in hippokampalen CA1 Neuronen zu hemmen und dass dieser Effekt auf einer Inhibition von $Ca_v2.3$ Ca^{2+}-Kanälen beruht. In dieser Neuronenpopulation konnte ferner nachgewiesen werden, dass $Ca_v2.3$ vermittelte Ca^{2+}-Ströme über Stimulation muskarinerger Rezeptoren, z.B. mittels Carbachol über G-Protein und PKC-vermittelte Effekte augmentieren (Leroy et al., 2003;Klöckner et al., 2004;Kuzmiski et al., 2005;Tai et al., 2006). Die so induzierten Plateau-Potentiale sind für die Genese epileptiformer *burst*-Prozesse von essentieller Bedeutung, was die Effekte des Topiramat auf anhaltende repetitive Feuerung, spontane epileptiforme *burst*-Aktivität und rekurrente Anfälle erklärt (DeLorenzo et al., 2000). Da $Ca_v2.3$ ein proiktogenes/proepileptogenes Potential aufweist (Tai et al., 2006), verdichten sich die Hinweise, dass eine Inhibition des $Ca_v2.3$ Ca^{2+}-Kanals antikonvulsive Wirkung haben könnte (Khosravani and Zamponi, 2006).

Einige Antiepileptika haben sich als typische T-Typ Ca^{2+}-Kanalblocker herausgestellt, wie z.B. die Suxinimide. Diese Substanzgruppe, allen voran das Ethosuximid, wird in der Therapie der Absencen-Epilepsie, v.a. bei Kindern unter dem 10. Lebensjahr eingesetzt. Zelluläre Elektrophysiologie an Hirnschnitten von Nagern hatte schon früh vermuten lassen, dass Suxinimide T-Typ Ca^{2+}-Ströme zu inhibieren vermögen. Doch erst die Klonierung der entsprechenden porenbildenen $Ca_v3.1$-3.3 Untereinheiten ermöglichte eine detaillierte pharmakologische Untersuchung, die bestätigte, dass z.B. das Ethosuximid im therapeutisch relevanten

Konzentrationsbereich sog. *low-threshold* Ca^{2+}-*spikes* zu inhibieren vermag und auf diese Weise thalamokortikale Hyperoszillationen hemmen kann (Gomora et al., 2001). Aber auch Mechanismen, wie die Hemmung eines persistierenden Na^{+}-Einstroms und eines Ca^{2+}-aktivierten K^{+}-Kanals werden als mögliche Erklärungsansätze des Anti-Absencen-Effekts der Suxinimide diskutiert (Leresche et al., 1998). Für Valproat, den zweiten Goldstandard in der Therapie typischer Absencen (Rogawski and Loscher, 2004), fällt der Ca^{2+}-Stromblock im therapeutisch relevanten Konzentrationsbereich gering aus (Sayer et al., 1993;Todorovic and Lingle, 1998). Auch die antiepileptische Aktivität des Zonisamid wurde u.a. auf die Inhibition von T-Typ Ca^{2+}-Kanälen zurückgeführt (Suzuki et al., 1992;Kito et al., 1996), wobei Untersuchungen an rekombinanten humanen $Ca_v3.1$-3.3 Ca^{2+}-Kanälen nur eine geringe Inhibition von 15 - 20 % im therapeutisch relevanten Konzentrationsbereich (50 – 100 μM) zeigten (Matar et al., 2009). Eine Hemmung der $Ca_v2.3$ Ca^{2+}-Kanalentität durch Zonisamid konnte nicht nachgewiesen werden (Matar et al., 2009). Einige Antiepileptika binden nicht direkt an die porenbildende Ca_v-α_1-, sondern an die $\alpha_2\delta$-Untereinheit. Hierzu gehören das Gabapentin und Pregabalin (Kavoussi, 2006;Sills, 2006). Pregabalin vermittelt seine Wirkung vermutlich über eine Hemmung der präsynaptischen Neurotransmitterfreisetzung (Joshi and Taylor, 2006) und wird nicht nur zur Therapie partieller Epilepsien, sondern auch zur Behandlung von generalisierten Angststörungen und chronisch-neuropathischen Schmerzen eingesetzt (Maneuf et al., 2006).

2. Wissenschaftliche Fragestellung

Basierend auf den oben dargestellten Zusammenhängen ergaben sich dezidierte Hinweise auf eine funktionelle Involvierung der $Ca_v2.3$ Ca^{2+}-Kanaluntereinheit bei konvulsiven wie auch nicht-konvulsiven Anfallsformen sowie exzitotoxischen Prozessen. Ausgehend hiervon sollte auf systemisch-elektrophysiologischer, pharmakologischer und morphologischer Ebene eruiert werden, welche Rolle der $Ca_v2.3$ Ca^{2+}-Kanal bei der Iktogenese und begleitendem neuronalen Zelluntergang spielt. Auch die Rolle der $Ca_v2.3$ und $Ca_v3.1$-3.3 Ca^{2+}-Kanäle als Zielstrukur für neuere Antiepileptika wurde in diesem Zusammenhang untersucht.

3. Ergebnisse

3.1. Identifikation neuronaler $Ca_v2.3$ Spleißvarianten im ZNS – funktionelle und regulative Implikationen

Die Distribution der $Ca_v2.3$ Ca^{2+}-Spleißvarianten in Abhängigkeit von der betreffenden Hirnregion ist äußerst variabel (Weiergräber et al., 2006a). Es zeigt sich, dass die Hirnregionen diesbezüglich in drei Gruppen eingeteilt werden können: 1. Hirnregionen, die primär die Ca^{2+}-sensitive $Ca_v2.3c$ Variante (kompletter II-III-*loop* und kurzer C-terminus ohne Exon 45) exprimieren, wie z.B. Kortex und Hippokampus; 2. Regionen, die dominant die $Ca_v2.3e$ Spleißvariante (II-III-*loop* ohne Insert 1 (Exon 19) und langer C-Terminus) exprimieren wie z.B. Zerebellum und Medulla; 3. Hirnregionen, wie Thalamus und Hypothalamus, die ein ausgeglichenes Verhältnis von $Ca_v2.3c$ und $Ca_v2.3e$ Spleißvarianten aufweisen (Weiergräber et al., 2006a). Die Betrachtung der Spleißvarianten-Verteilung ist von zentraler Bedeutung, da einige, wie $Ca_v2.3c$ und $Ca_v2.3d$ durch geringe Konzentrationen zytosolischen Ca^{2+} stimulierbar sind, andere wie z.B. $Ca_v2.3e$ hingegen nicht (Leroy et al., 2003;Klöckner et al., 2004). Gerade die Ca^{2+}-sensitiven Spleißvarianten sind im Rahmen epileptogener Prozesse von besonderem Interesse. Um zu eruieren, ob es in $Ca_v2.3$ defizienten Mäusen zu einer kompensatorischen Gegenregulation anderer Ca^{2+}-Kanäle kommt, wurden in einem semiquantitativen RT-PCR Ansatz alle verbliebenen Ca_v-α_1-Untereinheiten hinsichtlich ihrer Transkriptionsniveaus getestet. Es zeigte sich in allen untersuchten Hirnarealen zwar ein komplexes Spleißvarianten-Distributionsmuster, aber darüber hinaus kein signifikanter Unterschied zwischen Kontrolltieren und $Ca_v2.3^{-/-}$ Mäusen (Weiergräber et al., 2006a).

3.2. Histologische Analyse $Ca_v2.3$ defizienter Mäuse und Kontrolltiere

Mittels *Western-Blot* als auch immunhistochemischer Analyse zeigte sich, dass $Ca_v2.3$ nicht nur im Hippokampus (z.B. Pyramidenzellen) exprimiert wird, sondern auch in inhibitorischen Schlüsselpositionen, wie z.B. dem Nucleus reticularis thalami und kortikalen Interneuronen (Weiergräber et al., 2006a, 2006b; Weiergräber et al., 2008b). Histochemische Verfahren (HE, Nissl-Färbung) legten weiterhin dar, dass in den Hirnen $Ca_v2.3$ defizienter Mäuse keine morphologischen Alterationen wie z.B. Malformationen vorliegen, die mit dem unten dargelegten neurologischen Phänotyp funktionell in Beziehung gesetzt werden könnten (Weiergräber et al., 2006a, 2006b, Weiergräber et al., 2007; Weiergräber et al., 2008).

3.3. Telemetrisch-neurologische Charakterisierung $Ca_v2.3$ defizienter Mäuse

3.3.1. Methode zur Erfassung von Biopotentialen bei transgenen Mäusen

Zunächst wurde eine Methode zur Detektion von Biopotentialen bei kleinen Nagern entwickelt und etabliert (Weiergraber et al., 2005a; Weiergräber et al., 2005b). Nachdem bereits radiotelemetrische Aufzeichnungen zur elektrokardiographischen Charakterisierung $Ca_v2.3$ defizienter Mäuse erfolgreich durchgeführt worden waren (Weiergräber et al., 2005b), erfolgte im Rahmen der neurologischen Charakterisierung ein weiterer Ausbau der Methodik zur Aufnahme von Elektrokortikogrammen (ECoG) und tiefen, intrazerebralen EEG-Ableitungen unter Verwendung eines Stereotakten (Weiergräber et al., 2005a). Hiermit wurde es möglich, extrazelluläre Feldpotentiale aus spezifischen Hirnregionen in Kurz- und Langzeitmessungen sowie nach Administration verschiedener Pharmaka zu erfassen.

3.3.2. Neurologischer Phänotyp $Ca_v2.3$ defizienter Mäuse

Aufgrund der Untersuchungen zur Rolle von $Ca_v2.3$ beim Triggern epileptiformer Aktivität im Hippokampus, aber auch im thalamokortikalen Neuronenkreis und basierend auf seiner Expression in neuronalen Schlüsselstrukturen, wie hippokampalen Pyramidenzellen, aber auch gabaergen Interneuronen, stellte sich zunächst die Frage der systemischen Konsequenzen einer $Ca_v2.3$ Ablation. Visuelle Inspektion der $Ca_v2.3$ Tiere lieferte keine Anzeichen für ein spontanes epileptisches Geschehen oder eine andere neurologische Symptomatik, wie Ataxien oder Dyskinesien. Mittels der etablierten Methodik der oberflächlichen und tiefen Elektroenzephalographie wurden sodann $Ca_v2.3^{-/-}$ und Kontrolltiere eingehender neurologisch untersucht. Elektrokortikographische und tiefe, intrahippokampale Langzeitaufzeichnungen aus der CA1 und CA3 Region an generalisierten wie hirnspezifisch $Ca_v2.3$-inaktivierten Mäusen wiesen keine epileptiformen Graphoelemente auf, die ein indikatives Moment für konvulsive oder nicht-konvulsive Anfallsleiden hätten darstellen können. Auch Frequenzanalysen der Spontan-EEGs zeigten keine Unterschiede in der *Power*-Spektrumdichte der verschiedenen EEG-Frequenzbänder zwischen $Ca_v2.3$ defizienten Mäusen und Kontrolltieren.

3.3.3. Suszeptibilität gegenüber konvulsiven Anfallsformen und Anfallsarchitektur bei $Ca_v2.3^{-/-}$ Mäusen

Zur Induktion generalisiert tonisch-klonischer Anfälle wurden Pentylentetrazol (PTZ) und 4-Aminopyridin (4-AP), zum Triggeren hippokampaler Epilepsien Kainat und NMDA verwendet. Die final eingesetzten Versuchsdosen der einzelnen Konvulsiva entstammten Pilotversu-

chen, bei denen der LD_{50}-Wert der Kontrolltiere approximiert wurde. Es zeigte sich, dass $Ca_v2.3$ defiziente Mäuse eine generelle Resistenz gegenüber konvulsiven, generalisiert tonisch-klonischen und hippokampalen Anfällen aufwiesen. Nach PTZ-Administration (80 mg/kg) betrug die Letalität bei Kontrolltieren 70 %, während keines der $Ca_v2.3$ defizienten Tiere verstarb. Insbesondere die schweren Anfallsstadien (generalisierter Myoklonus und generalisiert tonisch-klonischer Anfall) waren hinsichtich Latenz, Dauer und Frequenz bei $Ca_v2.3^{-/-}$ Tieren signifikant vermindert (Weiergräber et al., 2006a). Da andere spannungsgesteuerte Ca^{2+}-Kanäle keine veränderten Expressionsmuster aufwiesen, muss davon ausgegangen werden, dass es sich hierbei um Effekte handelt, die originär auf die $Ca_v2.3$ Ablation zurückgehen und nicht auf kompensatorischen Prozessen anderer Ca^{2+}-Kanäle beruhen (Weiergräber et al., 2006a).

Studien zur Induktion hippokampaler Epilepsien mittels Kainat (30 mg/kg i.p.) und NMDA (150 mg/kg i.p.) zeigten weiterhin, dass hier die Anfallsresistenz bei $Ca_v2.3^{-/-}$ Mäusen noch drastischer ausfällt als dies bei PTZ und 4-AP beobachtet wurde (Weiergräber et al., 2007). Auch hier wurde deutlich, dass die Anfallsresistenz $Ca_v2.3$ defizienter Mäuse v.a. die höhergradigen Stadien wie den Status epilepticus und generalisiert tonisch-klonische Aktivität umfasst. Der $Ca_v2.3$ Ca^{2+}-Kanal übt damit ganz unmittelbar Effekte auf Anfallsinitiation, Propagation und die Anfallsgeneralisierung aus.

Neben der phänotypischen Evaluation von $Ca_v2.3^{+/+}$ und $Ca_v2.3^{-/-}$ Tieren nach Administration verschiedener Konvulsiva, wurde eine qualitative Analyse der Anfallsarchitektur nach PTZ, 4-AP-, Kainat- und NMDA-Gabe durchgeführt. Nach Gabe von PTZ und 4-AP durchliefen die Versuchstiere eine charakteristische Abfolge von Anfallstadien, die durch einen spezifischen EEG-Phänotyp gekennzeichnet sind. Vor allem das generalisiert tonisch-klonische Anfallsstadium ist initial durch das typische Auftreten von *spike*- und *spike-wave* Aktivität (4 - 4,5 Hz) und im Folgenden langsameren *spike-wave* Mustern von 1 - 1,5 Hz gekennzeichnet. Es zeigte sich, dass generalisierte Anfallsstadien bei $Ca_v2.3$ defizienten Tieren einen geringeren Organisationsgrad aufwiesen und disperser als bei Kontrolltieren waren. Isolierte, singuläre *spike*-Aktivität, die mit Ganzkörperkontraktionen (*whole body twitchings*) einhergeht, ist dagegen in $Ca_v2.3^{-/-}$ Tieren signifikant erhöht und fand sich in der interiktalen Phase (Weiergräber et al., 2006a). Die $Ca_v2.3$-Ablation schwächt somit auf systemischer Ebene die Etablierung schwer verlaufender iktaler Episoden und fördert im Gegenzug eine kontinuierliche aber isolierte *spike*-Aktivität auf niedrigerem Frequenzniveau in den interiktalen Perioden.

Tiefe intrahippokampale Ableitungen hatten gezeigt, dass $Ca_v2.3$ defiziente Mäuse auch im Hippokampus nicht spontan epileptisch aktiv sind. Zusätzlich wurde die hippokampale An-

fallssuzeptibilität mittels Kainat und NMDA getestet. Für die bei den Verhaltenuntersuchungen verwendete Kainat-Dosen von 30 mg/kg wiesen sowohl die $Ca_v2.3$ defizienten als auch die Kontrolltiere kontinuierliche Anfallsaktivität (Status epilepticus und exazerbierende *spike-wave* Aktivität mit nachfolgender kurzer postiktaler Depression auf. Beide Genotypen zeigten sowohl bei 30 als auch bei 10 mg/kg Kainat kontinuierliche *spike-wave* Aktivität im Theta-Frequenzbereich (4 - 8 Hz) auf, was unterstreicht, dass sich beide Konzentrationen über der hippokampalen Anfallsschwelle befinden (Weiergräber et al., 2007).
Da die Resistenzstudien zum Kainat bei einer Dosis von 30 mg/kg durchgeführt wurden, erfolgte auch eine detaillierte Untersuchung der intrahippokampalen EEG-Ableitungen bei dieser Dosis. Eine *Power*-Spektrumdichte-Analyse der iktalen Episoden sowie des gesamten zweistündigen Beobachtungszeitraumes zeigte keine signifikanten Unterschiede, obwohl sich bei letzterer ein vorzeitiges Auftreten von Theta- und Delta-Aktivität (stellvertretend für epileptiforme Tatigkeit) vorliegt (Weiergräber et al., 2007). Es zeigte sich, dass bei dieser hippokampal deutlich überschwelligen Kainat-Dosis die Hippokampi beider Genotypen vergleichbarer Hyperexzitabilität ausgesetzt waren, was für die Interpretation der exzitotoxischen Konsequenzen von zentraler Bedeutung war.

3.3.4. Suszeptibilität gegenüber nicht-konvulsiven Anfallsformen bei $Ca_v2.3^{-/-}$ Mäusen

Basierend auf der Expression des $Ca_v2.3$ Ca^{2+}-Kanals im thalamokoertikalen System erfolgte auch eine Anfallssuszeptibilitätstestung gegenüber nicht-konvulsiven Anfallsformen vom Absencen-Typ unter Verwendung von γ-Hydroxybutyrolacton (GHB, 70 mg/kg). Überraschenderweise präsentierten $Ca_v2.3$ defiziente Mäuse im Oberflächen-EEG eine erhöhte Suszeptibilität gegenüber GHB-induzierten *spike-wave* Graphoelementen sowie eine Veränderung der Anfallsarchitektur (Weiergräber et al., 2008a). Auch *Power*-Spektrumanalysen konnten diesen Sachverhalt bestätigen. Diese Ergebnisse legen nahe, dass $Ca_v2.3$ als mittel- bis hochspannungsaktivierter Ca^{2+}-Kanal im retikulär-thalamischen Kern den tonischen Aktivitätsmodus der Neurone fördert. Umgekehrt führt Ablation des Kanals zu einer thalamokortikalen Dysbalance mit funktionellem Übergewicht des *rebound burst*-Modus und folglich erhöhter Suszeptibilität zur Generation von *spike-wave* Elementen (Weiergräber et al., 2008a). Die Bedeutung der $Ca_v2.3$ Untereinheit bei thalamokortikalen Oszillationen zeigt sich weiterhin darin, dass Isoflurane als Inhibitor der $Ca_v2.3$-Untereinheit im Nucleus reticularis thalami das thalamokortikale *burst* und *burst suppression* Muster zu modulieren vermochte (Joksovic et al., 2009).

3.4. Der $Ca_v2.3$ Kalziumkanal und seine Bedeutung bei neuronaler Exzitoxizität und Apoptose

In Kenntnis der Ergebnisse von Suzuki et al. (2004) wurden mit histologischen Verfahren (HE-, Nissl-Färbung) die durch Kainat (30 mg/kg) induzierten exzitotoxischen Effekte sieben Tage nach systemischer Administration untersucht. In der CA3-Region von Kontrolltieren fand sich ein deutlicher Zelluntergang, der in den $Ca_v2.3$ defizienten Tieren nicht festzustellen war (Weiergräber et al., 2007). Da telemetrische Untersuchungen keine Unterschiede in der Anfallsaktivität beider Genotypen bei dieser überschwelligen Kainat-Dosis gezeigt haben und auch detaillierte Analyse der iktalen und interiktalen Episoden sowie eine zeitliche Analyse der *Power*-Spektrumdichte-Verteilung keine Unterschiede zwischen beiden Genotypen ergab, liegt es nahe, dass die $Ca_v2.3$ Ablation einen anti-exzitotoxischen Effekt hat (Weiergräber et al., 2007).

3.5. Ca^{2+}-Kanäle als Zielstruktur für Antiepileptika

Vorarbeiten anderer Arbeitsgruppen zeigten, dass einige Antiepileptika mit $Ca_v2.3$ blockierender Wirkung, wie das Topiramat, ein Sulfonamid-Strukturmotiv aufweisen (McNaughton et al., 2004, Kuzmiski et al., 2005). Basierend hierauf wurde v.a. das Zonisamid entsprechend seiner postulierten Wirkweise auf $Ca_v2.3$ aber auch $Ca_v3.1$-3.3 T-Typ Ca^{2+}-Kanäle getestet und elektrophysiologisch im heterologen Expressionssystem charakterisiert (Matar et al., 2009). Während die Effekte auf $Ca_v2.3$ im therapeutisch relevanten Konzentrationsbereich des Zonisamids vernachlässigbar waren, zeigte sich bei den T-Typen ein moderater Block, der jedoch deutlich hinter den in der Literatur zuvor berichteten Werten zurückbliebt (Matar et al., 2009).

Nachstehend sind wichtige, eigene Publikationen zu dem beschriebenen Themenkomplex angehängt:

Nervenarzt 2008 · 79:426–436
DOI 10.1007/s00115-007-2398-6
Online publiziert: 13. Januar 2008

M. Weiergräber[1, 2] · J. Hescheler[1, 2] · T. Schneider[1, 2]
[1] Institut für Neurophysiologie, Medizinische Einrichtungen, Universität zu Köln
[2] Zentrum für Molekulare Medizin Köln (ZMMK), Universität zu Köln

Kalziumkanalopathien des Menschen

Spannungsgesteuerte Ca^{2+}-Kanäle in Ätiologie, Pathogenese und Pharmakotherapie neurologischer Krankheitsbilder

Kanalopathien – im angloamerikanischen Sprachraum *channelopathies* genannt – stellen eine faszinierende neue Kategorie innerhalb der Neurologie, aber auch anderer Fachdisziplinen dar. Viele vormals enigmatische Krankheitsentitäten des Menschen wurden entmystifiziert und nach ätiopathogenetischen Gesichtspunkten neu klassifiziert, basierend auf Alterationen spannungs- oder ligandengesteuerter Ionenkanäle. Die Zahl identifizierter Kanalopathien hat v. a. in der letzten Dekade rapide zugenommen und ist das Ergebnis intensiver medizinischer Grundlagenforschung. Nicht zuletzt eröffnet gerade dieser molekularmedizinische Ansatz neue Perspektiven in der Pharmako- und Gentherapie und wird somit auch für den Patienten in der Zukunft einen deutlichen Benefit darstellen.

Spannungsgesteuerte Kalziumkanäle – Struktur und Funktion

Spannungsgesteuerte Ca^{2+}-Kanäle gehören zu einer Familie transmembranärer Kanalproteine, die in Reaktion auf eine Membrandepolarisation öffnen und Ca^{2+}-Ionen selektiv entlang ihres elektrochemischen Gradienten in Zellen einströmen lassen. Entsprechend der globalen Funktion des Ca^{2+}-Ions spielen spannungsgesteuerte Ca^{2+}-Kanäle eine entscheidende Rolle bei der Regulation einer Vielzahl zellulärer Prozesse, wie z. B. der Exzitations-Kontraktions-Kopplung, der Exzitations-Sekretions-Kopplung, der Hormon- und Transmitterfreisetzung sowie der Regulation der Genexpression. Spannungsgesteuerte Ca^{2+}-Kanalkomplexe sind hochmolekulare Strukturen (>400 kDa), die aus mindestens drei Untereinheiten (α_1-, $\alpha_2\delta$- und β-Untereinheit) in einer 1:1:1 Stöchiometrie zusammengesetzt sind (◘ **Abb. 1**) [2]. Zehn verschiedene porenbildende, ionenleitende Ca_v-α_1-Untereinheiten sind bis heute identifiziert worden, die strukturelle Homologien mit spannungsgesteuerten Na^+- und K^+-Kanälen aufweisen.

Nach klassischen pharmakologischen und elektrophysiologischen Gesichtspunk-

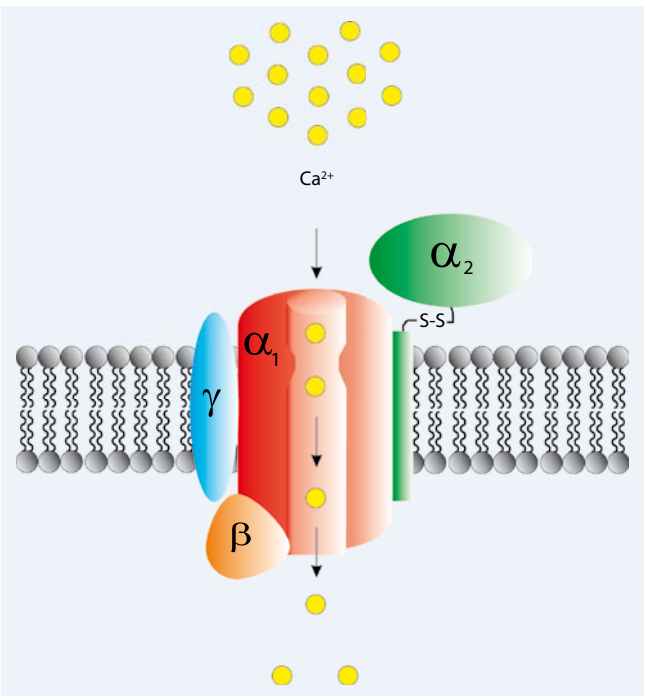

Abb. 1 ▶ Strukturelle Zusammensetzung eines spannungsgesteuerten Ca^{2+}-Kanals [30]

ten lassen sich die Ca_v-α_1-Untereinheiten in hochspannungsaktivierte (*high-voltage activated, HVA*) und niederspannungsaktivierte (*low-voltage activated, LVA*) unterteilen, wobei sich die hochspannungsaktivierten weiter in Dihydropyridin (DHP)-sensitive L-Typ („L" für *long-lasting*)-Kanäle und DHP-"unempfindlichere" Non-L-Typ Ca^{2+}-Kanäle differenzieren lassen. Die L-Typ (Ca_v1)-Fraktion umfasst hierbei gemäß der neuen IUPHAR-Nomenklatur die porenbildenen α_1-Untereinheiten $Ca_v1.1$ (α_1S), $Ca_v1.2$ (α_1C), $Ca_v1.3$ (α_1D) sowie $Ca_v1.4$ (α_1F), während die Non-L-Typ-Gruppe (Ca_v2) die Untereinheiten $Ca_v2.1$ (α_1A), $Ca_v2.2$ (α_1B) und $Ca_v2.3$ (α_1E) beinhaltet. Die niederspannungsaktivierten T-Typ („T" für *transient/tiny*)-Ca^{2+}-Kanäle setzen sich aus $Ca_v3.1$ (α_1G), $Ca_v3.2$ (α_1H) und $Ca_v3.3$ (α_1I) zusammen [2, 20] (**Tab. 1**).

Wie andere Ionenkanalfamilien umfasst auch ein Ca^{2+}-Kanalkomplex nicht nur die porenbildende α_1-Untereinheit, sondern weiterhin eine Vielzahl von Hilfsuntereinheiten, die sich aus den bislang klonierten $\alpha_2\delta_{1-4}$-, β_{1-4}-, und γ_{1-8}-Untereinheiten rekrutieren und in vielfältiger Weise die elektrophysiologischen und pharmakologischen Eigenschaften der zentralen α_1-Untereinheit des Ca^{2+}-Kanalkomplexes sowie deren Plasmamembranexpression zu modulieren vermögen (**Abb. 1**). Die $\alpha_2\delta$-Untereinheit kann z. B. direkt mit der porenbildenden Ca_v-α_1-Untereinheit interagieren und dient bemerkenswerterweise auch als Zielstruktur einer Reihe neuerer Antiepileptika, wie z. B. Gabapentin oder Pregabalin [6]. Die zytosolisch lokalisierte β-Untereinheit interagiert unmittelbar mit dem I-II-*Loop*, einer intrazellulär lokalisierten Schleife zwischen Domäne I und II der porenbildenden Ca_v-α_1-Untereinheit und scheint von besonderer Wichtigkeit für die Signalvermittlung und kinetischen Eigenschaften der α_1-Untereinheit zu sein. Die äußerst wichtige Funktion der β-Untereinheiten wird auch dadurch unterstrichen, dass *Knock-out*-Tiere entsprechend schwere physiologische Beeinträchtigungen aufweisen [13].

Ebenso wie die α_1-Untereinheit liegen auch die γ-Untereinheiten als membranintegrale Proteine vor, die als modulierende Hilfsuntereinheit vielfältige Funk-

Zusammenfassung · Summary

Nervenarzt 2008 · 79:426–436 DOI 10.1007/s00115-007-2398-6

M. Weiergräber · J. Hescheler · T. Schneider

Kalziumkanalopathien des Menschen. Spannungsgesteuerte Ca^{2+}-Kanäle in Ätiologie, Pathogenese und Pharmakotherapie neurologischer Krankheitsbilder

Zusammenfassung

Spannungsgesteuerte Ca^{2+}-Kanäle spielen eine Schlüsselrolle bei einer Vielzahl physiologischer Prozesse. Innerhalb des letzten Jahrzehnts hat die Zahl der als sog. Ca^{2+}-Kanalopathien definierten Krankheitsentitäten, die v. a. das neuronale und muskuläre System affizieren, dramatisch zugenommen. Beim Menschen finden sich hierbei v.a. Mutationen in den L-Typ $Ca_v1.2$- und $Ca_v1.4$-Ca^{2+}-Kanälen sowie in den Non-L-Typ $Ca_v2.1$- und T-Typ $Ca_v3.2$-Untereinheiten. Derartige Mutationen sind mit Alterationen grundlegender elektrophysiologischer Parameter assoziiert und somit von ätiopathologischer Relevanz. Basierend auf ihrer dominanten Expression im ZNS sind Ca^{2+}-Kanäle aber auch für Epilepsien sowie Erkrankungen aus dem neuropsychiatrischen Formenkreis von besonderer Bedeutung. In der vorliegenden Übersichtsarbeit werden die bis heute bekannten humanen Ca^{2+}-Kanalopathien im Detail erörtert und auf pathophysiologische wie klinische Aspekte besonders eingegangen.

Schlüsselwörter

Epilepsie · Kanalopathien · Neuromuskulär · Pharmakotherapie · Spannungsgesteuerte Ca^{2+}-Kanäle

Human calcium channelopathies. Voltage-gated Ca^{2+} channels in etiology, pathogenesis, and pharmacotherapy of neurologic disorders

Summary

Voltage-gated calcium channels are key components in a variety of physiological processes. Within the last decade an increasing number of voltage-gated Ca^{2+} channelopathies in both humans and animal models has been described, most of which are related to the neurologic and muscular system. In humans, mutations were found in L-type $Ca_v1.2$ and $Ca_v1.4$ Ca^{2+} channels as well as the non-L-type $Ca_v2.1$ and T-type $Ca_v3.2$ channels, resulting in altered electrophysiologic properties. Based on their widespread distribution within the CNS, voltage-gated calcium channels are of particular importance in the etiology and pathogenesis of various forms of epilepsy and neuropsychiatric disorders. In this review we characterise the different human Ca^{2+} channelopathies known so far, further illuminating basic pathophysiologic mechanisms and clinical aspects.

Keywords

Channelopathies · Epilepsy · Neuromuscular · Pharmacotherapy · Voltage-gated Ca^{2+} channels

Tab. 1 Kanalopathien der Ca_v-α_1-Untereinheiten

Untereinheit	Pharmakologie	Verteilung	Humane Kalziumkanalopathien
$Ca_v1.1$	Dihydropyridne, Benzothiazepine, Phenylalkylamine, TaiCatoxin, Calciseptine, Calcicludine, FS-2	Skelettmuskel	Hypokaliämische periodische Paralyse Typ 1 (HypoPP1) Maligne Hyperthermie Typ 5 (MH5)
$Ca_v1.2$		Ubiquitär	Timothy-Syndrom (LQT8, Epilepsien)
$Ca_v1.3$		Ubiquitär	Nicht bekannt
$Ca_v1.4$		Retina	X-*linked congenital stationary night blindness 2* (xCSNB2), X-*linked cone-rod dystrophy type* 3 (CORDX3), *Aland Island eye disease* (AIED)
$Ca_v2.1$	ω-Agatoxin IVA	ZNS	Absencen-Epilepsie, Episodische Ataxia Typ 2 (EA2), spinozerebelläre Ataxie Typ 6 (SCA6) Familiäre hemiplegische Migräne (FHM1) Lambert-Eaton Myastenie-Syndrom (LEMS)
$Ca_v2.2$	ω-Conotoxin GVIA	ZNS/PNS	Lambert-Eaton-Myastenie-Syndrom (LEMS)
$Ca_v2.3$	SNX-482, Ni^{2+}	ZNS/PNS	*Young onset* Typ 2 Diabetes mellitus
$Ca_v3.1$	Mibefradil, Kurtoxin, Ni^{2+}	ZNS/PNS	Nicht bekannt
$Ca_v3.2$		ZNS/Herz	Absencen-Epilepsie (CAE), idiopathisch generalisierte Epilepsien (IGE), autistischer Formenkreis
$Ca_v3.3$		ZNS	Nicht bekannt

ZNS zentrales Nervensystem, PNS peripheres Nervensystem.

tionen übernehmen. Sie können die Ca^{2+}-Kanalaktivität über eine Reduktion der Zahl funktioneller Ca^{2+}-Kanalkomplexe in der Plasmamembran vermindern oder auch zu einer -Begünstigung des thermodynamisch stabileren inaktivierten Kanalkonformationszustandes beitragen.

L-Typ-Ca^{2+}-Kanäle zeigen eine weite Verbreitung im ZNS, Skelettmuskel, Herzen und anderen Geweben und sind klassischerweise durch DHP, Phenylalkylamine und Benzothiazepine hemmbar. Die Non-L-Typ-Ca^{2+}-Kanäle werden dagegen vorwiegend im Nervensystem exprimiert und lassen sich durch eine Reihe von Schnecken- und Spinnentoxinen inhibieren. So lässt sich $Ca_v2.1$ durch ω-Agatoxin IVA und ω-Conotoxin MVIIC hemmen, $Ca_v2.2$ durch ω-Conotoxin GVIA sowie ebenfalls ω-Conotoxin MVIIC (**Tab. 1**). Auf den in klinischer Anwendung befindlichen $Ca_v2.1$-Blocker Ziconotid wird weiter unten in diesem Beitrag eingegangen. Für den lange Zeit als R (*resistant*)-Typ bezeichneten $Ca_v2.3$-Ca^{2+}-Kanal fand sich erst 1998 mit dem Taranteltoxin SNX-482 ein vergleichsweise spezifischer Blocker. Weiterhin besteht eine Empfindlichkeit gegenüber Ni^{2+}-Ionen, die der Kanal allerdings mit $Ca_v3.2$ teilt. Obwohl es mit Mibefradil und dem Skorpiontoxin Kurtoxin erste Erfolg versprechende Ansätze für vergleichsweise selektive T-Typ-Blocker gab, erreichen diese bis heute noch nicht das gewünschte pharmakologische Profil und finden daher v.a. in der Forschung Anwendung.

Neben spannungsgesteuerten können auch ligandengesteuerte Ca^{2+}-Kanäle Depolarisationen sowie einen Anstieg des zytosolischen Ca^{2+}-Spiegels vermitteln. Einige sind plasmamembranständig, wie z. B. NMDA-Glutamat-Rezeptoren oder hyperpolarisationsaktivierte und zyklisch-Nukleotid-gesteuerte Kanäle (sog. HCN-Kanäle). Sie sind jedoch nicht Ca^{2+}-selektiv, sondern auch gegenüber anderen Kationen, wie z. B. Na^+, permeabel und werden daher bevorzugt als nichtselektive Kationenkanäle bezeichnet. Zu den intrazellulär ligandengesteuerten Ca^{2+}-Kanäle werden u. a. die IP_3- und Ryanodin-Rezeptoren gezählt. Im Folgenden werden die spannungsgesteuerten Ca^{2+}-Kanalopathien detaillierter dargestellt.

Humane Ca^{2+}-Kanalopathien – eine Übersicht

Hochspannungsaktivierte L-Typ-Kalziumkanäle ($Ca_v1.1$–1.4)

$Ca_v1.1$ (α_1S)

Das die porenbildende Untereinheit $Ca_v1.1$ kodierende Gen CACNA1S findet sich beim Menschen auf Chromosom 1q31–32. Primärer Expressionsort sind die transversalen Tubuli des skelettmuskulären Apparates, in denen sie an der Exzitations-Kontraktions-Kopplung sowie der Ca^{2+}-Homöostase maßgeblich beteiligt sind. Bei Mäusen führt eine Leserastermutation (nt 4010) zu einer letal verlaufenden Form muskulärer Dysgenesie und stellte die erste In-vivo-Beobachtung einer Ca^{2+}-Kanal-Dysfunktion (Ca^{2+}-Kanalopathie) und ihrer fatalen pathophysiologischen Konsequenzen dar [1]. Beim Menschen sind zwei neurologische Krankheitsbilder ätiopathologisch mit $Ca_v1.1$-Mutationen assoziiert:

- die hypokaliämische periodische Paralyse Typ 1 sowie
- die maligne Hyperthermie Typ 5.

Hypokaliämische periodische Paralyse Typ 1. Die hypokaliämische periodische Paralyse Typ 1 (HypoPP1) stellt eine autosomal-dominant vererbte Muskelerkrankung dar, die durch episodische Muskelschwäche in Assoziation mit niedrigen K^+-Serumspiegeln gekennzeichnet ist. Mit einer Prävalenz von 1:100.000 stellt sie die häufigste periodische Paralyse dar, wobei es sich bei 1/3 der Fälle um De-novo-Mutationen handelt. Sie manifestiert sich i.d.R. in der 1. und 2. Lebensdekade mit kurzen Paralysen bei nächtlichem Erwachen und in den frühen Morgenstunden. Die Muskelschwäche kann fokal oder generalisiert auftreten, spart aber die faziale und respiratorische Muskulatur aus. Typische Trigger sind Erholungsphasen nach körperlicher Anstrengung, Stress, Schlafdeprivation, Infektionen, Menstruation sowie auch kohlenhydratreiche Mahlzeiten. Teilweise werden auch begleitende Paräs-

thesien, Müdigkeit sowie Verhaltens- und kognitive Änderungen beschrieben. Die paralytischen Attacken können Stunden, selten Tage andauern und lösen sich graduell. Bei ca. 3/4 der Patienten bleibt eine dauerhafte residuale Muskelschwäche. Eine Myotonie ist im EMG nicht nachweisbar, ebenso keine skelettmuskulären Entwicklungsstörungen. Die Muskelbiopsie kann unspezifische, vakuoläre Veränderungen zeigen. Der bei der HypoPP1 betroffene $Ca_v1.1$-Ca^{2+}-Kanal vermittelt nicht nur selbst einen Ca^{2+}-Einstrom, sondern auch die depolarisationsgekoppelte Ca^{2+}-Freisetzung aus dem sarkoplamatischen Retikulum.

Zwei der $Ca_v1.1$-Mutationen, die mit HypoPP1 in Verbindung gebracht wurden, liegen innerhalb desselben Codons und weisen einen Austausch eines hochkonservierten Arginins in S4 der Domäne IV durch ein Histidin bzw. Glyzin auf (R1239G, R1239H). Somit haben diese Mutationen deutliche Effekte auf den durch positiv geladene Argininreste aufgebauten Spannungssensor. Die genannten Mutationen führen zu einer reduzierten L-Typ-Ca^{2+}-Stromamplitude und verlangsamter Aktivierungskinetik, und auch Untersuchungen in menschlichen Myozyten zeigten eine Reduktion der Stromdichte. Ein Austausch positiver Arginine und damit verbunden Alterationen am Spannungssensor scheinen ein grundlegendes ätiopathogenetisches Element der HypoPP1 zu sein, da zwei weitere bekannte Mutationen ebenfalls in S4, nun jedoch in Domäne II (R528H, R528G) vorliegen [18].

Obwohl $Ca_v1.1$-Mutationen ursächlich der HypoPP1 zugrunde liegen, scheinen die pathophysiologischen Konsequenzen auch auf Interaktionen mit anderen Kanalentitäten zu beruhen. So zeigt sich in Patienten mit HypoPP eine abnorme Reduktion des ATP-sensitiven K^+-Kanals (K_{ATP}). Die Bedeutung des K_{ATP}-Kanals wird dadurch unterstrichen, dass der K^+-Kanal-Öffner Chromokalim die pathophysiologischen Manifestationen der HypoPP zu mindern vermag. Bei der Behandlung sind sowohl verhaltenstherapeutische wie pharmakologische Aspekte von besonderer Bedeutung. Neben der Vermeidung auslösender Faktoren und diätetischen Maßnahmen (häufige, kleine kohlenhydratarme Mahlzeiten) als Prophylaxe werden in der akuten Attacke K^+-Ionen verabreicht, bis die K^+-Spiegel wieder Normalwerte erreicht haben. Auch die Karboanhydrasehemmer Azetazolamid und Dichlorphenamid haben sich als wirksam erwiesen.

Maligne Hyperthermie. Die maligne Hyperthermie (MH) stellt ebenfalls eine autosomal-dominant vererbte skelettmuskuläre Störung dar und steht primär in Beziehung zu Mutationen am Ryanodin-Rezeptor Typ 1 (RYR1) im sarkoplasmatischen Retikulum (SR). Charakteristikum der malignen Hyperthermie ist hierbei eine deutliche Suszeptibilität gegenüber Inhalationsnarkotika und depolarisierenden Muskelrelaxanzien, die mit dramatischen und z. T. lebensbedrohlichen Hyperthermien vergesellschaftet sind. Weiterhin findet sich eine schwere Hypertonie der Willkürmuskulatur mit CPK-, PO_4^{3-}- und K^+-Anstieg als Zeichen der Rhabdomyolyse und Laktatazidose. Komplikationen wie Nierenversagen und Fälle von „sudden infant death syndrome" (SIDS) wurden mit maligner Hyperthermie in Verbindung gebracht.

Zur Diagnostik steht ein In-vitro-Kontrakturtest (nach Muskelbiopsie) oder In-vivo-Testverfahren mit intramuskulärer Injektion von z. B. Koffein zur Verfügung. Während Alterationen des RYR1 als Hauptursache bei der Mehrzahl betroffener Individuen gilt, gibt es Hinweise, dass auch Mutationen in $Ca_v1.1$ (MH Typ 5, R1086H) oder auch der $\alpha_2\delta$-Untereinheit für die Genese der malignen Hyperthermie verantwortlich sind [19]. Therapeutikum der Wahl ist das Dantrolen, welches im Akutfall intravenös, zur Prophylaxe auch oral verabreicht werden kann. Dantrolen hemmt hierbei die Freisetzung der Ca^{2+}-Ionen aus dem SR.

$Ca_v1.2$ (α_1C)

Die $Ca_v1.2$-Untereinheit wird durch CACNA1C auf Chromosom 12p13.3 kodiert. Diese Untereinheit findet sich im Herzmuskel sowie glatter Muskulatur, weiterhin auch in endokrin aktivem Gewebe sowie Nervenzellen. $Ca_v1.2$-defiziente Mäuse versterben bereits intrauterin aufgrund kardialer Dysfunktion [2]. Beim Menschen sind erst zwei De-novo-*Missense*-Mutationen bekannt, die zum sog. Timothy-Syndrom führen.

Timothy-Syndrom. Beim Timothy-Syndrom handelt sich um eine Multisystemerkrankung, die u. a. durch maligne kardiale Arrhythmien und komplexe Entwicklungsstörungen wie Syndaktylie gekennzeichnet ist. Des Weiteren finden sich bei betroffenen Patienten Zeichen einer Immundefizienz und häufig eine autistische Symptomatik. Kardial lassen sich neben einem LQT-Syndrom und ventrikulären Tachyarrhythmien ein persistierender Ductus arteriosus Botalli, ein offenes Foramen ovale, ventrikuläre Septumdefekte, eine Fallot-Tetralogie sowie eine Kardiomegalie finden. Die jungen Patienten versterben im Durchschnitt bereits mit 2 1/2 Jahren vornehmlich an malignen kardialen Arrhythmien. Interessanterweise handelt es sich um De-novo-*Gain-of-function-missense*-Mutationen (G406R, G402S) am C-terminalen Ende des IS6 der Domäne I der porenbildenden $Ca_v1.2$-Untereinheit [25]. Die Aminosäuresequenz in dieser Region ist speziesübergreifend und im Vergleich mit anderen spannungsgesteuerten Ca^{2+}-Kanälen zu 100% konserviert.

Die beschriebenen Mutationen führen zu einer deutlichen Verlangsamung der Inaktivierung und konnten so direkt für die kardialen Effekte, wie Prolongation des myokardialen Aktionspotenzials, QT-Zeit-Verlängerung und erhöhte Suszeptibilität für maligne Arrhythmien verantwortlich gemacht werden. Es ist damit die erste Ca^{2+}-Kanalopathie, die mit einem LQT-Syndrom in Verbindung gebracht werden konnte und trägt nun die Bezeichnung LQT8-Syndrom. Nicht unterschätzt werden dürfen die neurologischen und neuropsychiatrischen Implikationen dieser Multisystemerkrankung. So zeigen Timothy-Patienten rezidivierende epileptische Anfälle (21%), autistische Störungen (80%) sowie mentale Retardierung in 25% der Fälle [25]. Entsprechend ihrer multisystemischen Natur ist die Therapie vielschichtig pharmakologisch und zur Behandlung der diversen Entwicklungsstörungen auch chirurgisch.

$Ca_v1.3$ (α_1D)

Die $Ca_v1.3$-Untereinheit wird durch das Gen CACNA1D auf Chromosom 3p14.3 kodiert und findet sich primär in endokrin aktiven Geweben, wie z. B. der

Hypophyse, den β-Zellen des Pankreas und chromaffinen Zellen des Nebennierenmarks. Daneben ist sie in Sinneszellen (Photorezeptorzellen und Haarzellen der Kochlea) sowie in Schrittmacherregionen des Herzens und Neuronen exprimiert. Auf neuronaler Ebene zeigt $Ca_v1.3$ eine bevorzugte Expression auf den Somata und proximalen Dendriten [2]. Mutationen beim Menschen sind bislang nicht bekannt. Bei Mäusen führt die Ablation des $Ca_v1.3$-Ca^{2+}-Kanals zu Anakusis, Sinusbradykardie und Störungen der atrioventrikulären Überleitung (AV-Block II°).

$Ca_v1.4$ (α_1F)

Die $Ca_v1.4$-Untereinheit wird durch das Gen CACNA1F auf Chromosom Xp11.4 kodiert und zeigt eine Expression in retinalen Stäbchen und Bipolarzellen, aber auch im Rückenmark, in der Nebenniere sowie in Mastzellen. Die Zahl der $Ca_v1.4$-Alterationen, die mit der sog. *X-linked congenital stationary night blindness* (x-CSNB2) assoziiert sind, ist mit derzeit mehr als 73 bekannten Mutationen (51% *Nonsense*-, 32% *Missense*- und 8% Leserastermutationen) äußerst vielfältig [18]. Weiterhin bestehen Hinweise auf eine Assoziation zwischen Schizophrenie und dem CACNA1F-Genlokus [29].

X-chromosomal-gebundene angeborene Form der Nachtblindheit Typ 2 (X-CSNB2). Die CSNB2 ist eine X-chromosomal-rezessiv vererbte, nicht progressive retinale Funktionsstörung, die durch Nachtblindheit, Visusverlust, Myopie, Nystagmus und Strabismus charakterisiert sein kann und auf einer retinalen Neurotransmissionsstörung von Photorezeptorzellen zu Bipolarzellen beruht. Der Augenhintergrund ist i.d.R. unauffällig, bei starker Myopie sind myope Degenerationen möglich. Zur Funktionsdiagnostik zählen die Visusanalyse, der Farbsehtest und die Adaptometrie sowie die ERG-Analyse (Riggs-Typ oder Schubert-Bornschein-Typ).

Der L-Typ $Ca_v1.4$ findet sich in der Plasmamembran der Zellkörper retinaler Photorezeptorzellen und genetische Analysen haben bis heute mehr als 73 Mutationen des CACNA1F-Gens erbracht [27]. Diese Mutationen umfassen *Missense*-, *Nonsense*-, und Leserastermutationen. Einige führen zu trunkierten und damit funktionseingeschränkten $Ca_v1.4$-Varianten und stellen damit sog. *Loss-of-function*-Mutationen dar. Es wird allerdings vermutet, dass einige Mutationen sog. *Gain-of-function*-Alterationen darstellen oder eine verminderte Expression bei normaler Einzelkanalfunktion zur Folge haben [27]. Eine kausale Therapie ist nicht möglich. Bei starker Visusminderung erfolgt die Verordnung vergrößernder Sehhilfen oder, falls vorhanden, die Korrektur der Myopie.

X-chromosomal-gebundene Stäbchen-Zapfen-Dystrophie Typ 3 (CORDX3). Die CORDX3 (X-linked cone-rod dystrophy type 3) teilt eine Reihe von Symptomen mit der X-CSNB2 und beruht ebenfalls auf Mutationen in CACNA1F. Anders als die X-CSNB2 ist sie aber progressiv und weist i.d.R. keinen Nystagmus und nur einen geringen Astigmatismus auf. Hierbei führt ein alterierter Spleißprozess zum vorzeitigen Abbruch der Kanalproteinsynthese und zum Verlust des $Ca_v1.4$-Kanalproteins [10]. Eine kausale Therapie ist nicht möglich; bei Visusminderung kommen vergrößernde Sehhilfen zum Einsatz.

Aland Island eye disease (Forsius-Eriksson-Syndrom). Die *Aland Island eye disease* (AIED) ist eine ebenfalls X-chromosomal-rezessiv vererbte retinale Erkrankung, die mit Fundushypopigmentierung, Visusminderung, Nystagmus, Astigmatismus, progressiver Myopie und Störung der Dunkeladaptation einhergeht. Neueste Analysen zeigen, dass es sich um eine *In-frame*-Deletion des Exons 30 der $Ca_v1.4$-Untereinheit handelt, die im Verlust eines transmembranären Segmentes sowie einer extrazellulären Schleife der Domäne VI resultiert [9]. Das klinische Bild ähnelt der X-CSNB2, Diagnostik und Therapie folgen dem dort dargelegten.

Hochspannungsaktivierte Non-L-Typ-Kalziumkanäle ($Ca_v2.1$–2.3)

$Ca_v2.1$ (α_1A)

Die $Ca_v2.1$-kodierende Region befindet sich mit dem CACNA1A-Gen auf Chromosom 19p13. Der $Ca_v2.1$-Ca^{2+}-Kanal stellt derzeit die wohl bedeutendste α_1-Untereinheit dar, die mit Ca^{2+}-Kanalopathien in Verbindung gebracht werden konnte. Eine weite Verbreitung im ZNS und seine Involvierung in die schnelle Neurotransmitterfreisetzung unterstreichen dessen Relevanz. Aber auch in den Dendriten ausgewählter Neurone lässt sich $Ca_v2.1$ nachweisen und spielt hier bei integrativen dendritischen Prozessen eine wichtige Rolle [2]. Die Zahl beschriebener Maus-Modelle mit $Ca_v2.1$-Mutationen ist groß, wobei die pathophysiologischen Mechanismen der entsprechenden Phänotypen wie Ataxie, Absencen etc. noch weitgehend unbekannt sind.

Episodische Ataxie Typ-2. Die episodische Ataxie Typ 2 (EA2) stellt eine autosomal-dominant vererbte zerebrale Funktionsstörung dar, die durch das Auftreten von Ataxie, migräneähnlichen Symptomen, Nystagmus und zerebellärer Atrophie gekennzeichnet ist. Sie kann sich bereits im 2. bis 5. Lebensjahr manifestieren, am häufigsten in der 2. Lebensdekade mit variabler Anfallsfrequenz (3–4/Woche bis zu 1–2/Jahr). Stress, Emotionen, Fieber und Hitze können Attacken triggern, die neben den Kardinalsymptomen auch mit Schwächegefühl, Vertigo, Vomitus, Nausea und selten auch Dystonie vergesellschaftet sein können.

Insgesamt sind derzeit 19 Mutationen beim Menschen bekannt, die zu EA2 führen. Sie umfassen *Missense*-, *Nonsense*- und Leserastermutationen, aber auch fehlerhafte Spleißprozesse. Typischerweise kommt es zu einer Funktionseinschränkung der $Ca_v2.1$-Ca^{2+}-Kanäle. Deutlich zeigt sich dies an zerebellären Purkinje-Zellen, die $Ca_v2.1$ stark exprimieren und deren Dysfunktion bei EA2 u.a. für die ataktische Symptomatik mit verantwortlich gemacht werden kann. Wahrscheinlich spielt hier auch eine beeinträchtigte Neurotransmitterfreisetzung eine entscheidende Rolle. Während sich bei der Mehrzahl der bekannten Mutationen die Symptomatik bereits vor der Adoleszenz einstellt, gibt es einen bekannten Fall einer erst spät, im fortgeschrittenen Erwachsenenalter (61. Lebensjahr) aufgetretenen EA2, die auf einer 9 bp-Insertion im Bereich des II-III-*Loops* beruht [18]. Therapeutisch positive Reaktionen wurden bei

der EA2 mit dem Karboanhydrasehemmer Azetazolamid sowie dem K^+-Kanal-Blocker 4-Aminopyridin (4-AP) erzielt.

Familiäre hemiplegische Migräne Typ-1. Die familiäre hemiplegische Migräne Typ 1 (FHM1) ist eine seltene, ebenfalls autosomal-dominant vererbte Migräne mit Aura, die mit anfallsbegleitender Hemiparese sowie progressiver zerebellärer Atrophie vergesellschaftet ist. Schwere Migräneattacken können mehrere Tage anhalten und u. a. auch zu Fehldiagnosen wie Apoplex oder Epilepsie verleiten. FHM1 manifestiert sich i.d.R. im Alter von 5–30 Jahren. Die 30- bis 60-minütige Aura kann eine halbseitige Visusminderung, unilaterale Parästhesien, Taubheitsgefühl und Dysphasie umfassen. Hieran schließen sich massive pulsatile Kopfschmerzen mit Übelkeit, Erbrechen, Photo- und Phonophobie und u. U. Fieber und Verwirrtheit an, welche Stunden bis Tage andauern. In einigen Fällen können sich neuropsychiatrische Alterationen hinzugesellen, wie Aufmerksamkeitsstörungen, beeinträchtigtes Sprachgedächtnis, Dyskalkulie, paranoid-psychotische Attacken mit visuellen und akustischen Halluzinationen. Die Diagnosestellung erfolgt primär anamnestisch. Da es jedoch zu symptomatischen Überlagerungen mit der EA2 und Epilepsien kommen kann (s. unten) ist ein EEG, MRT oder evtl. CAT-Scan sinnvoll.

Bei FHM1-Patienten sind bislang 14 verschiedene *Missense*-Mutationen der $Ca_v2.1$-Untereinheit bekannt. Einige finden sich im S4-Segment der Domänen I, II und IV, die u.a. den Spannungssensor aufbauen, andere im Bereich des S5-S6-*Loops* der II. und III. Domäne, der teilweise die Poreninnenwand aufbaut. Derartige Mutationen beeinflussen die kinetischen Eigenschaften wie z. B. die Deinaktivierung *(Repriming)* des $Ca_v2.1$-Ca^{2+}-Kanals, allerdings abhängig von der Mutation in durchaus unterschiedliche Richtungen [15]. FHM1 stellt zusammen mit der EA2 die ersten bei Menschen detektierten hereditären Ca^{2+}-Kanalopathien dar. Die Tatsache, dass $Ca_v2.1$ eine zentrale Rolle bei der neuronalen Exzitabilität, Integration und Ca^{2+}-abhängigen Neurotransmitterfreisetzung spielt [2], legt nahe, dass $Ca_v2.1$-Kanalopathien primär synaptische Erkrankungen darstellen.

In einem Maus-Modell, dass die humane Mutation R192Q trägt, konnten van den Maagdenberg et al. [33] zeigen, dass diese Mutation zu einer erhöhten $Ca_v2.1$-Stromdichte sowie einer Kanalaktivierung bei negativeren Potenzialen führt als dies beim Wildtyp-Kanal der Fall ist. R192Q-Mäuse wiesen eine erhöhte Neurotransmission und eine erhöhte Suszeptibilität gegenüber kortikaler *spreading depression* auf. FHM-Mutationen beim Menschen scheinen demnach auf Einzelkanal- und synaptischer Ebene v.a. *Gain-of-function*-Mutationen zu sein. Es ist weiterhin interessant zu erwähnen, dass es bei FHM und EA2 auch zu symptomatischen Überlagerungen kommen kann [7]. Die Therapie der FHM1 orientiert sich an der Therapie der klassischen Migräne. Neben den Vertretern der NSAR/NSAID-Gruppe ist hier v. a. die Triptan-Familie zu nennen.

Spinozerebelläre Ataxie Typ 6. Bei der spinozerebellären Ataxie Typ 6 (SCA6) handelt es sich ebenfalls um eine autosomal-dominant vererbte zerebrale Funktionsstörung, deren Genlokus sich ebenso wie bei EA2 und FHM1 auf Chromosom 19p13.1 befindet. Die SCA6 ist eher spätmanifestierend, beginnend im fortgeschrittenen Erwachsenenalter (50. bis 60. Lebensjahr) und verläuft langsam progressiv über einen Zeitraum von mehr als 25 Jahren. Während des Krankheitsverlaufs nehmen die Symptome wie zerebelläre Atrophie (Purkinje-Zell-Degeneration), Dysarthrie, Nystagmus, Verlust des Vibrationssinns und der Propriozeption, Ataxie und Gangunsicherheit bis zum völligen Gehverlust zu. Anfänglich manifestiert sich die SCA6 nur in einer temporären Imbalance v. a. bei schnellen Bewegungswechseln, endet dann häufig final in starken Koordinationsstörungen und evtl. Rollstuhlpflichtigkeit.

Interessanterweise finden sich bei der SCA6 keine solitären *Missense*- oder *Nonsense*-Mutationen, sondern CAG-Wiederholungen *(repeats)* an Position 7213 im Bereich des C-terminal-kodierenden Bereiches. Derartige CAG-kodierte Polyglutamin (Poly-Q)-Sequenzen sind bei bislang 8 neurologischen Krankheitsbildern (sog. *CAG repeat expansion disorders*) detektiert worden [Morbus Huntington, dentatorubrale pallidolysiane Atrophie (DRPLA), spinobulbäre muskuläre Atrophie (SBMA) sowie bei den spinozerebellären Ataxien (SCA) Typ 1, 2, 3, 6 und 7]. Während bei den letztgenannten Krankheitsbildern die Auswirkungen dieser Poly-Q-Expansion auf das zugrunde liegende Protein nur bedingt bekannt sind, weiß man heute, dass Polyglutaminsequenzen die spannungsabhängige Aktivierung sowie die Inaktivierungskinetik der $Ca_v2.1$-Untereinheit zu modifizieren vermögen [24]. So führt eine Verschiebung der *Steady-state*-Inaktivierungskurve zu negativeren Potenzialen zu einer thermodynamischen Begünstigung des inaktivierten Kanalkonformationszustandes und letztlich zu einer Reduktion des Ca^{2+}-Einwärtsstromes. Untersuchungen in rekombinanten Expressionssystemen zeigten interessanterweise eine Zunahme der $Ca_v2.1$-Proteinexpression und folglich erhöhte Stromdichte [21]. Von zentraler Bedeutung in der Pathogenese der SCA6 ist aber die nukleäre Translokation der aus $Ca_v2.1$ freiwerdenden C-terminalen Poly-Q-Fragmente sowie die hieraus resultierenden zytotoxischen Effekte [14].

Idiopathische generalisierte Formen der Epilepsie. Idiopathische generalisierte Formen der Epilepsie umfassen u. a. generalisiert tonisch-klonische Anfälle, myoklonische Anfälle wie die juvenile Myoklonusepilepsie (JME), aber auch typische und atypische Absencen. Die Diagnosestellung erfolgt anamnestisch und elektroenzephalographisch. Eine Assoziation der $Ca_v2.1$-Untereinheit mit einzelnen Epilepsieentitäten beim Menschen ist noch weitgehend unklar, während es eine Vielzahl von Maus-Modellen mit einem Absencen-ähnlichen Phänotyp gibt. Es ist allerdings eine Tatsache, dass man EA2-Patienten mit generalisierten epileptischen Anfällen vorgefunden hat [11]. Ein von Jouvenceau et al. [11] beschriebener 11-jähriger Patient wies ataktische Episoden sowie pharmakologisch nur schwer kontrollierbare Absencen (CAE-ähnlich) sowie generalisiert tonisch-klonische Anfälle auf. Die hier vorliegende Mutation C5733T führte zu einer Trunkation mit komplettem Verlust des C-terminalen Kanalabschnitts von $Ca_v2.1$ mit entsprechender Funktionseinschränkung. Eine weitere Punktmutation in der Domäne I-

S2 bewirkt ebenfalls einen epileptischen/ataktischen Phänotyp und geht mit einem Verlust der $Ca_v2.1$-Ca^{2+}-Kanal-Funktionalität einher [8]. Dennoch, die Koinzidenz von EA2 und Absencen-Epilepsien ist eine Rarität. Das gemeinsame Auftreten von FHM1 und Absencen ist bislang nicht beschrieben, wohl jedoch die Koinzidenz mit anderen Anfallsformen. Die antiepileptische Therapie orientiert sich an den Empfehlungen der ILAE für generalisierte Anfallsformen vom konvulsiven und nichtkonvulsiven Typ. Neben einer Monotherapie stehen hier auch Antiepileptika der 2. und 3. Wahl sowie Kombinationen selbiger zur Verfügung.

$Ca_v2.2$ (α_1B)

Das für $Ca_v2.2$ kodierende Gen CACNA1B befindet sich beim Menschen auf Chromosom 9q34. Diese Untereinheit wird u.a. für die Neurotransmitterfreisetzung in zentralen und sympathischen Neuronen, die sympathische Regulation des Herz-Kreislauf-Systems, Aktivitäts- und Vigilanzkontrolle sowie die Schmerzweiterleitung verantwortlich gemacht [2]. $Ca_v2.2$-defiziente Mäuse weisen dementsprechend Störungen der Nozizeption auf, des Weiteren eine verminderte Sympathikusaktivität sowie veränderte Ethanol- und Anästhetikasensitivitäten [2]. Mit Ziconotid (SNX-111) wird seit kurzem ein $Ca_v2.2$-Ca^{2+}-Kanalblocker zur Therapie schwerer chronischer Schmerzen eingesetzt, insbesondere bei Patienten, die gegenüber Opiaten refraktär erscheinen oder mit Unverträglichkeit reagieren.

Autoimmunologische Erkrankungen. Autoantikörper gegen $Ca_v2.1$ aber auch $Ca_v2.2$ sind mit verantwortlich für die Genese des sog. Lambert-Eaton-Myasthenie-Syndroms (LEMS) [23]. In etwa 50% der Fälle ist LEMS mit einem identifizierbaren Neoplasma, wie kleinzelligem Lungenkarzinom, Lymphom, Prostatakarzinom oder Thymom assoziiert. Die sich einstellende progressive Muskelschwäche betrifft v.a. die proximalen Anteile der oberen und unteren Extremitäten während respiratorische und Gesichtsmuskulatur i.d.R. ausgespart bleiben. Da $Ca_v2.1$ und $Ca_v2.2$ an der myoneuralen Präsynapse über einen Ca^{2+}-Einstrom die vesikuläre Acethylcholin-Freisetzung vermitteln, bewirkt eine autoimmunologische Reaktion gegen diese Ionenkanäle eine Verminderung der Transmission an der motorischen Endplatte. Neben der Behandlung eines möglichen Neoplasmas stehen Kortikosteroide, Cholinesterasehemmer, 3,4-Diaminopyridin sowie die Plasmapherese therapeutisch zur Wahl.

$Ca_v2.3$ (α_1E)

Der den $Ca_v2.3$ Ca^{2+}-Kanal kodierende Genlokus befindet sich auf Chromosom 1q25–31. Im Gegensatz zu anderen Vertretern spannungsgesteuerter Ca^{2+}-Kanäle ist $Ca_v2.3$ resistent gegenüber gängigen Conotoxinen und Agatoxinen, jedoch empfindlich gegenüber dem Tarantoxin SNX-482 und Ni^{2+}-Ionen. Der $Ca_v2.3$-E/R-Typ-Ca^{2+}-Kanal weist ein recht breites Expressionsmuster im Organismus auf. Dennoch zeigte sich, dass er v. a. im ZNS, dem endokrinen, kardiovaskulären [31], Reproduktions- und gastrointestinalen System funktionell relevant ist. Im ZNS ist $Ca_v2.3$ an der Neurotransmitterfreisetzung und synaptischen Plastizität beteiligt [4], aber auch für die Modulation von Angst- und Schmerzverhalten sowie die Myelinogenese verantwortlich. Des Weiteren scheint $Ca_v2.3$ Einfluss auf den neuronalen Untergang im Rahmen ischämischer Prozesse sowie die vasospastische Aktivität nach Subarachnoidalblutung zu nehmen [2]. Zunehmend mehren sich auch die Hinweise, dass $Ca_v2.3$ eine Rolle bei der Initiation und Propagation von konvulsiven wie nichtkonvulsiven Anfallsleiden spielen könnte und dass eine Inhibition des $Ca_v2.3$-Ca^{2+}-Kanals eine anfallsprotektive Wirkung haben könnte [13, 30].

Mutationen in EFHC1, einem C-terminalen Interaktionspartner von $Ca_v2.3$ führen nachweislich zu juveniler Myoklonusepilepsie (JME) beim Menschen basierend auf verminderter neuronaler Apoptose [28]. Bislang sind allerdings noch keine $Ca_v2.3$-Mutationen im Tier-Modell beschrieben. Bei Pima-Indianern soll ein Einzelnukleotidpolymorphismus (*single-nucleotide polymorphism, SNP*) in der 3'-UTR-Region des CACNA1E-Gens für die Genese eines Typ-2-Diabetes in früher Adoleszenz verantwortlich sein [16].

Niederspannungsaktivierte T-Typ-Kalziumkanäle ($Ca_v3.1$–3.3)

$Ca_v3.1$ (α_1G)

Das für $Ca_v3.1$ kodierende Gen CACNA1G ist auf Chromosom 17q22 lokalisiert. Der $Ca_v3.1$-T-Typ-Ca^{2+}-Kanal zeigt eine dominante Expression im ZNS, speziell den Dendriten und ist u. a. der dominierende Ca^{2+}-Kanal im Thalamus, wenn man von der Expression von $Ca_v3.2$, $Ca_v3.3$ und $Ca_v2.3$ im Nucleus reticularis thalami absieht. Aber auch in den Ovarien, der Plazenta und in kardialen Schrittmacherzentren ist $Ca_v3.1$ von Bedeutung [2]. Obwohl Mutationen beim Menschen bislang nicht beschrieben sind, zeigen Untersuchungen an $Ca_v3.1$-defizienten Mäusen eine Bradykardie, Störungen der atrioventrikulären Überleitung [17] sowie komplexe Alterationen im thalamokortikalen Neuronenkreis, die sich in einer Resistenz gegenüber der Induktion von *Spike-wave*-Graphoelementen sowie Störungen des *Slow-wave*-Schlafes und der REM/NREM-Schlafarchitektur äußern [13].

$Ca_v3.2$ (α_1H)

Das $Ca_v3.2$-kodierende Gen CACNA1H ist beim Menschen auf Chromosom 16p13.3 lokalisiert. Ähnlich wie $Ca_v3.1$ findet sich diese Untereinheit im ZNS dominant exprimiert, aber auch in glatter Muskulatur, in der Leber und im Herzen [2]. Des Weiteren gibt es Hinweise auf eine funktionelle Rolle bei der Nozizeption sowie bei der Akrosomenreaktion der Spermien [20]. $Ca_v3.2$-defiziente Mäuse zeigen zwar keine EKG-Alterationen, jedoch findet sich eine koronare Dysregulation mit Vasokonstriktion und begleitenden fokalen myokardialen Fibrosen [3]. Interessanterweise können Mutationen bei $Ca_v3.2$ beim Menschen Epilepsien triggern. So werden 12 *Missense*-Mutationen in $Ca_v3.2$, die den Ca^{2+}-Einstrom mehrheitlich faszilitieren, für die *childhood absence epilepsy* (CAE) beim Menschen und 3 *Missense*-Mutationen für generalisiert idiopathische Epilepsieformen verantwortlich gemacht [12]. Viele der beschriebenen Mutationen liegen im I-II-*Loop* des Kanals. Zur Therapie der Absencen-Epilepsie stehen v. a. Ethosuximid (mit T-Typ-hemmender Wirkung) sowie Valproat zur Verfügung.

Es ist bemerkenswert festzustellen, dass 6 $Ca_v3.2$-*Missense*-Mutationen mit autistischen Störungen in Verbindung gebracht worden sind, die ausnahmslos mit einer Reduktion der $Ca_v3.2$-Aktivität einhergehen [26]. Der $Ca_v3.2$-Ca^{2+}-Kanal findet sich hierbei u. a. im Hippokampus, der Amygdala und dem Putamen und somit in Regionen, die mit der Genese autistischer Störungen in Verbindung gebracht worden sind. Bis zu 1/3 der autistischen Patienten weisen auch eine Epilepsie auf.

$Ca_v3.3$ (α_1I)

Das $Ca_v3.3$-kodierende Gen CACNA1I liegt auf Chromosom 22q12.3. Wie $Ca_v3.1$ und $Ca_v3.2$ weist der Kanal eine starke Expression im ZNS auf und scheint ebenfalls eine Rolle bei thalamischen Oszillationen zu spielen [20]. Genetische Defekte des $Ca_v3.3$-Kanals beim Menschen sind nicht bekannt. In Ätiologie und Pathogenese der Absencen-Epilepsie scheint $Ca_v3.3$ bislang keine belegbare Rolle zu spielen.

Akzessorische Ca^{2+}-Kanal-Untereinheiten

Während im Tier-Modell eine Reihe von Mutationen akzessorischer Untereinheiten gefunden wurden (s. unten), ist bislang beim Menschen nur eine einzelne Familie mit juveniler Myoklonusepilepsie (JME) beschrieben, die eine trunkierte Form der β_4-Untereinheit aufweist [5]. Des Weiteren wurde erst kürzlich eine Mutation in der $\alpha_2\delta_4$-Untereinheit des Menschen gefunden, die mit einer autosomal-rezessiven Form der Nachtblindheit, basierend auf einer Stäbchendystrophie, einhergeht [32]. Mutationen in der γ-Untereinheit sind beim Menschen bislang nicht bekannt.

Tier-Modelle mit Alterationen spannungsgesteuerter Ca^{2+}-Kanäle

Bis zum heutigen Zeitpunkt sind für die verschiedenen porenbildenden Ca_v-α_1 sowie akzessorischen Untereinheiten sowohl beim Menschen als auch in Tier-Modellen diverse Mutationen bekannt, die mit einem neurologischen Phänotyp assoziiert sind [22]. Interessanterweise finden sich eine Vielzahl von $Ca_v2.1$-Mutationen im Maus-Modell, wie z. B. der *tottering* (tg), *tottering leaner* (tg^l), *rolling* Nagoya (tg^{rol}) oder die *Rocker*-Maus, wobei sich hier ähnlich wie beim Menschen eine komplexe neurologische Symptomatik bestehend aus zerebellärer Ataxie, paroxysmaler Dyskinesie und Absencen-Epilepsie darstellt. Anders als beim Menschen sind jedoch bei der Maus auch eine Reihe von Mutationen akzessorischer Ca^{2+}-Kanal-Untereinheiten bekannt. Beispiele hierfür sind das *lethargic* (lh) Maus-Modell (β_4-Leserastermutation), das *stargazer* (stg) Maus-Modell (γ_2-Mutation) sowie Mutationen in der $\alpha_2\delta_2$-Untereinheit (sog. *ducky*- und *entla*-Phänotyp) [7].

$Ca_v2.1$-Mutationen rufen interessanterweise bei Nagern regelmäßig eine Funktionseinschränkung des Kanals hervor mit Beeinträchtigung der synaptischen Neurotransmission. Es ist wichtig hervorzuheben, dass in keinem der $Ca_v2.1$-Maus-Modelle Absencen isoliert auftreten, sondern stets in Kombination mit Ataxie, zerebellärer Atrophie, Dyskinesien etc. So bleibt die tatsächliche funktionelle Involvierung des $Ca_v2.1$-Ca^{2+}-Kanals bei Absencen noch immer ein Enigma.

Fazit für die Praxis

Kanalopathien sind mehr als nur ein medizinisches Klassifikationskriterium. Mit zunehmender Aufklärung der molekularbiologischen Grundlagen neuronaler Krankheitsbilder wird es für den klinisch tätigen Mediziner immer bedeutsamer, Kanalopathien zu erkennen und einen darauf abgestimmten spezifischen Therapieansatz zu wählen. Für den Patienten ist es wiederum essenziell, Informationen über die genetische Grundlagen seiner Erkrankung zu erhalten und in einer humangenetischen Beratung Aspekte der eigenen Familienplanung zu diskutieren.

Für eine genetische Analyse ist die Isolierung genomischer DNA z. B. aus einer Blutprobe notwendig. Unter Verwendung von Ca^{2+}-Kanal-spezifischen Primern erfolgt mittels Polymerasekettenreaktion (PCR) eine Amplifikation des entsprechenden cDNA-Fragmentes, dass durch anschließende Sequenzierung Aufschluss über Mutationen in den entsprechenden Ca^{2+}-Kanal-Genen geben kann. Häufig steht ein eigenes molekularbiologisches Labor zur genetischen Analyse nicht zur Verfügung, oder die Etablierung einer Eigenanalyse ist zu zeitaufwendig und kostspielig. Hier bietet sich die Einsendung von Blutproben an das nächstliegende humangenetisches Institut an. Daneben gibt es auf humane Kanalopathien spezialisierte Analyselabors wie z. B. das Institut für angewandte Physiologie der Universität Ulm. Auf eine akkurate Patienteninformation und eine Patienteneinwilligung zur genetischen Analyse ist zu achten. Obwohl bislang keine der beschriebenen Kanalopathien kausal therapierbar ist, stellt doch ihre molekularbiologische Charakterisierung die Grundlage für gentherapeutische Ansätze und damit die vollständige Genesung der Patienten in der Zukunft dar.

Buchtipps

- Ion Channels and Disease von Frances M. Ashcroft, Academic Press, 1999
- Channelopathies von Frank Lehmann-Horn, Karin Jurkat-Rott, Elsevier Science, 2000
- Channelopathies of the Nervous System von Michael R. Rose, Robert Griggs, Butterworth-Heinemann, 2001
- Voltage-Gated Calcium Channels von Gerald W. Zamponi, Springer Netherlands, 2005

Korrespondenzadresse

Dr. nat. med. Dr. med. M. Weiergräber
Institut für Neurophysiologie, Medizinische Einrichtungen, Universität zu Köln
Robert-Koch-Straße 39, 50931 Köln
akp74@uni-koeln.de

Interessenkonflikt. Der korrespondierende Autor gibt an, dass kein Interessenkonflikt besteht.

Literatur

1. Beam KG, Knudson CM, Powell JA (1986) A lethal mutation in mice eliminates the slow calcium current in skeletal muscle cells. Nature 320: 168–170
2. Catterall WA, Perez-Reyes E, Snutch TP, Striessnig J (2005) International Union of Pharmacology. XLVIII. Nomenclature and structure-function relationships of voltage-gated calcium channels. Pharmacol Rev 57: 411–425
3. Chen CC, Lamping KG, Nuno DW et al. (2003) Abnormal coronary function in mice deficient in alpha1H T-type Ca^{2+} channels. Science 302: 1416–1418

4. Dietrich D, Kirschstein T, Kukley M et al. (2003) Functional specialization of presynaptic $Ca_v2.3$ Ca^{2+} channels. Neuron 39: 483–496
5. Escayg A, De Waard M, Lee DD et al. (2000) Coding and noncoding variation of the human calcium-channel beta4- subunit gene CACNB4 in patients with idiopathic generalized epilepsy and episodic ataxia. Am J Hum Genet 66: 1531–1539
6. Felix R (2005) Molecular regulation of voltage-gated Ca^{2+} channels. J Recept Signal Transduct Res 25: 57–71
7. Felix R (2006) Calcium channelopathies. Neuromolecular Med 8: 307–318
8. Imbrici P, Jaffe SL, Eunson LH et al. (2004) Dysfunction of the brain calcium channel $Ca_v2.1$ in absence epilepsy and episodic ataxia. Brain 127: 2682–2692
9. Jalkanen R, Bech-Hansen NT, Tobias R et al. (2007) A Novel CACNA1F gene mutation causes Aland Island eye disease. Invest Ophthalmol Vis Sci 48: 2498–2502
10. Jalkanen R, Mantyjarvi M, Tobias R et al. (2006) X linked cone-rod dystrophy, CORDX3, is caused by a mutation in the CACNA1F gene. J Med Genet 43: 699–704
11. Jouvenceau A, Eunson LH, Spauschus A et al. (2001) Human epilepsy associated with dysfunction of the brain P/Q-type calcium channel. Lancet 358: 801–807
12. Khosravani H, Altier C, Simms B et al. (2004) Gating effects of mutations in the $Ca_v3.2$ T-type calcium channel associated with childhood absence epilepsy. J Biol Chem 279: 9681–9684
13. Khosravani H, Zamponi GW (2006) Voltage-gated calcium channels and idiopathic generalized epilepsies. Physiol Rev 86: 941–966
14. Kordasiewicz HB, Thompson RM, Clark HB, Gomez CM (2006) C-termini of P/Q-type Ca^{2+} channel alpha1A subunits translocate to nuclei and promote polyglutamine-mediated toxicity. Hum Mol Genet 15: 1587–1599
15. Kraus RL, Sinnegger MJ, Glossmann H et al. (1998) Familial hemiplegic migraine mutations change α_{1A} Ca^{2+} channel kinetics. J Biol Chem 273: 5586–5590
16. Li MY, Hanson RL, Zimmerman C et al. (2007) Variants in the $Ca_v2.3$ ({alpha}1E) subunit of voltage-activated Ca^{2+} channels are associated with insulin resistance and type 2 diabetes in Pima Indians. Diabetes 24
17. Mangoni ME, Traboulsie A, Leoni AL et al. (2006) Bradycardia and slowing of the atrioventricular conduction in mice lacking $Ca_v3.1$/alpha1G T-type calcium channels. Circ Res 98: 1422–1430
18. McKeown L, Robinson P, Jones OT (2006) Molecular basis of inherited calcium channelopathies: role of mutations in pore-forming subunits. Acta Pharmacol Sin 27: 799–812
19. Monnier N, Procaccio V, Stieglitz P, Lunardi J (1997) Malignant-hyperthermia susceptibility is associated with a mutation of the alpha 1-subunit of the human dihydropyridine-sensitive L-type voltage-dependent calcium-channel receptor in skeletal muscle. Am J Hum Genet 60: 1316–1325
20. Perez-Reyes E (2003) Molecular physiology of low-voltage-activated T-type calcium channels. Physiol Rev 83: 117–161
21. Piedras-Renteria ES, Watase K, Harata N et al. (2001) Increased expression of alpha1A Ca^{2+} channel currents arising from expanded trinucleotide repeats in spinocerebellar ataxia type 6. J Neurosci 21: 9185–9193
22. Pietrobon D (2005) Function and dysfunction of synaptic calcium channels: insights from mouse models. Curr Opin Neurobiol 15: 257–265
23. Pinto A, Moss F, Lang B et al. (1998) Differential effect of Lambert-Eaton myasthenic syndrome immunoglobulin on cloned neuronal voltage-gated calcium channels. Ann N Y Acad Sci 841: 687–690
24. Restituito S, Thompson RM, Eliet J et al. (2000) The polyglutamine expansion in spinocerebellar ataxia type 6 causes a β subunit-specific enhanced activation of P/Q-type calcium channels in Xenopus oocytes. J Neurosci 20: 6394–6403
25. Splawski I, Timothy KW, Sharpe LM et al. (2004) $Ca_v1.2$ calcium channel dysfunction causes a multisystem disorder including arrhythmia and autism. Cell 119: 19–31
26. Splawski I, Yoo DS, Stotz SC et al. (2006) CACNA1H mutations in autism spectrum disorders. J Biol Chem 281: 22085–22091
27. Striessnig J, Hoda JC, Koschak A et al. (2004) L-type Ca^{2+} channels in Ca^{2+} channelopathies. Biochem Biophys Res Commun 322: 1341–1346
28. Suzuki T, Delgado-Escueta AV, Aguan K et al. (2004) Mutations in EFHC1 cause juvenile myoclonic epilepsy. Nat Genet 36: 842–849
29. Wei J, Hemmings GP (2006) A further study of a possible locus for schizophrenia on the X chromosome. Biochem Biophys Res Commun 344: 1241–1245
30. Weiergräber M, Henry M, Krieger A et al. (2006) Altered seizure susceptibility in mice lacking the $Ca_v2.3$ E-type Ca^{2+} channel. Epilepsia 47: 839–850
31. Weiergräber M, Henry M, Südkamp M et al. (2005) Ablation of $Ca_v2.3$ / E-type voltage-gated calcium channel results in cardiac arrhythmia and altered autonomic control within the murine cardiovascular system. Basic Res Cardiol 100: 1–13
32. Wycisk KA, Zeitz C, Feil S et al. (2006) Mutation in the auxiliary calcium-channel subunit CACNA2D4 causes autosomal recessive cone dystrophy. Am J Hum Genet 79: 973–977
33. Van den Maagdenberg AM, Pietrobon D, Pizzorusso T et al. (2004) A Cacna1a knockin mi-graine mouse model with increased susceptibility to cortical spreading depression. Neuron 41: 701-710

Schmerzfiltration

Beteiligte GABAA-Rezeptorsubtypen identifiziert

Chronische Schmerzen sind häufig darauf zurückzuführen, dass das Rückenmark in seiner Funktion, Schmerzsignale zu filtern, beeinträchtigt ist. Im gesunden Zustand filtern inhibitorische Nervenzellen die Schmerzsignale, vermittelt durch Subtypen von GABAA-Rezeptoren. Wissenschaftler der ETH Zürich und der Universität Zürich konnten nun zwei Subtypen identifizieren, welche die Weiterleitung von Schmerzsignalen im Rückenmark beeinflussen. Sie induzierten in Mäusen, deren GABAA-Rezeptoren genetisch verändert waren, Entzündungen oder reizten den Nervus ischiaticus. Wenige Tage später erhielten die Mäuse eine Benzodiazepin-Injektion im Bereich des Rückenmarks. Daraufhin überprüften die Forscher den Einfluss der Rezeptormutationen auf die schmerzstillende Wirkung.

Benzodiazepine verstärken die Aktivierung von GABAA-Rezeptoren unspezifisch. Ein weiterer Nachteil dieser Wirkstoffgruppe bei der Behandlung chronischer Schmerzen ist, dass die Wirkung im Laufe der Therapie nachlässt. Als Alternative könnten sich verschiedene Wirkstoffe erweisen, deren Spezifität für die identifizierten Subtypen bereits in Tierversuchen nachgewiesen wurde und die bei längerer Verwendung nicht ihre Wirkung verlieren.

Originalpublikation:
Knabl J, Witschi R, Hösl K et al. (2008) Reversal of pathological pain through specific spinal GABAA receptor subtypes. Nature 451(7176):330-4

Quelle: ETH Zürich

Available online at www.sciencedirect.com

SCIENCE DIRECT

Brain Research Protocols 14 (2005) 154–164

BRAIN RESEARCH PROTOCOLS

www.elsevier.com/locate/brainresprot

Protocol

Electrocorticographic and deep intracerebral EEG recording in mice using a telemetry system

Marco Weiergräber[a,b,*], Margit Henry[a], Jürgen Hescheler[a,b], Neil Smyth[b,c], Toni Schneider[a,b]

[a]*Institute of Neurophysiology, University of Cologne, Robert-Koch-Street 39, 50931 Cologne, Germany*
[b]*Center for Molecular Medicine in Cologne (CMMC), Germany*
[c]*Center for Biochemistry, Medical Faculty, University of Cologne, Germany*

Accepted 22 December 2004
Available online 5 February 2005

Abstract

Telemetric EEG recording plays a crucial role in the neurological characterization of various transgenic mouse models giving valuable information about epilepsies and sleep disorders in humans. In the past different experimental approaches have been described using tethered systems and jacket systems containing recorders. A main disadvantage of these is their sometimes unphysiological, restraining character. Telemetric EEG recording overcomes most of these disadvantages and allows precise and highly sensitive measurement under various physiological and pathophysiological conditions and different stages of consciousness, as during seizure activity and different sleep stages.

Here we present the first contiguous, detailed description of a successful and quick technique for intraperitoneal implantation or subcutaneous pouch implantation of a radiofrequency transmitter in mice and subsequent lead placement in both epidural and deep intracerebral position. Preoperative preparation of the mice, suitable anesthesia, as well as postoperative treatment including pain management are described in detail to provide optimal postoperative recovery. Finally, we display examples of electrocorticograms and deep intracerebral recordings, present strategies to maximize signal-to-noise ratio, paying special attention to major pitfalls and possible artefacts occurring in telemetric EEG recording in mice.

Theme: Disorders of the nervous system
Topic: Epilepsy: human studies and animal models

Keywords: Electroencephalogram; Electrocorticogram; Deep electrodes; Telemetry; Stereotaxic implantation; Epilepsy

1. Type of research

Biotelemetry is a useful tool for measuring a variety of behavioral and physiological parameters (EEG, ECG, EMG, blood pressure, body core temperature, activity, etc.) in conscious, unrestrained animals of various sizes. In the past it has been shown to be valuable in the characterization of various animal models of human specific diseases, such as epilepsies and sleep disorders [6,7]. Previously, a number of methods collecting physiological data even from mice have been described: tethered systems, physical restraint methods, worn in jacket recorder systems, or non-implanted radiotransmitters [11]. Currently, a number of systems are commercially available for radiotelemetric implantation.

Telemetry recordings from conscious animals are superior to those from anesthetized or restrained animals, since they represent the normal state and are more predictive of the results that would be achieved in humans [8]. Restraining methods induce stress artefacts

Abbreviations: EEG, electroencephalogram; ECoG, electrocorticogram; EMG, electromyogram; ECG, electrocardiogram

* Corresponding author. University of Cologne, Institute of Neurophysiology, Robert-Koch-Str. 39, D-50931 Cologne, Germany. Fax: +49 221 478 6965.
E-mail address: akp74@uni-koeln.de (M. Weiergräber).

1385-299X/$ - see front matter © 2005 Elsevier B.V. All rights reserved.
doi:10.1016/j.brainresprot.2004.12.006

and severely influence basic physiological parameters, such as heart rate, blood pressure, body core temperature, and food intake [8]. A classical restraining approach in EEG recording is the use of tethered systems [2] in which electrodes are connected to a miniature socket anchored to the skull and exposed for attachment of a cable. Although tethered systems allow relatively free movement of the animal, one of its disadvantages is, that it is still semi-restraining, and that there is a risk of infection, as the electrode implantation site serves as a potential entry for infection.

Although wireless radiotelemetry technology for monitoring larger laboratory animals has existed for some time, it has only become recently that affordable, reliable, and relatively easy-to-use in mice [14]. Small transmitters are now commercially available (TA10ETA-F20; DSI), which can be implanted in mice greater than 20 g (~10 weeks), so that animal size is no longer an absolute limitation. Implantable transmitter systems are capable of minimizing most disadvantages related to potential recording-associated stress by restraining systems. Mice are able to show a complete repertoire of physiological behavior including resting, locomotor activity (exploration), and sleep (REM, slow-wave sleep) [9,13]. Furthermore, telemetry leads to a strong reduction of animal use [8].

This is the first contiguous, detailed description of a successful, quick, and simple surgical procedure for both intraperitoneal and subcutaneous pouch implantation of a radiofrequency transmitter in mice and subsequent lead placement in both epidural and deep intracerebral position. Examples of high-quality electrocorticograms (ECoGs) as well as deep recordings are displayed and special attention is paid to detect and analyze EEG artefacts. Finally, strategies for reduction of trauma and optimization of pain management during postoperative recovery are presented.

2. Time required

Total time for radiofrequency transmitter implantation and surface as well as deep electrode implantation is ~1 h. High-quality short- and long-term EEGs can be reliably recorded over a period of 5 weeks.

3. Materials

3.1. Animals and housing

Male C57Bl/6 mice between 3 and 9 months of age ranging from 22.3 to 31.2 g have been used in this study. All animals were housed individually in clear makrolon type 2 cages (26.7 × 20.7 × 14.0 cm, area 410 cm^2) before and after the implantation. Animals were kept under temperature-controlled conditions with an ambient temperature of 20–22 °C with light cycle from 6 a.m. to 6 p.m. The bedding of the cages consisted of wood shavings, food, and water were presented ad libitum. All animal experimentation was undertaken according to the local institutional guidelines for the care and use of laboratory animals.

3.2. Telemetry system

The telemetry system used consists of a telemetry implant (PhysioTel® transmitter TA10ETA-F20 (technical specification: 3.9 g, 1.9 cc; Data Science International

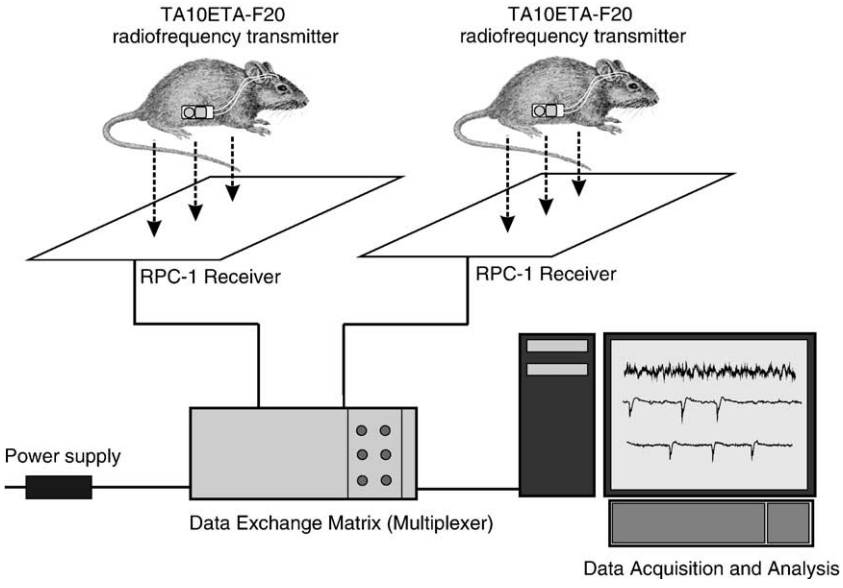

Fig. 1. Radiotelemetry set-up for EEG monitoring. The TA10ETA-F20 transmitter implant (DSI) telemeters EEG data from mice to the receiver (RPC-1, DSI), further processed to a data exchange matrix (DSI) which serves as a multiplexer. Data were finally transferred to a data acquisition and analysis system (DSI).

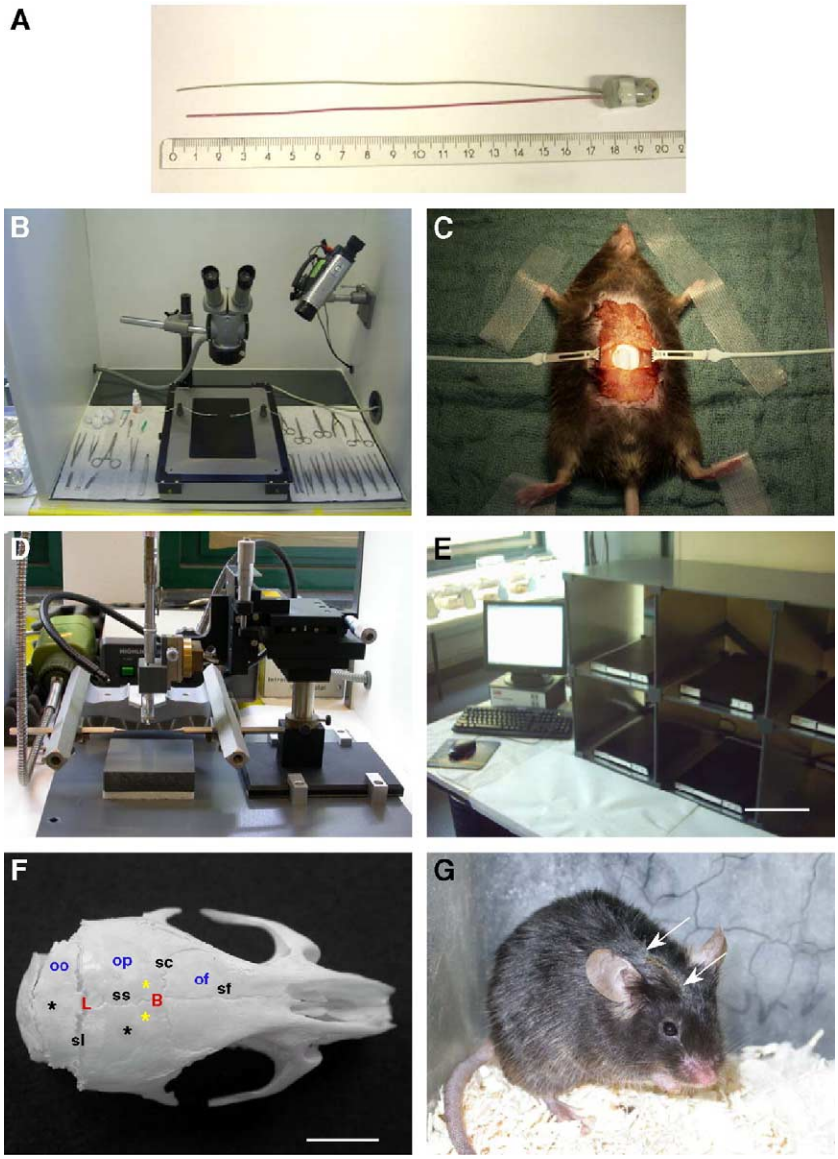

Fig. 2. Intraperitoneal implantation of the radiofrequency transmitter. (A) TA10ETA-F20 transmitter used in this study (technical specification: volume 1.9 cc, weight 3.9 g, lead length: 20 cm). (B) Surgical equipment, dissecting microscope, external temperature support with base plate, fixators, elastomers, and wound retractors and a video monitoring system. (C) After removal of body hair, a 1.5- to 2-cm midline abdominal incision is performed and the transmitter is placed directly onto the GI tract (a Teflon dummy is shown). Note 5 mm wound retractors that help push aside the abdominal skin. After the abdominal wall is closed using non-absorbable sutures, the abdominal skin incision is finally closed using wound clips. (D) Stereotaxic device with base frame, ear bars, nose clamp, and dental drill mounted on a calibrated 3-axis precision micromanipulator for drilling 0.7 mm holes. (E) Multiple receiver plates connected to a data exchange matrix (multiplexer, DSI). Each housing chamber is shielded with stainless steel to avoid cross-talk. (F) Anatomic structures and landmarks of the murine skull. Apical view of a C57Bl/6 mouse skull which has been prepared in 30%H_2O_2. Note cranial bones (os frontale (of), os parietale (op), os occipitale (oo)) and sutures (sutura frontalis (sf), sutura saggitalis (ss), sutura coronaria (sc), and sutura lambdoidea (sl)) which determine the major anatomic landmarks bregma (B) and lamda (L). Surface electrodes (bipolar) were implanted at the following stereotaxic coordinates: (−)-lead: caudal of bregma 1 mm, lateral of bregma 1 mm (left hemisphere); (+)-lead: caudal of bregma 1 mm, lateral of bregma 1 mm (right hemisphere, yellow stars); deep electrodes in the positions: (+)-lead: caudal of bregma 2 mm, lateral of bregma 2 mm (right hemisphere), dorsoventral 2 mm; (−)-lead: caudal of bregma 6.2 mm, lateral of bregma 0 mm, dorsoventral 0 mm (black stars). (G) Dorsal view of the skull 4 weeks after electrode implantation and fixation using glass ionomer cement. Note that no skin necrosis occurred after closure of the scalp (arrows).

(DSI), Lexington, USA, Figs. 1 and 2A) capable of measuring biopotentials (electroencephalogram (EEG), electrocardiogram (ECG), electromyogram (EMG), physical activity, and temperature). This was transmitted to a receiver (RPC-1, DSI), which picks up the telemetered data from the implant and forwarded them to a data exchange matrix (DSI) serving as a multiplexer (Fig. 1).

4. Detailed procedure

4.1. Surgical instrumentation—general aspects

Mice present an anesthetic challenge because of their small size and varied responses to anesthetic drugs within strains and between genders. Furthermore, they are predis-

posed to hypothermia. Therefore, during and postsurgery warming plates are necessary to maintain body core temperature which should be 37–38 °C (98.6–100.4 °F). To avoid corneal desiccation, eyes were covered with dexpanthenole (Bepanthen®, Hoffmann-La Roche AG) during the whole implantation period and early recovery.

4.2. Anesthesia

Animals were anesthetized with esketaminhydrochloride (Ketanest®, Parke-Davis/Pfizer, Germany, 100 mg/kg) and xylazinehydrochloride (Rompun® 2% BayerVital, Leverkusen Germany, 10 mg/kg). This dose is usually sufficient for the implantation duration with xylazine providing a good muscle relaxation. Artificial respiration was not required.

4.3. Transmitter implantation

Body hair was removed from the abdomen using a clipper and the shaved areas were scrubbed with Mercuchrom® (Merbromin, Krewel Meuselbach, Eitorf, Germany). No depilation cream was applied due to skin irritation and possible wound healing defects later on. Animals were placed on a sterile drape on a heating pad (37–38 °C) under an operation microscope (Fig. 2B). All surgical instruments necessary for implantation were heat sterilized. Sterile conditions were further maximized using masks, surgical gloves, and surgical gown.

Following a 1.5- to 2-cm midline abdominal incision, the abdominal skin and wall was opened and both incision borders were held aside using a 5-mm wound retractor (together with elastomers, fixators, and a base frame (Fine Science Tools, FST, Heidelberg, Germany); Fig. 2C). The transmitter was placed carefully into the peritoneal cavity on top of the gastrointestinal tract. Care was taken not to impinge bladder or diaphragm. Anatomical forceps were preferred to surgical forceps, as they produce less damage to the tissue, particularly when manipulating the bowel. In case of local bleeding from the abdominal wound edges a thermocauter (Heiland, Germany) was used.

Next, both leads were tunneled through the abdominal wall at the cranial part of the incision using a 14-gauge needle. A trocar together with a plastic sleeve can be tunneled subcutaneously along the lateral thoracic wall to the intended position at the neck, where a second skin incision was made before. The trocar can than be withdrawn from the sleeve and the leads are tunneled through it. Alternatively, a thin trocar with a short silicon tubing attached at its tip can be used to tunnel the leads subcutaneously to the neck. In this case, the sensing electrodes can be tied mechanically to the silicon tubing or by attaching them with glue. The latter method is much faster to perform and causes less damage to the subcutaneous tissue than using trocar and plastic sleeve, which is important for rapid postoperative recovery. Leads were secured on the underlying muscle layer using a non-absorbable interrupted stay suture (Ethilon® II, 4-0, M-2, Ethicon, Germany). If not tacked, the intrinsic elasticity of the electrodes will make implantation of the electrodes more difficult later.

The transmitter was fixed in the peritoneal cavity using its suture tab to avoid intraabdominal movement. Finally, the abdominal wall was closed using non-absorbable suture material (Ethilon® II, 4-0, M-2, Ethicon, Germany), the ventral skin incision was closed using wound clips (Michel, 7.5 × 1.75 mm, Heiland, Germany), as mice tend to bite sutures. Wound clips drop off later during wound healing process. The wound area was once again cleaned with Mercuchrom®.

4.4. Surface electrode implantation

A midline skin incision, 10 mm on the head and 5–10 mm down the neck, was made and the subcutaneous tissue was bluntly separated. The periosteum was cleaned using cotton tips without damaging the temporal and occipital muscles. The superficial thin layer of the skull was pretreated with 10% H_2O_2. This pretreatment removes any tissue from the skull and assures strong contact of the glass ionomer cement (Kent Dental®, Kent Express, UK) used later on. It also accentuates the sutures as well as bregma and lambda landmarks of the skull, which are essential for precise stereotaxic lead placement (Fig. 2F). This should be done carefully as the procedure can produce severe oxidative damage to the surrounding tissue. Two burr holes, each 0.7 mm in diameter, were positioned with an electric high-speed dental drill at the coordinates of choice.

Hemorrhage reflecting intraosseous bleeding from the cut edge of the skull was easily controlled with a cotton tampon. Fatal bleeding was never observed as positioning of the electrodes was different from localization of dural sinuses (e.g., the superior sagittal sinus). Furthermore, after H_2O_2 treatment of the calvaria, small vessels like meningeal arteries or superficial cerebral arteries or veins can easily be detected under an operation microscope as the calvaria is rather transparent, even in adult mice. Thus, damage of these structures can be avoided.

The silicone insulation was removed from the terminal part of the sensing leads of the TA10ETA-F20 transmitter. Both electrodes were shortly bend at the tip and placed directly on the dura mater (epidural lead placement) in a bipolar deflection at the following coordinates: (+)-lead: caudal of bregma 1 mm, lateral of bregma 1 mm (right hemisphere); (−)-lead: caudal of bregma 1 mm, lateral of bregma 1 mm (left hemisphere, see recordings from this deflection in Fig. 5). Electrodes were fixed with glass ionomer cement (Kent Dental®, Kent Express, UK) which is extremely hard and gives strong adhesion to the underlying neurocranium. After the cement has dried (5 min), the scalp was closed using over-and-over sutures with non-absorbable 6-0 suture material (Ethilon® polyamid, Ethicon, Germany) (Fig. 2G). In contrast to other reports, no cortical screw electrodes are necessary [10,12,13].

4.5. Stereotaxic device

The standard stereotaxic frame was modified to fit the mouse skull anatomy. It was necessary to adapt teeth holder and nose clamp as well as ear bars (Figs. 2D and 3). A stereotaxic frame was combined with a high-speed dental drill (20000 rpm, KaVo EWL, Germany) mounted to a three-axis micromanipulator. This procedure enables precise electrode placement according to stereotaxic coordinates. Manual handling of a dental drill is not suitable. The thickness of the murine cranial bones severely varies depending on the localization (*os frontale*: midline section: 320–390 μm, lateral section: 300–430 μm; *os parietale*: midline section: 210–250 μm, lateral section: 200–210 μm; *os occipitale*: midline section: 600–730 μm, lateral section: 380–420 μm). Although the head has to be fixed tightly, damage of the inner ear can be avoided by covering ear bars with cotton balls. For some experimental purposes, like screening for audiogenic seizures or seizure susceptibility, this is of especially high importance. Holes must be drilled at maximum velocity. This avoids an applanation of the skull which may result in a sudden breakthrough of the drill head and therefore might cause severe brain damage.

4.6. Intracerebral (deep) electrode implantation

Here we have performed an experimental modification of the DSI telemetry system. Holes were drilled as described above and positioned at the following coordinates: (+)-lead: caudal of bregma 2 mm, lateral of bregma 2 mm (right hemisphere), dorsoventral (depth) 2 mm (related to the dorsal surface of the calvaria and corresponding to the final targeting region CA3 (hippocampus)). The (−)-lead was positioned at caudal of bregma 6.2 mm, lateral of bregma 0 mm; dorsoventral 0 mm (epidural reference electrode localized on the cerebellum), by simply bending the electrodes 90°. This is easy to perform as sensing leads consist of high-grade stainless steel helix which provides flexibility and resistance to breakage. Proper lead placement was confirmed histologically at postmortem. Electrodes were fixed and scalp was closed as described earlier.

Fig. 3. Stereotaxic device for mouse surface and deep intracerebral electrode implantation. Teeth holder and nose clamp were adapted for mouse size. Note the dental drill which is mounted on a calibrated 3-axis precision micromanipulator. Ear bars were covered with cotton prior to positioning of the mouse head (not shown).

4.7. Postoperative care and pain management

After implantation, animals were placed back into the cage and within the first 3–4 days postsurgery, body core temperature was maintained using a thermal lamp and/or warming plate. External temperature support was not removed until mice were able to maintain physiological body core temperature themselves.

Metamizole–sodium (Novaminsulfon-ratiopharm 1, ratiopharm, Germany), which was used for postoperative pain management at 100 mg/kg body weight for 4 days postsurgery, was administered intraperitoneally with 0.3 ml of 5% glucose in Ringer solution or 0.9% NaCl. Alternatively, tramadolhydrochloride (Tramal®, Grünenthal, Germany) can be applied directly on the tongue or be added to the drinking water. However, the latter approach might be insufficient as water consumption is restricted, particularly early after implantation. Postoperatively, animals were fed moistened food pellets. Systemic administration or local application of antibiotics is often recommended but was not performed in this study and no signs of meningitis, encephalitis, or other local or generalized infection was detected at postmortem examination of any mouse analyzed.

Although animals recovered quickly, they should be given 10–14 days to fully recover before starting EEG recordings for further analysis.

Transmitters are sterilely packaged as provided by the manufacturer. However, they can be reused after explantation. Using a biodetergent (neodisher® medizym, Weigert, Germany) for removing tissue debris (24 h at RT) and glutaraldehyde (2%, Roth, Germany) for resterilization (2 h at RT) they were prepared for reimplantation.

4.8. Pharmacological injection experiments

Intraperitoneal administration of R/S-baclofen (Sigma, Germany) was performed at 20 mg/kg and bicucullinemethobromide (BMB, Sigma, Germany) at 10 mg/kg to induce spike/spike-wave activity originating from the thalamocortical–corticothalamic circuitry. Generalized tonic–clonic seizures were provoked by ip administration of 4-aminopyridine (4-AP) at a dose of 10 mg/kg. Control recordings of at least 1 h were performed prior to injection.

4.9. Data acquisition and analysis

To acquire and analyze EEG data the Dataquest™ A.R.T.™ 2.2 software (DSI) was used. EEG recordings

were done each day for at least 30–45 min between 9 a.m. and 6 p.m.; at days 7 and 14 postsurgery overnight recordings were performed for long-term analysis. EEG activity was sampled at 1000 Hz with a filter cut-off of 50 Hz. Optionally, also higher frequencies up to 150 Hz can be recorded.

5. Results

5.1. Postoperative recovery

Postoperative recovery after intraperitoneal placement of the transmitter was evaluated by monitoring postsurgical development of body weight. A maximum reduction in body weight was observed around days 4–5 postsurgery followed by a slight, but steady increase of weight during a 10- to 14-day recovery period after which it remained constant. The time pattern of recovery is consistent with the postoperative development of body weight after intraperitoneal implantation for ECG recording (Fig. 4). To obtain valid EEG recordings, a minimum period of 10–14 days of recovery is therefore recommended, as also suggested in literature [8].

5.2. Signal-to-noise ratio

EEG recording systems which make use of a tethering system require special connectors to attach the sensing leads to the implanted wire which is capable of introducing significant noise to the system. Radiotelemetry systems using screw electrodes [13] or isolated stainless steel wires for implantation [1] might therefore exhibit similar susceptibilities. Our approach does not make use of connectors; sensing leads are simply bend 90° and implanted to the desired stereotaxic coordinates reducing the background noise in our recordings after implantation to a range of 100 nV–1 μV. Additionally, as the EEG signal is small compared to both electromyographic and electrocardiographic signals, it is important to eliminate or maximally reduce the influence of these biopotentials on the electroencephalogram (see also Figs. 7B and C).

5.3. EEG recordings after subcutaneous (pouch) implantation of the transmitter

A major concern when implanting the radiofrequency transmitter in a subcutaneous pouch on the back is reduced signal strength (monitored by the Dataquest™ A.R.T.™ software) due to increased distance from the receiver plate. Therefore, we implanted the transmitter subcutaneously at the flank close to the ventral abdominal region and fixed the transmitter at the skin using a single stitch. In this position, a reduction in signal strength was not observed compared to the intraperitoneal implantation procedure. It should be noted that after a subcutaneous placement the telemetered temperature values do not represent the body core temperature.

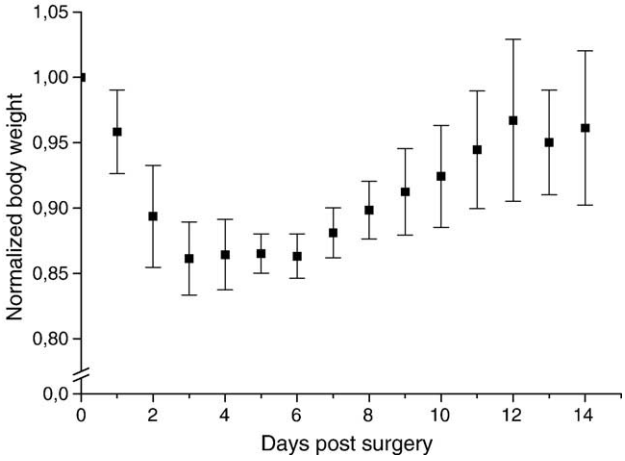

Fig. 4. Postoperative recovery of body weight. Typical changes in body weight after intraperitoneal implantation of radiofrequency TA10ETA-F20 transmitter (results taken from intraperitoneal ECG implantation). Maximum decrease in body weight is observed around days 4–5 postsurgery. Test measurements for EEG implantation showed the same trend in weight loss.

5.4. Electrocorticogram (ECoG)

After the implantation and fixation of the tip of the sensing lead using glass ionomer cement, no severe inflammatory reactions either of the cerebrum, the cerebellum, the meninges, or skin were observed. However, skin necrosis due to an increased pressure caused by the underlying cement was occasionally detected during the observation period of 4–6 weeks; thus, a minimum of cement should be used to prevent this.

In C57Bl/6 control mice rare single spikes were observed. However, it is hard to determine whether these are an intrinsic feature or due to implantation-related damage of the brain. Slight cortical impression was found adjacent to the implantation site at postmortem examination. This observation underlines the relevance of valid control experiments. Alterations in behavior after recovery that might be related to the transmitter or electrode implantation were not observed.

5.5. Electroencephalogram after the ip administration of R/S-baclofen and bicuculline

Systemic administration of baclofen and bicuculline was performed to check for quality of the EEG signal. Both substances, baclofen, serving as a GABA(B) receptor agonist, as well as bicuculline, which exerts antagonistic effects on GABA(A) receptors, are capable of provoking spikes/spike-waves in the ECoG based on hypersynchronization processes within the thalamocortical–corticothalamic circuitry [4]. Figs. 5B and C illustrate a surface EEG after the ip administration of R/S-baclofen and bicuculline-methobromide (BMB). The bipolar deflection exhibits prominent spike/spike-wave signals with high signal-to-noise ratio.

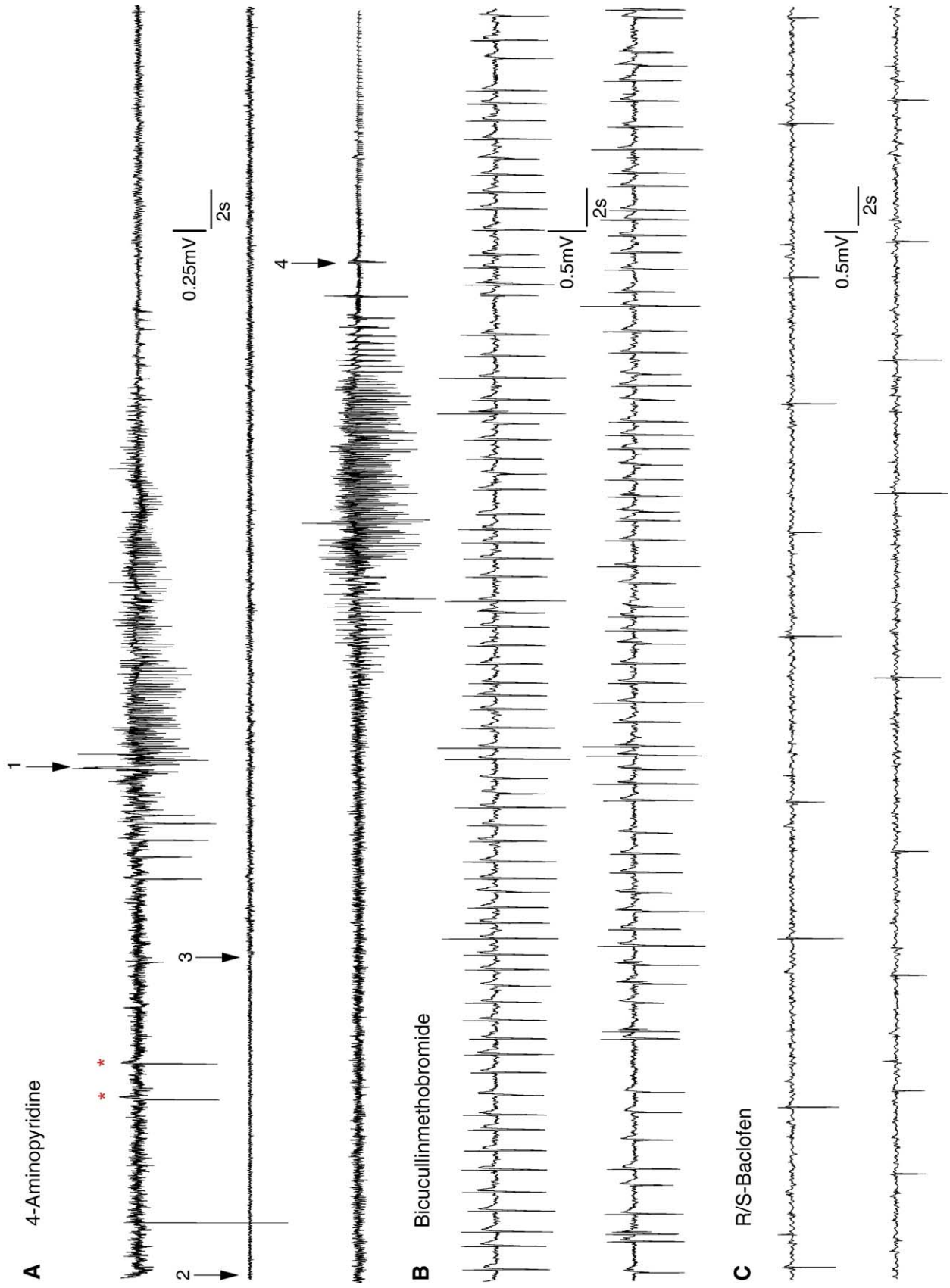
A
4-Aminopyridine
1
2
3
4
0.25mV
2s
B
Bicuculinmethobromide
0.5mV
2s
C
R/S-Baclofen
0.5mV
2s

5.6. Electroencephalogram after ip administration of 4-aminopyridine (4-AP)

Systemic administration of 4-aminopyridine (4-AP) or pentylenetetrazole [5] in mice provokes generalized tonic–clonic seizures with the animals developing a typical progressive sequence of seizure activity of increasing severity. Shortly after the injection, mice are hypoactive, followed by a mild (partial) myoclonus displaying clonic seizure activity affecting the face (vibrissal twitching), the head, and/or forelimbs. This state evolves into a generalized clonus characterized by loss of upright posture, whole body clonus involving all four limbs, jumping, wild running, and finally a tonic extension of the hindlimbs. Fig. 5A illustrates a typical recording after 4-AP administration (10 mg/kg). At the early stages of seizure development (myoclonus of the head, face and forelimbs) the EEG exhibits only marginal EMG contamination. Following sporadic spike activity (*) the generalized clonus starts with a characteristic deflection (1) and a subsequent episode of continuous spike activity. Although this period is characterized by massive muscle activity (whole body clonus), spike activity of the brain can clearly be determined and EMG contamination is surprisingly low, indicating that the implantation procedure is capable of exhibiting electroencephalographic signals selectively even under generalized seizure conditions, when EEG signals might expected to be masked by EMG artefacts. After the first generalized clonus an EEG depression of uncertain cause (2–3) was observed which was then followed by a second generalized clonus which ended in a tonic extension of hindlimbs (4).

5.7. Deep intracerebral (hippocampal) EEG recordings and postimplantational histology

In this study, deep intracerebral recordings were obtained after placing the lead into the CA3 region of the hippocampus (Fig. 6A). Within the hippocampus theta-wave activity appears to be of striking regularity, especially if the mouse is engaged in exploratory behavior, but also during rapid-eye movement (REM) sleep. Theta activity could be provoked by experimental environmental changes by placing the mouse into a new cage. Dominance of theta activity during exploratory behavior was confirmed by power spectrum density (PSD) analysis using the Data-quest™ A.R.T™ system (Figs. 6B and C).

As for surface electrode implantation no traces of infection were observed around the implanted materials for several weeks. By this technique, EEGs can be stably recorded for at least 5–6 weeks. After this time, proliferative reaction of the connective tissue as well as ossification in the burr holes [11] begins and tends to disconnect the electrodes from the underlying dura mater or simply tear the deep electrodes out of the brain, which might then be associated with EMG or ECG contamination (Figs. 7B and C). However, the implant never dropped off.

5.8. Electromyographic and electrocardiographic contamination of the electroencephalogram

The implantation technique described above provides a reliable tool of recording EEG with a high signal-to-noise ratio. However, as the EEG signal is weak, it is highly susceptible towards electrocardiographic and electromyographic contamination, both of which can evolve into a severe problem. This often occurs if the sensing lead is not properly secured or isolated from extracranial tissues by glass ionomer cement or if the silicone insulation of the sensing leads is damaged during the implantation procedure. ECG contamination can be easily identified due to its very regular pattern (7–9 Hz according to 420–540 bpm in Fig. 7B).

6. Discussion

Here we present an optimized surgical technique for telemetric EEG recordings in mice using surface or deep electrodes and offering stable recordings for several weeks.

Sophisticated telemetric systems have been developed in the past especially for larger animals, in particular rats [1,3] and guinea pigs [10], but telemetry has not been widely used in mice due to the large size of the older transmitting systems. However, with the miniaturization of new radiotransmitters and with the vast and growing number of transgenic mouse models requiring characterization, this method will undoubtedly become more widespread.

There are two different positions for transmitter placement, intraperitoneally or subcutaneously. Neither of them exhibited marked alterations in the signal strength. However, there are drawbacks for each. In the latter position, there is a risk that by exerting subcutaneous pressure, the transmitter can induce skin necrosis, which was occasionally observed. Furthermore, without proper fixation, movement of the transmitter might place tension on the electrodes. However, placement on the back does not result in pressure on the bowel, a phenomenon which may cause mechanical/paralytic ileus after intraperitoneal implantation. Therefore, a minimal animal weight of ~20 g (10 weeks of

Fig. 5. Pharmacological induction of epileptic discharges. (A) Bipolar surface EEG displaying ictal discharges after ip administration of 4-aminopyridine (10 mg/kg). Initially the EEG exhibits single, sporadic spikes (*) evolving into a transitory period of continuous spiking (1), ending up in an EEG depression (decreased amplitude, 2–3). Shortly after this episode a second train of spikes concomitant to the development of a generalized tonic–clonic seizure with wild running and jumping becomes apparent which finally results in a tonic extension of the hindlimbs (4) and death. Note that the remaining tiny signal after brain death represents an ECG contamination. (B) After ip administration of bicucullinemethobromide (BMB, 10 mg/kg) mice display trains of characteristic spikes/spike waves. (C) Administration of baclofen (20 mg/kg) showing sporadic occurrence of spiking activity.

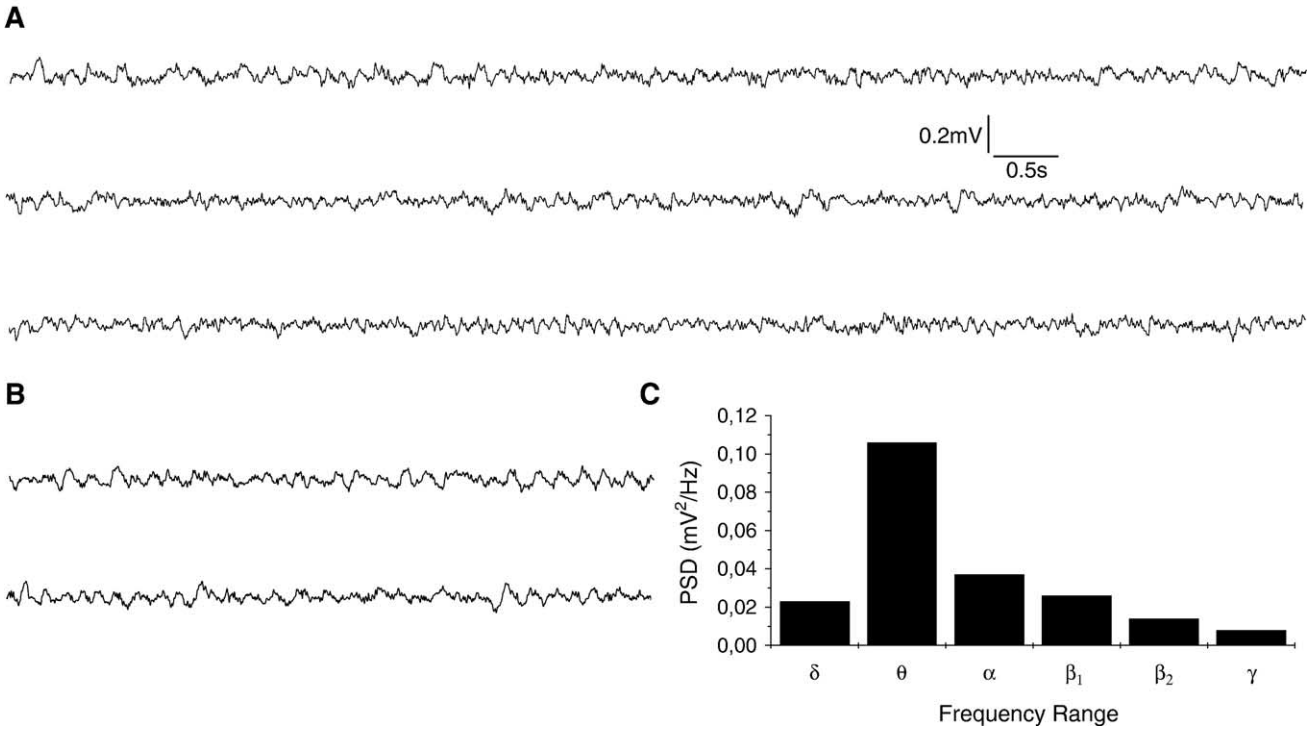

Fig. 6. Deep intracerebral (hippocampal) EEG recordings. (A) This figure illustrates a representative intrahippocampal recording within the CA3 region from a C57Bl/6 mouse. (B) During exploratory behavior after placing the mouse into a new cage (environmental change) power spectrum analysis (C) reveals predominance of theta-wave activity (4–8 Hz). PSD, power spectrum density; frequency rages: δ, 1–4 Hz; θ, 4–8 Hz; α, 8–12 Hz; β_1, 12–16 Hz, β_2, 16–32 Hz; γ, 32–50 Hz).

age) was required when intraperitoneal placement was used while subcutaneous placement can be carried out in smaller mice. Given an accurate intraabdominal transmitter placement, authors suggest this localization for long-term implantation whereas subcutaneous implantation is favored for short-term experiments.

The transmitters used in this study had 20 cm leads which offers the advantage of multiple implantations (Fig. 2A); however, it is therefore necessary to secure the excessive lead length either intraabdominally or subcutaneously by forming loops. Although intraperitoneal implantation and intraabdominal looping is more complex and time consuming, we never encountered any postoperative effects (e.g., interference with gastrointestinal motility, etc.) while subcutaneous looping occasionally resulted in skin necrosis. Neither of the implantation procedures causes severe alterations in behavioral characteristics with implanted mice showing a full range of activities including grooming, running, and climbing.

Different recording techniques of the mouse EEG have been described, involving electrodes formed by silver beads, silver wires, stainless steel, screws, etc. [11,13]. In contrast to recent studies in mice [13] and rats [1] using screw electrodes or stainless steel electrodes that need to be attached to the transmitters sensing leads, we have described a technique in which the sensing leads are directly attached to the dura mater (ECoG) or deep intracerebral structures (like the hippocampus) lacking any connectors or connecting cable system. This reduces the impedance and lowers attachment artefacts and thus providing higher signal-to-noise ratios. However, this approach might exhibit experimental limitations in specific brain regions that are less accessible (e.g., the brainstem).

Loosening of electrodes may occur at the implantation site due to the reactive proliferation of surrounding connective tissue, suggesting that there is a time window in which the EEG is most meaningful. However, in our experiments carried out over 6 weeks postimplantation the EEG signal remained strong and distinct. Other biopotential signals can contaminate the EEG recordings; however, electromyographic contamination (Fig. 7C) can often be avoided by proper lead placement. Recently, a new transmitter was released (F20-EET, DSI) with two differential leads for EEG and EMG recording which makes it possible to directly correlate both biopotentials.

ECG contamination can be of varying severity and in one occasion major contamination was observed when the shielding silicon insulation was damaged (Fig. 7B); hence, care should be given when manipulating the leads.

In contrast to these intrinsic EMG/ECG contaminations, the EEG is also highly susceptible to various types of extrinsic artefact, which can occur in both tethered and telemetry systems. As receiver plates in telemetry are very sensitive, they readily pick up electrical noise. We effi-

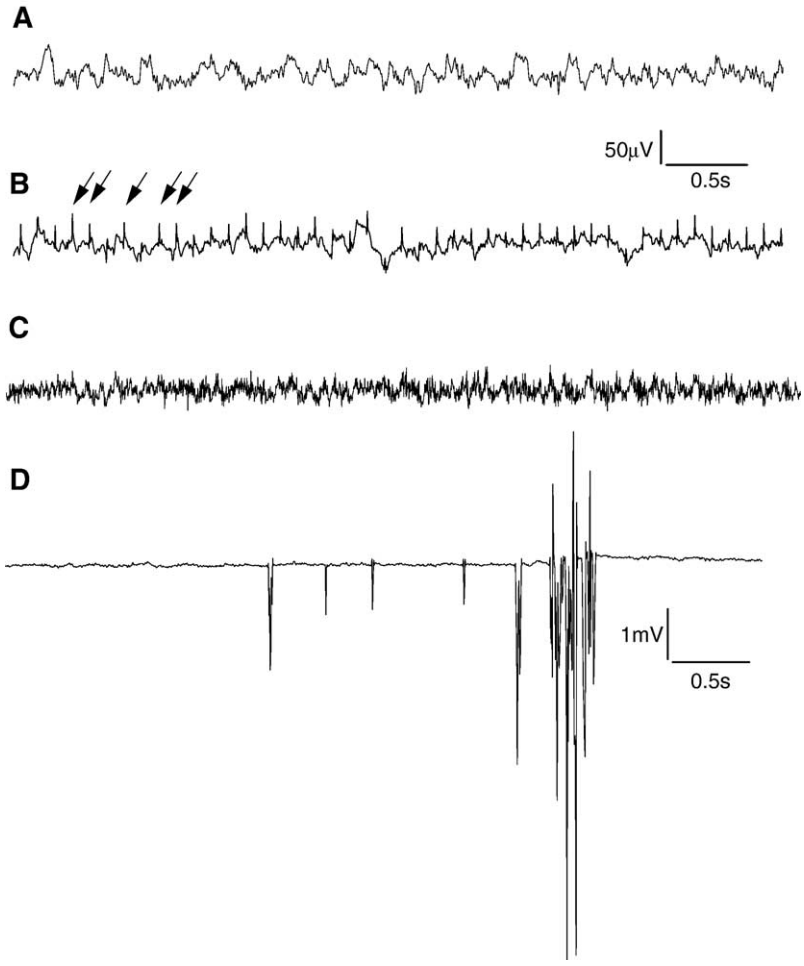

Fig. 7. Electrocardiographic/electromyographic and system artefacts contaminating the EEG (deep electrodes (A–C), surface electrodes (D), vertical bar: 50 μV in A–C, 1 mV in D). (A) Intrahippocampal EEG recording from control mouse. (B) Damaged silicone insulation of the leads as well as ossification processes originating from drilled holes can result in severe contamination of the electroencephalographic recording. Note regular pattern of interfering ECG signal (arrows). Although ECG contamination cannot always be avoided, the implantation procedure presented here will reduce it to a minimum. (C) Example of an electromyographic contamination of the EEG. (D) Artefacts can originate from cross-talk between receiver plates or from electrical noise evolving from room lights or various other electrical devices close to the receiver. An effective way of preventing the system picking up noise is to shield receiver plate and home cage using a Faraday cage.

ciently reduced this phenomenon by shielding each telemetered mouse with a Faraday cage.

In summary, telemetry can be used to reliably record both surface and deep EEG signals in the mouse allowing further characterization for the increasing numbers of mutant mouse strains available.

7. Quick procedure

(i) Anesthesia of mice using esketamin/xylazine (100/10 mg/kg).
(ii) Placing anesthetized animal on a heating surface (Fig. 2B); removal of body hair and disinfection of the abdomen (Mercuchrom®).
(iii) Intraperitoneal or subcutaneous pouch implantation of radiofrequency transmitter (Fig. 2C). Fixation of the transmitter using 4-0 suture material.
(iv) Longitudinal midline incision of the scalp; removal of additional connective tissue using 10% H_2O_2.
(v) Drilling holes using a stereotaxic device with a high-speed dental drill mounted on a three-axis micromanipulator (Figs. 1 and 2D).
(vi) Epidural placement or deep insertion of electrodes followed by fixation with glass ionomer cement.
(vii) Closure of the scalp using 6-0 suture material. Final disinfection with Mercuchrom® (Fig. 2G).
(viii) Postoperative pain management (100 mg/kg metamizole) and temperature support.

8. Essential literature references

Refs. [1,2,8,14]

Acknowledgments

The authors would like to thank Prof. Dr. Edward Bertram for helpful discussions and Dr. Oliver Weiergräber for careful reading of the manuscript. We thank the physical plant facility (Mr. Harald Metzner) and the animal keepers of the central facility and Dr. Winfried Oswald for their assistance. The work was financially supported by the Köln Fortune Program of the Faculty of Medicine, University of Cologne, and the Center of Molecular Medicine Cologne (CMMC) (Bundesministerium für Bildung, Wissenschaft, Forschung und Technologie, Förderkennzeichen 01 KS 9502, to TS and JH).

References

[1] J.F. Bastlund, P. Jennum, P. Mohapel, V. Vogel, W.P. Watson, Measurement of cortical and hippocampal epileptiform activity in freely moving rats by means of implantable radiotelemetry, J. Neurosci. Methods 138 (2004) 65–72.

[2] E.H. Bertram, J.M. Williamson, J.F. Cornett, S. Spradlin, Z.F. Chen, Design and construction of a long-term continuous video-EEG monitoring unit for simultaneous recording of multiple small animals, Brain Res. Brain Res. Protoc. 2 (1997) 85–97.

[3] M. Cotugno, P. Mandile, D. DAngiolillo, P. Montagnese, A. Giuditta, Implantation of an EEG telemetric transmitter in the rat, Ital. J. Neurol. Sci. 17 (1996) 131–134.

[4] L. Danober, C. Deransart, A. Depaulis, M. Vergnes, C. Marescaux, Pathophysiological mechanisms of genetic absence epilepsy in the rat, Prog. Neurobiol. 55 (1998) 27–57.

[5] T.N. Ferraro, G.T. Golden, G.G. Smith, P. St Jean, N.J. Schork, N. Mulholland, C. Ballas, J. Schill, R.J. Buono, W.H. Berrettini, Mapping loci for pentylenetetrazol-induced seizure susceptibility in mice, J. Neurosci. 19 (1999) 6733–6739.

[6] N.F. Guler, E.D. Ubeyli, Theory and applications of biotelemetry, J. Med. Syst. 26 (2002) 159–178.

[7] D.C. Jeutter, Biomedical telemetry techniques, Crit. Rev. Biomed. Eng. 7 (1982) 121–174.

[8] K. Kramer, L.B. Kinter, Evaluation and applications of radiotelemetry in small laboratory animals, Physiol. Genomics 13 (2003) 197–205.

[9] R.P. Louis, J. Lee, R. Stephenson, Design and validation of a computer-based sleep-scoring algorithm, J. Neurosci. Methods 133 (2004) 71–80.

[10] H. Mumford, J.R. Wetherell, A simple method for measuring EEG in freely moving guinea pigs, J. Neurosci. Methods 107 (2001) 125–130.

[11] H. Nakano, K. Saito, K. Suzuki, Chronic implantation technique for monopolar EEG monitoring of epileptic seizures in mice, Brain Res. Bull. 35 (1994) 261–268.

[12] L.D. Sanford, L.H. Yang, X.D. Tang, Influence of contextual fear on sleep in mice: a strain comparison, Sleep 26 (2003) 527–540.

[13] X.D. Tang, L.D. Sanford, Telemetric recording of sleep and home cage activity in mice, Sleep 25 (2002) 691–699.

[14] V. Vogel, C. Sanchez, P. Jennum, EEG measurements by means of radiotelemetry after intracerebroventricular (ICV) cannulation in rodents, J. Neurosci. Methods 118 (2002) 89–96.

Epilepsia, **47**(5):839–850, 2006
Blackwell Publishing, Inc.

Altered Seizure Susceptibility in Mice Lacking the $Ca_V2.3$ E-type Ca^{2+} Channel

*†Marco Weiergräber, *Margit Henry, *†Andreas Krieger, *Marcel Kamp, *†Kayalvizhi Radhakrishnan, *†Jürgen Hescheler, and *†Toni Schneider

*Institute of Neurophysiology, and †Center of Molecular Medicine Cologne (CMMC), University of Cologne, Köln, Germany

Summary: *Purpose:* Recently the $Ca_v2.3$ (E/R-type) voltage-gated calcium channel (VGCC) has turned out to be not only a potential target for different antiepileptic drugs (e.g., lamotrigine, topiramate) but also a crucial component in the pathogenesis of absence epilepsy, human juvenile myoclonic epilepsy (JME), and epileptiform activity in CA1 neurons. The aim of our study was to perform an electroencephalographic analysis, seizure-susceptibility testing, and histomorphologic characterization of $Ca_v2.3^{-/-}$ mice to unravel the functional relevance of $Ca_v2.3$ in ictogenesis.

Methods: Generalized and brain-specific $Ca_v2.3$ knockout animals were analyzed for spontaneous epileptiform discharges by using both electrocorticographic and deep intracerebral recordings. In addition, convulsive seizure activity was induced by systemic administration of either 4-aminopyridine (4-AP; 10 mg/kg, i.p.) or pentylenetetrazol (PTZ; 80 mg/kg, s.c.) to reveal possible alterations in seizure susceptibility. Besides histomorphologic analysis, expression studies of other voltage-gated Ca^{2+} channels in $Ca_v2.3^{-/-}$ brains were carried out by using semiquantitative reverse transcription–polymerase chain reaction (RT-PCR).

Results: Both electrocorticographic and deep intrahippocampal recordings exhibited no spontaneous epileptiform discharges indicative of convulsive or nonconvulsive seizure activity during long-term observation. Gross histology and expression levels of other voltage-gated Ca^{2+} channels remained unchanged in various brain regions. Surprisingly, PTZ-induced seizure susceptibility was dramatically reduced in $Ca_v2.3$-deficient mice, whereas 4-AP sensitivity remained unchanged.

Conclusions: $Ca_v2.3$ ablation results in seizure resistance, strongly supporting recent findings in CA1 neurons that $Ca_v2.3$ triggers epileptiform activity in specialized neurons via plateau potentials and afterdepolarizations. We provide novel insight into the functional involvement of $Ca_v2.3$ in ictogenesis and seizure susceptibility on the whole-animal level.
Key Words: $Ca_v2.3$—Electroencephalogram—Ictogenesis—Pentylenetetrazol—Seizure susceptibility.

Voltage-gated calcium channels (VGCCs) are key components in the etiology and pathogenesis of various forms of epilepsies (1). In the past, mutations within the pore-forming $\alpha 1$ subunits, accessory subunits (β, $\alpha_2\delta$, and γ), as well as interaction partners of VGCCs, were shown to be responsible for different types of convulsive and nonconvulsive seizure activities not only in animal models but also particularly in humans, like childhood absence epilepsy (CAE) or juvenile myoclonus epilepsy (JME) (2,3). A major focus in clinical and basic epilepsy research has been on the HVA $Ca_v2.1$ channel, with different mutations in this channel exhibiting various combinations of absence epilepsy, episodic ataxia type 2 (EA2), and spinocerebellar ataxia type 6 (SCA6) in humans (4–6). LVA T-type calcium channels, particularly $Ca_v3.2$, were shown to be crucial for the etiology of CAE (7,8) and display an important target for a variety of antiepileptic drugs [AEDs; e.g., suxinimides lamotrigine (LTG) and zonisamide (ZNS)] (9–11). However, the functional relevance of the $Ca_v2.3$ VGCC has been underestimated for a long time. $Ca_v2.3$-containing E/R-type Ca^{2+} channels are widely expressed in the central nervous system, including those regions that are involved in the generation of spike–wave discharges, such as neocortex and thalamus, including the reticular thalamic nucleus (RTN) (12–14). In hippocampal pyramidal neurons, $Ca_v2.3$ significantly contributes to the E/R-type Ca^{2+} current component (15,16). In CA1 neurons, E/R-type Ca^{2+} currents were related to the current component in distal apical dendrites (17) and were shown to be implicated not only in dendritic burst firing (18) but also in the generation of spontaneous carbachol-induced oscillations, which resemble epileptiform activity in animal models of epilepsy (19). Recently it also was shown that $Ca_v2.3$ is not only involved in processes such as anxiety (20), pain behavior

Accepted December 22, 2005.
Address correspondence and reprint requests to Dr. M. Weiergräber at Institute of Neurophysiology & Center of Molecular Medicine Cologne (CMMC), Robert-Koch-Str. 39, D-50931 Köln, Germany. E-mail: akp74@uni-koeln.de

The first two authors contributed equally to this study.

Present address of Mr. Krieger: Department of Dermatology and Venerology, University of Cologne, Kerpener Str. 62, 50937 Köln, Germany.

(21), presynaptic long-term potentiation (LTP) and post-tetanic potentiation (22) and myelinogenesis (23), but particularly serves as a potent target for a number of AEDs, like LTG (11) or topiramate (TPM) (24). Significantly, it turned out that $Ca_v2.3$ is substantially inhibited by therapeutic brain concentrations of LTG, whereas $Ca_v3.1$ and $Ca_v3.3$ exhibit only minor sensitivities (11,25). Thus inhibition of E/R-type calcium currents, rather than T-type currents, is likely to be involved in the antiabsence action of LTG and therefore suggests functional relevance of $Ca_v2.3$ in the pathogenesis of absence epilepsy. These results are further supported by the observation that different rat models of absence epilepsy exhibit alterations in $Ca_v2.3$ channel expression. In genetic absence epilepsy rats from Strasbourg (GAERS), for example, $Ca_v2.3$ transcripts were reported to be significantly reduced in cerebellum and medulla compared with controls (26,27), with both regions projecting to different components of the thalamocortical circuitry (28) that modifies oscillatory behavior (29,30). Furthermore, van de Bovenkamp-Janssen et al. (31) showed that development of spike–wave discharges (SWDs) in WAG/Rij rats is concomitant with a lack of increase of $Ca_v2.3$ expression in the RTN. Therefore $Ca_v2.3$ might be related to the generation of SWDs and, hence, also of absence epilepsy. However, increasing evidence indicates that $Ca_v2.3$ also is related to the pathophysiology of convulsive seizure activity. Just recently, mutations in the EFHC1 protein, a novel C-terminal interaction partner of the $Ca_v2.3$ VGCC, were reported to cause JME in humans (3). Normally, EFHC1 induces neuronal apoptosis by interaction with $Ca_v2.3$, whereas mutations in EFHC1 disrupt C-terminal binding. It is assumed that the lack of apoptosis results in an increased cell density (32), producing hyperexcitable circuits as a result of altered neuronal connectivity (3). In addition, recent findings strongly suggest that $Ca_v2.3$ can trigger epileptiform activity in specialized neurons by modulating afterdepolarizations (ADPs) and plateau potentials (PPs) (24,33). As stated by Suzuki et al. (3), the EEG phenotype of $Ca_v2.3^{-/-}$ mice has not been described, and as-yet undetected minor seizure sensitivities or brain microdysgenesis might be present. Our results on electroencephalographic characterization of both generalized and brain-specific $Ca_v2.3^{-/-}$ mice and seizure-susceptibility testing shed new light on the functional relevance of $Ca_v2.3$ in the etiology and pathogenesis of epilepsy.

METHODS

RNA isolation and RT-PCR

Total RNA was isolated from different regions of the CNS (cortex, hippocampus, thalamus, mesencephalon, cerebellum, medulla) from $Ca_v2.3^{+/+}$ and $Ca_v2.3^{-/-}$ mice by using standard protocols (Tri-reagent; Sigma, Munich, Germany). Fragments of cDNA were amplified by polymerase chain reaction (PCR; Biometra, Göttingen, Germany) after reverse transcription (RT) of RNA (14,34). The sequences of primer pairs and annealing temperatures used for PCR reactions of VGCC $\alpha 1$ subunits and for hypoxanthine guanine phosphoribosiltransferase (HPRT) have been summarized (35) and were adapted for murine tissue (36). Transcript levels were analyzed semiquantitatively by using GelScan V3.1 software (BioSciTec, Frankfurt/Main, Germany).

Western blot analysis

Brain microsomes from $Ca_v2.3^{+/+}$ and $Ca_v2.3^{-/-}$ mice were isolated and stored at -80°C (37). For immunoblotting, a $Ca_v2.3$-specific polyclonal serum was used as primary antibody (37) at a dilution of 1:500, and proteins were visualized by ECL detection reagent (Amersham LifeScience, Munich, Germany). The peptide $Ca_v2.3$-com, SGILEGFDPPHPCGVQGC, is part of the loop between IS5 and the pore region (aa 256–273, GB L27745), and the peptide $Ca_v2.3$-spec, GIYLPSDTQEHAG[C], is located in the carboxy-terminal domain (aa 1981–1993, in the extended splice variant $Ca_v2.3$d). Peptide $Ca_v2.3$-spec contains one additional cysteine residue at its carboxy terminus for coupling to a matrix, as shown in brackets. Microsomes from untransfected HEK-293 cells and from stably transfected HEK-2C6 cells expressing $Ca_v2.3$d were used as negative and positive controls, respectively.

Brain histology and histochemistry

Paraffin embedding of the rat brain, as well as immunohistochemistry, was carried out as described previously (38). The polyclonal antibodies anti-$Ca_v2.3$-com and anti-$Ca_v2.3$-spec were used at a working dilution of 1:20. Two negative controls were included. Either the primary antibodies were replaced by the preimmune serum or the serum was preincubated with an excess of the peptide (20 m*M*) used for immunization. Sections from a multitissue block were used to verify appropriate positive and negative reactions. Histology of brain slices from $Ca_v2.3^{+/+}$ and $Ca_v2.3^{-/-}$ mice was investigated by using standard Nissl staining.

Study animals

The cacna1e gene encoding $Ca_v2.3$ was targeted by homologous recombination in E14.1 embryonic stem (ES) cells. A loxP-flanked neomycin cassette was inserted into the *Nsi*I site of intron 2, and a third loxP site was inserted downstream of the *Hin*dIII site. The cyclic DNA-producing recombinase (Cre-recombinase) was transiently expressed in correctly targeted ES cells, from which the clone Tα1E1E8 was identified by Southern blotting of its genomic DNA. From the ES cells surviving under puromycin, those cells were selected that had lost their neomycin cassette (type II deletion), leading to a recombined cacna1e gene, in which exon 2 was flanked

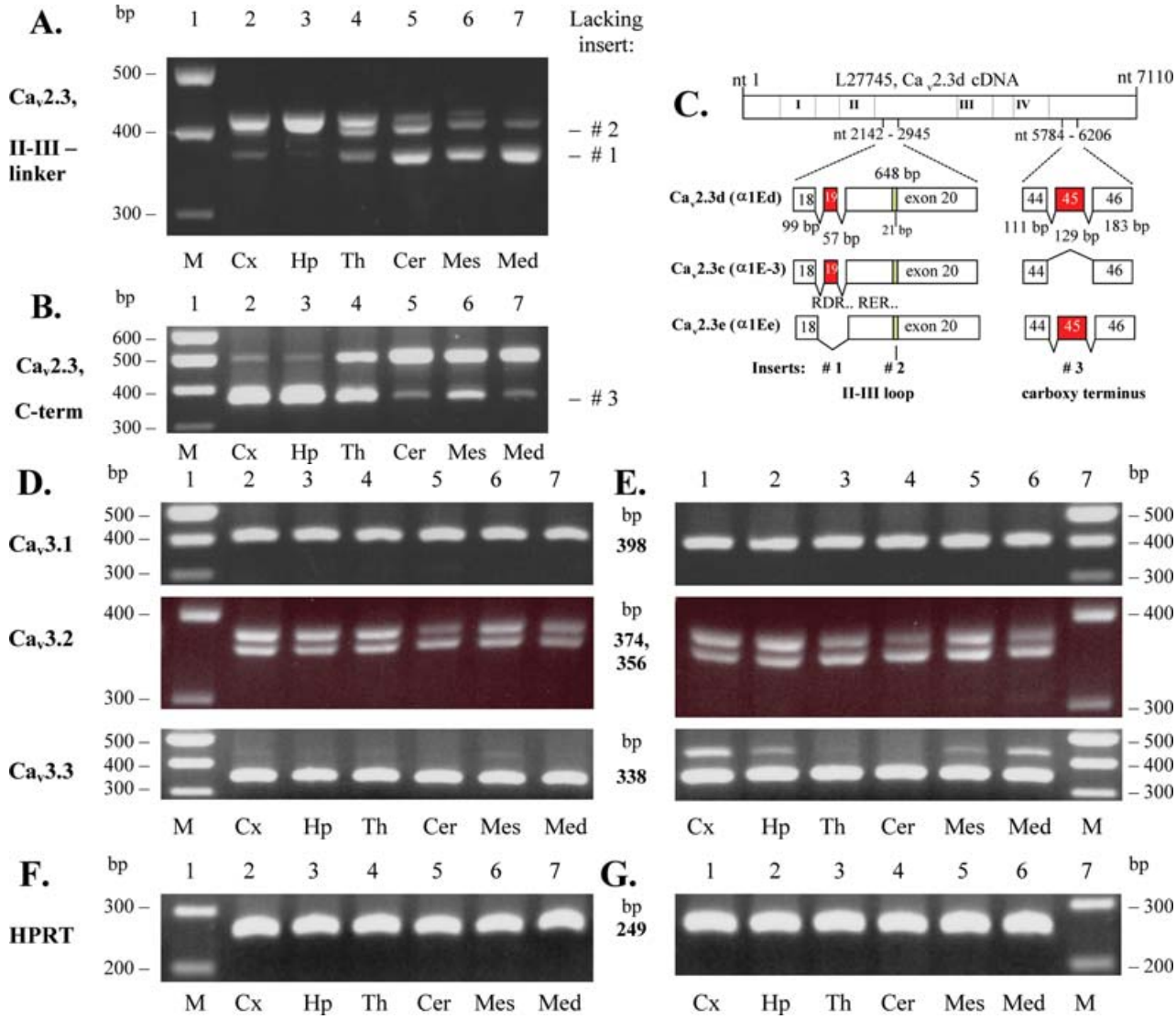

FIG. 1. Detection of $Ca_v2.3$ in control mice and comparison of T-type voltage-gated calcium–channels (VGCC) transcripts from different brain regions of control and $Ca_v2.3$-deficient mice. Total RNA was isolated from neocortex (Cx), hippocampus (Hp), the thalamus and hypothalamus (Th), cerebellum (Cer), mesencephalon (Mes), and the medulla (Med). Known $Ca_v2.3$ splice variants were identified by reverse transcriptase–polymerase chain reaction (RT-PCR) after amplifying indicative fragments of the II-III loop and the C-terminus. **A:** With the oligonucleotide primer pairs that are flanking the segment containing exon 19 (insert 1) and the adjacent insert 2 (in exon 20) led to the detection of indicative patterns of the II-III loop. The expected sizes of cDNA fragments are 363 bp (lacking exon 19), 399 bp (lacking insert 2), and 420 bp, representing the full-length segment within the II-III loop. **B:** With the oligonucleotide, primer pair that is flanking exon 45 (insert 3) leads to the detection of indicative patterns of carboxy-terminal fragments of $Ca_v2.3$. **C:** Diagram of indicative fragments of $Ca_v2.3$ and their relation to gene structure. **D**, **E:** Amplification of indicative cDNA fragments for the T-type VGCCs $Ca_v3.1 - 3.3$. No compensatory changes could be detected. **F**, **G:** Amplification of cDNA fragments for hypoxanthine-guanine phosphoribosyltransferase (HPRT).

by two loxP sites (39). Exon 2 represents nts 269–375 of the murine $Ca_v2.3$ subunit (GB L29346).

Exon-2 loxP-flanked ES cells were injected into C57Bl/6 blastocysts. Resulting male chimeras were bred to C57Bl/6 females, and the $Ca_v2.3^{fl/+}$ genotype of agouti-colored offspring was determined by Southern blot analysis. The cacna1e gene was ablated in vivo by mating $Ca_v2.3^{fl/+}$ and Cre-deleter mice expressing cyclic DNA-producing recombinase (Cre-recombinase) constitutively under the control of the cytomegalovirus promoter. For details see (40). $Ca_v2.3$ null mutant was backcrossed into C57Bl/6 as previously described (40). The brain-specific inactivation of cacna1e was achieved by mating $Ca_v2.3^{fl/+}$ and nestin-Cre mice expressing Cre-recombinase under the control of the nestin promoter (39). $Ca_v2.3^{+/+}$ control animals and $Ca_v2.3^{-/-}$ mice were generated from $Ca_v2.3^{+/-}$ littermates by inbreeding two parallel mouse lines with identical genetic backgrounds, and $Ca_v2.3$ deficient and control mice from both genders were used in this study. Mice

were housed in Makrolon cages type II and maintained on a conventional light/dark cycle with food and water available ad libitum. All animal experimentation was approved by the local institutional committee on animal care. All efforts were made to minimize animal suffering and to use only the number of animals necessary to produce reliable scientific data.

Telemetric EEG and EMG recordings

Both TA10ETA-F20 and TL11M2-F20-EET transmitters (DSI, St. Paul, MN, U.S.A.) were used for electrocorticographic and deep intracerebral recordings in mice. Electromyogram (EMG) electrodes (F20-EET transmitter) were placed 2–3 mm apart within the cervical region of the trapezius muscle. The telemetry system, anesthesia, implantation procedure, and postoperative treatment have been described in detail previously (41).

Surface electrode implantation (ECoG)

In total, eight $Ca_v2.3^{+/+}$ mice (29.3 ± 0.9 g) and seven $Ca_v2.3^{-/-}$ animals (30.4 ± 1.9 g) were analyzed. Epidural leads were positioned above the somatosensory cortex at the following stereotaxic coordinates: (+)-lead, bregma −1 mm, lateral of bregma −2.5 mm (right hemisphere); (−)-lead, bregma −1 mm, lateral of bregma −2.5 mm (left hemisphere) and fixed at the neurocranium by using dental cement.

Intracerebral (deep) electrode implantation

For deep intrahippocampal recordings, two mice with neuronal progenitor specific ablation of $Ca_v2.3$ ($Ca_v2.3^{(fl/fl)nestin-Cre+}$) were used. As control animals, either a nestin-Cre negative ($Ca_v2.3^{(fl/fl)nestin-Cre-}$) or an animal still containing one wild-type allele of the cacna1e was used ($Ca_v2.3^{(fl/+)nestin-Cre+}$). The electrodes were positioned as follows: (+)-lead, bregma −2 mm, lateral of bregma 2 mm (right hemisphere), dorsoventral (depth) 2 mm (final targeting region CA3); (−)-lead, bregma −6.2 mm, lateral of bregma 0 mm; dorsoventral 0 mm (epidural reference electrode localized on the cerebellum).

Seizure-susceptibility testing

Experimental design

4-Aminopyridine (4-AP, Sigma, Munich, Germany), as well as pentylenetetrazole (PTZ, Sigma), was freshly dissolved in 0.9% NaCl before each injection. All animals were placed singly for ≥30 min before administration of convulsants.

4-AP–induced seizures

The K^+-channel blocker 4-AP was administered intraperitoneally (i.p.) to $Ca_v2.3^{+/+}$ mice [n = 9 (all ♀), 24.8 ± 5.1 g, 11.8 ± 3.2 wk] and $Ca_v2.3^{-/-}$ mice [n = 8 (all ♂), 22.9 ± 2.7 g, 11.9 ± 1.2 wk] at a dose of 10 mg/kg. After injection, animals were immediately placed back into their home cage, observed, and videomonitored for 60 min. The 4-AP–induced convulsive phenotype correlates with phases 1–4 outlined below for PTZ-induced seizure activity (42).

PTZ-induced seizures

Seizures were induced by subcutaneous (s.c.) administration of PTZ at a dose of 80 mg/kg. Ten $Ca_v2.3^{+/+}$ mice (six ♂, four ♀; 24.7g ± 1.4 g, 18.3 ± 1.9 wk) and nine $Ca_v2.3^{-/-}$ mice (all ♂; 24.8 ± 1.5 g, 16.2 ± 0.9 wk) were used in this study and videomonitored for 45 min after injection. Four different stages of seizure activity are differentiated in the literature, which we have slightly modified and further subdivided:

Phase 1: Nonseizure activity. This phase represents a nonconvulsive state characterized by reduced motor activity (hypoactive state) with mice exhibiting a prone or crouched posture and a characteristic direct contact of the abdomen with the cage bottom.

Phase 2: Partial clonus. During this phase, mice display typical partial clonic activity affecting the face, head, vibrissae, and forelimbs. Jerks of head and forelimbs are sometimes accompanied with vocalization (however, the latter can also occur in phases 3 and 4). Principally, partial clonic events are short, lasting 1–2 s, but they can occur repetitively over time.

Phase 3: Generalized myoclonus. This phase is characterized by a generalized (whole-body) clonus involving all four limbs and the tail. According to its severity, it can be further subdivided into (a) whole-body clonus without loss of upright posture, (b) whole-body clonus with loss of upright posture, and (c) whole-body clonus with complete loss of motoric control (wild running and jumping). Typically, this phase is initiated by isolated whole-body twitching with increasing frequency, finally evolving into a generalized myoclonus that often lasts for ≤30 s. After clonic activity, animals remain in a tonic posture (either opistotonus-like with uplifted tail or emprostotonus-like) of variable duration, which ends in a quiescent period (postictal depression). Often, rearing and autonomic signs such as hypersalivation and defecation can be observed. Mice are capable of exhibiting several generalized myoclonic events of various severities.

Phase 4: Generalized (maximal) tonic–clonic seizure (with tonic extension of hindlimbs). Initially, this stage is indistinguishable from phase 3. However, when evolving to phase 4, mice exhibit maximal seizure activity characterized by tonic extension of hindlimbs normally associated with death due to respiratory insufficiency. Nevertheless, some mice can spontaneously recover and perform a number of phase 4 seizures.

Collecting data for the analysis of seizure susceptibility

Latencies were calculated as the time from the initial 4-AP or PTZ injection to the first observation of phases 1–4. If the animal did not undergo a specific seizure phase during the observation period, it was assigned a latency of 60 min (4-AP) or 45 min (PTZ), respectively. In addition, the frequency with which an animal entered the various phases 1–4 was counted. Time points and frequencies were noted in real time and rechecked by using mouse video recordings. Further, the duration of phase 1–4 was analyzed during the observation period. If an animal entered into a phase of seizure more than once, the durations of the incidents were summed. If an animal did not enter into a specific seizure phase, it was assigned a duration and frequency of zero. Total seizure activity was calculated by adding time durations of phase 2–4.

Statistical analysis

To acquire and analyze EEG data, the Dataquest A.R.T. 3.1 software (DSI) was used. EEG recordings were performed each day for ≥30–45 min between 9 a.m. and 6 p.m.; at days 7 and 14 after surgery, overnight recordings were performed for long-term analysis. EEG activity was sampled at 1000 Hz with a filter cutoff of 50 Hz. EMG sampling rate was also 1000 Hz. All data are calculated and displayed as the mean ± SEM. Statistical comparison was performed by using the Student *t* test, with a value of $p < 0.05$ considered significant (*) or $p < 0.01$ as highly significant (**). Lethality and number of animals entering individual seizure stages were analyzed by using Fisher's exact probability test.

RESULTS

Distribution of $Ca_v2.3$ splice variants and transcripts of T-type Ca^{2+} channels in different brain regions. Mouse brains were dissected and analyzed for expression of $Ca_v2.3$ splice variants (Fig. 1 A and B) as well as other voltage-gated calcium channels (Fig. 1D and E). Indicative cDNA patterns of $Ca_v2.3$ splice variants were investigated in detail (Fig. 1), because the splice variants $Ca_v2.3c$ and $Ca_v2.3d$ are stimulated by low cytosolic Ca^{2+} concentrations, differently from $Ca_v2.3e$ (34,35,43). Assuming that the Ca^{2+}-sensitive splice variants are most important for signaling in thalamocortical circuits, their transcripts were defined in different brain regions. The pattern of $Ca_v2.3$ cDNA fragments from the II-III–loop (Fig. 1A) and the carboxy terminal tail (Fig. 1B) was found to be different for the brain regions investigated in our study. Concerning the $Ca_v2.3$ splice variant expression pattern (Fig. 1C), brain regions can be subdivided into three groups (Fig. 1A): first, regions that mainly express fragments indicative of the Ca^{2+}-sensitive $Ca_v2.3c$, the splice variant in neocortex and hippocampus that contains a full length II-III–loop, and a smaller C-terminus lacking exon 45–encoded insert 3 (34,35,43); second, regions that predominantly express fragments related to the splice variant $Ca_v2.3e$ lacking exon 19–encoded insert 1 of the II-III loop but containing exon 45–encoded insert 3 of the C-terminus, as depicted for cerebellum (34) and medulla (present report). Finally, brain regions such as thalamus and hypothalamus including the RTN express fragments of both variants at a similar density, suggesting that both major splice variants, $Ca_v2.3c$ and $Ca_v2.3e$, may contribute to neuronal signaling in this region. Furthermore, other VGCCs were analyzed for compensatory changes in transcript levels by using a semiquantitative RT-PCR approach ($n = 3$). No significant changes could be detected for the T-type channels $Ca_v3.1$–3.3 (Fig. 1D and E) as well as the L-Type channels $Ca_v1.2$ and $Ca_v1.3$ and the non–L-type $Ca_v2.1$ and $Ca_v2.2$ (not shown) in different brain regions from controls and $Ca_v2.3^{-/-}$ mice.

Polyclonal sera directed either against a common epitope of all splice variants or against a specific one in the insert 3 of the carboxy terminus (Fig. 2A and B) were used to stain brain slices from rat. Immunoreactive cells were detected in the neocortex (Fig. 2D and E) and with high density in the RTN (Fig. 2C) and hippocampal pyramidal cells (Fig. 2F).

Inactivation of $Ca_v2.3$ does not impair the macroscopic histology of the brain

After gene inactivation (15,22,40), the $Ca_v2.3$ protein cannot be detected by Western blotting (Fig. 2A and B). Histology of brain slices was investigated for control and $Ca_v2.3$-deficient mice by using Nissl staining (Fig. 3). In serial sections throughout the whole mouse brain, no apparent differences in gross histology were detected in age-matched mice of the same sex, suggesting that the ablation of $Ca_v2.3$ did not cause macroscopic dysmorphologies.

Electroencephalographic characterization of control and $Ca_v2.3$-deficient mice

EEGs from epidural and deep electrodes were recorded and evaluated from conscious unrestrained mice starting 2 weeks after surgery (41,44). Qualitative analysis of long-term electrocorticograms (ECoGs) from eight $Ca_v2.3^{+/+}$ and seven $Ca_v2.3^{-/-}$ did not display any epileptiform discharges indicative of convulsive or non-convulsive seizure activity (Fig. $4A_{I-II}$ and B_{I-II}). In addition, brain-specifically inactivated mice ($n = 2$) did not exhibit any epileptic graphoelements in deep intrahippocampal recordings (Fig. $4A_{III-V}$ and B_{III-V}). Occasionally, isolated low-amplitude spikes have been recorded in both controls and $Ca_v2.3$-inactivated mice, probably related to the surgical implantation procedure itself (41).

Electrocorticogram after 4-AP and PTZ administration

Generalized convulsive seizures were reflected in the surface EEG by high-amplitude polyspike and

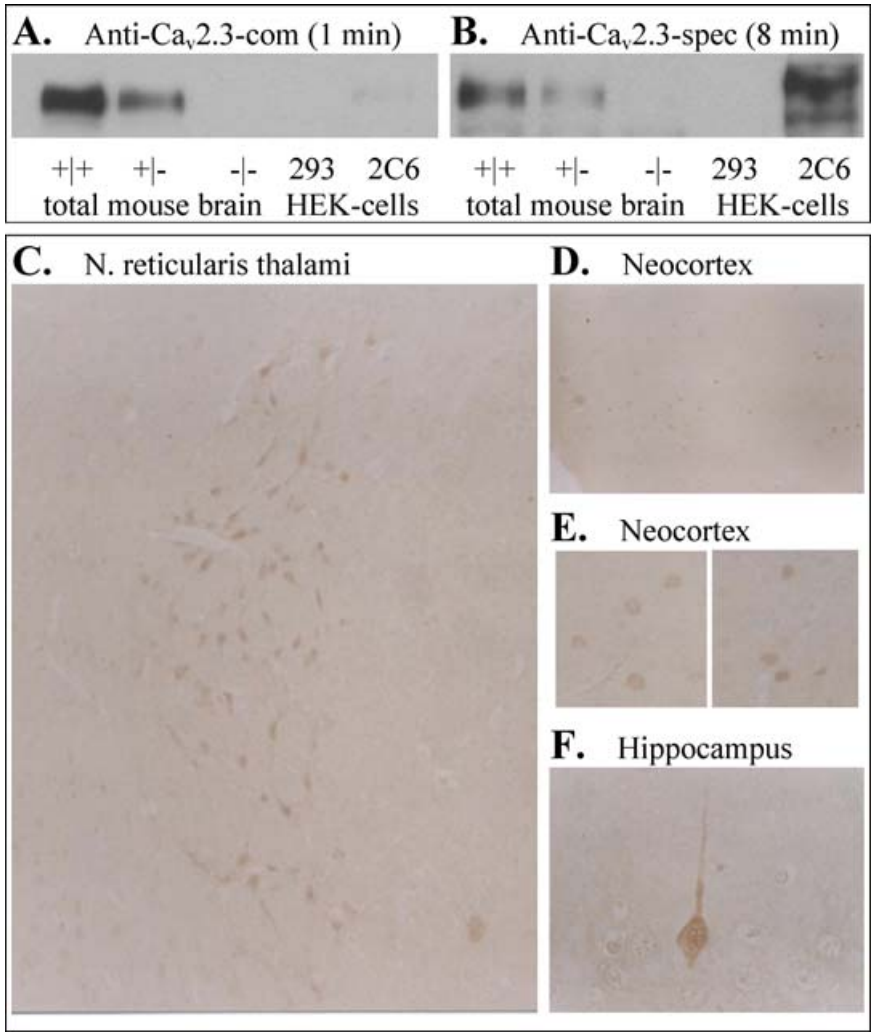

FIG. 2. Detection of $Ca_v2.3$ in the neocortex, reticular thalamic nucleus, and hippocampus. **A**, **B:** With two different antibodies, $Ca_v2.3$ could be detected in brains from control and heterozygous but not in $Ca_v2.3^{-/-}$ mice by using standard Western blot technique. **C–F:** A polyclonal serum directed against part of the carboxy-terminal insertion 3 was used as the primary antibody to unravel $Ca_v2.3$ expression in the rat brain. The strongest staining was detected in the reticular thalamic nucleus (RTN), suggesting the expression of $Ca_v2.3$ splice variants with an extended carboxy terminus as, for example, $Ca_v2.3e$.

polyspikes–wave discharges (Fig. $5A_{III-IV}$ and B_{II}) lasting ≤90 s. Initial spikes with a frequency of 4.5–5 Hz are typically followed by trains of low-frequency SWDs (1–1.5 Hz) during generalized myoclonic activity in both 4-AP– and PTZ-treated animals from both genotypes. Concomitant behavioral manifestations were characterized by chronic contractions of the limbs and of the axial muscles, ranging in intensity from barely perceptible body twitches to severe convulsions. No qualitative EEG differences were observed between $Ca_v2.3^{+/+}$ and $Ca_v2.3^{-/-}$ mice, and no subclinical electrographic seizure could be detected at the site of implantation. However, subclinical seizure activity in other brain regions cannot be absolutely excluded, as telemetric multiple channel recordings are not yet available in mice.

4-Aminopyridine sensitivity of $Ca_v2.3$-deficient mice

Analysis of latencies to the different seizure phases 1, 3, and 4 after i.p. administration of the K^+-channel blocker 4-AP revealed no difference between $Ca_v2.3^{+/+}$ and $Ca_v2.3^{-/-}$ mice. However, latency to partial myoclonic activity (phase 2) was significantly reduced in $Ca_v2.3^{-/-}$ mice compared with controls (473.4 ± 23.9 s vs. 592.5 ± 32.6 s; $p = 0.0132$). Besides, no further differences in seizure parameters and lethality ($Ca_v2.3^{+/+}$: 50.0% vs. $Ca_v2.3^{-/-}$: 55.6%) could be detected.

Altered PTZ seizure susceptibility in $Ca_v2.3^{-/-}$ mice

$Ca_v2.3$-deficient mice were shown to be more resistant to seizures induced by the chemoconvulsant PTZ, which impairs γ-aminobutyric acid $(GABA)_A$ neurotransmission. In particular, $Ca_v2.3^{-/-}$ mice exhibited a significantly lower lethality after s.c. administration of 80 mg/kg PTZ combined with a significant reduction of phase 4 latency, duration, and frequency (Table 1). This phenomenon seems to be independent of animal gender, as additional lethality analysis in female $Ca_v2.3^{-/-}$ mice confirmed reduced PTZ sensitivity (20%; n = 5) compared with female $Ca_v2.3^{+/+}$ mice (100%; n = 4). These data also suggest that PTZ lethality is slightly increased in females. No difference between both genotypes was observed for the various generalized myoclonic phases

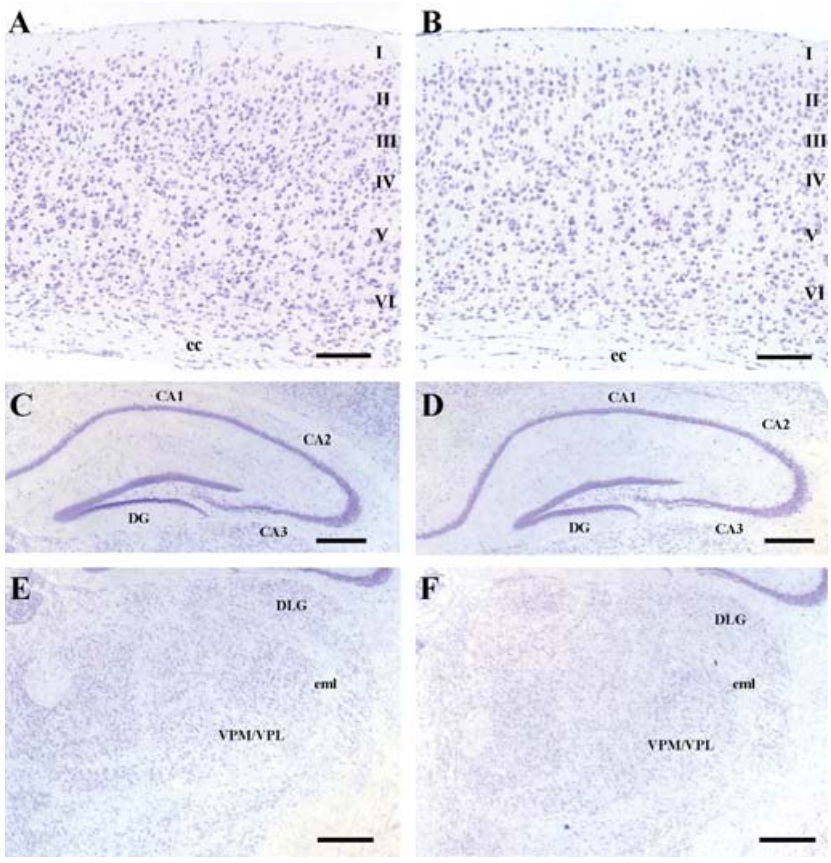

FIG. 3. Histochemical characterization of mouse brains from $Ca_v2.3^{+/+}$ (left) and $Ca_v2.3^{-/-}$ mice (right) by using Nissl staining. **A**, **B**: Neocortical segment of the primary somatosensory cortex (trunk region/barrel field). Cortical layers are indicated: I, molecular layer; II, external granular layer; III, external pyramidal layer; IV, internal granular layer; V, internal pyramidal layer; VI, multiform polymorphic layer; ec, external capsule; bar: 200 μm. **C**, **D**: Hippocampus; DG, dentate gyrus; bar: 400 μm. **E**, **F**: Thalamus; eml, external medullary lamina; DLG, dorsal lateral geniculate nucleus; VPL/VPM, ventral posterolateral/medial nucleus; bar: 400 μm.

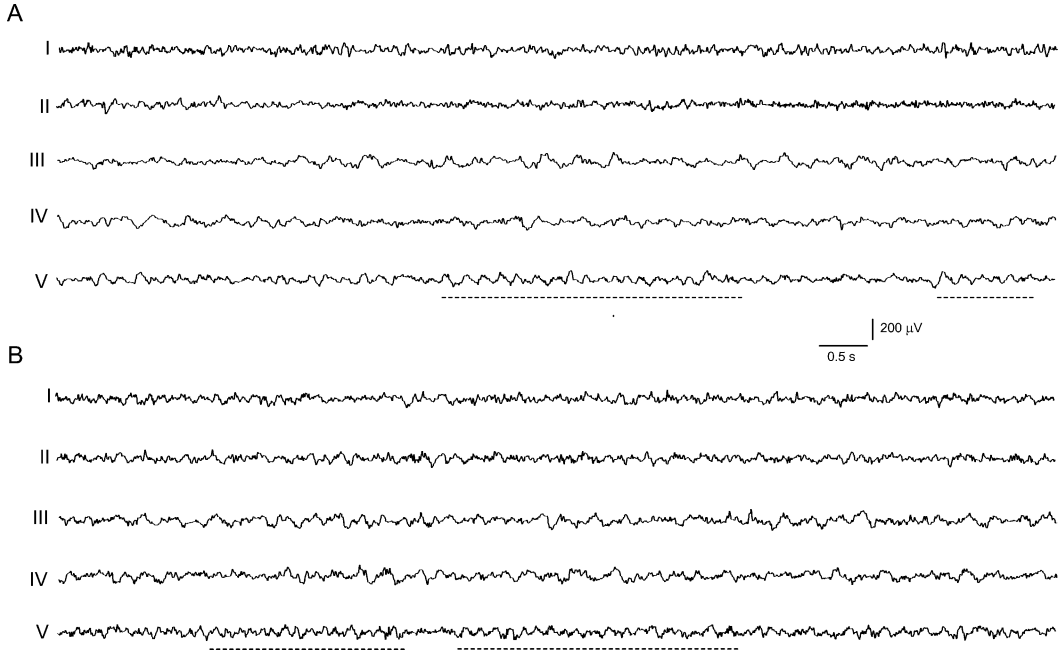

FIG. 4. Electrocorticographic (ECoG) and deep intracerebral recordings from C57Bl/6 control mice **(A)** and $Ca_v2.3$-deficient animals **(B)** (I-II: ECoGs, III: deep intrahippocampal recordings (CA3), IV-V: deep recordings after induction of exploratory behavior). No EEG abnormalities are detectable in $Ca_v2.3^{fl/fl,cre}$ or $Ca_v2.3^{fl/fl,nestin-cre-}$ control mice ($\mathbf{A}_{I-V}$). Generalized $Ca_v2.3^{-/-}$ mice ($Ca_v2.3^{fl/fl,cre+}$) did not exhibit epileptiform discharges in ECoG recordings ($\mathbf{B}_{I-II}$), nor did brain-specific $Ca_v2.3$-inactivated animals ($Ca_v2.3^{fl/fl,nestin-cre+}$, $\mathbf{B}_{III}$) in deep recordings during long-term observation. After induction of exploratory behavior (changing cages), both controls ($\mathbf{A}_{IV-V}$) and brain-specific $Ca_v2.3^{-/-}$ mice exhibit marked theta-wave activity (*dashed lines*).

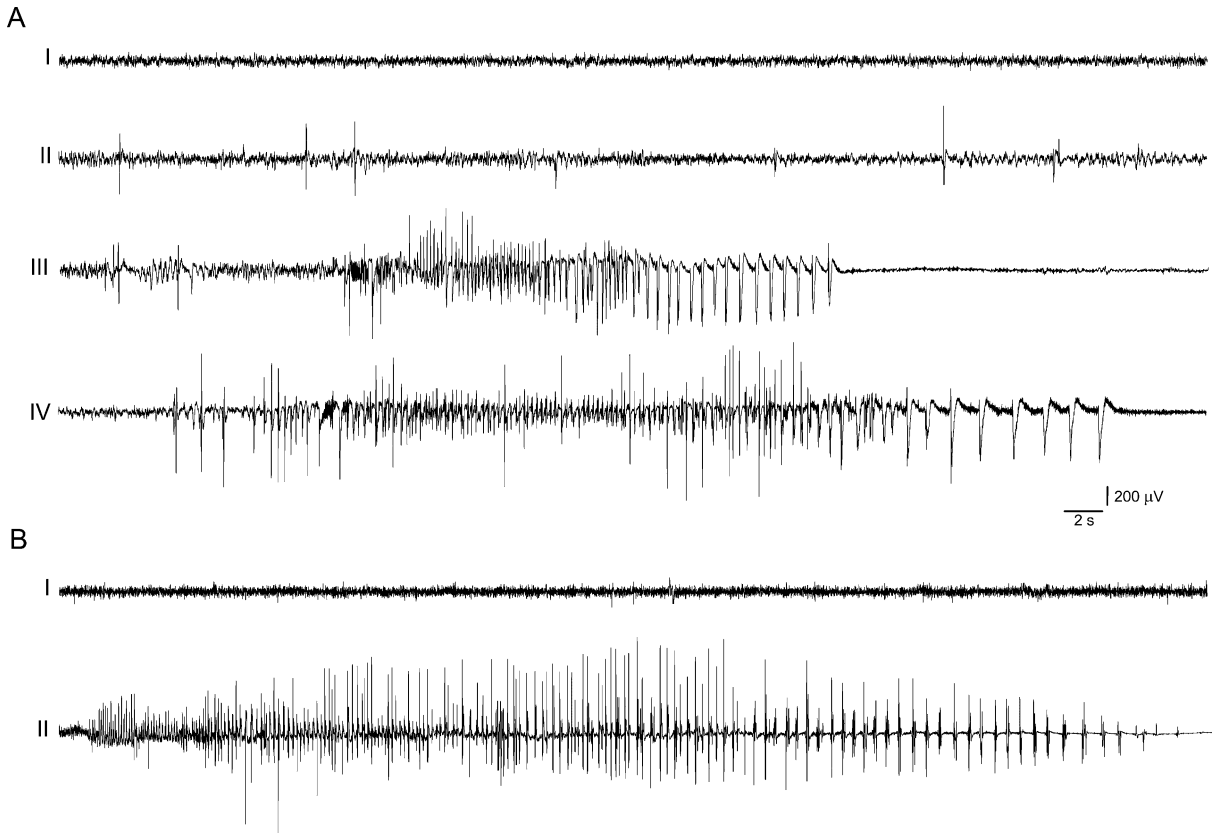

FIG. 5. Electrocorticographic (ECoG) characteristics after administration of pentylenetetrazol ($\mathbf{A}_{I-IV}$) and 4-aminopyridine ($\mathbf{B}_{I-II}$) in C57Bl/6 control mice. No ictal discharges are recorded during the hypoactive stage ($\mathbf{A}_{I}$). Phase 2 is characterized by repetitive occurrence of single spikes ($\mathbf{A}_{II}$) that correlate with whole-body twitching (confirmed by simultaneous Video–ECoG–EMG recordings using the F20-EET transmitter (DSI, not shown). Finally, single spiking gains frequency evolving into a generalized myoclonus (phase 3, $\mathbf{A}_{III}$) characterized by continuous trains of spikes and/or spike–waves. If seizure activity exhibits maximal spread, a generalized tonic–clonic event occurs (phase 4, $\mathbf{A}_{IV}$), causing death in most cases due to respiratory insufficiency. Although PTZ– and 4-AP–treated mice pass through the similar seizure stages, ECoG did not show prominent spike activity in stage 1–3 ($\mathbf{B}_{I}$), but only during maximal generalized clonic–tonic seizure activity (stage 4, $\mathbf{B}_{II}$).

(3a–b), although the number of $Ca_v2.3$-deficient mice exhibiting phases 3a and 3b was reduced compared with controls and close to significance. Interestingly, control animals as well as $Ca_v2.3$-deficient mice did not display isolated phase 3c events. However, seven of 10 controls entered generalized tonic–clonic seizures with tonic extension of hindlimbs via phase 3c, suggesting that maximal epileptic excitatory progression is restricted in $Ca_v2.3^{-/-}$ mice (Table 1). In contrast, whole-body twitchings, which were perceived to correlate with isolated cortical spike activity by using simultaneous video-EEG-EMG monitoring (Fig. 6A–C), were significantly increased in $Ca_v2.3^{-/-}$ mice (148.1 ± 29.1 vs. 55.9 ± 7.9; $p = 0.0051$). This supports the observation that convulsive activity displays a higher degree of fragmentation in $Ca_v2.3$-deficient mice and therefore is less organized and continuous in generalized seizure stages of higher severity. Interestingly, similar to phase 2 results described earlier for 4-AP–induced seizures, latency to partial myoclonic activity was reduced in $Ca_v2.3$-inactivated animals compared with controls (202.4 ± 23.9 s vs. 280.8 ± 30.9 s), approaching significance ($p = 0.0681$)

DISCUSSION

Within recent years, the focus regarding the involvement of VGCCs in etiology and pathogenesis of epilepsies has been on the non–L-type $Ca_v2.1$ and the T-type $Ca_v3.2$ channel. However, increasing evidence suggests that the E/R-type calcium channel $Ca_v2.3$ also is of tremendous importance in both ictogenesis and propagation of epileptic discharges. In the present report, we have demonstrated that mice lacking the $Ca_v2.3$ VGCCs do not exhibit spontaneous epileptiform discharges and, in addition, are less susceptible to PTZ- induced convulsive seizure activity, whereas 4-AP sensitivity remained unchanged. This difference in seizure susceptibility is probably due to the different convulsive mechanisms of 4-AP and PTZ: the first enhancing synaptic transmission by reducing K^+ currents, whereas the latter serves as a $GABA_A$-receptor antagonist in various brain regions [e.g., the hippocampus (see later)]. As other VGCC expression is not significantly altered in $Ca_v2.3^{-/-}$ mice, reduced PTZ-seizure susceptibility is directly related to $Ca_v2.3$ ablation and not due to compensatory changes.

TABLE 1. *Effects of pentylenetetrazol (80 mg/kg s.c.) on the latency (L), duration (D), and frequency (F, for complete observation period) of the different seizure stages (phases 1–4)*

	$Ca_v2.3^{+/+}$	$Ca_v2.3^{-/-}$	
Hypoactivity (phase 1)			
L1	175.9 ± 30.0	174.3 ± 21.9	ns
D1	286.1 ± 65.9	340.4 ± 76.9	ns
	9/10	9/9	p = 0.3428
Partial clonus (phase 2)			
L2	280.8 ± 30.9	202.4 ± 23.9	p = 0.0681[a]
	9/9	8/8	ns[b]
Generalized myoclonus (phase 3)			
L3a	509.60 ± 102.14	1,391.89 ± 328.91	p = 0.0158
L3b	762.10 ± 242.98	1,665.11 ± 334.03	p = 0.0405
L3c	2,540 ± 159.60	2459.11 ± 240.89	ns
D3a	34.50 ± 15.66	20.00 ± 8.87	ns
D3b	191.10 ± 128.97	14.33 ± 6.07	ns
D3c	8.10 ± 8.11	23.00 ± 23.00	ns
F3a	8.10 ± 2.11	5.67 ± 2.17	ns
	10/10	6/9	p = 0.0867[ab]
F3b	3.80 ± 1.04	3.22 ± 1.62	ns
	9/10	5/9	ns[b]
F3c	0.10 ± 0.10	0.11 ± 0.11	ns
	1/10	1/9	ns[b]
Tonic–clonic seizure (phase 4)			
L4	1,781.3 ± 187.7	2,700	p = 0.0002[c]
D4	39.7 ± 8.7	0	p = 0.0005[c]
F4	0.90 ± 0.18	0	p = 0.0002[c]
Hindlimb extension	7/10	0/9	p = 0.0024[b]
Lethality	7/10	0/9	p = 0.0024[b]
WBT	55.9 ± 7.9	148.1 ± 29.1	p = 0.0051

Time values (in seconds) are presented as mean ± SEM. WBT, whole-body twitchings. The p values <0.05 are considered significant; ns, not significant.

[a]Parameters approaching significance.

[b]Lethality and number of animals entering individual seizure stages were analyzed by using Fisher's exact probability test.

[c]No $Ca_v2.3^{-/-}$ mouse exhibited phase 4 and was therefore assigned a maximal latency and zero values for phase 4 duration and frequency.

However, as suggested by the widespread distribution of various $Ca_v2.3$ splice variants throughout the brain, its functional implications in ictogenesis/epileptogenesis and particularly seizure propagation might be more complex than actually expected. Three current aspects of epileptic functionality of $Ca_v2.3$ are discussed here.

First, mutations in the EFHC1 protein, an interaction partner of $Ca_v2.3$, were proven to cause JME in humans, as such mutations prevent EFHC1 from binding to and activating $Ca_v2.3$, which prohibits apoptosis (3). Consequently, an increased neuronal cell density is supposed to be responsible for the establishment of altered neuronal connectivity and hyperexcitable circuits. However, as depicted here, ablation of $Ca_v2.3$ provokes not hyperexcitability but rather a reduced sensitivity toward the epileptogenic drug PTZ. Therefore a reduced apoptosis during CNS ontogenesis cannot account for altered seizure susceptibility in $Ca_v2.3^{-/-}$ mice, indicating that as-yet unknown mechanisms might regulate apoptosis and trigger hyperexcitability in JME patients with EFHC1 mutations.

Second, GABAergic interneurons were shown to express $Ca_v2.3$ (this study, also see ref. 31) and are probably of high importance for GABA homeostasis and excitation–inhibition balance within the CNS. Consequently, diminished GABAergic neurotransmission in the cortex results in the emergence of epileptiform activity (45). Besides $GABA_B$-receptor–mediated effects, inhibitory action of GABA can basically occur via postsynaptic $GABA_A$-receptor stimulation, exhibiting phasic inhibition, or via peri- or extrasynaptic $GABA_A$ receptors exerting tonic inhibition (46). The tonic inhibition is based on ambient GABA probably released by GABA transporters (47). Interestingly, expression studies in cultured mouse cortical GABAergic neurons have revealed that $Ca_v2.3$ is expressed on neuronal cell bodies and proximal dendrites, but not presynaptically (48,49); thus $Ca_v2.3$ may not be directly involved in vesicular GABA release. However, its somatodendritic expression pattern points to a role in the generation of conducted calcium action potentials and local calcium signals and may thereby exert indirect functions on GABA release. Its influence on ambient GABA and tonic inhibition is to some extent speculative, although astrocytes, which strongly support tonic inhibition, display a strong expression of R-type calcium current (50). Expression of $Ca_v2.3$ within the RTN, which is part of the thalamocortical–corticothalamic circuitry, also

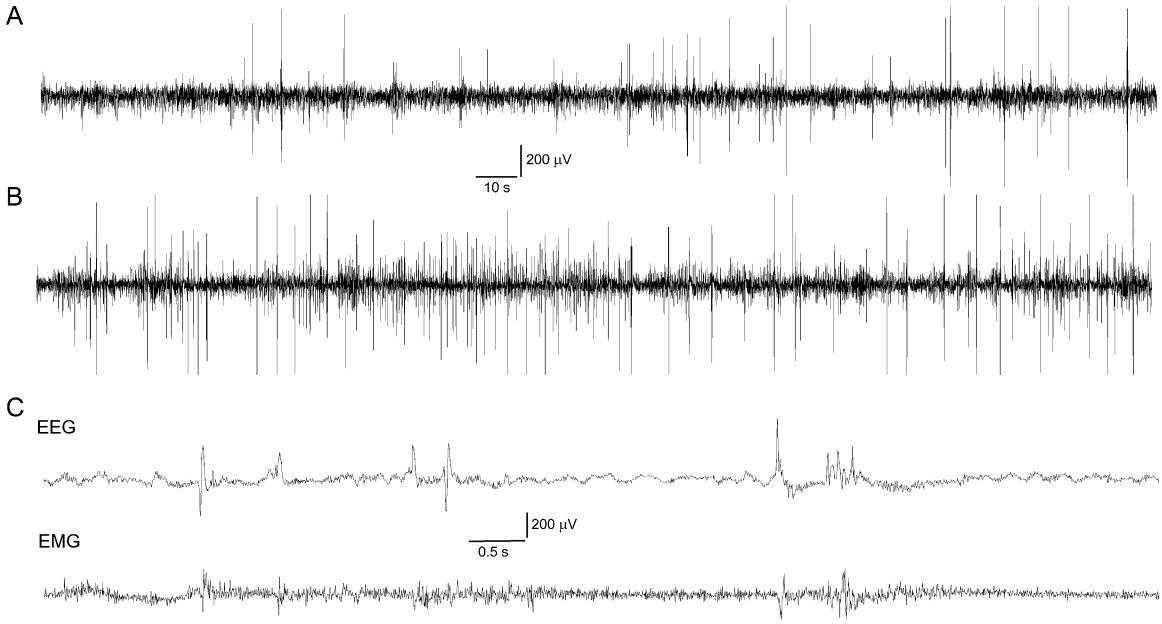

FIG. 6. Isolated spike activity in electrocorticograms (ECoGs) from $Ca_v2.3^{+/+}$ and $Ca_v2.3^{-/-}$ mice after PTZ administration, and its relation to simultaneous EMG recordings. **A**: ECoGs from $Ca_v2.3^{+/+}$ mice. **B**: ECoGs from $Ca_v2.3^{-/-}$ mice. Note: whole-body twitching (spike activity) was shown to be significantly increased in $Ca_v2.3$-deficient mice compared with controls (**A**), suggesting that seizure activity is more disperse and less severe in $Ca_v2.3^{-/-}$ mice. **C**: Simultaneous video-EEG–EMG monitoring using an F20-EET transmitter (DSI) revealed that single-spike activity in surface EEG recordings (**C**, upper trace) correlates with whole-body twitching (see EMG, lower trace; recordings were obtained from a $Ca_v2.3^{-/-}$ mouse).

suggests a functional role in nonconvulsive seizure susceptibility and sleep homeostasis. The observation that $Ca_v2.3$ channels play a protective role in ischemic neuronal injury by a mechanism in which GABAergic neuronal actions are involved (51) further supports a functional involvement of $Ca_v2.3$ in the GABAergic neurotransmission. In addition, a number of antiepileptics, like sipatrigine 202W92, are neuroprotective under ischemic conditions (11,52), as well as TPM in several models of global and focal ischemia (53). Nevertheless, we are still lacking detailed information on $Ca_v2.3$ influence on GABA neurotransmission, and thus explanatory models for altered PTZ-seizure susceptibility remain speculative.

Recent data, however, point to an even more intriguing role of $Ca_v2.3$ in epileptogenesis. $Ca_v2.3$ VGCCs are widely expressed throughout the brain, including neocortical and striatal neurons (54), cerebellar granule neurons (55–58), and CA1 neurons in the hippocampus (55). In CA1 neurons, the distribution of R-type VGCCs is restricted to distal apical dendrites, and they were shown to be involved in dendritic burst firing (59,60). Lately it was demonstrated that muscarinic-receptor stimulation dramatically enhances R-type Ca^{2+} spikes in CA1 hippocampal neurons and that enhanced R-type Ca^{2+} spiking plays an important role in the generation of carbachol-induced oscillations, which resemble epileptiform activity in various animal models of epilepsy (19). In addition, R-type Ca^{2+} spikes contributed to the initiation of complex spikes during trains of action potentials, similar to those prominent during epileptiform bursting (61). Just recently, Metz et al. (33) showed that R-type calcium currents underlie ADPs in CA1 neurons and are important contributors to intrinsic burst activity. This phenomenon seems to be widespread, as $\leq$78% of pyramidal cells in the subiculum display ADPs and bursting activity (62,63). TPM was now found to reduce ictal-like activity based on PPs in CA1 neurons through a novel inhibitory action on R-type calcium channels (24). Interestingly, plateau potentials are not restricted to hippocampal neurons. Indeed, a plethora of other neuronal cell types exhibit this phenomenon, such as suprachiasmatic neurons of the hypothalamus (64), spinal interneurons (65), dorsal horn neurons (66,67), and striatal cholinergic neurons (68,69), in which $Ca_v2.3$ could exert similar functions. Thus removal of $GABA_A$- receptor inhibition by PTZ might trigger plateau potentials and afterdepolarizations in various brain regions and might therefore be responsible for reduced PTZ-seizure susceptibility in $Ca_v2.3^{-/-}$mice. This is further supported by the observation that $GABA_A$-receptor–mediated inhibition attenuates primary and secondary bursting within the hippocampus (61). In addition, preliminary data indicate that kainate seizure susceptibility is also significantly reduced in $Ca_v2.3^{-/-}$ mice (Weiergräber et al., unpublished data), supporting our hypothesis. Furthermore, increased latency data and altered, fragmented seizure architecture in $Ca_v2.3^{-/-}$ mice after PTZ administration point to a critical role of $Ca_v2.3$ in the propagation of epileptic discharges and seizure generalization.

4-AP, which enhances neurotransmission by presynaptic accumulation of Ca^{2+} via reduction of K^+ currents, probably exerts more-global effects on a huge variety of different neuronal cell populations and therefore did not reveal changes in seizure susceptibility between both genotypes.

Our findings, that $Ca_v2.3$ inactivated mice do not exhibit spontaneous epileptiform discharges and display reduced PTZ-seizure susceptibility, strongly support a functional role of $Ca_v2.3$ in seizure initiation and propagation (24). Thus $Ca_v2.3$ will serve as an important target for development of AEDs in the future.

Acknowledgment: We thank Mrs. Renate Clemens, Ms. Evelyn Süss, Ms. Claudia Zyntek, the animal keepers of the central facility, and Dr. W. Oswald for their excellent and permanent assistance. The work was financially supported by the Köln Fortune Program and the Center of Molecular Medicine Cologne (CMMC), both Faculty of Medicine, University of Cologne.

REFERENCES

1. Turnbull J, Lohi H, Kearney JA, et al. Sacred disease secrets revealed: the genetics of human epilepsy. *Hum Mol Genet* 2005.
2. Escayg A, De Waard M, Lee DD, et al. Coding and noncoding variation of the human calcium-channel beta4-subunit gene CACNB4 in patients with idiopathic generalized epilepsy and episodic ataxia. *Am J Hum Genet* 2000;66:1531–1539.
3. Suzuki T, Delgado-Escueta AV, Aguan K, et al. Mutations in EFHC1 cause juvenile myoclonic epilepsy. *Nat Genet* 2004;36:842–849.
4. Ophoff RA, Terwindt GM, Vergouwe MN, et al. Familial hemiplegic migraine and episodic ataxia type-2 are caused by mutations in the Ca2+ channel gene CACNL1A4. *Cell* 1996;87:543–552.
5. Jodice C, Mantuano E, Veneziano L, et al. Episodic ataxia type 2 (EA2) and spinocerebellar ataxia type 6 (SCA6) due to CAG repeat expansion in the CACNA1A gene on chromosome 19p. *Hum Mol Genet* 1997;6:1973–1978.
6. Chioza B, Wilkie H, Nashef L, et al. Association between the alpha(1a) calcium channel gene CACNA1A and idiopathic generalized epilepsy. *Neurology* 2001;56:1245–1246.
7. Chen Y, Lu J, Pan H, et al. Association between genetic variation of CACNA1H and childhood absence epilepsy. *Ann Neurol* 2003;54:239–243.
8. Vitko I, Chen Y, Arias JM, et al. Functional characterization and neuronal modeling of the effects of childhood absence epilepsy variants of CACNA1H, a T-type calcium channel. *J Neurosci* 2005;25:4844–4855.
9. Kito M, Maehara M, Watanabe K. Mechanisms of T-type calcium channel blockade by zonisamide. *Seizure* 1996;5:115–119.
10. Gomora JC, Daud AN, Weiergraber M, et al. Block of cloned human T-type calcium channels by succinimide antiepileptic drugs. *Mol Pharmacol* 2001;60:1121–1132.
11. Hainsworth AH, McNaughton NC, Pereverzev A, et al. Actions of sipatrigine, 202W92, and lamotrigine on R-type and T-type Ca2+ channel currents. *Eur J Pharmacol* 2003;467:77–80.
12. Soong TW, Stea A, Hodson CD, et al. Structure and functional expression of a member of the low voltage-activated calcium channel family. *Science* 1993;260:1133–1136.
13. Williams ME, Marubio LM, Deal CR, et al. Structure and functional characterization of neuronal α_{1E} calcium channel subtypes. *J Biol Chem* 1994;269:22347–22357.
14. Schneider T, Wei X, Olcese R, et al. Molecular analysis and functional expression of the human type E α1 subunit. *Receptors Channels* 1994;2:255–270.
15. Sochivko D, Pereverzev A, Smyth N, et al. α1E Calcium channel subunit underlies R-type calcium current in hippocampal and cortical pyramidal neurons. *J Physiol* 2002;542:699–710.
16. Sochivko D, Chen J, Becker A, et al. Blocker-resistant Ca2+ currents in rat CA1 hippocampal pyramidal neurons. *Neuroscience* 2003;116:629–638.
17. Magee JC, Johnston D. Characterization of single voltage-gated Na^+ and Ca^{2+} channels in apical dendrites of rat CA1 pyramidal neurons. *J Physiol (Lond)* 1995;487:67–90.
18. Magee JC, Carruth M. Dendritic voltage-gated ion channels regulate the action potential firing mode of hippocampal CA1 pyramidal neurons. *J Neurophysiol* 1999;82:1895–1901.
19. Williams JH, Kauer JA. Properties of carbachol-induced oscillatory activity in rat hippocampus. *J Neurophysiol* 1997;78:2631–2640.
20. Lee SC, Choi S, Lee T, et al. Molecular basis of R-type calcium channels in central amygdala neurons of the mouse. *Proc Natl Acad Sci U S A* 2002;99:3276–3281.
21. Saegusa H, Kurihara T, Zong SQ, et al. Altered pain responses in mice lacking α_{1E} subunit of the voltage-dependent Ca^{2+} channel. *Proc Natl Acad Sci U S A* 2000;97:6132–6137.
22. Dietrich D, Kirschstein T, Kukley M, et al. Functional specialization of presynaptic Cav2.3 Ca2+ channels. *Neuron* 2003;39:483–496.
23. Chen S, Ren YQ, Bing RJ, et al. Alpha 1E subunit of the R-type calcium channel is associated with myelinogenesis. *J Neurocytol* 2000;29:719–28.
24. Kuzmiski JB, Barr W, Zamponi GW, et al. Topiramate inhibits the initiation of plateau potentials in CA1 neurons by depressing R-type calcium channels. *Epilepsia* 2005;46:481–489.
25. Leach JP, Brodie MJ. New antiepileptic drugs: an explosion of activity. *Seizure* 1995;4:5–17.
26. De Borman B, Lakaye B, Minet A, et al. Expression of mRNA encoding alpha1E and alpha1G subunit in the brain of a rat model of absence epilepsy. *Neuroreport* 1999;10:569–574.
27. Lakaye B, Thomas E, Minet A, et al. The genetic absence epilepsy rat from Strasbourg (GAERS), a rat model of absence epilepsy: computer modeling and differential gene expression. *Epilepsia* 2002;43(suppl 5):123–129.
28. Cornwall J, Cooper JD, Phillipson OT. Projections to the rostral reticular thalamic nucleus in the rat. *Exp Brain Res* 1990;80:157–171.
29. Filakovszky J, Gerber K, Bagdy G. A serotonin-1A receptor agonist and an N-methyl-D-aspartate receptor antagonist oppose each others effects in a genetic rat epilepsy model. *Neurosci Lett* 1999;261:89–92.
30. Deransart C, Landwehrmeyer GB, Feuerstein TJ, et al. Upregulation of D3 dopaminergic receptor mRNA in the core of the nucleus accumbens accompanies the development of seizures in a genetic model of absence-epilepsy in the rat. *Brain Res Mol Brain Res* 2001;94:166–177.
31. van de Bovenkamp-Janssen MC, Scheenen WJ, Kuijpers-Kwant FJ, et al. Differential expression of high voltage-activated Ca2+ channel types in the rostral reticular thalamic nucleus of the absence epileptic WAG/Rij rat. *J Neurobiol* 2004;58:467–478.
32. Woermann FG, Free SL, Koepp MJ, et al. Abnormal cerebral structure in juvenile myoclonic epilepsy demonstrated with voxel-based analysis of MRI. *Brain* 1999;122:2101–2108.
33. Metz AE, Jarsky T, Martina M, et al. R-type calcium channels contribute to afterdepolarization and bursting in hippocampal CA1 pyramidal neurons. *J Neurosci* 2005;25:5763–5773.
34. Pereverzev A, Klöckner U, Henry M, et al. Structural diversity of the voltage-dependent Ca^{2+} channel α1E subunit. *Eur J Neurosci* 1998;10:916–925.
35. Vajna R, Schramm M, Pereverzev A, et al. New isoform of the neuronal Ca^{2+} channel α1E subunit in islets of Langerhans, and kidney: distribution of voltage-gated Ca^{2+} channel α1 subunits in cell lines and tissues. *Eur J Biochem* 1998;257:274–285.
36. Weiergräber M, Henry M, Südkamp M, et al. Ablation of $Ca_v2.3$/E-type voltage-gated calcium channel results in cardiac arrhythmia and altered autonomic control within the murine cardiovascular system. *Basic Res Cardiol* 2005;100:1–13.
37. Weiergräber M, Pereverzev A, Vajna R, et al. Immunodetection of α1E voltage-gated Ca^{2+} channel in chromogranin-positive muscle cells of rat heart, and in distal tubules of human kidney. *J Histochem Cytochem* 2000;48:807–819.
38. Grabsch H, Pereverzev A, Weiergräber M, et al. Immunohistochemical detection of α1E voltage-gated Ca^{2+} channel isoforms in

cerebellum, INS-1 cells, and neuroendocrine cells of the digestive system. *J Histochem Cytochem* 1999;47:981–993.
39. Tronche F, Kellendonk C, Kretz O, et al. Disruption of the glucocorticoid receptor gene in the nervous system results in reduced anxiety. *Nat Genet* 1999;23:99–103.
40. Pereverzev A, Mikhna M, Vajna R, et al. Disturbances in glucose-tolerance, insulin-release and stress-induced hyperglycemia upon disruption of the Cav2.3 (α1E) subunit of voltage-gated Ca2+ channels. *Mol Endocrinol* 2002;16:884–895.
41. Weiergräber M, Henry M, Hescheler J, et al. Electrocorticographic and deep intracerebral EEG recording in mice using a telemetry system. *Brain Res Brain Res Protoc* 2005;14:154–164.
42. Ferraro TN, Golden GT, Smith GG, et al. Mapping loci for pentylenetetrazol-induced seizure susceptibility in mice. *J Neurosci* 1999;19:6733–6739.
43. Pereverzev A, Leroy J, Krieger A, et al. Alternate splicing in the cytosolic II-III loop and the carboxy terminus of human E-type voltage-gated Ca^{2+} channels: electrophysiological characterization of isoforms. *Mol Cell Neurosci* 2002;21:352–365.
44. Kramer K, Kinter LB. Evaluation and applications of radiotelemetry in small laboratory animals. *Physiol Genomics* 2003;13:197–205.
45. Jacobs KM, Donoghue JP. Reshaping the cortical motor map by unmasking latent intracortical connections. *Science* 1991;251:944–947.
46. Richerson GB. Looking for GABA in all the wrong places: the relevance of extrasynaptic GABA(A) receptors to epilepsy. *Epilepsy Curr* 2004;4:239–242.
47. Richerson GB, Wu Y. Role of the GABA transporter in epilepsy. *Adv Exp Med Biol* 2004;548:76–91.
48. Rhee JS, Ishibashi H, Akaike N. Calcium channels in the GABAergic presynaptic nerve terminals projecting to Meynert neurons of the rat. *J Neurochem* 1999;72:800–807.
49. Timmermann DB, Westenbroek RE, Schousboe A, et al. Distribution of high-voltage-activated calcium channels in cultured gamma-aminobutyric acidergic neurons from mouse cerebral cortex. *J Neurosci Res* 2002;67:48–61.
50. Latour I, Hamid J, Beedle AM, et al. Expression of voltage-gated Ca2+ channel subtypes in cultured astrocytes. *GLIA* 2003;41:347–353.
51. Toriyama H, Wang L, Saegusa H, et al. Role of Ca(v) 2.3 (alpha1E) Ca^{2+} channel in ischemic neuronal injury. *Neuroreport* 2002;13:261–265.
52. Caputi L, Hainsworth AH, Lavaroni F, et al. Neuroprotective actions in vivo and electrophysiological actions in vitro of 202W92. *Brain Res* 2001;919:259–268.
53. Edmonds HL Jr, Jiang YD, Zhang PY, et al. Topiramate as a neuroprotectant in a rat model of global ischemia-induced neurodegeneration. *Life Sci* 2001;69:2265–2277.
54. Foehring RC, Mermelstein PG, Song WJ, et al. Unique properties of R-type calcium currents in neocortical and neostriatal neurons. *J Neurophysiol* 2000;84:2225–2236.
55. Ishibashi H, Rhee JS, Akaike N. Regional difference of high voltage-activated Ca^{2+} channels in rat CNS neurones. *Neuroreport* 1995;6:1621–1624.
56. Forti L, Tottene A, Moretti A, et al. Three novel types of voltage-dependent calcium channels in rat cerebellar neurons. *J Neurosci* 1994;14:5243–5256.
57. Tottene A, Moretti A, Pietrobon D. Functional diversity of P-type and R-type calcium channels in rat cerebellar neurons. *J Neurosci* 1996;16:6353–6363.
58. Tottene A, Volsen S, Pietrobon D. alpha1E subunits form the pore of three cerebellar R-type calcium channels with different pharmacological and permeation properties. *J Neurosci* 2000;20:171–178.
59. Magee JC, Johnston D. Synaptic activation of voltage-gated channels in the dendrites of hippocampal pyramidal neurons. *Science* 1995;268:301–304.
60. Magee JC. Dendritic integration of excitatory synaptic input. *Nat Rev Neurosci* 2000;1:181–190.
61. McCormick DA, Contreras D. On the cellular and network bases of epileptic seizures. *Annu Rev Physiol* 2001;63:815–846.
62. Staff NP, Jung HY, Thiagarajan T, et al. Resting and active properties of pyramidal neurons in subiculum and CA1 of rat hippocampus. *J Neurophysiol* 2000;84:2398–2408.
63. Jung HY, Staff NP, Spruston N. Action potential bursting in subicular pyramidal neurons is driven by a calcium tail current. *J Neurosci* 2001;21:3312–3321.
64. Pierson PM, Liu X, Raggenbass M. Suppression of potassium channels elicits calcium-dependent plateau potentials in suprachiasmatic neurons of the rat. *Brain Res* 2005;1036:50–59.
65. Hounsgaard J, Kjaerulff O. Ca2+-mediated plateau potentials in a subpopulation of interneurons in the ventral horn of the turtle spinal cord. *Eur J Neurosci* 1992;4:183–188.
66. Russo RE, Nagy F, Hounsgaard J. Modulation of plateau properties in dorsal horn neurones in a slice preparation of the turtle spinal cord. *J Physiol* 1997;499:459–474.
67. Morisset V, Nagy F. Ionic basis for plateau potentials in deep dorsal horn neurons of the rat spinal cord. *J Neurosci* 1999;19:7309–7316.
68. Dunia R, Buckwalter G, Defazio T, et al. Decreased duration of Ca(2+)-mediated plateau potentials in striatal neurons from aged rats. *J Neurophysiol* 1996;76:2353–2363.
69. Pisani A, Bonsi P, Catania MV, Metabotropic glutamate 2 receptors modulate synaptic inputs and calcium signals in striatal cholinergic interneurons. *J Neurosci* 2002;22:6176–6185.

J Neurophysiol 97: 3660–3669, 2007.
First published March 21, 2007; doi:10.1152/jn.01193.2006.

Hippocampal Seizure Resistance and Reduced Neuronal Excitotoxicity in Mice Lacking the $Ca_v2.3$ E/R-Type Voltage-Gated Calcium Channel

Marco Weiergräber,[1,2] Margit Henry,[1] Kayalvizhi Radhakrishnan,[1,2] Jürgen Hescheler,[1,2] and Toni Schneider[1,2]
[1]*Institute of Neurophysiology and* [2]*Center of Molecular Medicine Cologne, University of Cologne, Cologne, Germany*

Submitted 10 November 2006; accepted in final form 13 March 2007

Weiergräber M, Henry M, Radhakrishnan K, Hescheler J, Schneider T. Hippocampal seizure resistance and reduced neuronal excitotoxicity in mice lacking the $Ca_v2.3$ E/R-type voltage-gated calcium channel. *J Neurophysiol* 97: 3660–3669, 2007. First published March 21, 2007; doi:10.1152/jn.01193.2006. Voltage-gated calcium channels are key components in the etiology and pathogenesis of epilepsies. Former studies mainly focused on P/Q-type $Ca_v2.1$ and T-type $Ca_v3.2$ Ca^{2+} channels involved in absence epileptogenesis, but recent findings also point to an intriguing role of the $Ca_v2.3$ E/R-type Ca^{2+} channel in ictogenesis and seizure propagation. Based on the observation that $Ca_v2.3$ is thought to induce plateau potentials in CA1 pyramidal cells, which can trigger epileptiform activity, our recent investigation revealed reduced PTZ-seizure susceptibility and altered seizure architecture in $Ca_v2.3^{-/-}$ mice compared with controls. In the present study we tested hippocampal seizure susceptibility in $Ca_v2.3$-deficient mice using surface and deep intrahippocampal telemetric EEG recordings as well as phenotypic seizure video analysis. Administration of kainic acid (30 mg/kg ip) revealed clear alteration in behavioral seizure architecture and dramatic resistance to limbic seizures in $Ca_v2.3^{-/-}$ mice compared with controls, whereas no difference in hippocampal EEG seizure activity between both genotypes could be detected at this suprathreshold dosage. The same tendency was observed for NMDA seizure susceptibility (150 mg/kg ip) approaching the level of significance. In addition, histochemical analysis within the hippocampus revealed that excitotoxic effects after kainic acid administration are absent in $Ca_v2.3^{-/-}$ mice, whereas $Ca_v2.3^{+/+}$ animals exhibited clear and typical signs of excitotoxic cell death. These findings clearly indicate that the $Ca_v2.3$ voltage-gated calcium channel plays a crucial role in both hippocampal ictogenesis and seizure generalization and is of central importance in neuronal degeneration after excitotoxic events.

INTRODUCTION

Voltage-gated calcium channels (VGCCs) are of tremendous importance in etiology and pathogenesis of various forms of epilepsies capable of modulating seizure initiation, propagation, termination, and kindling (Khosravani and Zamponi 2006; McKeown et al. 2006; Remy and Beck 2006). Interestingly, only a restricted number of these channels has been directly associated with epileptic disorders in humans and animal models so far, including $Ca_v2.1$ and $Ca_v3.2$ (Khosravani and Zamponi 2006). Recently, however, it turned out that the $Ca_v2.3$ E/R-type VGCC also harbors a potential proictogenic/proepileptogenic capacity that has been underestimated for a long time (Tai et al. 2006; Weiergräber et al. 2006a,b). Being resistant to most other VGCC antagonists, such as dihydropyridines (DHPs), ω-conotoxin GVIA, ω-conotoxin MVIIC, and ω-agatoxin IVA (Catterall et al. 2005), $Ca_v2.3$ E/R-type VGCCs exhibit a significant sensitivity toward Ni^{2+} (IC_{50} = 30 μM) (Schneider et al. 1994; Tottene et al. 2000) and the tarantula toxin SNX-482 (IC_{50} = 15–30 nM) (Newcomb et al. 1998).

Recent findings in hippocampal CA1 neurons elucidated that R-type channels can trigger epileptiform activity by contributing to plateau potentials after cholinergic stimulation (Kuzmiski et al. 2005; Tai et al. 2006). Muscarinic activation by M_1/M_3-cholinergic receptors was shown to enhance both $Ca_v2.3$ and R-type currents (Bannister et al. 2004; Melliti et al. 2000; Meza et al. 1999), but not T-type Ca^{2+} currents in rat hippocampal CA1 pyramidal neurons after P/Q-, N-, and L-type Ca^{2+} currents were selectively blocked (Tai et al. 2006). This muscarinic stimulation (e.g., using carbachol) is capable of inducing plateau potentials on the cellular level by $G\alpha_{q/11}$ and protein kinase C (PKC) but also theta bursts in extracellular recordings from the CA1 region (Tai et al. 2006). The epileptogenic capacity of $Ca_v2.3$ in triggering hippocampal seizure activity is further supported by the observation that M_1 receptor knockout mice exhibit decreased seizure susceptibility after pilocarpine administration (Hamilton et al. 1997).

Interestingly, R-type Ca^{2+} channels exhibit a complex functional modulation based on internal Ca^{2+} levels and PKC-mediated phosphorylation. At lower cytosolic Ca^{2+} concentrations, a positive feedback mechanism, which includes activation through PKC, slows down inactivation and speeds up recovery from short-term inactivation (Klöckner et al. 2004; Leroy et al. 2003). Also, the pattern of $Ca_v2.3$ splice variant distribution in different brain regions is important for neuronal mechanisms underlying ictogenesis, seizure propagation, but also neuroprotection (Weiergräber et al. 2006a). In concordance with these findings, recent electroencephalographic characterization of $Ca_v2.3$-inactivated mice exhibited no indications of spontaneous epileptiform graphoelements. In contrast, pentylenetetrazol (PTZ)-seizure susceptibility was reduced and seizure architecture exhibited appreciable alterations in $Ca_v2.3^{-/-}$ mice compared with controls, supporting a proconvulsive capacity of $Ca_v2.3$ (Weiergräber et al. 2006a,b).

Given its contribution to plateau potential generation in CA1 hippocampal neurons capable of triggering epileptiform activity, we investigated the role of $Ca_v2.3$ in hippocampal seizure susceptibility and seizure architecture by means of electroencephalography (EEG) and behavioral analysis in both $Ca_v2.3^{+/+}$ and $Ca_v2.3^{-/-}$ mice using kainic acid (KA) and *N*-methyl-D-aspartate (NMDA). We further performed histo-

Address for reprint requests and other correspondence: M. Weiergräber, Institute of Neurophysiology and Center of Molecular Medicine Cologne (CMMC), Robert-Koch-Str. 39, D-50931 Cologne, Germany (E-mail: akp74@uni-koeln.de).

The costs of publication of this article were defrayed in part by the payment of page charges. The article must therefore be hereby marked "*advertisement*" in accordance with 18 U.S.C. Section 1734 solely to indicate this fact.

logical analysis to unravel differences in hippocampal excitotoxicity. Our results demonstrate that $Ca_v2.3^{-/-}$ mice exhibit a pronounced resistance to hippocampal seizures and reduced excitotoxicity.

METHODS

Study animals

Generation of the $Ca_v2.3$ null mutant, which was backcrossed into C57Bl/6, was previously described in detail (Pereverzev et al. 2002; Weiergräber et al. 2006a). $Ca_v2.3$-deficient and control mice (with identical genetic backgrounds) from both genders were used in this study. Mice were housed in makrolon cages type II and maintained on a conventional 12-h light/dark cycle with food and water available without restriction. All animal experimentation was approved by the local institutional committee on animal care.

Hippocampal seizure-susceptibility testing: experimental design

Kainic acid (KA) and NMDA (both from Sigma, Munich, Germany) were freshly dissolved in physiological 0.9% NaCl before injection. Each animal was isolated for ≥30 min before administration of convulsants.

Kainic acid–induced hippocampal seizures

The non-NMDA receptor agonist KA was administered intraperitoneally (ip) to $Ca_v2.3^{+/+}$ ($n = 18$; 24.0 ± 0.7 g; 16.1 ± 0.8 wk) and $Ca_v2.3^{-/-}$ mice ($n = 18$; 25.5 ± 1.1 g; 22.9 ± 1.5 wk) at a dose of 30 mg/kg. Genders were exactly balanced with nine ♂ and nine ♀ in each study group. After injection animals were immediately placed back into their home cage, observed, and videomonitored for 2 h. Administration of KA causes a well-characterized hippocampal seizure syndrome that was analyzed according to a slightly modified seizure score from Baran et al. 1994: *stage 1*, no behavioral change; *stage 2*, facial clonus; *stage 3*, forlimb clonus; *stage 4*, rearing; *stage 5*, falling; *stage 6*, status epilepticus; *stage 7a*, jumping, tonic seizure <30 s; *stage 7b*, jumping, tonic seizure 30–60 s; *stage 8*, maximum generalized seizure activity, respiratory arrest, and death.

NMDA-induced hippocampal seizures

Seizures were induced by ip administration of NMDA at a dose of 150 mg/kg. Twenty $Ca_v2.3^{+/+}$ (21.7 ± 0.8 g; 18.1 ± 1.9 wk) and 20 $Ca_v2.3^{-/-}$ (23.4 ± 0.9 g; 16.4 ± 1.2 wk) mice were used in this study and videomonitored for 2 h after injection. Genders were again balanced with seven ♂ and 13 ♀ in each population. In NMDA-treated mice, seizures developed through a sequence of paroxysmal scratching, hypermotility and circling, tonic–clonic convulsions, and, occasionally, death. The following semiquantitative scale was used for the examination of seizure severity slightly modified according to Marganella et al. 2005: *stage 0*, no response; *stage 1*, excessive grooming and paroxysmal scratching; *stage 2*, mild hypermotility; *stage 3*, extensive hypermotility and circling; *stage 4*, forepaw clonus and tail hypertonus; *stage 5*, generalized tonic–clonic convulsions; *stage 6*, status epilepticus; *stage 7*, death.

Collecting data for seizure-susceptibility analysis

Latencies were calculated as the time from injection of KA and NMDA to the first observation of the individual seizure phase. If animals did not undergo a specific seizure phase during the observation period, it was assigned a latency of 120 min for both substances. In addition, the frequencies with which an animal entered the various phases during the observation period were also counted. Time points and frequencies were noted on-line and rechecked using mouse video recordings.

Telemetric surface and intrahippocampal EEG recordings

Both TA10ETA-F20 and TL11M2-F20-EET transmitters (DSI, St. Paul, MN) were used for electrocorticographic and deep intrahippocampal EEG recordings in $Ca_v2.3^{+/+}$ and $Ca_v2.3^{-/-}$ mice. The telemetry system, implantation procedure, and postoperative treatment were previously described in detail (Weiergräber et al. 2005).

SURFACE ELECTRODE IMPLANTATION (ELECTROCORTICOGRAM, ECOG). Epidural leads were positioned at the border of primary to secondary motor cortex (M_1/M_2) at the following stereotaxic coordinates: (+)-lead, bregma +1 mm, lateral of bregma 1 mm (left hemisphere); (−)-lead, bregma +1 mm, lateral of bregma 1 mm (right hemisphere) and fixed at the neurocranium using dental cement.

INTRACEREBRAL ELECTRODE IMPLANTATION. For deep intrahippocampal recordings targeting the CA1 region electrodes were positioned as follows: (+)-lead, bregma −2 mm, lateral of bregma 1.5 mm (left hemisphere), dorsoventral (depth) 1.3 mm; (−)-lead, bregma −2 mm, lateral of bregma 1.5 mm (right hemisphere); dorsoventral 1.3 mm. In total, nine $Ca_v2.3^{+/+}$ (28.0 ± 0.8 g, 17.5 ± 1.7 wk, all ♂) and nine $Ca_v2.3^{-/-}$ mice (28.8 ± 1.2 g, 20.1 ± 1.6 wk, all ♂) were analyzed that did not belong to the behavioral study groups. After recovery (7–10 days post-implantation) animals were administered KA at 10 mg/kg ip ($n = 3$ for each genotype) and 30 mg/kg ip ($n = 6$ for each genotype) and EEGs recorded for ≥2 h. In addition, daily recordings (minimum 1 h) were carried out in controls for 1 wk after injection.

Brain histology and histochemistry

Brains from KA (30 mg/kg ip) treated $Ca_v2.3^{+/+}$ ($n = 3$, all ♂) and $Ca_v2.3^{-/-}$ ($n = 3$, all ♂) mice were exstirpated 7 days post-injection and fixed in 4% formaldehyde. Hippocampal sections (bregma: −1.7 mm) were analyzed for KA-induced excitotoxic effects using standard hematoxylin-eosin (HE) and Nissl-staining.

Statistical analysis

To acquire and analyze EEG data, the Dataquest A.R.T. 3.1 software (DSI) was used. EEG recordings were obtained as outlined earlier. In addition long-term deep intrahippocampal EEG recordings (>24 h) were performed 7–10 days post-surgery. EEG activity was sampled at 1,000 Hz with no filter cutoff. Absolute power spectrum density (PSD, mV^2/Hz) was calculated from 5-min segments using the periodogram function (FFT based with Hanning windowing method). Frequency ranges were defined as follows: sub-δ (0–1 Hz), δ (1–4 Hz), θ (4–8 Hz), α (8–12 Hz), β (12–32 Hz), γ (32–50 Hz). All data were calculated and displayed as the means ± SE. Statistical comparison of categorical variables (e.g., occurrence of seizure stages, lethality) was performed using Fisher's exact probability test (two-tailed), whereas continuous variables (e.g., seizure latencies, frequencies) were analyzed using the parametric Student's *t*-test, considering $P < 0.05$ as significant.

RESULTS

Hippocampal KA seizure susceptibility in $Ca_v2.3$-deficient and control mice

Analysis of $Ca_v2.3^{+/+}$ and $Ca_v2.3^{-/-}$ mice after KA administration revealed a complex alteration in behavioral seizure architecture with $Ca_v2.3$-deficient animals exhibiting pro-

nounced seizure resistance (Table 1). The most prominent observation is that a significantly higher number of control mice exhibit severe status epilepticus (56.3 vs. 0%; $P = 0.0017$) and maximum generalized seizure activity associated with death (50 vs. 0%; $P = 0.0010$) compared with $Ca_v2.3$-deficient animals. This is concomitant with a significant reduction in stage 6 and stage 8 frequency and increase in latency for controls (Table 1A). Furthermore, stage 5 latency was significantly increased but frequency nonsignificantly reduced in $Ca_v2.3^{-/-}$ mice. No difference was observed between the two genotypes for both generalized seizure stages (stages 7a and 7b) characterized by jumping and tonic events except an increase in stage 7a frequency in $Ca_v2.3^{-/-}$ mice. Interestingly, some parameters of lower seizure severity (e.g., stage 2 and 3 frequency) were significantly increased in $Ca_v2.3^{-/-}$ mice similar to results obtained previously (Weiergräber et al. 2006a). However, similar to our prior studies using PTZ and 4-AP, KA-induced seizure severity is clearly reduced in $Ca_v2.3$-deficient mice (Table 1A). In particular, results from stages 6 and 8 point to a functional role of $Ca_v2.3$ in seizure perturbation and generalization.

Parameters known to affect seizure susceptibility (e.g., age and body weight) were approximated at the best possible rate and genders were exactly balanced. Although KA but not NMDA study groups differed significantly in age ($P = 0.0003$ and $P = 0.4547$, respectively) there is no information given in the literature that such minor differences (6–7 wk) cause significant alterations in seizure susceptibility. We strictly avoided to use inappropriately aged animals (juvenile <3 wk and old mice >1 yr). In our study KA-induced lethality was slightly higher in male compared with female controls (55.6 vs. 44.4%), similar to results obtained in rats (Mejias-Aponte et al. 2002), although not reaching level of significance.

Hippocampal NMDA seizure susceptibility in $Ca_v2.3$-deficient and control mice

NMDA seizure analysis of 20 controls and 20 $Ca_v2.3^{-/-}$ mice revealed a tendency similar to that observed for KA. Again, $Ca_v2.3^{-/-}$ mice exhibited reduced seizure susceptibility, particularly to stages of higher seizure severity. The survival rate of $Ca_v2.3$-deficient mice was 90%, but only 60% in control animals not reaching the level of significance ($P = 0.0648$). In addition, occurrence of generalized tonic–clonic convulsions and status epilepticus are also reduced in $Ca_v2.3^{-/-}$ mice close to the level of significance (Table 1B). Latency data for stages 5–7 are also increased in knockouts, although not significantly. It is also worthwhile to note that lethality in female $Ca_v2.3^{+/+}$ mice was higher compared with males (46.2 vs. 28.6%), although not significant ($P = 0.6424$).

Electrocorticogram (ECoG) and deep intracerebral EEG recordings after KA administration

Analysis of deep intrahippocampal long-term EEG recordings from the CA1 region of both $Ca_v2.3^{+/+}$ and $Ca_v2.3^{-/-}$ mice did not reveal any spontaneous ictal-like discharges that are indicative of limbic seizure activity (Fig. 1, *A* and *B*). Because seizure-susceptibility studies (see above) were carried out at 30 mg/kg to obtain behavioral phenomena, subsequent EEG recordings were also performed at that dosage (Figs. 1, *C–F* and 2, *A* and *B*). Initially, pilot studies were carried out to validate that intrahippocampal EEG recordings can be reliably distinguished from cortical EEG activity after KA administration by simultaneous recordings from the CA1 and M1/M2 region using a TL11M2-F20-EET transmitter (Fig. 2*B*). Unlike PTZ-induced seizure activity (Weiergräber et al. 2006a), we did not observe any indications of altered KA-induced seizure architecture. Analysis of ictal episode duration in $Ca_v2.3^{+/+}$ (7.1 ± 2.3 min, $n = 6$) and $Ca_v2.3^{-/-}$ mice (6.5 ± 1.6 min, $P = 0.8174$, $n = 6$) did not reveal any difference (Fig. 3*A*) and similar results were obtained for interictal phases (3.9 ± 0.4 vs. 2.5 ± 0.7 min, $P = 0.0868$, $n = 6$, Fig. 3*B*). As depicted in Fig. 2, *A* and *B* both controls and $Ca_v2.3$-deficient mice exhibit contiguous spike and spike-wave activity throughout the 2-h observation period. This epileptic activity is within the delta- and theta-wave range (1–8 Hz), as confirmed by power spectrum analysis. At 30 and 10 mg/kg KA, no major differences in hippocampal seizure activity could be detected between both genotypes (Figs. 2 and 3). PSD analysis of ictal episodes (30 s) did not reveal any differences between both genotypes (Fig. 3*C*). Although analysis of the entire 2-h EEG recording period after KA (30 mg/kg) administration revealed a more rapid onset of theta, delta, and particularly subdelta activity in controls compared with $Ca_v2.3^{-/-}$ mice (Fig. 3*D*), these differences did not reach the level of significance. In addition, latency to first onset of exacerbating EEG seizure activity did not differ significantly between $Ca_v2.3^{+/+}$ and $Ca_v2.3^{-/-}$ mice (7.2 ± 1.6 vs. 7.0 ± 2.7 min; $P = 0.9351$) and no alteration in latencies to peak PSD values for the individual frequency ranges could be detected (Fig. 3*E*). Thus hippocampal EEG seizure activity does not vary between $Ca_v2.3^{+/+}$ and $Ca_v2.3^{-/-}$ mice at 30 mg/kg KA. Even at 10 mg/kg mice from both genders appeared to be behaviorally normal, although exhibiting a hippocampal status (Fig. 2, *C* and *D*). Thus both dosages turned out to be far beyond hippocampal seizure threshold in either genotype.

However, seizure generalization including motoric components (e.g., clonic events and status epilepticus) could be induced only with higher doses (30 mg/kg). Thus the pronounced KA-induced seizure resistance in $Ca_v2.3^{-/-}$ mice points not only to an ictogenic potential of $Ca_v2.3$ but also to its role in seizure spreading and generalization.

Kainic acid–induced hippocampal excitotoxicity in $Ca_v2.3^{+/+}$ and $Ca_v2.3^{-/-}$ mice

To unravel the role of $Ca_v2.3$ in modulating excitotoxic cell death we performed histochemical analysis of brains derived from $Ca_v2.3^{-/-}$ and $Ca_v2.3^{+/+}$ mice 1 wk after ip administration of KA (30 mg/kg). In rodents, peripheral injections of KA result in recurrent seizures and subsequent degeneration of selected populations of neurons within the hippocampus. EEG recordings for a 1-wk period after KA administration revealed that, although decreasing, hippocampal seizure activity still persists (Fig. 1, *C–F*). This leads to a time-dependent, hyperexcitability-mediated neuronal degeneration within the hippocampus, particularly CA3, paving the way for further excitotoxic damage. Both Nissl and HE staining exhibit prominent neuronal cell loss and neurodegeneration in the CA3 region of

TABLE 1. *Effects of KA (A, 30 mg/kg, ip) and NMDA (B, 150 mg/kg) on occurrence, latency (L), and frequency (F) of the individual seizure stages*

Stage	$Ca_v2.3^{+/+}$ ($n = 18$)	$Ca_v2.3^{-/-}$ ($n = 18$)	
	A. KA seizure susceptibility		
1 (no behavioral change)			
	0/16[a]	2/18	ns[b]
L1	7,200[c]	7,200[c]	ns
2 (facial clonus)			
	13/16[a]	16/18	ns[b]
L2	2,453 ± 628	2,379 ± 428	ns
F2	3.4 ± 1.0	8.9 ± 1.2	$P = 0.0025$
3 (forelimb clonus)			
	12/16[a]	15/18	ns[b]
L3	2,876 ± 691	3,286 ± 493	ns
F3	4.7 ± 1.4	10.7 ± 2.1	$P = 0.0331$
4 (rearing)			
	9/16[a]	10/18	ns[b]
L4	4,090 ± 736	5,193 ± 449	ns
F4	7.7 ± 3.7	7.1 ± 1.9	ns
5 (falling)			
	9/16[a]	8/18	ns[b]
L5	3,919 ± 764	5,7239 ± 424	$P = 0.0445$
F5	4.3 ± 1.4	2.2 ± 0.8	ns
6 (status epilepticus > 3 min)			
	9/16[a]	0/18	$P = 0.0017$[b]
L6	3,777 ± 794	7,200[c]	$P < 0.0001$
F6	0.7 ± 0.2	0[c]	$P = 0.0002$
7a (jumping, tonic seizure < 30 s)			
	9/16[a]	14/18	ns[b]
L7a	3,797 ± 779	3,568 ± 487	ns
F7a	1.6 ± 0.7	4.7 ± 1.0	$P = 0.0255$
7b (jumping, tonic seizure > 30 s)			
	5/16[a]	8/18	ns[b]
L7b	5,494 ± 669	5,576 ± 463	ns
F7b	0.6 ± 0.3	1.2 ± 0.6	ns
8 (maximum seizure activity and death)			
	9/18	0/18	$P = 0.0010$[b]
L8	4,338 ± 696	7,200[c]	$P = 0.0001$
F8	0.6 ± 0.1	0[c]	$P < 0.0001$
Stage	$Ca_v2.3^{+/+}$ ($n = 20$)	$Ca_v2.3^{-/-}$ ($n = 20$)	
	B. NMDA seizure susceptibility		
0 (no response)			
	0/19[a]	0/16[a]	ns
L0	7,200	7,200	ns
1 (excessive grooming and paroxysmal scratching)			
	13/19[a]	13/16[a]	ns[b]
L1	3,794 ± 532	3,314 ± 543	ns
F1	5.3 ± 1.6	6.5 ± 1.4	ns
2 (mild hypermotility)			
	11/19[a]	8/16[a]	ns[b]
L2	3,895 ± 720	4,162 ± 814	ns
F2	1.5 ± 0.4	1.4 ± 0.5	ns
3 (extensive hypermotility and circling)			
	6/19[a]	6/16[a]	ns[b]
L3	5,596 ± 645	5,169 ± 719	ns
F3	0.8 ± 0.4	0.6 ± 0.2	ns
4 (forepaw clonus and tail hypertonus)			
	13/19[a]	8/16[a]	ns[b]
L4	2,918 ± 702	3,883 ± 857	ns
F4	22.6 ± 8.6	50.0 ± 19.3	ns
5 (generalized tonic-clonic convulsions)			
	5/19[a]	0/16[a]	$P = 0.0493$[b]
L5	5,601 ± 638	6,358 ± 575	ns
F5	0.4 ± 0.2	0	$P = 0.05314$[d]
6 (status epilepticus)			
	7/19[a]	2/16[a]	ns[b]
L6	5,110 ± 725	6,394 ± 551	ns
F6	0.5 ± 0.2	0.1 ± 0.1	$P = 0.07739$[d]
7 (death)			
	8/20	2/20	$P = 0.0648$[b,d]
L7	4,974 ± 690	6,398 ± 548	ns

Latency values (s) and frequency data (s^{-1}) are presented as means ± SE. Values of $P < 0.05$ are considered significant; ns, not significant. Values of P approaching the level of significance are mentioned explicitly. [a]A few animals could not be video-analyzed completely, which explains the difference in number. [b]Lethality and number of animals entering individual seizure stages were analyzed using Fisher's exact probability test. [c]Mice exhibiting no individual seizure phase were assigned a maximum latency and zero values for frequency. [d]Parameters approaching significance.

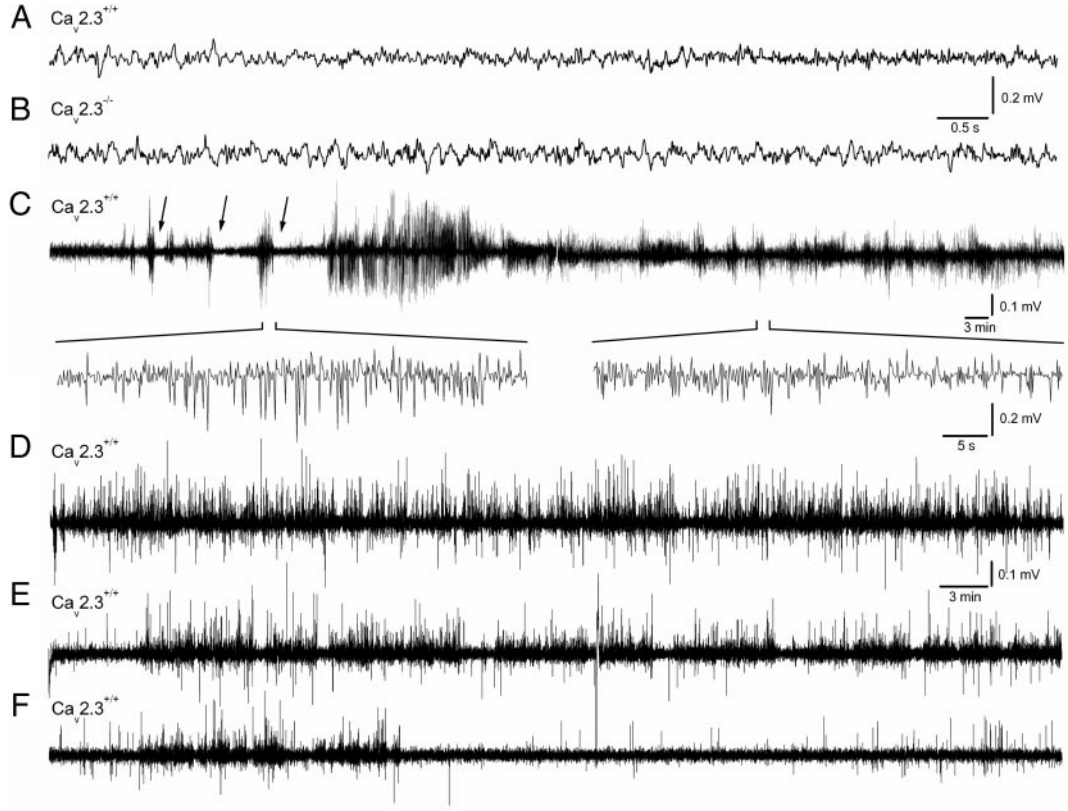

FIG. 1. Intrahippocampal electroencephalographic (EEG) recordings after intraperitoneal administration of kainic acid (KA, 30 mg/kg). *A* and *B*: representative spontaneous EEG traces (10 s) obtained from the CA1 region of the hippocampus from $Ca_v2.3^{+/+}$ ($n = 9$, *A*) and $Ca_v2.3^{-/-}$ mice ($n = 9$, *B*) before injection. No epileptiform discharges indicative of spontaneous hippocampal seizure activity could be detected in $Ca_v2.3$-deficient mice. *C*: deep CA1 recording from a $Ca_v2.3^{+/+}$ mouse for 2 h immediately after KA administration. At 30 mg/kg KA contiguous hippocampal seizure activity is presented occasionally interrupted by postictal depression (arrows). Ictal discharges are characterized by spike and/or spike-wave activity (see *insets*) in the delta- and theta-wave range (4–8 Hz). *D–F*: At days 1, 3, and 5 post-injection 1-h CA1 EEG recordings illustrate slightly declining but still continuous ictiform activity related to neuronal excitotoxic degeneration depicted in Fig. 4.

$Ca_v2.3^{+/+}$ mice but not in $Ca_v2.3$-deficient animals (Fig. 4, *A–D*). In $Ca_v2.3^{+/+}$ mice, only 11% of neurons within the stratum pyramidale (CA3) exhibit an intact morphology after Nissl or HE staining (Fig. 4*C*). However in $Ca_v2.3^{-/-}$ mice, 89 and 90% of neurons reveal an intact cell shape after Nissl and HE staining, respectively. In addition, the number of countable (intact and degenerating) cells is reduced by 13.4% in $Ca_v2.3^{+/+}$ mice compared with $Ca_v2.3^{-/-}$ mice. Note also the fading appearance of condensed chromatin in $Ca_v2.3^{+/+}$ CA3 pyramidal neurons compared with $Ca_v2.3$-deficient animals (Fig. 4*C*, two *left panels* vs. *right panels*). As hippocampal seizure activity emerged to be similar in both genotypes at 30 mg/kg, reduced excitotoxicity in $Ca_v2.3^{-/-}$ mice also points to an intriguing role of $Ca_v2.3$ in neuronal cell degeneration and apoptosis.

DISCUSSION

Voltage-gated Ca^{2+} channels are key regulators in neuronal excitability and turn out to be important components in ictogenesis and epileptogenesis (Khosravani and Zamponi 2006; Weiergräber et al. 2006b). Most studies in the past focused on $Ca_v2.1$ and $Ca_v3.2$ VGCCs. However, recent findings indicate that the $Ca_v2.3$ E/R-type Ca^{2+} channel can also serve as a proictogenic factor. Within the CNS $Ca_v2.3$ is widely distributed and preferentially localized either presynaptically or homogeneously on the soma and dendrites depending on the cell type (Weiergräber et al. 2006b; Westenbroek et al. 1995). Presynaptically, only a smaller fraction of $Ca_v2.3$ is restricted to the active zone of the vesicle fusion machinery and thus involved in neurotransmission (Wu et al. 1999), whereas a larger fraction is localized more distant in the synapse responsible for synaptic plasticity, e.g., long-term potentiation (LTP) (Breustedt et al. 2003; Dietrich et al. 2003). The somatic and dendritic expression of $Ca_v2.3$ is highly organized in space and contributes to the genesis of electrical phenomena resembling epileptiform activity (Magee 2000; McCormick and Contreras 2001; Williams and Kauer 1997). In addition, $Ca_v2.3$ is capable of inducing plateau potentials that underlie ictiform burst activity in various neuronal cell types (Kuzmiski et al. 2005; Tai et al. 2006). Its functional contribution to afterdepolarizations, which are also involved in epileptiform bursting, was previously reported (Metz et al. 2005) but remains controversial (Yue et al. 2005). In addition, $Ca_v2.3$ channels exhibit a complex regulation by G-protein–coupled signal transduction pathways, PKC, and internal Ca^{2+} levels, thus harboring remarkable but typical features of a seizure-susceptibility candidate (Weiergräber et al. 2006b).

We previously demonstrated that neither $Ca_v2.3^{-/-}$ mice nor control animals exhibit spontaneous epileptiform discharges in

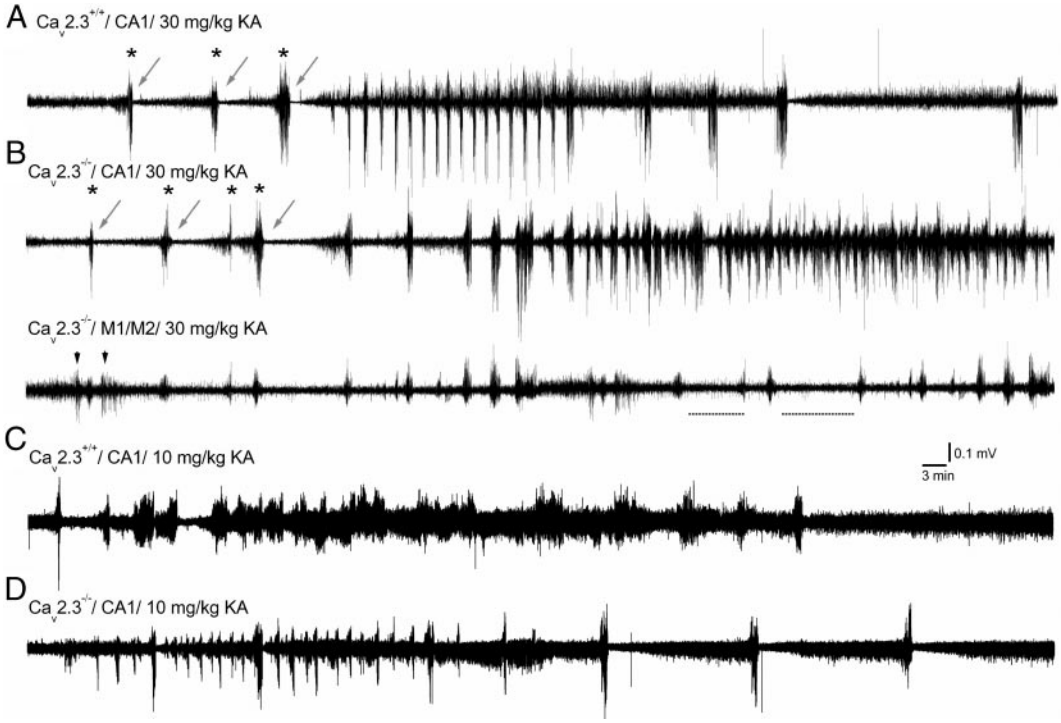

FIG. 2. Intrahippocampal EEG recording from $Ca_v2.3^{+/+}$ and $Ca_v2.3^{-/-}$ mice after KA administration (30 mg/kg, *A*, *B*; 10 mg/kg, *C*, *D*). Deep CA1 EEG recording from control (*A*) and $Ca_v2.3$-deficient mice for 2 h (*B*). In some animals seizure activity is predominantly characterized by repetitive and delimitable high-amplitude exacerbation of spike and/or spike-wave activity (*) usually followed by postictal depression (red arrows), whereas in other mice this activity seems to merge resulting in continuous seizure activity. However, detailed EEG analysis of 6 animals from each genotype revealed no differences in seizure architecture at this suprathreshold KA concentration. *B*: simultaneous deep CA1 and surface EEG recordings from the motor cortex (M1/M2) reveal partially overlapping but also distinct patterns of neuronal hyperexcitability in the different regions (see black arrows and dashed lines), pointing out the regional specificity of EEG recordings. *C* and *D*: even 10 mg/kg KA turned out to be far beyond hippocampal seizure threshold ($n = 3$ for each genotype).

surface and deep intracerebral EEG recordings indicative of convulsive or nonconvulsive seizure activity. Interestingly, $Ca_v2.3^{-/-}$ mice turned out to be more resistant to PTZ-induced seizures, whereas 4-AP–induced seizure susceptibility remained unchanged (Weiergräber et al. 2006a). Based on recent electrophysiological studies in CA1 neurons pointing to a functional role of $Ca_v2.3$ in plateau potential generation in the hippocampus, we investigated the systemic effects of $Ca_v2.3$ ablation on hippocampal seizure activity using KA and NMDA. Behavioral analysis of 36 animals in total demonstrates that KA-induced seizure susceptibility (e.g., status epilepticus and lethality) is dramatically reduced in $Ca_v2.3^{-/-}$ versus control mice, supporting recent observations in CA1 neurons and validating the proconvulsive effect of $Ca_v2.3$ on the systemic, whole animal level. Similar findings were obtained for NMDA seizure susceptibility (40 animals in total), further strengthening the role of $Ca_v2.3$ in seizure initiation and generalization.

These results suggest that $Ca_v2.3$ acts solely as an electrophysiological regulator in triggering seizure initiation and propagation. However, studies by Suzuki et al. (2004) elucidated that $Ca_v2.3$ is likely to be involved in neuronal apoptotic processes related to excitotoxicity as well. Mutations in EFHC1, a novel interaction partner of the $Ca_v2.3$ VGCC, were reported to cause juvenile myoclonic epilepsy (JME) in humans. Normally, EFHC1 induces neuronal apoptosis by interaction with $Ca_v2.3$, whereas mutations in EFHC1 disrupt C-terminal binding and consequently result in lack of apoptosis and increased cell density, exhibiting hyperexcitable circuits as a result of altered neuronal connectivity (Suzuki et al. 2004). This functional role of $Ca_v2.3$ in neuronal degeneration is further supported by the observation that antiepileptic drugs (AEDs) known to block $Ca_v2.3$ (e.g., topiramate and lamotrigine) also exert strong neuroprotective effects (Caputi et al. 2001; Edmonds Jr et al. 2001; Hainsworth et al. 2003). Normal neuronal computation in the brain requires intense ongoing excitatory transmission. However, excessive excitatory activity results in neuronal damage and death, through a mechanism known as excitotoxicity (Ben Ari and Cossart 2000).

A major contributor to both hyperexcitability and excitotoxicity within the CNS is the glutamate system. Spreading of excessive glutamatergic neurotransmission eventually leads to sustained, paroxysmal network activity that can emerge into behaviorally observable symptoms. L-Glutamate is a neurotransmitter in a majority of excitatory synapses within the brain and acts on three classes of ionotropic receptors: NMDA, AMPA (α-amino-3-hydroxy-5-methyl-4-isoxazolepropionic acid), and KA receptors. In excessive concentrations, glutamate has the potential to induce serious cell damage and even death to neurons, with NMDA and KA receptors located on neuronal cell bodies but also the pre- and postsynapse (Nicoll and Schmitz 2005). Kainic acid in particular is a well-characterized excitotoxin in the hippocampus and induces degeneration of cornu ammonis pyramidal neurons but also hyperexcitability in surviving CA neurons, provoking epileptiform activity and thereby serving as a model of complex partial seizure activity. Kainic acid–induced limbic seizure activity is initiated by paroxysmal discharges within the hippocampus and further spread to other limbic structures and finally to nonlimbic areas

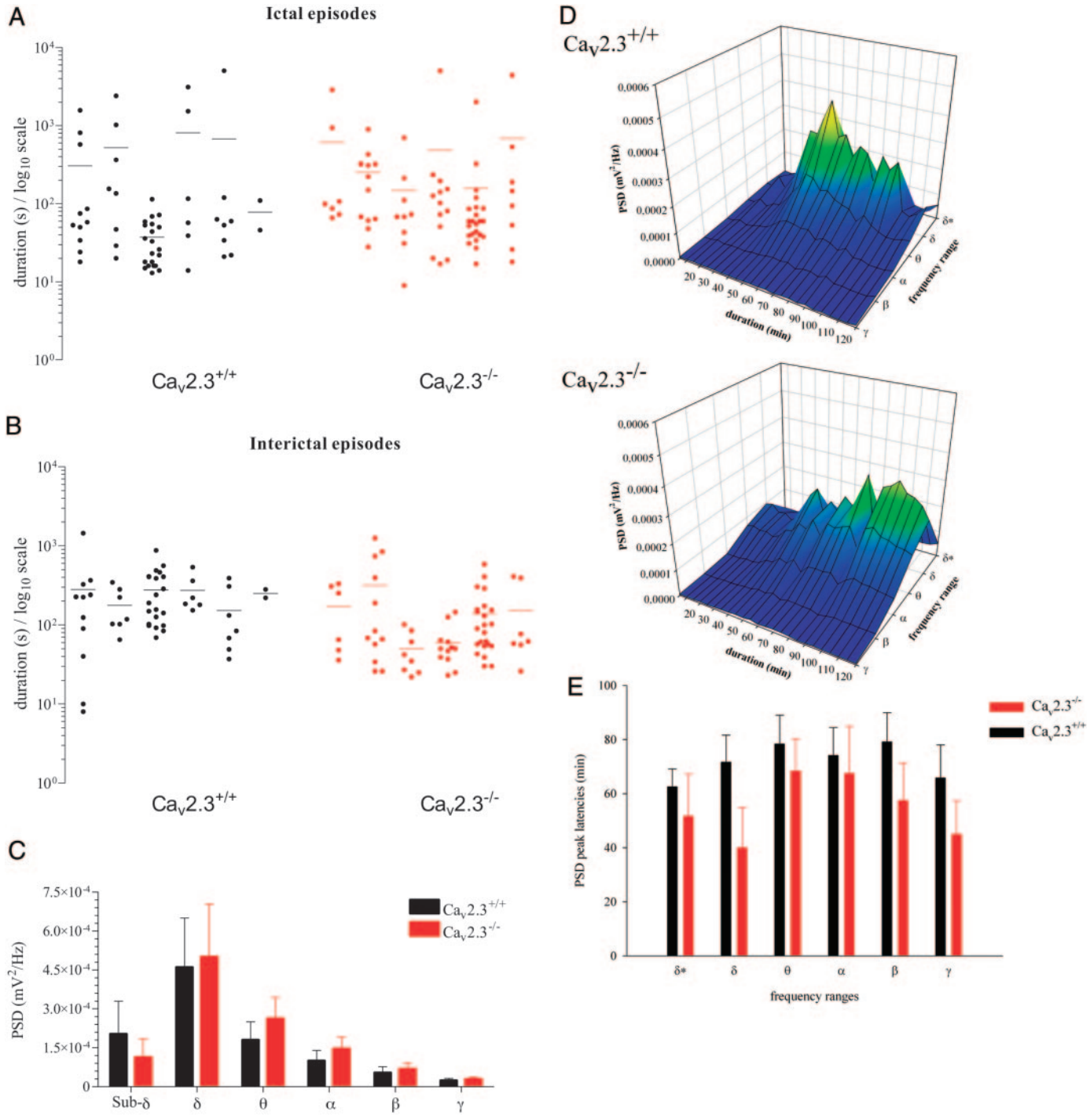

FIG. 3. Analysis of hippocampal EEG seizure activity in $Ca_v2.3^{+/+}$ and $Ca_v2.3^{-/-}$ mice after KA (30 mg/kg) administration. Six $Ca_v2.3^{+/+}$ and six $Ca_v2.3^{-/-}$ mice deeply implanted in the CA1 region were used for this analysis. *A* and *B*: scatterplot illustrating duration and frequency of ictal episodes (*A*) and interictal phases (*B*) in $Ca_v2.3^{+/+}$ and $Ca_v2.3^{-/-}$ mice. Horizontal bars indicate mean values. No significant differences could be detected between both genotypes. Note that short-term ictal episodes are frequent early after KA injection, whereas long-term hippocampal EEG seizure activity representing limbic status epilepticus occurs at later time points. *C*: power-spectrum density (PSD) analysis of ictal episodes (30-s segments) for the various frequency ranges. *D*: 3D plot of averaged absolute PSD from $Ca_v2.3^{+/+}$ and $Ca_v2.3^{-/-}$ mice ($n = 6$ for each genotype) for the different frequency ranges. A total observation period of 2 h was plotted using 5-min EEG segments for analysis. No significant difference between both genotypes could be detected. *E*: measurement of peak PSD latencies for the individual frequency ranges after KA administration; δ*, subdelta range.

(Ben Ari 1985), resulting in various motor signs such as staring, head nodding, wet-dog shakes, recurrent limbic motor seizures, status epilepticus, and death. Both NMDA- and KA-receptor activation is associated with activation of VGCCs by prolonged depolarization and Ca^{2+}-mediated excitotoxicity that might in part be responsible for neuronal cell death. However, the exact mechanisms yet have to be illuminated.

Interestingly, it was recently shown that KA receptors are expressed not only postsynaptically at the mossy fiber synapse,

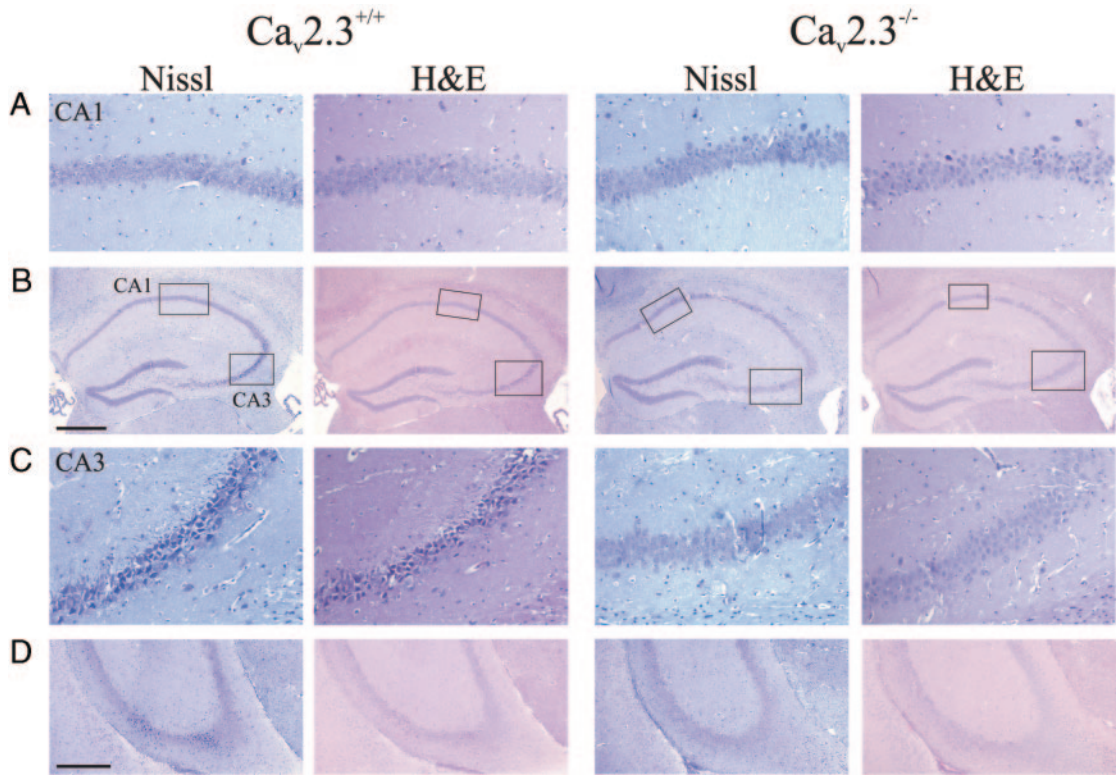

FIG. 4. Assessment of excitotoxic cell injury and neuronal degeneration in the hippocampus of $Ca_v2.3^{+/+}$ ($n = 3$) and $Ca_v2.3^{-/-}$ mice ($n = 3$) after systemic KA (30 mg/kg) treatment. Seven days after injection brains from $Ca_v2.3^{+/+}$ (*left panels*) and $Ca_v2.3^{-/-}$ mice (*right panels*) were exstirpated and both Nissl- and HE-stained. In $Ca_v2.3^{+/+}$ mice neuronal cell degeneration is present in both the rostral-middle hippocampus (*B*, bregma: −1.7 mm) as well as in the more caudal parts (*D*, bregma: −2.5 mm), but absent in corresponding sections of $Ca_v2.3^{-/-}$ animals. Enlargements of individual areas (labeled by boxes in *B*) are shown for the CA1 region in *A* and for the CA3 region in *C*. Note, the strong granulation of cells and gaps between pyramidal neurons in the CA3 region shown in *C*. Bars in *B* and *D*: 500 μm.

but also presynaptically together with $Ca_v2.3$ modulating neurotransmission in the CA3 region, probably related to the profound excitotoxic effects in this hippocampal region (Nicoll and Schmitz 2005). In addition, it turns out that more and more neuroprotectants and neurotransmitters that are upregulated after KA-induced seizures (Hunsberger et al. 2005) interact with or functionally modulate $Ca_v2.3$, e.g., hsp70 (Krieger et al. 2006) or neurokinin 1 (Meza et al. 2007).

Excitotoxic neurodegeneration clearly differs between the individual mouse strains. Studies by Schauwecker and Steward (1997) using 30 mg/kg KA revealed that 129/SvEMS and FVB/N mice exhibit excitotoxic cell death in the CA3 and CA1 regions of the hippocampus at lower doses. However, C57Bl/6 and BALB/c mice display neuronal cell death only at higher doses of KA in restricted areas (predominantly CA3), although the severity of seizures is comparable. Histochemical analysis of $Ca_v2.3^{+/+}$ and $Ca_v2.3^{-/-}$ mice revealed clear indications of reduced excitotoxic cell death in the CA3 region of $Ca_v2.3$-deficient mice exhibiting a characteristic distribution pattern as reported previously (Schauwecker and Steward 1997). Because detailed analysis of hippocampal EEG seizure activity did not reveal differences between both genotypes at 30 mg/kg KA (Fig. 2, *A* and *B*), the explicit hippocampal invulnerability of $Ca_v2.3^{-/-}$ mice is likely to be a direct result of $Ca_v2.3$ ablation and not because of decreased limbic seizure intensity at that dosage. Given the complex distribution pattern of functionally divergent $Ca_v2.3$ splice variants in the CNS (Weiergräber et al. 2006) one can hypothesize that hyperexcitability and neuronal degeneration are mediated by different $Ca_v2.3$ splice entities in a direct or indirect way. Interestingly, the major, near-exclusive splice variant in hippocampus and neocortex corresponds to the $Ca_v2.3c$ variant, which contains the exon 19 encoded insert 1 of the cytosolic II–III loop. This segment provides a novel Ca^{2+} and phorbolester sensitivity to $Ca_v2.3c$. Further, the II–III loop of $Ca_v2.3$ (with or without insert 1) represents the interaction site for the molecular chaperone hsp70 (Krieger et al. 2006). Hsp70 in particular was proved to be involved in neuroprotection. The investigation of disturbances of $Ca_v2.3$–hsp70 signaling may be an important target to understand neurodegeneration in epileptiform disorders.

Power spectrum density analysis did not reveal any differences in frequency distribution between both genotypes after KA administration (Fig. 3), particularly not in ictal discharges within the delta and theta range, which were reported to correlate with hippocampal atrophy and sclerosis in humans (Vossler et al. 1998).

This observation is of tremendous relevance because cell death associated with glutamate neurotoxicity contributes to the devastating secondary effects of epileptic disorders (Malva et al. 1998).

In summary, our recent findings point to a fascinating dual role of $Ca_v2.3$ in both ictogenesis and excitotoxicity. Electrophysiological studies on both the cellular and the systemic level of $Ca_v2.3^{-/-}$ mice strongly support a proictogenic capacity of the

$Ca_v2.3$ VGCC. Moreover, the channel also mediates excitotoxic effects as first reported by Suzuki et al. (2004) in JME patients, now further validated by the observation of reduced KA excitotoxic susceptibility in $Ca_v2.3^{-/-}$ mice. Finally, $Ca_v2.3$ serves as a potent target for various AEDs, which exert neuroprotective effects. Clearly, these remarkable features bring the $Ca_v2.3$ VGCC into focus of pharmacotherapeutic research in epilepsy and neurodegeneration in the future.

ACKNOWLEDGMENTS

We thank R. Clemens, C. Zyntek, A. Müller, and the animal keepers of the central facility for excellent and permanent assistance.

GRANTS

The work was financially supported by the Center of Molecular Medicine Cologne, University of Cologne.

REFERENCES

Bannister RA, Melliti K, Adams BA. Differential modulation of $Ca_v2.3$ Ca^{2+} channels by Gαq/11-coupled muscarinic receptors. *Mol Pharmacol* 65: 381–388, 2004.

Baran H, Loscher W, Mevissen M. The glycine/NMDA receptor partial agonist D-cycloserine blocks kainate-induced seizures in rats. Comparison with MK-801 and diazepam. *Brain Res* 652: 195–200, 1994.

Ben Ari Y. Limbic seizure and brain damage produced by kainic acid: mechanisms and relevance to human temporal lobe epilepsy. *Neuroscience* 14: 375–403, 1985.

Ben Ari Y, Cossart R. Kainate, a double agent that generates seizures: two decades of progress. *Trends Neurosci* 23: 580–587, 2000.

Breustedt J, Vogt KE, Miller RJ, Nicoll RA, Schmitz D. Alpha1E-containing Ca^{2+} channels are involved in synaptic plasticity. *Proc Natl Acad Sci USA* 100: 12450–12455, 2003.

Caputi L, Hainsworth AH, Lavaroni F, Leach MJ, McNaughton NC, Mercuri NB, Randall AD, Spadoni F, Swan JH, Stefani A. Neuroprotective actions in vivo and electrophysiological actions in vitro of 202W92. *Brain Res* 919: 259–268, 2001.

Catterall WA, Perez-Reyes E, Snutch TP, Striessnig J. International Union of Pharmacology. XLVIII. Nomenclature and structure–function relationships of voltage-gated calcium channels. *Pharmacol Rev* 57: 411–425, 2005.

Dietrich D, Kirschstein T, Kukley M, Pereverzev A, von der Brelie C, Schneider T, Beck H. Functional specialization of presynaptic $Ca_v2.3$ Ca^{2+} channels. *Neuron* 39: 483–496, 2003.

Edmonds HL Jr, Jiang YD, Zhang PY, Shank R. Topiramate as a neuroprotectant in a rat model of global ischemia-induced neurodegeneration. *Life Sci* 69: 2265–2277, 2001.

Hainsworth AH, McNaughton NC, Pereverzev A, Schneider T, Randall AD. Actions of sipatrigine, 202W92 and lamotrigine on R-type and T-type Ca^{2+} channel currents. *Eur J Pharmacol* 467: 77–80, 2003.

Hamilton SE, Loose MD, Qi M, Levey AI, Hille B, McKnight GS, Idzerda RL, Nathanson NM. Disruption of the m_1 receptor gene ablates muscarinic receptor-dependent M current regulation and seizure activity in mice. *Proc Natl Acad Sci USA* 94: 13311–13316, 1997.

Hunsberger JG, Bennett AH, Selvanayagam E, Duman RS, Newton SS. Gene profiling the response to kainic acid induced seizures. *Brain Res Mol Brain Res* 141: 95–112, 2005.

Khosravani H, Zamponi GW. Voltage-gated calcium channels and idiopathic generalized epilepsies. *Physiol Rev* 86: 941–966, 2006.

Klöckner U, Pereverzev A, Leroy J, Krieger A, Vajna R, Hescheler J, Pfitzer G, Malecot CO, Schneider T. The cytosolic II–III loop of $Ca_v2.3$ provides an essential determinant for the phorbol ester-mediated stimulation of E-type Ca^{2+} channel activity. *Eur J Neurosci* 19: 2659–2668, 2004.

Krieger A, Radhakrishnan K, Pereverzev A, Siapich SA, Banat M, Kamp MA, Leroy J, Klockner U, Hescheler J, Weiergräber M, Schneider T. The molecular chaperone hsp70 interacts with the cytosolic II–III loop of the $Ca_v2.3$ E-type voltage-gated Ca^{2+} channel. *Cell Physiol Biochem* 17: 97–110, 2006.

Kuzmiski JB, Barr W, Zamponi GW, MacVicar BA. Topiramate inhibits the initiation of plateau potentials in CA1 neurons by depressing R-type calcium channels. *Epilepsia* 46: 481–489, 2005.

Leroy J, Pereverzev A, Vajna R, Qin N, Pfitzer G, Hescheler J, Malécot CO, Schneider T, Klöckner U. Ca^{2+}-sensitive regulation of E-type Ca^{2+} channel activity depends on an arginine rich region in the cytosolic II–III loop. *Eur J Neurosci* 18: 841–855, 2003.

Magee JC. Dendritic integration of excitatory synaptic input. *Nat Rev Neurosci* 1: 181–190, 2000.

Malva JO, Carvalho AP, Carvalho CM. Kainate receptors in hippocampal CA3 subregion: evidence for a role in regulating neurotransmitter release. *Neurochem Int* 32: 1–6, 1998.

Marganella C, Bruno V, Matrisciano F, Reale C, Nicoletti F, Melchiorri D. Comparative effects of levobupivacaine and racemic bupivacaine on excitotoxic neuronal death in culture and N-methyl-D-aspartate-induced seizures in mice. *Eur J Pharmacol* 518: 111–115, 2005.

McCormick DA, Contreras D. On the cellular and network bases of epileptic seizures. *Annu Rev Physiol* 63: 815–846, 2001.

McKeown L, Robinson P, Jones OT. Molecular basis of inherited calcium channelopathies: role of mutations in pore-forming subunits. *Acta Pharmacol Sin* 27: 799–812, 2006.

Mejias-Aponte CA, Jimenez-Rivera CA, Segarra AC. Sex differences in models of temporal lobe epilepsy: role of testosterone. *Brain Res* 944: 210–218, 2002.

Melliti K, Meza U, Adams B. Muscarinic stimulation of a1E Ca channels is selectively blocked by the effector antagonist function of RGS2 and phospholipase C-b1. *J Neurosci* 20: 7167–7173, 2000.

Metz AE, Jarsky T, Martina M, Spruston N. R-type calcium channels contribute to afterdepolarization and bursting in hippocampal CA1 pyramidal neurons. *J Neurosci* 25: 5763–5773, 2005.

Meza U, Bannister R, Melliti K, Adams B. Biphasic, opposing modulation of cloned neuronal a1E Ca channels by distinct signaling pathways coupled to M2 muscarinic acetylcholine receptors. *J Neurosci* 19: 6806–6817, 1999.

Meza U, Thapliyal A, Bannister RA, Adams BA. Neurokinin 1 receptors trigger overlapping stimulation and inhibition of $Ca_v2.3$ (R-type) calcium channels. *Mol Pharmacol* 71: 284–293, 2007.

Newcomb R, Szoke B, Palma A, Wang G, Chen XH, Hopkins W, Cong R, Miller J, Urge L, Tarczy-Hornoch K, Loo JA, Dooley DJ, Nadasdi L, Tsien RW, Lemos J, Miljanich G. Selective peptide antagonist of the class E calcium channel from the venom of the tarantula *Hysterocrates gigas. Biochemistry* 37: 15353–15362, 1998.

Nicoll RA, Schmitz D. Synaptic plasticity at hippocampal mossy fibre synapses. *Nat Rev Neurosci* 6: 863–876, 2005.

Pereverzev A, Mikhna M, Vajna R, Gissel C, Henry M, Weiergräber M, Hescheler J, Smyth N, Schneider T. Disturbances in glucose-tolerance, insulin-release and stress-induced hyperglycemia upon disruption of the $Ca_v2.3$ (a1E) subunit of voltage-gated Ca^{2+} channels. *Mol Endocrinol* 16: 884–895, 2002.

Remy S, Beck H. Molecular and cellular mechanisms of pharmacoresistance in epilepsy. *Brain* 129: 18–35, 2006.

Schauwecker PE, Steward O. Genetic determinants of susceptibility to excitotoxic cell death: implications for gene targeting approaches. *Proc Natl Acad Sci USA* 94: 4103–4108, 1997.

Schneider T, Wei X, Olcese R, Costantin JL, Neely A, Palade P, Perez-Reyes E, Qin N, Zhou J, Crawford GD, Smith RG, Appel SH, Stefani E, Birnbaumer L. Molecular analysis and functional expression of the human type E a1 subunit. *Receptors Channels* 2: 255–270, 1994.

Suzuki T, Delgado-Escueta AV, Aguan K, Alonso ME, Shi J, Hara Y, Nishida M, Numata T, Medina MT, Takeuchi T, Morita R, Bai D, Ganesh S, Sugimoto Y, Inazawa J, Bailey JN, Ochoa A, Jara-Prado A, Rasmussen A, Ramos-Peek J, Cordova S, Rubio-Donnadieu F, Inoue Y, Osawa M, Kaneko S, Oguni H, Mori Y, Yamakawa K. Mutations in EFHC1 cause juvenile myoclonic epilepsy. *Nat Genet* 36: 842–849, 2004.

Tai C, Kuzmiski JB, MacVicar BA. Muscarinic enhancement of R-type calcium currents in hippocampal CA1 pyramidal neurons. *J Neurosci* 26: 6249–6258, 2006.

Tottene A, Volsen S, Pietrobon D. alpha1E Subunits form the pore of three cerebellar R-type calcium channels with different pharmacological and permeation properties. *J Neurosci* 20: 171–178, 2000.

Weiergräber M, Henry M, Hescheler J, Smyth N, Schneider T. Electrocorticographic and deep intracerebral EEG recording in mice using a telemetry system. *Brain Res Brain Res Protoc* 14: 154–164, 2005.

Weiergräber M, Henry M, Krieger A, Kamp M, Radhakrishnan K, Hescheler J, Schneider T. Altered seizure susceptibility in mice lacking the $Ca_v2.3$ E-type Ca^{2+} channel. *Epilepsia* 47: 839–850, 2006a.

Weiergräber M, Kamp MA, Radhakrishnan K, Hescheler J, Schneider T. The $Ca_v2.3$ voltage-gated calcium channel in epileptogenesis—shedding new light on an enigmatic channel. *Neurosci Biobehav Rev* 30: 1122–1144, 2006b.

Westenbroek RE, Sakurai T, Elliott EM, Hell JW, Starr TVB, Snutch TP, Catterall WA. Immunochemical identification and subcellular distribution of the a_{1A} subunits of brain calcium channels. *J Neurosci* 15: 6403–6418, 1995.

Williams JH, Kauer JA. Properties of carbachol-induced oscillatory activity in rat hippocampus. *J Neurophysiol* 78: 2631–2640, 1997.

Wu LG, Westenbroek RE, Borst JGG, Catterall WA, Sakmann B. Calcium channel types with distinct presynaptic localization couple differentially to transmitter release in single calyx-type synapses. *J Neurosci* 19: 726–736, 1999.

Yue C, Remy S, Su H, Beck H, Yaari Y. Proximal persistent Na^+ channels drive spike afterdepolarizations and associated bursting in adult CA1 pyramidal cells. *J Neurosci* 25: 9704–9720, 2005.

Molecular and Cellular Neuroscience 39 (2008) 605–618

Contents lists available at ScienceDirect

Molecular and Cellular Neuroscience

journal homepage: www.elsevier.com/locate/ymcne

Altered thalamocortical rhythmicity in $Ca_v2.3$-deficient mice

Marco Weiergräber [a,c,*], Margit Henry [a], Matthew S.P. Ho [b,c], Henrik Struck [a], Jürgen Hescheler [a,c], Toni Schneider [a,c]

[a] Institute of Neurophysiology, Faculty of Medicine, University of Cologne, Germany
[b] Center for Biochemistry, Faculty of Medicine, University of Cologne, Germany
[c] Center for Molecular Medicine Cologne (CMMC), University of Cologne, Germany

ARTICLE INFO

Article history:
Received 7 April 2008
Revised 28 July 2008
Accepted 13 August 2008
Available online 4 September 2008

Keywords:
$Ca_v2.3$
Electroencephalogram
Hyperoscillation
Thalamocortical circuitry
Non-convulsive seizure
Absence epilepsy

ABSTRACT

Voltage-gated calcium channels (VGCCs) are key regulators of neuronal excitability and important factors in epileptogenesis and neurodegeneration. Recent findings suggest a novel, important proictogenic and proneuroapoptotic role of the $Ca_v2.3$ E/R-type VGCCs in convulsive generalized tonic–clonic and hippocampal seizures. Though $Ca_v2.3$ is also expressed in key structures of the thalamocortical circuitry, their functional relevance in non-convulsive absence seizure activity remains unknown. To this end, we investigated absence specific spike–wave discharge (SWD) susceptibility in control and $Ca_v2.3$-deficient mice by systemic administration of γ-hydroxybutyrolactone (GBL, 70 mg/kg i.p.), followed by electrocorticographic radio-telemetric recordings, behavioral analysis and histomorphological characterization. Based on motoric studies, SWD and power-spectrum density (PSD) analysis, our results demonstrate that $Ca_v2.3^{-/-}$ mice exhibit increased absence seizure susceptibility and altered absence seizure architecture compared to control animals. This study provides evidence for the first time that $Ca_v2.3$ E/R-type Ca^{2+} channels are important in modulating thalamocortical hyperoscillation exerting anti-epileptogenic effects in non-convulsive absence seizures.

Introduction

Voltage-gated calcium channels (VGCCs) mediate Ca^{2+} influx into living cells triggering various cellular processes, such as excitation–contraction coupling (Bers, 2002), excitation–secretion coupling (Yang and Berggren, 2005; Kisilevsky and Zamponi, 2008), neurotransmitter and hormone release (Catterall et al., 2005), and also regulation of gene expression (Bito et al., 1997; Hofmann et al., 1999). In the last decade, VGCCs, in particular $Ca_v2.1$ P/Q-type and $Ca_v3.2$ T-type channels, were shown to be functionally relevant in the etiopathogenesis of various forms of epilepsies in both humans and animal models exhibiting convulsive and non-convulsive seizure phenotypes (Kullmann, 2002; Turnbull et al., 2005). Recently, another VGCC entity, the $Ca_v2.3$ E/R-type channel, was also proven to exert proictogenic and proepileptogenic effects in convulsive seizures. Cellular electrophysiology of hippocampal CA1 neurons revealed that $Ca_v2.3$ is capable of triggering plateau potentials with superimposed epileptiform bursting following muscarinergic M_1/M_3 receptor stimulation (Kuzmiski et al., 2005; Tai et al., 2006). There are further indications, though controversially discussed, that $Ca_v2.3$ is involved in epileptogenic afterdepolarizations (ADH) in hippocampal CA1 neurons as well (Metz et al., 2005; Yue et al., 2005). In addition, some anti-epileptic drugs, e.g. lamotrigine, sipatrigine and topiramate, are efficient $Ca_v2.3$ E/R-type Ca^{2+} channel blockers, among which topiramate is capable of suppressing $Ca_v2.3$ mediated epileptiform bursting in the CA1 hippocampal region at therapeutically relevant plasma concentrations (Kuzmiski et al., 2005).

The functional properties of $Ca_v2.3$ E/R-type Ca^{2+} channels in convulsive seizures in vivo have been studied in detail recently by gene inactivation of *Cacna1E*, expressing $Ca_v2.3$ (Pereverzev et al., 2002). Electroencephalographic analysis of $Ca_v2.3$-deficient mice revealed no spontaneous epileptiform discharges indicative of convulsive seizure activity. Instead, ablation of $Ca_v2.3$ resulted in reduced seizure susceptibility to generalized tonic–clonic seizures provoked by pentylenetetrazol (PTZ) and to hippocampal seizures induced by kainic acid (KA) or *N*-methyl-D-aspartate (NMDA) (Weiergraber et al., 2006a; Weiergraber et al., 2006b; Weiergraber et al., 2007). Intriguingly, $Ca_v2.3$ deficiency provides additional neuroprotective effects by suppressing hyperexcitability and excitotoxicity in the CNS (Weiergraber et al., 2007). Furthermore, mutation analysis of EFHC1, a $Ca_v2.3$ interaction partner supports that $Ca_v2.3$ may mediate epileptogenesis and neurodegeneration (Suzuki et al., 2004). In addition, the molecular chaperone hsp70 known to be involved in neurodegenera-

Abbreviations: GBL, γ-hydroxybutyrolactone; RTN, reticular thalamic nucleus; SWD, spike–wave discharge; VGCC, voltage-gated calcium channel.

* Corresponding author. Institute of Neurophysiology and Center for Molecular Medicine Cologne (CMMC), Robert-Koch-Str. 39, D-50931 Cologne, Germany. Fax: +49 0221 478 6965.
E-mail address: akp74@uni-koeln.de (M. Weiergräber).

1044-7431/$ – see front matter © 2008 Elsevier Inc. All rights reserved.
doi:10.1016/j.mcn.2008.08.007

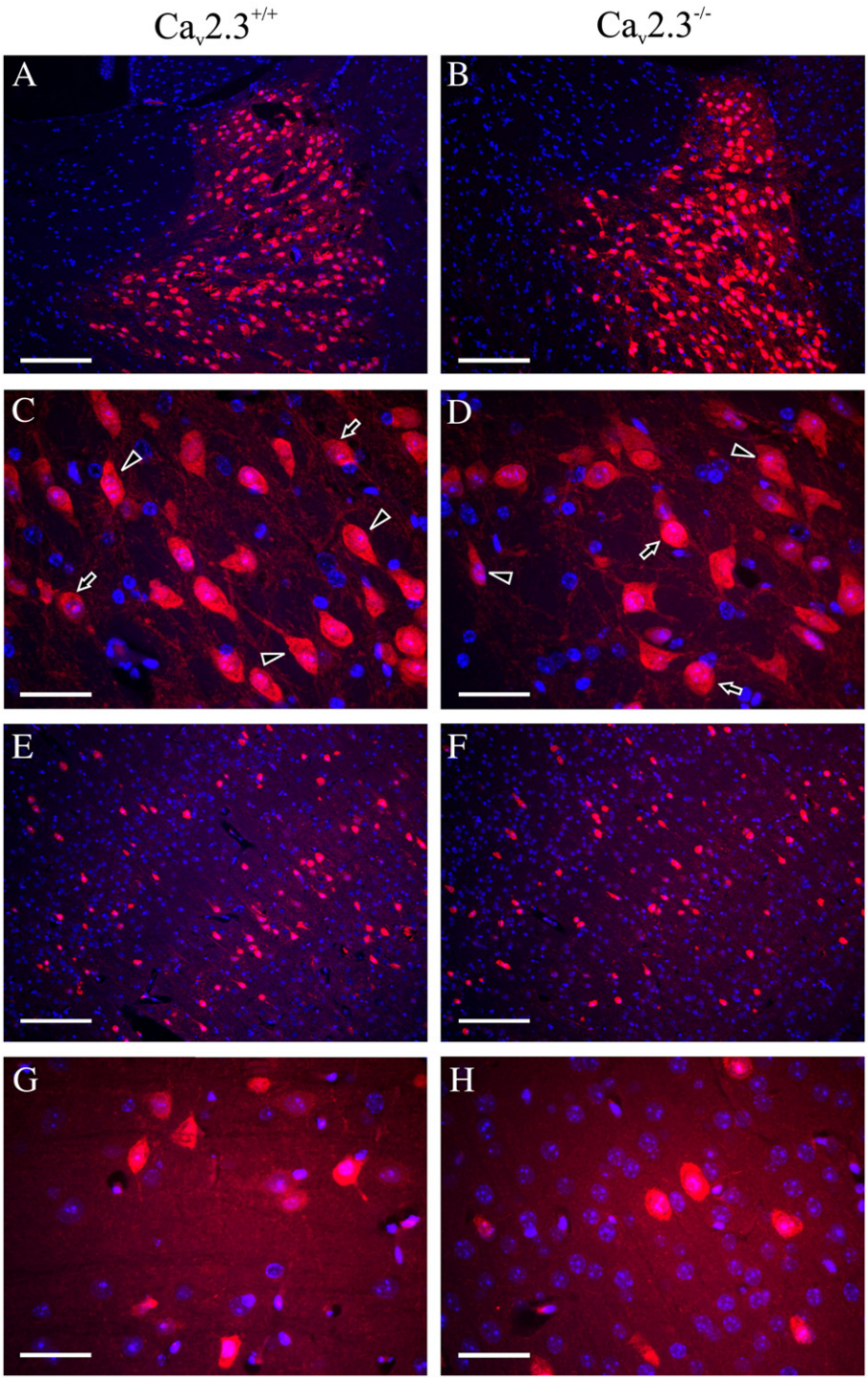

Fig. 1. Immunodetection of GABAergic interneurons in the thalamocortical circuitry. (A–H) Coronal sections (Bregma: −0.1 to −1.0 mm) from control (left) and $Ca_v2.3^{-/-}$ mice (right) were stained for parvalbumin (1:4000) using indirect immunofluorescent labeling revealing typical staining of the reticular thalamic nucleus (A–D). No obvious structural differences in RTN histomorphology between both genotypes were observed (arrows indicate round "R" neurons; arrowheads point at large fusiform "F" cells; small fusiform cells "f" are rarely present in the RTN). Other than the thalamic region, parvalbumin-positive cells were also detected in the neocortex (E–H). Similar to the RTN, immunofluorescent labeling of cortical GABAergic neurons does not suggest structural alterations in both regions expressing the $Ca_v2.3$ E/R-type VGCC. Bar (A, B, E, F): 200 μm; bar (C, D, G, H): 50 μm.

tion functionally interacts with the II–III loop of the $Ca_v2.3$ E/R-type VGCC and contributes to the protein kinase C mediated effects on this channel (Krieger et al., 2006). Finally, divalent trace metals target $Ca_v2.3$ Ca^{2+} channels (Mathie et al., 2006; Sun et al., 2007) capable of modulating hippocampal seizure susceptibility and neurotoxicity (Dominguez et al., 2003; Takeda et al., 2003a; Takeda et al., 2003b; Takeda et al., 2005). Although the functional involvement of $Ca_v2.3$ E/R-type Ca^{2+} channels in convulsive seizures has been elicited lately, their functional implications in generalized non-convulsive seizures of the absence type are still largely unknown to date.

Absence seizures are characterized behaviorally by a paroxysmal loss of consciousness that is normally accompanied with bilateral synchronous spike–wave discharge (SWD) activity, of which the frequency is species specific (Manning et al., 2003). The pathophysiological substrate of absence seizure activity is aberrant hyperoscillation in the underlying thalamocortical–corticothalamic network.

Within this circuitry, glutamatergic thalamic relay cells innervate cortical pyramidal neurons which finally resynapse onto the ventrobasal thalamic region. Both structures also exhibit glutamatergic input onto reticular thalamic nucleus (RTN) neurons with the latter providing GABAergic projections not only onto the RTN neurons themselves, i.e. lateral inhibition, but also onto thalamic relay cells (Danober et al., 1998; Khosravani and Zamponi, 2006). Both relay neurons of the ventrobasal thalamus and RTN neurons have the intriguing capability to shift between two functional modes, the tonic and burst firing mode, which strongly regulates transmission of external information to the cortex (Blumenfeld and McCormick, 2000). Oscillatory behavior within the thalamocortical circuitry is substantially driven by the RTN which serves as a key modulator of information transfer between thalamus and cortex. It is noteworthy that various extrathalamocortical structures capable of modulating thalamocortical rhythmicity and absence SWD generation project to that circuitry (Danober et al., 1998; Lakaye et al., 2002).

Most studies on absence epileptogenesis in humans and animal models in the past predominantly focused on T- and P/Q-type VGCCs. The $Ca_v3.1$ VGCC knock-out mouse model lacks rebound burst firing in thalamocortical relay neurons, thus displaying resistance to absence seizures (Kim et al., 2001) and altered sleep architecture (Lee et al., 2004). In addition, Genetic Absence Epilepsy Rats from Strasbourg (GAERS) exhibit increased T-type Ca^{2+}-current in RTN neurons (Tsakiridou et al., 1995) and also alterations in $Ca_v3.1$ and $Ca_v3.2$ VGCC expression in the adult ventroposterior thalamic nuclei and juvenile RTN neurons, respectively (Talley et al., 2000). Finally, the gene encoding $Ca_v3.2$ T-type Ca^{2+} channel (CACNA1H) was identified as a susceptibility locus of absence epilepsy in humans with gain-of-function mutations triggering thalamocortical hyperoscillation and absence epilepsy (Khosravani et al., 2004; Khosravani et al., 2005; Shin, 2006; Arias-Olguin et al., 2008). $Ca_v2.1^{-/-}$ mice and various $Ca_v2.1$ mouse mutants, e.g. tottering, tottering leaner and rocker, are also prone to absence epilepsy, the mechanism of which still remains poorly understood (Jun et al., 1999; Kullmann, 2002). However, within the thalamocortical circuitry, T- and P/Q-type VGCCs are not the only players.

GABAergic interneurons of the RTN and cortex as well as extrathalamocortical structures were clearly shown to express $Ca_v2.3$ E/R-type Ca^{2+} channels (De Borman et al., 1999; Talley et al., 2000; van de Bovenkamp-Janssen et al., 2004; Weiergraber et al., 2006b). Interestingly, de Borman et al. (1999) and Lakaye et al. (2002) detected a significant reduction of $Ca_v2.3$ transcript levels in both cerebellum and medulla of GAERS, pointing to a functional involvement of $Ca_v2.3$ VGCCs in absence epileptogenesis. Furthermore, the development of SWDs in Wistar Albino Glaxo (WAG/Rij) rats, another model of absence epilepsy, is accompanied with an increased $Ca_v2.1$ expression in the reticular thalamic nucleus but reduced $Ca_v2.3$ expression in the RTN at the age of absence seizure onset (van de Bovenkamp-Janssen et al., 2004). These observations suggest a functional role of $Ca_v2.3$ in the etiopathogenesis of absence epilepsy. In the present study we provide evidence that activation of $Ca_v2.3$ can exert anti-absence effects, probably by facilitating the tonic mode of action, and thus being involved in the regulation of thalamocortical rhythmicity and hyperoscillation. These findings provide novel perspectives for $Ca_v2.3$ as a potent target in the treatment of absence epilepsy and sleep related disorders.

Results

Histomorphological characterization of $Ca_v2.3$ positive neurons in the reticular thalamic nucleus and neocortex from control and $Ca_v2.3$-deficient mice

Previously, serial sections of whole brains stained by both Nissl- and Klüver–Barrera revealed no apparent alteration in gross histomorphology in $Ca_v2.3$-deficient mouse brains suggesting that ablation of $Ca_v2.3$ VGCCs does not disrupt thalamocortical formation in the murine brain (Weiergraber et al., 2006a). Since immunohistochemistry and in situ hybridization has revealed that $Ca_v2.3$ E/R-type VGCCs are expressed in GABAergic interneurons within the RTN and the cortex (Talley et al., 2000; Weiergraber et al., 2006a), we looked into any possible subtle alteration on the cytoarchitectural level in $Ca_v2.3^{-/-}$ mouse brains compared to controls. One of the molecular markers for GABAergic interneurons is parvalbumin, a calcium-binding protein. Immunofluorescent staining on brain sections of both $Ca_v2.3^{+/+}$ and $Ca_v2.3^{-/-}$ mice displayed a similar staining pattern, with GABAergic RTN interneurons exhibiting intensively positive immunoreactivity (Figs. 1 A–D). The RTN generally appears as a thin layer interposed between the internal capsule and the external medullary lamina, crossed over by bundles of the thalamocortical–corticothalamic fibers, which becomes particularly obvious by using Kluver–Barrera staining (see Supplementary data). The presence of these bundles results in fragmentation of the nucleus into numerous mediolaterally oriented strips of cell bodies. The RTN can be generally divided into three parts, the dorsal (see also Figs. 1A, B), the ventral and the lateral part, exhibiting together a clear shell-like morphology. Parvalbumin staining of the RTN from $Ca_v2.3^{+/+}$ (Figs. 1A, C) and $Ca_v2.3^{-/-}$ mice (Figs. 1B, D) clearly exhibited that different reticular thalamic cell types can be distinguished (Spreafico et al., 1991; Battaglia et al., 1994; Nagaeva and Akhmadeev, 2006): 1. round neurons ("R") that make up about 37% of RTN neurons predominantly localized in the rostral pole of the RTN harboring 4–8 principal dendrites; 2. large fusiform neurons (F) contributing to about 49% to the RTN cell mass being equally represented throughout the nucleus with 2–4 dendrites from two poles) and finally small fusiform neurons (f) contributing app. 14% of the RTN cell mass mainly distributed in the medial and lateral border of the RTN with two polar dendrites (Figs. 1C, D). The parvalbumin antibody provided specific and intense staining not only of the soma but also the axonal and dendritic processes (Figs. 1C, D). Similarly, intense parvalbumin immunoreactivity in GABAergic interneurons was observed in the neocortex of $Ca_v2.3^{+/+}$ and $Ca_v2.3^{-/-}$ mice (Figs. 1E, F). These neurons are also known to express $Ca_v2.3$ forming part of the thalamocortical circuitry. In summary, detailed investigation of parvalbumin stained sections from both controls and $Ca_v2.3^{-/-}$ brains did not show alterations in cell-type specific composition of the RTN or structural connectivity between the GABAergic interneurons.

To directly prove that $Ca_v2.3$ is coexpressed with parvalbumin in GABAergic interneurons within the RTN and the cortex, double immunofluorescent labeling of the brain section from control and $Ca_v2.3^{-/-}$ mice was performed. However, two different antibodies against $Ca_v2.3$ (see Experimental methods) exhibited non-specific staining throughout the whole mouse brain sections of both genotypes. In stark contrast, the anti-$Ca_v2.3$ 195A antibody (Grabsch et al., 1999; Weiergraber et al., 2000) exhibited a distinct staining pattern in the RTN on rat brain sections (Figs. $2A_{II,V}$–$C_{II,V}$). These $Ca_v2.3$ positively stained cells are in fact GABAergic as they were co-immunostained for parvalbumin (Fig. $2A_{III,VI}$). In contrast, there were low numbers of calretinin positive neurons in the rat RTN (Fig. $2B_{I,IV}$) that were only partially $Ca_v2.3$ positive (Fig. $2B_{III,VI}$). No immunoreactivity of calbindin was seen in the rat RTN (Fig. $2C_{I,IV}$).

$Ca_v2.3$-deficient mice do not exhibit spontaneous SWDs indicative of absence seizure activity

We previously reported that both video analysis and radiotelemetric electrocorticographic and deep, intracerebral electroencephalographic recordings from $Ca_v2.3^{-/-}$ mice did not exhibit spontaneous epileptiform behavior or ictal discharges indicative of convulsive seizure activity (Weiergraber et al., 2006a; Weiergraber et al., 2006b). Furthermore, a detailed qualitative and quantitative analysis of long-term ECoG recordings from various cortical regions,

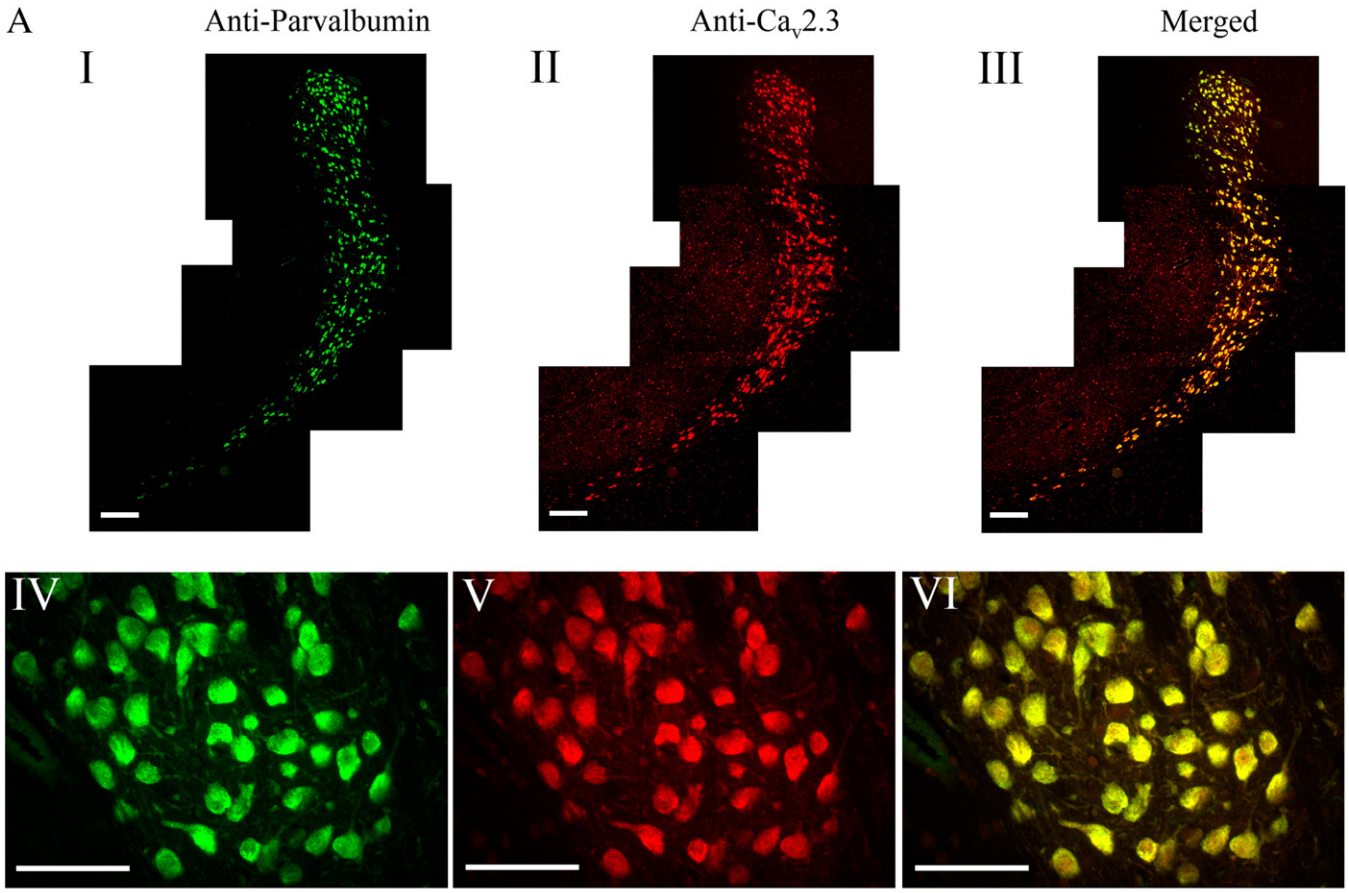
A
Anti-Parvalbumin
Anti-Cav2.3
Merged
I
II
III
IV
V
VI

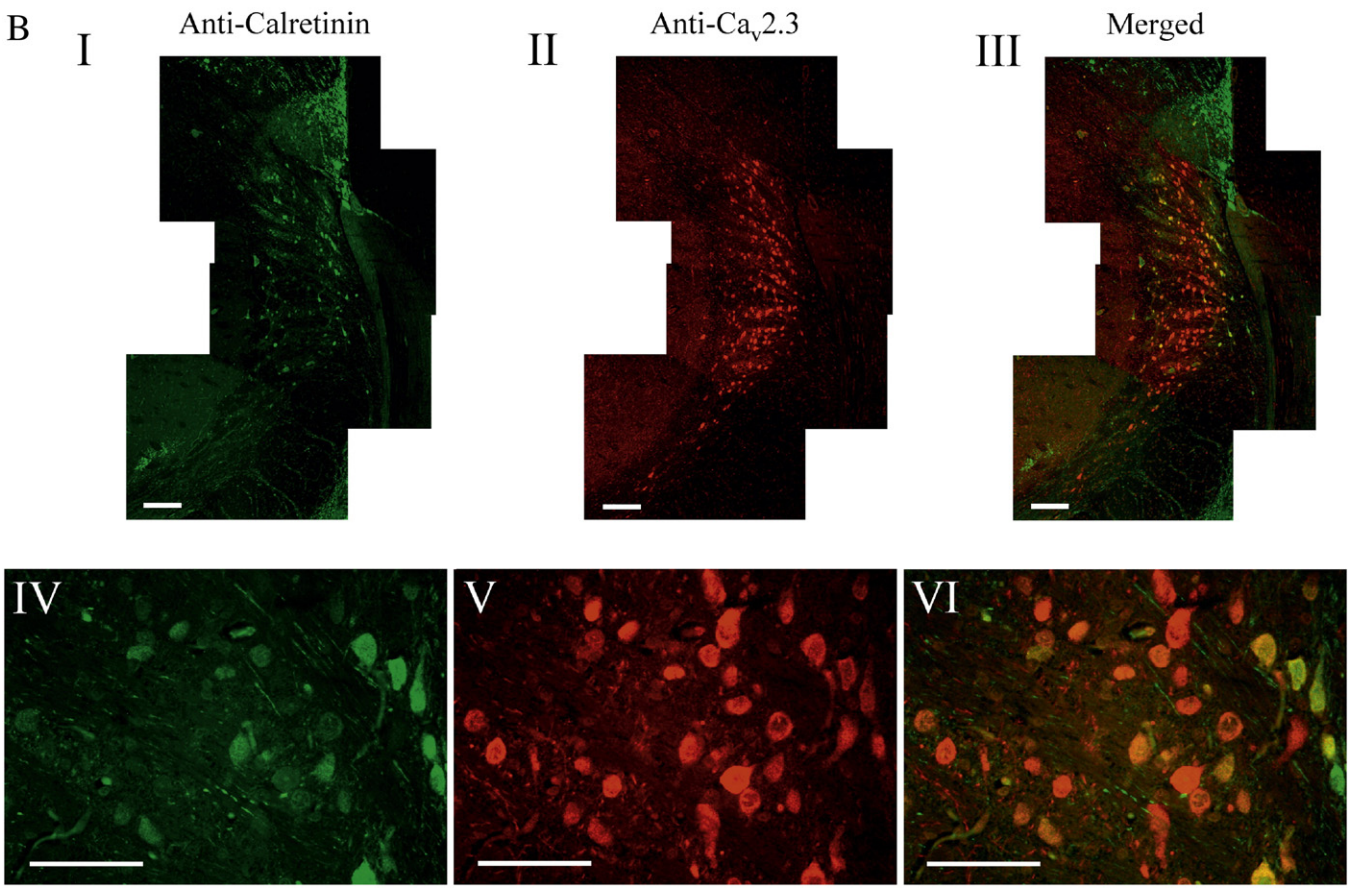
B
Anti-Calretinin
Anti-Cav2.3
Merged
I
II
III
IV
V
VI

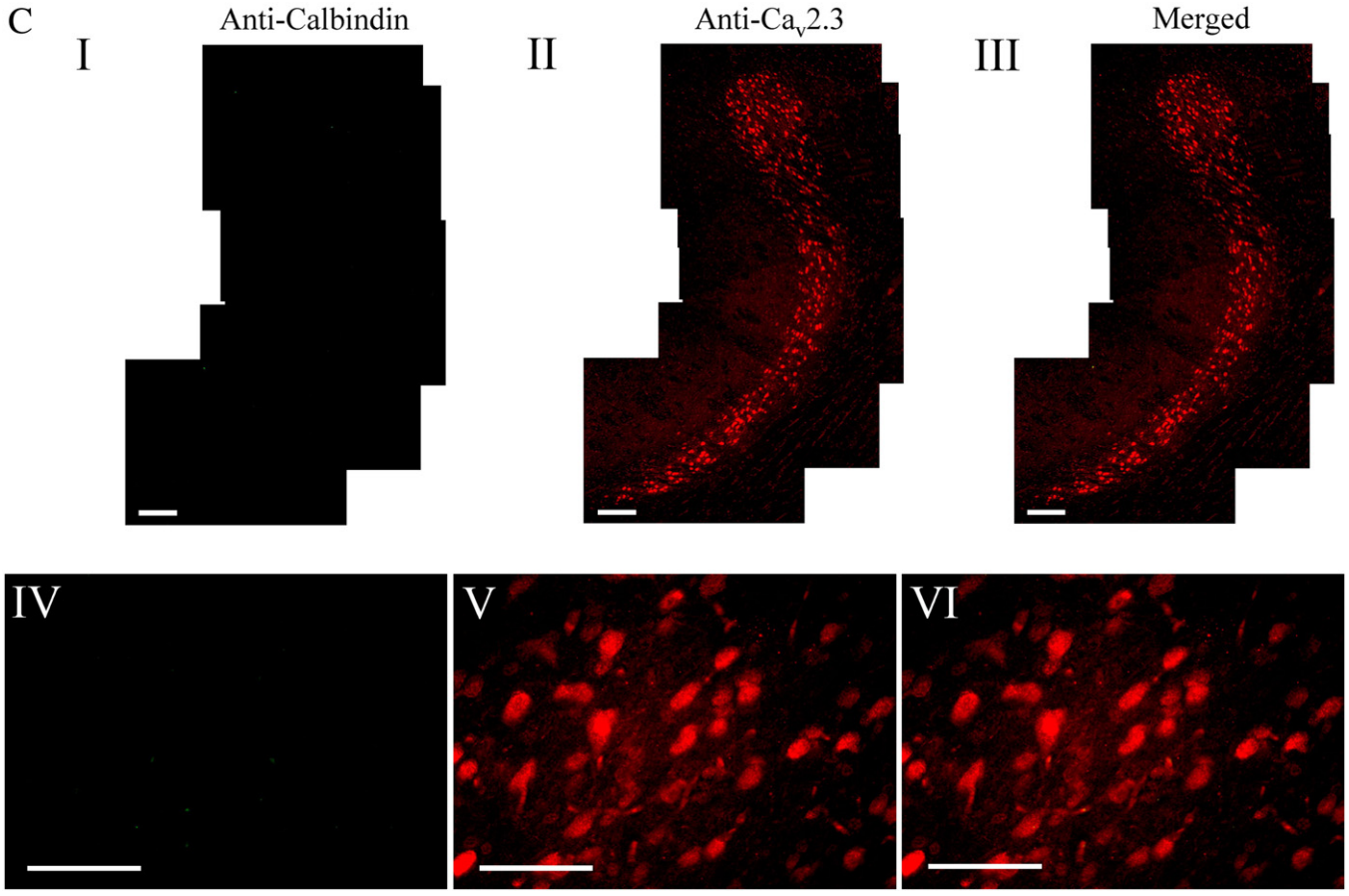

Fig. 2. Immunolocalization of $Ca_v2.3$ E/R-type calcium channels in the rat RTN and coexpression with calcium-binding proteins. As $Ca_v2.3$ antibodies failed to exhibit specific staining on murine brain sections, we performed immunofluorescent double staining for the calcium-binding proteins parvalbumin (A), calretinin (B) and calbindin (C) together with $Ca_v2.3$ Ca^{2+} channels on rat brain sections using the anti-$Ca_v2.3$ 195A antibody. Parvalbumin staining ($A_{I,IV}$) displays the characteristic shell-shaped structure of the RTN localized at the lateral edge of the thalamic region. The number of calretinin positive RTN neurons is considerably less ($B_{I,IV}$) and there was hardly any immunopositive reaction for calbindin ($C_{I,IV}$). Immunolocalization of $Ca_v2.3$ E/R-type Ca^{2+} channels ($A_{II,V}$–$C_{II,V}$) revealed almost complete staining of the RTN with double staining exhibiting strong colocalization of $Ca_v2.3$ Ca^{2+} channels with parvalbumin ($A_{III,\ VI}$) but to a much lesser extent with calretinin ($B_{III,VI}$). Bar ($A_{I–III}$–$C_{I–III}$): 200 μm; bar ($A_{IV–VI}$–$C_{IV–VI}$): 75 μm.

such as the motor cortex (M1/M2) or the somatosensory cortex (Fig. 3$A_{c1,c2}$, Fig. 4$A_{c1,c2}$) clearly demonstrates that $Ca_v2.3$-deficient mice do not spontaneously exhibit SWDs indicative of non-convulsive absence seizure activity.

Increased SWD activity in $Ca_v2.3$-deficient mice following γ-hydroxybutyrolactone (GBL) administration

To investigate the functional relevance of the $Ca_v2.3$ E/R-type Ca^{2+} channel in SWD generation in vivo, we systemically administered γ-hydroxybutyrolactone (GBL), a prodrug of γ-hydroxybutyric acid (GHB), into control mice (27.86±1.78 g, 16.36±1.24 weeks, n=8, all ♂) and $Ca_v2.3$-deficient animals (32.16±0.99 g, 15.09±1.05 weeks, n=8, all ♂). Both genotypes were given at least 7 days after implantation to allow for full recovery ($Ca_v2.3^{+/+}$: 13.75±1.33 days; $Ca_v2.3^{-/-}$: 12.00±0.82 days). GBL is a moderate $GABA_B$-receptor agonist but exerts also strong agonistic effects on the newly characterized GBL-receptors (Andriamampandry et al., 2007) probably via G-protein coupled pathways (Snead, 2000). It is known that $GABA_B$-receptor agonists exacerbate absence seizures, whereas $GABA_B$-receptor antagonists suppress them (Snead, 1992; Hosford et al., 1992; Smith and Fisher, 1996). Thus, GBL injection results in highly organized bilaterally synchronous SWD activity typically associated with behavioral phenomena, such as facial myoclonus, vibrissal twitching and most importantly, motoric arrest (Snead et al., 2000).

In controls, administration of GBL at 70 mg/kg results in typical paroxysmal SWD activity (Figs. 3A, B_3) predominantly in the frequency range of 2–5 Hz. As depicted in Fig. 4A, $Ca_v2.3^{-/-}$ mice are capable of exhibiting SWD activity at earlier stage following GBL injection compared to control animals (see also Fig. 5A). Statistical analysis revealed that ictal SWD latency was significantly shorter in $Ca_v2.3^{-/-}$ mice compared to controls ($Ca_v2.3^{-/-}$: 149.8±20.4 s, n=8 versus $Ca_v2.3^{+/+}$: 723.5±136.3 s, n=8, p<0.001; Fig. 5A). Furthermore, the total number of SWD episodes within the entire one-hour observation period was increased in $Ca_v2.3^{-/-}$ mice (22.13±1.01, n=8) versus controls (7.00±0.46, n=8, p<0.001, Fig. 5B) and the same trend held for the total duration of SWD epochs ($Ca_v2.3^{+/+}$: 1179.4±122.3 s; n=8 versus $Ca_v2.3^{-/-}$: 2264.4±188.8 s; n=8; p<0.001, Fig. 5D). On the contrary, the average duration of each SWD events was reduced in $Ca_v2.3$-deficient animals (105.1±12.2 s; n=8) compared to controls (173.7±22.9 s; n=8 p=0.019, Fig. 5C). Intriguingly, these results demonstrate that systemic ablation of the $Ca_v2.3$ E/R-type Ca^{2+} channel results in increased absence seizure susceptibility and altered absence seizure architecture unravelled by the modified electroencephalographic SWD parameters.

γ-hydroxybutyrolactone (GBL) induced motoric arrest in $Ca_v2.3^{-/-}$ mice and controls

Gamma-hydroxybutyrolactone, which is metabolized to GHB, is known to cause a typical biphasic motoric phenotype characterized by initial cessation of activity accompanied with dominant absence seizure activity which is then followed by irregular and increasing locomotion again. We therefore investigated the motoric activity

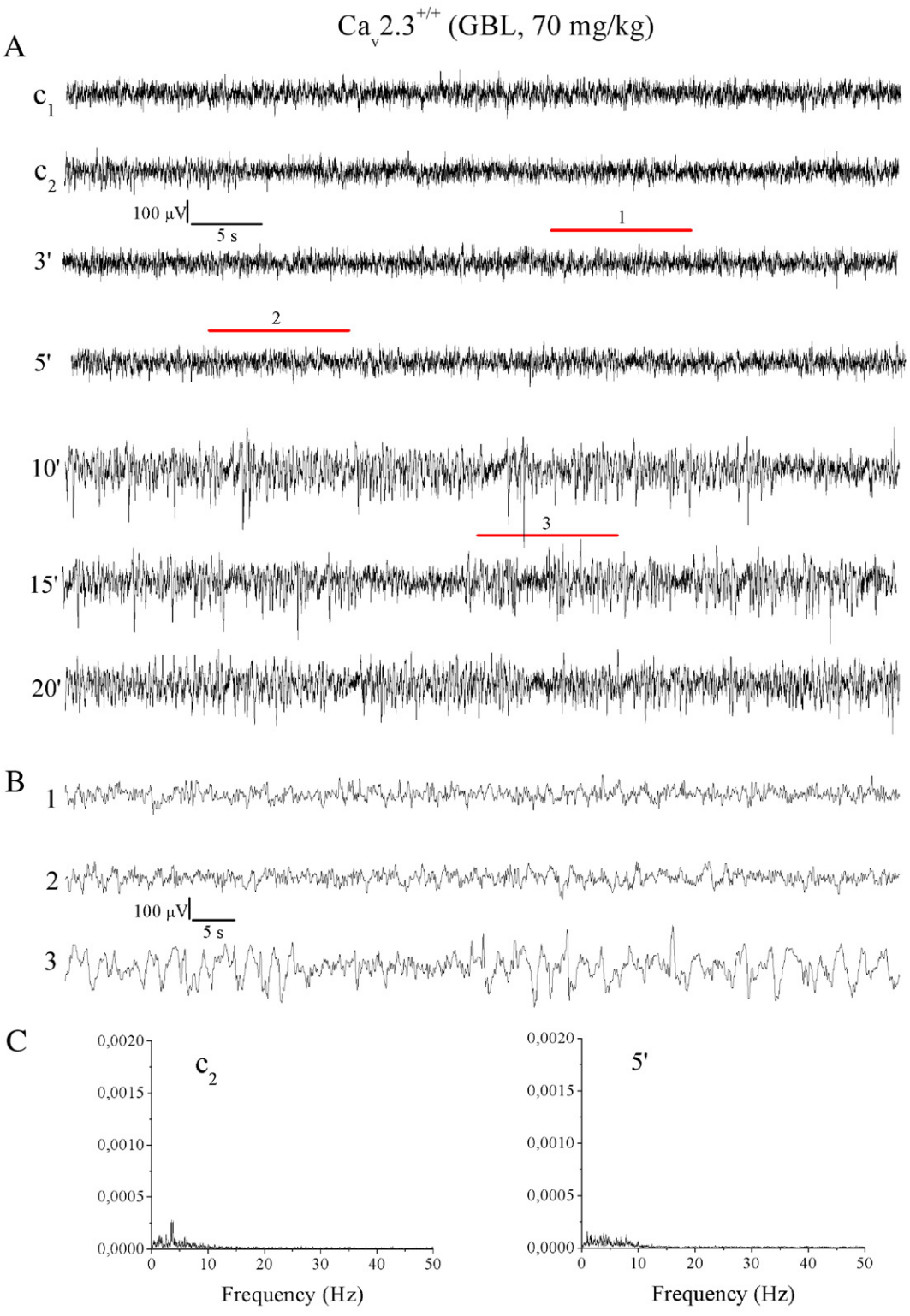

Fig. 3. Spike–wave discharges induced by γ-hydroxybutyrolactone (GBL) in control and $Ca_v2.3^{-/-}$ mice (Fig. 4). (A) Representative 1 min radiotelemetric ECoG recordings before (c_1, c_2) and after the administration of GBL (70 mg/kg i.p.) at the time points indicated. Horizontal bars (labeled 1–3) represent EEG segments that are displayed with an expanded time scale in B_{1-3}. In $Ca_v2.3^{+/+}$ (B_3) and $Ca_v2.3^{-/-}$ (Fig. 4B_{1-3}) typical bilaterally synchronous SWD activity becomes apparent. (C) Power-spectrum density analysis of a control segment (Ac_2) and EEG epoch 5 min after GBL injection exhibits typical theta- and delta-wave activity due to SWDs in $Ca_v2.3^{-/-}$ mice (Fig. 4C). Note that latency till first occurrence of absence seizure activity is reduced in $Ca_v2.3$-deficient animals (Fig. 4$A_{3'}$, see also Fig. 5A).

(activity index) of controls and $Ca_v2.3$-deficient mice on a horizontal plane using the implantable radiotelemetry. Although both genotypes exhibit the characteristic biphasic locomotion profile, there are marked differences in their initial hypoactive segment (Fig. 6A). Whereas control animals displayed only a moderate reduction in motoric activity, administration of GBL in $Ca_v2.3^{-/-}$ mice results in a total cessation of activity for at least 20–25 min following injection (Fig. 6A). Detailed analysis demonstrated that the mean activity index is reduced in $Ca_v2.3^{-/-}$ mice compared to controls approaching a level of significance (2.46±0.66 rel. units, n=8 versus 6.90±2.08 rel. units,

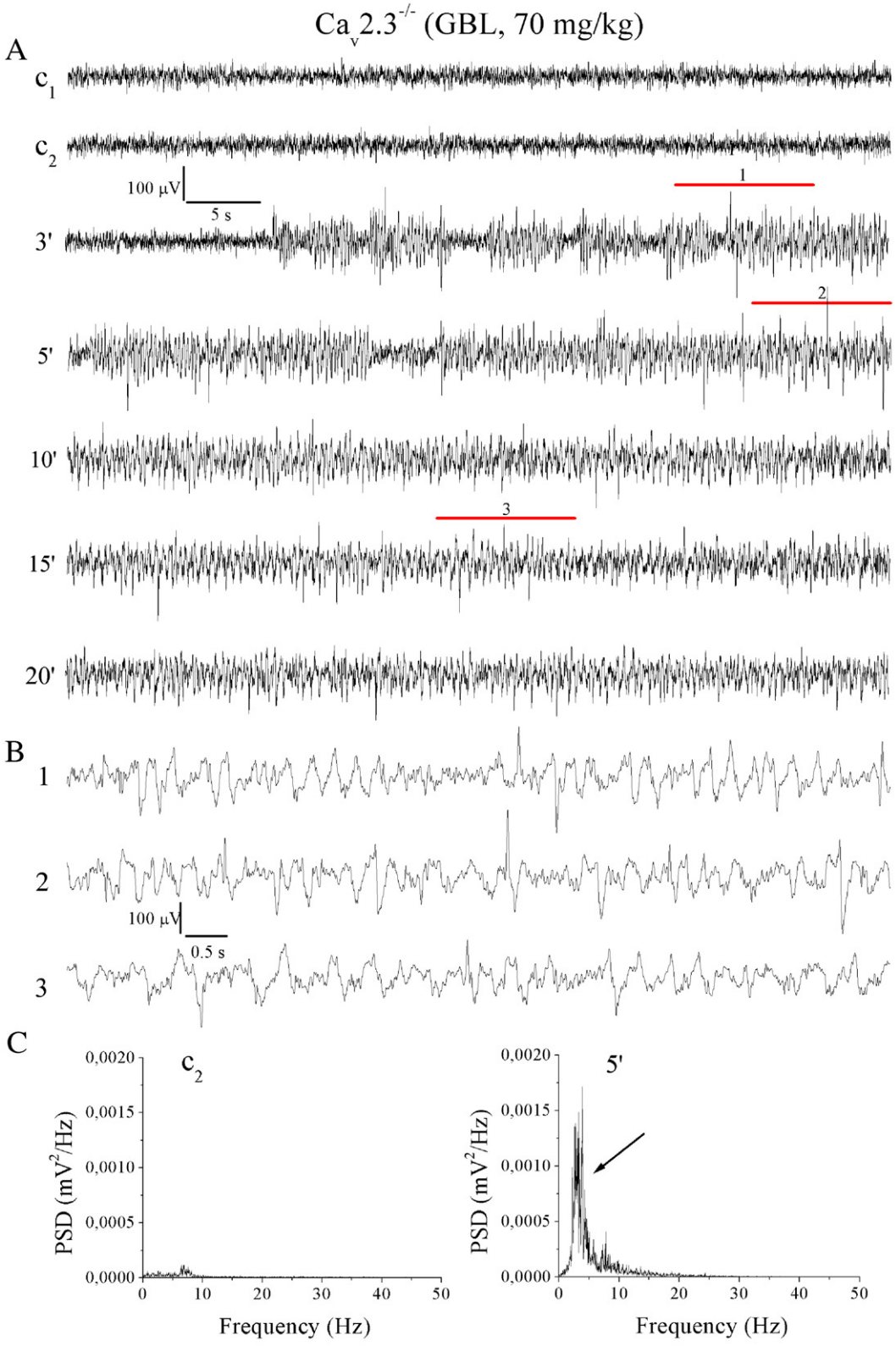

Fig. 4. Spike–wave discharges induced by γ-hydroxybutyrolactone (GBL) in control (Fig. 3) and Ca$_v$2.3$^{-/-}$ mice. (A) Representative 1 min radiotelemetric ECoG recordings before (c$_1$, c$_2$) and after the administration of GBL (70 mg/kg i.p.) at the time points indicated. Horizontal bars (labeled 1–3) represent EEG segments that are displayed with an expanded time scale in B$_{1-3}$. In Ca$_v$2.3$^{+/+}$ (Fig. 3B$_3$) and Ca$_v$2.3$^{-/-}$ (B$_{1-3}$) typical bilaterally synchronous SWD activity becomes apparent. (C) Power-spectrum density analysis of a control segment (Ac$_2$) and EEG epoch 5 min after GBL injection exhibits typical theta- and delta-wave activity due to SWDs in Ca$_v$2.3$^{-/-}$ mice (C). Note that latency till first occurrence of absence seizure activity is reduced in Ca$_v$2.3-deficient animals (A$_3$, see also Fig. 5A).

$n=8$, $p=0.061$, Fig. 6C). Specifically, the time of total inactivation is significantly increased in Ca$_v$2.3-deficient animals (46.13±2.81 min, $n=8$ versus 25.00±2.43 min, $n=8$, $p<0.001$, Fig. 6B). In addition, GBL-induced hypolocomotion was typically accompanied by transient hypothermia which was also measured by radiotelemetry (data not shown). These results clearly illustrate that the increased SWD activity

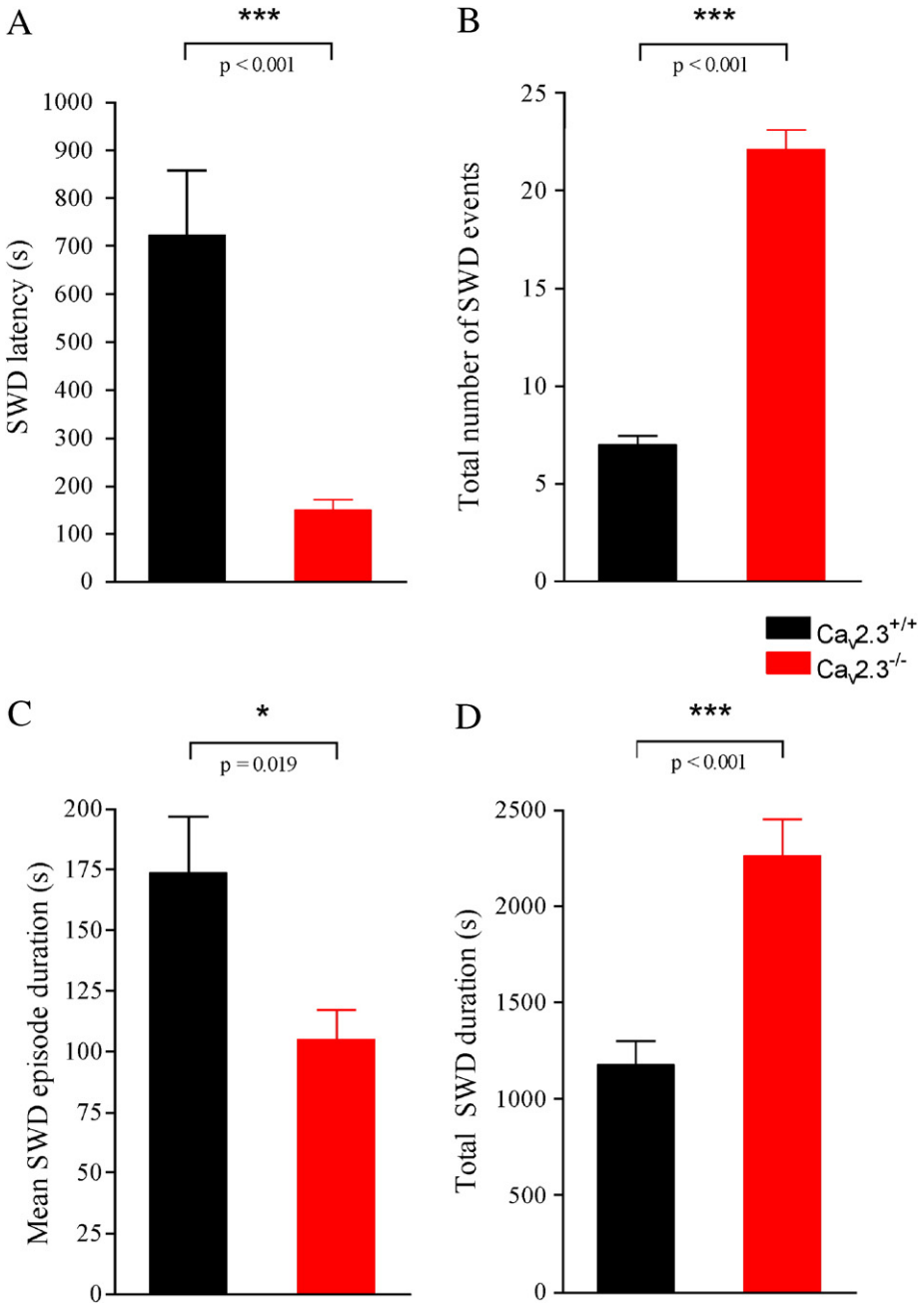

Fig. 5. Quantitative SWD analysis in controls and $Ca_v2.3^{-/-}$ mice following GBL administration. Latency till first occurrence of SWD is shortened in $Ca_v2.3^{-/-}$ mice (A). Furthermore, the total number of SWD episodes as well as the total SWD duration is increased in $Ca_v2.3$-deficient mice compared to controls (B, D). However, the average SWD duration in transgenic mice was reduced (C), indicating increased SWD susceptibility and altered SWD architecture in $Ca_v2.3^{-/-}$ mice.

observed in $Ca_v2.3^{-/-}$ mice coincides with enhanced motoric arrest typical of GBL-induced absence seizure activity.

Power-spectrum density analysis of GBL-induced absence seizure activity in $Ca_v2.3^{-/-}$ mice and controls

In addition to the analysis of SWD activity by visual inspection of the EEG and quantification of indirect behavioral phenomena, e.g. motoric activity, we used a third independent mathematical approach based on power-spectrum density (PSD) analysis to further validate increased bilaterally synchronous SWD activity in $Ca_v2.3$-deficient mice. In the primary analysis, we performed both continuous and discontinuous PSD analysis of 30 s ECoG segments before and after GBL administration to ascertain that GBL-induced SWD activity is embodied in the theta- and delta-wave frequency range (not shown, but see also Fig. 4C, Figs. 7A, B). Based on these findings, we performed a three-dimensional PSD plot for the total one-hour observation period following GBL injection for the different EEG frequency ranges, δ, θ, α, β and γ. Most importantly, the theta and particularly the delta frequency range known to represent SWDs typical of absence seizure activity are strongly increased in $Ca_v2.3^{-/-}$ mice compared to controls, particularly within the first 25 min after GBL administration (Figs. 7A, B). During this early period, the enhanced ictal theta- and delta-wave activity in $Ca_v2.3^{-/-}$ mice was again accompanied by complete cessation of locomotive activity in these animals, whereas there was only moderate theta and delta PSD increase associated with minor hypolocomotion in the control group (Figs. 6A, B).

These results were further supported by the analysis of PSD peak latencies of the individual frequency bands (Fig. 7C). In agreement

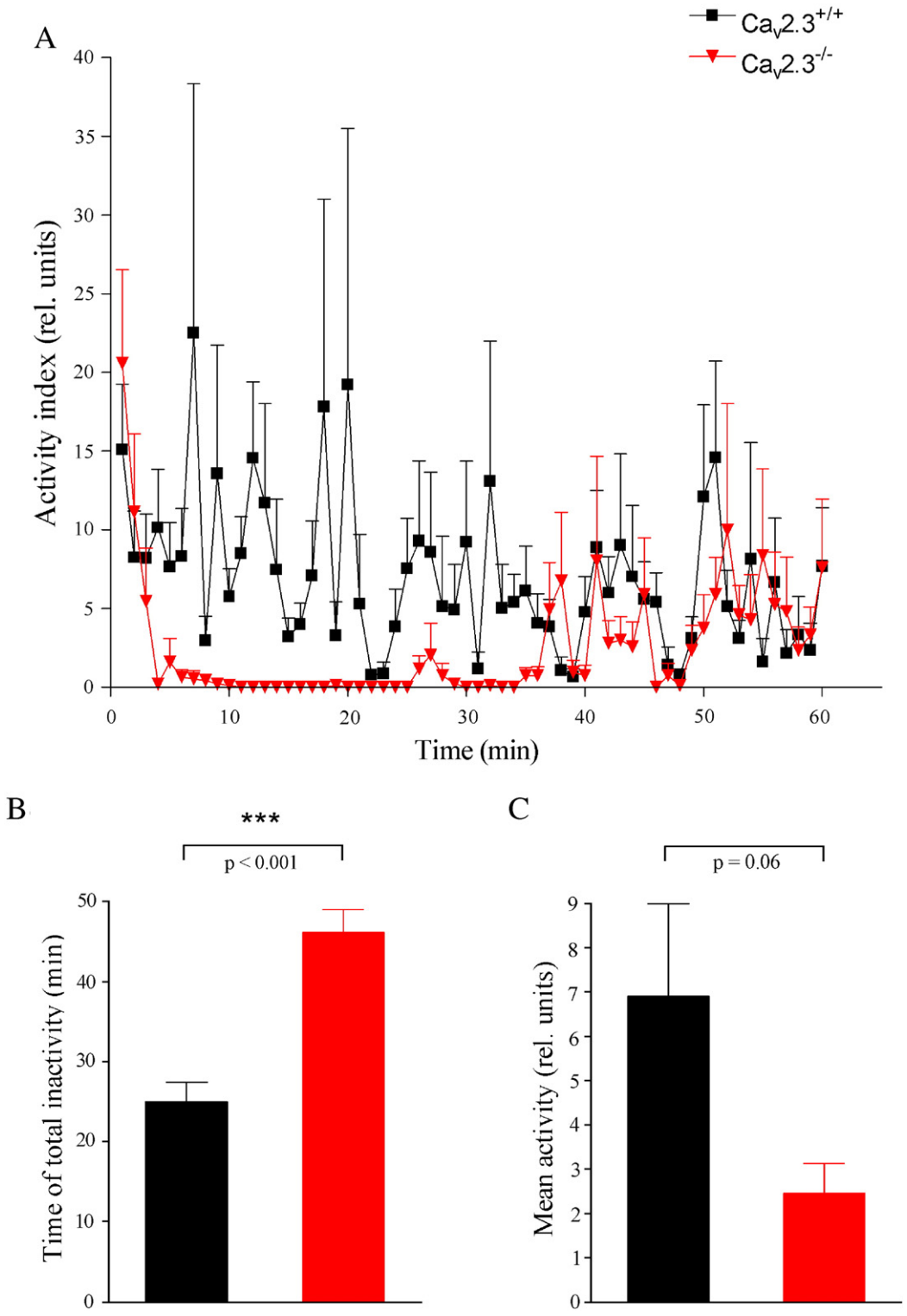

Fig. 6. Hypolocomotion in control and Ca$_v$2.3$^{-/-}$ mice following GBL administration. (A) Continuous plot of the activity index (representing movement on the horizontal plane) for one-minute episodes averaged for control and Ca$_v$2.3$^{-/-}$ mice. Ca$_v$2.3$^{-/-}$ mice display a complete cessation of activity within the first 20–25 min after GBL administration, which is only moderate in control mice. Whereas the mean activity does not differ significantly between both genotypes (C), the time of complete inactivity is markedly increased in Ca$_v$2.3 deficient animals (B).

with three-dimensional PSD analysis (Figs. 7A, B), the delta EEG frequency band reaches its PSD peak much earlier in Ca$_v$2.3$^{-/-}$ mice compared to control animals (delta, 0–4 Hz: 10.50±0.82 min in Ca$_v$2.3$^{-/-}$ mice, n=8 versus 16.25±1.94 min in Ca$_v$2.3$^{+/+}$, n=8, p=0.016) and the theta band (4–8 Hz) approaches a level of significance (13.00±4.28 min in Ca$_v$2.3$^{-/-}$ mice, n=8 versus 24.75±4.47 min in Ca$_v$2.3$^{+/+}$, n=8, p=0.078, Fig. 7C). For the other frequency ranges, alpha (8–12 Hz), beta (12–32 Hz) and gamma (32 – 50 Hz), there was no difference in PSD activity between both genotypes (Figs. 7A, B). In addition, the peak latency for alpha and beta PSD activity remained unchanged. The significant reduction in gamma PSD peak latency in control animals compared to Ca$_v$2.3$^{-/-}$ mice is

based on fluctuating low level PSD values (see also Figs. 7A, B) of which the biological relevance remains to be determined (18.25±8.02 min in $Ca_v2.3^{+/+}$, $n=8$ versus 51.25±3.18 min in $Ca_v2.3^{-/-}$, $n=8$, $p=0.002$, Fig. 7C).

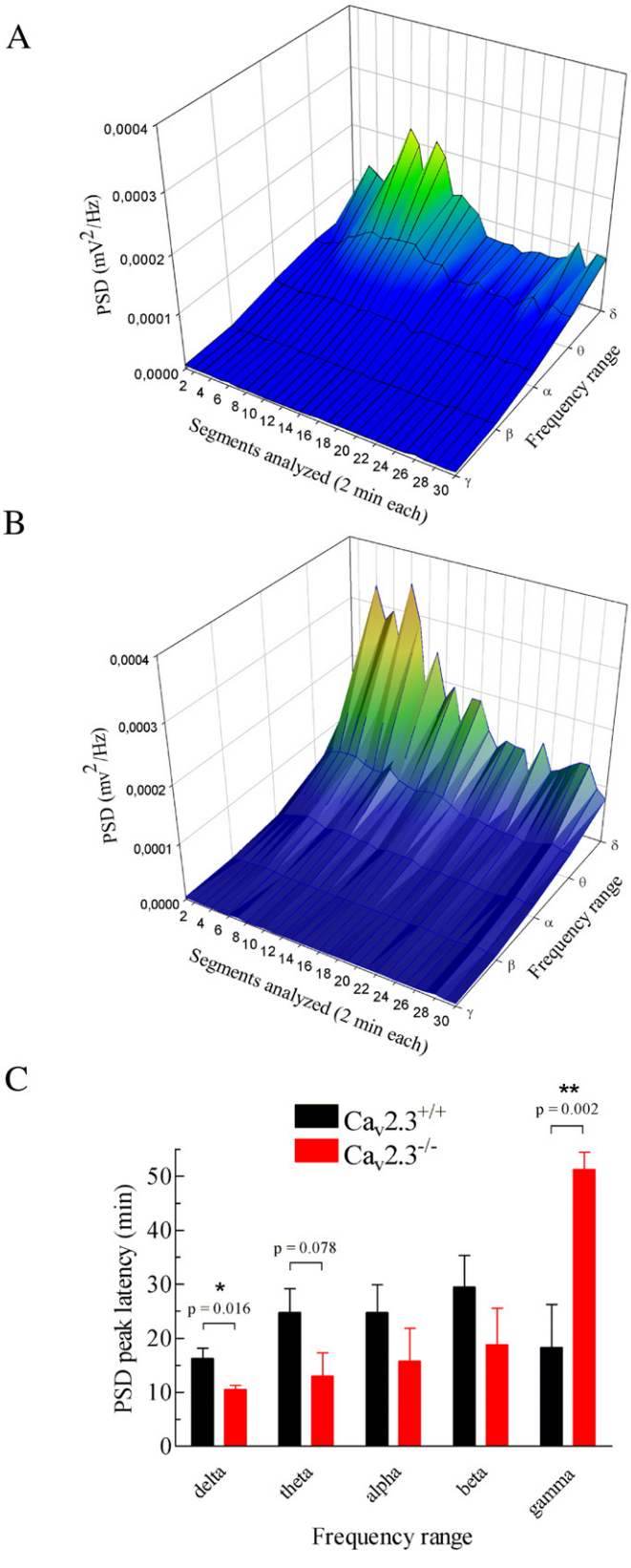

Frequency distribution of GBL-induced thalamocortical hyperoscillation in control and $Ca_v2.3$-deficient mice

In order to investigate the frequency distribution of thalamocortical hyperoscillation, we performed a continuous PSD analysis of 5 s SWD epochs ranging from 0 to 12 Hz in both controls and $Ca_v2.3^{-/-}$ mice. Figs. 8A and B illustrates the spectral distribution with PSD normalized to peak values. Both plots display that GBL-induced SWDs characteristic of absence seizure activity predominate in the theta and particularly the delta frequency range. Furthermore, the SWD peak frequency is slightly reduced in $Ca_v2.3^{-/-}$ mice compared to controls (2.79±0.23 Hz in $Ca_v2.3^{-/-}$, $n=8$ versus 3.34±0.24 Hz in $Ca_v2.3^{+/+}$, $n=8$), however, not reaching the level of significance ($p=0.128$, Fig. 8C). Previous studies in $Ca_v3.1^{-/-}$ and control mice have revealed similar frequencies of 3–4 Hz of paroxysmal SWDs in epidural EEG recordings (Kim et al., 2001).

Discussion

The thalamocortical circuitry is part of a complex neural system that is involved in the control of different stages of vigilance. Within this circuitry thalamic relay cells project to cortical pyramidal neurons that finally reproject to the ventrobasal thalamus. An important structural component in this circuitry is the RTN formation, which is composed of GABAergic interneurons receiving not only collateral glutamatergic projections from cortical pyramidal and thalamic relay cells but also GABAergic projections from other RTN neurons (Manning et al., 2003; Khosravani and Zamponi, 2006). Other than GABA, somatostatin, acetylcholine, CCK and serotonin are also found in RTN terminals (Nagaeva and Akhmadeev, 2006). An intriguing feature of these neurons is that they can exhibit two different modes of action characteristic of different stages of vigilance. At high vigilance, deeper brain structures, e.g. the reticular formation exerts excitatory input on thalamic relay cells and inhibitory effects on RTN neurons. The cells slightly depolarize resulting in the so-called tonic mode of action. Under these conditions, spiking frequency and pattern codes for the information perceived in the periphery which is finally processed to the cortex via ventrobasal thalamic relay cells (Llinas and Steriade, 2006). The ECoG correlate of this tonic behavior is a typical low-amplitude, high-frequency pattern as observed in the beta- and gamma-wave band. With decreasing activity from deeper activating brain structures the thalamic neurons re- and hyperpolarize, passing the intermediate state finally exhibiting the burst mode of action. At hyperpolarizing membrane potentials, low-voltage-activated T-type Ca^{2+} channels deinactivate, a process known as repriming which allows these channels to be activated upon small depolarization steps due to hyperpolarization and cyclic-nucleotide gated channels (HCN2, HCN4). This results in the generation of low-threshold calcium spikes (LTCSs) superimposed with sodium bursting (Llinas and Steriade, 2006). This rebound burst firing mode in ventrobasal thalamic cells and RTN neurons is a major cellular electrophysiological phenomenon typical of low stages of vigilance, e.g. during slow-wave sleep (Shin, 2006). Subsequent oscillatory thalamocortical activity triggers characteristic low-frequency, high-amplitude theta- and delta-wave EEG

Fig. 7. Power-spectrum density analysis of GBL-induced SWD activity in control and $Ca_v2.3$-deficient mice. Three-dimensional plot of averaged absolute PSD (mV^2/Hz) from controls (A) and $Ca_v2.3^{-/-}$ mice (B). PSD was calculated for 2 min ECoG epochs. Both genotypes predominately differ in theta- and delta-wave activity representing ictal SWDs. The steep increase in theta and particularly the delta PSD within the first 20 min after GBL administration in $Ca_v2.3^{-/-}$ mice coincides with enhanced hypolocomotion up to complete motoric cessation in this genotype (Fig. 6A). (C) Power-spectrum density peak latency of different EEG frequency bands following GBL administration. The mean latencies till the occurrence of peak PSD for the individual frequency ranges were calculated by analyzing 2 min ECoG epochs. The ictal delta power-spectrum density peak exhibits reduced latency in $Ca_v2.3^{-/-}$ mice compared to controls as depicted in (A) and (B).

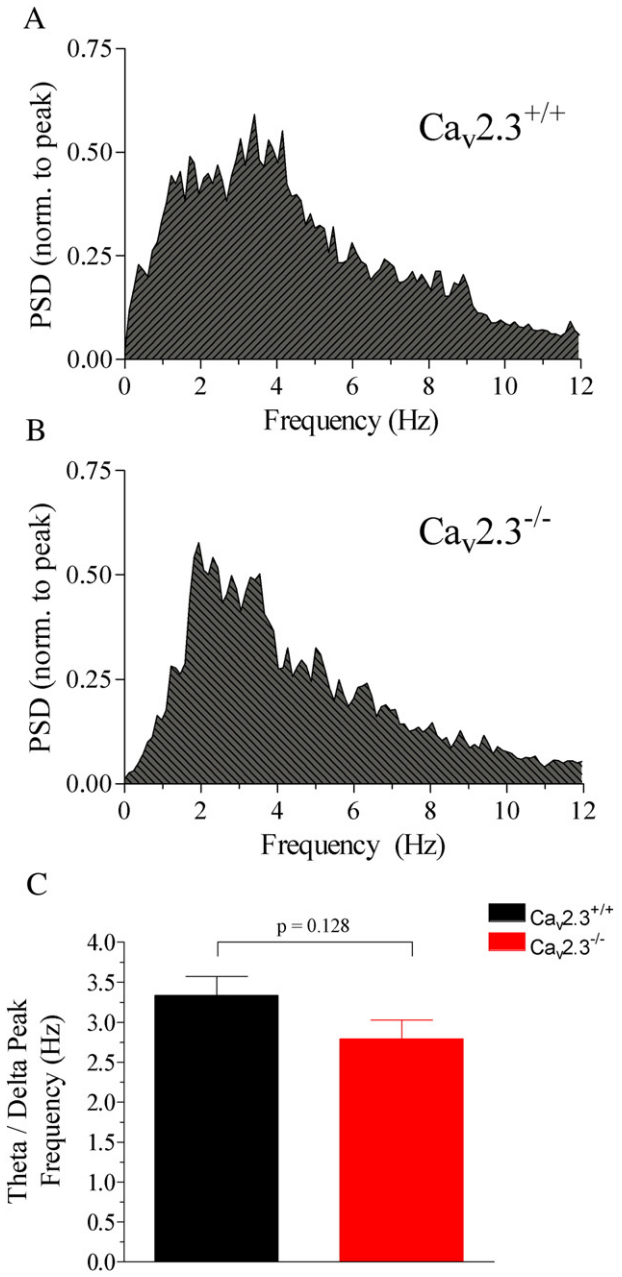

Fig. 8. Frequency distribution of SWD activity in controls and $Ca_v2.3^{-/-}$ mice. Three representative 30 s SWD segments from each control and $Ca_v2.3$-deficient mouse were analyzed by continuous PSD analysis and plotted as mean normalized PSD distribution in a frequency range from 0–12 Hz (A, B). GBL-induced SWD activity is predominant in the upper delta to lower theta wave range (3–6 Hz) as reported previously. Though slightly reduced, thalamocortical peak oscillation frequency during absence seizure activity does not differ significantly from control mice.

activity. Enhanced rebound burst firing of thalamic relay neurons and RTN cells has been clearly implicated to play a crucial role in the etiopathogenesis of absence epilepsy (Shin, 2006).

Within the last decade VGCCs have gained major relevance in the etiopathogenesis of absence epilepsy due to their unique electrophysiological properties and cellular distribution (Weiergraber et al., 2006b). The $Ca_v2.3$ E/R-type VGCC is expressed in GABAergic interneurons in the cortex and also in the RTN where $Ca_v3.2$ and $Ca_v3.3$ T-type Ca^{2+} channels can also be found (Fig. 1; Talley et al., 2000; Weiergraber et al., 2006a). In contrast, thalamic relay cells do not express considerable $Ca_v2.3$ amounts, whereas $Ca_v3.1$ displays high transcript levels (Talley et al., 1999; Talley et al., 2000). In accordance with its selective expression in the thalamic relay nucleus, Kim et al. (2001) and Lee at al. (2004) demonstrated that $Ca_v3.1$ null mutants are resistant to absence seizures induced by GBL or baclofen, exhibiting strong reduction of slow-wave sleep and alteration of sleep architecture. In addition, crossbreeding $Ca_v3.1^{-/-}$ mice with various $Ca_v2.1$ mouse mutants (e.g. tottering, tottering leaner, rocker, rolling Nagoya, lethargic) or $Ca_v2.1^{-/-}$ mice that display spontaneous absence seizure activity resulted in offspring that were either free from absence seizures or displayed significant reduction in SWD activity (Song et al., 2004). These findings demonstrate that the $Ca_v3.1$ T-type Ca^{2+} channel is of functional relevance in thalamocortical rhythmicity and absence epileptogenesis by contributing to low-threshold Ca^{2+} spikes and rebound bursting in ventrobasal thalamic neurons. Most interestingly, reticular thalamic neurons were also reported to generate spontaneous oscillations, such as rhythmic spike-burst activities (Von Krosigk et al., 1993; Kim et al., 1995) which exert severe inhibitory input to ventrobasal relay neurons serving as a major driving force for rebound burst firing due to hyperpolarization. Thus, SWD activity in absence epilepsy can originate from RTN neurons. Although gene ablation studies on $Ca_v3.2$ and $Ca_v3.3$ T-type Ca^{2+} channel involvement in absence epilepsy in mice have not been published yet, preliminary data suggest a significant contribution of $Ca_v3.2$ to the generation of SWD induced by baclofen (Shin, 2006). In addition, several $Ca_v3.2$ gain-of-function mutations have been reported in humans associated with childhood absence epilepsy (CAE) (Khosravani et al., 2004; Khosravani et al., 2005; Shin, 2006). Therefore, low-voltage activated T-type Ca^{2+}-current enhancement in both thalamic relay cells and RTN neurons is involved in SWD generation and thus absence epileptogenesis.

Though expressed in the RTN, the functional implications of $Ca_v2.3$ in thalamocortical rhythmicity still remain unknown. In this study we analyzed $Ca_v2.3$-deficient mice with respect to their propensity to generate SWDs using a well-established pharmacological GBL model of absence seizure activity. Our results provide the first and conclusive evidence for a critical role of $Ca_v2.3$ E/R-type Ca^{2+} channels in the generation of and prevention from absence seizures and thalamocortical hyperoscillation. We demonstrated that $Ca_v2.3$ ablation results in increased absence seizure susceptibility and altered absence seizure architecture. The increased SWDs activity in $Ca_v2.3^{-/-}$ mice compared to controls was further shown to coincide with enhanced motoric arrest in $Ca_v2.3$-deficient animals, which is typical of simple absence epilepsy not only in humans but also in rodents. There is a general agreement that the $Ca_v2.3$ non-L-type Ca^{2+} channel exhibits mid- to high-voltage activated behavior (Catterall et al., 2005; Kisilevsky and Zamponi, 2008). Thus, activation of $Ca_v2.3$ Ca^{2+} channels would further depolarize RTN neurons facilitating the tonic firing mode and preventing the cells from exhibiting rebound burst firing (Fig. 9A). This antihyperoscillatory and SWD activity suppressing effect of high-voltage activated Ca^{2+} channel activation has been reported for GAERS, a rat model of absence epilepsy, in which SWDs are effectively diminished by BayK-8644 administration, an L-type Ca^{2+} channel agonist or increased by L-type Ca^{2+} channel blockers, e.g. dihydropyridines (van Luijtelaar et al., 2000). As normal thalamocortical rhythmicity is based on a functional equilibrium of low- and high-voltage activated Ca^{2+}-current in RTN neurons, ablation of $Ca_v2.3$ Ca^{2+} channels is likely to result in a functional overbalance of the low-voltage activated T-type Ca^{2+} channel fraction and would thus facilitate rebound burst firing as it is unmasked in $Ca_v2.3$-deficient mice following GBL administration (Fig. 9B). Furthermore, our findings clearly parallel data obtained by van de Bovenkamp-Janssen et al. (2004) in WAG/Rij rats, illustrating that occurrence of SWDs in this rat model of absence epilepsy is accompanied by a lack of expression of the $Ca_v2.3$ E/R-type VGCC in the RTN at the age of absence seizure onset. In addition, de Borman et al. (1999) and Lakaye et al. (2002) detected a significant reduction of $Ca_v2.3$ transcript levels in both cerebellum

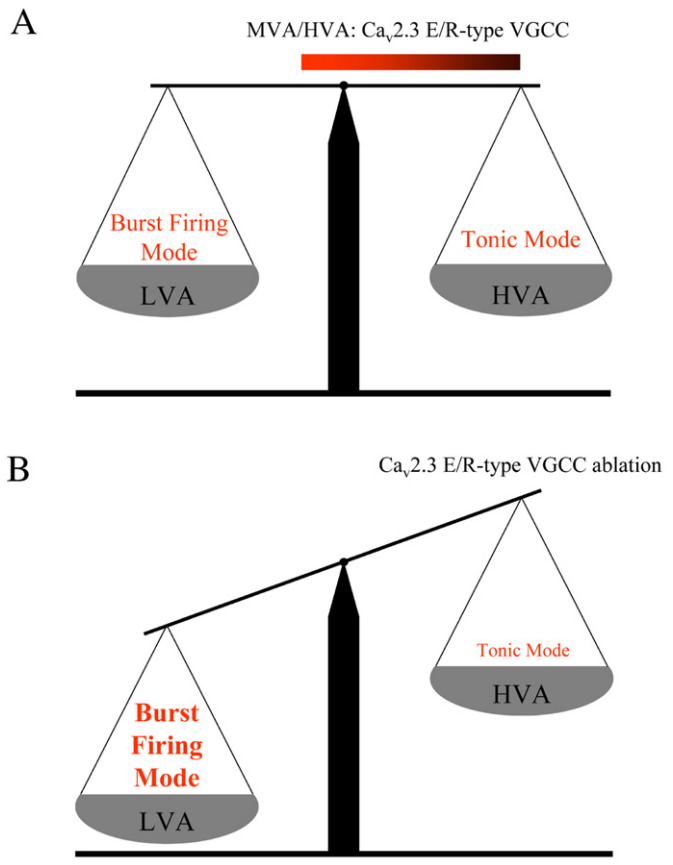

Fig. 9. Voltage-gated Ca^{2+} channels as functional regulators of thalamocortical burst activity. Depending on the depolarizing or hyperpolarizing input, thalamic relay cells and RTN neurons can switch between different modes, the tonic, intermediate and burst mode of action. Activation of high-voltage activated Ca^{2+} channels is supposed to result in further depolarization of the cell, thus facilitating the tonic mode of action. In contrast, enhanced low-voltage-activated T-type Ca^{2+}-currents or reduced high-voltage activated Ca^{2+} channel activity facilitates the burst mode of action. As $Ca_v2.3$ E/R-type channels exhibit mid- to high-voltage activated properties (A), ablation of this channel results in functional overbalance of the T-type Ca^{2+} channel population which would subsequently favor thalamocortical burst activity in $Ca_v2.3^{-/-}$ mice (B). As $Ca_v2.3$ is also expressed in extrathalamocortical structures, modulatory influence on RTN membrane potential cannot be excluded.

and medulla of GAERS, pointing to a functional involvement of $Ca_v2.3$ in absence epileptogenesis and further stressing the role of $Ca_v2.3$ positive extrathalamocortical structures projecting to the thalamocortical circuitry.

It is conceivable that the lack of $Ca_v2.3$ in the neocortex may also contribute to the increased absence seizure susceptibility in $Ca_v2.3^{-/-}$ mice. The neocortex has been well documented to be involved in the generation of SWDs. Interestingly, athalamic animals are also capable of exhibiting SWDs in the cortex following bicuculline administration, indicating an important role of the cortex in the genesis of SWDs (Steriade and Contreras, 1998). This might be of particular relevance as $Ca_v2.3$ is also expressed in GABAergic cortical interneurons (Rhee et al., 1999; Timmermann et al., 2002). However, GBL-induced absence seizures are predominantly thalamus-dependent due to $GABA_B$ and GBL receptor agonistic effects (Steriade and Contreras, 1998; Seidenbecher et al., 1998; Manning et al., 2004; Shin, 2006).

Finally, it cannot be excluded that there may be compensatory changes in other VGCC expression in thalamic relay neurons or RTN cells. However, previous investigation of VGCC transcript levels isolated from total thalamic preparation did not reveal significant differences between controls and $Ca_v2.3$-deficient animals (Weiergraber et al., 2006a). Furthermore, other mechanisms, such as reduced excitatory but normal inhibitory synaptic transmission as reported in $\beta_4^{lh/lh}$ and $Ca_v2.1^{tg/tg}$ mice thalami (Caddick et al., 1999), or enhanced $GABA_B$-receptor expression (Hosford et al., 1992), could also result in relatively enhanced GABAergic input and thus facilitate burst firing.

Some anti-epileptics such as lamotrigine exert inhibitory actions on $Ca_v2.3$ VGCCs (Hainsworth et al., 2003) and were proven to effectively suppress SWDs in both GAERS and WAG/Rij rats (van Luijtelaar et al., 2002; Manning et al., 2003) and thalamocortical burst complexes in rat brain slices (Gibbs et al., 2002). However, lamotrigine strongly inhibits T-type Ca^{2+} channels (Hainsworth et al., 2003) thus its anti-absence effect is likely due to its predominant inhibitory effect on low-voltage-activated T-type Ca^{2+} channels.

In summary, $Ca_v2.3$ E/R-type VGCCs exhibit a Janus-faced behavior in epileptogenesis. Whereas previous studies have demonstrated that the $Ca_v2.3$ VGCC is proepileptogenic in convulsive seizures (Weiergraber et al., 2006a; Weiergraber et al., 2007), such as generalized tonic–clonic and hippocampal seizures, it clearly exhibits anti-epileptogenic capacity in typical non-convulsive absence epilepsy. These findings illustrate that the channel per se is neither pro- nor anti-epileptogenic. Indeed, it is the functional and structural integration within specific neuronal circuitries that endows its pathophysiological implications. Finally, our results shed new light on $Ca_v2.3$ as a possible therapeutic target in absence epilepsy treatment and the involvement of this ion channel in the physiology of slow-wave sleep.

Experimental methods

Study animals

$Ca_v2.3$-deficient mice backcrossed into C57Bl/6 have been generated and described previously (Pereverzev et al., 2002; Weiergraber et al., 2006a). Male $Ca_v2.3$-deficient animals and male control mice (with identical genetic C57Bl/6 background) were used in this study. Mice were housed in Makrolon cages type II and maintained at a conventional 12-h light/dark cycle with food and water available ad libitum. All animal experimentation was approved by the local institutional committee on animal care.

Antibodies

Mouse monoclonal parvalbumin and calbindin antibodies (both 1: 4000) were purchased from Sigma (Germany), the monoclonal murine calretinin antibody (1:15) was obtained from Acris Antibodies (Germany). Two different sources of antibodies against $Ca_v2.3$ were used to detect for the channel on both murine and rat brain sections, namely, the polyclonal anti-$Ca_v2.3$ 195A antibody (1:100) raised in rabbit with the target epitope being localized in pore-loop (IS5-6) of domaine I (Grabsch et al., 1999; Weiergraber et al., 2000), and a commercially available $Ca_v2.3$ antibody (1:50) raised in rabbits and directed against the II–III loop of the channel (Alomone Labs, Israel).

Immunofluorescence and immunohistochemistry

Brains from $Ca_v2.3^{+/+}$ and $Ca_v2.3^{-/-}$ mice were fixed by perfusion with 4% formaldehyde in 0.1 M PB-buffer (pH 7.4) and embedded in paraffin. The paraffin sections (6 μm) were dewaxed, cleared in xylene, rehydrated in decreasing percentage of ethanol and finally transferred into TBS (50 mM Tris–HCl, pH 7.4; 150 mM NaCl). Microwave antigen retrieval was performed in 0.1 M sodium citrate buffer (pH 6.0). Sections were blocked either by non-serum based blocking reagent (DAKO, Germany) or M.O.M blocking reagent (Vector Lab., USA), depending on the secondary antibodies used. For immunofluorescent staining using the mouse parvalbumin, calbindin and calretinin monoclonal antibodies, the M.O.M. blocking reagent was applied on sections for 2 h at RT. The primary mouse monoclonal antibodies against parvalbumin and calbindin (Sigma, Germany) were diluted

1:4000, the calretinin antibody 1:15 in TBS solution containing 10% normal goat serum and 0.5% Triton X-100 and was incubated at RT for 1.5 h. A goat-anti-mouse secondary antibody (1:1000) conjugated with Alexa 546 (Invitrogen, Germany) was diluted in the same solution and incubated on sections at RT for 1.5 h. Unbounded antibodies were removed by rinsing sections 3×5 min in TBS buffer. The nuclei were stained by 0.1% Hoechst 33258 (1:500, Invitrogen, Germany) for 10 min. Sections were finally mounted with coverslips using DAKO fluorescent mounting medium.

For enzyme-linked indirect immunohistochemical labeling, DAKO Envision$^+$ (mouse Ig) kit was used and the staining was performed according to the manufacturer's instruction. The primary parvalbumin antibody was diluted in 3% (w/v) BSA/TBS and the color development of DAB chromogen was controlled by checking its intensity under the light microscope. DAB-stained sections were counter-stained by Haematoxylin (Sigma), dehydrated in ethanol series and cleared in xylene. The sections were mounted with coverslips using DAPX mounting medium (Fluka, Germany). Negative controls were carried out using normal mouse serum. Histology of brain slices from $Ca_v2.3^{+/+}$ and $Ca_v2.3^{-/-}$ mice was further investigated using standard Nissl and Klüver–Barrera staining.

For double immunostaining of $Ca_v2.3$ and parvalbumin on rat brain, sections were first incubated with anti-parvalbumin antibody according to the above mentioned procedure, and then followed by incubation of anti-$Ca_v2.3$ 195A antibody at RT for 1 h. The immunoreactivity was detected by goat-anti mouse Ig conjugated with Alexa 488 (Invitrogen) and goat-anti rabbit Ig conjugated with Alexa 546 (Invitrogen), respectively.

Radiotelemetric surface EEG recordings (Electrocorticograms, ECoG)

The TA10ETA-F20 transmitter (DSI, St. Paul, MN, USA) was used for electrocorticographic (surface) recordings in $Ca_v2.3^{+/+}$ and $Ca_v2.3^{-/-}$ mice. The radiotelemetry system, implantation procedure, and post-operative treatment including pain management are as previously described (Weiergraber et al., 2005; Weiergraber et al., 2006a; Weiergraber et al., 2007). Epidural leads were positioned at the primary somatosensory cortex (S1), the transition zone of barrel field, dysgranular region and shoulder region at the following stereotaxic coordinates: (+)-lead, Bregma −1 mm, lateral of Bregma 2.5 mm (right hemisphere); (−)-lead, Bregma −1 mm, lateral of Bregma 2.5 mm (left hemisphere) and finally fixed at the neurocranium using dental cement. Animals were given at least 10 days to fully recover before initiating injection experiments (Kramer and Kinter, 2003).

Thalamocortical hyperoscillation induced by GBL administration

To evaluate the impact of $Ca_v2.3$ in SWD generation, γ-hydroxybutyrolactone (GBL, Sigma, Germany), a prodrug of γ-hydroxybutyric acid (GHB) was systemically administered to a radiotransmitter implanted $Ca_v2.3^{+/+}$ (27.86±1.78 g, 16.36±1.24 weeks, n=8, all ♂) and $Ca_v2.3^{-/-}$ mice (32.16±0.99 g, 15.09±1.05 weeks, n=8, all ♂) at a dosage of 70 mg/kg. GBL provokes electroencephalographically recordable absence seizures in rodents which are associated with behavioural arrest (Snead et al., 2000). Gamma-hydroxybutyrolactone was freshly dissolved in physiological 0.9% NaCl before injection. Both genotypes received GBL injection at least 10 days after implantation to ensure full recovery from radiotransmitter implantation ($Ca_v2.3^{+/+}$: 15.50±0.92 days; $Ca_v2.3^{-/-}$: 12.60±1.12 days). Each animal was isolated for >30 min before intraperitoneal (i.p.) administration of the non-convulsant epileptogenic agent.

Collecting data for absence seizure susceptibility analysis

SWD latencies were calculated as the time interval from the moment of GBL injection to the first electroencephalographic observation of SWDs. If an animal did not exhibit SWDs, it was assigned the maximum latency of the total observation period, i.e. 60 min. In addition, the frequencies and total duration of SWD episodes (ictal phases) and interictal epochs during the 1 h observation period were evaluated using radiotelemetric ECoG recordings. SWD episodes with an interictal period >3 s were regarded as separate events.

Evaluation of EEG data and statistical analysis

To acquire and analyze EEG data, the Dataquest A.R.T. 4.1 software (DSI) was used. In addition to EEG recordings following GBL administration, 24 h control recordings were carried out at day 7 and day 10 post-implantation for each individual animal. EEG activity was sampled at 1000 Hz with no a priori filter cut-off. Absolute power-spectrum density (PSD, mV^2/Hz) was calculated from 2 min segments using the periodogram function (FFT based with Hamming windowing method). Frequency ranges were defined as follows: delta, δ (1–4 Hz), theta, (4–8 Hz), alpha, α (8–12 Hz), beta, β (12–32 Hz), and gamma, γ (32–50 Hz). Additional to this discontinuous PSD evaluation, continuous PSD analysis was also performed to elicit the SWD frequency distribution. All data are calculated and displayed as means±SEM. Continuous variables were analyzed using the parametric Student's t-test, considering $p<0.05$ as statistically significant.

Acknowledgments

We thank Mrs. Renate Clemens and the animal keepers of the central facility and Dr. B. Wagner for their excellent and permanent assistance. The work was financially supported by the Center of Molecular Medicine Cologne (CMMC, to MW, JH, and TS, Faculty of Medicine, University of Cologne).

Appendix A. Supplementary data

Supplementary data associated with this article can be found, in the online version, at doi:10.1016/j.mcn.2008.08.007.

References

Andriamampandry, C., Taleb, O., Kemmel, V., Humbert, J.P., Aunis, D., Maitre, M., 2007. Cloning and functional characterization of a gamma-hydroxybutyrate receptor identified in the human brain. FASEB J. 21, 885–895.

Arias-Olguin, I.I., Vitko, I., Fortuna, M., Baumgart, J.P., Sokolova, S., Shumilin, I.A., Van Deusen, A., Soriano-Garcia, M., Gomora, J.C., Perez-Reyes, E., 2008. Characterization of the gating brake in the I–II loop of Cav3.2 T-type Ca2+ channels. J. Biol. Chem. 283, 8136–8144.

Battaglia, G., Lizier, C., Colacitti, C., Princivalle, A., Spreafico, R., 1994. A reticuloreticular commissural pathway in the rat thalamus. J. Comp. Neurol. 347, 127–138.

Bers, D.M., 2002. Cardiac excitation–contraction coupling. Nature 415, 198–205.

Bito, H., Deisseroth, K., Tsien, R.W., 1997. Ca2+-dependent regulation in neuronal gene expression. Curr. Opin. Neurobiol. 7, 419–429.

Blumenfeld, H., McCormick, D.A., 2000. Corticothalamic inputs control the pattern of activity generated in thalamocortical networks. J. Neurosci. 20, 5153–5162.

Caddick, S.J., Wang, C., Fletcher, C.F., Jenkins, N.A., Copeland, N.G., Hosford, D.A., 1999. Excitatory but not inhibitory synaptic transmission is reduced in lethargic (Cacnb4 (lh)) and tottering (Cacna1atg) mouse thalami. J. Neurophysiol. 81, 2066–2074.

Catterall, W.A., Perez-Reyes, E., Snutch, T.P., Striessnig, J., 2005. International Union of Pharmacology. XLVIII. Nomenclature and structure–function relationships of voltage-gated calcium channels. Pharmacol. Rev. 57, 411–425.

Danober, L., Deransart, C., Depaulis, A., Vergnes, M., Marescaux, C., 1998. Pathophysiological mechanisms of genetic absence epilepsy in the rat. Prog. Neurobiol. 55, 27–57.

De Borman, B., Lakaye, B., Minet, A., Zorzi, W., Vergnes, M., Marescaux, C., Grisar, T., 1999. Expression of mRNA encoding a1E and a1G subunit in the brain of a rat model of absence epilepsy. NeuroReport 10, 569–574.

Dominguez, M.I., Blasco-Ibanez, J.M., Crespo, C., Marques-Mari, A.I., Martinez-Guijarro, F.J., 2003. Zinc chelation during non-lesioning overexcitation results in neuronal death in the mouse hippocampus. Neuroscience 116, 791–806.

Gibbs III, J.W., Zhang, Y.F., Ahmed, H.S., Coulter, D.A., 2002. Anticonvulsant actions of lamotrigine on spontaneous thalamocortical rhythms. Epilepsia 43, 342–349.

Grabsch, H., Pereverzev, A., Weiergräber, M., Schramm, M., Henry, M., Vajna, R., Beattie, R.E., Volsen, S.G., Klöckner, U., Hescheler, J., Schneider, T., 1999. Immunohistochemical detection of a1E voltage-gated Ca2+ channel isoforms in cerebellum, INS-1

cells, and neuroendocrine cells of the digestive system. J. Histochem. Cytochem. 47, 981–993.
Hainsworth, A.H., McNaughton, N.C., Pereverzev, A., Schneider, T., Randall, A.D., 2003. Actions of sipatrigine, 202W92 and lamotrigine on R-type and T-type Ca2+ channel currents. Eur. J. Pharmacol. 467, 77–80.
Hofmann, F., Lacinová, L., Klugbauer, N., 1999. Voltage-dependent calcium channels: from structure to function. Rev. Physiol. Biochem. Pharmacol. 139, 33–87.
Hosford, D.A., Clark, S., Cao, Z., Wilson Jr., W.A., Lin, F.H., Morrisett, R.A., Huin, A., 1992. The role of GABAB receptor activation in absence seizures of lethargic (lh/lh) mice. Science 257, 398–401.
Jun, K., Piedras-Renteria, E.S., Smith, S.M., Wheeler, D.B., Lee, S.B., Lee, T.G., Chin, H.M., Adams, M.E., Scheller, R.H., Tsien, R.W., Shin, H.S., 1999. Ablation of P/Q-type Ca2+ channel currents, altered synaptic transmission, and progressive ataxia in mice lacking the a1A-subunit. Proc. Natl. Acad. Sci. U. S. A. 96, 15245–15250.
Khosravani, H., Zamponi, G.W., 2006. Voltage-gated calcium channels and idiopathic generalized epilepsies. Physiol. Rev. 86, 941–966.
Khosravani, H., Altier, C., Simms, B., Hamming, K.S., Snutch, T.P., Mezeyova, J., McRory, J.E., Zamponi, G.W., 2004. Gating effects of mutations in the Cav3.2 T-type calcium channel associated with childhood absence epilepsy. J. Biol. Chem. 279, 9681–9684.
Khosravani, H., Bladen, C., Parker, D.B., Snutch, T.P., McRory, J.E., Zamponi, G.W., 2005. Effects of Cav3.2 channel mutations linked to idiopathic generalized epilepsy. Ann. Neurol. 57, 745–749.
Kim, D., Song, I., Keum, S., Lee, T., Jeong, M.J., Kim, S.S., McEnery, M.W., Shin, H.S., 2001. Lack of the burst firing of thalamocortical relay neurons and resistance to absence seizures in mice lacking a1G T-type Ca2+ channels. Neuron 31, 35–45.
Kim, U., Bal, T., McCormick, D.A., 1995. Spindle waves are propagating synchronized oscillations in the ferret LGNd in vitro. J. Neurophysiol. 74, 1301–1323.
Kisilevsky, A.E., Zamponi, G.W., 2008. Presynaptic calcium channels: structure, regulators, and blockers. Handb. Exp. Pharmacol. 45–75.
Kramer, K., Kinter, L.B., 2003. Evaluation and applications of radiotelemetry in small laboratory animals. Physiol. Genomics 13, 197–205.
Krieger, A., Radhakrishnan, K., Pereverzev, A., Siapich, S.A., Banat, M., Kamp, M.A., Leroy, J., Klockner, U., Hescheler, J., Weiergraber, M., Schneider, T., 2006. The molecular chaperone hsp70 interacts with the cytosolic II–III loop of the Cav2.3 E-type voltage-gated Ca2+ channel. Cell. Physiol. Biochem. 17, 97–110.
Kullmann, D.M., 2002. The neuronal channelopathies. Brain 125, 1177–1195.
Kuzmiski, J.B., Barr, W., Zamponi, G.W., MacVicar, B.A., 2005. Topiramate inhibits the initiation of plateau potentials in CA1 neurons by depressing R-type calcium channels. Epilepsia 46, 481–489.
Lakaye, B., Thomas, E., Minet, A., Grisar, T., 2002. The genetic absence epilepsy rat from Strasbourg (GAERS), a rat model of absence epilepsy: computer modeling and differential gene expression. Epilepsia 43 (Suppl. 5), 123–129.
Lee, J., Kim, D., Shin, H.S., 2004. Lack of delta waves and sleep disturbances during non-rapid eye movement sleep in mice lacking alpha1G-subunit of T-type calcium channels. Proc. Natl. Acad. Sci. U. S. A. 101, 18195–18199.
Llinas, R.R., Steriade, M., 2006. Bursting of thalamic neurons and states of vigilance. J. Neurophysiol. 95, 3297–3308.
Manning, J.P., Richards, D.A., Bowery, N.G., 2003. Pharmacology of absence epilepsy. Trends Pharmacol. Sci. 24, 542–549.
Manning, J.P., Richards, D.A., Leresche, N., Crunelli, V., Bowery, N.G., 2004. Cortical-area specific block of genetically determined absence seizures by ethosuximide. Neuroscience 123, 5–9.
Mathie, A., Sutton, G.L., Clarke, C.E., Veale, E.L., 2006. Zinc and copper: pharmacological probes and endogenous modulators of neuronal excitability. Pharmacol. Ther. 111, 567–583.
Metz, A.E., Jarsky, T., Martina, M., Spruston, N., 2005. R-type calcium channels contribute to afterdepolarization and bursting in hippocampal CA1 pyramidal neurons. J. Neurosci. 25, 5763–5773.
Nagaeva, D.V., Akhmadeev, A.V., 2006a. Structural organization, neurochemical characteristics, and connections of the reticular nucleus of the thalamus. Neurosci. Behav. Physiol 36, 987–995.
Pereverzev, A., Mikhna, M., Vajna, R., Gissel, C., Henry, M., Weiergräber, M., Hescheler, J., Smyth, N., Schneider, T., 2002. Disturbances in glucose-tolerance, insulin-release and stress-induced hyperglycemia upon disruption of the Cav2.3 (a1E) subunit of voltage-gated Ca2+ channels. Mol. Endocrinol. 16, 884–895.
Rhee, J.S., Ishibashi, H., Akaike, N., 1999. Calcium channels in the GABAergic presynaptic nerve terminals projecting to Meynert neurons of the rat. J. Neurochem. 72, 800–807.
Seidenbecher, T., Staak, R., Pape, H.C., 1998. Relations between cortical and thalamic cellular activities during absence seizures in rats. Eur. J. Neurosci. 10, 1103–1112.
Shin, H.S., 2006. T-type Ca2+ channels and absence epilepsy. Cell Calcium 40, 191–196.
Smith, K.A., Fisher, R.S., 1996. The selective GABAB antagonist CGP-35348 blocks spike–wave bursts in the cholesterol synthesis rat absence epilepsy model. Brain Res. 729, 147–150.
Snead III, O.C., 1992. Evidence for GABAB-mediated mechanisms in experimental generalized absence seizures. Eur. J. Pharmacol. 213, 343–349.
Snead III, O.C., 2000. Evidence for a G protein-coupled gamma-hydroxybutyric acid receptor. J. Neurochem. 75, 1986–1996.
Snead III, O.C., Banerjee, P.K., Burnham, M., Hampson, D., 2000. Modulation of absence seizures by the GABA(A) receptor: a critical role for metabotropic glutamate receptor 4 (mGluR4). J. Neurosci. 20, 6218–6224.
Song, I., Kim, D., Choi, S., Sun, M., Kim, Y., Shin, H.S., 2004. Role of the alpha1G T-type calcium channel in spontaneous absence seizures in mutant mice. J. Neurosci. 24, 5249–5257.
Spreafico, R., Battaglia, G., Frassoni, C., 1991. The reticular thalamic nucleus (RTN) of the rat: cytoarchitectural, Golgi, immunocytochemical, and horseradish peroxidase study. J. Comp. Neurol. 304, 478–490.
Steriade, M., Contreras, D., 1998. Spike–wave complexes and fast components of cortically generated seizures. I. Role of neocortex and thalamus. J. Neurophysiol. 80, 1439–1455.
Sun, H.S., Hui, K., Lee, D.W., Feng, Z.P., 2007. Zn2+ sensitivity of high- and low-voltage activated calcium channels. Biophys. J. 93, 1175–1183.
Suzuki, T., Delgado-Escueta, A.V., Aguan, K., Alonso, M.E., Shi, J., Hara, Y., Nishida, M., Numata, T., Medina, M.T., Takeuchi, T., Morita, R., Bai, D., Ganesh, S., Sugimoto, Y., Inazawa, J., Bailey, J.N., Ochoa, A., Jara-Prado, A., Rasmussen, A., Ramos-Peek, J., Cordova, S., Rubio-Donnadieu, F., Inoue, Y., Osawa, M., Kaneko, S., Oguni, H., Mori, Y., Yamakawa, K., 2004. Mutations in EFHC1 cause juvenile myoclonic epilepsy. Nat. Genet. 36, 842–849.
Tai, C., Kuzmiski, J.B., MacVicar, B.A., 2006. Muscarinic enhancement of R-type calcium currents in hippocampal CA1 pyramidal neurons. J. Neurosci. 26, 6249–6258.
Takeda, A., Hirate, M., Tamano, H., Nisibaba, D., Oku, N., 2003a. Susceptibility to kainate-induced seizures under dietary zinc deficiency. J. Neurochem. 85, 1575–1580.
Takeda, A., Minami, A., Seki, Y., Oku, N., 2003b. Inhibitory function of zinc against excitation of hippocampal glutamatergic neurons. Epilepsy Res. 57, 169–174.
Takeda, A., Tamano, H., Nagayoshi, A., Yamada, K., Oku, N., 2005. Increase in hippocampal cell death after treatment with kainate in zinc deficiency. Neurochem. Int. 47, 539–544.
Talley, E.M., Cribbs, L.L., Lee, J.H., Daud, A., Perez-Reyes, E., Bayliss, D.A., 1999. Differential distribution of three members of a gene family encoding low voltage-activated (T-type) calcium channels. J. Neurosci. 19, 1895–1911.
Talley, E.M., Solórzano, G., Depaulis, A., Perez-Reyes, E., Bayliss, D.A., 2000. Low-voltage-activated calcium channel subunit expression in a genetic model of absence epilepsy in the rat. Mol. Brain Res. 75, 159–165.
Timmermann, D.B., Westenbroek, R.E., Schousboe, A., Catterall, W.A., 2002. Distribution of high-voltage-activated calcium channels in cultured gamma-aminobutyric acidergic neurons from mouse cerebral cortex. J. Neurosci. Res. 67, 48–61.
Tsakiridou, E., Bertollini, L., de Curtis, M., Avanzini, G., Pape, H.C., 1995. Selective increase in T-type calcium conductance of reticular thalamic neurons in a rat model of absence epilepsy. J. Neurosci. 15, 3110–3117.
Turnbull, J., Lohi, H., Kearney, J.A., Rouleau, G.A., Delgado-Escueta, A.V., Meisler, M.H., Cossette, P., Minassian, B.A., 2005. Sacred disease secrets revealed: the genetics of human epilepsy. Hum. Mol. Genet. 14, 2491–2500.
van de Bovenkamp-Janssen, M., Scheenen, W.J., Kuijpers-Kwant, F.J., Kozicz, T., Veening, J.G., van Luijtelaar, E.L., McEnery, M.W., Roubos, E.W., 2004. Differential expression of high voltage-activated Ca2+ channel types in the rostral reticular thalamic nucleus of the absence epileptic WAG/Rij rat. J. Neurobiol. 58, 467–478.
van Luijtelaar, G., Wiaderna, D., Elants, C., Scheenen, W., 2000. Opposite effects of T- and L-type Ca2+ channels blockers in generalized absence epilepsy. Eur. J. Pharmacol. 406, 381–389.
van Luijtelaar, E.L., Drinkenburg, W.H., van Rijn, C.M., Coenen, A.M., 2002. Rat models of genetic absence epilepsy: what do EEG spike–wave discharges tell us about drug effects? Methods Find. Exp. Clin. Pharmacol. 24 (Suppl. D), 65–70.
Von Krosigk, M., Bal, T., McCormick, D.A., 1993. Cellular mechanisms of a synchronized oscillation in the thalamus. Science 261, 361–364.
Weiergraber, M., Pereverzev, A., Vajna, R., Henry, M., Schramm, M., Nastainczyk, W., Grabsch, H., Schneider, T., 2000. Immunodetection of alpha1E voltage-gated Ca2+ channel in chromogranin-positive muscle cells of rat heart, and in distal tubules of human kidney. J. Histochem. Cytochem. 48, 807–819.
Weiergraber, M., Henry, M., Hescheler, J., Smyth, N., Schneider, T., 2005. Electrocorticographic and deep intracerebral EEG recording in mice using a telemetry system. Brain Res. Brain Res. Protoc. 14, 154–164.
Weiergraber, M., Henry, M., Krieger, A., Kamp, M., Radhakrishnan, K., Hescheler, J., Schneider, T., 2006a. Altered seizure susceptibility in mice lacking the Cav2.3 E-type Ca2+ channel. Epilepsia 47, 839–850.
Weiergraber, M., Kamp, M.A., Radhakrishnan, K., Hescheler, J., Schneider, T., 2006b. The Cav2.3 voltage-gated calcium channel in epileptogenesis—shedding new light on an enigmatic channel. Neurosci. Biobehav. Rev. 30, 1122–1144.
Weiergraber, M., Henry, M., Radhakrishnan, K., Hescheler, J., Schneider, T., 2007. Hippocampal seizure resistance and reduced neuronal excitotoxicity in mice lacking the Cav2.3 E/R-type voltage-gated calcium channel. J. Neurophysiol. 97, 3660–3669.
Yang, S.N., Berggren, P.O., 2005. {beta}-Cell CaV channel regulation in physiology and pathophysiology. Am. J. Physiol. Endocrinol. Metab. 288, E16–E28.
Yue, C., Remy, S., Su, H., Beck, H., Yaari, Y., 2005. Proximal persistent Na+ channels drive spike afterdepolarizations and associated bursting in adult CA1 pyramidal cells. J. Neurosci. 25, 9704–9720.

Available online at www.sciencedirect.com
ScienceDirect
Neuroscience and Biobehavioral Reviews 30 (2006) 1122–1144
NEUROSCIENCE AND BIOBEHAVIORAL REVIEWS
www.elsevier.com/locate/neubiorev

Review

The $Ca_v2.3$ voltage-gated calcium channel in epileptogenesis—Shedding new light on an enigmatic channel

Marco Weiergräber[a,b,*], Marcel A. Kamp[a], Kayalvizhi Radhakrishnan[a,b], Jürgen Hescheler[a,b], Toni Schneider[a,b]

[a]*Institute for Neurophysiology, University of Cologne, Robert-Koch-Str. 39, D 50931 Cologne, Germany*
[b]*Center for Molecular Medicine Cologne (CMMC), University of Cologne, Robert-Koch-Str. 39, D 50931 Cologne, Germany*

Received 16 May 2006; received in revised form 5 July 2006; accepted 6 July 2006

Abstract

The $Ca_v2.3$ encoded Ca^{2+} channel is probably one of the least well-understood voltage-gated calcium channels in terms of physiology, pharmacology and clinical relevance. Here we provide a detailed insight into the functional involvement of $Ca_v2.3$ in etiology and pathogenesis of both convulsive and non-convulsive seizures. In the CNS, $Ca_v2.3$ containing E/R-type Ca^{2+} channels are involved in triggering epileptiform discharges by significantly contributing to plateau potentials and afterdepolarisations. Pharmacological analysis further revealed that various antiepileptic drugs specifically target $Ca_v2.3$ VGCCs capable of blocking epileptiform burst activity. Whereas electroencephalographic recordings in $Ca_v2.3^{-/-}$ mice did not reveal any ictal-like discharges, seizure susceptibility was dramatically reduced in $Ca_v2.3^{-/-}$ animals compared to controls, further supporting the observation that $Ca_v2.3$ is an important factor in triggering epileptiform activity in neuronal populations. Although some aspects of its relationship to epilepsy have been uncovered, further functional characterization of $Ca_v2.3$ in etiology and pathogenesis of human epileptic syndromes as well as development of new antiepileptic drugs specifically targeting $Ca_v2.3$ turns out to become indispensable.

Keywords: Antiepileptic drugs; Channelopathies; Epileptogenesis; E/R-type Ca^{2+}-channel; Pharmacoresistant; Plateau potential

Contents

Abbreviations: Ca^{2+}, calcium; Cl^-, chloride; CNS, central nervous system; GABA, γ-aminobutyric acid; GAERS, genetic absence epilepsy rats from Strasbourg; K^+, potassium; Na^+, sodium; VGCC, voltage-gated calcium channel; WAG/Rij, Wistar Albino Glaxo strain, bred in Rijswijk

*Corresponding author. Institute for Neurophysiology, University of Cologne, Robert-Koch-Str. 39, D 50931 Cologne, Germany.
Tel.: +49 221 478 6968; fax: +49 221 478 6965.
E-mail address: akp74@uni-koeln.de (M. Weiergräber).

0149-7634/$ - see front matter © 2006 Elsevier Ltd. All rights reserved.
doi:10.1016/j.neubiorev.2006.07.004

1. Voltage-gated calcium channels (VGCCs) in neuronal calcium channelopathies—animal models of epilepsy and human disorders

In contemporary society, the frequency, importance and sociocultural effects of epilepsy can hardly be overestimated. Manifest epilepsy affects around 0.5–1% of the population in Europe and North America (Forsgren et al., 2005), 5% of the population perceive a single seizure in their lifetime and about 10% display an increased seizure susceptibility. Furthermore, epilepsy is characterized by a strong heterogeneity concerning etiology, age of onset, seizure type, responsiveness to pharmacological treatment, prognosis and occurrence of additional disorders. Principally, epileptic disorders can be differentiated into primary, idiopathic forms as well as secondary forms, e.g. due to neoplasms, cerebral ischemia or brain macro-/microdysgenesis. Regardless of the underlying cause, the fundamental electrophysiological basis for hyperexcitability associated with ictogenesis/epileptogenesis are paroxysmal depolarization shifts in neuronal cell populations and within the last decade a number of epileptic disorders originally termed idiopathic turned out to be due to ion channel dysfunctions triggering depolarization shifts. These ion channel entities comprise both voltage-gated Na^+-, K^+-, Ca^{2+}-, Cl^--channels and ligand-gated ion channels (GABA, glutamate, glycine, acetylcholine receptors) (Kullmann, 2002; Mulley et al., 2005). Among these candidates, VGCCs significantly contribute to etiology and pathogenesis of epilepsies, such as absence epilepsy or juvenile myoclonic epilepsy (Turnbull et al., 2005). Besides, mutations in neuropeptides, vesicle docking complex proteins, transporters, signal transduction molecules and extracellular matrix proteins were also reported to be linked to an epileptic phenotype (Puranam and McNamara, 1999).

Physiologically, VGCCs regulate Ca^{2+} influx into living cells and thereby trigger a number of cellular processes, such as excitation–contraction coupling (Bers, 2002), excitation–secretion coupling (Yang and Berggren, 2005), neurotransmitter/hormonal release (Catterall, 1999) and regulation of gene expression (Bito et al., 1997; Hofmann et al., 1999). Ten different pore-forming α1-subunits of VGCCs have been cloned so far which are subdivided based on electrophysiological and pharmacological properties into high-voltage activated L-type ($Ca_v1.1$–1.4) and Non-L-Type ($Ca_v2.1$–2.3) Ca^{2+} channels, and low-voltage activated T-type channels ($Ca_v3.1$–3.3) (Catterall, 2000; Perez-Reyes, 2003). Besides, a number of auxiliary subunits (β_{1-4}, $\alpha_2\delta_{1-4}$, γ_{1-8}) are associated with the ion-conducting $Ca_v\alpha1$-subunit capable of modulating basic electrophysiological and pharmacological properties of the Ca^{2+} channel complex (Lacinova, 2005). Recent studies elicited an increasing number of mutations in both, ion-conducting and auxiliary subunits, associated with various cardiovascular, muscular and neurological diseases not only in different animal models but particularly in humans, the so-called calcium channelopathies (Clapham, 1997; Lehmann-Horn and Jurkat-Rott, 1999; Pietrobon, 2005). So far, neuronal calcium channelopathies in humans are primarily restricted to the $Ca_v2.1$ and $Ca_v3.2$ VGCCs resulting in absence epilepsy like activity, episodic ataxia type 2 (EA-2), spinocerebellar ataxia type 6 (SCA-6) or familial hemiplegic migraine (FHM) (Pietrobon, 2005) in $Ca_v2.1$ or absence epilepsy in patients with $Ca_v3.2$ mutations (Chen et al., 2003). In addition, not only autoantibodies against $Ca_v2.1$ but also those against $Ca_v2.2$ are associated with Lambert-Eaton myasthenic syndrome (Pinto et al., 1998) and may be of significance in sporadic amyotrophic lateral sclerosis too (Missiaen et al., 2000). In the retina ontogenetically originating from the diencephalon, mutations in the $Ca_v1.4$ VGCC are reported to cause congenital stationary night blindness (CSNB) in humans (Bech-Hansen et al., 1998). Furthermore, a gain-of-function missense mutation (G406R) of $Ca_v1.2$ was recently described to cause Timothy syndrome, a multi-system disorder in humans including complex neuropsychatric symptoms such as autism (60%), autism spectrum disorders (80%), mental retardation (25%) and seizures (21%) (Splawski et al., 2004).

In addition, several animal models with complex neurological disorders, e.g. cerebellar ataxia, paroxysmal dyskinesia and absence epilepsy have been described in the past based on mutations either in the pore-forming $Ca_v\alpha1$-subunit or auxiliary subunits. Most of these mutations are again restricted to the $Ca_v2.1$ VGCC, e.g. the *tottering* (tg) (Fletcher et al., 1996), *tottering leaner* (tg^l) (Fletcher et al., 1996), *rolling Nagoya* (tg^{rol}) (Mori et al., 2000) and *rocker* (rkr) (Zwingman et al., 2001) mouse model, whereas others are related to mutations in accessory subunits, e.g. the β_4-subunit mutation in *lethargic* (lh) mice (Burgess et al., 1997), γ_2-subunit mutation in *stargazer* (stg) mice (Letts et al., 1998) and the $\alpha_2\delta_2$-subunit mutations associated with the *ducky* (du) and *entla* (ent) phenotype (Burgess and Noebels, 1999; Gao et al., 2000; Barclay et al., 2001; Brill et al., 2003). This turns out to be an astonishing observation, particularly as other VGCCs are also widely distributed throughout the brain, e.g. the $Ca_v2.3$ E/R-type channel

which is present in most basal ganglia regions, the thalamus, hypothalamus, amygdala, hippocampus and cortex (Soong et al., 1993; Williams et al., 1994). The L-type Ca^{2+} channels $Ca_v1.1$–1.4 are not reported to be directly associated with primary or secondary forms of epilepsy despite incidental occurrence of seizures in Timothy patients as outlined above. In addition, no seizure phenotype has been associated with mutations in the $Ca_v2.2$ and $Ca_v2.3$ VGCC itself yet. Nevertheless, both high-voltage and low-voltage activated Ca^{2+} channels represent potent targets for antiepileptic drugs, as blockade of these channels can inhibit neurotransmitter release (Turner, 1998) or interfere with neuronal firing patterns such as burst activity or intrinsic oscillations (Rogawski and Loscher, 2004). Some newer antiepileptic drugs directly target the pore-forming $Ca_v\alpha1$-subunit of Ca^{2+} channel complexes, e.g. lamotrigine, felbamate, topiramate and levetiracetam for high-voltage activated channels and ethosuximide or zonisamide for low-voltage activated T-type Ca^{2+} channels (Gomora et al., 2001; Rogawski and Loscher, 2004; Remy and Beck, 2006). Other antiepileptic drugs however were shown to interact with auxiliary subunits, e.g. gabapentin and pregabalin that interfere with the $\alpha_2\delta$ subunit of VGCCs (Sills, 2006).

Constrictively, one has to state that most of these antiepileptic drugs are broad-spectrum pharmacons that also exert modulating effects on other voltage- and ligand-gated ion channels. In this review, we elaborate remarkable new findings on the functional relevance of the $Ca_v2.3$ VGCC in etiology and pathogenesis of both convulsive and non-convulsive seizures. Based on biochemical, molecular, electrophysiological and pharmacological analysis given, we will develop an integrative view of how $Ca_v2.3$ is capable of triggering epileptiform activity and why $Ca_v2.3$ is getting more and more important as a novel target in antiepileptic drug treatment in humans.

2. Functional characteristics of the $Ca_v2.3$ E/R-type VGCC—what makes $Ca_v2.3$ an interesting player in ictogenesis/epileptogenesis and seizure propagation?

The $Ca_v2.3$ VGCC is widely distributed throughout the organism, not only in the peripheral and central nervous system (CNS), but also the endocrine (Jing et al., 2005; Pereverzev et al., 2005), cardiovascular (Lu et al., 2004; Weiergräber et al., 2005), reproductive (Sakata et al., 2002) and gastrointestinal system (Grabsch et al., 1999). Generation of mice lacking the $Ca_v2.3$ VGCC has provided detailed insight into the functional relevance of this intractable channel in the last few years. Within the CNS, $Ca_v2.3$ is involved in neurotransmitter release and presynaptic plasticity (Breustedt et al., 2003; Dietrich et al., 2003). In addition, $Ca_v2.3$ was reported to be involved in the physiology of fear (Lee et al., 2002), control of pain behavior (Saegusa et al., 2000) and myelinogenesis (Chen et al., 2000). Furthermore, $Ca_v2.3$ seems to exert a protective role in ischemic neuronal injury (Toriyama et al., 2002) and be involved in vasospasms following subarachnoid hemorrage in humans (Ishiguro et al., 2005) (Table 1).

2.1. Cellular distribution and functional implications

The $Ca_v2.3$ VGCC exhibits a dominant presynaptic expression, e.g. in mossy fibers of the hippocampus (Day et al., 1996) and the pallidal globe (Hanson and Smith, 2002) (Table 2), besides $Ca_v2.1$ (Wu et al., 1999) and $Ca_v2.2$ (Westenbroek et al., 1992) and it can also be found at the neuromuscular junction (Day et al., 1997). Presynaptically, a smaller fraction of $Ca_v2.3$ is restricted to the active zone of the vesicle fusion machinery and thus involved in neurotransmission (Wu et al., 1999) whereas a larger fraction is localized more distant in the synapse responsible for synaptic plasticity, e.g. long-term potentiation (LTP) (Dietrich et al., 2003; Kamp et al., 2005). E/R-type Ca^{2+} channels also exhibit a prominent expression on the soma and dendrites.

Localization experiments revealed that $Ca_v2.3$ is preferentially distributed homogenously on the cell soma and the dendritic arbor. Dendritic expression appears to be most complex and only certain CNS nuclei and specific cell types exhibit positive staining in dendrites, e.g. CA1 neurons, which will be discussed in more detail below. Depending on the cell type a distribution in proximal or distal dendrites is preferred, an observation that differs from other high-voltage activated Ca^{2+} channels pointing out the highly organized spatial distribution of $Ca_v2.3$ (Westenbroek et al., 1995). Consequently, $Ca_v2.3$ was found to be involved in the generation of Ca^{2+}-dependent action potentials that are conducted along the length of the dendritic arbor which is an important site of Ca^{2+} entry and electrogenesis in neurons (Tank et al., 1988). This somatic and dendritic role of $Ca_v2.3$ is of special interest and likely to contribute to a number of electrical phenomena characteristic for ictiform/epileptiform activity, which are discussed later in more detail.

2.2. Novel mechanisms of $Ca_v2.3$ Ca^{2+}-sensitivity

Numerous splice variants of the $Ca_v2.3$ Ca^{2+} subunit have been described (Pereverzev et al., 2002) and this diversity could potentially be further amplified by partnering with the various isoforms of the $\alpha_2\delta$, β, and γ Ca^{2+} channel accessory subunits. On the biochemical level, $Ca_v2.3$ is subject to complex regulatory mechanisms, including phosphorylation and dephosphorylation. Such mechanisms are of particular importance as they may alter basic electrophysiological properties of a channel and induce epileptiform burst activity in neurons (Remy and Beck, 2006). Surprisingly, Ca^{2+} influx through $Ca_v2.3$ E/R-type Ca^{2+} channels has opposite effects on the channel activity itself. At lower cytosolic Ca^{2+} concentrations, a positive feedback mechanism, which includes

Table 1
$Ca_v2.3$ deficient mouse models

Mouse model	Gene inactivation	Location of mutation	Phenotype of $Ca_v2.3$-deficient mice or cells	Miscellaneous	Ref.
A. *Miller/Chicago*	Homologous recombination in CJ7 ES cells, and breeding into C57Bl/6J mice	S4—S6 regions of domain II were replaced	Cultivated cerebellar granule cells loose their SNX-482 sensitive component	Even in cultured cerebellar granule cells from $Ca_v2.3^{-/-}$ mice, 31% of Ba^{2+} current is pharmaco-''resistant''	Wilson et al. (2000)
			Increase in the threshold for inducing mossy fiber long term potentiation	(see also: Brenowitz and Regehr, 2003	Breustedt et al. (2003)
B. *Tanabe/Tokyo*	Homologous recombination in J1 ES cells (derived from 129/Sv mice)	Deletion of a 2.3 kb NotI - SstI fragment containing exon 1 (= full N-terminus) and part of intron 1	Normal pain behaviour in $Ca_v2.3^{+/-}$ and $Ca_v2.3^{-/-}$ mice against acute mechanical, thermal, and chemical stimuli, but reduced responses to somatic inflammatory pain in $Ca_v2.3^{+/-}$, and increased responses to a somatic inflammatory pain in $Ca_v2.3^{-/-}$mice when presensitized with visceral noxious stimuli.	β-galactosidase as reporter in the inactivated allele by an in-frame insertion of *nlacZ*	Saegusa et al. (2000)
			Impaired spatial memory (Morris water-maze test)	Long term potentiation in CA1 region was not impaired; also, $Ca_v2.3^{-/-}$ mice were able to establish and to maintain fear memories	Kubota et al. (2001)
			After occlusion of middle cerebral artery (focal ischemia), $Ca_v2.3^{-/-}$ mice suffer from increased neuronal injuries	$Ca_v2.3$ is neuroprotective during ischemia by a mechanism which includes GABergic neuronal activities	Toriyama et al. (2002)
			Control of sperm function: the rising rates of Ca^{2+} transients in the head region of sperms were lower than in control sperms	$Ca_v2.3$ plays some roles for the control of flagellar movement	Sakata et al. (2001), Sakata et al. (2002)
			Altered cocaine effects (missing enhancement of locomotor activity, no response to acute cocaine administration)		Han et al. (2002)
			Decreased sensitivities for propofol and halothane	Propofol enhances GABAergic effects	Takei et al. (2003)
			Enhanced morphine analgesia, but reduced morophine tolerance	Inhibition of R-type Ca^{2+} current may lead to high-efficiency opioid therapy without tolerance.	Yokoyama et al. (2004)
C. *Shin/Seoul*		Deletion of the 0.5 kb XbaI—ClaI fragment in exon 1	Loss of pharmacoresistant type Ca^{2+} current in central amygdala neurons, and exhibited signs of enhanced fear in vivo (vigorous escaping behavior and aversion to open-field conditions)	GFP as reporter in the inactivated allele by an in-frame insertion	Lee et al. (2002)
D. *Schneider/Cologne*	Homologous recombination in R1 ES cells, and breeding into C57Bl/6J mice	Deletion of exon 2 (= trans-membrane segment IS1 and loop to IS2)	Disturbance in glucose-tolerance, insulin release, and stress-induced hyperglycemia; suppressed second phase insulin release concomitant with a reduced oscillatory Ca^{2+} signaling; impaired glucose-mediated suppression of glucagons secretion; coexpression of insulin and glucagons in a fraction of islets		Jing et al. (2005), Pereverzev et al. (2002a), Pereverzev et al. (2002b), Pereverzev et al. (2005), Vajna et al. (1998, 2001), Lu et al. (2004), Weiergräber et al. (2005)
			Cardiac arrhythmia in isolated prenatal hearts, and adult mice as well as altered autonomic control in the cardiovascular system		

Table 1 (*continued*)

Mouse model	Gene inactivation	Location of mutation	Phenotype of $Ca_v2.3$-deficient mice or cells	Miscellaneous	Ref.
			Impairment of mossy fiber CA3 long term potentiation in hippocampus		Dietrich et al. (2003), Sochivko et al. (2002)
			Reduced pentylene-tetrazol (PTZ)—induced seizure susceptibility	Seizure sensitivity towards 4-aminopyridine was unchanged	Weiergräber et al. (2006)

The cacna1e gene encoding the $Ca_v2.3$ containing E-/R-type voltage-gated Ca^{2+} channels has been inactivated by homologous recombination in 4 different laboratories (Miller-Chicago-lab, Tanabe-Tokyo-lab, Shin-Seoul-lab, Schneider-Cologne-lab). In all four mouse models the mice are fertile and show a normal life span although male $Ca_v2.3$-deficient mice suffer from their increased aggression which may be based on their enhanced fear.

References

Brenowitz, S.D., Regehr, W.G., 2003. ''Resistant'' channels reluctantly reveal their roles. Neuron 39, 391–394.

Breustedt, J., Vogt, K.E., Miller, R.J., Nicoll, R.A., Schmitz, D., 2003. Alpha1E-containing Ca^{2+} channels are involved in synaptic plasticity. Proceedings of the National Academy of Sciences of the United States of America 100, 12450–12455.

Dietrich, D., Kirschstein, T., Kukley, M., Pereverzev, A., von der Brelie, C., Schneider, T., Beck, H., 2003. Functional specialization of presynaptic $Ca_v2.3$ Ca^{2+} channels. Neuron 39, 483–496.

Han, W., Saegusa, H., Zong, S., Tanabe, T., 2002. Altered cocaine effects in mice lacking $Ca_v2.3$ (alpha1E) calcium channel. Biochemical and Biophysical Research Communications 299, 299–304.

Jing, X., Li, D. Q., Olofsson, C. S., Salehi, A., Surve, V. V., Caballero, J., Ivarsson, R., Lundquist, I., Pereverzev, A., Schneider, T., Rorsman, P., Renstrom, E., 2005. $Ca_v2.3$ calcium channels control second-phase insulin release. Journal of Clinical Investigation 115, 146–154.

Kubota, M., Murakoshi, T., Saegusa, H., Kazuno, A., Zong, S., Hu, Q., Noda, T., Tanabe, T., 2001. Intact LTP and Fear Memory but Impaired Spatial Memory in Mice Lacking $Ca_v2.3$ (α1E) Channel. Biochemical and Biophysical Research Communications 282, 242–248.

Lee, S. C., Choi, S., Lee, T., Kim, H. L., Chin, H., Shin, H. S., 2002. Molecular basis of R-type calcium channels in central amygdala neurons of the mouse. Proceedings of the National Academy of Sciences of the United States of America 99, 3276–3281.

Lu, Z.-L., Pereverzev, A., Liu, H.-L., Weiergraber, M., Henry, M., Krieger, A., Smyth, N., Hescheler, J., Schneider, T., 2004. Arrhythmia in isolated prenatal hearts after ablation of the $Ca_v2.3$ (α1E) subunit of voltage-gated Ca^{2+} channels. Cellular Physiology and Biochemistry 14, 11–22.

Pereverzev, A., Mikhna, M., Vajna, R., Gissel, C., Henry, M., Weiergräber, M., Hescheler, J., Smyth, N., Schneider, T., 2002a. Disturbances in glucose-tolerance, insulin-release and stress-induced hyperglycemia upon disruption of the $Ca_v2.3$ (α1E) subunit of voltage-gated Ca^{2+} channels. Molecular Endocrinology 16, 884–895.

Pereverzev, A., Salehi, A., Mikhna, M., Renstrom, E., Hescheler, J., Weiergraber, M., Smyth, N., Schneider, T., 2005. The ablation of the $Ca_v2.3$/E-type voltage-gated Ca^{2+} channel causes a mild phenotype despite an altered glucose induced glucagon response in isolated islets of Langerhans. European Journal of Pharmacology 511, 65–72.

Pereverzev, A., Vajna, R., Pfitzer, G., Hescheler, J., Klöckner, U., Schneider, T., 2002b. Reduction of insulin secretion in the insulinoma cell line INS-1 by overexpression of a calcium channel antisense-alpha1E cassette. European Journal of Endocrinology 146, 881–889.

Saegusa, H., Kurihara, T., Zong, S. Q., Minowa, O., Kazuno, A. A., Han, W. H., Matsuda, Y., Yamanaka, H., Osanai, M., Noda, T., Tanabe, T., 2000. Altered pain responses in mice lacking α_{1E} subunit of the voltage-dependent Ca^{2+} channel. Proceedings of the National Academy of Sciences of the United States of America 97, 6132–6137.

Sakata, Y., Saegusa, H., Zong, S. Q., Osanai, M., Murakoshi, T., Shimizu, Y., Noda, T., Aso, T., Tanabe, T., 2001. Analysis of Ca^{2+} currents in spermatocytes from mice lacking $Ca_v2.3$ (α_{1E}) Ca^{2+} channel. Biochemical and Biophysical Research Communications 288, 1032–1036.

Sakata, Y., Saegusa, H., Zong, S. Q., Osanai, M., Murakoshi, T., Shimizu, Y., Noda, T., Aso, T., Tanabe, T., 2002. $Ca_v2.3$ (α_{1E}) Ca^{2+} channel participates in the control of sperm function. FEBS Letters 516, 229–233.

Sochivko, D., Pereverzev, A., Smyth, N., Gissel, C., Schneider, T., Beck, H., 2002. The α1E calcium channel subunit underlies R-type calcium current in hippocampal and cortical pyramidal neurons. Journal of Physiology 542, 699–710.

Takei, T., Saegusa, H., Zong, S., Murakoshi, T., Makita, K., Tanabe, T., 2003. Anesthetic sensitivities to propofol and halothane in mice lacking the R-Type ($Ca_v2.3$) Ca^{2+} channel. Anesthesia and Analgesia 97, 96–103.

Toriyama, H., Wang, L., Saegusa, H., Zong, S., Osanai, M., Murakoshi, T., Noda, T., Ohno, K., Tanabe, T., 2002. Role of $Ca_v2.3$ (alpha1E) Ca^{2+} channel in ischemic neuronal injury. Neuroreport 13, 261–265.

Vajna, R., Klöckner, U., Pereverzev, A., Weiergräber, M., Chen, X. H., Miljanich, G., Klugbauer, N., Hescheler, J., Perez-Reyes, E., Schneider, T., 2001. Functional coupling between 'R-type' calcium channels and insulin secretion in the insulinoma cell line INS-1. European Journal of Biochemistry 268, 1066–1075.

Vajna, R., Schramm, M., Pereverzev, A., Arnhold, S., Grabsch, H., Klöckner, U., Perez-Reyes, E., Hescheler, J., Schneider, T., 1998. New isoform of the neuronal Ca^{2+} channel α1E subunit in Islets of Langerhans, and kidney. Distribution of voltage-gated Ca^{2+} channel α1 subunits in cell lines and tissues. European Journal of Biochemistry 257, 274–285.

Weiergräber, M., Henry, M., Krieger, A., Kamp, M. A., Radhakrishnan, K., Hescheler, J., Schneider, T., 2006. Altered seizure susceptibility in mice lacking the $Ca_v2.3$ E-type Ca^{2+} channel. Epilepsia, in press.

Weiergräber, M., Henry, M., Südkamp, M., De Vivie, E. R., Hescheler, J., Schneider, T., 2005. Ablation of $Ca_v2.3$/E-type voltage-gated calcium channel results in cardiac arrhythmia and altered autonomic control within the murine cardiovascular system. Basic Research in Cardiology 100, 1–13.

Wilson, S. M., Toth, P. T., Oh, S. B., Gillard, S. E., Volsen, S., Ren, D., Philipson, L. H., Lee, E. C., Fletcher, C. F., Tessarollo, L., Copeland, N. G., Jenkins, N. A., Miller, R. J., 2000. The status of voltage-dependent calcium channels in alpha1E knock-out mice. Journal of Neuroscience 20, 8566–8571.

Yokoyama, K., Kurihara, T., Saegusa, H., Zong, S., Makita, K., Tanabe, T., 2004. Blocking the R-type ($Ca_v2.3$) Ca channel enhanced morphine analgesia and reduced morphine tolerance. European Journal of Neuroscience 20, 3516–3519.

Table 2
Localization of the $Ca_v2.3$ VGCC in the brain

Location	Species	Method of detecting $Ca_v2.3$	Reference
Telencephalon			
Neocortex	Mouse	PC	Sochivko et al. (2002)
	Mouse	RT-PCR	Weiergräber et al. (2006)
Layers II–VI	Rat	ISH	Soong et al. (1993)
Pyramidal cells	Rat	PC; RT-PCR	Foehring et al. (2000)
GABAergig neurons	Mouse	IHC	Timmermann et al. (2002)
Frontal cortex	Mouse	ISH	Williams et al. (1994)
Dorsal cortex (layers I–VI)	Rat	IHC	Yokoyama et al. (1995)
Cingulate cortex	Mouse	ISH	Williams et al. (1994)
Endopiriform nucleus	Guinea pig	PC	Brevi et al. (2001)
Hippocampus	Mouse	RT-PCR	Weiergräber et al. (2006)
Dentate gyrus	Human	IHC, ISH	Day et al. (1996)
	Human	PC	Sochivko et al. (2002)
	Mouse	ISH	Williams et al. (1994)
	Rat	IHC	Yokoyama et al. (1995)
	Rat	ISH	Soong et al. (1993)
Field CA3	Mouse	ISH	Williams et al. (1994)
pyramidal cell layer	Human	IHC	Day et al. (1996)
	Rat	IHC	Yokoyama et al. (1995)
Stratum lucidum/	Human	IHC	Day et al. (1996)
Mossy fiber terminals	Mouse	PC	Gasparini et al. (2001)
			Dietrich et al. (2003)
			Breustedt et al. (2003)
Field CA2	Human	IHC	Day et al. (1996)
	Mouse	ISH	Williams et al. (1994)
	Rat	IHC	Yokoyama et al. (1995)
Field CA1	Human	IHC	Day et al. (1996)
	Mouse	ISH	Williams et al. (1994)
	Mouse	PC	Sochivko et al. (2002)
	Rat	IHC	Yokoyama et al. (1995)
	Rat	PC	Metz et al. (2005)
	Rat	PC	Yasuda et al. (2003)
Parahippocampal gyrus	Human	IHC	Day et al. (1996)
Entorhinal cortex	Human	IHC	Day et al. (1996)
	Rat	ISH	Soong et al. (1993)
Olfactory bulb	Rat	IHC	Yokoyama et al. (1995)
	Rat	ISH	Soong et al. (1993)
	Mouse	ISH	Williams et al. (1994)
Amygdala	Rat	IHC	Yokoyama et al. (1995)
	Rat	ISH	Soong et al. (1993)
Central amygdala	Mouse	PC	Lee et al. (2002)
	Rat	PC	Yu and Shinnick-Gallagher (1997)
Claustrum	Mouse	ISH	Williams et al. (1994)
Striatum	Rat	IHC	Yokoyama et al. (1995)
	Rat	ISH	Soong et al. (1993)
	Rat	PC; RT-PCR	Foehring et al. (2000)
	Rat	MD; PC	Bergquist and Nissbrandt (2003)
Diencephalon			
Globus pallidus	Rat	IHC	Hanson and Smith (2002)
	Rat	IHC	Yokoyama et al. (1995)
Habenula (medial part)	Rat	ISH	Soong et al. (1993)
	Mouse	ISH	Williams et al. (1994)
Thalamus	Mouse	ISH	Williams et al. (1994)
	Mouse	RT-PCR	Weiergräber et al. (2006)
	Rat	IHC	Yokoyama et al. (1995)
	Rat	ISH	Soong et al. (1993)
Reticular thalamic nucleus	Mouse	RT-PCR/IHC	Weiergräber et al. (2006)
Subthalamic nucleus	Rat	IHC	Yokoyama et al. (1995)
Medial geniculate body	Mouse	ISH	Williams et al. (1994)
Hypothalamus	Mouse	RT-PCR	Weiergräber et al. (2006)
	Rat	IHC	Yokoyama et al. (1995)
	Rat	ISH	Soong et al. (1993)

Table 2 (*continued*)

Location	Species	Method of detecting $Ca_v2.3$	Reference
Supraoptic nucleus	Rat	ISH	Soong et al. (1993)
Ventromedial nucleus	Mouse	ISH	Williams et al. (1994)
Dorsomedial nucleus	Mouse	ISH	Williams et al. (1994)
Pituitary gland	Rat	ISH	Soong et al. (1993)
Oxytocin-releasing neurons	Rat	PC, RIA	Wang et al. (1999)
AtT-20-Cells (pituitary gland)	Mouse	RT-PCR	Vajna et al. (1998)
			Williams et al. (1994)
Pineal gland	Rat	ISH	Soong et al. (1993)
Cerebellum			
	Mouse	ISH	Williams et al. (1994)
	Human/Mouse/Rat	RT-PCR	Vajna et al. (1998)
Granule cell layer	Rat	PC	Randall and Tsien (1995)
			Tottene et al. (1996)
			D'Angelo et al. (1997)
	Rat	ISH	Soong et al. (1993)
	Rat	IHC	Grabsch et al. (1999)
Purkinje cell layer	Rat	IHC	Yokoyama et al. (1995)
	Rat	IHC	Grabsch et al. (1999)
	Rat	ISH	Soong et al. (1993)
	Human	IHC	Volsen et al. (1995)
Deep cerbellar nuclei	Rat	IHC	Yokoyama et al. (1995)
Midbrain and mesencephalon			
Substantia nigra, pars compacta	Rat	ISH	Soong et al. (1993)
	Rat	MD, PC	Bergquist and Nissbrandt (2003)
Dorsal raphe nucleus	Rat	ISH	Soong et al. (1993)
Medulla	Mouse	RT-PCR	Weiergräber et al. (2006)
Periaqueductal gray	Mouse	ISH	Williams et al. (1994)
Pontine nuclei	Rat	ISH	Soong et al. (1993)
	Mouse	ISH	Williams et al. (1994)
Locus coeruleus	Mouse	ISH	Williams et al. (1994)
	Rat	PC	Chieng and Bekkers (1999)
Dorsal vagal complex	Mouse	ISH	Williams et al. (1994)
Dorsal lateral and medial parabrachial nuclei	Mouse	ISH	Williams et al. (1994)
Posterior cochlear nucleus	Guinea pig	PC	Molitor and Manis (1999)
Calyx of held	Rat	IHC, PC	Wu et al. (1998), Wu et al. (1999)
Nucleus n. facialis	Rat	IHC	Yokoyama et al. (1995)
Spinal tegmental nucleus	Mouse	ISH	Williams et al. (1994)
Area postrema			reviewed by Hay (2001)

Abbreviations: IHC—immunohistochemistry; ISH—in situ hybridization; MD—microdialysis; PC—patch clamp technique; RIA—radioimmunoassay; RT-PCR—reverse transcription–polymerase chain reaction

References

Bergquist, F., Nissbrandt, H., 2003. Influence of R-type ($Ca_v2.3$) and t-type ($Ca_v3.1$-3.3) antagonists on nigral somatodendritic dopamine release measured by microdialysis. Neuroscience 120, 757–764.

Breustedt, J., Vogt, K. E., Miller, R.J., Nicoll, R.A., Schmitz, D., 2003. Alpha1E-containing Ca^{2+} channels are involved in synaptic plasticity. Proceedings of the National Academy of Sciences of the United States of America 100, 12450–12455.

Brevi, S., de Curtis, M., Magistretti, J., 2001. Pharmacological and biophysical characterization of voltage-gated calcium currents in the endopiriform nucleus of the guinea pig. Journal of Neurophysiology 85, 2076–2087.

Chieng, B., Bekkers, J. M., 1999. $GABA_B$, opioid and α_2 receptor inhibition of calcium channels in acutely-dissociated locus coeruleus neurones. British Journal of Pharmacology 127, 1533–1538.

D'Angelo, E., De Filippi, G., Rossi, P., Taglietti, V., 1997. Synaptic activation of Ca^{2+} action potentials in immature rat cerebellar granule cells in situ. Journal of Neurophysiology 78, 1631–1642.

Day, N.C., Shaw, P.J., McCormack, A.L., Craig, P.J., Smith, W., Beattie, R., Williams, T.L., Ellis, S.B., Ince, P.G., Harpold, M.M., Lodge, D., Volsen, S.G., 1996. Distribution of α 1A, α 1B AND α 1E voltage-dependent calcium channel subunits in the human hippocampus and parahippocampal gyrus. Neuroscience 71, 1013–1024.

Dietrich, D., Kirschstein, T., Kukley, M., Pereverzev, A., von der Brelie, C., Schneider, T., Beck, H., 2003. Functional specialization of presynaptic $Ca_v2.3$ Ca^{2+} channels. Neuron 39, 483–496.

Foehring, R.C., Mermelstein, P.G., Song, W.J., Ulrich, S., Surmeier, D.J., 2000. Unique properties of R-type calcium currents in neocortical and neostriatal neurons. Journal of Neurophysiology 84, 2225–2236.

Gasparini, S., Kasyanov, A. M., Pietrobon, D., Voronin, L. L., Cherubini, E., 2001. Presynaptic R-type calcium channels contribute to fast excitatory synaptic transmission in the rat hippocampus. Journal of Neuroscience 21, 8715–8721.

Grabsch, H., Pereverzev, A., Weiergräber, M., Schramm, M., Henry, M., Vajna, R., Beattie, R. E., Volsen, S. G., Klöckner, U., Hescheler, J., Schneider, T., 1999. Immunohistochemical detection of α1E voltage-gated Ca^{2+} channel isoforms in cerebellum, INS-1 cells, and neuroendocrine cells of the digestive

system. Journal of Histochemistry & Cytochemistry 47, 981–993.
Hanson, J. E., Smith, Y., 2002. Subcellular distribution of high-voltage-activated calcium channel subtypes in rat globus pallidus neurons. Journal of Comparative Neurology 442, 89–98.
Hay, M., 2001. Subcellular mechanisms of area postrema activation. Clinical and Experimental Pharmacology And Physiology 28, 551–557.
Lee, S. C., Choi, S., Lee, T., Kim, H. L., Chin, H., Shin, H. S., 2002. Molecular basis of R-type calcium channels in central amygdala neurons of the mouse. Proceedings of the National Academy of Sciences of the United States of America 99, 3276–3281.
Metz, A. E., Jarsky, T., Martina, M., Spruston, N., 2005. R-type calcium channels contribute to afterdepolarization and bursting in hippocampal CA1 pyramidal neurons. Journal of Neuroscience 25, 5763–5773.
Molitor, S.C., Manis, P.B., 1999. Voltage-gated Ca^{2+} conductances in acutely isolated guinea pig dorsal cochlear nucleus neurons. Journal of Neurophysiology 81, 985–998.
Randall, A., Tsien, R. W., 1995. Pharmacological dissection of multiple types of Ca^{2+} channel XX currents in rat cerebellar granule neurons. Journal of Neuroscience 15, 2995–3012.
Sochivko, D., Pereverzev, A., Smyth, N., Gissel, C., Schneider, T., Beck, H., 2002. The α1E calcium channel subunit underlies R-type calcium current in hippocampal and cortical pyramidal neurons. Journal of Physiology 542, 699–710.
Soong, T. W., Stea, A., Hodson, C. D., Dubel, S. J., Vincent, S. R., Snutch, T. P., 1993. Structure and functional expression of a member of the low voltage-activated calcium channel family. Science 260, 1133–1136.
Timmermann, D. B., Westenbroek, R. E., Schousboe, A., Catterall, W. A., 2002. Distribution of high-voltage-activated calcium channels in cultured gamma-aminobutyric acidergic neurons from mouse cerebral cortex. Journal of Neuroscience Research 67, 48–61.
Tottene, A., Moretti, A., Pietrobon, D., 1996. Functional diversity of P-type and R-type calcium channels in rat cerebellar neurons. Journal of Neuroscience 16, 6353–6363.
Vajna, R., Schramm, M., Pereverzev, A., Arnhold, S., Grabsch, H., Klöckner, U., Perez-Reyes, E., Hescheler, J., Schneider, T., 1998. New isoform of the neuronal Ca^{2+} channel α1E subunit in Islets of Langerhans, and kidney. distribution of voltage-gated Ca^{2+} channel α1 subunits in cell lines and tissues. European Journal of Biochemistry 257, 274–285.
Volsen, S.G., Day, N.C., McCormack, A.L., Smith, W., Craig, P.J., Beattie, R., Ince, P.G., Shaw, P.J., Ellis, S.B., Gillespie, A., Harpold, M.M., Lodge, D., 1995. The expression of neuronal voltage-dependent calcium channels XX in human cerebellum. Molecular Brain Research 34, 271–282.
Wang, G., Dayanithi, G., Newcomb, R., Lemos, J. R., 1999. An R-Type Ca^{2+} Current in Neurohypophysial Terminals Preferentially Regulates Oxytocin Secretion. J.Neurosci. 19, 9235–9241.
Weiergräber, M., Henry, M., Krieger, A., Kamp, M. A., Radhakrishnan, K., Hescheler, J., Schneider, T., 2006. Altered seizure susceptibility in mice lacking the $Ca_v2.3$ E-type Ca^{2+} channel. Epilepsia, in press.
Williams, M.E., Marubio, L.M., Deal, C.R., Hans, M., Brust, P.F., Philipson, L.H., Miller, R.J., Johnson, E.C., Harpold, M.M., Ellis, S.B., 1994. Structure and functional characterization of neuronal α_{1E} calcium channel subtypes. Journal of Biology Chemistry 269, 22347–22357.
Wu, L.G., Borst, J.G., Sakmann, B., 1998. R-type Ca^{2+} currents evoke transmitter release at a rat central synapse. . Proceedings of the National Academy of Sciences of the United States of America 95, 4720–4725.
Wu, L.G., Westenbroek, R.E., Borst, J.G.G., Catterall, W.A., Sakmann, B., 1999. Calcium channel types with distinct presynaptic localization couple differentially to transmitter release in single calyx-type synapses. Journal of Neuroscience 19, 726–736.
Yasuda, R., Sabatini, B.L., Svoboda, K., 2003. Plasticity of calcium channels in dendritic spines. Nature Neuroscience 6, 948–955.
Yokoyama, C.T., Westenbroek, R.E., Hell, J.W., Soong, T.W., Snutch, T.P., Catterall, W.A., 1995. Biochemical properties and subcellular distribution of the XX neuronal class E calcium channel α_1 subunit. Journal of Neuroscience 15, 6419–6432.
Yu, B., Shinnick-Gallagher, P., 1997. Dihydropyridine- and neurotoxin-sensitive and -insensitive calcium currents in acutely dissociated neurons of the rat central amygdala. Journal of Neurophysiology 77, 690–701.

activation through protein kinase C (PKC) slows down inactivation and speeds up recovery from short-term inactivation (Leroy et al., 2003; Klöckner et al., 2004). Such a positive feedback is dependent on the presence of the exon 19 encoded arginine rich insert 1 in the cytosolic II–III loop (Pereverzev et al., 2002). For $Ca_v2.3e$ E/R-type Ca^{2+} channels, which are lacking exon 19 encoded insert 1, a minor but still significant phorbol ester mediated stimulation is left. We interpreted this as a reduced affinity for scaffolding proteins, which bind PKC to the II–III loop of the $Ca_v2.3d$ splice variant containing insert 1 (Fig. 1). (Krieger et al., 2006). This model is supported by the observation that coexpression of PKCα with $Ca_v2.3e$ leads to similar kinetics of inactivation and recovery as recorded for the full length II–III loop splice variant $Ca_v2.3d$. Thus, the pattern of $Ca_v2.3$ splice variants in different brain regions is likely to be of tremendous importance for neuronal mechanisms underlying neuroprotection, icto-/epileptogenesis and seizure propagation (Weiergräber et al., 2006) (Fig. 1). Besides $Ca_v2.3$, a positive feedback mechanism by incoming Ca^{2+} was also reported for L-type Ca^{2+} channels and is mediated through Ca^{2+}/calmodulin kinase II (Dzhura et al., 2000). However, at elevated cytosolic Ca^{2+} concentrations, a prominent Ca^{2+}-dependent inactivation renders the channel activity to further increase (for overview see Liang et al., 2003).

PKC-mediated phosphorylation is of substantial physiological relevance, mediating hormonal effects and those of intracellular messengers. Voltage-gated Ca^{2+} channels are effectors in various regulatory neurotransmitter and hormonal pathways initiated by G-proteins. Principally, this G-protein dependent regulation of VGCCs can either be indirect via second messengers and/or protein kinases or direct via physical interaction between G-protein subunits and the Ca_v-α1 subunit. Functional studies elicited that G-protein interaction reversibly inhibits neuronal non-L-type Ca^{2+}-channels. Peak current amplitude is reduced and activation kinetics are slowed. The effects of the hetereotrimeric G-proteins on VGCC are well described for the $G_{\beta\gamma}$ dimer (Herlitze et al., 1996; Ikeda, 1996), whereas the role of G_α is yet not well understood. There is evidence

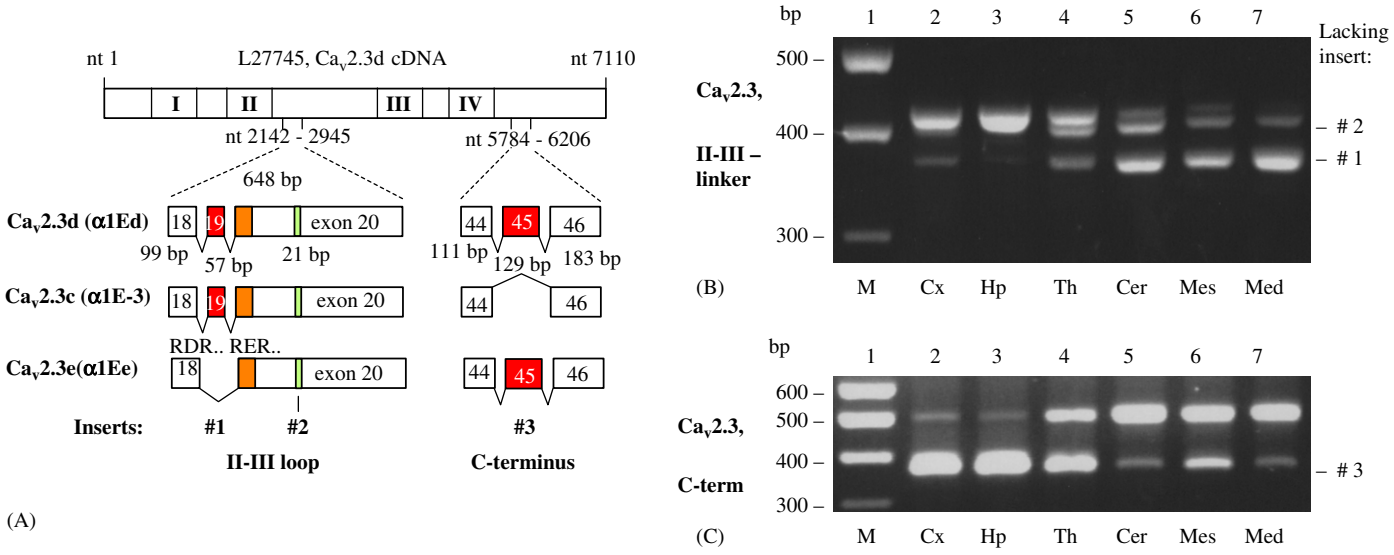

Fig. 1. Distribution of neuronal $Ca_v2.3$ splice variants. Major neuronal $Ca_v2.3$ splice variants differ by exon skipping either in the II–III loop (exon 19) or in the C-terminus (exon 45). Both exons are only expressed in the splice variant $Ca_v2.3d$ which was cloned from human fetal brain. (A) Cartoon for indicative fragments of $Ca_v2.3$ and their relation to gene structure. (B) Total RNA was isolated from neocortex (Cx), hippocampus (Hp), the thalamus and hypothalamus (Th), cerebellum (Cer), mesencephalon (Mes) and the medulla (Med). Known $Ca_v2.3$ splice variants were identified by RT-PCR after amplifying indicative fragments of the II–III loop and the C-terminus. Using the oligonucleotide primer pairs which are flanking the segment containing exon 19 (insert # 1) and the adjacent insert # 2 (in exon 20) leads to the detection of indicative patterns of the II–III loop. The expected sizes of cDNA fragments are 363 bp (lacking exon 19), 399 bp (lacking insert 2), and 420 bp representing the full-length segment within the II–III loop. (C) Using the oligonucleotide primer pair which is flanking exon 45 (insert # 3) leads to the detection of indicative patterns of carboxy terminal fragments of $Ca_v2.3$.

that $G_{\beta\gamma}$ directly interacts with the I–II linker of the Ca_v α1-subunit (De Waard et al., 1997; Zamponi et al., 1997). In addition, the N-terminus of Ca_v2-α1 subunits also seems to be involved in G-protein coupled channel modulation (Dolphin, 2003b) including $Ca_v2.3$. As the $G_{\beta\gamma}$ interaction site within the I–II linker partially overlaps the AID (α_1-interacting domain) where β subunits bind, this mechanism suggests a physical competition between the agonistic β-subunits (De Waard and Campbell, 1995; Dolphin, 2003a) and the antagonistic effects of $G_{\beta\gamma}$ (Sandoz et al., 2004). Interestingly, $G_{\beta\gamma}$ seems to exert inhibitory effects on low-voltage-activated T-type Ca^{2+}-channels via interaction with the II–III-loop (Wolfe et al., 2003). In addition, there are hints of a complex interdependence between PKC and G-protein pathways as activation of PKC antagonizes adjacent receptor-mediated G-protein inhibition of VGCC (Zamponi et al., 1997; Doering et al., 2004).

Accumulation of internal Ca^{2+} at low concentrations therefore leads to tonic activation of $Ca_v2.3d$ resulting in augmented responses, slowed inactivation and accelerated recovery from inactivation (Leroy et al., 2003). According to Dietrich et al. (2003) $Ca_v2.3$ contributes selectively to the so-called residual $[Ca^{2+}]_i$ which also underlies various forms of synaptic plasticity but contributes less to neurotransmitter release. However, this residual internal background Ca^{2+} reaches concentration of up to 0.5 μM (Brenowitz and Regehr, 2003) and is in the same range as has been shown to facilitate Ca^{2+} currents through $Ca_v2.3d$ channels (Leroy et al., 2003). Initial positive feedback mechanisms based on PKC activity might later be attenuated by negative feedback loops involving N-lobe calmodulin-dependent modulation as described previously by Liang et al. (2003) and therefore help to maintain physiological $[Ca^{2+}]_i$ concentrations.

2.3. Internal cell calcium and neuronal excitability

A number of cell functions are regulated by the free cytosolic Ca^{2+} concentration. Calcium ions can enter the cell via different types of Ca^{2+} channels, the Na^+/Ca^{2+}-exchanger, and through release channels from internal Ca^{2+} stores. The resulting Ca^{2+} signal is highly organized in space, frequency and amplitude because the localization and the integrated free cytosolic Ca^{2+} concentration over time contains specific information (Missiaen et al., 2000). Action potentials induce Ca^{2+} entry through high-voltage activated Ca^{2+} channels in pyramidal cells (Markram et al., 1995; Helmchen et al., 1999). Until buffering mechanisms restore resting Ca^{2+} levels (Markram et al., 1995; Kannurpatti et al., 2000; Gibney et al., 2002), cytoplasmic free Ca^{2+} regulates critical cellular functions, including neurotransmitter release, gene transcription and channel modulation. Cytoplasmic Ca^{2+} may also provide the cell with an index of recent spiking activity (Helmchen et al., 1999).

The calcium hypothesis of epileptogenesis claims that alterations in internal Ca^{2+} play a crucial role in the development of epilepsy (Albowitz et al., 1997; DeLorenzo

et al., 1998; Sun et al., 2002). Consequently, the extracellular Ca^{2+} concentrations deceases during epileptiform activity (Hamon and Heinemann, 1986). Although a number of studies provide clear evidence for increased neuronal Ca^{2+} influx during epileptiform activity, direct visualizations and measurements of the underlying $[Ca^{2+}]_i$ are rare and the structural/molecular background of Ca^{2+} influx is only partially known. High-voltage activated Ca^{2+} channels are likely to be predominant candidates for $[Ca^{2+}]_i$ elevation during epileptiform activity (Albowitz et al., 1997; Pisani et al., 2004), contributing to both seizure initialization and propagation. In hippocampal tissue for example, Ca^{2+} current density was reported to be upregulated during epileptogenesis (Beck et al., 1998) and blockade of these channels also depressed epileptiform activity (Straub et al., 1990). Furthermore, Berg et al. (1995) proved that seizure activity induced by kainate, e.g. in the hippocampus is strongly based on internal Ca^{2+} which also plays a crucial role in seizure-related excitotoxicity. Consequently, various antiepileptic drugs were reported to exert neuroprotective effects in different animal models by inhibiting components of the excitotoxic cascade (Sullivan, 2005). By regulating internal Ca^{2+}-levels and given the functional interdependence of $Ca_v2.3$ channel activation and cellular Ca^{2+} modulated via Ca^{2+}/calmodulin and PKC, $Ca_v2.3$ becomes a key regulator in neuronal excitability and consequently in triggering of epileptiform activity, as discussed later for CA1 neurons (Section 4).

3. $Ca_v2.3$ in non-convulsive seizures—functional interdependence with the $Ca_v2.1$ and $Ca_v3.1$ VGCC in absence epileptogenesis

Typical absence epilepsy is characterized behaviourally by a paroxysmal loss of consciousness of sudden onset and termination that is normally accompanied with bilateral synchronous spike-wave discharges activity of species specific frequency (Manning et al., 2003). The involvement of the thalamocortical circuit, particularly the contribution of the ventrobasal thalamus and the reticular thalamic nucleus in establishment and propagation of absence seizures has been established for several years (Steriade, 2005). Furthermore, various extrathalamocortical structures such as the reticular formation, laterodorsal tegmental nucleus, pedunculopontine tegmental nucleus, raphe nuclei, locus coeruleus, basal nucleus of Meynert as well as cerebellar structures project to that circuitry. Some brain structures like hippocampus or cerebellum classically not known to be involved in the production of absence spike-wave discharges could in fact participate in the development of this phenotype (Lakaye et al., 2002). Pathophysiologically, aberrant corticothalamic rhythms are believed to be the substrate of spike-wave discharges. Thalamic neurons have the intriguing capability to shift between two functional modes, the tonic and burst firing mode, which strongly regulates transmission of external information to the cortex (Blumenfeld and McCormick, 2000). Oscillatory behavior within the thalamocortical circuitry is substantially driven by the reticular thalamic nucleus which serves as a key modulator of information transfer between thalamus and cortex. These reticular thalamic nucleus neurons are gabaergic, strategically localized lateral to the ventrobasal thalamic relay neurons exerting inhibitory action on each other as well as thalamic relay cells (Steriade, 2005).

It is interesting to note that the majority of single-mutation mouse models of absence epilepsy are associated with defects in genes encoding subunits of VGCCs, indicating the central role that such channels might play in absence epileptogenesis. Particularly, $Ca_v2.1$ as well as T-type Ca^{2+} channels have been reported to play a major role in this field. The $Ca_v3.1$ VGCC knock-out mouse model was reported to lack burst firing in thalamocortical neurons and displays resistance to absence seizures (Kim et al., 2001). In addition, $Ca_v3.1^{-/-}$ mice are characterized by altered sleep architecture and lack of delta waves (Lee et al., 2004). $Ca_v3.1$ is dominantly expressed within thalamic relay neurons and the results obtained from $Ca_v3.1^{-/-}$ mice strongly indicate the functional relevance of VGCCs and also $Ca_v2.3$ within the thalamocortical circuitry. In contrast to $Ca_v3.1$ deficient animals, $Ca_v2.1^{-/-}$ mice are prone to absence epilepsy with spike-wave discharges and motoric arrest (Jun et al., 1999). Furthermore, the ablation of P/Q-type Ca^{2+} channel currents resulted in altered synaptic transmission and progressive ataxia in these mice. Interestingly, T-type Ca^{2+} currents were increased in thalamocortical relay neurons from these mice (Zhang et al., 2002). Double knock-out experiments further revealed that $Ca_v2.1^{-/-}$ $Ca_v3.1^{-/-}$ mice do not exhibit spontaneous spike-wave discharges and no T-type Ca^{2+} current in thalamocortical neurons was observed (Song et al., 2004). However, in some mouse models, e.g. $Ca_v2.1$ leaner, $Ca_v3.1$ is down regulated in the cerebellar granule cells while expression in Purkinje cells is increased and might therefore be involved in complex movement disorders such as ataxia and paroxysmal dyskinesia (Nahm et al., 2005; Pietrobon 2005). Thus, increased T-type Ca^{2+} currents in various structural components of the thalamocortical circuitry seem to be a common feature in absence epileptogenesis though it is not an absolute must (Song et al., 2004).

However, within the thalamocortical circuitry T- and P/Q-type VGCCs are not the only players. Gabaergic interneurons of the reticular thalamic nucleus and cortex as well as extrathalamocortical structures were clearly shown to express $Ca_v2.3$ (Soong et al., 1993; De Borman et al., 1999; Talley et al., 2000; van de Bovenkamp-Janssen et al., 2004; Weiergräber et al., 2006). Most studies on the role of $Ca_v2.3$ in absence epileptogenesis were carried out on the Genetic Absence Epilepsy Rats from Strasbourg (GAERS) and the Wistar Albino Glaxo rats (WAG/Rij). In GAERS an increase of T-type Ca^{2+} current in reticular thalamic

nucleus neurons has been reported (Tsakiridou et al., 1995) and later on also alterations in $Ca_v3.1$ and $Ca_v3.2$ expression in the adult ventroposterior thalamic nuclei and reticular thalamic nucleus neurons, respectively (Talley et al., 2000).

Astonishingly, de Borman et al. (1999) and Lakaye et al. (2002) detected a significant reduction of $Ca_v2.3$ transcript levels in both cerebellum and medulla of GAERS, two extrathalamocortical brain structures, the brainstem and cerebellum which project to the thalamocortical circuitry, capable of modifying its oscillatory behavior (Filakovszky et al., 1999; Deransart et al., 2001). On the other hand, the WAG/Rij rat model of absence epilepsy was also reported to exhibit altered VGCC expression. Development of spike-wave discharges in these rats is concomitant with an increased expression of $Ca_v2.1$ in the reticular thalamic nucleus. Furthermore, van de Bovenkamp-Janssen et al. (2004) demonstrated that normal control rats exhibit an increase of $Ca_v2.3$ expression within the RTN during development (from 3 to 6 months of age) whereas WAG/Rij rats were lacking this $Ca_v2.3$ increase concomitant with the establishment of SWDs. These observations clearly point to a functional role of $Ca_v2.3$ in etiology and pathogenesis of absence epilepsy like activity and, in addition might be related to sleep disorders.

Pharmacological studies further support this observation. Lamotrigine for example, which exerts inhibitory actions on $Ca_v2.3$ VGCCs (Hainsworth et al., 2003) was proven to be effective in suppressing spike-wave discharges in both GAERS and WAG/Rij rats (van Luijtelaar et al., 2002; Manning et al., 2003) and thalamocortical burst complexes in rat brain slices (Gibbs III et al., 2002). However, the electrophysiological properties and functional implications of $Ca_v2.3$ expression within reticular thalamic nucleus cells, gabaergic interneurons of the cortex and extrathalamocortical structures on thalamocortical oscillations have not been described yet. In conclusion, there are strong hints that $Ca_v2.3$ might play a primary or secondary role in the establishment of spike-wave discharges.

4. The $Ca_v2.3$ VGCC in convulsive seizures

4.1. $Ca_v2.3$ in neuronal apoptosis

In a recent study, Suzuki et al. (2004) characterized five missense mutations within EFHC1, an EF-hand protein interacting with the C-terminus of the $Ca_v2.3$ VGCC. This protein is primarily localized on the soma and dendrites of pyramidal neurons and Purkinje cells. Surprisingly, patients carrying these mutations were reported to exhibit juvenile myoclonic epilepsy, a common form of generalized epilepsy in humans. Suzuki et al. (2004) deduced that EFHC1 normally controls neuronal apoptosis via $Ca_v2.3$ mediated Ca^{2+} influx further supported by the observation that apoptosis was suppressed by 30 nM SNX-482 in mouse hippocampal primary culture but not by other Ca^{2+} channel antagonists. Interestingly, mutations in EFHC1 were shown to prevent EFHC1 from binding to and activating $Ca_v2.3$, thus prohibiting neuronal apoptosis in patients suffering from juvenile myoclonic epilepsy. However, EFHC1 does not only bind to $Ca_v2.3$, but also interacts with other proteins capable of modifying the seizure phenotype. The intriguing aspect of these findings is that mutations in EFHC1 result in lack of neuronal apoptosis during early brain development and consequently, increased neuronal cell density leads to the establishment of altered neuronal connectivity and hyperexcitable circuits proposing a completely new mechanism of epileptogenesis in juvenile myoclonic epilepsy patients. Most common, epileptogensis is related to primary or secondary forms of neuronal degeneration. However, increased neuronal density in association with epilepsy is rarely described in literature (Andres et al., 2005). Principally, apoptosis involves a genetic reprogramming of the cell to promote a cascade of biochemical and morphological changes that finally result in cell death and elimination. Different stimuli, e.g. Ca^{2+} influx through VGCCs could serve this function. So far, no reports on markers of neuronal apoptosis in $Ca_v2.3^{-/-}$ and control mice are available. However, as $Ca_v2.3^{-/-}$ mice did not exhibit spontaneous epileptiform discharges in electroencephalographic (EEG) recordings and turned out to be more seizure resistant than their $Ca_v2.3^{+/+}$ counterparts (Weiergräber et al., 2006), the functional involvement of $Ca_v2.3$ in neuronal apoptosis is obviously more complex than actually expected and definitely needs further investigation in the future.

4.2. The $Ca_v2.3$ VGCC in neuronal epileptiform activity

Abnormal burst activity is a characteristic feature of epileptiform, neuronal activity. Each cellular burst is sustained by a slow, persistent depolarization, the so-called plateau potential (Andrew and Dudek, 1983), which is initiated at the beginning of the burst and lasts for several hundred milliseconds to seconds (Andrew, 1987). The plateau is spike dependent and regenerative and is triggered by the summation of depolarizing action potentials (Andrew and Dudek, 1984). The depolarizing action potentials that follow two or more closely spaced spikes sum up to a much larger afterpotential, and the resulting depolarization can take the cell above spike threshold. Additionally, a concomitant increase in internal Ca^{2+} after multiple spikes further supports this process by inhibiting $I_{K,leak}$ and so more strongly depolarizes the cell. If the resulting summed depolarizing action potentials are then sufficient to carry the cell above spike threshold, the resulting action potential brings in more Ca^{2+} eliciting further depolarizing action potentials via a positive feedback mechanism. Consequently, this process repeats resulting in a sustained plateau potential which supports repetitive spiking (Andrew and Dudek, 1983). After several seconds of activity, but long before termination, $[Ca^{2+}]_i$ attains a plateau that is typically >200 nM above rest.

However, the plateau potential quickly collapses, once the electrical activity has ceased and the membrane repolarizes again (Andrew and Dudek, 1984). The cause of plateau potential termination has not yet been fully established, although an accumulation of $[Ca^{2+}]_i$ and the subsequent activation of a hyperpolarizing Ca^{2+}-dependent K^+-mediated afterhyperpolarisation has been proposed (Hlubek and Cobbett, 2000; Roper et al., 2003). A shift from Ca^{2+}-dependent facilitation to Ca^{2+} dependent inactivation of VGCCs at elevated $[Ca^{2+}]_i$ might also play a role. In neocortical pyramidal cells, Abel et al. (2004) have shown that there is a linear relationship between plateau $[Ca^{2+}]_i$ and firing frequency in soma and proximal dendrites and the rise in $[Ca^{2+}]_i$ finally activates K^+ channels underlying the afterhyperpolarization, consisting of two Ca^{2+}-dependent components, medium and slow afterhyperpolarisation.

Principally, plateau potentials as outlined above, but also afterdepolarisations are a common feature of different neuronal cell types in various brain regions, e.g. spinal and brainstem motoneurons, spinal interneurons, dorsal horn neurons, subthalamic nucleus neurons, suprachiasmatic neurons, striatal cholinergic neurons, hippocampal pyramidal cells, subicular and entorhinal cortical cells (Pierson et al., 2005).

Though a common phenomenon within the CNS, plateau potentials and afterdepolarisations still harbor a plethora of secrets as the underlying ion channel entities are still not fully described. However, recent studies more and more point to the fact that $Ca_v2.3$ indeed is a potent player in plateau potential and afterdepolarisation generation. In lumbar spinal cord motor neurons, plateau potentials were originally reported to be driven by L-type Ca^{2+} channels in dendrites (Simon et al., 2003). Li and Bennett (2003) have argued that a TTX-sensitive persistent sodium and L-type Ca^{2+} current are responsible for plateau potentials in these cells. Both Cd^{2+} (400 μM), a non-specific Ca^{2+} channel blocker, and nimodipine (10–20 μM), a specific L-type Ca^{2+} channel blocker, completely abolished this TTX-resistant plateau and therefore Li and Bennett (2003) concluded that it was mediated by L-type Ca^{2+} channels. However, the nimodipine-sensitive Ca^{2+} current in this preparation was low-voltage activated (−50 mV) and concluded to be associated with the $Ca_v1.3$ Ca^{2+} channel with low-voltage behavior. This L-type current was usually fully activated at <-40 mV. Additionally, the authors clearly ruled out that the high-voltage activated Ca^{2+} channels $Ca_v2.1$ and $Ca_v2.2$ are related to the persistent low-threshold inward Ca^{2+} current by using various Ca^{2+} channel blockers, e.g. ω-conotoxin GVIA (2 μM) and ω-conotoxin MVIIC (1 μM). Although L-type Ca^{2+} channels are conventionally considered as high-voltage activated channels, Li and Bennett (2003) demonstrated that the threshold of L-type Ca^{2+} channels in their preparation is around the firing threshold of the motoneurons, which is similar to the low-threshold obtained in other studies of plateaus in neurons (i.e., −45 to −55 mV; Hounsgaard and Kiehn, 1989; Mills and Pitman, 1997; Morisset and Nagy, 1999; Voisin and Nagy, 2001; Zhang and Harris-Warrick, 1995). Amazingly, many other studies further elicited that these L-type like Ca^{2+} channels involved in generation of plateau potentials require a higher concentration of dihydropyridines, e.g. 10 μM nimodipine (Li and Bennett, 2003), 15 μM nifedipine (Hounsgaard and Kiehn, 1989); 10 μM nifedipine (Voisin and Nagy, 2001) or 50 μM nifedipine (Mills and Pitman, 1997) to be completely blocked than actually do conventional L-type Ca^{2+} channels (<1 μM) (Fanelli et al., 1994; McCarthy and TanPiengco, 1992). However, one has to consider that these data were obtained from different tissue preparations from various species and that dihydropyridine action on VGCCs is further influenced by experimental conditions, such as cell membrane potential or penetration depth of these drugs in CNS slices.

Similar studies were carried out by Vergara et al. (2003) in striatal medium spiny neurons of the rat. Again, L-type Ca^{2+} channels were reported to be necessary for promoting the generation of plateau potentials from relatively depolarized holding potentials if elicited from the soma (−60 to −55 mV) (Hernandez-Lopez et al., 1997; Hernandez-Lopez et al., 2000). The application of the L-type Ca^{2+} channel antagonist nitrendipine (5 μM) reduced plateau potentials in these and other cells tested (Vergara et al., 2003). A central question remains: what's the nature of this low-dihydropyridine sensitive, L-type like Ca^{2+} current?

Fascinatingly, not only neurological but also cardiovascular studies suggest that $Ca_v1.3$ is a possible candidate for a low-threshold and low-dihydropyridine sensitive L-type Ca^{2+} current component (Koschak et al., 2001; Xu and Lipscombe, 2001) and thus is likely to promote generation of plateau potentials in different studies on neuronal cell types. Whereas the characteristics of a low-voltage activated behavior of $Ca_v1.3$ have recently been described (Koschak et al., 2001; Michna et al., 2003), $Ca_v2.3$ has already been reported to conduct transient Ca^{2+} currents with both activation and steady-state inactivation occurring at relatively negative membrane potentials, thus sometimes called a low- to mid-voltage activated channel (Soong et al., 1993).

To determine, whether $Ca_v2.3$ might be indeed a possible candidate for a low dihydropyridine sensitive VGCC, we recently performed dose–response analyses of isradipine effects on two $Ca_v2.3$ splice variants, $Ca_v2.3d$ and $Ca_v2.3e$ yielding IC_{50} values of 9.1 and 14.6 μM, respectively (Lu et al., 2004) (Fig. 2). Furthermore, when $Ca_v2.3$ was coexpressed with $\alpha_2\delta$ and β_{1b} in COS-7 cells the dihydropyridine nicardipine was reported to exert a $51 \pm 7\%$ inhibition of Ca^{2+} influx at 1 μM (Stephens et al., 1997). In contrast, other studies failed to show an inhibitory effect of nifedipine or isradipine on $Ca_v2.3$ VGCCs expressed in *Xenopus* oocytes (Soong et al., 1993; Wakamori et al., 1994; Williams et al., 1994) indicating that the expression system, splice variants and subunit distribution might be of central importance for

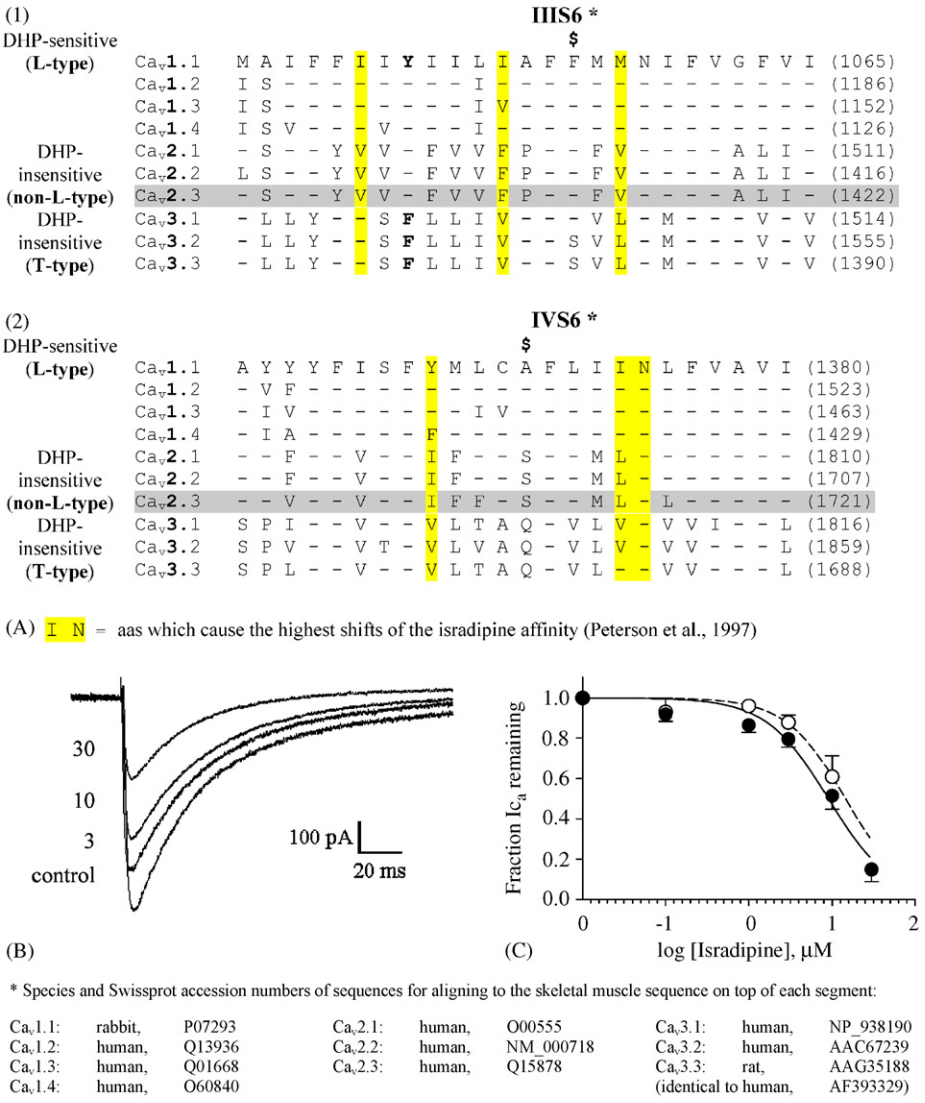

Fig. 2. High-affinity dihydropyridine binding. Alignment of sequences from non-L- and T-type voltage-gated Ca^{2+} channels with the two most important segments for high affinity dihydropyridine binding in L-type Ca^{2+} channels. (A) Initially, the dihydropyridine receptor binding site was analyzed by covalent drug binding (Striessnig et al., 1998) and alanine-scanning (Peterson et al., 1997), which helped to identify critical amino acid residues for high-affinity drug binding. The consecutive molecular modeling of the dihydropyridine binding site with the inner pore of L-type Ca^{2+} channels (Lipkind and Fozzard, 2003) strengthened the idea that within domain III and IV the transmembrane segments S6 are most important for high-affinity drug binding. Dihydropyridines are thought to dock to a crevice, which may be formed by two neighboring tilted S6 helices of domains III and IV below the selectivity filter. According to this model, the dihydropyridine ring may be located between Phe-1176 (homolog to mouse Phe-1159) of IIIS6 (see panel A1, labeled by a $-sign) and Ala-1512 (homolog Ala-1467 in mouse $Ca_v1.2$) of IVS6 (see panel A2, $-sign), parallel to the pore axis. In addition, non-polar interactions with hydrophobic side chains of Ile-1173, Ile-1180, and Ile1516 (in mouse: Ile-1156, Ile-1163, and Ile-1471) on the bottom of the binding cavity may stabilize the channel's closed/inactivated state (Lipkind and Fozzard 2003). Interestingly, the amino acid residue in IIIS6, which binds to the dihydropyridine ring, is identical in L- and non-L-type channels. Similar, one of the two Ile-residues, also is identical in both subfamilies but different in T-type channels. In total, the reduced affinity of the non-L-type $Ca_v2.3$ channel for dihydropyridines arises from multiple differences within the other critical residues as highlighted in panel A. (B) Whole cell recordings with 5 mM extracellular Ca^{2+} as charge carrier from stably transfected HEK-293 cells expressing the ion-conducting subunit $Ca_v2.3d$ of human E-/R-type Ca^{2+} channels. Superimposed traces of Ca^{2+} inward currents are shown which were activated from a holding potential of −50 mV to test potentials of 30 mV. (C) After normalizing the peak inward currents, the dose-response relationship for (±)isradipine is shown for either $Ca_v2.3d$ (closed circles) or the cardiac/endocrine splice variant $Ca_v2.3e$ (open circles). Data were fitted using the Hill equation yielding an IC_{50} value of 9.1 and 14.6 µM for $Ca_v2.3d$ and $Ca_v2.3e$, respectively (Lu et al., 2004).

dihydropyridine-sensitivity. Nevertheless, it is highly questionable whether low micromolar concentrations of dihydropyridines should be regarded as diagnostic for L-type Ca^{2+} channels. Considering, that $Ca_v1.3$ and $Ca_v2.3$ are coexpressed in most regions capable of exhibiting neuronal plateau potentials, it becomes obvious, that $Ca_v2.3$ is likely to contribute significantly to plateau potential and after-depolarisation generation.

In 2005 Pierson et al., further corroborated this hypothesis by demonstrating that E/R-type Ca^{2+} channels are likely to play a major role in the genesis of plateau potentials in hypothalamic suprachiasmatic neurons from

rat (Pierson et al., 2005). In contrast to most other studies carried out before, the authors used low doses of isradipine (2 μM) which clearly failed to prevent or reduce Ca^{2+}-dependent plateau potentials, whereas ω-conotoxin GVIA (1 μM) and ω-agatoxin IVA (200 nM) caused only a slight reduction in plateau potential duration. Based on this observation, Pierson et al. (2005) concluded that E/R-type Ca^{2+} channels significantly contribute to plateau potential generation, particularly, as suprachiasmatic neurons seem to express large E/R-type Ca^{2+} currents of up to 50% (Cloues and Sather, 2003). Thus, by contributing to sustained plateau potentials, E/R-type Ca^{2+} channels might enhance neuronal excitability and contribute to epileptogenic processes.

Moreover, two recent publications directly proved that $Ca_v2.3$ is involved in generation of plateau potentials and afterdepolarisations and contributes to epileptiform burst activity in CA1 neurons of the hippocampus (Kuzmiski et al., 2005; Metz et al., 2005). Early studies by Fraser and MacVicar (1996) and Fraser et al. (2001) already elicited that cholinergic stimulation of hippocampal CA1 neurons using carbachol results in slow afterdepolarisation and long-lasting plateau potentials resembling epileptiform activity. Principally, triggering the cholinergic system is one well-known mechanism to induce limbic seizure activity in vitro and in vivo (Lothman et al., 1991; Wasterlain et al., 1993) and plateau potentials are supposed to play an important role in this field by Ca^{2+} entry through VGCCs as well as muscarinic receptor-mediated activation of guanylate cyclase activity and subsequent increase in cGMP (Kuzmiski and MacVicar, 2001). It is further known that E/R-type Ca^{2+} channels are primarly responsible for the Ca^{2+} influx in dendrites and spines of CA1 neurons (Yasuda et al., 2003) and therefore reduction of E/R-type Ca^{2+} current results in reduction of postsynaptic Ca^{2+} accumulation, especially during repetitive synaptic activation (Qian and Noebels, 2001, 2003). The role of $Ca_v2.3$ seems to be particularly important during cholinergic stimulation, as in the absence of carbachol large plateau Ca^{2+} spikes are based on L-, N-, and P/Q-type Ca^{2+} channels, with E/R-type Ca^{2+} channels exhibiting only minor contribution (Magee and Johnston, 1995a, b; Westenbroek et al., 1990). However, when carbachol is present, L-, N-, and P/Q-type VGCCs are depressed (Gahwiler and Brown, 1987; Toselli et al., 1989) whereas E/R-type-dependent spiking is unmasked and dramatically enhanced.

In 2000 Palmieri et al., reported that topiramate can depress carbachol-induced plateau potentials in subicular bursting cells (Palmieri et al., 2000). Whereas the authors did not further investigate the ionic background of plateau potentials, Kuzmiski et al. (2005) directly proved that topiramate inhibits generation of plateau potentials by depressing E/R-type VGCCs. Topiramate itself is a newer antiepileptic drug, used in treatment of partial seizures, primary generalized tonic-clonic seizures and seizures associated with Lennox-Gastaut-syndrome (LaRoche and Helmers, 2004). On the molecular level, topiramate is supposed to interfere with different systems, e.g. block of voltage-gated sodium channels, VGCCs, AMPA/kainite receptors or GABA(A) receptors, although there are also contradictory reports (Waugh and Goa, 2003; Kuzmiski et al., 2005). Using $Ca_v2.3$ expressing tsA-201 cells cotransfected with β_{1b} and $\alpha_2\delta$ subunits, Kuzmiski et al. (2005) revealed that topiramate is capable of inhibiting $Ca_v2.3$ mediated Ca^{2+} currents at therapeutically relevant concentrations ($IC_{50} = 50.9\,\mu M$) and, in addition shifts the steady-state inactivation curve to more negative potentials supporting transition of the channel into the inactivated state. Interestingly, topiramate had no effect on Ca^{2+} spikes under control conditions, but it reduced Ca^{2+} spikes after cholinergic receptor stimulation which is in accordance with increased E/R-type activity after carbachol application. Carbachol-induced plateau potentials in CA1 neurons were completely depressed by topiramate at therapeutically relevant concentrations (50 μM). Calcium spikes elicited in this study were high-threshold activated, transient Ca^{2+}-dependent action potential. Using a cocktail of TTX and various VGCC blockers (i.a. nifedipine 10 μM) the remaining Ca^{2+} spike was E/R-type based and shown to be increased by carbachol, besides an increase in spike frequency and decrease in threshold for $Ca_v2.3$-mediated spiking. Again, topiramate resulted in a highly significant reduction of E/R-type Ca^{2+} spike amplitude. Although Kuzmiski et al. (2005) did not try to block this E/R-type Ca^{2+} current component by SNX-482, a selective blocker of E/R-type Ca^{2+} channels (Newcomb et al., 1998), it is known that $Ca_v2.3$ contributes at around 80% to the blocker-resistant E/R-type Ca^{2+} current in CA1 neurons (Sochivko et al., 2002) and in addition the E/R-type component turned out to be sensitive to low concentrations of Ni^{2+} (50 μM). Considering the fact that 10 μM nifedipine is likely to exert inhibitory effects on $Ca_v2.3$ (Stephens et al., 1997; Lu et al., 2004) one could imagine that the real $Ca_v2.3$-mediated topiramate effect on carbachol-induced Ca^{2+} spikes is even more dramatic.

Studies by Melliti et al. (2000) and Bannister et al. (2004) have provided first detailed information how $Ca_v2.3$ is actually regulated by M_1, M_3 and M_5 muscarinergic receptors, e.g. via carbachol. All three muscarinic receptors were proven to exert various effects on $Ca_v2.3$ VGCCs. The $G_{\beta\gamma}$ subunit was reported to mediate inhibition of $Ca_v2.3$ whereas the stimulation of $Ca_v2.3$ involves a pertussis toxin-insensitive $G_{\alpha q/11}$ subunit, PLCβ, DAG and a Ca^{2+} independent PKC mechanism. This PKC mediated stimulation might also have severe pharmacological implications regarding topiramate effects on $Ca_v2.3$ (Curia et al., 2004). It is also possible that VGCCs, e.g. $Ca_v2.3$ trigger further intracellular cascades that effect other channel and receptor systems. In rats deep dorsal horn interneurons, it has been described that after initiation of plateau potentials, activation of a Ca^{2+}-activated non-selective cation current can prolong existing plateau potentials (Morisset and Nagy, 1999).

Recently, muscarinic activation via M_1/M_3-cholinergic receptors was shown to enhance R-type, but not T-type, Ca^{2+} currents in rat hippocampal CA1 pyramidal neurons after N-, P/Q-, and L-type Ca^{2+} currents were selectively blocked (Tai et al., 2006). This muscarinic stimulation, e.g. using carbachol is capable of inducing sADP and PP on the cellular level but also θ bursts in extracellular recordings from the CA1 region. Hippocampal pyramidal neurons express high levels of postsynaptic M_1 and M_3 receptors (Levey et al., 1995) which are $G\alpha_{q/11}$ coupled. Their activation results in the generation of DAG and IP_3 following PLC activation. Subsequently, DAG activates Ca^{2+}-independent group II PKCs, most probably PKCδ (Tai et al., 2006). In the presence of PKC inhibitors R-type Ca^{2+}-currents were inhibited by muscarinic stimulation in CA1 neurons probably mediated by activation of pertussis toxin-sensitive G-protein-coupled M_2/M_4 receptors and $G_{\beta\gamma}$ (Meza et al., 1999; Bannister et al., 2004). The functional epileptogenic capacity of $Ca_v2.3$ in triggering hippocampal seizure activity is further supported by the observation that M1 receptor knock-out mice exhibit decreased seizure susceptibility to pilocarpine-induced seizures (Hamilton et al., 1997).

To provide a global view of $Ca_v2.3$ involvement in epileptogenesis one also has to consider secondary effects of VGCCs. In the rat hippocampus for example, the establishment of a focus of epileptiform activity was reported to lead to enhanced voltage-dependent Ca^{2+} conductance of CA1 pyramidal neurones (Vreugdenhil and Wadman, 1994). Hendriksen et al. (1997) induced epileptogenesis by application of electrical tetanic stimulation of the Schaffer collateral/commissural fibre pathway in the hippocampus. Interestingly, during the initial stages of epileptogenesis, $Ca_v2.1$, $Ca_v1.3$- and particularly, $Ca_v2.3$ subunit mRNA levels were significantly increased in the different hippocampal subareas compared to levels in control animals (Hendriksen et al., 1997). Similar results were obtained from the hippocampus of seizure-prone gerbils (Kang et al., 2004).

It becomes obvious that the complex regulation of the $Ca_v2.3$ VGCC by muscarinic receptors, including PKC-mediated and Ca^{2+}-dependent channel activation, harbors a potent and outstanding epileptogenic mechanism that will also enable pharmacological interference in the future.

5. Electroencephalographic characterization and seizure susceptibility testing in $Ca_v2.3$ deficient mice

Our electroencephalographic studies in both generalized and brain-specifically $Ca_v2.3$ inactivated mice revealed no spontaneous epileptiform discharges indicative of convulsive or non-convulsive seizure activity (Fig. 3). However, $Ca_v2.3^{-/-}$ mice turned out to be less susceptible to PTZ-induced convulsive seizures, whereas 4-AP sensitivity remained unchanged (Weiergräber et al., 2006). This difference in seizure susceptibility is probably related to the different convulsive mechanisms of 4-AP and PTZ. 4-Aminopyridine enhances synaptic transmission by reducing K^+ currents, whereas PTZ serves as a GABA(A) receptor antagonist in various brain regions. Expression of other VGCCs was not significantly altered in $Ca_v2.3^{-/-}$ mice indicating that reduced PTZ-seizure susceptibility is directly related to $Ca_v2.3$ ablation and not due to compensatory changes. In addition, EEG analysis revealed that $Ca_v2.3$ deficient animals display less organized and continuous generalized seizure stages of higher severity whereas isolated spike activity in the interictal phase was significantly increased. These results point to a severe alteration in seizure architecture in $Ca_v2.3^{-/-}$ mice compared to controls (Fig. 3). Whereas most other studies carried out before were performed on the cellular level, these are the first results exhibiting the functional consequences of $Ca_v2.3$ ablation on spontaneous electroencephalographic activity and seizure susceptibility thus providing first insight into the intriguing mechanisms of $Ca_v2.3$ on the systemic level.

Principally, three different systemic aspects of $Ca_v2.3$ have to be discussed: Considering the functional involvement of EFHC1 and $Ca_v2.3$ in neuronal apoptosis as outlined above one might speculated that $Ca_v2.3^{-/-}$ mice display increased neuronal cell density associated with altered neuronal connectivity and hyperexcitable circuits (Suzuki et al., 2004). Although markers of neuronal apoptosis have not been tested yet in brains from $Ca_v2.3^{-/-}$ mice, this mechanisms cannot account for reduced seizure susceptibility in $Ca_v2.3^{-/-}$ mice further indicating that there are yet unknown mechanisms which might regulate apoptosis and trigger hyperexcitability in juvenile myoclonic epilepsy patients with EFHC1 mutations.

The second system that $Ca_v2.3$ is involved in is the GABAergic system. GABAergic interneurons are well known to express $Ca_v2.3$ (van de Bovenkamp-Janssen et al., 2004; Weiergräber et al., 2006) and are probably of high importance for GABA homeostasis and excitation–inhibition balance within the CNS. Consequently, diminished GABAergic neurotransmission in the cortex results in the emergence of epileptiform activity (Jacobs and Donoghue, 1991). Besides GABA(B) receptor mediated effects, inhibitory action of GABA can basically occur via postsynaptic GABA(A) receptor stimulation, exhibiting phasic inhibition or via peri- or extrasynaptic GABA(A) receptors exerting tonic inhibition (Richerson, 2004). The tonic inhibition is based on ambient GABA probably released by GABA-transporters (Richerson and Wu, 2004). Interestingly, expression studies in cultured mouse cortical GABAergic neurons have revealed that $Ca_v2.3$ is expressed on neuronal cell bodies and proximal dendrites, but not presynaptically (Rhee et al., 1999), thus, $Ca_v2.3$ may not be directly involved in vesicular GABA release. However, its somatodendritic expression pattern points to a role in the generation of conducted Ca^{2+} action potentials and local Ca^{2+} signals, and may thereby exert indirect functions on GABA release. Its influence on

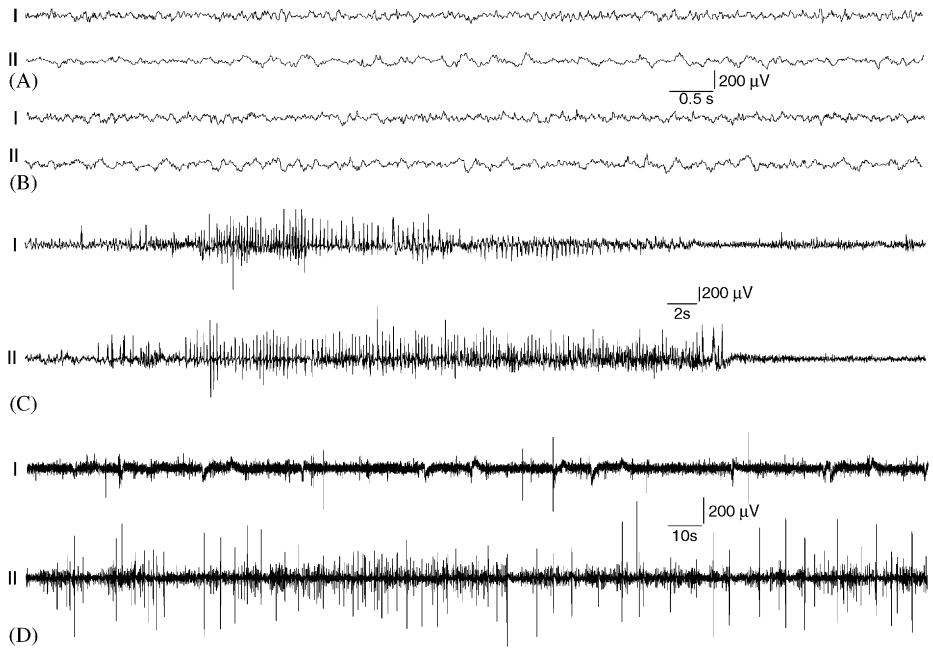

Fig. 3. Susceptibility testing and seizure architecture in $Ca_v2.3^{-/-}$ and control mice by electroencephalography. (A and B) Electrocorticographic recordings (I) and deep intrahippocampal (CA3) recordings (II) from generalized $Ca_v2.3^{-/-}$ mice ($Ca_v2.3^{fl/fl,cre+}$, BI) and brain-specific $Ca_v2.3$ inactivated animals ($Ca_v2.3^{fl/fl,nestin-cre+}$, BII) compared to controls (A). $Ca_v2.3$ inactivated mice did not exhibit any epileptiform discharges indicative of convulsive or non-convulsive seizure susceptibility. (C) Electrocorticographic characteristics following administration of pentylenetetrazol (80 mg/kg s.c.) in control mice. (CI) Generalized myoclonus characterized by continuous trains of spikes and/or spike-waves. If seizure activity exhibits maximum spread a generalized tonic-clonic event (CII) occurs causing death in most cases due to respiratory insufficiency. $Ca_v2.3^{-/-}$ mice exhibited a significant resistance to generalized tonic-clonic seizures following PTZ administration. (D) Isolated spike activity in ECoGs from $Ca_v2.3^{+/+}$ (DI) and $Ca_v2.3^{-/-}$ (DII) mice following PTZ administration. Whole body twitchings (spike activity) were shown to be significantly increased and disperse in $Ca_v2.3$ deficient mice compared to controls suggesting altered seizure architecture in $Ca_v2.3^{-/-}$ mice.

ambient GABA and tonic inhibition is to some extent speculative although astrocytes, which strongly support tonic inhibition, display a strong expression of E/R-type Ca^{2+} current (Latour et al., 2003). Expression of $Ca_v2.3$ within the reticular thalamic nucleus, which is part of the thalamocortical–corticothalamic circuitry, also suggests a functional role in non-convulsive seizure susceptibility and sleep homeostasis. The observation that $Ca_v2.3$ channels play a protective role in ischemic neuronal injury by a mechanism in which GABAergic neuronal actions are involved (Toriyama et al., 2002) further supports a functional involvement of $Ca_v2.3$ in the GABAergic neurotransmission. In addition, a number of antiepileptics, like sipatrigine, 202W92 are neuroprotective under ischemic conditions (Caputi et al., 2001; Hainsworth et al., 2003) as well as topiramate in several models of global and focal ischemia (Edmonds Jr. et al., 2001). Nevertheless, we are still lacking detailed information on $Ca_v2.3$ influence on GABA neurotransmission and thus, explanatory models for altered PTZ-seizure susceptibility remain to some extent speculative.

Recent data however, point to an even more intriguing role of $Ca_v2.3$ in epileptogenesis. In CA1 neurons, the distribution of E/R-type VGCCs is restricted to distal apical dendrites and they were shown to be involved in dendritic burst firing (Magee and Johnston, 1995b). Lately it was demonstrated that muscarinic-receptor stimulation dramatically enhances E/R-type Ca^{2+} spikes in CA1 hippocampal neurons and that enhanced E/R-type Ca^{2+} spiking plays an important role in the generation of carbachol-induced oscillations, which resemble epileptiform activity in various animal models of epilepsy (Williams and Kauer, 1997). In addition, E/R-type Ca^{2+} spikes contributed to the initiation of complex spikes during trains of action potentials which were similar to those prominent during epileptiform bursting (McCormick and Contreras, 2001). The ictogenic potential of the $Ca_v2.3$ VGCC is directly related to its basic biochemical features and complex electrophysiological modulation via G-proteins, internal Ca^{2+} and PKC, as discussed in Section 2. Recently, Metz et al. (2005) have shown that E/R-type Ca^{2+} currents underlie afterdepolarisation in CA1 neurons and are important contributors to intrinsic burst activity. This phenomenon seems to be widely spread as up to 78% of pyramidal cells in the subiculum display afterdepolarisation and burst activity. Topiramate was now found to reduce ictal-like activity based on plateau potentials in CA1 neurons through a novel inhibitory action on E/R-type Ca^{2+} channels (Kuzmiski et al., 2005) and it also protects against seizures induced by AMPA, 4-AP and PTZ (Russo et al., 2004). Interestingly, plateau potentials are not restricted to hippocampal neurons. Indeed, a plethora of other neuronal cell types exhibit this phenomenon such as suprachiasmatic neurons of the

hypothalamus (Pierson et al., 2005), spinal interneurons (Hounsgaard and Kjaerulff, 1992), dorsal horn neurons (Russo et al., 1997; Morisset and Nagy, 1999) and striatal cholinergic neurons (Dunia et al., 1996; Pisani et al., 2002) in which $Ca_v2.3$ could exert similar functions. Thus, removal of GABA(A) receptor inhibition by PTZ might trigger plateau potentials and afterdepolarisations in various brain regions and might therefore be responsible for reduced PTZ-seizure susceptibility in $Ca_v2.3^{-/-}$mice. This is further supported by the observation that GABA(A) receptor-mediated inhibition attenuates primary and secondary bursting within the hippocampus (McCormick and Contreras, 2001). Indeed, PTZ-treatment was reported to enhance cholinergic–muscarinic neurotransmission in the CA3 hippocampal area and a number of studies illustrate that potentiation of hippocampal cholinergic transmission is related to epilepsy (Meilleur et al., 2003). Therefore, cholinergic epileptogeneity is at least partly related to the $Ca_v2.3$ VGCC.

Vergara et al. (2003) also reported that NMDA and AMPA/kainate receptor stimulation can induce plateau potentials in corticostriatal slice preparations, whereas inhibition via GABA(A) receptors reduces this effect. In accordance with these findings, preliminary data also indicate that kainate seizure susceptibility is also significantly reduced in $Ca_v2.3^{-/-}$ mice (Weiergräber et al., 2006) supporting our hypothesis that $Ca_v2.3$ exhibits an outstanding function in triggering epileptiform activity. Furthermore, increased latency data and altered, fragmented seizure architecture in $Ca_v2.3^{-/-}$ mice following PTZ administration point to a critical role of $Ca_v2.3$ in the propagation of epileptic discharges and seizure generalization. Thus, our findings that $Ca_v2.3$ deficient mice exhibit reduced PTZ-seizure susceptibility, strongly support a functional role of $Ca_v2.3$ in seizure initiation and propagation (Kuzmiski et al., 2005).

Principally, idiopathic epilepsies are primarily genetic and etiologically heterogenous. Among these, monogenic channelopathies associated with epilepsy syndromes are still rare (Mulley et al., 2005) and strongly based on voltage- and ligand-gated ion channels. However, the majority of complex idiopathic epilepsies is supposed to be polygenic harboring various susceptibility gene candidates. Hyperexcitable, epileptiform neuronal activity includes triggering and initiation, perturbation/propagation as well as remission of ictal-like discharges and numerous studies have demonstrated VGCCs to be significantly involved in these processes. The fundamental basis is their intriguing proictogenic/proepileptogenic electrophysiological capacity when dysfunctioning or being dysregulated. Low-voltage activated T-type Ca^{2+} channels for example can perform low-threshold Ca^{2+} spikes and rebound burst firing in intact neuronal populations. In mouse models of epilepsy and human childhood absence epilepsy patients increased T-type Ca^{2+}-channel activity results in thalamocortical hyperoscillation and generation of spike-wave discharges. High-voltage activated L-Type channels on the other hand, harbor the capability to induce and maintain two other proictogenic electrophysiological events, plateau potentials and afterdepolarisation. As reviewed here, $Ca_v2.3$ significantly contributes to plateau potentials and afterdepolarisations as well, besides its involvement in synaptic plasticity. Though we know, that VGCCs are of functional relevance in etiology and pathogenesis of epileptiform activity and conconcomitant neurotoxicity, our knowledge on functional interaction of individual subtypes during seizure activity is still fragmented. Initiation of seizure activity might be triggered by neurotransmitters, e.g. acethylcholine via muscarinic receptors within the CA1 hippocampal region leading to a shift in Ca^{2+}-entry from P/Q-, N- and L-type Ca^{2+}-channels to the $Ca_v2.3$ R-type VGCC, now triggering epileptiform burst activity in these neurons as described above (Gahwiler and Brown, 1987; Tai et al., 2006). In contrast, the pathological burst mode of thalamic relay neurons or reticular thalamic nucleus neurons are strongly based on low-threshold Ca^{2+} spikes mediated by T-type channels. Interestingly, activation of high-voltage activated Ca^{2+}-channel via BayK8644 can force T-Type channel to inactivate and is thus capable of reducing spike-wave discharges dose-dependently, whereas consequently, L-type channel antagonists, e.g. nimodipine, facilitate spike-wave discharges (van Luijtelaar et al., 2000; Russo et al., 2004). Thus, depending on the seizure entities and neuronal cell types involved, VGCCs can exert proictogenic as well as antiictogenic effects. An all-illuminating integrative view of VGCCs in epilepsy still remains a challenging task for the future.

6. The $Ca_v2.3$ VGCC as a target in convulsive and non-convulsive seizure therapy

VGCCs represent important molecular targets for a number of antiepileptic drugs (Rogawski and Loscher, 2004; Remy and Beck, 2006). Most antiepileptic drugs described in the past were reported to inhibit low-voltage or high-voltage activated channels others than $Ca_v2.3$. However, there is increasing evidence that the $Ca_v2.3$ VGCC indeed serves as an important target in both convulsive and non-convulsive seizure therapy. Lamotrigine for example, is a broad-spectrum antiepileptic drug used to treat typical absence seizures but also Lennox-Gastaut syndrome (Matsuo, 1999; McCabe, 2000). The principle mechanism of action is the blockade of both voltage-gated sodium and calcium channels (Xie and Hagan, 1998). Within the VGCC family it targets $Ca_v2.1$- and $Ca_v2.2$ channels (Stefani et al., 1996; Wang et al., 1996), but also $Ca_v2.3$ E/R-type and T-type VGCCs (Hainsworth et al., 2003). As lamotrigine inhibits E/R-type Ca^{2+} currents rather than T-type currents, $Ca_v2.3$ is likely to be involved in the anti-absence action of lamotrigine and therefore suggests a functional involvement of $Ca_v2.3$ in the pathogenesis of absence epilepsy. Hainsworth et al. (2003) clearly demonstrated that lamotrigine (10 μM) is capable of inhibiting recombinately

expressed human $Ca_v2.3$-α1 (coexpressed with β_3) by 30% at therapeutically relevant brain concentrations (4–40 μM). In contrast, $Ca_v3.1$ and $Ca_v3.3$ exhibited only minor sensitivity to lamotrigine. Thus, given the distribution of $Ca_v2.3$ within the thalamocortical circuitry, it is likely that inhibition of E/R-type Ca^{2+} channels contributes to the anti-absence effect of lamotrigine. In addition, lamotrigine can clearly inhibit transient elevations in neuronal $[Ca^{2+}]_i$ in rat pyramidal neurons. Alterations in neuronal Ca^{2+} homeostasis are believed to play an essential role in generation and propagation of epileptiform events. Transient elevations in neuronal $[Ca^{2+}]_i$ correlate to epileptiform discharges and antagonistic effects of lamotrigine on $[Ca^{2+}]_i$ might represent the basis for its anticonvulsant efficacy and could preserve neuronal viability (Pisani et al., 2004). Besides, structurally related agents, such as sipatrigine or 202W92 also exert inhibitory effects on $Ca_v2.3$ with IC_{50} values of 10 μM (therapeutically relevant brain concentration: 20–100 μM (sipatrigine) and 56 μM (202W92). In addition, both sipatrigine and 202W92 are neuroprotective agents in animal models of ischemia (Caputi et al., 2001; Hainsworth et al., 2000) and interestingly, were shown to exert anticonvulsant effects in genetically epilepsy-prone rats and DBA/2 audiogenic mice (Hainsworth et al., 2003; Reddy et al., 1998).

Recently, McNaughton et al. (2004) revealed that carbonic anhydrase inhibitors such as ethoxyzolamide, acetazolamide and dichlorphenamide are capable of blocking the $Ca_v2.3$ E/R-type VGCC. Although carbonic anhydrase inhibitors display a variety of possible clinical applications such as induction of diuresis in congestive heart failure, reduction of ocular hypertension and relief from altitude sickness (Sun and Alkon, 2002; Supuran et al., 2003), epidemiological studies indicate that carbonic anhydrase inhibitors are also effective in patients with absence epilepsy (Sun and Alkon, 2002) and protect against provoked seizures in adults. Ethoxyzolamide application resulted in a $66 \pm 4\%$ reduction of E/R-type currents at 10 μM, whereas dichlorphenamide (10 μM), also used to treat generalized epilepsies exhibited a reduction of $24 \pm 6\%$ (McNaughton et al., 2004). Interestingly, topiramate, one of the most favoured and popular broad-spectrum antiepileptic drugs in clinic shares structural similarities, particularly the sulfonamide moiety with classical carbonic anhydrase inhibitors and also exerts residual carbonic anhydrase inhibitory activity. Previously, topiramate was reported to inhibit L-type currents (Zhang et al., 2000). Recently however, it was clearly shown in two independent publications (McNaughton et al., 2004; Kuzmiski et al., 2005) that topiramate exerts a strong inhibitory effect on $Ca_v2.3$ of $68 \pm 7\%$ at therapeutically relevant concentrations (10 μM). In addition, Kuzmiski et al. (2005) demonstrated that topiramate is capable of blocking plateau potentials in CA1 neurons of the hippocampus strongly based on its inhibitory effect on $Ca_v2.3$. These plateau potentials are of particular importance in the generation of epileptiform burst activity and blocking of $Ca_v2.3$ by topiramate is therefore involved in the decrease of sustained repetitive firing, spontaneous epileptiform burst firing and spontaneous recurrent seizures, as described previously (DeLorenzo et al., 2000). Though antiepileptic drugs, such as lamotrigine and topiramate were clearly shown to inhibit $Ca_v2.3$ in heterologous expression systems, one has to consider that they do not solely act on $Ca_v2.3$ but also a variety of other channels mediating the anticonvulsant effect.

7. Perspectives

Within the recent years, studies on the involvement of VGCCs in etiology and pathogenesis of epilepsies have mainly focused on the non-L-type $Ca_v2.1$ and the T-type $Ca_v3.2$ VGCCs. However, recent biochemical, molecular and electrophysiological findings on the cellular and whole animal level together with pharmacological analyses point to an outstanding role of the $Ca_v2.3$ E/R-type Ca^{2+} channel in epileptogenesis and seizure propagation further supported by $Ca_v2.3$ splice variant distribution throughout the brain and its biochemical regulation via muscarinic receptors, PKC and Ca^{2+}-dependent activation and inactivation processes. Its therefore plausible that mutations in $Ca_v2.3$ will turn out to be responsible for different forms of epilepsies in humans in the future. Thus, generation of new antiepileptic drugs specifically targeting $Ca_v2.3$ becomes absolutely indispensable.

Acknowledgements

The authors would like to thank Margit Henry, Ms. Claudia Zynthek and Andreas Krieger for performing injection experiments and Mrs. Renate Clemens for genotyping and mouse breeding. This work was financially supported by the Köln Fortune Program/Faculty of Medicine, University of Köln by a stipend to MAK and the Center for Molecular Medicine Cologne (CMMC) (Bundesministerium für Bildung, Wissenschaft, Forschung und Technologie, Förderkennzeichen 01 KS 9502, to TS and JH).

References

Abel, H.J., Lee, J.C., Callaway, J.C., Foehring, R.C., 2004. Relationships between intracellular calcium and afterhyperpolarizations in neocortical pyramidal neurons. Journal of Neurophysiology 91, 324–335.

Albowitz, B., Konig, P., Kuhnt, U., 1997. Spatiotemporal distribution of intracellular calcium transients during epileptiform activity in guinea pig hippocampal slices. Journal of Neurophysiology 77, 491–501.

Andres, M., Andre, V.M., Nguyen, S., Salamon, N., Cepeda, C., Levine, M.S., Leite, J.P., Neder, L., Vinters, H.V., Mathern, G.W., 2005. Human cortical dysplasia and epilepsy: an ontogenetic hypothesis based on volumetric MRI and NeuN neuronal density and size measurements. Cerebral Cortex 15, 194–210.

Andrew, R.D., 1987. Endogenous bursting by rat supraoptic neuroendocrine cells is calcium dependent. Journal of Physiology 384, 451–465.

Andrew, R.D., Dudek, F.E., 1983. Burst discharge in mammalian neuroendocrine cells involves an intrinsic regenerative mechanism. Science 221, 1050–1052.

Andrew, R.D., Dudek, F.E., 1984. Analysis of intracellularly recorded phasic bursting by mammalian neuroendocrine cells. Journal of Neurophysiology 51, 552–566.

Bannister, R.A., Melliti, K., Adams, B.A., 2004. Differential Modulation of $Ca_v2.3$ Ca^{2+} Channels by G{alpha}q/11-Coupled Muscarinic Receptors. Molecular Pharmacology 65, 381–388.

Barclay, J., Balaguero, N., Mione, M., Ackerman, S.L., Letts, V.A., Brodbeck, J., Canti, C., Meir, A., Page, K.M., Kusumi, K., Perez-Reyes, E., Lander, E.S., Frankel, W.N., Gardiner, R.M., Dolphin, A.C., Rees, M., 2001. Ducky mouse phenotype of epilepsy and ataxia is associated with mutations in the *Cacna2d2* gene and decreased calcium channel current in cerebellar Purkinje cells. Journal of Neuroscience 21, 6095–6104.

Bech-Hansen, N.T., Naylor, M.J., Maybaum, T.A., Pearce, W.G., Koop, B., Fishman, G.A., Mets, M., Musarella, M.A., cott, K.M., 1998. Loss-of-function mutations in a calcium-channel α1-subunit gene in Xp11.23 cause incomplete X-linked congenital stationary night blindness. Nature Genetics 19, 264–267.

Beck, H., Steffens, R., Elger, C.E., Heinemann, U., 1998. Voltage-dependent Ca^{2+} currents in epilepsy. Epilepsy Research 32, 321–332.

Berg, M., Bruhn, T., Frandsen, A., Schousboe, A., Diemer, N.H., 1995. Kainic acid-induced seizures and brain damage in the rat: role of calcium homeostasis. Journal of Neuroscience Research 40, 641–646.

Bers, D.M., 2002. Cardiac excitation–contraction coupling. Nature 415, 198–205.

Bito, H., Deisseroth, K., Tsien, R.W., 1997. Ca^{2+}-dependent regulation in neuronal gene expression. Current Opinion in Neurobiology 7, 419–429.

Blumenfeld, H., McCormick, D.A., 2000. Corticothalamic inputs control the pattern of activity generated in thalamocortical networks. Journal of Neuroscience 20, 5153–5162.

Brenowitz, S.D., Regehr, W.G., 2003. "Resistant" channels reluctantly reveal their roles. Neuron 39, 391–394.

Breustedt, J., Vogt, K.E., Miller, R.J., Nicoll, R.A., Schmitz, D., 2003. Alpha1E-containing Ca^{2+} channels are involved in synaptic plasticity. Proceedings of the National Academy of Sciences of the United States of America 100, 12450–12455.

Brill, J., Klocke, R., Paul, D., Boison, D., Gouder, N., Klugbauer, N., Hofmann, F., Becker, C.M., Becker, K., 2003. Entla: a novel epileptic and ataxic Cacna2d2 mutant of the mouse. Journal of Biological Chemistry.

Burgess, D.L., Noebels, J.L., 1999. Single gene defects in mice: the role of voltage-dependent calcium channels in absence models. Epilepsy Research 36, 111–122.

Burgess, D.L., Jones, J.M., Meisler, M.H., Noebels, J.L., 1997. Mutation of the Ca^{2+} channel beta subunit gene Cchb4 is associated with ataxia and seizures in the lethargic (lh) mouse. Cell 88, 385–392.

Caputi, L., Hainsworth, A.H., Lavaroni, F., Leach, M.J., McNaughton, N.C., Mercuri, N.B., Randall, A.D., Spadoni, F., Swan, J.H., Stefani, A., 2001. Neuroprotective actions in vivo and electrophysiological actions in vitro of 202W92. Brain Research 919, 259–268.

Catterall, W.A., 1999. Interactions of presynaptic Ca^{2+} channels and snare proteins in neurotransmitter release. Annals of the New York Academy of Sciences 868, 144–159.

Catterall, W.A., 2000. Structure and regulation of voltage-gated Ca^{2+} channels. Annual Review of Cell and Developmental Biology 16, 521–555.

Chen, S., Ren, Y.Q., Bing, R.J., Hillman, D.E., 2000. Alpha1E subunit of the R-type calcium channel is associated with myelinogenesis. Journal of Neurocytology 29, 719–728.

Chen, Y., Lu, J., Pan, H., Zhang, Y., Wu, H., Xu, K., Liu, X., Jiang, Y., Bao, X., Yao, Z., Ding, K., Lo, W.H., Qiang, B., Chan, P., Shen, Y., Wu, X., 2003. Association between genetic variation of CACNA1 H and childhood absence epilepsy. Annals of Neurology 54, 239–243.

Clapham, D.E., 1997. Some like it hot: spicing up ion channels. Nature 389, 783–784.

Cloues, R.K., Sather, W.A., 2003. Afterhyperpolarization regulates firing rate in neurons of the suprachiasmatic nucleus. Journal of Neuroscience 23, 1593–1604.

Curia, G., Aracri, P., Sancini, G., Mantegazza, M., Avanzini, G., Franceschetti, S., 2004. Protein-kinase C-dependent phosphorylation inhibits the effect of the antiepileptic drug topiramate on the persistent fraction of sodium currents. Neuroscience 127, 63–68.

Day, N.C., Shaw, P.J., McCormack, A.L., Craig, P.J., Smith, W., Beattie, R., Williams, T.L., Ellis, S.B., Ince, P.G., Harpold, M.M., Lodge, D., Volsen, S.G., 1996. Distribution of α 1A, α 1B AND α 1E voltage-dependent calcium channel subunits in the human hippocampus and parahippocampal gyrus. Neuroscience 71, 1013–1024.

Day, N.C., Wood, S.J., Ince, P.G., Volsen, S.G., Smith, W., Slater, C.R., Shaw, P.J., 1997. Differential localization of voltage-dependent calcium channel α_1 subunits at the human and rat neuromuscular junction. Journal of Neuroscience 17, 6226–6235.

De Borman, B., Lakaye, B., Minet, A., Zorzi, W., Vergnes, M., Marescaux, C., Grisar, T., 1999. Expression of mRNA encoding alpha1E and alpha1G subunit in the brain of a rat model of absence epilepsy. Neuroreport 10, 569–574.

DeLorenzo, R.J., Pal, S., Sombati, S., 1998. Prolonged activation of the N-methyl-D-aspartate receptor-Ca^{2+} transduction pathway causes spontaneous recurrent epileptiform discharges in hippocampal neurons in culture. Proceedings of the National Academy of Sciences of the United States of America 95, 14482–14487.

DeLorenzo, R.J., Sombati, S., Coulter, D.A., 2000. Effects of topiramate on sustained repetitive firing and spontaneous recurrent seizure discharges in cultured hippocampal neurons. Epilepsia 41 (Suppl. 1), S40–S44.

Deransart, C., Landwehrmeyer, G.B., Feuerstein, T.J., Lucking, C.H., 2001. Up-regulation of D3 dopaminergic receptor mRNA in the core of the nucleus accumbens accompanies the development of seizures in a genetic model of absence-epilepsy in the rat. Brain Research Molecular Brain Research 94, 166–177.

De Waard, M., Campbell, K.P., 1995. Subunit regulation of the neuronal a_{1A} Ca^{2+} channel expressed in *Xenopus* oocytes. Journal of Physiology (London) 485, 619–634.

De Waard, M., Liu, H., Walker, D., Scott, V.E.S., Gurnett, C.A., Campbell, K.P., 1997. Direct binding of G-protein β gamma complex to voltage-dependent calcium channels. Nature 385, 446–450.

Dietrich, D., Kirschstein, T., Kukley, M., Pereverzev, A., von der Brelie, C., Schneider, T., Beck, H., 2003. Functional specialization of presynaptic $Ca_v2.3$ Ca^{2+} channels. Neuron 39, 483–496.

Doering, C.J., Kisilevsky, A.E., Feng, Z.P., Arnot, M.I., Peloquin, J., Hamid, J., Barr, W., Nirdosh, A., Simms, B., Winkfein, R.J., Zamponi, G.W., 2004. A single Gbeta subunit locus controls cross-talk between protein kinase C and G protein regulation of N-type calcium channels. Journal of Biological Chemistry 279, 29709–29717.

Dolphin, A.C., 2003a. Beta subunits of voltage-gated calcium channels. Journal of Bioenergetics and Biomembranes 35, 599–620.

Dolphin, A.C., 2003b. G protein modulation of voltage-gated calcium channels. Pharmacological Reviews 55, 607–627.

Dunia, R., Buckwalter, G., Defazio, T., Villar, F.D., McNeill, T.H., Walsh, J.P., 1996. Decreased duration of Ca^{2+}-mediated plateau potentials in striatal neurons from aged rats. Journal of Neurophysiology 76, 2353–2363.

Dzhura, I., Wu, Y., Colbran, R.J., Balser, J.R., Anderson, M.E., 2000. Calmodulin kinase determines calcium-dependent facilitation of L-type calcium channels. Nature Cell Biology 2, 173–177.

Edmonds Jr., H.L., Jiang, Y.D., Zhang, P.Y., Shank, R., 2001. Topiramate as a neuroprotectant in a rat model of global ischemia-induced neurodegeneration. Life Sciences 69, 2265–2277.

Fanelli, R.J., McCarthy, R.T., Chisholm, J., 1994. Neuropharmacology of nimodipine: from single channels to behavior. Annals of the New York Academy of Sciences 747, 336–350.

Filakovszky, J., Gerber, K., Bagdy, G., 1999. A serotonin-1A receptor agonist and an *N*-methyl-D-aspartate receptor antagonist oppose each

others effects in a genetic rat epilepsy model. Neuroscience Letters 261, 89–92.

Fletcher, C.F., Lutz, C.M., O'Sullivan, T.N., Shaughnessy Jr., J.D., Hawkes, R., Frankel, W.N., Copeland, N.G., Jenkins, N.A., 1996. Absence epilepsy in tottering mutant mice is associated with calcium channel defects. Cell 87, 607–617.

Forsgren, L., Beghi, E., Oun, A., Sillanpaa, M., 2005. The epidemiology of epilepsy in Europe—a systematic review. European Journal of Neurology 12, 245–253.

Fraser, D.D., MacVicar, B.A., 1996. Cholinergic-dependent plateau potential in hippocampal CA1 pyramidal neurons. Journal of Neuroscience 16, 4113–4128.

Fraser, D.D., Doll, D., MacVicar, B.A., 2001. Serine/threonine protein phosphatases and synaptic inhibition regulate the expression of cholinergic-dependent plateau potentials. Journal of Neurophysiology 85, 1197–1205.

Gahwiler, B.H., Brown, D.A., 1987. Muscarine affects calcium-currents in rat hippocampal pyramidal cells in vitro. Neuroscience Letters 76, 301–306.

Gao, B.N., Sekido, Y., Maximov, A., Saad, M., Forgacs, E., Latif, F., Wei, M.H., Lerman, M., Lee, J.H., Perez-Reyes, E., Bezprozvanny, I., Minna, J.D., 2000. Functional properties of a new voltage-dependent calcium channel $\alpha_2\delta$ auxiliary subunit gene (CACNA2D2). Journal of Biological Chemistry 275, 12237–12242.

Gibbs III, J.W., Zhang, Y.F., Ahmed, H.S., Coulter, D.A., 2002. Anticonvulsant actions of lamotrigine on spontaneous thalamocortical rhythms. Epilepsia 43, 342–349.

Gibney, G.T., Zhang, J.H., Douglas, R.M., Haddad, G.G., Xia, Y., 2002. Na^+/Ca^{2+} exchanger expression in the developing rat cortex. Neuroscience 112, 65–73.

Gomora, J.C., Daud, A.N., Weiergräber, M., Perez-Reyes, E., 2001. Block of cloned human T-type calcium channels by succinimide antiepileptic drugs. Molecular Pharmacology 60, 1121–1132.

Grabsch, H., Pereverzev, A., Weiergräber, M., Schramm, M., Henry, M., Vajna, R., Beattie, R.E., Volsen, S.G., Klöckner, U., Hescheler, J., Schneider, T., 1999. Immunohistochemical detection of α1E voltage-gated Ca^{2+} channel isoforms in cerebellum, INS-1 cells, and neuroendocrine cells of the digestive system. Journal of Histochemistry & Cytochemistry 47, 981–993.

Hainsworth, A.H., Stefani, A., Calabresi, P., Smith, T.W., Leach, M.J., 2000. Sipatrigine (BW 619C89) is a neuroprotective agent and a sodium channel and calcium channel inhibitor. CNS Drug Reviews 6, 111–134.

Hainsworth, A.H., McNaughton, N.C., Pereverzev, A., Schneider, T., Randall, A.D., 2003. Actions of sipatrigine, 202W92 and lamotrigine on R-type and T-type Ca^{2+} channel currents. European Journal of Pharmacology 467, 77–80.

Hamilton, S.E., Loose, M.D., Qi, M., Levey, A.I., Hille, B., McKnight, G.S., Idzerda, R.L., Nathanson, N.M., 1997. Disruption of the m1 receptor gene ablates muscarinic receptor- dependent M current regulation and seizure activity in mice. Proceedings of the National Academy of Sciences of the United States of America 94, 13311–13316.

Hamon, B., Heinemann, U., 1986. Effects of GABA and bicuculline on *N*-methyl-D-aspartate- and quisqualate-induced reductions in extracellular free calcium in area CA1 of the hippocampal slice. Experimental Brain Research 64, 27–36.

Hanson, J.E., Smith, Y., 2002. Subcellular distribution of high-voltage-activated calcium channel subtypes in rat globus pallidus neurons. Journal of Comparative Neurology 442, 89–98.

Helmchen, F., Svoboda, K., Denk, W., Tank, D.W., 1999. In vivo dendritic calcium dynamics in deep-layer cortical pyramidal neurons. Nature Neuroscience 2, 989–996.

Hendriksen, H., Kamphuis, W., Lopes da Silva, F.H., 1997. Changes in voltage-dependent calcium channel alpha1-subunit mRNA levels in the kindling model of epileptogenesis. Molecular Brain Research 50, 257–266.

Herlitze, S., Garcia, D.E., Mackie, K., Hille, B., Scheuer, T., Catterall, W.A., 1996. Modulation of Ca^{2+} channels by G-protein βgamma subunits. Nature 380, 258–262.

Hernandez-Lopez, S., Bargas, J., Surmeier, D.J., Reyes, A., Galarraga, E., 1997. D1 receptor activation enhances evoked discharge in neostriatal medium spiny neurons by modulating an L-type Ca^{2+} conductance. Journal of Neuroscience 17, 3334–3342.

Hernandez-Lopez, S., Tkatch, T., Perez-Garci, E., Galarraga, E., Bargas, J., Hamm, H., Surmeier, D.J., 2000. D2 dopamine receptors in striatal medium spiny neurons reduce L-type Ca^{2+} currents and excitability via a novel PLC[beta]1-IP3-calcineurin-signaling cascade. Journal of Neuroscience 20, 8987–8995.

Hlubek, M.D., Cobbett, P., 2000. Differential effects of K^+ channel blockers on frequency-dependent action potential broadening in supraoptic neurons. Brain Research Bulletin 53, 203–209.

Hofmann, F., Lacinova, L., Klugbauer, N., 1999. Voltage-dependent calcium channels: from structure to function. Reviews of Physiology Biochemistry and Pharmacology 139, 33–87.

Hounsgaard, J., Kiehn, O., 1989. Serotonin-induced bistability of turtle motoneurones caused by a nifedipine-sensitive calcium plateau potential. Journal of Physiology 414, 265–282.

Hounsgaard, J., Kjaerulff, O., 1992. Ca^{2+}-mediated plateau potentials in a subpopulation of interneurons in the ventral horn of the turtle spinal cord. European Journal of Neuroscience 4, 183–188.

Ikeda, S.R., 1996. Voltage-dependent modulation of N-type calcium channels by G-proteins $\beta\tau$ subunits. Nature 380, 255–258.

Ishiguro, M., Wellman, T.L., Honda, A., Russell, S.R., Tranmer, B.I., Wellman, G.C., 2005. Emergence of a R-type Ca^{2+} channel (CaV 2.3) contributes to cerebral artery constriction after subarachnoid hemorrhage. Circulation Research 96, 419–426.

Jacobs, K.M., Donoghue, J.P., 1991. Reshaping the cortical motor map by unmasking latent intracortical connections. Science 251, 944–947.

Jing, X., Li, D.Q., Olofsson, C.S., Salehi, A., Surve, V.V., Caballero, J., Ivarsson, R., Lundquist, I., Pereverzev, A., Schneider, T., Rorsman, P., Renstrom, E., 2005. $Ca_v2.3$ calcium channels control second-phase insulin release. Journal of Clinical Investigation 115, 146–154.

Jun, K., Piedras-Renteria, E.S., Smith, S.M., Wheeler, D.B., Lee, S.B., Lee, T.G., Chin, H.M., Adams, M.E., Scheller, R.H., Tsien, R.W., Shin, H.S., 1999. Ablation of P/Q-type Ca^{2+} channel currents, altered synaptic transmission, and progressive ataxia in mice lacking the α_{1A}-subunit. Proceedings of the National Academy of Sciences of the United States of America 96, 15245–15250.

Kamp, M.A., Krieger, A., Henry, M., Hescheler, J., Weiergraber, M., Schneider, T., 2005. Presynaptic '$Ca_v2.3$-containing' E-type Ca channels share dual roles during neurotransmitter release. European Journal of Neuroscience 21, 1617–1625.

Kang, T.C., Kim, D.S., Yoo, K.Y., Hwang, I.K., Kwak, S.E., Kim, J.E., Jung, J.Y., Won, M.H., Suh, J.G., Oh, Y.S., 2004. Elevated voltage-gated Ca^{2+} channel immunoreactivities in the hippocampus of seizure-prone gerbil. Brain Research 1029, 168–178.

Kannurpatti, S.S., Joshi, P.G., Joshi, N.B., 2000. Calcium sequestering ability of mitochondria modulates influx of calcium through glutamate receptor channel. Neurochemical Research 25, 1527–1536.

Kim, D., Song, I., Keum, S., Lee, T., Jeong, M.J., Kim, S.S., McEnery, M.W., Shin, H.S., 2001. Lack of the burst firing of thalamocortical relay neurons and resistance to absence seizures in mice lacking alpha1G T-type Ca^{2+} channels. Neuron 31, 35–45.

Klöckner, U., Pereverzev, A., Leroy, J., Krieger, A., Vajna, R., Hescheler, J., Pfitzer, G., Malecot, C.O., Schneider, T., 2004. The cytosolic II–III loop of $Ca_v2.3$ provides an essential determinant for the phorbol ester-mediated stimulation of E-type Ca^{2+} channel activity. European Journal of Neuroscience 19, 2659–2668.

Koschak, A., Reimer, D., Huber, I., Grabner, M., Glossmann, H., Engel, J., Striessnig, J., 2001. α1D ($Ca_v1.3$) subunits can form L-type Ca^{2+} channels activating at negative voltages. Journal of Biological Chemistry 276, 22100–22106.

Krieger, A., Radhakrishnan, K., Pereverzev, A., Siapich, S.A., Banat, M., Kamp, M.A., Leroy, J., Klockner, U., Hescheler, J., Weiergraber, M.,

Schneider, T., 2006. The molecular chaperone hsp70 interacts with the cytosolic II–III loop of the $Ca_v2.3$ E-type voltagegated Ca^{2+} channel. Cell Physiology and Biochemistry 17, 97–110.

Kullmann, D.M., 2002. The neuronal channelopathies. Brain 125, 1177–1195.

Kuzmiski, J.B., MacVicar, B.A., 2001. Cyclic nucleotide-gated channels contribute to the cholinergic plateau potential in hippocampal CA1 pyramidal neurons. Journal of Neuroscience 21, 8707–8714.

Kuzmiski, J.B., Barr, W., Zamponi, G.W., MacVicar, B.A., 2005. Topiramate inhibits the initiation of plateau potentials in CA1 neurons by depressing R-type calcium channels. Epilepsia 46, 481–489.

Lacinova, L., 2005. Voltage-dependent calcium channels. General Physiology and Biophysics 24 (Suppl. 1), 1–78.

Lakaye, B., Thomas, E., Minet, A., Grisar, T., 2002. The genetic absence epilepsy rat from Strasbourg (GAERS), a rat model of absence epilepsy: computer modeling and differential gene expression. Epilepsia 43 (Suppl. 5), 123–129.

LaRoche, S.M., Helmers, S.L., 2004. The new antiepileptic drugs: scientific review. JAMA 291, 605–614.

Latour, I., Hamid, J., Beedle, A.M., Zamponi, G.W., MacVicar, B.A., 2003. Expression of voltage-gated Ca^{2+} channel subtypes in cultured astrocytes. GLIA 41, 347–353.

Lee, S.C., Choi, S., Lee, T., Kim, H.L., Chin, H., Shin, H.S., 2002. Molecular basis of R-type calcium channels in central amygdala neurons of the mouse. Proceedings of the National Academy of Sciences of the United States of America 99, 3276–3281.

Lee, J., Kim, D., Shin, H.S., 2004. Lack of delta waves and sleep disturbances during non-rapid eye movement sleep in mice lacking alpha1G-subunit of T-type calcium channels. Proceedings of the National Academy of Sciences of the United States of America 101, 18195–18199.

Lehmann-Horn, F., Jurkat-Rott, K., 1999. Voltage-gated ion channels and hereditary disease. Physiological Reviews 79, 1317–1372.

Leroy, J., Pereverzev, A., Vajna, R., Qin, N., Pfitzer, G., Hescheler, J., Malécot, C.O., Schneider, T., Klöckner, U., 2003. Ca^{2+}-sensitive regulation of E-type Ca^{2+} channel activity depends on an arginine rich region in the cytosolic II–III loop. European Journal of Neuroscience 18, 841–855.

Letts, V.A., Felix, R., Biddlecome, G.H., Arikkath, J., Mahaffey, C.L., Valenzuela, A., Bartlett II, F.S., Mori, Y., Campbell, K.P., Frankel, W.N., 1998. The mouse stargazer gene encodes a neuronal Ca^{2+}-channel gamma subunit. Nature Genetics 19, 340–347.

Levey, A.I., Edmunds, S.M., Koliatsos, V., Wiley, R.G., Heilman, C.J., 1995. Expression of m1–m4 muscarinic acetylcholine receptor proteins in rat hippocampus and regulation by cholinergic innervation. Journal of Neuroscience 15, 4077–4092.

Li, Y., Bennett, D.J., 2003. Persistent sodium and calcium currents cause plateau potentials in motoneurons of chronic spinal rats. Journal of Neurophysiology 90, 857–869.

Liang, H., DeMaria, C.D., Erickson, M.G., Mori, M.X., Alseikhan, B.A., Yue, D.T., 2003. Unified mechanisms of Ca^{2+} regulation across the Ca^{2+} channel family. Neuron 39, 951–960.

Lipkind, G.M., Fozzard, H.A., 2003. Molecular modeling of interactions of dihydropyridines and phenylalkylamines with the inner pore of the L-type Ca^{2+} channel. Molecular Pharmacology 63, 499–511.

Lothman, E.W., Bertram III, E.H., Stringer, J.L., 1991. Functional anatomy of hippocampal seizures. Progress in Neurobiology 37, 1–82.

Lu, Z.J., Pereverzev, A., Liu, H.L., Weiergraber, M., Henry, M., Krieger, A., Smyth, N., Hescheler, J., Schneider, T., 2004. Arrhythmia in isolated prenatal hearts after ablation of the $Ca_v2.3$ (alpha1E) subunit of voltage-gated Ca^{2+} channels. Cell Physiology and Biochemistry 14, 11–22.

Magee, J.C., Johnston, D., 1995a. Characterization of single voltage-gated Na^+ and Ca^{2+} channels in apical dendrites of rat CA1 pyramidal neurons. Journal of Physiology (London) 487, 67–90.

Magee, J.C., Johnston, D., 1995b. Synaptic activation of voltage-gated channels in the dendrites of hippocampal pyramidal neurons. Science 268, 301–304.

Manning, J.P., Richards, D.A., Bowery, N.G., 2003. Pharmacology of absence epilepsy. Trends in Pharmacological Sciences 24, 542–549.

Markram, H., Helm, P.J., Sakmann, B., 1995. Dendritic calcium transients evoked by single back-propagating action potentials in rat neocortical pyramidal neurons. Journal of Physiology 485 (Pt1), 1–20.

Matsuo, F., 1999. Lamotrigine. Epilepsia 40 (Suppl. 5), S30–S36.

McCabe, P.H., 2000. New anti-epileptic drugs for the 21st century. Expert Opinion on Pharmacotherapy 1, 633–674.

McCarthy, R.T., TanPiengco, P.E., 1992. Multiple types of high-threshold calcium channels in rabbit sensory neurons: high-affinity block of neuronal L-type by nimodipine. Journal of Neuroscience 12, 2225–2234.

McCormick, D.A., Contreras, D., 2001. On the cellular and network bases of epileptic seizures. Annual Review of Physiology 63, 815–846.

McNaughton, N.C., Davies, C.H., Randall, A., 2004. Inhibition of alpha1E Ca^{2+} channels by carbonic anhydrase inhibitors. Journal of Pharmacological Sciences 95, 240–247.

Meilleur, S., Aznavour, N., Descarries, L., Carmant, L., Mamer, O.A., Psarropoulou, C., 2003. Pentylenetetrazol-induced seizures in immature rats provoke long-term changes in adult hippocampal cholinergic excitability. Epilepsia 44, 507–517.

Melliti, K., Meza, U., Adams, B., 2000. Muscarinic stimulation of α1E Ca channels is selectively blocked by the effector antagonist function of RGS2 and phsopholipase C-β1. Journal of Neuroscience 20, 7167–7173.

Metz, A.E., Jarsky, T., Martina, M., Spruston, N., 2005. R-type calcium channels contribute to afterdepolarization and bursting in hippocampal CA1 pyramidal neurons. Journal of Neuroscience 25, 5763–5773.

Meza, U., Bannister, R., Melliti, K., Adams, B., 1999. Biphasic, opposing modulation of cloned neuronal α1E Ca channels by distinct signaling pathways coupled to m2 muscarinic acetylcholine receptors. Journal of Neuroscience 19, 6806–6817.

Michna, M., Knirsch, M., Hoda, J.C., Muenkner, S., Langer, P., Platzer, J., Striessnig, J., Engel, J., 2003. $Ca_v1.3$ (alpha1D) Ca^{2+} currents in neonatal outer hair cells of mice. Journal of Physiology 553, 747–758.

Mills, J.D., Pitman, R.M., 1997. Electrical properties of a cockroach motor neuron soma depend on different characteristics of individual Ca components. Journal of Neurophysiology 78, 2455–2466.

Missiaen, L., Robberecht, W., Van Den Bosch, L., Callewaert, G., Parys, J.B., Wuytack, F., Raeymaekers, L., Nilius, B., Eggermont, J., De Smedt, H., 2000. Abnormal intracellular Ca^{2+} homeostasis and disease. Cell Calcium 28, 1–21.

Mori, Y., Wakamori, M., Oda, S., Fletcher, C.F., Sekiguchi, N., Mori, E., Copeland, N.G., Jenkins, N.A., Matsushita, K., Matsuyama, Z., Imoto, K., 2000. Reduced voltage sensitivity of activation of P/Q-type Ca^{2+} channels is associated with the ataxic mouse mutation rolling nagoya (tg^{rol}). Jounal of Neuroscience 20, 5654–5662.

Morisset, V., Nagy, F., 1999. Ionic basis for plateau potentials in deep dorsal horn neurons of the rat spinal cord. Journal of Neuroscience 19, 7309–7316.

Mulley, J.C., Scheffer, I.E., Harkin, L.A., Berkovic, S.F., Dibbens, L.M., 2005. Susceptibility genes for complex epilepsy. Human Molecular Genetics 14, R243–R249.

Nahm, S.S., Jung, K.Y., Enger, M.K., Griffith, W.H., Abbott, L.C., 2005. Differential expression of T-type calcium channels in P/Q-type calcium channel mutant mice with ataxia and absence epilepsy. Journal of Neurobiology 62, 352–360.

Newcomb, R., Szoke, B., Palma, A., Wang, G., Chen, X.H., Hopkins, W., Cong, R., Miller, J., Urge, L., Tarczy-Hornoch, K., Loo, J.A., Dooley, D.J., Nadasdi, L., Tsien, R.W., Lemos, J., Miljanich, G., 1998. Selective peptide antagonist of the class E calcium channel from the venom of the tarantula *Hysterocrates gigas*. Biochemistry 37, 15353–15362.

Palmieri, C., Kawasaki, H., Avoli, M., 2000. Topiramate depresses carbachol-induced plateau potentials in subicular bursting cells. Neuroreport 11, 75–78.

Pereverzev, A., Leroy, J., Krieger, A., Malecot, C.O., Hescheler, J., Pfitzer, G., Klockner, U., Schneider, T., 2002. Alternate splicing in the

cytosolic II-III loop and the carboxy terminus of human E-type voltage-gated Ca^{2+} channels: electrophysiological characterization of isoforms. Molecular and Cellular Neuroscience 21, 352–365.

Pereverzev, A., Salehi, A., Mikhna, M., Renstrom, E., Hescheler, J., Weiergraber, M., Smyth, N., Schneider, T., 2005. The ablation of the $Ca_v2.3$/E-type voltage-gated Ca^{2+} channel causes a mild phenotype despite an altered glucose induced glucagon response in isolated islets of Langerhans. European Journal of Pharmacology 511, 65–72.

Perez-Reyes, E., 2003. Molecular physiology of low-voltage-activated T-type calcium channels. Physiological Reviews 83, 117–161.

Peterson, B.Z., Johnson, B.D., Hockerman, G.H., Acheson, M., Scheuer, T., Catterall, W.A., 1997. Analysis of the dihydropyridine receptor site of L-type calcium channels by alanine-scanning mutagenesis. Journal of Biological Chemistry 272, 18752–18758.

Pierson, P.M., Liu, X., Raggenbass, M., 2005. Suppression of potassium channels elicits calcium-dependent plateau potentials in suprachiasmatic neurons of the rat. Brain Research 1036, 50–59.

Pietrobon, D., 2005. Function and dysfunction of synaptic calcium channels: insights from mouse models. Current Opinion in Neurobiology 15, 257–265.

Pinto, A., Gillard, S., Moss, F., Whyte, K., Brust, P., Williams, M., Stauderman, K., Harpold, M., Lang, B., Newsom-Davis, J., Bleakman, D., Lodge, D., Boot, J., 1998. Human autoantibodies specific for the α_{1A} calcium channel subunit reduce both P-type and Q-type calcium currents in cerebellar neurons. Proceedings of the National Academy of Sciences of the United States of America 95, 8328–8333.

Pisani, A., Bonsi, P., Catania, M.V., Giuffrida, R., Morari, M., Marti, M., Centonze, D., Bernardi, G., Kingston, A.E., Calabresi, P., 2002. Metabotropic glutamate 2 receptors modulate synaptic inputs and calcium signals in striatal cholinergic interneurons. Journal of Neuroscience 22, 6176–6185.

Pisani, A., Bonsi, P., Martella, G., De Persis, C., Costa, C., Pisani, F., Bernardi, G., Calabresi, P., 2004. Intracellular calcium increase in epileptiform activity: modulation by levetiracetam and lamotrigine. Epilepsia 45, 719–728.

Puranam, R.S., McNamara, J.O., 1999. Seizure disorder in mutant mice: relevance to human epilepsies. Current Opinion in Neurobiology 9, 281–287.

Qian, J., Noebels, J.L., 2001. Presynaptic Ca^{2+} channels and neurotransmitter release at the terminal of a mouse cortical neuron. Journal of Neuroscience 21, 3721–3728.

Qian, J., Noebels, J.L., 2003. Topiramate alters excitatory synaptic transmission in mouse hippocampus. Epilepsy Research 55, 225–233.

Reddy, N.L., Fan, W., Magar, S.S., Perlman, M.E., Yost, E., Zhang, L., Berlove, D., Fischer, J.B., Burke-Howie, K., Wolcott, T., Durant, G.J., 1998. Synthesis and pharmacological evaluation of *N,N′*-diarylguanidines as potent sodium channel blockers and anticonvulsant agents. Journal of Medicinal Chemistry 41, 3298–3302.

Remy, S., Beck, H., 2006. Molecular and cellular mechanisms of pharmacoresistance in epilepsy. Brain 129, 18–35.

Rhee, J.S., Ishibashi, H., Akaike, N., 1999. Calcium channels in the GABAergic presynaptic nerve terminals projecting to Meynert neurons of the rat. Journal of Neurochemistry 72, 800–807.

Richerson, G.B., 2004. Looking for GABA in all the wrong places: the relevance of extrasynaptic GABA(A) receptors to epilepsy. Epilepsy Currents 4, 239–242.

Richerson, G.B., Wu, Y., 2004. Role of the GABA transporter in epilepsy. Advances in Experimental Medicine and Biology 548, 76–91.

Rogawski, M.A., Loscher, W., 2004. The neurobiology of antiepileptic drugs. Nature Reviews Neuroscience 5, 553–564.

Roper, P., Callaway, J., Shevchenko, T., Teruyama, R., Armstrong, W., 2003. AHP's, HAP's and DAP's: how potassium currents regulate the excitability of rat supraoptic neurones. Journal of Computational Neuroscience 15, 367–389.

Russo, R.E., Nagy, F., Hounsgaard, J., 1997. Modulation of plateau properties in dorsal horn neurones in a slice preparation of the turtle spinal cord. Journal of Physiology 499 (Pt. 2), 459–474.

Russo, E., Constanti, A., Ferreri, G., Citraro, R., De Sarro, G., 2004. Nifedipine affects the anticonvulsant activity of topiramate in various animal models of epilepsy. Neuropharmacology 46, 865–878.

Saegusa, H., Kurihara, T., Zong, S.Q., Minowa, O., Kazuno, A.A., Han, W.H., Matsuda, Y., Yamanaka, H., Osanai, M., Noda, T., Tanabe, T., 2000. Altered pain responses in mice lacking α_{1E} subunit of the voltage-dependent Ca^{2+} channel. Proceedings of the National Academy of Sciences of the United States of America 97, 6132–6137.

Sakata, Y., Saegusa, H., Zong, S.Q., Osanai, M., Murakoshi, T., Shimizu, Y., Noda, T., Aso, T., Tanabe, T., 2002. $Ca_v2.3$ (α_{1E}) Ca^{2+} channel participates in the control of sperm function. FEBS Letters 516, 229–233.

Sandoz, G., Lopez-Gonzalez, I., Grunwald, D., Bichet, D., Altafaj, X., Weiss, N., Ronjat, M., Dupuis, A., De Waard, M., 2004. Ca_vbeta-subunit displacement is a key step to induce the reluctant state of P/Q calcium channels by direct G protein regulation. Proceedings of the National Academy of Sciences of the United States of America 101, 6267–6272.

Sills, G.J., 2006. The mechanisms of action of gabapentin and pregabalin. Current Opinion in Pharmacology 6, 108–113.

Simon, M., Perrier, J.F., Hounsgaard, J., 2003. Subcellular distribution of L-type Ca^{2+} channels responsible for plateau potentials in motoneurons from the lumbar spinal cord of the turtle. European Journal of Neuroscience 18, 258–266.

Sochivko, D., Pereverzev, A., Smyth, N., Gissel, C., Schneider, T., Beck, H., 2002. The α1E calcium channel subunit underlies R-type calcium current in hippocampal and cortical pyramidal neurons. Journal of Physiology 542, 699–710.

Song, I., Kim, D., Choi, S., Sun, M., Kim, Y., Shin, H.S., 2004. Role of the alpha1G T-type calcium channel in spontaneous absence seizures in mutant mice. Journal of Neuroscience 24, 5249–5257.

Soong, T.W., Stea, A., Hodson, C.D., Dubel, S.J., Vincent, S.R., Snutch, T.P., 1993. Structure and functional expression of a member of the low voltage-activated calcium channel family. Science 260, 1133–1136.

Splawski, I., Timothy, K.W., Sharpe, L.M., Decher, N., Kumar, P., Bloise, R., Napolitano, C., Schwartz, P.J., Joseph, R.M., Condouris, K., Tager-Flusberg, H., Priori, S.G., Sanguinetti, M.C., Keating, M.T., 2004. $Ca_v1.2$ calcium channel dysfunction causes a multisystem disorder including arrhythmia and autism. Cell 119, 19–31.

Stefani, A., Spadoni, F., Siniscalchi, A., Bernardi, G., 1996. Lamotrigine inhibits Ca^{2+} currents in cortical neurons: functional implications. European Journal of Pharmacology 307, 113–116.

Stephens, G.J., Page, K.M., Burley, J.R., Berrow, N.S., Dolphin, A.C., 1997. Functional expression of rat brain cloned alpha1E calcium channels in COS-7 cells. Pflugers Archive 433, 523–532.

Steriade, M., 2005. Sleep, epilepsy and thalamic reticular inhibitory neurons. Trends in Neurosciences 28, 317–324.

Straub, H., Speckmann, E.J., Bingmann, D., Walden, J., 1990. Paroxysmal depolarization shifts induced by bicuculline in CA3 neurons of hippocampal slices: suppression by the organic calcium antagonist verapamil. Neuroscience Letters 111, 99–101.

Striessnig, J., Grabner, M., Mitterdorfer, J., Hering, S., Sinegger, M.J., Glossmann, H., 1998. Structural basis of drug binding to L Ca^{2+} channels. TIPS 19, 108–115.

Sullivan, P.G., 2005. Interventions with neuroprotective agents: novel targets and opportunities. Epilepsy Behaviour 7 (Suppl. 3), S12–S17.

Sun, M.K., Alkon, D.L., 2002. Carbonic anhydrase gating of attention: memory therapy and enhancement. Trends in Pharmacological Sciences 23, 83–89.

Sun, D.A., Sombati, S., Blair, R.E., DeLorenzo, R.J., 2002. Calcium-dependent epileptogenesis in an in vitro model of stroke-induced "epilepsy". Epilepsia 43, 1296–1305.

Supuran, C.T., Scozzafava, A., Casini, A., 2003. Carbonic anhydrase inhibitors. Medicinal Research Reviews 23, 146–189.

Suzuki, T., Delgado-Escueta, A.V., Aguan, K., Alonso, M.E., Shi, J., Hara, Y., Nishida, M., Numata, T., Medina, M.T., Takeuchi, T., Morita, R., Bai, D., Ganesh, S., Sugimoto, Y., Inazawa, J., Bailey, J.N., Ochoa, A., Jara-Prado, A., Rasmussen, A., Ramos-Peek, J.,

Cordova, S., Rubio-Donnadieu, F., Inoue, Y., Osawa, M., Kaneko, S., Oguni, H., Mori, Y., Yamakawa, K., 2004. Mutations in EFHC1 cause juvenile myoclonic epilepsy. Nature Genetics 36, 842–849.

Tai, C., Kuzmiski, J.B., MacVicar, B.A., 2006. Muscarinic enhancement of R-type calcium currents in hippocampal CA1 pyramidal neurons. Journal of Neuroscience 26, 6249–6258.

Talley, E.M., Solórzano, G., Depaulis, A., Perez-Reyes, E., Bayliss, D.A., 2000. Low-voltage-activated calcium channel subunit expression in a genetic model of absence epilepsy in the rat. Molecular Brain Research 75, 159–165.

Tank, D.W., Sugimori, M., Connor, J.A., Llinas, R.R., 1988. Spatially resolved calcium dynamics of mammalian Purkinje cells in cerebellar slice. Science 242, 773–777.

Toriyama, H., Wang, L., Saegusa, H., Zong, S., Osanai, M., Murakoshi, T., Noda, T., Ohno, K., Tanabe, T., 2002. Role of $Ca_v2.3$ (alpha1E) Ca^{2+} channel in ischemic neuronal injury. Neuroreport 13, 261–265.

Toselli, M., Lang, J., Costa, T., Lux, H.D., 1989. Direct modulation of voltage-dependent calcium channels by muscarinic activation of a pertussis toxin-sensitive G-protein in hippocampal neurons. Pflugers Archive 415, 255–261.

Tsakiridou, E., Bertollini, L., de Curtis, M., Avanzini, G., Pape, H.C., 1995. Selective increase in T-type calcium conductance of reticular thalamic neurons in a rat model of absence epilepsy. Journal of Neuroscience 15, 3110–3117.

Turnbull, J., Lohi, H., Kearney, J.A., Rouleau, G.A., Delgado-Escueta, A.V., Meisler, M.H., Cossette, P., Minassian, B.A., 2005. Sacred disease secrets revealed: the genetics of human epilepsy. Human Molecular Genetics 14, 2491–2500.

Turner, T.J., 1998. Calcium channels coupled to glutamate release. Progress in Brain Research 116, 3–14.

van de Bovenkamp-Janssen, M., Scheenen, W.J., Kuijpers-Kwant, F.J., Kozicz, T., Veening, J.G., van Luijtelaar, E.L., McEnery, M.W., Roubos, E.W., 2004. Differential expression of high voltage-activated Ca^{2+} channel types in the rostral reticular thalamic nucleus of the absence epileptic WAG/Rij rat. Journal of Neurobiology 58, 467–478.

van Luijtelaar, G., Wiaderna, D., Elants, C., Scheenen, W., 2000. Opposite effects of T- and L-type Ca^{2+} channels blockers in generalized absence epilepsy. European Journal of Pharmacology 406, 381–389.

van Luijtelaar, E.L., Drinkenburg, W.H., van Rijn, C.M., Coenen, A.M., 2002. Rat models of genetic absence epilepsy: what do EEG spike-wave discharges tell us about drug effects? Methods and Findings in Experimental and Clinical Pharmacology 24 (Suppl. D), 65–70.

Vergara, R., Rick, C., Hernandez-Lopez, S., Laville, J.A., Guzman, J.N., Galarraga, E., Surmeier, D.J., Bargas, J., 2003. Spontaneous voltage oscillations in striatal projection neurons in a rat corticostriatal slice. Journal of Physiology 553, 169–182.

Voisin, D.L., Nagy, F., 2001. Sustained L-type calcium currents in dissociated deep dorsal horn neurons of the rat: characteristics and modulation. Neuroscience 102, 461–472.

Vreugdenhil, M., Wadman, W.J., 1994. Kindling-induced long-lasting enhancement of calcium current in hippocampal CA1 area of the rat: relation to calcium-dependent inactivation. Neuroscience 59, 105–114.

Wakamori, M., Niidome, T., Rufutama, D., Furuichi, T., Mikoshiba, K., Fujita, Y., Tanaka, I., Katayama, K., Yatani, A., Schwartz, A., Mori, Y., 1994. Distinctive functional properties of the neuronal BII (Class E) calcium channel. Receptors & Channels 2, 303–314.

Wang, S.J., Huang, C.C., Hsu, K.S., Tsai, J.J., Gean, P.W., 1996. Inhibition of N-type calcium currents by lamotrigine in rat amygdalar neurones. Neuroreport 7, 3037–3040.

Wasterlain, C.G., Fujikawa, D.G., Penix, L., Sankar, R., 1993. Pathophysiological mechanisms of brain damage from status epilepticus. Epilepsia 34 (Suppl. 1), S37–S53.

Waugh, J., Goa, K.L., 2003. Topiramate: as monotherapy in newly diagnosed epilepsy. CNS Drugs 17, 985–992.

Weiergräber, M., Henry, M., Südkamp, M., De Vivie, E.R., Hescheler, J., Schneider, T., 2005. Ablation of $Ca_v2.3$/E-type voltage-gated calcium channel results in cardiac arrhythmia and altered autonomic control within the murine cardiovascular system. Basic Research in Cardiology 100, 1–13.

Weiergräber, M., Henry, M., Krieger, A., Kamp, M.A., Radhakrishnan, K., Hescheler, J., Schneider, T., 2006. Altered seizure susceptibility in mice lacking the $Ca_v2.3$ E-type Ca^{2+} channel. Epilepsia 47, 839–850.

Westenbroek, R.E., Ahlijanian, M.K., Catterall, W.A., 1990. Clustering of L-type Ca^{2+} channels at the base of major dendrites in hippocampal pyramidal neurons. Nature 347, 281–284.

Westenbroek, R.E., Hell, J.W., Warner, C., Dubel, S.J., Snutch, T.P., Catterall, W.A., 1992. Biochemical properties and subcellular distribution of an N-type calcium channel $\alpha 1$ subunit. Neuron 9, 1099–1115.

Westenbroek, R.E., Sakurai, T., Elliott, E.M., Hell, J.W., Starr, T.V.B., Snutch, T.P., Catterall, W.A., 1995. Immunochemical identification and subcellular distribution of the α_{1A} subunits of brain calcium channels. Journal of Neuroscience 15, 6403–6418.

Williams, J.H., Kauer, J.A., 1997. Properties of carbachol-induced oscillatory activity in rat hippocampus. Journal of Neurophysiology 78, 2631–2640.

Williams, M.E., Marubio, L.M., Deal, C.R., Hans, M., Brust, P.F., Philipson, L.H., Miller, R.J., Johnson, E.C., Harpold, M.M., Ellis, S.B., 1994. Structure and functional characterization of neuronal α_{1E} calcium channel subtypes. Journal of Biological Chemistry 269, 22347–22357.

Wolfe, J.T., Wang, H., Howard, J., Garrison, J.C., Barrett, P.Q., 2003. T-type calcium channel regulation by specific G-protein betagamma subunits. Nature 424, 209–213.

Wu, L.G., Westenbroek, R.E., Borst, J.G.G., Catterall, W.A., Sakmann, B., 1999. Calcium channel types with distinct presynaptic localization couple differentially to transmitter release in single calyx-type synapses. Journal of Neuroscience 19, 726–736.

Xie, X., Hagan, R.M., 1998. Cellular and molecular actions of lamotrigine: possible mechanisms of efficacy in bipolar disorder. Neuropsychobiology 38, 119–130.

Xu, W., Lipscombe, D., 2001. Neuronal $Ca_v1.3$ alpha1 L-type channels activate at relatively hyperpolarized membrane potentials and are incompletely inhibited by dihydropyridines. Journal of Neuroscience 21, 5944–5951.

Yang, S.N., Berggren, P.O., 2005. {beta}-Cell Ca_v channel regulation in physiology and pathophysiology. American Journal of Physiology Endocrinology and Metabolism 288, E16–E28.

Yasuda, R., Sabatini, B.L., Svoboda, K., 2003. Plasticity of calcium channels in dendritic spines. Nature Neuroscience 6, 948–955.

Zamponi, G.W., Bourinet, E., Nelson, D., Nargeot, J., Snutch, T.P., 1997. Crosstalk between G proteins and protein kinase C mediated by the calcium channel $\alpha 1$ subunit. Nature 385, 442–446.

Zhang, B., Harris-Warrick, R.M., 1995. Calcium-dependent plateau potentials in a crab stomatogastric ganglion motor neuron. I. Calcium current and its modulation by serotonin. Journal of Neurophysiology 74, 1929–1937.

Zhang, X., Velumian, A.A., Jones, O.T., Carlen, P.L., 2000. Modulation of high-voltage-activated calcium channels in dentate granule cells by topiramate. Epilepsia 41 (Suppl. 1), S52–S60.

Zhang, Y., Mori, M., Burgess, D.L., Noebels, J.L., 2002. Mutations in high-voltage-activated calcium channel genes stimulate low- voltage-activated currents in mouse thalamic relay neurons. Journal of Neuroscience 22, 6362–6371.

Zwingman, T.A., Neumann, P.E., Noebels, J.L., Herrup, K., 2001. Rocker is a new variant of the voltage-dependent calcium channel gene Cacna1a. Journal of Neuroscience 21, 1169–1178.

Epilepsy Research (2009) **83**, 224—234

journal homepage: www.elsevier.com/locate/epilepsyres

Zonisamide block of cloned human T-type voltage-gated calcium channels

Nora Matar[a], **Wei Jin**[a], **Heiko Wrubel**[a], **Jürgen Hescheler**[a,b], **Toni Schneider**[a,b], **Marco Weiergräber**[a,b,*]

[a] *Institute of Neurophysiology, University of Cologne, Robert-Koch-Str. 39, D-50931 Cologne, Germany*
[b] *Center for Molecular Medicine Cologne (CMMC), University of Cologne, Robert-Koch-Str. 21, D-50931 Cologne, Germany*

Received 28 April 2008; received in revised form 7 November 2008; accepted 11 November 2008
Available online 4 January 2009

KEYWORDS
Antiepileptic drug;
Ca_v3;
Low-voltage activated;
T-type;
Voltage-gated calcium channel;
Zonisamide

Summary Zonisamide (ZNS) is a multi-target antiepileptic drug reported to be efficient in the treatment of both partial and generalized seizures, with T-type Ca^{2+} channel blockade being one of its proposed mechanisms of action. In this study, we systematically investigated electrophysiological effects of ZNS on cloned human $Ca_v3.1$—3.3 Ca^{2+} channels in a heterologous HEK-293 expression system using whole cell patch-clamp technique. Concentration-response studies were performed in the range from 5 μM to 2 mM for $Ca_v3.2$ Ca^{2+} channels exhibiting a 15.4—30.8% reduction of Ca^{2+} influx within the maximum therapeutic plasma range (50—200 μM ZNS). The other T-type Ca^{2+} channel entities, $Ca_v3.1$ and $Ca_v3.3$, were even less sensitive to ZNS. Both voltage- and concentration-dependence of inactivation kinetics remained unchanged for $Ca_v3.2$ VGCC, whereas $Ca_v3.1$ and $Ca_v3.3$ exhibited minor, though significant reduction of inactivation-*tau*. Interestingly, ZNS block of $Ca_v3.2$ VGCCs was not use-dependent and remained unaffected by changes in the holding potential. Steady-state inactivation studies did not display a significant shift in steady-state availability of $Ca_v3.2$ channels at 100 μM ZNS ($\Delta V_{1/2} = 3.1$ mV, $p = 0.071$). Our studies indicate that ZNS is a moderate blocker of human Ca_v3 T-type Ca^{2+} channels with little or no effect on $Ca_v3.2$ Ca^{2+} channel inactivation kinetics, use- and state-dependence of blockade. These results suggest that T-type Ca^{2+} channel inhibition only partially contributes to the anti-absence activity of ZNS antiepileptic drug.

Abbreviations: AED, antiepileptic drug; CAI, carbonic anhydrase inhibitor; FBS, fetal bovine serum; HEK, human embryonic kidney; LTCS, low-threshold calcium spike; LVA, low-voltage activated; VGCC, voltage-gated calcium channel; VGSC, voltage-gated sodium channel; ZNS, zonisamide.

* Corresponding author at: Institute of Neurophysiology & Center for Molecular Medicine Cologne (CMMC), University of Cologne, Robert-Koch-Str. 39, D-50931 Cologne, Germany. Tel.: +49 221 478 6968; fax: +49 221 478 6965.
E-mail address: akp74@uni-koeln.de (M. Weiergräber).

0920-1211/$ — see front matter © 2008 Elsevier B.V. All rights reserved.
doi:10.1016/j.eplepsyres.2008.11.010

Introduction

Zonisamide (ZNS) is a synthetic 1,2-benzisoxazole derivative (1,2-benzisoxazole-3-methanesulfonamide, $C_8H_8N_2O_3S$) with a non-arylamine sulphonamide moiety, and it is chemically unrelated to other common antiepileptic drugs (AEDs). It was first synthesized in 1972 by Uno and later approved in Japan (1989), the US (2000) and recently also in Europe (2005) with more than two million patients per year being treated with ZNS (Leppik, 2004; Baulac, 2006). Since then, ZNS emerged as a widely used, broad-spectrum, multi-target AED. As part of its pharmacodynamic profile, ZNS mediates enhancement of neuronal inhibition via modulation of neurotransmission in the dopaminergic, GABAergic and serotonergic systems (Mimaki et al., 1990; Kaneko et al., 1993; Okada et al., 1995; Ueda et al., 2003). Zonisamide also inhibits excitatory glutamate-mediated transmission (Okada et al., 1998; Zhu and Rogawski, 1999) which may be related to secondary effects on voltage-gated sodium channels (VGSCs) and voltage-gated Ca^{2+} channels (VGCCs) (Ueda et al., 2003). Similar to other sulfonamides, ZNS also serves as a carbonic anhydrase inhibitor (CAI), but its efficacy remains controversial (Masuda and Karasawa, 1993; De Simone et al., 2005; Thone et al., 2008). Furthermore, ZNS inhibits nitric oxide and hydroxyl radical formation by serving as a free radical scavenger and thus being neuroprotective (Hayakawa et al., 1994; Minato et al., 1997; Owen et al., 1997; Mori et al., 1998). The central aspect of ZNS antiepileptic action, however, is blockade of VGSCs and VGCCs (Schauf, 1987; Mimaki et al., 1990; Zhu et al., 2002). Studies carried out on the Myxicola giant axon suggested that ZNS preferentially binds to inactivated VGSCs, producing use- and voltage-dependent blockade and slowing the rate of recovery from inactivation (Schauf, 1987; Rock et al., 1989). Thus, ZNS is effective in inhibiting high-frequency repetitive firing and epileptiform burst activity that is likely to account for its efficacy in the treatment of partial seizures in humans (Thone et al., 2008). In addition, ZNS was recently found to enhance the activity of a large-conductance Ca^{2+}-activated potassium channel (BK_{Ca}) (Huang et al., 2007).

Interestingly, two early studies favored the idea that ZNS is a potent T-type VGCC blocker. Suzuki et al. (1992) reported that ZNS could inhibit T-type currents in cultured neurons of the rat cerebral cortex by $59.5 \pm 7.2\%$ at 500 μM without effecting L-type Ca^{2+} current. The second study, investigating ZNS effects on T-type Ca^{2+} current in the human neuroblastoma cell line NB-I, revealed a $38.3 \pm 5.8\%$ reduction at 50 μM but without changes in inactivation kinetics and voltage-dependence of activation (Kito et al., 1996). However, ZNS shifted the steady-state inactivation curve by approximately −20 mV to more negative potentials, re-equilibrating the distribution of Ca^{2+} channel conformation to the favored inactivated state (Kito et al., 1995, 1996). In addition, ZNS was reported to reduce L-type Ca^{2+} current by $41.9 \pm 8.0\%$ at 50 μM in the human NB-I cell line (Kito et al., 1994).

Concerning pharmacokinetics, the reported therapeutic ZNS plasma levels differ from 6.7 to 40 μg/ml (Wilensky et al., 1985; Rock et al., 1989; Seino et al., 1991; Yagi and Seino, 1992; Mimaki, 1998; Oommen and Mathews, 1999; Leppik, 1999). Approximately 40–50% of ZNS is bound to plasma proteins and the ZNS concentrations in the cerebrospinal fluid was reported not to differ significantly from plasma levels (Mimaki, 1998).

Zonisamide is effective in the antiepileptic treatment of both experimental animal models and humans (Leppik, 2004) and it was approved in the US in 2000 (Wilfong, 2005) as adjunctive treatment of refractory partial seizures in adults (Schmidt et al., 1993; Faught et al., 2001; Sackellares et al., 2004; Brodie et al., 2005). It is also an effective drug for the treatment of typical and atypical absence epilepsy (Yagi and Seino, 1992; Kotani et al., 1994; Wilfong and Schultz, 2005). Furthermore, ZNS is used in patients suffering from secondarily generalized tonic-clonic seizures, myoclonic seizures, West-syndrome, Lennox-Gastaut syndrome and infantile spasms (Leppik, 1999; Kothare et al., 2004; Seino, 2004; Yagi, 2004; Hitiris and Brodie, 2006) by suppressing not only ictal activity, but also interictal discharges (Perucca and Bialer, 1996).

Up to now, various AEDs have been shown to partially block T-type Ca^{2+} channels, including phenytoin, valproic acid, phenobarbital and suxinimides, such as ethosuximide and methylphenylsuxinimide (Coulter et al., 1990; Gomora et al., 2001; Heady et al., 2001; Stefan and Feuerstein, 2007). Only two studies have been carried out so far to investigate ZNS effects on T-type Ca^{2+} currents (Suzuki et al., 1992; Kito et al., 1996) revealing rather divergent concentration-dependent blockade in cultured rat cortical neurons and human neuroblastoma (NB-I) cells under different, but non-standardized experimental conditions. As the amount of experimental evidence has been limited so far, the antiepileptic action of ZNS has thus been predominantly attributed to its inhibitory effect on T-type Ca^{2+} channels. However, the major restriction in interpreting previous results arises from the difficulty in pharmacological and electrophysiological isolation of native T-type Ca^{2+} current, species-specific differences and the cell-specific subunit composition of voltage-gated T-type Ca^{2+} channel complexes, that still remains largely unknown. Thus, the aim of the present study is to unravel ZNS effects on cloned human $Ca_v3.1$–3.3 T-type Ca^{2+} channels in the standardized, heterologous HEK-293 expression system using the whole-cell patch-clamp technique.

Materials and methods

Chemicals and drugs

All drugs, chemicals and solutions used for cell culture (DMEM, FBS, penicillin, streptomycin, geneticin (G418), non-essential amino acids and trypsin) were from Invitrogen (Karlsruhe, Germany). Ultrapure chemicals necessary for electrophysiological measurements were purchased from Sigma–Aldrich (Munich, Germany), Merck (Darmstadt, Germany) and Roth (Karlsruhe, Germany). Zonisamide was also obtained from Sigma (Munich, Germany).

Generation and culturing of Ca_v3 stably transfected cell lines

$Ca_v3.1$–3.3 α_1-subunit stably transfected HEK-293 cell lines were used in our study: α1G-3, containing the human $Ca_v3.1a$ channel (Cribbs et al., 2000); hh8-5, containing the plasmid construct of human $Ca_v3.2$ (Cribbs et al., 1998); and LT9-8, containing the plasmid construct of human $Ca_v3.3$. Stable cell lines were a gift from

Dr. E. Perez-Reyes and had been constructed by transfecting HEK-293 cells using the calcium phosphate method (CalPhos Maximizer Transfection Kit, CLONTECH) as described previously (Gomora et al., 2001). Transfected cells were cultured in DMEM (Dulbecco's Modified Eagle's Medium) supplemented with 15% fetal bovine serum (FBS), 50 U/ml penicillin, 50 μg/ml streptomycin, 1 mg/ml geneticin (G418) and 10 μl/ml non-essential amino acids. Cells were incubated in 100 mm culture dishes at 37 °C in an atmosphere of 95%air/5% CO_2 and split 2—3 times per week. Prior to electrophysiological recordings, cells were washed with 5 ml PBS and dissociated by digestion with 1 ml 0.05% (m/v) trypsin for 90 s; 3 ml DMEM were added following removal of trypsin. The triturated cell suspension was centrifuged for 5 min at 2000 rpm (580×*g*) using a IEC Centra CL2 centrifuge (Thermo Electron Corporation, Waltham, MA, USA), rediluted 1.6—2-fold in DMEM/FBS medium and plated on round cover slips (12 mm, Marienfeld GmbH, Lauda-Königshoven, Germany) in 30 mm culture dishes. Cells were placed in an incubator for at least 4 h up to 1 day prior to electrophysiological recordings.

Electrophysiological measurements of Ca_v3 stably transfected HEK-293 cells

Whole cell currents were recorded from stably transfected HEK-293 cells using the ruptured patch method on an electrophysiological set-up with an inverted microscope Axiovert S100 (Zeiss, Göttingen, Germany), three-axis hydraulic micromanipulator (MH0-103, Narishige, Japan) and an EPC9 patch clamp amplifier (HEKA Elektronik, Lambrecht, Germany). The standard internal pipette solution contained 135 mM CsCl, 10 mM EGTA and 10 mM HEPES. The pH was adjusted to 7.3 with CsOH and osmolality ranged from 269 to 276 mosmol/kg. In addition, 4 mM $Mg_3(ATP)_2$ and 0.3 mM Na_3GTP were freshly prepared and directly added to the internal solution (kept at 4 °C) prior to experiments. The bath solution was composed of 5 mM $CaCl_2$, 155 mM tetraethylammonium (TEA) chloride, and 10 mM HEPES with pH adjusted to 7.4 using TEA-OH and a mean osmolality of 310 mosmol/kg. Osmolalities were measured by using a cryoscope (Osmomat 030, Gonotec, Berlin, Germany) and adapted if necessary. All solutions were prepared with deionized Milli-Q water (Millipore, Schwalbach, Germany), sterile filtrated and stored at 4 °C before use. Prior to cell attachment, the recording electrode was adjusted to give zero current. The liquid junction potential for internal and external solution was calculated as 8.8 mV and compensated. Currents were filtered with a three-pole analog Bessel filter set as a cut-off (−3 dB) at 10 kHz. Patch-clamp electrodes were pulled from thick wall borosilicate glass (OD/ID: 2.0 mm/1.12 mm, 1B200F-4, World Precision Instruments, Sarasota, USA) using a model P-97 Flaming-Brown pipette puller (Sutter Instrument Co., Novato, CA, USA). Once filled with internal solution, the pipette resistance was typically between 2.5 and 5.5 MΩ and series resistance ranged from 7.1 to 7.9 MΩ and was compensated 50—70% using fast (10 μs) compensation. The mean cell capacitance was 21.8 ± 1.1 pF (n = 96 cells analyzed) and on-line P/N leak subtraction was done. All experiments were performed at room temperature (22—24 °C).

Experimental design

Zonisamide was freshly dissolved in external solution at concentrations ranging from 5 μM to 2 mM. The recording chamber was a RC-25 equivalent (13 mm diameter, Warner Instruments, Hamden, CT, USA) with cells plated on 12 mm microscope cover slips (Marienfeld GmbH, Lauda-Königshofen, Germany). Gravitation driven perfusion of ZNS test solutions was performed using a precision perfusion controlling system (Sarstedt, Nürnberg, Germany) at 2.2 ml/min. The electrophysiological set-up was used to analyze concentration-response behavior, use-dependence of block, inactivation kinetics, voltage-dependence of activation and steady-state inactivation properties of Ca_v3 VGCCs in the presence of ZNS.

Data analysis and statistical procedures

Peak current analysis, exponential fits to currents and analysis of current—voltage relationships were carried out by using PULSEFIT and FITMASTER (HEKA Elektronik, Lambrecht, Germany). Concentration-response analysis and graphing of the data were performed with Prism (Graph-Pad, San Diego, CA). The following equation was used to fit concentration-response data assuming a monophasic sigmoidal curve progression with variable slope:

$$Y = \frac{1}{1 + 10^{(\log IC_{50} - X) \times n)}}$$

where X is the logarithm of concentration, Y the response (current fraction remaining) and n the slope (Hill coefficient) of the approximated curve.

For the analysis of voltage-dependence of activation the following Goldman—Hodgkin—Katz based equation was used:

$$I(V) = \mathrm{Cond} * \frac{1 - \exp(-(V - E_{rev})/kT\varepsilon^{-1})}{1 - \exp(-V/kT\varepsilon^{-1})} * \frac{1}{(1 + \exp(-(V - V_{1/2})/\mathrm{Slope}))^3}$$

where V is the test potential; Cond, the conductance; E_{rev}, the reversal potential; $V_{1/2}$, the mid-point of activation; k, the Boltzmann constant; T, the absolute temperature; and ε, the elementary charge.

Calculation of inactivation kinetics was performed by using an exponential fit according to the following equation:

$$I(t) = a_0 + a_1 * \exp\left(\frac{-t}{\tau}\right)$$

with τ as the time constant of inactivation.

Finally, analysis of steady-state inactivation parameters was performed using a Boltzmann equation:

$$\frac{G}{G_{max}} = \frac{1}{1 + \exp\left(\frac{V_{1/2} - V}{k}\right)}$$

where $V_{1/2}$ is the voltage at half-maximum inactivation and k the slope factor.

All data were calculated and displayed as the means ± S.E.M. Statistical comparison of continuous variables was performed using the parametric Student's t-test, considering $p < 0.05$ as significant.

Results

Concentration-dependent inhibition of Ca_v3 T-type voltage-gated calcium channels by zonisamide antiepileptic drug

HEK-293 cells stably transfected with human $Ca_v3.1$—3.3 VGCCs were studied using the whole-cell patch-clamp configuration and continuously superfused with various zonisamide concentrations in a cumulative mode (Figs. 1 and 2). The amplitude of the currents was stable for most recordings (10—15 min), although there was some initial run-down observed immediately after establishment of the whole-cell

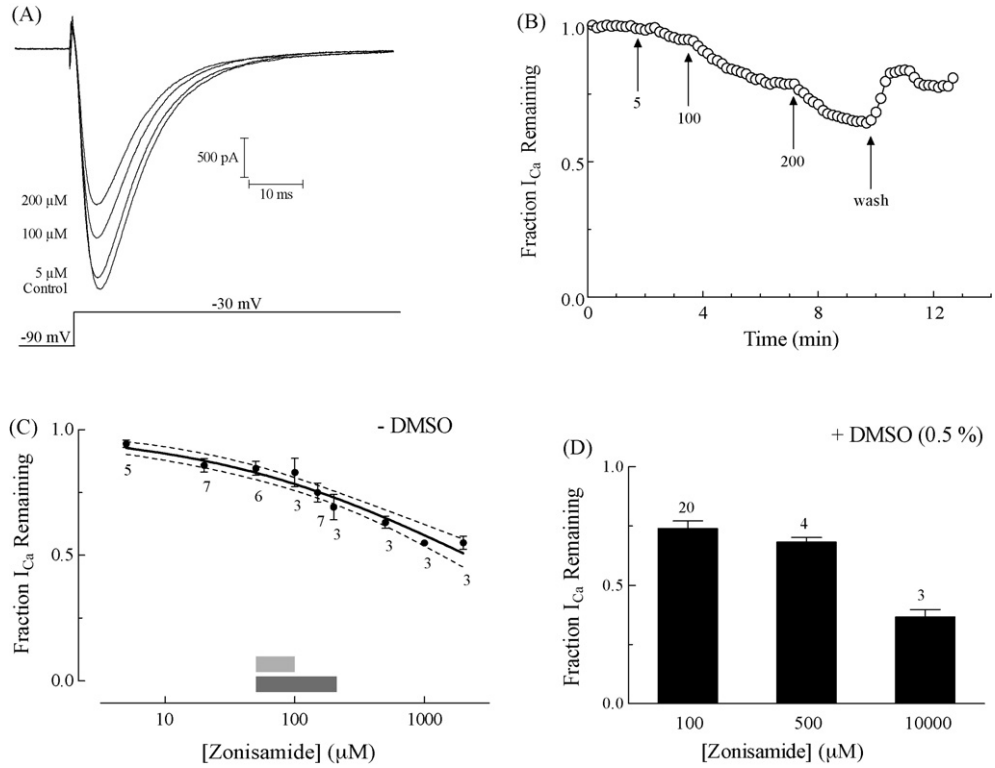

Figure 1 Inhibition of human $Ca_v3.2$ (α_1H) T-type Ca^{2+}-channels by zonisamide. (A) Representative whole-cell recordings displaying the effects of various ZNS concentrations on $Ca_v3.2$ T-type Ca^{2+}-currents. (B) Time course of peak currents normalized to control for the same cell shown in A. Ordinate axis, peak current during steady-state exposure to zonisamide normalized by the peak current before drug exposure, defined as the fraction of I_{Ca} remaining. (C) Concentration-response relationship for ZNS block of $Ca_v3.2$ VGCC. The remaining fractional peak current is plotted against ZNS concentration. Numbers of cells investigated for each concentration is indicated next to each data point. Due to limited ZNS solubility and the lack of fractional block >0.5, no IC_{50} value could be determined in the absence of DMSO. D) ZNS block of $Ca_v3.2$ mediated Ca^{2+}-current in the presence of 0.5% DMSO. Light gray: average therapeutic range (50—100 µM ZNS); dark gray: maximum therapeutic range (50—200 µM ZNS).

patch clamp. Long-term stability of Ca^{2+} currents was monitored in all experiments and only cells exhibiting negligible run-down (less than 2%/min) were used. Recorded Ca^{2+} currents were further corrected for run-down. Test pulses under control, ZNS and washout conditions were applied till Ca^{2+} peak currents reached a stable plateau lasting for 50—100 s. For determination of fractional T-type blockade by ZNS only plateau values were analyzed. Due to its predominant effect in epileptogenesis, concentration-response studies were initiated on $Ca_v3.2$ VGCCs. Applying rectangular test pulses from −90 to −30 mV for 150 ms at a frequency of 0.1 Hz, $Ca_v3.2$ stably transfected HEK-293 cells exhibited maximum peak currents of 1.58 ± 0.14 nA with a mean current density of 99.8 ± 10.5 pA/pF (Fig. 1A). Cell capacitance varied from 5.8 to 35.6 pF and the mean series resistance R_s was 7.9 ± 0.5 MΩ. In contrast to $Ca_v3.1$ and $Ca_v3.3$ (see below), $Ca_v3.2$ exhibited a higher ZNS sensitivity with a Ca^{2+} current reduction of $15.4 \pm 2.8\%$ ($n = 6$) to $25.0 \pm 3.7\%$ ($n = 7$) at therapeutically relevant concentrations of 50—150 µM (Fig. 1B and C, Table 1). In total, ZNS concentrations ranging from 5 µM to 2 mM were used and significant reduction of Ca^{2+} current occurred at 5 µM ($p = 0.002$) and higher concentrations (Table 1). The maximum ZNS concentration used in this study was 2 mM as higher concentrations approach the

Table 1 Inhibition of cloned human Ca_v3 T-type VGCCs by various ZNS concentrations (percentage reduction as mean ± S.E.M.). All ZNS concentrations listed resulted in a significant reduction of Ca^{2+}-current.

Percentaged Ca^{2+} current reduction			
ZNS (µM)	$Ca_v3.1$	$Ca_v3.2$	$Ca_v3.3$
50	13.6 ± 2.6 ($n = 7$)	15.4 ± 2.8 ($n = 6$)	10.3 ± 1.9 ($n = 6$)
100		17.0 ± 5.6 ($n = 3$)	
150	15.1 ± 6.3 ($n = 5$)	25.0 ± 3.7 ($n = 7$)	16.7 ± 2.9 ($n = 6$)
200		30.8 ± 5.1 ($n = 3$)	17.2 ± 4.1 ($n = 3$)

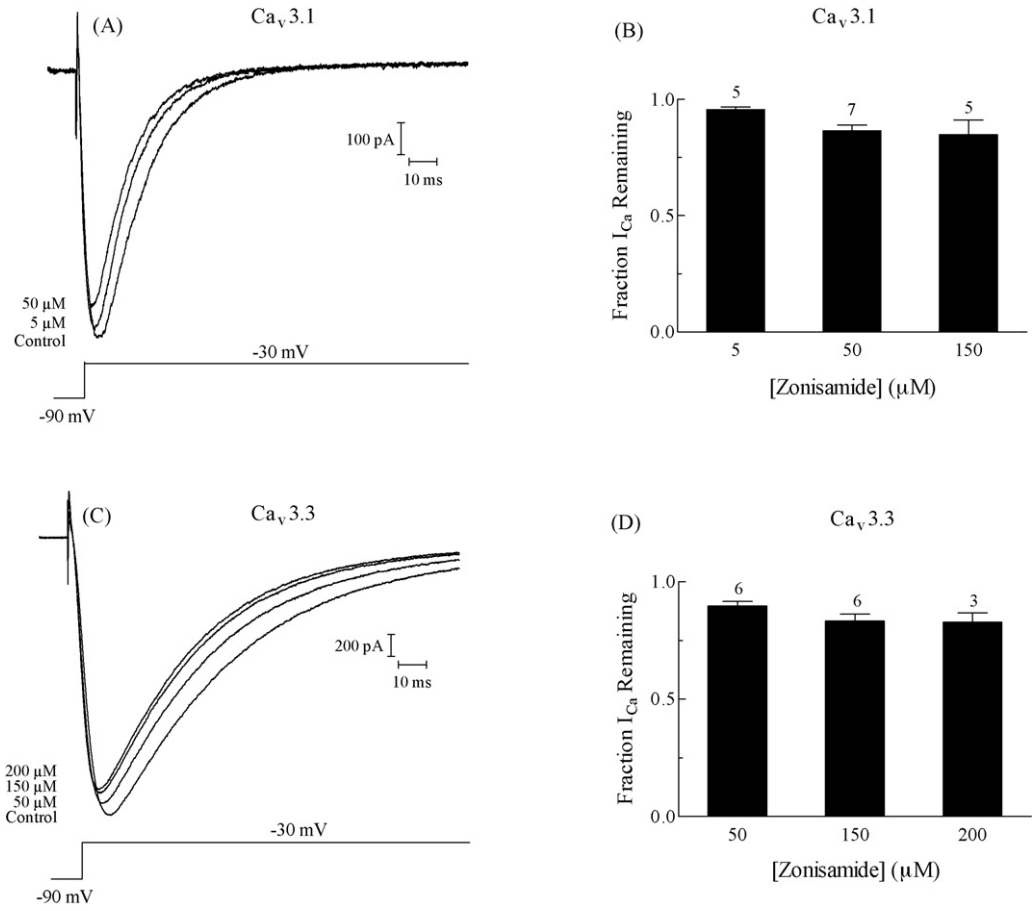

Figure 2 Inhibition of human $Ca_v3.1$ (α_1G) and $Ca_v3.3$ ($\alpha1I$) T-type Ca^{2+}-channels by zonisamide. Representative whole-cell Ca^{2+}-currents recorded from a HEK-293 cell stably transfected with the $Ca_v3.1$ (A) and $Ca_v3.3$ (B) α_1-subunit in response to voltage-steps to −30 mV from a holding potential of −90 mV applied every 10 s. Current traces before and after application of various ZNS concentrations are depicted. Concentration-response studies for ZNS block of $Ca_v3.1$ (B) and $Ca_v3.3$ VGCCs (D) are depicted on the right. Fraction of unblocked peak current is plotted against drug concentration. Numbers of cells investigated for each concentration is indicated next to each data point.

maximum water-solubility of ZNS. Interestingly, application of 100 µM ZNS at a holding potential of −75 mV did not result in increased $Ca_v3.2$ Ca^{2+} current blockade compared to a holding potential of −90 mV (20.4 ± 5.0% (n = 3) vs. 17.0 ± 5.6% (n = 8, p = 0.716), suggesting that ZNS does not significantly shift steady-state inactivation at this concentration (Fig. 6C). Given the higher ZNS sensitivity of $Ca_v3.2$ as compared to $Ca_v3.1$ and $Ca_v3.3$ (as outlined below), further experiments involving use-dependence of block, IV- and steady-state inactivation studies were carried out on $Ca_v3.2$ VGCCs. It is noteworthy that in the absence of DMSO as a solvent, which represents the real pharmacological situation in patients, fractional blockade of $Ca_v3.2$ Ca^{2+} currents greater than 0.5 could not be achieved. Thus, Hill—Langmuir approximation of concentration-response data and subsequent specification of IC_{50} values is invalid and practically impossible. Consequently, the concentration-response behavior, i.e. a mono- or polyphasic, remains speculative. It is noteworthy that previous experiments on ZNS block of T-type Ca^{2+} current were carried in external solution with final concentration of 0.5% DMSO. To elucidate the potential interference of DMSO with ZNS action on $Ca_v3.2$ VGCCs, we also tested effects of 100 µM, 500 µM and 10 mM ZNS dissolved in 0.5% (v/v) DMSO revealing a 26.0 ± 0.03% (n = 20), 31.7 ± 0.02% (n = 4) and 63.3 ± 3.1% (n = 3) reduction in Ca^{2+} current, respectively. These inhibitory effects of ZNS on cloned human $Ca_v3.2$ channels in the presence of DMSO are about 10—20 times lower than those described for T-type Ca^{2+} current in the rat cortex or NB-I cell line before (Suzuki et al., 1992; Kito et al., 1996).

Following the same test pulse regime, ZNS concentration-responses on $Ca_v3.1$ and $Ca_v3.3$ VGCC were also recorded. $Ca_v3.1$ stably transfected HEK-293 cells displayed maximum peak currents of 595.5 ± 50.1 pA with an average current density of 42.9 ± 5.0 pA/pF and cell capacitance ranging from 6.5 to 20.2 pF (Fig. 2A). The mean series resistance was 7.1 ± 0.9 MΩ. ZNS exhibited only minor reduction of $Ca_v3.1$ mediated Ca^{2+} currents of 13.6 ± 2.6% (n = 7) and 15.1 ± 6.3% (n = 5) at pharmacologically relevant concentrations of 50 and 150 µM (Fig. 2B, Table 1). A significant reduction of Ca^{2+} current was observed at 5 µM ZNS (p = 0.017) and higher concentrations (Table 1). Furthermore, whole-cell patch-clamp experiments of $Ca_v3.3$ stably transfected HEK-293 cells displayed peak currents of 2.88 ± 0.50 nA with an average current density of 148.3 ± 20.3 pA/pF, cell capacitance ranging from 14.3 to 28.6 pF and a mean R_s of

7.6 ± 0.9 MΩ. Test pulses were applied from −90 to −30 mV for 150 ms at a frequency of 0.1 Hz (Fig. 2C) and ZNS superfused at concentrations from 50 to 200 μM. Similar to $Ca_v3.1$, ZNS only exerted minor inhibitory effects on $Ca_v3.3$ mediated Ca^{2+}-currents of 10.3 ± 1.9 ($n = 6$) and 16.7 ± 2.9% ($n = 6$) at pharmacologically relevant concentrations (50 and 150 μM ZNS) (Fig. 2D, Table 1) with significant reduction of Ca^{2+}-current observed at 50 μM ($p = 0.003$) and higher concentrations. In order to rule out that potential run-down effects interfere with low-concentration ZNS effects on $Ca_v3.1$−3.3 Ca^{2+} channels during long-term recordings, both cumulative and singular ZNS application regimes were performed which however, did not exhibit differences at low ZNS concentration levels.

ZNS inhibitory effects on Ca_v3 stably transfected HEK-293 cells turned out to be partially (25−75%) reversible in 40% of cells analyzed and completely (>75%) reversible in only 14.3% of the cells. The remaining fraction exhibited washout effects less than 25%. Interestingly, in ZNS/DMSO treated $Ca_v3.2$ stably transfected HEK cells there was hardly any washout possible. Given the fact that ZNS shares a sulfonamide moiety with other AEDs, such as topiramate or CAIs that were previously shown to block the $Ca_v2.3$ E/R-type VGCCs (McNaughton et al., 2004; Kuzmiski et al., 2005) we also checked for antagonistic effects on this Ca^{2+} channel entity. However, ZNS did not exert a detectable reduction of $Ca_v2.3$ mediated Ca^{2+}-current in the 2C6 cell line (stably transfected with the human $Ca_v2.3$ α_1-subunit) or the 1C5 cell line (stably co-expressing the same pore-forming $Ca_v2.3$ α_1- and the human β_3 auxiliary subunit) even at 500 μM ZNS (unpublished results).

Use-dependence of block

In order to investigate whether T-type Ca^{2+} current blockade by ZNS is use-dependent, repetitive test pulses from −110 to −30 mV (duration 100 ms) were applied to $Ca_v3.2$ transfected HEK-293 cells every 0.3 and 5 s in the presence of 100 μM ZNS. Both time course of fractional Ca^{2+} current block and mean steady-state values of ZNS block are depicted in Fig. 3. At a recovery interval of 5 s the obtained fractional block was 0.014 ± 0.012 ($n = 3$). Although reduction of recovery interval to 0.3 s resulted in a significant increase in fractional block (0.065 ± 0.012, $n = 4$, $p = 0.031$; Fig. 3), the impact of 100 μM ZNS on use-dependence of block is minor. Thus, ZNS mediated inhibition of $Ca_v3.2$ Ca^{2+}-current is not substantially facilitated by repetitive high-frequency activation of the pore-forming α_1 subunit.

Concentration- and voltage-dependence of inactivation kinetics

ZNS effects on inactivation kinetics were studied for both voltage- and concentration-dependence using an exponential fit (see *Data analysis*) in the range of 90−10% of Ca^{2+}-current amplitude. For $Ca_v3.2$, as the most intensively studied T-type VGCC candidate in this study, only minor effects on voltage-dependence of inactivation-*tau* could be detected not reaching level of significance at 100 μM ZNS (Fig. 4B). A detailed investigation of current traces revealed that ZNS is hardly capable of affecting the decay of $Ca_v3.2$

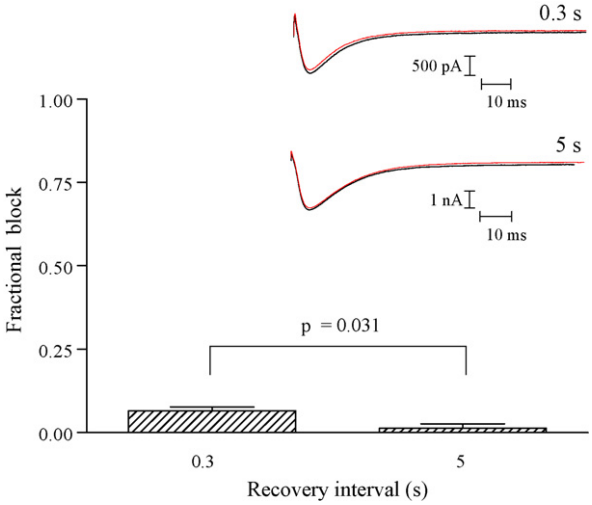

Figure 3 Use-dependence of ZNS mediated $Ca_v3.2$ T-type Ca^{2+} channel blockade. Fractional block by 100 μM ZNS significantly, but slightly increased as the interval between repetitive 100-ms depolarisation steps from −110 to −30 mV decreased (5 s, $n = 3$; 0.3 s, $n = 4$). Inset, representative current traces in the absence (black) and presence (red) of 100 μM ZNS. Currents recorded with recovery intervals of 0.3 and 5 s are depicted. (For interpretation of the references to color in this figure legend, the reader is referred to the web version of the article.)

Ca^{2+}-currents which was tested during a command pulse from −90 to −30 mV (Fig. 4A, scaled and superimposed traces). The washout was not able to restore the inactivation kinetics obtained under control conditions. In addition, we investigated the concentration-dependent effects of ZNS on $Ca_v3.1$−3.3 inactivation-*tau* using test potentials to −30 mV. Whereas $Ca_v3.2$ inactivation kinetics turned out to be unaffected by therapeutically relevant ZNS concentrations, $Ca_v3.1$ and $Ca_v3.3$ exhibited slight, though significant reduction of inactivation-*tau* (Fig. 4C).

Current−voltage relationship

Current−voltage studies were carried out for $Ca_v3.2$ stably transfected HEK-293 cells from a holding potential of −90 mV to +50 mV in 10 mV steps lasting for 100 ms. Fig. 5A displays averaged IV-traces from four cells under control conditions (■), following application of 100 μM ZNS (▲) and after washout (▼). Interestingly, 100 μM ZNS caused a significant shift in the half-activating voltage $Va_{1/2}$ from −44.2 ± 3.1 mV to −48.5 ± 2.3 mV ($n = 4$; $p = 0.0098$), which slightly increased even during washout procedure ($Va_{1/2} = -53.5 \pm 2.1$ mV). The peak current voltage also shifted from −34.9 ± 3.8 mV to −38.3 ± 3.1 mV ($n = 4$; $p = 0.0234$) with the slope factor and reversal potential unaffected. This is in contrast to earlier studies by Kito et al. (1996) that failed to detect changes in voltage-dependence of activation. Similar to concentration-response studies, the washout was only partially effective. Performing the same approach in presence of DMSO (0.5% final concentration) revealed similar results (Fig. 5B). The $Va_{1/2}$ value changed from −56.2 ± 0.9 mV under control conditions to −61.3 ± 1.0 mV after ZNS (100 μM) application

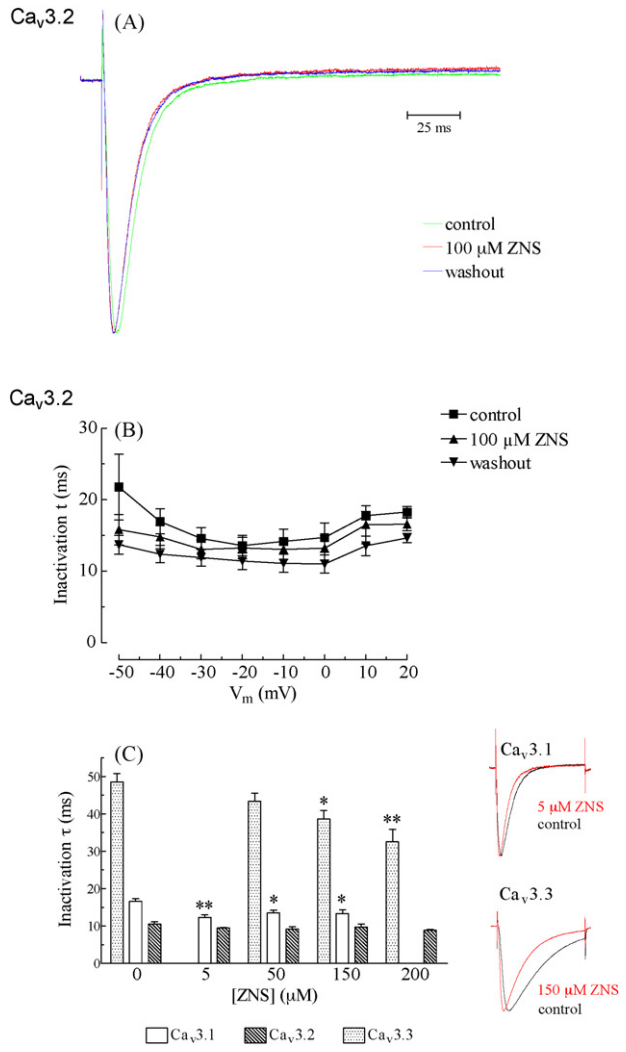

Figure 4 Zonisamide effects on Ca$_v$3.2 T-type Ca^{2+}-channel inactivation kinetics. (A) Superimposed current traces at −30 mV from the same cell as illustrated in Fig. 1A and B. Control-, ZNS- (100 μM) and wash-traces were normalized to the amplitude of the control trace. (B) Voltage-dependence of the inactivation-τ under control (■)-, ZNS- (100 μM, ▲) and washout (▼)-conditions ($n = 4$). Current traces obtained from IV-studies were analyzed using an exponential fit and the resulting inactivation time constants were plotted as function of voltage. (C) Concentration-dependent ZNS-effects on Ca$_v$3.1−3.3 Ca^{2+} channel inactivation kinetics. Inactivation time constants were analyzed from concentration-response current traces using test pulses from −90 mV to −30 mV and plotted versus the ZNS concentration ($n = 20$). *Right*, exemplary normalized current traces from Ca$_v$3.1 and Ca$_v$3.3 transfected HEK cells displaying alteration in inactivation kinetics at various ZNS concentrations.

($n = 8$; $p < 0.001$) and further increased during washout (-63.5 ± 1.1 mV). One cannot rule out that the continuous shift in $Va_{1/2}$ under ZNS and washout conditions is also due to potential Ca^{2+} current run-down during prolonged recordings. Peak current voltage shifted from -38.8 ± 1.4 to -47.4 ± 2.1 mV ($n = 8$; $p < 0.001$). In addition, DMSO caused a prominent reduction of peak current amplitude as reported previously (Suzuki et al., 1992).

Steady-state inactivation studies

The modulated receptor model is based on the observation that specific drugs exhibit different affinities to the closed/resting state, the open state and the inactivated channel state. Many pharmaceuticals, e.g. dihydropyridines and suxinimides display increased affinity to the inactivated state which serves as an important criterion of selectivity of action (Triggle, 1999; Gomora et al., 2001). Voltage-gated Ca^{2+}-channels harbor the capability to directly switch from the closed/resting state to the inactivated state analyzed by applying long-lasting subthreshold prepulses followed by a short test pulse. This so-called double-pulse experiment provides data for steady-state inactivation (h_∞)-studies. Drugs that preferentially bind to the inactivated state shift the equilibrium from the closed to the inactivated state and finally cause a shift of the steady-state inactivation curve to more negative potentials (Bean et al., 1983). The effect of 100 μM ZNS on steady-state inactivation of Ca$_v$3.2 T-type Ca^{2+} channels was determined by using a 5 s prepulse followed by a test pulse from −90 mV to −30 mV for 150 ms (Fig. 6A and B). Control recordings exhibited a half-maximum inactivation voltage ($V_{1/2}$) of -66.5 ± 1.1 mV ($k = 5.27 \pm 0.41$ mV) and $V_{1/2} = -69.6 \pm 1.1$ mV ($k = 4.43 \pm 0.22$ mV) at 100 μM ZNS with an apparent shift of Ca$_v$3.2 steady-state inactivation of 3.1 mV not reaching level of significance ($p = 0.071$, $n = 4$) (Fig. 6C). An attempt to reverse such effect by washing out ZNS was again found ineffective, probably related to secondary, intracellular effects of ZNS (see *Discussion*). The observation that 100 μM ZNS does not significantly shift the steady-state inactivation curve and thus does not favor the inactivated state at the upper therapeutic range, is consistent with our finding that changing the holding potential from −90 mV to −75 mV has no effect on ZNS block of Ca$_v$3.2 VGCCs at 100 μM ($17.0 \pm 5.6\%$ vs. $20.4 \pm 5.0\%$ reduction in Ca^{2+}-current, $p = 0.716$, Fig. 6C). As the electrophysiological and pharmacological properties of the T-type Ca^{2+} currents reported in NB-I cells (Kito et al., 1995, 1996) resemble those known from Ca$_v$3.2 Ca^{2+} channels (Perez-Reyes, 2003; Catterall et al., 2005), steady-state inactivation studies were not extended to Ca$_v$3.1 and Ca$_v$3.3 Ca^{2+} channels.

Discussion

The present study describes the effects of zonisamide antiepileptic drug on Ca$_v$3.1−3.3 T-type voltage-gated Ca^{2+} channels. Previously, only two electrophysiological studies have addressed the question of ZNS block of T-type Ca^{2+} channels, with one using cultured cortical neurons from rat (Suzuki et al., 1992) and the second one analyzing its effects in the human neuroblastoma cell line NB-I (Kito et al., 1996). However, ZNS sensitivity of cloned human Ca$_v$3 T-type Ca^{2+} channels has not been investigated till now. This is of particular relevance as low-voltage activated (LVA) Ca^{2+} channels were repetitively claimed to serve as a primary target for ZNS, although inter-species sequence variations are known to severely influence pharmacological properties of T-type channels (Lee et al., 1999; Cribbs et al., 2000). A closer look into previous studies reveals some of the aspects that might account for the apparent discrepancy in ZNS sensitivity of

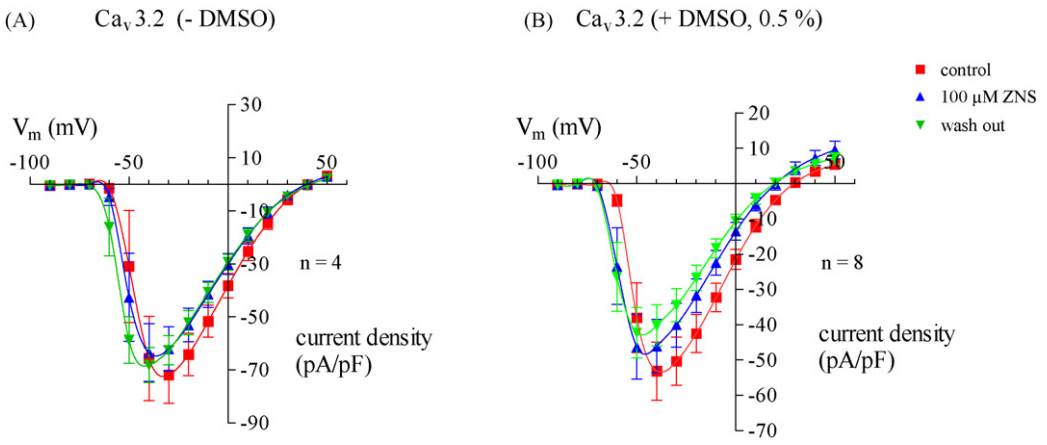

Figure 5 ZNS effects on current—voltage relationship. Current traces were obtained from HEK-293 cells stably expressing $Ca_v3.2$ in the absence ($n = 4$) and in the presence of 100 µM ZNS ($n = 8$) stepping from −90 mV to the indicated voltages for 100 ms with 5 mM Ca^{2+} as a charge carrier. Current—voltage relationships of $Ca_v3.2$ VGCCs before administration of (■), in the presence of 100 µM (▲) and after washout of ZNS (▼) are displayed (A). An identical current—voltage regime was performed in presence of 0.5% DMSO (B). The smooth lines are spline curves fit to the calculated values of current using the product of the Goldman—Hodgkin—Katz and Boltzmann equation (see also *Data analysis*).

T-type Ca^{2+} currents. Studies by Kito et al. (1996) suggested a 38.3 ± 5.8% reduction of T-type Ca^{2+}-current in NB-I cells at 50 µM and an IC_{50} approaching 100 µM with a preferential binding to the inactivated channel state. In contrast, an early study by Suzuki et al. (1992) using ZNS application via pressure ejection elicited a much lower ZNS sensitivity with 59.5 ± 7.2% Ca^{2+} current reduction at 1 mM ZNS similar to the rather weak ZNS effects on $Ca_v3.2$ VGCC in the presence of DMSO observed in our study (Fig. 1C and D). In contrast to the high ZNS sensitivity of T-type Ca^{2+} currents

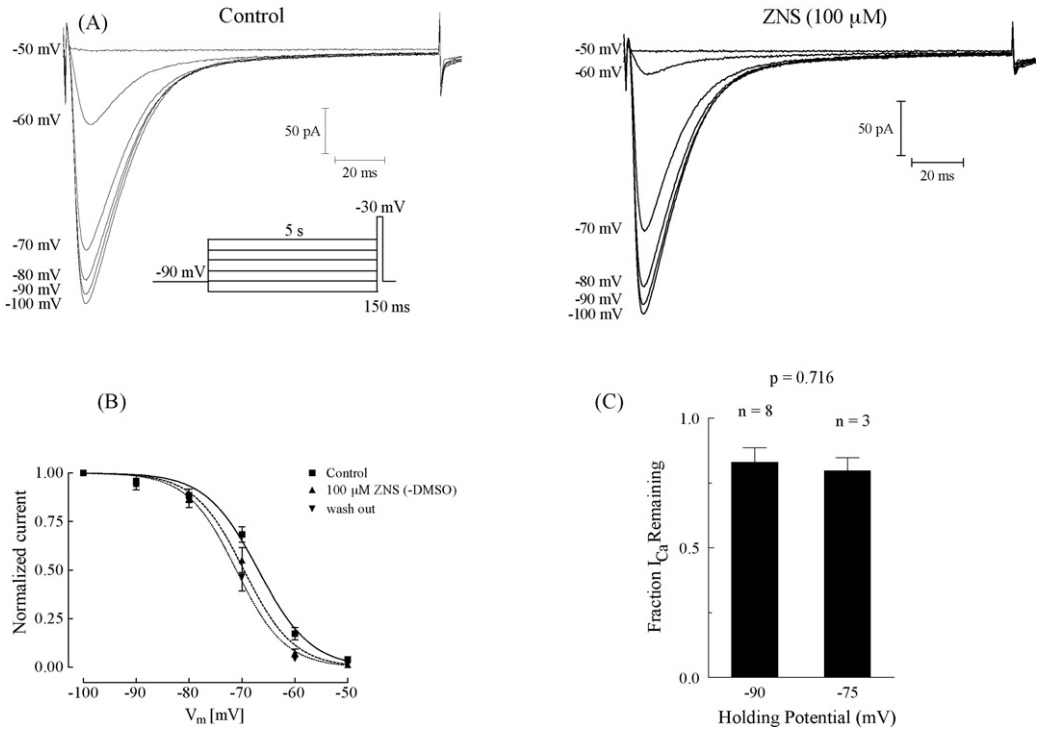

Figure 6 ZNS effects on voltage-dependence of steady-state inactivation of the human $Ca_v3.2$ T-type Ca^{2+} channel. (A) Representative traces recorded from double-pulse experiments with a 5 s prepulse to the indicated voltages followed by a test pulse to −30 mV for 150 ms under control conditions (*left*) and 100 µM ZNS (*right*). (B) Steady-state inactivation curves obtained before (■), during (▲) and after (▼) exposure to 100 µM ZNS using 5 mM Ca^{2+} as a charge carrier. ZNS was capable of shifting the h_∞-curve non-significantly by 3.1 mV ($p = 0.071$, $n = 4$). (C) Changing the holding potential from −90 mV to −75 mV did not result in significant increase of Ca^{2+}-current block following ZNS (100 µM) application, further indicating that the inactivated state is not significantly favored by ZNS at therapeutically relevant concentrations.

in NB-I cells (Kito et al., 1996), our data demonstrate that ZNS application on cloned human $Ca_v3.1-3.3$ α_1-subunits does not result in profound reduction of Ca^{2+} influx within the therapeutic range. Two major reasons might account for this divergent observation: first, differences in electrophysiological recording conditions and second, variations in Ca^{2+} channel complex subunit composition in cultured neurons. In previous studies (Suzuki et al., 1992; Kito et al., 1996), T-type Ca^{2+} currents were elicited by voltage steps from either −60 to −10 mV or −80 to −20 mV resulting in partial LVA Ca^{2+} channel inactivation or contamination with L- or non-L-type Ca^{2+} currents due to the lack of proper pharmacological isolation. In both studies, ZNS was further dissolved in DMSO (0.5% final) and cells were pre-incubated for at least 5 min prior to recordings. The pre-incubation and DMSO mediated cytosolic accumulation of ZNS might give rise to secondary intracellular effects of ZNS that are likely to interfere with T-type Ca^{2+} channel activity. These effects may include modulation of nitric oxid/hydroxyl radical formation, redox potentials and pH changes (due to ZNS interference on CAs) (Owen et al., 1997; Mori et al., 1998; Leppik, 2004) that are known to interfere with T-type Ca^{2+} channel activity (Gottfried and Chesler, 1995; Zhang et al., 2000; Tabet et al., 2004). The hypothesis that intracellular effects influence ZNS blockade of T-type Ca^{2+} channels is further strengthened by the observation that inhibitory effects on VGSCs are at least partially dependent on intracellular ZNS and not on extracellular concentrations of the drug (Schauf, 1987).

Apart from experimental parameters, the differences in subunit composition of T-type voltage-gated Ca^{2+} channel complexes needs to be considered, though it has not been well documented. Co-expression of cloned β-subunits with cloned Ca_v3-subunits did not alter the electrophysiological properties (Dolphin et al., 1999), whereas coexpression with either $\alpha_2\delta1$ or $\alpha_2\delta2$ was found to double the size of the $Ca_v3.1$ mediated Ca^{2+} current (Dolphin et al., 1999; Gao et al., 2000). Furthermore, γ-subunits were reported to exert no or minor effects on cloned Ca_v3 Ca^{2+} channels (Klugbauer et al., 2000; Green et al., 2001). The γ_6-subunit, however, exerts strong inhibitory effects on $Ca_v3.1$ VGCCs (Hansen et al., 2004). In contrast to the distinct over-expression of Ca_v3 α_1-subunits in HEK-293 cells in this study, T-type subunit composition in rat cortical neurons and human NB-I cells is unknown and might influence ZNS efficacy due to its interaction with auxiliary subunits as has been reported previously for other AEDs, such as gabapentin or pregabalin that mediate blockade via $\alpha_2\delta$-subunit interaction (Felix, 2005).

Our detailed investigation of ZNS effects on inactivation kinetics of $Ca_v3.2$ revealed no significant voltage- and concentration-dependence, whereas $Ca_v3.1$ and $Ca_v3.3$ displayed minor yet significant concentration-dependent reduction in inactivation-*tau*. In contrast to previous reports (Suzuki et al., 1992; Kito et al., 1996), current–voltage relationships of $Ca_v3.2$ stably transfected HEK-293 cells exhibited a slight, yet significant shift following ZNS (100 μM) administration. Furthermore, therapeutically relevant ZNS concentrations (100 μM) did not result in a significant shift of the steady-state inactivation curve and consequently, ZNS block was also unaffected by changes in holding potentials (Fig. 6B and C).

Ca_v3 T-type Ca^{2+} channels are responsible for mediation of low-threshold Ca^{2+}-spikes (LTCS) in various neuronal cell types, e.g. thalamic relay neurons or reticular thalamic neurons. LTCS capable of triggering burst activity are the functional background of neuronal pacemaking activity in these cells and hyperoscillation in the thalamocortical-corticothalamic circuitry is known to underlie spike-wave discharge activity in the EEG during non-convulsive absence seizures and slow-wave sleep (Steriade, 2005). During the awake state, thalamic relay neurons are normally slightly depolarized switching from the burst into the tonic mode characterized by repetitive, tonic Na^+-spiking (Steriade and Llinás, 1988). Thus, AEDs that effectively block T-type Ca^{2+} channels succeed in stabilizing the tonic mode. Our results demonstrate that ZNS is capable of blocking human Ca_v3 T-type Ca^{2+} channels of up to 25% in the therapeutic range. Although $Ca_v3.2$ Ca^{2+} current blockade is minor at therapeutically relevant concentrations, previous studies using mock LTCS waveforms and suxinimides indicate that even partial block of low-threshold Ca^{2+} current can be sufficient to effectively suppress thalamic burst activity (Gomora et al., 2001). Narahashi (2000) has suggested that even a 10% block of T-type current might be sufficient to substantially inhibit action potential burst activity (Narahashi, 2000). Therefore, ZNS block of human T-type Ca^{2+} channels may exert limited effects in absence epilepsy treatment (Mimaki, 1998; Wilfong and Schultz, 2005).

From all three T-type Ca^{2+}-channels investigated in this study, $Ca_v3.2$ is the most sensitive one, similar to other AEDs such as phenytoin (Heady et al., 2001). This is of particular interest as $Ca_v3.2$ VGCC emerged as a potential susceptibility gene in the etiopathogenesis of various forms of epilepsies in both animal models and humans (Tsakiridou et al., 1995; Talley et al., 2000; Khosravani et al., 2004; Vitko et al., 2007).

As the amount of experimental evidence has been limited in the past, the antiepileptic action of ZNS had been predominantly attributed to its inhibitory effect on T-type Ca^{2+} channels. However, our current knowledge including this study clearly demonstrates that ZNS is a multi-target AED with only moderate T-type Ca^{2+} channel block being one of the pharmacodynamic properties that might account for its anti-absence activity. Similar to other AEDs with only partially inhibitory effect on T-type Ca^{2+}-current that does not represent its total function, block of Na^+- and K^+-channels or interference with various neurotransmitter systems may also contribute to the broad-spectrum antiepileptic character of zonisamide.

Acknowledgements

We thank Matthew S.P. Ho for comments on the manuscript. This work was financially supported by the Köln Fortune Program (No. 2680089301 to NM, TS and MW), and the Center for Molecular Medicine Cologne (CMMC, to JH, TS and MW), Faculty of Medicine, University of Cologne.

References

Baulac, M., 2006. Introduction to zonisamide. Epilepsy Res. 68 (Suppl. 2), S3–S9.

Bean, B.P., Cohen, C.J., Tsien, R.W., 1983. Lidocaine block of cardiac sodium channels. J. Gen. Physiol. 81, 613—642.

Brodie, M.J., Duncan, R., Vespignani, H., Solyom, A., Bitenskyy, V., Lucas, C., 2005. Dose-dependent safety and efficacy of zonisamide: a randomized, double-blind, placebo-controlled study in patients with refractory partial seizures. Epilepsia 46, 31—41.

Catterall, W.A., Perez-Reyes, E., Snutch, T.P., Striessnig, J., 2005. International Union of Pharmacology. XLVIII. Nomenclature and structure-function relationships of voltage-gated calcium channels. Pharmacol. Rev. 57, 411—425.

Coulter, D.A., Huguenard, J.R., Prince, D.A., 1990. Differential effects of petit mal anticonvulsants and convulsants on thalamic neurones: GABA current blockade. Br. J. Pharmacol. 100, 807—813.

Cribbs, L.L., Gomora, J.C., Daud, A.N., Lee, J.H., Perez-Reyes, E., 2000. Molecular cloning and functional expression of $Ca_v3.1c$, a T-type calcium channel from human brain. FEBS Lett. 466, 54—58.

Cribbs, L.L., Lee, J.-H., Yang, J., Satin, J., Zhang, Y., Daud, A., Barclay, J., Williamson, M.P., Fox, M., Rees, M., Perez-Reyes, E., 1998. Cloning and characterization of α1H from human heart, a member of the T-type calcium channel gene family. Circ. Res. 83, 103—109.

De Simone, G., Di Fiore, A., Menchise, V., Pedone, C., Antel, J., Casini, A., Scozzafava, A., Wurl, M., Supuran, C.T., 2005. Carbonic anhydrase inhibitors. Zonisamide is an effective inhibitor of the cytosolic isozyme II and mitochondrial isozyme V: solution and X-ray crystallographic studies. Bioorg. Med. Chem. Lett. 15, 2315—2320.

Dolphin, A.C., Wyatt, C.N., Richards, J., Beattie, R.E., Craig, P., Lee, J.-H., Cribbs, L.L., Volsen, S.G., Perez-Reyes, E., 1999. The effect of α2-delta and other accessory subunits on expression and properties of the calcium channel α1G. J. Physiol. (Lond.) 519, 35—45.

Faught, E., Ayala, R., Montouris, G.G., Leppik, I.E., 2001. Randomized controlled trial of zonisamide for the treatment of refractory partial-onset seizures. Neurology 57, 1774—1779.

Felix, R., 2005. Molecular regulation of voltage-gated Ca^{2+} channels. J. Receptors Signal Transduct. 25, 57—71.

Gao, B.N., Sekido, Y., Maximov, A., Saad, M., Forgacs, E., Latif, F., Wei, M.H., Lerman, M., Lee, J.H., Perez-Reyes, E., Bezprozvanny, I., Minna, J.D., 2000. Functional properties of a new voltage-dependent calcium channel $\alpha_2\delta$ auxiliary subunit gene (CACNA2D2). J. Biol. Chem. 275, 12237—12242.

Gomora, J.C., Daud, A.N., Weiergraber, M., Perez-Reyes, E., 2001. Block of cloned human T-type calcium channels by succinimide antiepileptic drugs. Mol. Pharmacol. 60, 1121—1132.

Gottfried, J.A., Chesler, M., 1995. Benzolamide inhibits low-threshold calcium currents in hippocampal pyramidal neurons. J. Neurophysiol. 74, 2774—2777.

Green, P.J., Warre, R., Hayes, P.D., McNaughton, N.C.L., Medhurst, A.D., Pangalos, M., Duckworth, D.M., Randall, A.D., 2001. Kinetic modification of the α_{1I} subunit-mediated T-type Ca^{2+} channel by a human neuronal Ca^{2+} channel gamma subunit. J. Physiol. 533, 467—478.

Hansen, J.P., Chen, R.S., Larsen, J.K., Chu, P.J., Janes, D.M., Weis, K.E., Best, P.M., 2004. Calcium channel gamma6 subunits are unique modulators of low voltage-activated $Ca_v3.1$ calcium current. J. Mol. Cell Cardiol. 37, 1147—1158.

Hayakawa, T., Higuchi, Y., Nigami, H., Hattori, H., 1994. Zonisamide reduces hypoxic-ischemic brain damage in neonatal rats irrespective of its anticonvulsive effect. Eur. J. Pharmacol. 257, 131—136.

Heady, T.N., Gomora, J.C., Macdonald, T.L., Perez-Reyes, E., 2001. Molecular pharmacology of T-type Ca^{2+} channels. Jpn. J. Pharmacol. 85, 339—350.

Hitiris, N., Brodie, M.J., 2006. Modern antiepileptic drugs: guidelines and beyond. Curr. Opin. Neurol. 19, 175—180.

Huang, C.W., Huang, C.C., Wu, S.N., 2007. Activation by zonisamide, a newer antiepileptic drug, of large-conductance calcium-activated potassium channel in differentiated hippocampal neuron-derived H19-7 cells. J. Pharmacol. Exp. Ther. 321, 98—106.

Kaneko, S., Okada, M., Hirano, T., Kondo, T., Otani, K., Fukushima, Y., 1993. Carbamazepine and zonisamide increase extracellular dopamine and serotonin levels in vivo, and carbamazepine does not antagonize adenosine effect in vitro: mechanisms of blockade of seizure spread. Jpn. J. Psychiatry Neurol. 47, 371—373.

Khosravani, H., Altier, C., Simms, B., Hamming, K.S., Snutch, T.P., Mezeyova, J., McRory, J.E., Zamponi, G.W., 2004. Gating effects of mutations in the $Ca_v3.2$ T-type calcium channel associated with childhood absence epilepsy. J. Biol. Chem. 279, 9681—9684.

Kito, M., Maehara, M., Watanabe, K., 1994. Antiepileptic drugs—calcium current interaction in cultured human neuroblastoma cells. Seizure 3, 141—149.

Kito, M., Maehara, M., Watanabe, K., 1996. Mechanisms of T-type calcium channel blockade by zonisamide. Seizure 5, 115—119.

Kito, M., Maehara, M., Watanbe, K., 1995. Three types of voltage-dependent calcium currents in cultured human neuroblastoma cells. Nagoya J. Med. Sci. 58, 29—33.

Klugbauer, N., Dai, S.P., Specht, V., Lacinová, L., Marais, E., Bohn, G., Hofmann, F., 2000. A family of gamma-like calcium channel subunits. FEBS Lett. 470, 189—197.

Kotani, H., Hirai, K., Nishiki, T., Yamazoe, I., Okano, S., Takeuchi, Y., Yoshioka, H., Sawada, T., 1994. Zonisamide monotherapy against absence attacks: report of two cases. No To Hattatsu 26, 349—354.

Kothare, S.V., Valencia, I., Khurana, D.S., Hardison, H., Melvin, J.J., Legido, A., 2004. Efficacy and tolerability of zonisamide in juvenile myoclonic epilepsy. Epileptic. Disord. 6, 267—270.

Kuzmiski, J.B., Barr, W., Zamponi, G.W., MacVicar, B.A., 2005. Topiramate inhibits the initiation of plateau potentials in CA1 neurons by depressing R-type calcium channels. Epilepsia 46, 481—489.

Lee, J.-H., Gomora, J.C., Cribbs, L.L., Perez-Reyes, E., 1999. Nickel block of three cloned T-type calcium channels: low concentrations selectively block alpha1H. Biophys. J. 77, 3034—3042.

Leppik, I.E., 1999. Zonisamide. Epilepsia 40 (Suppl. 5), S23—S29.

Leppik, I.E., 2004. Zonisamide: chemistry, mechanism of action, and pharmacokinetics. Seizure 13 (Suppl. 1), S5—S9.

Masuda, Y., Karasawa, T., 1993. Inhibitory effect of zonisamide on human carbonic anhydrase in vitro. Arzneimittelforschung 43, 416—418.

McNaughton, N.C., Davies, C.H., Randall, A., 2004. Inhibition of alpha(1E) Ca^{2+} channels by carbonic anhydrase inhibitors. J. Pharmacol. Sci. 95, 240—247.

Mimaki, T., 1998. Clinical pharmacology and therapeutic drug monitoring of zonisamide. Ther. Drug Monit. 20, 593—597.

Mimaki, T., Suzuki, Y., Tagawa, T., Karasawa, T., Yabuuchi, H., 1990. Interaction of zonisamide with benzodiazepine and GABA receptors in rat brain. Med. J. Osaka Univ. 39, 13—17.

Minato, H., Kikuta, C., Fujitani, B., Masuda, Y., 1997. Protective effect of zonisamide, an antiepileptic drug, against transient focal cerebral ischemia with middle cerebral artery occlusion-reperfusion in rats. Epilepsia 38, 975—980.

Mori, A., Noda, Y., Packer, L., 1998. The anticonvulsant zonisamide scavenges free radicals. Epilepsy Res. 30, 153—158.

Narahashi, T., 2000. Neuroreceptors and ion channels as the basis for drug action: past, present, and future. J. Pharmacol. Exp. Ther. 294, 1—26.

Okada, M., Kaneko, S., Hirano, T., Mizuno, K., Kondo, T., Otani, K., Fukushima, Y., 1995. Effects of zonisamide on dopaminergic system. Epilepsy Res. 22, 193—205.

Okada, M., Kawata, Y., Mizuno, K., Wada, K., Kondo, T., Kaneko, S., 1998. Interaction between Ca^{2+}, K^+, carbamazepine and zonisamide on hippocampal extracellular glutamate monitored

with a microdialysis electrode. Br. J. Pharmacol. 124, 1277—1285.
Oommen, K.J., Mathews, S., 1999. Zonisamide: a new antiepileptic drug. Clin. Neuropharmacol. 22, 192—200.
Owen, A.J., Ijaz, S., Miyashita, H., Wishart, T., Howlett, W., Shuaib, A., 1997. Zonisamide as a neuroprotective agent in an adult gerbil model of global forebrain ischemia: a histological, in vivo microdialysis and behavioral study. Brain Res. 770, 115—122.
Perucca, E., Bialer, M., 1996. The clinical pharmacokinetics of the newer antiepileptic drugs. Focus on topiramate, zonisamide and tiagabine. Clin. Pharmacokinet. 31, 29—46.
Perez-Reyes, E., 2003. Molecular physiology of low-voltage-activated T-type calcium channels. Physiol. Rev. 83, 117—161.
Rock, D.M., Macdonald, R.L., Taylor, C.P., 1989. Blockade of sustained repetitive action potentials in cultured spinal cord neurons by zonisamide (AD 810, CI 912), a novel anticonvulsant. Epilepsy Res. 3, 138—143.
Sackellares, J.C., Ramsay, R.E., Wilder, B.J., Browne III, T.R., Shellenberger, M.K., 2004. Randomized, controlled clinical trial of zonisamide as adjunctive treatment for refractory partial seizures. Epilepsia 45, 610—617.
Schauf, C.L., 1987. Zonisamide enhances slow sodium inactivation in Myxicola. Brain Res. 413, 185—188.
Schmidt, D., Jacob, R., Loiseau, P., Deisenhammer, E., Klinger, D., Despland, A., Egli, M., Bauer, G., Stenzel, E., Blankenhorn, V., 1993. Zonisamide for add-on treatment of refractory partial epilepsy: a European double-blind trial. Epilepsy Res. 15, 67—73.
Seino, M., 2004. Review of zonisamide development in Japan. Seizure 13 (Suppl. 1), S2—S4.
Seino, M., Miyazaki, H., Ito, T., 1991. Zonisamide. Epilepsy Res. Suppl. 3, 169—174.
Stefan, H., Feuerstein, T.J., 2007. Novel anticonvulsant drugs. Pharmacol. Ther. 113, 165—183.
Steriade, M., 2005. Sleep, epilepsy and thalamic reticular inhibitory neurons. Trends Neurosci. 28, 317—324.
Steriade, M., Llinás, R.R., 1988. The functional states of the thalamus and the associated neuronal interplay. Physiol. Rev. 68, 649—742.
Suzuki, S., Kawakami, K., Nishimura, S., Watanabe, Y., Yagi, K., Seino, M., Miyamoto, K., 1992. Zonisamide blocks T-type calcium channel in cultured neurons of rat cerebral cortex. Epilepsy Res. 12, 21—27.
Tabet, F., Savoia, C., Schiffrin, E.L., Touyz, R.M., 2004. Differential calcium regulation by hydrogen peroxide and superoxide in vascular smooth muscle cells from spontaneously hypertensive rats. J. Cardiovasc. Pharmacol. 44, 200—208.
Talley, E.M., Solórzano, G., Depaulis, A., Perez-Reyes, E., Bayliss, D.A., 2000. Low-voltage-activated calcium channel subunit expression in a genetic model of absence epilepsy in the rat. Mol. Brain Res. 75, 159—165.
Thone, J., Leniger, T., Splettstosser, F., Wiemann, M., 2008. Antiepileptic activity of zonisamide on hippocampal CA3 neurons does not depend on carbonic anhydrase inhibition. Epilepsy Res. 79, 105—111.
Triggle, D.J., 1999. The pharmacology of ion channels: with particular reference to voltage-gated Ca^{2+} channels. Eur. J. Pharmacol. 375, 311—325.
Tsakiridou, E., Bertollini, L., de Curtis, M., Avanzini, G., Pape, H.C., 1995. Selective increase in T-type calcium conductance of reticular thalamic neurons in a rat model of absence epilepsy. J. Neurosci. 15, 3110—3117.
Ueda, Y., Doi, T., Tokumaru, J., Willmore, L.J., 2003. Effect of zonisamide on molecular regulation of glutamate and GABA transporter proteins during epileptogenesis in rats with hippocampal seizures. Brain Res. Mol Brain Res. 116, 1—6.
Vitko, I., Bidaud, I., Arias, J.M., Mezghrani, A., Lory, P., Perez-Reyes, E., 2007. The I—II loop controls plasma membrane expression and gating of $Ca_v3.2$ T-type Ca^{2+} channels: a paradigm for childhood absence epilepsy mutations. J. Neurosci. 27, 322—330.
Wilensky, A.J., Friel, P.N., Ojemann, L.M., Dodrill, C.B., McCormick, K.B., Levy, R.H., 1985. Zonisamide in epilepsy: a pilot study. Epilepsia 26, 212—220.
Wilfong, A., Schultz, R., 2005. Zonisamide for absence seizures. Epilepsy Res. 64, 31—34.
Wilfong, A.A., 2005. Zonisamide monotherapy for epilepsy in children and young adults. Pediatr. Neurol. 32, 77—80.
Yagi, K., 2004. Overview of Japanese experience-controlled and uncontrolled trials. Seizure 13 (Suppl. 1), S11—S15.
Yagi, K., Seino, M., 1992. Methodological requirements for clinical trials in refractory epilepsies—our experience with zonisamide. Prog. Neuropsychopharmacol. Biol. Psychiatry 16, 79—85.
Zhang, X., Velumian, A.A., Jones, O.T., Carlen, P.L., 2000. Modulation of high-voltage-activated calcium channels in dentate granule cells by topiramate. Epilepsia 41 (Suppl. 1), S52—S60.
Zhu, G., Okada, M., Murakami, T., Kawata, Y., Kamata, A., Kaneko, S., 2002. Interaction between carbamazepine, zonisamide and voltage-sensitive Ca^{2+} channel on acetylcholine release in rat frontal cortex. Epilepsy Res. 49, 49—60.
Zhu, W.J., Rogawski, M.A., 1999. Zonisamide depresses excitatory synaptic transmission by a presynaptic action. Epilepsia 40, 245.

Cellular/Molecular

Isoflurane-Sensitive Presynaptic R-Type Calcium Channels Contribute to Inhibitory Synaptic Transmission in the Rat Thalamus

Pavle M. Joksovic,[1] Marco Weiergräber,[4,5] WooYong Lee,[1,3] Henrik Struck,[4,5] Toni Schneider,[4,5] and Slobodan M. Todorovic[1,2]

Departments of [1]Anesthesiology and [2]Neuroscience, University of Virginia School of Medicine, Charlottesville, Virginia 22908-0710, [3]Department of Anesthesiology and Pain Medicine, InJe University, Sanggyepaik Hospital, Seoul 139-707, South Korea, and [4]Department of Neurophysiology and [5]Center for Molecular Medicine Cologne, University of Cologne, D-50931 Cologne, Germany

Because inhibitory synaptic transmission is a major mechanism of general anesthesia, we examined the effects of isoflurane on properties of GABAergic inhibitory currents in the reticular thalamic nucleus (nRT) in brain slices. The evoked IPSCs (eIPSCs) and spontaneous miniature synaptic currents (mIPSCs) of visualized nRT cells in young and adult rats were recorded. Consistent with postsynaptic effects on $GABA_A$ receptors, isoflurane prolonged the decay-time constants of both eIPSCs and mIPCSs. Surprisingly, isoflurane completely inhibited the amplitude of eIPSCs at clinically relevant concentrations (IC_{50} of 240 ± 20 μM), increased the paired-pulse ratio, and decreased the frequency of mIPSCs, indicating that presynaptic mechanisms may also contribute to the effects of isoflurane on IPSCs. The overall effect of isoflurane on eIPSCs in nRT cells was a decrease of net charge-transfer across the postsynaptic membrane. The application of 100 μM nickel (Ni^{2+}) and the more specific R-type Ca^{2+} channel blocker SNX-482 (0.5 μM) decreased eIPSC amplitudes, increased the paired-pulse ratio, and attenuated isoflurane-induced inhibition of eIPSCs. In addition, isoflurane potently blocked currents in recombinant human $Ca_V2.3$ (α1E) channels with an IC_{50} of 206 ± 22 μM. Importantly, *in vivo* electroencephalographic (EEG) recordings in adult $Ca_V2.3$ knock-out mice demonstrated alterations in isoflurane-induced burst-suppression activity. Because the thalamus has a key function in processing sensory information, sleep, and cognition, modulation of its GABAergic tone by presynaptic R-type Ca^{2+} channels may contribute to the clinical effects of general anesthesia.

Key words: **anesthesia; calcium channels; calcium current; $GABA_A$ receptor; GABAergic neuron; thalamus**

Introduction

Recent studies have suggested that general anesthetics act through specific ion channels to inhibit neuronal excitability. It is now known that some ligand-gated channels such as $GABA_A$ (Franks, 2008), NMDA (Jevtović-Todorović et al., 1998; Mennerick et al., 1998), as well as background (leak) potassium channels (Franks, 2008), are sensitive to anesthetics. Furthermore, some studies (Herrington et al., 1991; Takenoshita and Steinbach, 1991; Study, 1994; McDowell et al., 1996; Todorovic and Lingle, 1998) indicate that voltage-gated Ca^{2+} channels are also affected by volatile general anesthetics at concentrations that occur under clinical conditions. On the basis of the membrane potential at which they activate, these channels are subdivided into high-voltage-activated (HVA) and low-voltage-activated (LVA), or transient (T-type) Ca^{2+} channels. Pharmacological and physiological experiments support the existence of multiple types of native HVA Ca^{2+} channels (Catterall, 2000). These channels are products of different genes, which give rise to α1 subunits that form the pores of the neuronal Ca^{2+} channels named Ca_V1 family (former α1S, α1C, α1D, α1F) encoding L-type; $Ca_V2.1$ (α1A) encoding P/Q-type; $Ca_V2.2$ (α1B) encoding N-type; and $Ca_V2.3$ (α1E) encoding R-type. These channels in neurons have a central function in sensory, cognitive, and motor pathways by controlling cell excitability and neurotransmitter release. Despite the determined sensitivities of certain Ca^{2+} channels to anesthetic blockade, previous studies have not conclusively established that presynaptic Ca^{2+} channels in neurons are sites of anesthetic action. This is important because small changes in Ca^{2+} influx into presynaptic terminals can result in profound changes in transmitter release and synaptic efficacy (Wu and Saggau, 1997). Thus, even if Ca^{2+} channels are only partially blocked by anesthetics at concentrations within the clinically relevant range, it is important to determine the effects of anesthetics on presynaptic neuronal Ca^{2+} channels.

There is growing recognition that thalamic nuclei are important in awareness and cognitive functions (Kinney et al., 1994; McCormick and Bal, 1997; Llinás et al., 1999; Alkire et al., 2000). The rhythmicity of this complex circuitry depends to a great ex-

Received Nov. 20, 2008; revised Dec. 29, 2008; accepted Jan. 6, 2009.

This work was supported in part by National Institutes of Health Grant GM070726 to S.M.T. We thank Dr. Steven Mennerick for helpful comments on this manuscript and Dr. Karthik Rajasekaran, Dr. Howard Goodkin, and Matt Rannals for help with data analysis.

Correspondence should be addressed to Slobodan M. Todorovic, Department of Anesthesiology, University of Virginia Health System, Mail Box 800710, Charlottesville, VA 22908-0710. E-mail:st9d@virginia.edu.

DOI:10.1523/JNEUROSCI.5574-08.2009

 0270-6474/09/291434-12$15.00/0

tent on the ability of thalamic cells to burst in oscillatory patterns. A key element in rhythm generation within the thalamus is the GABAergic nucleus reticularis thalami (nRT), which is not only reciprocally connected to thalamocortical relay neurons of dorsal thalamic nuclei, but also receives collateral excitatory connections from corticothalamic and thalamocortical fibers (Jones, 1985). In addition, nRT neurons create numerous axonal and dendrodendritic synapses that can inhibit one another (Sanchez-Vives et al., 1997; Shu and McCormick, 2002) and may receive GABAergic inputs from other forebrain structures as well (Jourdain et al., 1989; Paré et al., 1990; Asanuma, 1994). Earlier *in vivo* extracellular recordings have shown that volatile general anesthetics modulate synaptic transmission and depress the excitability of thalamic neurons, which in turn causes blockade of thalamocortical information transfer (Angel, 1991; Detsch et al., 2002; Vahle-Hinz et al., 2007a,b). Thus, we hypothesized that voltage-gated Ca^{2+} channels that support fast synaptic transmission in nRT neurons may be affected by isoflurane, the prototypical volatile general anesthetic.

Materials and Methods

In vitro *tissue slice preparation*

Most experiments were done on transverse rat brain slices taken through the middle anterior portion of the nRT (Paxinos and Watson, 1986). Sprague Dawley rats were housed in the local animal facility in accordance with protocols approved by the University of Virginia Animal Use and Care Committee. All treatment of rats adhered to the guidelines in the *NIH Guide for the Care and Use of Laboratory Animals*.

Rats [postembryonic day 7 (P7–28)] were briefly anesthetized with isoflurane and decapitated. The brains were rapidly removed and placed in chilled (4°C) cutting solution consisting, in mM, of 2 $CaCl_2$, 260 sucrose, 26 $NaHCO_3$, 10 glucose, 3 KCl, 1.25 NaH_2PO_4, and 2 $MgCl_2$ equilibrated with a mixture of 95% O_2 and 5% CO_2. A block of tissue containing the thalamus was glued to the chuck of a vibratome (World Precision Instruments) and 250–300 μm slices were cut in a transverse plane. The slices were incubated in 36°C oxygenated saline for 1 h, then placed in a recording chamber that had been superfused with extracellular saline at a rate of 1.5 cc/min. Incubating saline consisted, in mM, of 124 NaCl, 4 KCl, 26 $NaHCO_3$, 1.25 NaH_2PO_4, 2 $MgCl_2$, 10 glucose, and 2 $CaCl_2$ equilibrated with a mixture of 95% O_2 and 5% CO_2. Slices were maintained in the recording chamber at room temperature and remained viable for at least 1 h. Because the half-life of halogenated volatile anesthetics in nerve tissue after induction of anesthesia is only ~10 min (Stevens and Kingston 1992), it is unlikely that the isoflurane used to euthanize animals could have interfered with the results of our experiments, which were performed at least 2 h later.

Recording procedures

The standard extracellular saline for recording of IPSCs and voltage-gated Ca^{2+} currents in brain slices consisted, in mM, of 2 $CaCl_2$, 130 NaCl, 1 $MgCl_2$, 10 glucose, 26 $NaHCO_3$, 1.25 NaH_2PO_4, and 2 mM KCl equilibrated with a mixture of 95% O_2 and 5% CO_2. For recording $GABA_A$ evoked (eIPSC) and miniature (mIPSC) IPSCs, we used internal solution containing, in mM, 130 KCl, 4 NaCl, 0.5 $CaCl_2$, 5 EGTA, 10 HEPES, 2 $MgATP_2$, and 0.5 Tris-GTP. For recording mIPSC, 5 mM Lidocaine *N*-ethyl bromide was added to the internal solution and 0.5 μM TTX was added to the external solution to prevent the influence of action potentials on neurotransmitter release. To eliminate glutamatergic excitatory currents, all recordings of IPSCs were done in the presence of 5 μM NBQX (2,3-dihydroxy-6-nitro-7-sulfamoyl-benzo[f]quinoxaline-2,3-dione) and 50 μM D-APV ((2*R*)-amino-5-phosphonovaleric acid; AP5 (2*R*)-amino-5 phosphonopentanoate). For a subset of recordings of eIPSCs from nRT neurons, we included in our external solution 100 nM CGP55845A [(2*S*)-3-[[(1*S*)-1-(3,4-dichlorophenyl)ethyl]amino-2-hydroxypropyl](phenylmethyl)phosphinic acid], a specific $GABA_B$ receptor antagonist.

For recordings of HVA Ca^{2+} current in HEK recombinant cells and intact brain slices, we used internal solution containing, in mM, 110 Cs-methane sulfonate, 14 phosphocreatine, 10 HEPES, 9 EGTA, 5 MgATP, and 0.3 Tris-GTP, pH adjusted to 7.15–7.20 with CsOH. The external solution used to record recombinant $Ca_V2.3$ Ca^{2+} currents contained, in mM, 2 $BaCl_2$, 152 TEA-Cl, and 10 HEPES adjusted to pH 7.4 with TEA-OH. Whole-cell recordings were obtained from nRT neurons visualized with an IR DIC camera (Hammamatsu, C2400) on the Zeiss 2 FS Axioscope (Carl Zeiss) with a 40× lens.

Electrophysiological recordings

We recorded $GABA_A$-evoked and miniature IPSCs in thalamic slices from a total of 193 visually identified nRT and 6 thalamocortical (TC) relay neurons (*R* values <20 MΩ). Synaptic stimulation of nRT neurons was achieved with a Constant Current Isolated Stimulator DS3 (Digitimer Ltd.) and electrical field stimulation achieved either by placing a stimulating electrode in the outer region of the internal capsule (see Fig. 1*A*) or within the nRT soma layer. Recordings were made with standard whole-cell voltage clamp technique. Electrodes were fabricated from thin-walled microcapillary glass with final resistances of 3–6 MΩ; membrane currents were recorded with an Axoclamp 200B amplifier (Molecular Devices). Voltage commands and digitization of membrane currents were done with Clampex 8.2 of the pClamp software package (Molecular Devices) running on an IBM-compatible computer. Neurons were typically held at −70 mV.

Currents were filtered at 5 kHz. Series resistance was typically compensated by 50–80% during experiments. In most experiments, during recordings of recombinant and native HVA currents, a P/5 protocol was used for on-line leakage subtractions. HEK293 cells were stably transfected with both the α1E ($Ca_V2.3$) and β3 Ca^{2+} channel subunits as described previously (Nakashima et al., 1998). Cells were typically used 1–4 d after plating. Steps used to activate $Ca_V2.3$-generated currents in HEK cells in whole-cell experiments were typically from a holding potential (V_h) of −70 mV to test potentials (V_t) at 0 mV.

Analysis of current

Current waveforms or extracted data were fitted using Clampfit 8.2 (Molecular Devices), Mini Analysis Program 6.0 (Synaptosoft) and Origin 7.0 (OriginLab). The decay of eIPSCs and mIPSCs was estimated by a single-or double-exponential term. If double exponential function was done, we used weighted averages for our analyses. The limit for mIPSCs detection was set in most recordings at three times the root mean square of baseline noise. The accuracy of detection was visually verified. The amplitudes of all mIPSCs greater than the detection criteria were included in the amplitude analysis.

The percentage reduction in peak current at a given blocker concentration was used to generate concentration–response curves. For each concentration–response curve, all points are averages of multiple determinations from at least six different cells. Mean values in concentration–response curves were fitted to the following (Hill-equation) function: $PB([Drug]) = PB_{max}/1 + (IC_{50}/[Drug])^n$, where PB_{max} is the maximal percentage block of peak eIPSCs or IBa^{2+}, the IC_{50} is the concentration that produced 50% of maximal inhibition, and n is the apparent Hill coefficient for blockade. Fitted values were typically reported with 95% linear confidence limits. Fitting was done with Origin 7.0. Numerical values are given in the text as means ± SEM unless stated otherwise. Statistical analysis was done with paired or unpaired Student's t test where indicated, with statistical significance determined with $p < 0.05$.

Drugs and chemicals

Tetrodotoxin (TTX) was obtained from Alomone Labs. SNX-482, Omega-Agatoxin IVA, and Omega-Conotoxin MVIIC were obtained from Peptides International. Isoflurane was obtained from Abbott. All other salts and chemicals were obtained from Sigma Chemical. The following drugs were prepared as stock solutions: TTX, 5 μM; NBQX and APV, 5 mM; SNX-482, Omega-Agatoxin IVA and Omega-Conotoxin MVIIC, 500 μM; Ni^{2+}, 100 mM and picrotoxin, 20 mM. Drugs were freshly diluted to the appropriate concentrations at the time of experiments. All stocks were prepared in H_2O except for NBQX and picrotoxin, which were prepared in DMSO. The maximum final concentration of

DMSO in any one experiment was 0.1%; at that concentration, DMSO has no effect on eIPSCs in nRT cells ($n = 3$, data not shown).

Solutions

A glass syringe served as a reservoir for a gravity-driven perfusion system consisting of multiple independently controlled glass capillary tubes.

Manually controlled valves allowed switching between solutions. All experiments were done at room temperature (20–24°C). Aliquots of anesthetic solutions were prepared from saturated saline solutions incubated with isoflurane (60 cc of saline with 40 cc of isoflurane in a closed 100 cc vial) for at least 24 h (Todorovic and Lingle, 1998; Todorovic et al., 2000; Joksovic et al., 2005). To quantify the actual anesthetic concentrations in solutions, we had analyzed samples of saturated stock solutions and aliquots in a gas chromatograph calibrated with appropriate volatile anesthetic standards (Todorovic and Lingle, 1998; Joksovic et al., 2005). By measuring actual concentrations, we found a loss of <10% if the solution was used within 30 min after preparation. Thus, all anesthetic solutions were used within 30 min after preparation. Test solutions were maintained in all-glass syringes tightly sealed with Parafilm punctured with a small escape hole when a whole-cell was obtained that allowed anesthetic solution to fall by gravity. All stock solutions were freshly diluted to appropriate concentrations at the time of an experiment. During an experiment, solution was removed from the end of the recording chamber opposite the glass capillary tubes by constant suction. Changes in current amplitudes in response to rapidly acting drugs or ionic changes are typically complete in 2–4 min. Switching between separate perfusion syringes, each containing control saline, resulted in no changes in the amplitude of IPCSs, IBa^{2+} or ICa^{2+}.

Methodological considerations

By necessity, thalamic slices were obtained from young rats. With current technology, direct visualization of nRT neurons in this heavily reticulated region of the thalamus of adult animals is difficult. Importantly, we performed a limited number of recordings in slices from adult rats (older than P21) as shown in Figure 3*B*, demonstrating qualitatively similar results of isoflurane modulation of eIPSCs.

Because voltage control is compromised in whole-cell recordings from slices because of the presence of extensive cell processes, we paid close attention to good voltage control, ensuring that there was no extensive delay in the onset of current and that the onset and offset kinetics depended on voltage, not on the amplitude of current. Because intact nRT neurons have long processes, rapid components of recorded current, such as fast-activation kinetics or tail currents, are not likely to reflect the true amplitude and time course of Ca^{2+} current behavior. However, all our measurements of amplitudes from holding, peak, and steady-state currents were made at time points sufficient to ensure reasonably well clamped current conditions. Furthermore, using brain slices from young animals, in which dendritic processes are not fully developed, ameliorated the space-clamp problem.

We applied all drugs in intact brain slices until an apparent equilibrium was reached. Delivery of lipid-soluble substances such as isoflurane to intact tissue slices is compromised by a decline in drug concentrations along the length of the bath and diffusion through the tissue. Thus, although our method allowed investigation of the effects of anesthetic agents in intact native cells, all quantitative assessments should be taken with caution. Actual effective concentrations of all drugs are likely to be lower than those reported.

In vivo *EEG recordings*

Study animals. Generation of the $Ca_v2.3$ null mutant, which was backcrossed into C57BL/6, has been described in detail (Pereverzev et al., 2002; Weiergräber et al., 2006). Mice were housed in Makrolon cages type II and maintained on a conventional 12 h light/dark cycle with food and water available *ad libitum*. All animal experimentation was approved by the Committee on Animal Care of the University of Cologne. All efforts were made to minimize animal suffering and to use only the number of animals necessary to produce reliable data.

Telemetric EEG recordings. The TA10ETA-F20 radiotransmitter (Data Sciences International, Transsoma Medical) was used for electrocorticographic (ECoG) recordings in $Ca_v2.3^{-/-}$ and control mice. The telemetry system, anesthesia, implantation procedure and postoperative treatment have been described in detail (Weiergräber et al., 2005).

Surface electrode implantation. In all, three $Ca_v2.3^{+/+}$ mice (21.62 ± 2.71 weeks old) and three $Ca_v2.3^{-/-}$ animals (22.14 ± 0.29 weeks old) were studied. Epidural leads were positioned above the somatosensory cortex at the following stereotaxic coordinates: (+)-lead, bregma −1 mm, lateral of bregma 2.5 mm (right hemisphere); (−)-lead, bregma −1 mm, lateral of bregma 2.5 mm (left hemisphere). Leads were fixed at the underlying neurocranium with glass ionomer cement. Radiotransmitter-implanted $Ca_v2.3^{-/-}$ and control mice were given at least 11 d (16.00 ± 2.65, $n = 3$ vs 14.67 ± 1.86, $n = 3$) to fully recover after surgery.

Isoflurane treatment of EEG-radiotransmitter implanted mice. Isoflurane was given at 1%, using a calibrated vaporizer in the presence of oxygen (2 l/min flow). Mice were given 30 min of equilibration time after the administration of isoflurane, followed by a 30-min ECoG recording used for later analysis. During the complete experimental procedure, mice's body temperature was maintained using a heating support with a semicircular recess and continuously monitored by the implanted radiotransmitter.

Data acquisition and analysis. We used A.R.T. 4.1 software (Data Sciences International) to acquire and analyze EEG data. Dataquest EEG recordings under isoflurane treatment were obtained throughout the complete 2 h exposure period. In addition, long-term ECoGs (up to 24 h) were obtained before isoflurane treatment. EEG activity was sampled at 1000 Hz with no filter cutoff. After the isoflurane equilibration phase, mice exhibited typical EEG patterns of repetitive transient sequences of high-voltage slow waves intermingled with sharp waves, or bursts; these episodes alternated with periods of depressed background activity or complete EEG flatness, termed suppression. The time of individual bursts and suppression episodes was analyzed together with their frequencies; the suppression to burst ratio was also calculated. Burst episodes of 2 s duration were analyzed by power spectrum density (PSD) analysis (Dataquest A.R.T. 4.1 software, Data Sciences International) to reveal frequency distribution and burst peak frequency. All data were calculated and are shown as the means ± SEM with $p < 0.05$ considered to be significant.

Results

Electrophysiological characterization of evoked $GABA_A$ IPSCs in nRT cells

The thalamic nRT is a thin layer of cells that surrounds the thalamus and segregates it from the internal capsule (IC). Stimulation of fibers in close proximity to the internal capsule (~200 μm from recorded cells) (Fig. 1*A*) evokes picrotoxin-sensitive $GABA_A$ IPSCs (eIPSCs) in nRT neurons. Figure 1*B* shows an example of eIPSCs with characteristic slow decay (Zhang et al., 1997; Huntsman and Huguenard, 2000) in which 20 μM picrotoxin, a potent noncompetitive $GABA_A$ receptor antagonist, has completely blocked the amplitude of eIPSCs. The time course for the same experiment is shown on the right side of Figure 1*B*. It has been established that synaptic transmission is triggered by Ca^{2+} ion entry into presynaptic nerve terminals (Katz and Miledi, 1970). To confirm the Ca^{2+} dependency of eIPSC in nRT neurons, we made recordings in a solution containing 1 mM Ca^{2+}, finding that the size of eIPSCs decreased by 37 ± 8% ($n = 5$, $p < 0.05$) (Fig. 1*C*). Furthermore, elimination of Ca^{2+} ions from extracellular media (within an average of 2–4 min) almost completely and reversibly eliminated the development of eIPSCs on introduction of nominal Ca^{2+}-free recording solution. A same-strength stimulus evoked IPSCs on reintroduction of 2 mM Ca^{2+} into our recording medium (Fig. 1*D*).

Previous recordings of HVA Ca^{2+} currents in acutely isolated nRT neurons demonstrated that a significant portion of current was sensitive to Ni^{2+} (Huguenard and Prince, 1992), a preferential blocker of R-type voltage-gated Ca^{2+} channels (Zamponi et al., 1996). Thus, we reasoned that eIPSCs in these cells could depend on R-type Ca^{2+} channels. To test this hypothesis, we

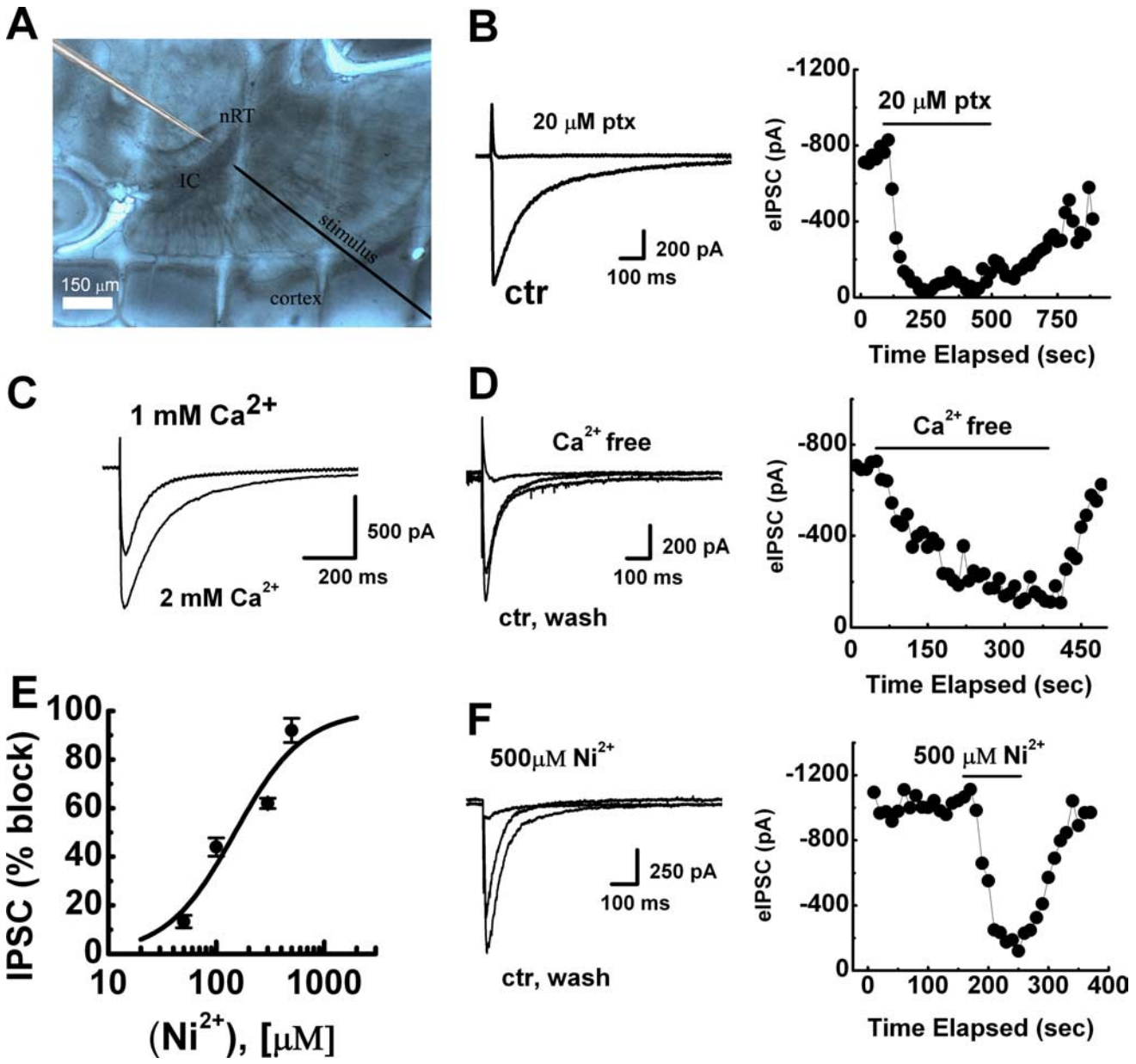

Figure 1. Isolation of eIPSCs in nRT cells in intact brain slices. ***A***, Images showing stimulating (outer part of IC) and recording electrode (nRT). Evoked $GABA_A$-ergic IPSCs were elicited by stimulating fibers on the outer part of the IC opposite to the recording electrode. Horizontal bar indicates calibration. ***B***, Representative traces of evoked $GABA_A$ IPSCs recorded in control conditions and in the presence of 20 μM picrotoxin (ptx), a selective $GABA_A$ and receptor antagonist (on the left). Time course from the same cell showing the partially reversible, potent, and fast blocking effect of picrotoxin (on the right). ***C***, eIPSCs traces recorded in the presence of 1 and 2 mM external calcium. Note faster current decay with 1 mM than 2 mM Ca^{2+}. The decay time constant decreased to 88 ms with 1 mM Ca^{2+} compared with 149 $\pm$ 9 ms in control recorded with 2 mM Ca^{2+}. ***D***, Traces (on the left) and time course (on the right) showing evoked $GABA_A$ IPSCs recorded before, during, and after the application of nominal Ca^{2+}-free external solution. ***E***, Concentration–response curve showing the blocking effect of 50, 100, 300, and 500 μM Ni^{2+} on eIPSC in nRT neurons, yielding IC_{50} of 150 $\pm$ 33 μM and slope constant 1.4 $\pm$ 0.4. Each point represents mean value calculated from at least 6 neurons. Vertical bars represent mean SEs. ***F***, Traces on the left and time course on the right show the reversible effect of 500 μM Ni^{2+} on evoked IPSCs. Horizontal bar represents duration of application.

recorded eIPSCs in the presence of different concentrations of Ni^{2+} in the external solution. We found that Ni^{2+} at 50, 100, 300, and 500 μM reversibly and almost completely inhibited the amplitude of total eIPSCs in these cells, yielding an IC_{50} of 150 $\pm$ 33 μM and a slope factor n of 1.4 $\pm$ 0.4 ($n = 27$ cells). Concentration—response curve and representative traces and time course of the effect of Ni^{2+} on eIPSC in nRT cells are shown in Figure 1, *E* and *F*.

The effect of isoflurane on IPSCs in nRT cells

We tested the effect of clinically relevant concentrations (75, 150, 300, and 600 μM) of isoflurane on $GABA_A$-dependent eIPSCs in the nucleus reticularis thalami. Isoflurane reversibly and almost completely decreased the peak of eIPSCs evoked via stimulating electrode under constant-strength current injections (Fig. 2*A*,*B*), with an IC_{50} of 240 $\pm$ 20 μM and a slope factor n of 1.43 $\pm$ 0.19 ($n = 28$ cells) (Fig. 2*C*). In addition, 300 μM isoflurane increased the decay-time constant of eIPSCs by 40 $\pm$ 2% (Fig. 2*A*) ($n = 9$ cells, $p < 0.05$; note the criss-crossing pattern of eIPSCs decay). However, despite the effects on decay-time constant, total charge transfer was decreased in the presence of isoflurane by 40 $\pm$ 7% ($n = 14$, $p < 0.01$). Also, at concentrations of 75 and 150 μM, isoflurane did not significantly affect the decay-time constant of eIPSCs (data not shown). In the presence of the specific $GABA_B$

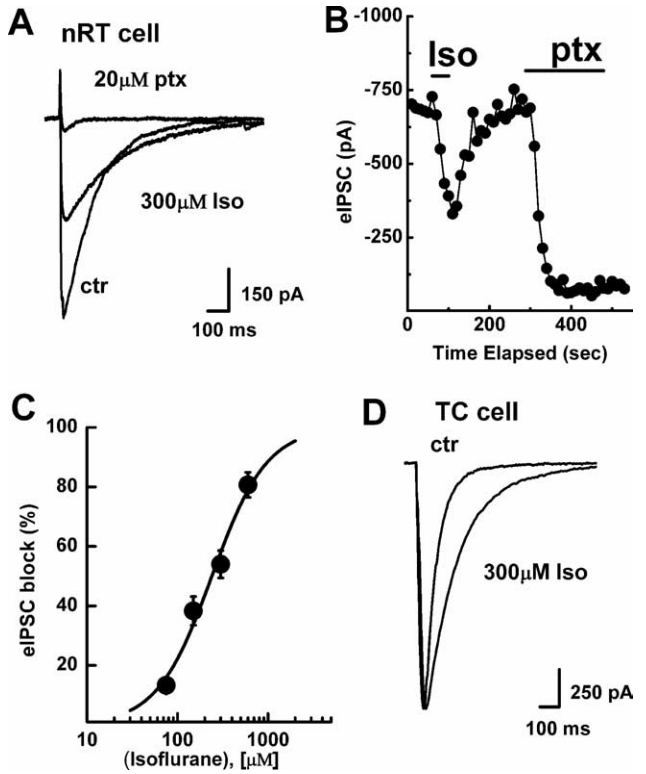

Figure 2. Nucleus-specific effects of isoflurane applications on eIPSCs in the thalamus. Panel shows representative traces (***A***) and time course (***B***) of the effects of isoflurane (Iso) and picrotoxin (ptx) on eIPSCs in an nRT neuron. Peak values of eIPSCs were plotted as a function of time showing the reversible blocking effect of 300 μM isoflurane and the almost complete block of eIPSCs with 20 μM picrotoxin. Horizontal bars indicate duration of isoflurane and picrotoxin application. Note that isoflurane caused a slight prolongation of eIPSC decay as shown by criss-crossing of current traces before and during its application. ***C***, Concentration–response curve showing the blocking effect of isoflurane on eIPSCs in nRT neurons. The curve is best fitted with Hill function, yielding an IC_{50} of 240 ± 20 μM and a slope constant of 1.4 ± 0.2. Each point represents mean value calculated from at least 6 neurons. Vertical bars represent mean SEs. ***D***, Representative traces of eIPSCs in a TC cell in control conditions and during application of 300 μM isoflurane. Note that isoflurane had minimal effect on the amplitude of current but increased decay time >2-fold (from 66 to 161 ms).

receptor antagonist CGP55845A (100 nM), 300 μM isoflurane inhibited the amplitude of eIPSCs to a similar degree (57 ± 7%, $n = 3$, $p < 0.05$; data not shown).

Next we examined the effects of isoflurane on eIPSCs in thalamocortical (TC) relay cells of the ventrobasal complex, which receives most of the inhibitory projections from nRT cells. We placed the stimulating electrode within the nRT layer and recorded eIPSCs from cells in the ventrobasal complex up to 250 μm from nRT. Figure 2*D* shows traces of typical eIPSCs before and during the application of 300 μM isoflurane. In contrast to its effects in nRT cells, isoflurane caused minimal change in the amplitude of eIPSCs (9 ± 5%, $n = 6$, $p > 0.05$), but induced an approximately twofold prolongation of the decay-time constant from 71 ± 10 to 145 ± 12 ms ($n = 6$, $p < 0.01$). As a result, total charge transfer was increased in the presence of isoflurane for 85 ± 13% in TC cells ($p < 0.01$). This finding argues that the inhibitory effect of isoflurane on eIPSCs is synapse-specific for nRT.

To discern the site of isoflurane's action on eIPSCs in nRT neurons, we used paired-pulse analysis to examine the potential synaptic effects of presynaptic modulators (e.g., blockers of voltage-gated Ca^{2+} channels). This sensitive test is done by analyzing changes in the ratio of eIPSCs elicited by two identical presynaptic stimuli delivered in rapid succession. In nRT neurons (Bessaïh et al., 2006) and other synapses (reviewed by Zucker and Regehr, 2002), stimulation with a paired-pulse stimulus interval of 0.01–10 s usually resulted in depression of the second (test) eIPSC compared with the first (conditioning) eIPSC. This depression of the test eIPSCs relative to the conditioning eIPSCs is believed to be caused by depletion of a fraction of readily available synaptic vesicles by the conditioning pulse (Zucker and Regehr, 2002). Presynaptic depressants that change the probability of transmitter release from presynaptic terminals will cause a smaller fraction of the readily releasable pool of vesicles to undergo exocytosis and therefore will decrease paired-pulse depression. This means that in the presence of presynaptic modulators, the ratio of test IPSCs to conditioning IPSCs becomes larger. However, if a modulator simply eliminates a fraction of the vesicle pool from availability or acts exclusively on postsynaptic sites, paired-pulse depression should remain unchanged.

Paired stimulation of afferent fibers resulted in paired-pulse depression, a highly characteristic finding for nRT neurons (Fig. 3*A*,*B*). We found that 300 μM isoflurane reversibly decreased the size of eIPSCs by ~54% from the control level and significantly changed the paired-pulse ratio (PPR, eIPSC-2:eIPSC-1 ratio) from 0.86 ± 0.02 in controls to 0.95 ± 0.02, strongly suggesting its presynaptic effect ($n = 10$ cells, $p < 0.05$) (Fig. 3*A*,*B*). Being concerned about the fact that we were doing our recordings on neonatal and juvenile rats (P7–14), we next recorded the effects of isoflurane in slices older than P21. Figure 3*C* shows the effects of 300 μM isoflurane in thalamic slices from a P23 rat. The results were similar to those in younger rats, with isoflurane inhibiting ~50% (average of 47 ± 9%, $p < 0.01$, $n = 5$) of the amplitude of eIPSCs and increasing PPR from 0.77 ± 0.06 in controls to 0.92 ± 0.02 in experimental rats ($n = 5$, $p < 0.05$) (Fig. 3*D*). Isoflurane in these experiments also increased the decay-time constant of eIPSCs by 56 ± 5% ($p < 0.001$), but decreased net charge transfer for 29 ± 7% ($p < 0.05$). Hence, it appears that there are not important developmental changes in the effects of isoflurane on nRT eIPSCs.

To investigate the contribution of local axonal and dendrodendritic synapses, we recorded eIPSCs from decorticated slice preparations while stimulating neurons directly within nRT (typically closer than 40 μm). However, the addition of 300 μM isoflurane to the external solution not only reversibly blocked eIPSCs by 55 ± 4% ($p < 0.05$, $n = 5$ cells), but prolonged the decay-time constant by 20 ± 2% ($p < 0.05$) and increased paired-pulse ratio from 0.70 ± 0.08 to 0.86 ± 0.02 ($p < 0.05$; data not shown). Overall, our data from decorticated slices are consistent with our previous finding from intact thalamic slice preparations, suggesting that, regardless of the method of stimulation, isoflurane inhibits eIPSCs by a presynaptic mechanism.

To confirm that all the inhibitory effects of isoflurane on IPSCs are likely to be the result of actions on the presynaptic terminal, we also examined the effects of isoflurane on the $GABA_A$-evoked amplitude, duration, and frequency of spontaneous miniature synaptic currents (mIPSCs) in nRT neurons. In miniature synaptic currents, presynaptic effects alter the frequency of events, whereas postsynaptic effects alter the amplitude and/or duration. Thus, we recorded $GABA_A$ picrotoxin-sensitive mIPSCs (Fig. 4*D*) in the same cells in the presence and absence of 300 μM isoflurane (Fig. 4*A–C*). Histograms on Figure 4*E* indicate that isoflurane significantly increased the decay-time constant

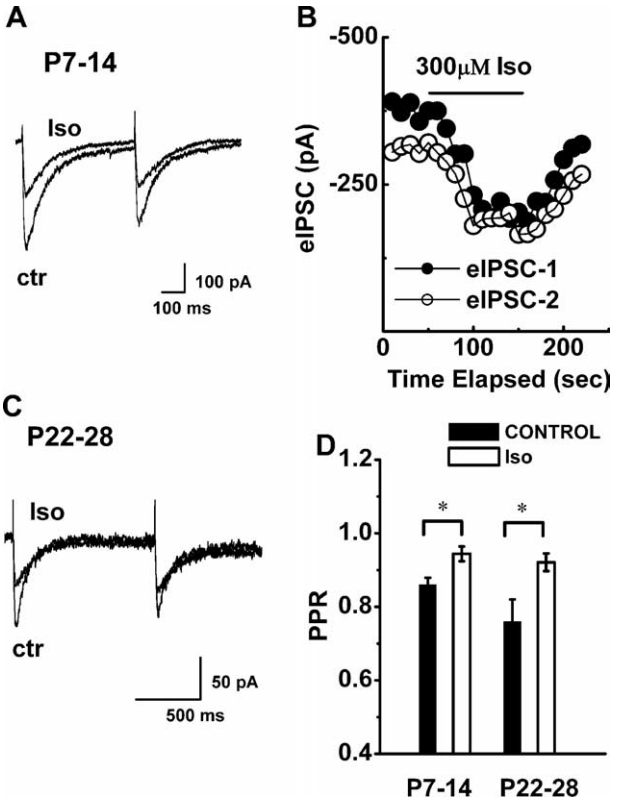

Figure 3. Presynaptic effects of isoflurane applications on eIPSCs in nRT neurons. ***A***, Representative traces of evoked $GABA_A$ receptor IPSCs obtained during recording in a paired-pulse protocol before and during application of 300 μM isoflurane in an nRT cell from an immature rat. Isoflurane reversibly blocked ~50% of eIPSCs without changing the holding current. Paired-pulse depression was observed in 98% of neurons from nRT. ***B***, Time course from the same cell as that in ***A***. Peak values of first (black circles) and second (white circles) evoked IPSCs (at 20 s intervals) were plotted as a function of time showing the reversible blocking effect of 300 μM isoflurane. Horizontal bar indicates duration of isoflurane application. Note that isoflurane more efficiently depressed the first eIPSC. Interval between conditioning and test pulse was 500 ms. ***C***, Representative traces of evoked $GABA_A$ receptor IPSCs obtained during recording in a paired-pulse protocol (interval 1.1 s) before and during application of 300 μM isoflurane in an nRT cell from an adult rat. Isoflurane blocked ~50% of eIPSCs without changing the holding current. Paired-pulse depression was observed in all neurons in this age group. ***D***, Histogram bars indicate PPR obtained by dividing the amplitude of eIPSC2/eIPSC1 in control conditions (black bars) and during application of 300 μM isoflurane (open bars) in nRT cells from immature (P7–14, $n = 10$) and adult (P22–28, $n = 5$) slices. Isoflurane in both groups increased paired-pulse ratio, strongly suggesting its presynaptic site of action. Asterisks indicate $p < 0.05$.

from 52 ± 3 ms in controls to 72 ± 4 ms ($p < 0.01$) and decreased the frequency of single mIPSC-events from 0.50 ± 0.06 Hz to 0.30 ± 0.06 Hz ($p < 0.05$), but had no significant effect on the amplitude of mIPSCs in these cells (control 17.7 ± 1.4 pA, isoflurane 18.3 ± 1.2 pA, $p > 0.05$, $n = 12$). The effect of isoflurane on frequency of mIPSCs appears to be strongly correlated with its presynaptic action as described in paired-pulse experiments. However, the increased decay-time constant of mIPSCs and eIPSCs argues for the postsynaptic effect of isoflurane on $GABA_A$ receptors.

Is there a common presynaptic target for isoflurane and Ni^{2+}?

Different types of voltage-gated Ca^{2+} channels have an important function in the sensory system and are targeted by many clinically relevant pharmacological agents. It appears that HVA Ca^{2+} channels (N-, P-, Q-, L-, and R-type) are principally responsible for supporting synaptic transmission (for review, see Catterall, 2000). We found that Ni^{2+}, thought to be selective for R-type in preference to other subtypes of HVA Ca^{2+} channels (Schneider et al., 1994; Zamponi et al., 1996), when used at a concentration of 100 μM, reversibly blocked eIPSCs while increasing paired-pulse ratio (Fig. 5*A*,*B*). On average, Ni^{2+} changed the PPR from 0.72 ± 0.08 in controls to 0.85 ± 0.02 ($n = 5$ cells, $p < 0.01$), strongly suggesting the presynaptic site as a possible target for Ni^{2+} modulation of eIPSCs.

Our recordings with isoflurane and Ni^{2+} both showed high potency effects on eIPSCs and PPR suggesting that these agents affect common targets on the presynaptic membrane. To test this possibility, we applied 300 μM isoflurane after the exposure of intact slices to 100 μM Ni^{2+}, which blocked ~50% of amplitude of eIPSCs. In this occlusion experiment, we found that 300 μM isoflurane had a less prominent effect on the remaining eIPSCs (Fig. 5*C*,*D*, representative traces and time course are shown). Overall, isoflurane blocked significantly fewer eIPSC currents after the administration of Ni^{2+} (31 ± 5%, $n = 8$ cells) than it did in control conditions (54 ± 6%, $n = 10$ cells, $p < 0.05$). Thus, it appears that isoflurane and Ni^{2+} affect common presynaptic targets in nRT cells. At a concentration of 100 μM, Ni^{2+} was less effective in inhibiting eIPSCs in TC cells (13 ± 7%; $n = 6$; $p < 0.001$, data not shown).

Next we tested whether, in intact slice preparations, 100 μM Ni^{2+} and 300 μM isoflurane can significantly block HVA Ca^{2+} current, which supports synaptic transmission. Because at least some of the inhibitory synapses in nRT neurons are recurrent connections from the same cells (Cox et al., 1996), we recorded HVA Ca^{2+} currents from the soma of these neurons. In support of our hypothesis, we found that Ni^{2+} reversibly decreased total HVA Ca^{2+} current amplitude in nRT neurons by 30 ± 3% ($n = 5$ cells, $p < 0.01$) (Fig. 5*E*,*F*) and that isoflurane similarly inhibited 38 ± 9% of total HVA current amplitude ($n = 5$, $p < 0.01$, data not shown).

Isoflurane-sensitive R-type Ca^{2+} channels contribute to inhibitory synaptic transmission in the reticular thalamic nucleus

The potent blocking effects of Ni^{2+} on eIPSCs in our experiments were highly suggestive of the possibility that R-type Ca^{2+} channels are involved in inhibitory synaptic transmission in the thalamus. To investigate the contribution of R-type Ca^{2+} channels to inhibitory synaptic transmission, we recorded eIPSCs in the presence of SNX-482, a selective R-type channel blocker. Previous studies documented the existence of SNX-482-sensitive R-type current (up to 0.5–1 μM SNX-482) (Newcomb et al., 1998; Tottene et al., 2000). In an earlier study, we found that 0.5 μM SNX-482 selectively blocked HVA but not T-type Ca^{2+} currents in nRT neurons (Joksovic et al., 2005). That is why, in these experiments, we recorded eIPSCs in the presence of 0.5 μM SNX-482. We found that in most cells 0.5 μM SNX-482 blocked evoked eIPSCs by 40 ± 4% ($n = 9$, $p < 0.001$) (Fig. 6*A*,*B*), apparently irreversibly. SNX-482, similar like isoflurane and Ni^{2+}, increased paired-pulse ratio from 0.70 ± 0.03 to 0.83 ± 0.04 ($n = 4$, $p < 0.01$, data not shown), strongly suggesting a presynaptic site of action. Overall, our results indicate that SNX-482-sensitive R-type Ca^{2+} channels contribute to vesicular GABA release in inhibitory synapses in the thalamus.

Based on our results, we hypothesized that the effect of isoflurane on eIPSCs may be related to its effect on R-type Ca^{2+} currents. To test this hypothesis, we did two sets of experiments.

First, in the same neurons, we recorded the effects of 300 μM isoflurane on eIPSCs before and after exposure to 0.5 μM SNX-482. Typical traces and the time course of eIPSCs from this experiment are shown in Figure 6, *C* and *D*. In seven cells studied with this method, the peak amplitude of eIPSCs blocked by 300 μM isoflurane was markedly reduced after the application of SNX-482 to 25 ± 7%. For comparison, 300 μM isoflurane blocked 54 ± 6% of eIPSCs in control conditions ($p < 0.01$). Thus, a substantial portion of the eIPSCs blocked by isoflurane was removed by the irreversible blocking action of SNX-482 on presynaptic R-type Ca^{2+} current. Our results strongly suggest that isoflurane modulates eIPSCs in nRT neurons by blocking presynaptic R-type Ca^{2+} currents.

We then studied the effect of isoflurane on recombinant $Ca_V2.3$ R-type Ca^{2+} channels stably transfected in HEK cells (Nakashima et al., 1998). We found that isoflurane potently and reversibly blocked recombinant human $Ca_V2.3$ currents in concentration-dependent manner, yielding an IC_{50} of 206 ± 22 μM and a Hill slope constant *n* of 1.66 ± 0.35 (Fig. 7*A–C*). The slope of the curve and the potency of isoflurane in blocking recombinant $Ca_V2.3$ currents were similar to the isoflurane inhibition of eIPSCs shown in Figure 2*C*.

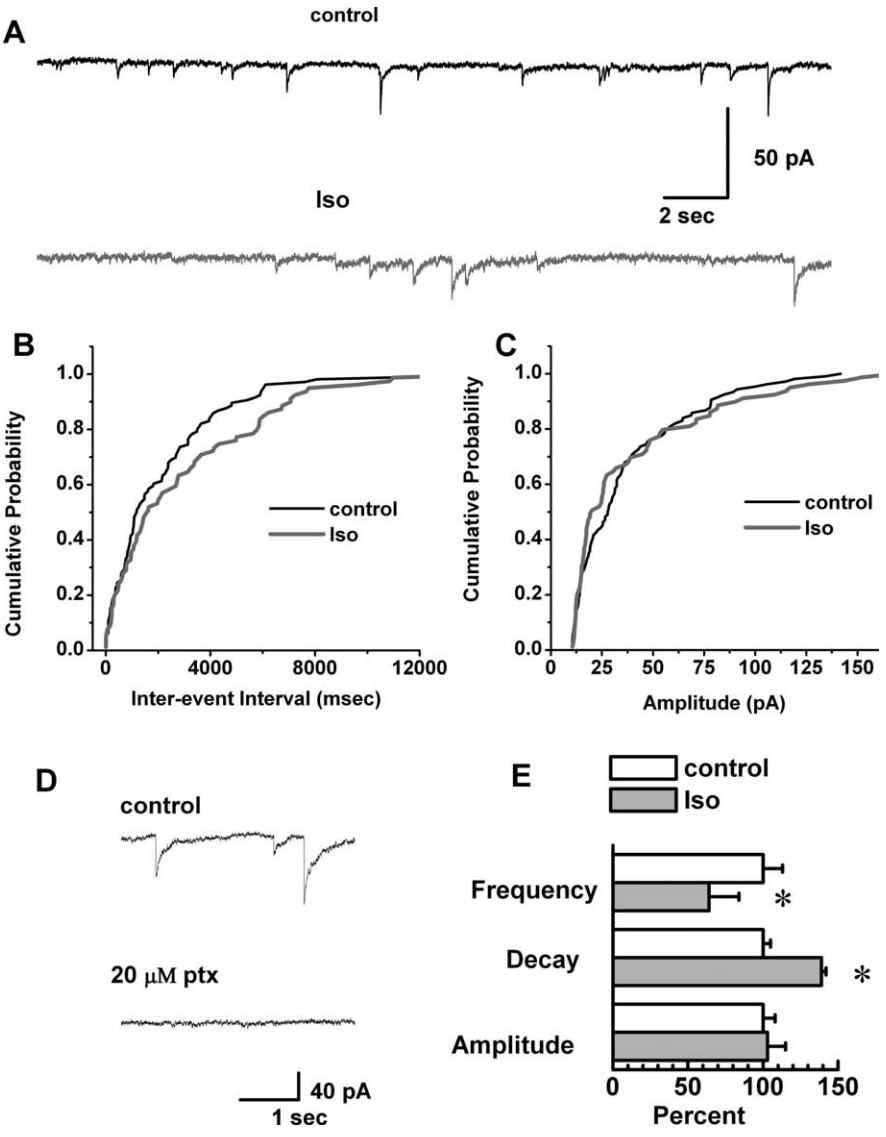

Figure 4. The effect of isoflurane application on mIPSCs in nRT cells. ***A***, Traces from representative recording of mIPSCs in control conditions (black trace) and in the presence of 300 μM isoflurane (gray trace). Holding potential was set at −70 mV. ***B***, ***C***, Cumulative probability of interevent intervals (***B***) and amplitudes (***C***) of mIPSCs in the absence (black trace) and presence (gray trace) of 300 μM isoflurane in the same cell as that shown in ***A***. Note the very small effect of isoflurane on the amplitude distributions, and more pronounced effect on interevent interval distributions in this cell. ***D***, Traces of mIPSCs recorded in control conditions and in the presence of 20 μM picrotoxin (specific $GABA_A$ receptor antagonist). Note that 20 μM picrotoxin completely prevented the development of mIPSCs. ***E***, Histogram summarizes the effect of 300 μM isoflurane (gray columns) on frequency, decay time, and amplitude of mIPSCs compared with controls (white columns). Isoflurane significantly decreased the frequency of mIPSCs (from 100 ± 13% to 64 ± 20%, $p < 0.05$) and increased the decay time constant (from 100 ± 5% to 139 ± 3%, $p < 0.01$), but had no significant effect on the mIPSCs peak amplitudes. Data were analyzed and calculated for each cell in a time frame of 250 s per condition ($n = 12$ cells).

Under isoflurane anesthesia, alterations of thalamocortical rhythmicity occur *in vivo* in mice lacking $Ca_V2.3$ channels

Under a variety of experimental and clinical conditions thalamocortical circuitry *in vivo* may generate rhythmic oscillations of bursts and blackout sequences (suppressions). This burst-suppression pattern, which is often induced by various volatile anesthetics, including isoflurane (Akrawi et al., 1996), is generally thought to correlate with the blockage of sensory information flow at the thalamic sensory gate (Steriade et al., 1994). Thus, to test the role of $Ca_V2.3$ channels in isoflurane anesthesia *in vivo*, we performed EEG analyses of adult $Ca_V2.3$ KO mice and WT littermates by systemically determining the number and duration of single-burst or suppression episodes within a representative 10-min episode after the equilibration period. We performed our *in vivo* study with 1% isoflurane, because this concentration approximately correlates with an IC_{50} for *in vitro* inhibition of eIPSCs and recombinant $Ca_V2.3$ currents.

The representative traces from these experiments are shown in Figure 8, *A* and *B*. At 1% isoflurane there was a marked, significant difference in duration of suppression episodes between controls (3.63 ± 0.62 s, $n = 3$) and $Ca_v2.3$-deficient mice (1.58 ± 0.39 s, $n = 3$, $p < 0.05$) (Fig. 8*C*, left). In addition, the suppression to burst ratio in $Ca_v2.3^{-/-}$ mice was reduced with isoflurane compared with that in controls (0.211 ± 0.029 vs 0.391 ± 0.049, $n = 3$, $p < 0.05$) (Fig. 8*C*, right). The total number of burst and suppression episodes, as well as duration of burst episodes in the presence of isoflurane did not differ significantly between genotypes (data not shown). From each WT and $Ca_v2.3$ KO mouse, five 2 s burst episodes were analyzed by PSD in the range from 0 to 100 Hz to obtain frequency distribution and burst peak frequency. The dominant frequency according to PSD analysis during burst activity was 14.9 ± 0.9 Hz ($n = 3$) in WT and 16.0 ± 2.6 Hz ($n = 3$) in $Ca_v2.3$ deficient mice ($p > 0.05$, data not shown). Overall, our data strongly suggest that $Ca_V2.3$ channels contribute to the inhibitory effects of isoflurane on sensory information transfer in corticothalamic circuitry.

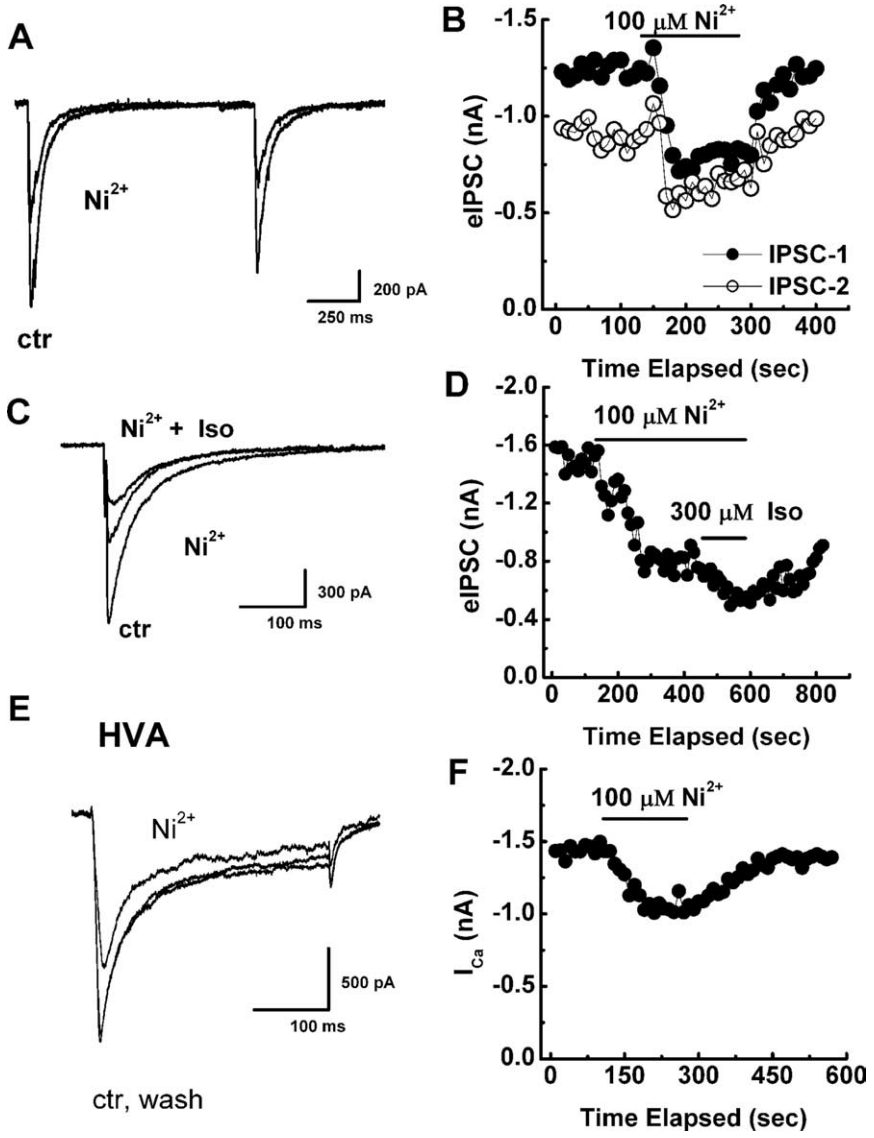

Figure 5. The effect of Ni^{2+} on eIPSCs in nRT neurons in intact slice preparation. ***A***, Representative eIPSC traces recorded in paired-pulse protocol in control conditions and in the presence of 100 μM Ni^{2+}. Nickel depressed the amplitudes of eIPSCs by ~50% without apparent effect on kinetics of current decay. Interval between conditioning and test pulse was 1100 ms. ***B***, Time course from the same nRT cell shows the effect of Ni^{2+} on eIPSC1 (filled symbols) and eIPSC2 (open symbols). Peak eIPSCs amplitudes were plotted as a function of time. The horizontal bar represents duration of Ni^{2+} application. ***C***, ***D***, eIPSC traces (left) and the corresponding time course (right) showing the occlusive effect of 100 μM Ni^{2+} and 300 μM isoflurane on the eIPSCs in nRT. Although 300 μM isoflurane in the presence of 100 μM Ni^{2+} further decreased the size of eIPSC, its overall effect was diminished. ***E***, ***F***, Representative traces (left) and time course (right) showing the effect of 100 μM Ni^{2+} on HVA Ca^{2+} currents in the same nRT neuron (V_h −60 mV, V_t 0 mV). Ni^{2+} reversibly blocked ~30% of peak HVA Ca^{2+} current. Horizontal bar represents duration of Ni^{2+} application.

Discussion

Isoflurane-sensitive R-type Ca^{2+} channels contribute to vesicular release in an inhibitory central synapse

One of our major findings is that R-type Ca^{2+} channels support inhibitory $GABA_A$ transmission in nRT neurons; another is that isoflurane inhibits both evoked and spontaneous inhibitory transmission in these neurons. We also demonstrated that this effect is at least partly mediated by the ability of isoflurane to interact with presynaptic R-type Ca^{2+} channels.

Depending on the synaptic system being studied, P/Q-, L-, N-, and R-subtypes of HVA currents may contribute to the Ca^{2+} influx that results in transmitter release (Catterall, 2000). It is generally accepted that most of the fast synaptic transmission in CNS neurons is supported by P/Q and N-type Ca^{2+} channels (Catterall, 2000; Zucker and Regehr, 2002). Because of the paucity of selective blockers, the function of R-type current remains poorly understood. However, it has been shown that this subtype can also support fast excitatory transmitter release in the brainstem (Wu et al., 1998) and in hippocampal (Gasparini et al., 2001) and cerebellar (Brown et al., 2004) neurons. We found that both inhibitory synaptic transmission and recombinant R-type Ca^{2+} channels are potently inhibited by isoflurane, a commonly used volatile anesthetic. In mammals, the aqueous concentration of isoflurane that correspond to 1 MAC (minimum alveolar concentration that prevents response to a surgical stimulus in 50% of human subjects) at room temperature is ~320 μM (Franks and Lieb, 1994). Therefore, isoflurane concentrations that inhibit IPSCs in nRT cells and recombinant R-type $Ca_V2.3$ current are well within the range required for surgical anesthesia.

An early theory of anesthetic mechanisms proposed that nonspecific alteration of the lipid membrane in nerve cells accounts for the anesthetic state (Meyer, 1899; Overton, 1901). However, over the last two decades there has been increasing recognition that specific classes of ion channels in the neuronal membrane are the major cellular targets of general anesthetics. Among the class of ligand-gated ion channels, it appears that the $GABA_A$ receptor-ion channel complex is central to many effects of general anesthetics. For example, intravenous anesthetics like etomidate and propofol markedly potentiate $GABA_A$-gated currents; they also prolong decay of GABAergic eIPSCs in CNS neurons as much as fourfold (for review, see Rudolph and Antkowiak, 2004; Urban 2002). Thus, it appears reasonable that modulation of neuronal GABAergic IPSCs may mediate the clinical effects, such as loss of consciousness, of some general anesthetics. In contrast, volatile anesthetic agents such as isoflurane have variable effects on postsynaptic currents mediated by $GABA_A$ receptors. We found that at 300 μM, isoflurane caused an increase of ~40–50% in the decay time constant of mIPSCs and eIPSCs in nRT neurons. However, it seems that inhibition of presynaptic R-type Ca^{2+} currents and a consequent decrease in the amplitude of eIPSCs with the same concentration of isoflurane can overcome these effects, because it resulted in an overall decrease of net-charge transfer. However, even though *in situ* hybridization studies have demonstrated presence of mRNA for $Ca_V2.3$ channels in nRT neurons (Williams et al., 1994), direct substantiation of functional presynaptic $Ca_V2.3$ proteins in nRT

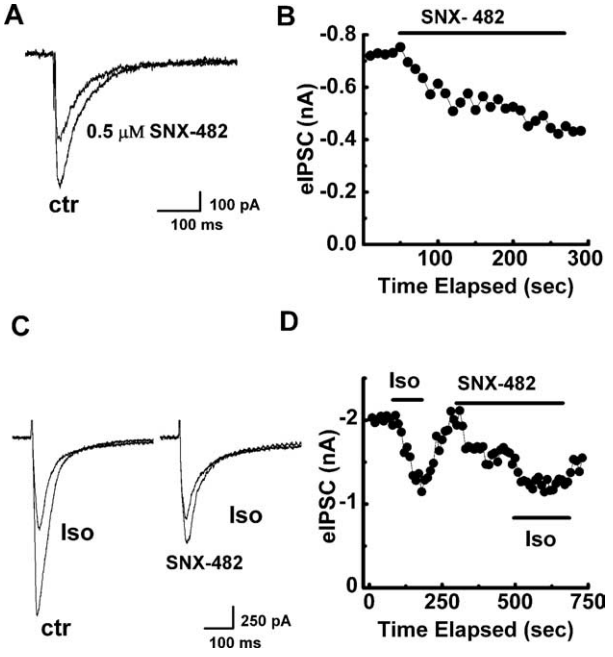

Figure 6. SNX-482-sensitive R-type Ca^{2+} channels contribute to generation of eIPSCs in nRT neurons. ***A***, ***B***, Representative eIPSC traces and time course on right recorded before and during application of 0.5 μM SNX-482, showing its effect on peak amplitude of eIPSCs. The effect of SNX-482 slowly reached a stable maximal level. There was little effect on the kinetics of eIPSCs. ***C***, Representative eIPSCs traces showing the effect of isoflurane on an nRT neuron exposed to SNX-482. After control application of 300 μM isoflurane, 0.5 μM SNX-482 was applied until stable eIPSCs were obtained, after which the neuron was reexposed to the same concentration of isoflurane. Traces originate from the same cell and are separated for clarity. Isoflurane blocked fewer eIPSCs after SNX-sensitive current was blocked. ***D***, Peak eIPSC amplitudes from the same cell as that depicted in panel C are plotted as a function of time. The reversible blocking effect of isoflurane on the amplitude of eIPSCs was diminished ~60% in the presence of SNX-482.

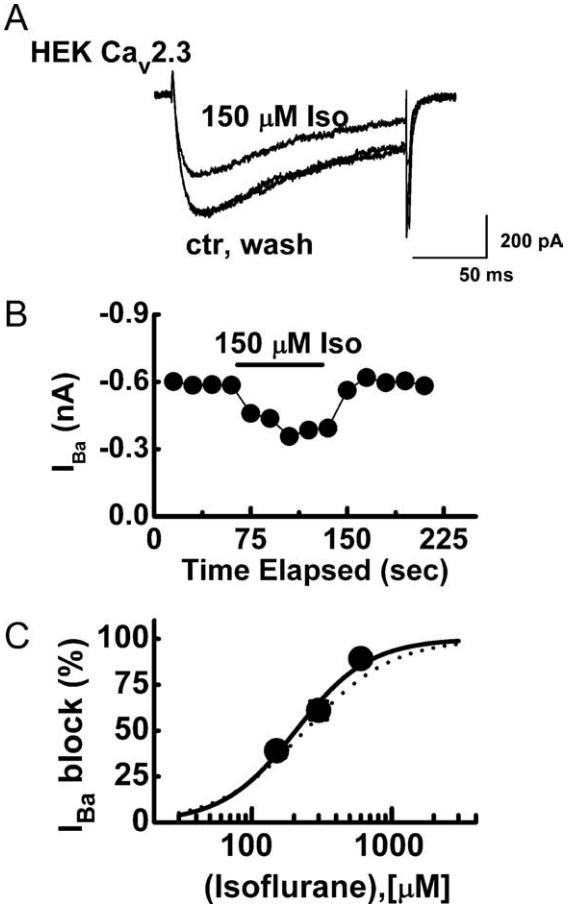

Figure 7. Isoflurane blocks human recombinant $Ca_V2.3$ currents in HEK cells. ***A***, Family of inward barium currents (V_h −70 mV, V_t 0 mV) recorded from HEK cells stably transfected with $Ca_V2.3$ channels before, during, and after application of 150 μM isoflurane. ***B***, Time course from the same cell illustrating the reversible blocking effect of 150 μM isoflurane on recombinant human $Ca_V2.3$ currents. Horizontal bar indicates the time of isoflurane application. ***C***, Solid line represents concentration–response curve best fitted with Hill function showing the effect of isoflurane on recombinant $Ca_V2.3$ currents, which yielded an IC_{50} of 206 ± 22 μM and a slope constant n of 1.66 ± 0.35. Each point on the curve is calculated as a mean from at least 6 cells. Dashed line represents concentration–response curve for isoflurane inhibition of eIPSCs in intact nRT neurons in brain slices (from Fig. 2*C*). Note that the two lines almost overlap.

neurons is difficult because nerve terminals are too small for patch-clamping and validated subtype-specific $Ca_V2.3$ antibodies are not readily available.

Previous studies have indicated that at clinically relevant concentrations isoflurane has smaller effects on other subtypes of HVA Ca^{2+} channels. For example, P-type Ca^{2+} currents in cerebellar Purkinje neurons were inhibited to <10% by 350 μM isoflurane (Hall et al., 1994). At 310 μM, isoflurane inhibited ~14% of recombinant N-type Ca^{2+} current in HEK cells (White et al., 2005). In contrast, we found that at 300 μM, isoflurane inhibited >50% of recombinant $Ca_V2.3$ R-type current and, with similar potency, inhibited vesicular release in nRT neurons. In agreement with our results, Kamatchi et al. (1999) found that 350 μM isoflurane inhibited ~45% of recombinant $Ca_V2.3$ current in *Xenopus* oocytes.

Thus, it appears that among other HVA Ca^{2+} channels, $Ca_V2.3$ have unique sensitivity to isoflurane. However, the relationship between Ca^{2+} ions and synaptic release is nonlinear (Katz and Miledi, 1970; Catterall, 2000; Zucker and Regehr, 2002). Also, neither SNX-482 nor Ni^{2+} completely occluded the effects of isoflurane on eIPSCs in our experiments. One possibility that cannot be ruled out is that blockade of P/Q or N-type, along with R-type Ca^{2+} currents, by isoflurane also contributes to the inhibition of eIPSCs in nRT neurons. This is particularly important in cases in which multiple Ca^{2+} channel subtypes contribute to vesicular release in the same synapse. We previously reported that recombinant and native T-type Ca^{2+} channels (T-channels) are potently inhibited by volatile anesthetics, including isoflurane (Todorovic and Lingle, 1998; Todorovic et al., 2000; Joksovic et al., 2005). However, T-channels are usually localized at somatic and dendritic compartments of neurons in CNS and are less likely to contribute to synaptic vesicular release. Furthermore, whereas Ni^{2+} blocks both families of channels with similar potency (Randall and Tsien, 1997), our results with SNX-482, which does not block T-currents in nRT neurons (Joksovic et al., 2005), argue that R-type channels are involved in vesicular release.

Is there functional significance in the inhibition of IPSCs by isoflurane in nRT neurons?

A complete anesthetic state involves loss of consciousness (hypnosis), movement (immobilization), pain sensation (analgesia), and recollection of the event (amnesia). In addition, most volatile general anesthetics, including isoflurane, have muscle relaxant and anticonvulsant properties. New theories propose that multiple end-points of anesthesia are mediated by multiple relevant cellular mechanisms (Urban, 2002; Rudolph and Antkowiak, 2004; Franks, 2008). According to this hypothesis, which molec-

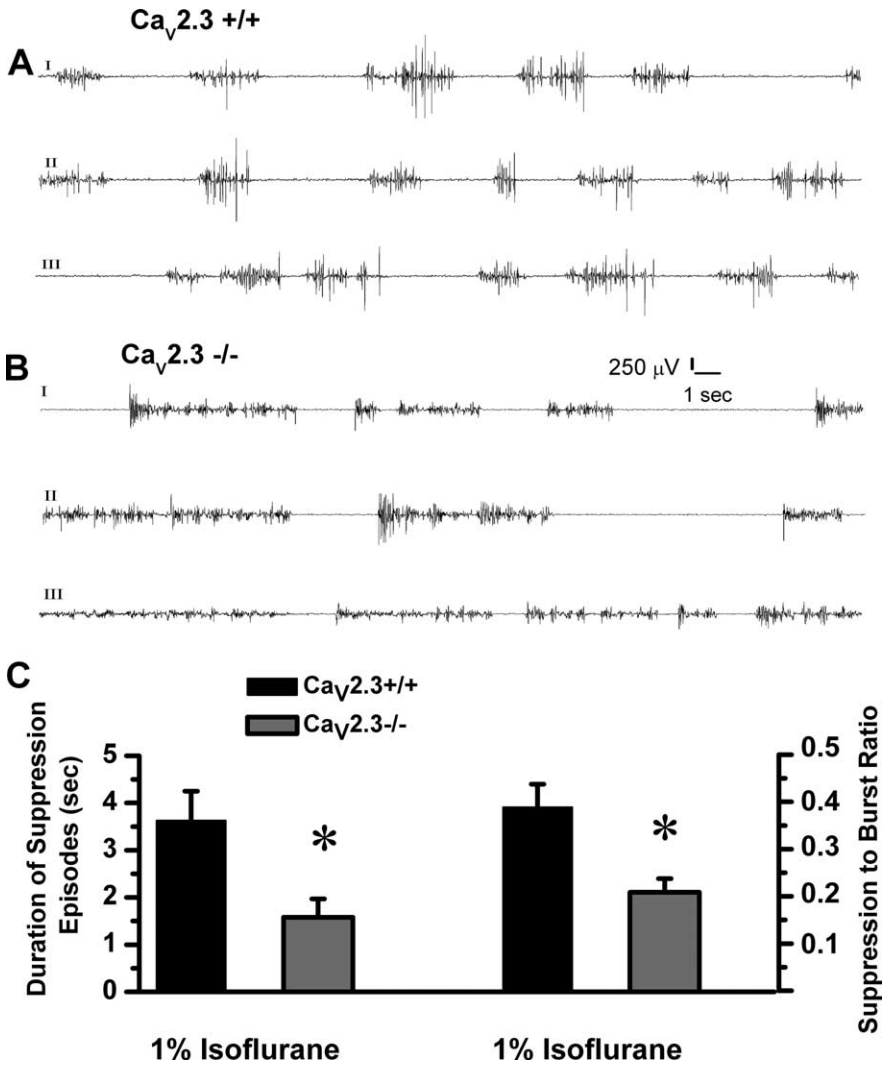

Figure 8. Alterations of isoflurane-induced burst-suppression EEG pattern in $Ca_V2.3$ KO mice. ***A***, Representative traces of EEG recordings under anesthesia with 1% isoflurane in a wild-type ($Ca_V2.3^{+/+}$) mouse. Note periods of alternating bursting activity and flatness (suppression) in recordings. ***B***, Representative traces of EEG recordings under anesthesia with 1% isoflurane in a $Ca_V2.3^{-/-}$ mouse. Note shorter periods of suppression pattern (flat line) compared with ***A***. Calibration bars pertain to ***A*** and ***B*** of this figure. ***C***, On the left, suppression episodes have been analyzed for their average duration within a 10-min period after equilibration of isoflurane. The suppression duration with isoflurane is significantly decreased in $Ca_V2.3^{-/-}$ mice (gray filled bars) compared with WT littermates (black filled bars) (asterisk indicates $p < 0.05$). On the right, the suppression to burst ratio is significantly reduced in $Ca_V2.3$-deficient mice (gray filled bars) compared with controls (black filled bars), which correlates with the strong reduction in suppression duration. Asterisk indicates $p < 0.05$.

ular target is important depends on the specific anesthetic and the specific end point in consideration.

The thalamus is a major "gateway" of corticothalamocortical functional connections. These functions are essential for awareness and cognitive functions, such as learning and memory, as well as sleep-wake cycles and epileptogenesis (Kinney et al., 1994; Llinás et al., 1999; McAlonan and Brown, 2002). Functional imaging studies in both humans and other animals have led to the theory that direct and indirect depression of thalamocortical neurons provide a convergent point for neural pathways of anesthetic action leading to a sleep-like state (Alkire et al., 2000). Mutually interconnected cortical, nRT, and thalamic relay neurons exhibit phasic behaviors such as tonic and burst firing that represent different functional modes (McCormick and Bal, 1997). During tonic firing, which predominates during awake states, there is a faithful transfer of sensory information to cortical neurons. In contrast, during slow oscillations that occur with a T-channel-dependent burst firing pattern of these neurons, there is impairment of sensory transfer and transition to sleep states. In agreement with this, $Ca_V3.1$ T-channel knock-out mice not only show slower anesthetic induction (Petrenko et al., 2007), but have an abnormal natural sleep phenotype that likely results from the lack of T-channels and underlying burst firing in thalamic relay neurons (Lee et al., 2004; Anderson et al., 2005).

Inhibitory GABAergic nRT neurons are crucial in these oscillations because their activation provides hyperpolarization of membrane potential in thalamic relay neurons. This, in turn, initiates transition to a bursting mode by deinactivating T-channels. It is difficult to predict what the particular consequence of inhibition of $Ca_V2.3$ channels and IPSCs per se in nRT cells might be in this complicated loop. However, given that nRT neurons are uniformly inhibitory, it is likely that decreasing feedback inhibition to these cells with isoflurane would initially favor a slow oscillatory mode of thalamic neurons. However, with the progressive hyperpolarization of neuronal membrane and the consequent shunting of action potentials associated with deeper anesthetic states, this could contribute to a suppression pattern and eventually lead to a completely flat line on EEG, which generally correlates with a block of sensory information at the level of the thalamic sensory gate (Steriade et al., 1994). In support of this view, we found a decrease in the duration of suppression episodes in EEG under *in vivo* isoflurane anesthesia in $Ca_V2.3$ KO mice. However, if we are to obtain a comprehensive picture, more information will be needed regarding the effects of isoflurane on ion channels other than $GABA_A$ in corticothalamic circuitry in both normal animals and $Ca_V2.3$ KO animals. For example, it is possible that the effects of anesthetics on both $GABA_A$ and K^+ conductance could contribute to suppression episodes in EEG (Steriade et al., 1994). Additionally, because molecular studies indicate that $Ca_V2.3$ is ubiquitously expressed in neurons including cerebral cortex (Williams et al., 1994), the alterations in EEG pattern could have been the result of effects of isoflurane on thalamic and/or cortical $Ca_V2.3$ R-type channels. Future studies with thalamus-specific $Ca_V2.3$ KO mice would be useful to address this issue.

In conclusion, we found that isoflurane at clinically relevant concentrations inhibits functional presynaptic R-type Ca^{2+} channels in the nRT neurons. Furthermore, these channels are ubiquitously expressed in neurons, where they have a crucial function in regulating fundamental properties of synaptic transmitter release. Thus, the potential involvement of presynaptic HVA Ca^{2+} channels as molecular targets for volatile general anesthetics warrants consideration.

References

Akrawi WP, Drummond JC, Kalkman CJ, Patel PM (1996) A comparison of the electrophysiologic characteristics of EEG burst-suppression as produced by isoflurane, thiopental, etomidate, and propofol. J Neurosurg Anesthesiol 8:40–46.

Alkire MT, Haier RJ, Fallon JH (2000) Toward a unified theory of narcosis: brain imaging evidence for a thalamocortical switch as the neurophysiologic basis of anesthetic-induced unconsciousness. Conscious Cogn 9:370–386.

Anderson MP, Mochizuki T, Xie J, Fischler W, Manger JP, Talley EM, Scammell TE, Tonegawa S (2005) Thalamic Cav3.1 T-type Ca2+ channel plays a crucial role in stabilizing sleep. Proc Natl Acad Sci U S A 102:1743–1748.

Angel A (1991) Adventures in anesthesia. Exp Physiol 76:1–38.

Asanuma C (1994) GABAergic and pallidal terminals in the thalamic reticular nucleus of squirrel monkeys. Exp Brain Res 101:439–451.

Bessaïh T, Bourgeais L, Badiu CI, Carter DA, Toth TI, Ruano D, Lambolez B, Crunelli V, Leresche N (2006) Nucleus-specific abnormalities of GABAergic synaptic transmission in a genetic model of absence seizures. J Neurophysiol 96:3074–3081.

Brown SP, Safo PK, Regehr WG (2004) Endocannabinoids inhibit transmission at granule cell to Purkinje cell synapses by modulating three types of presynaptic calcium channels. J Neurosci 24:5623–5631.

Catterall WA (2000) Structure and regulation of voltage-gated Ca^{2+} channels. Annu Rev Cell Dev Biol 16:521–555.

Cox CL, Huguenard JR, Prince DA (1996) Heterogeneous axonal arborizations of rat thalamic reticular neurons in the ventrobasal nucleus. J Comp Neurol 366:416–430.

Detsch O, Kochs E, Siemers M, Bromm B, Vahle-Hinz C (2002) Differential effects of isoflurane on excitatory and inhibitory synaptic inputs to thalamic neurones in vivo. Br J Anaesth 89:294–300.

Franks NP (2008) General anaesthesia: from molecular targets to neuronal pathways of sleep and arousal. Nat Rev Neurosci 9:370–386.

Franks NP, Lieb WR (1994) Molecular and cellular mechanisms of general anesthesia. Nature 367:607–614.

Franks NP, Dickinson R, de Sousa SL, Hall AC, Lieb WR (1998) How does xenon produce anaesthesia? Nature 396:324.

Gasparini S, Kasyanov AM, Pietrobon D, Voronin LL, Cherubini E (2001) Presynaptic R-type calcium channels contribute to fast excitatory synaptic transmission in the rat hippocampus. J Neurosci 21:8715–8721.

Hall AC, Lieb WR, Franks NP (1994) Insensitivity of P-type calcium channels to inhalational and intravenous general anesthetics. Anesthesiology 81:117–123.

Herrington J, Stern RC, Evers AS, Lingle CJ (1991) Halothane inhibits two components of calcium current in clonal (GH_3) pituitary cells. J Neurosci 11:2226–2240.

Huntsman MM, Huguenard JR (2000) Nucleus-specific differences in $GABA_A$-receptor-mediated inhibition are enhanced during thalamic development. J Neurophysiol 83:350–358.

Huguenard JR, Prince DA (1992) A novel T-type current underlies prolonged Ca^{2+}-dependent burst firing in GABAergic neurons of rat thalamic reticular nucleus. J Neurosci 12:3804–3817.

Jevtović-Todorović V, Todorović SM, Mennerick S, Powell S, Dikranian K, Benshoff N, Zorumski CF, Olney JW (1998) Nitrous oxide (laughing gas) is an NMDA antagonist, neuroprotectant and neurotoxin. Nat Med 4:460–463.

Joksovic PM, Bayliss DA, Todorovic SM (2005) Different kinetic properties of two T-type Ca^{2+} currents of rat reticular thalamic neurons and their modulation by enflurane. J Physiol 566:125–142.

Jones EG (1985) The thalamus. New York: Plenum.

Jourdain A, Semba K, Fibiger HC (1989) Basal forebrain and mesopontine tegmental projections of the reticular thalamic nucleus: an axonal collateralization and immunohistological study in the rat. Brain Res 505:55–65.

Kamatchi GL, Chan CK, Snutch T, Durieux ME, Lynch C 3rd (1999) Volatile anesthetic inhibition of neuronal Ca channel currents expressed in *Xenopus* oocytes. Brain Res 831:85–96.

Katz B, Miledi R (1970) Further study of the role of calcium in synaptic transmission. J Physiol 207:789–801.

Kinney HC, Korein J, Panigrahy A, Dikkes P, Goode R (1994) Neuropathological findings in the brain of Karen Ann Quinlan: the role of the thalamus in the persistent vegetative state. N Engl J Med 330:1469–1475.

Lee J, Kim D, Shin HS (2004) Lack of delta waves and sleep disturbances during non-rapid eye movement sleep in mice lacking alpha1G-subunit of T-type calcium channels. Proc Natl Acad Sci U S A 101:18195–18199.

Llinás RR, Ribary U, Jeanmonod D, Kronberg E, Mitra PP (1999) Thalamocortical dysrhythmia: a neurological and neuropsychiatric syndrome characterized by magnetoencephalography. Proc Natl Acad Sci U S A 96:15222–15227.

McAlonan K, Brown VJ (2002) The thalamic reticular nucleus: more than a sensory nucleus? Neuroscientist 8:302–305.

McCormick DA, Bal T (1997) Sleep and arousal: thalamocortical mechanisms. Annu Rev Neurosci 20:185–215.

McDowell TS, Pancrazio JJ, Lynch C 3rd (1996) Volatile anesthetics reduce low-voltage-activated calcium currents in a thyroid C-cell line. Anesthesiology 85:1167–1175.

Mennerick S, Jevtovic-Todorovic V, Todorovic SM, Shen W, Olney JW, Zorumski CF (1998) Effects of nitrous oxide (laughing gas) on excitatory and inhibitory synaptic transmission in hippocampal cultures. J Neurosci 18:9716–9726.

Meyer H (1899) Zur Theorie der Alcoholnarkose. Arch Exp Pathol Pharmacol 42:109–118.

Nakashima YM, Todorovic SM, Pereverzev A, Hescheler J, Schneider T, Lingle CJ (1998) Properties of Ca^{2+} currents arising from human α_{1E} and $\alpha_{1E}\beta_3$ constructs expressed in HEK293 cells: physiology, pharmacology, and comparison to native T-type Ca^{2+} currents. Neuropharmacology 37:957–972.

Newcomb R, Szoke B, Palma A, Wang G, Chen X, Hopkins W, Cong R, Miller J, Urge L, Tarczy-Hornoch K, Loo JA, Dooley DJ, Nadasdi L, Tsien RW, Lemos J, Miljanich G (1998) Selective peptide antagonist of the class E calcium channel from the venom of the tarantula *Hysterocrates gigas.* Biochemistry 37:15353–15362.

Overton S (1901) Studien Uber die Narkose Zugleich Ein Beitrag Zur Allgemeinen Pharmakologie. Jena: Verlag von Gustav Fischer.

Paré D, Hazrati LN, Parent A, Steriade M (1990) Substantia nigra pars reticulate projects to the reticular thalamic nucleus of the cat: a morphological and electrophysiological study. Brain Res 535:139–146.

Paxinos G, Watson C (1986) The rat brain in stereotaxic coordinates. Sydney: Academic.

Pereverzev A, Mikhna M, Vajna R, Gissel C, Henry M, Weiergräber M, Hescheler J, Smyth N, Schneider T (2002) Disturbances in glucose-tolerance, insulin-release, and stress-induced hyperglycemia upon disruption of the Ca(v) 2.3 (alpha 1E) subunit of voltage-gated Ca(2+) channels. Mol Endocrinol 16:884–895.

Petrenko AB, Tsujita M, Kohno T, Sakimura K, Baba H (2007) Mutation of alpha1G T-type calcium channels in mice do not change the anesthetic requirements for loss of righting reflex and minimum alveolar concentration but delays the onset of anesthetic induction. Anesthesiology 106:1177–1185.

Randall AD, Tsien RW (1997) Contrasting biophysical and pharmacological properties of T-type and R-type calcium channels. Neuropharmacology 36:879–893.

Rudolph U, Antkowiak B (2004) Molecular and neuronal substrates for general anaesthetics. Nat Rev Neurosci 5:709–720.

Sanchez-Vives MV, Bal T, McCormick DA (1997) Inhibitory interactions between perigeniculate GABAergic neurons. J Neurosci 17:8894–8908.

Schneider T, Wei X, Olcese R, Costantin JL, Neely A, Palade P, Perez-Reyes E, Qin N, Zhou J, Crawford GD, Smith RG, Appel SH, Stefani E, Birnbaumer L (1994) Molecular analysis and functional expression of the human type E neuronal Ca^{2+} channel alpha 1 subunit. Receptors Channels 2:255–270.

Shu Y, McCormick DA (2002) Inhibitory interactions between ferret thalamic reticular neurons. J Neurophysiol 87:2571–2576.

Steriade M, Amzica F, Contreras D (1994) Cortical and thalamic cellular correlates of electroencephalographic burst-suppression. Electroencephalogr Clin Neurophysiol 90:1–16.

Stevens WC, Kingston HGG (1992) Inhalation anesthesia. In: Clinical anesthesia, Ed 2 (Barash PG, ed), pp 429–465. Philadelphia: Lippincott.

Study RE (1994) Isoflurane inhibits multiple voltage-gated calcium current in hippocampal pyramidal neurons. Anesthesiology 81:104–116.

Takenoshita M, Steinbach JH (1991) Halothane blocks low-voltage-activated calcium current in rat sensory neurons. J Neurosci 11:1404–1412.

Todorovic SM, Lingle CJ (1998) Pharmacological properties of T-type

Ca^{2+} current in adult rat sensory neurons: effects of anticonvulsant and anesthetic agents. J Neurophysiol 79:240–252.

Todorovic SM, Perez-Reyes E, Lingle CJ (2000) Anticonvulsants but not general anesthetics have differential blocking effects on different T-type current variants. Mol Pharmacol 58:98–108.

Tottene A, Volsen S, Pietrobon D (2000) Alpha (1E) subunits form the pore of three cerebellar R-type calcium channels with different pharmacological and permeation properties. J Neurosci 20:171–178.

Urban BW (2002) Current assessment of targets and theories of anaesthesia. Br J Anaesth 89:167–183.

Vahle-Hinz C, Detsch O, Hackner C, Kochs E (2007a) Corresponding minimum alveolar concentrations of isoflurane and isoflurane/nitrous oxide have divergent effects on thalamic nociceptive signalling. Br J Anaesth 98:228–235.

Vahle-Hinz C, Detsch O, Siemers M, Kochs E (2007b) Contributions of GABAergic and glutamatergic mechanisms to isoflurane-induced suppression of thalamic somatosensory information transfer. Exp Brain Res 176:159–172.

Weiergräber M, Henry M, Hescheler J, Smyth N, Schneider T (2005) Electrocorticographic and deep intracerebral EEG recording in mice using a telemetry system. Brain Res Brain Res Protoc 14:154–164.

Weiergräber M, Henry M, Krieger A, Kamp M, Radhakrishnan K, Hescheler J, Schneider T (2006) Altered seizure susceptibility in mice lacking the Ca(v) 2.3 E-type Ca2+ channel. Epilepsia 47:839–850.

White IL, Franks NP, Dickinson R (2005) Effects of isoflurane and xenon on Ba2+-currents mediated by N-type calcium channels. Br J Anaesth 94:784–790.

Williams ME, Marubio LM, Deal CR, Hans M, Brust PF, Philipson LH, Miller RJ, Johnson EC, Harpold MM, Ellis SB (1994) Structure and functional characterization of neuronal alpha 1E calcium channel subtypes. J Biol Chem 269:22347–22357.

Wu LG, Saggau P (1997) Presynaptic inhibition of elicited neurotransmitter release. Trends Neurosci 20:204–212.

Wu LG, Borst JG, Sakmann B (1998) R-type Ca^{2+} currents evoke transmitter release at a rat central synapse. Proc Natl Acad Sci U S A 95:4720–4725.

Zamponi GW, Bourinet E, Snutch TP (1996) Nickel block of a family of neuronal calcium channels: subtype- and subunit-dependent action at multiple sites. J Membr Biol 151:77–90.

Zhang SJ, Huguenard JR, Prince DA (1997) $GABA_A$ receptor-mediated Cl^- currents in rat thalamic reticular and relay neurons. J Neurophysiol 78: 22890–22896.

Zucker RS, Regehr WG (2002) Short-term synaptic plasticity. Annu Rev Physiol 64:355–405.

4. Abschließende Bemerkungen und Ausblick

Die vorliegenden Originalarbeiten dokumentieren, dass $Ca_v2.3$ Ca^{2+}-Kanäle eine wichtige, bislang unbekannte Rolle bei der Anfallsuszeptibilität sowohl konvulsiver und nicht-konvulsiver Anfallsformen spielen. Während $Ca_v2.3$ Defizienz zu einer Resistenz gegenüber konvulsiven Anfallsformen führt und mit reduzierter Exzitotoxizität einhergeht, zeigt sich bei nicht-konvulsiven Versuchskautelen eine erhöhte Anfallssuszeptibilität. Das Fehlen kompensatorischer Regulation anderer spannungsgesteuerter Ca^{2+}-Kanäle und fehlende morphologische Alterationen bei $Ca_v2.3^{-/-}$ Mäusen unterstreichen darüber hinaus, dass die beschriebenen Effekte dem $Ca_v2.3$ Ca^{2+}-Kanal selbst zuzurechnen sind. Nicht zuletzt erinnert die diametral entgegengesetzte Beeinflussung konvulsiver und nicht-konvulsiver Anfallsformen durch $Ca_v2.3$ Ca^{2+}-Kanäle daran, dass Ionenkanalentitäten nicht per se proiktogen oder antiiktogene Kapazität in sich tragen. Hingegen ist das physiologische und pathophysiologische Potential abhängig von der funktionellen und strukturellen Integration in spezifische neuronale Schaltkreise. Der $Ca_v2.3$ Ca^{2+}-Kanal ist damit auch als potentielle Zielstruktur neuer Antiepileptika und Neuroprotektiva von zentraler Bedeutung in der Zukunft.

5. Literatur

Albowitz B, Konig P, Kuhnt U (1997) Spatiotemporal distribution of intracellular calcium transients during epileptiform activity in guinea pig hippocampal slices. J Neurophysiol 77: 491-501.

Andres M, Andre VM, Nguyen S, Salamon N, Cepeda C, Levine MS, Leite JP, Neder L, Vinters HV, Mathern GW (2005) Human cortical dysplasia and epilepsy: an ontogenetic hypothesis based on volumetric MRI and NeuN neuronal density and size measurements. Cereb Cortex 15: 194-210.

Andrew RD, Dudek FE (1984) Analysis of intracellularly recorded phasic bursting by mammalian neuroendocrine cells. J Neurophysiol 51: 552-566.

Arikkath J, Campbell KP (2003) Auxiliary subunits: essential components of the voltage-gated calcium channel complex. Curr Opin Neurobiol 13: 298-307.

Bannister RA, Melliti K, Adams BA (2004) Differential Modulation of $Ca_v2.3$ Ca^{2+} Channels by G(alpha)q/11-Coupled Muscarinic Receptors. Mol Pharmacol 65: 381-388.

Bech-Hansen NT, Naylor MJ, Maybaum TA, Pearce WG, Koop B, Fishman GA, Mets M, Musarella M.A., cott KM (1998) Loss-of-function mutations in a calcium-channel α_1-subunit gene in Xp11.23 cause incomplete X-linked congenital stationary night blindness. Nature Genet 19: 264-267.

Beck H, Steffens R, Elger CE, Heinemann U (1998) Voltage-dependent Ca^{2+} currents in epilepsy. Epilepsy Res 32: 321-332.

Bers DM (2002) Cardiac excitation-contraction coupling. Nature 415: 198-205.

Bidaud I, Mezghrani A, Swayne LA, Monteil A, Lory P (2006) Voltage-gated calcium channels in genetic diseases. Biochim Biophys Acta 1763: 1169-1174.

Bito H, Deisseroth K, Tsien RW (1997) Ca^{2+}-dependent regulation in neuronal gene expression. Curr Opin Neurobiol 7: 419-429.

Black JL, III (2003) The voltage-gated calcium channel gamma subunits: a review of the literature. J Bioenerg Biomembr 35: 649-660.

Bloodgood BL, Sabatini BL (2007) Nonlinear regulation of unitary synaptic signals by $Ca_v2.3$ voltage-sensitive calcium channels located in dendritic spines. Neuron 53: 249-260.

Brenowitz SD, Regehr WG (2003) "Resistant" channels reluctantly reveal their roles. Neuron 39: 391-394.

Breustedt J, Vogt KE, Miller RJ, Nicoll RA, Schmitz D (2003) Alpha1E-containing Ca^{2+} channels are involved in synaptic plasticity. Proc Natl Acad Sci U S A 100: 12450-12455.

Brown SG, Thomas A, Dekker LV, Tinker A, Leaney JL (2005) PKC-delta sensitizes $K_{ir}3.1/3.2$ channels to changes in membrane phospholipid levels after M_3 receptor activation in HEK-293 cells. Am J Physiol Cell Physiol 289: C543-C556.

Buzsaki G (2006) Rhythms of the brain. Oxford University Press.

Byrne J.H. and Roberts J.L. From Molecules to Networks: An Introduction to Cellular and Molecular Neuroscience. Elsevier Academic Press.

Caputi L, Hainsworth AH, Lavaroni F, Leach MJ, McNaughton NC, Mercuri NB, Randall AD, Spadoni F, Swan JH, Stefani A (2001) Neuroprotective actions in vivo and electrophysiological actions in vitro of 202W92. Brain Res 919: 259-268.

Cassel JC, Kelche C, Will BE (1987) Susceptibility to pentylenetetrazol-induced and audiogenic seizures in rats with selective fimbria-fornix lesions and intrahippocampal septal grafts. Exp Neurol 97: 564-576.

Catterall WA (1999) Interactions of presynaptic Ca^{2+} channels and snare proteins in neurotransmitter release. Ann N Y Acad Sci 868: 144-159.

Catterall WA (2000) Structure and Regulation of Voltage-Gated Ca^{2+} Channels. Annu Rev Cell Dev Biol 16: 521-555.

Catterall WA, Perez-Reyes E, Snutch TP, Striessnig J (2005) International Union of Pharmacology. XLVIII. Nomenclature and structure-function relationships of voltage-gated calcium channels. Pharmacol Rev 57: 411-425.

Chen S, Ren YQ, Bing RJ, Hillman DE (2000) Alpha1E subunit of the R-type calcium channel is associated with myelinogenesis. J Neurocytol 29: 719-728.

Chen Y, Lu J, Pan H, Zhang Y, Wu H, Xu K, Liu X, Jiang Y, Bao X, Yao Z, Ding K, Lo WH, Qiang B, Chan P, Shen Y, Wu X (2003) Association between genetic variation of CACNA1H and childhood absence epilepsy. Ann Neurol 54: 239-243.

Chuang RS, Jaffe H, Cribbs L, Perez-Reyes E, Swartz KJ (1998) Inhibition of T-type voltage-gated calcium channels by a new scorpion toxin. Nature Neurosci 1: 668-674.

Cloues RK, Sather WA (2003) Afterhyperpolarization regulates firing rate in neurons of the suprachiasmatic nucleus. J Neurosci 23: 1593-1604.

Coulter DA, Huguenard JR, Prince DA (1989) Specific petit mal anticonvulsants reduce calcium currents in thalamic neurons. Neurosci Lett 98: 74-78.

Danober L, Deransart C, Depaulis A, Vergnes M, Marescaux C (1998) Pathophysiological mechanisms of genetic absence epilepsy in the rat. Prog Neurobiol 55: 27-57.

Day NC, Shaw PJ, McCormack AL, Craig PJ, Smith W, Beattie R, Williams TL, Ellis SB, Ince PG, Harpold MM, Lodge D, Volsen SG (1996) Distribution of α_1A, α_1B and α_1E voltage-dependent calcium channel subunits in the human hippocampus and parahippocampal gyrus. Neuroscience 71: 1013-1024.

Day NC, Wood SJ, Ince PG, Volsen SG, Smith W, Slater CR, Shaw PJ (1997) Differential localization of voltage-dependent calcium channel α_1 subunits at the human and rat neuromuscular junction. J Neurosci 17: 6226-6235.

De Borman B, Lakaye B, Minet A, Zorzi W, Vergnes M, Marescaux C, Grisar T (1999) Expression of mRNA encoding α_1E and α_1G subunit in the brain of a rat model of absence epilepsy. Neuroreport 10: 569-574.

DeLorenzo RJ, Pal S, Sombati S (1998) Prolonged activation of the N-methyl-D-aspartate receptor-Ca^{2+} transduction pathway causes spontaneous recurrent epileptiform discharges in hippocampal neurons in culture. Proc Natl Acad Sci U S A 95: 14482-14487.

DeLorenzo RJ, Sombati S, Coulter DA (2000) Effects of topiramate on sustained repetitive firing and spontaneous recurrent seizure discharges in cultured hippocampal neurons. Epilepsia 41 Suppl 1: S40-S44.

Deransart C, Le Pham BT, Hirsch E, Marescaux C, Depaulis A (2001) Inhibition of the substantia nigra suppresses absences and clonic seizures in audiogenic rats, but not tonic seizures: evidence for seizure specificity of the nigral control. Neuroscience 105: 203-211.

Dietrich D, Kirschstein T, Kukley M, Pereverzev A, von der Brelie C, Schneider T, Beck H (2003) Functional specialization of presynaptic $Ca_v2.3$ Ca^{2+} channels. Neuron 39: 483-496.

Dirksen RT (2002) Bi-directional coupling between dihydropyridine receptors and ryanodine receptors. Front Biosci 7: d659-d670.

Dirksen RT, Beam KG (1995) Single calcium channel behavior in native skeletal muscle. J Gen Physiol 105: 227-247.

Dirksen RT, Nakai J, Gonzalez A, Imoto K, Beam KG (1997) The S5-S6 linker of repeat I is a critical determinant of L-type Ca^{2+} channel conductance. Biophys J 73: 1402-1409.

Dolphin AC (2003) Beta subunits of voltage-gated calcium channels. J Bioenerg Biomembr 35: 599-620.

Ertel EA, Campbell KP, Harpold MM, Hofmann F, Mori Y, Perez-Reyes E, Schwartz A, Snutch TP, Tanabe T, Birnbaumer L, Tsien RW, Catterall WA (2000) Nomenclature of voltage-gated calcium channels. Neuron 25: 533-535.

Escayg A, De Waard M, Lee DD, Bichet D, Wolf P, Mayer T, Johnston J, Baloh R, Sander T, Meisler MH (2000) Coding and noncoding variation of the human calcium-channel beta4- subunit gene CACNB4 in patients with idiopathic generalized epilepsy and episodic ataxia. Am J Hum Genet 66: 1531-1539.

Eskazan E, Aker R, Onat F, Koseoglu S, Goren MZ, Hasanoglu A (1999) Effect of pirenzepine, a muscarinic M1 receptor antagonist, on amygdala kindling in rat. Epilepsy Res 37: 133-140.

Fanelli RJ, McCarthy RT, Chisholm J (1994) Neuropharmacology of nimodipine: from single channels to behavior. Ann N Y Acad Sci 747: 336-350.

Felix R (2002) Insights from mouse models of absence epilepsy into Ca^{2+} channel physiology and disease etiology. Cellular and Molecular Neurobiology 22: 103-120.

Felix R (2005) Molecular regulation of voltage-gated Ca^{2+} channels. Journal of Receptors and Signal Transduction 25: 57-71.

Felix R (2006) Calcium channelopathies. Neuromolecular Med 8: 307-318.

Filakovszky J, Gerber K, Bagdy G (1999) A serotonin-1A receptor agonist and an N-methyl-D-aspartate receptor antagonist oppose each others effects in a genetic rat epilepsy model. Neurosci Lett 261: 89-92.

Fontaine B, Vale-Santos J, Jurkat-Rott K, Reboul J, Plassart E, Rime C-S, Elbaz A, Heine R, Guimaraes J, Weissenbach J, Baumann N, Fardeau M, Lehmann-Horn F (1994) Mapping of the hypokalaemic periodic paralysis (HypoPP) locus to chromosome 1q31-32 in three European families. Nature Genet 6: 267-272.

Fraser DD, MacVicar BA (1996) Cholinergic-dependent plateau potential in hippocampal CA1 pyramidal neurons. J Neurosci 16: 4113-4128.

Freise D, Held B, Wissenbach U, Pfeifer A, Trost C, Himmerkus N, Schweig U, Freichel M, Biel M, Hofmann F, Hoth M, Flockerzi V (2000) Absence of the gamma subunit of the skeletal muscle dihydropyridine receptor increases L-type Ca^{2+} currents and alters channel inactivation properties. J Biol Chem 275: 14476-14481.

Gahwiler BH, Brown DA (1987) Muscarine affects calcium-currents in rat hippocampal pyramidal cells in vitro. Neurosci Lett 76: 301-306.

Glossmann H, Striessnig J (1988) Structure and pharmacology of voltage-dependent calcium channels. ISI Atlas pharmacol 2: 202-210.

Gomora JC, Daud AN, Weiergraber M, Perez-Reyes E (2001) Block of cloned human T-type calcium channels by succinimide antiepileptic drugs. Mol Pharmacol 60: 1121-1132.

Grabsch H, Pereverzev A, Weiergräber M, Schramm M, Henry M, Vajna R, Beattie RE, Volsen SG, Klöckner U, Hescheler J, Schneider T (1999) Immunohistochemical detection of α_1E voltage-gated Ca^{2+} channel isoforms in cerebellum, INS-1 cells, and neuroendocrine cells of the digestive system. J Histochem Cytochem 47: 981-993.

Green JD (1964) THE HIPPOCAMPUS. Physiol Rev 44: 561-608.

Hainsworth AH, McNaughton NC, Pereverzev A, Schneider T, Randall AD (2003) Actions of sipatrigine, 202W92 and lamotrigine on R-type and T-type Ca^{2+} channel currents. Eur J Pharmacol 467: 77-80.

Hainsworth AH, Stefani A, Calabresi P, Smith TW, Leach MJ (2000) Sipatrigine (BW 619C89) is a neuroprotective agent and a sodium channel and calcium channel inhibitor. Cns Drug Reviews 6: 111-134.

Hamilton SE, Loose MD, Qi M, Levey AI, Hille B, McKnight GS, Idzerda RL, Nathanson NM (1997) Disruption of the M_1 receptor gene ablates muscarinic receptor- dependent M current regulation and seizure activity in mice. Proc Natl Acad Sci USA 94: 13311-13316.

Hamon B, Heinemann U (1986) Effects of GABA and bicuculline on N-methyl-D-aspartate- and quisqualate-induced reductions in extracellular free calcium in area CA1 of the hippocampal slice. Exp Brain Res 64: 27-36.

Hanson JE, Smith Y (2002) Subcellular distribution of high-voltage-activated calcium channel subtypes in rat globus pallidus neurons. J Comp Neurol 442: 89-98.

Hell JW, Westenbroek RE, Warner C, Ahlijanian MK, Prystay W, Gilbert MM, Snutch TP, Catterall WA (1993) Identification and differential subcellular localization of the neuronal class C and class D L-type calcium channel α_1 subunits. J Cell Biol 123: 949-962.

Hendriksen H, Kamphuis W, Lopes da Silva FH (1997) Changes in voltage-dependent calcium channel alpha1-subunit mRNA levels in the kindling model of epileptogenesis. Mol Brain Res 50: 257-266.

Herzig S, Khan IF, Grundemann D, Matthes J, Ludwig A, Michels G, Hoppe UC, Chaudhuri D, Schwartz A, Yue DT, Hullin R (2007) Mechanism of $Ca_v1.2$ channel modulation by the amino terminus of cardiac (beta)2-subunits. FASEB J 21: 1527-1538.

Hlubek MD, Cobbett P (2000) Differential effects of K^+ channel blockers on frequency-dependent action potential broadening in supraoptic neurons. Brain Res Bull 53: 203-209.

Hofmann F, Lacinová L, Klugbauer N (1999) Voltage-dependent calcium channels: From structure to function. Rev Physiol Biochem Pharmacol 139: 33-87.

Holmkvist J, Tojjar D, Almgren P, Lyssenko V, Lindgren CM, Isomaa B, Tuomi T, Berglund G, Renstrom E, Groop L (2007) Polymorphisms in the gene encoding the voltage-dependent Ca^{2+} channel $Ca_v2.3$ (CACNA1E) are associated with type 2 diabetes and impaired insulin secretion. Diabetologia 50: 2467-2475.

Hounsgaard J, Kiehn O (1989) Serotonin-induced bistability of turtle motoneurones caused by a nifedipine-sensitive calcium plateau potential. J Physiol 414: 265-282.

Hu H, Marban E (1998) Isoform-specific inhibition of L-type calcium channels by dihydropyridines is independent of isoform-specific gating properties. Mol Pharmacol 53: 902-907.

Ishiguro M, Wellman TL, Honda A, Russell SR, Tranmer BI, Wellman GC (2005) Emergence of a R-type Ca^{2+} channel $Ca_v2.3$ contributes to cerebral artery constriction after subarachnoid hemorrhage. Circ Res 96: 419-426.

Jacobs MP, Fischbach GD, Davis MR, Dichter MA, Dingledine R, Lowenstein DH, Morrell MJ, Noebels JL, Rogawski MA, Spencer SS, Theodore WH (2001) Future directions for epilepsy research. Neurology 57: 1536-1542.

Jalkanen R, Mantyjarvi M, Tobias R, Isosomppi J, Sankila EM, Alitalo T, Bech-Hansen NT (2006) X-linked cone-rod dystrophy, CORDX3, is caused by a mutation in the CACNA1F gene. J Med Genet 43: 699-704.

Jing X, Li DQ, Olofsson CS, Salehi A, Surve VV, Caballero J, Ivarsson R, Lundquist I, Pereverzev A, Schneider T, Rorsman P, Renstrom E (2005) $Ca_v2.3$ calcium channels control second-phase insulin release. J Clin Invest 115: 146-154.

Joksovic PM, Weiergräber M, Lee WY, Struck H, Schneider T, Todorovic SM (2009) Isoflurane-sensitive presynaptic R-type calcium channels contribute to inhibitory synaptic transmission in the rat thalamus. J Neurosci in press.

Joshi I, Taylor CP (2006) Pregabalin action at a model synapse: Binding to presynaptic calcium channel alpha(2)-delta subunit reduces neurotransmission in mice. Eur J Pharmacol 553: 82-88.

Jouvenceau A, Eunson LH, Spauschus A, Ramesh V, Zuberi SM, Kullmann DM, Hanna MG (2001) Human epilepsy associated with dysfunction of the brain P/Q-type calcium channel. Lancet 358: 801-807.

Jun K, Piedras-Renteria ES, Smith SM, Wheeler DB, Lee SB, Lee TG, Chin HM, Adams ME, Scheller RH, Tsien RW, Shin HS (1999) Ablation of P/Q-type Ca^{2+} channel currents, altered synaptic transmission, and progressive ataxia in mice lacking the α_{1A}- subunit. Proc Natl Acad Sci USA 96: 15245-15250.

Kamp MA, Krieger A, Henry M, Hescheler J, Weiergraber M, Schneider T (2005) Presynaptic $Ca_v2.3$-containing E-type Ca channels share dual roles during neurotransmitter release. Eur J Neurosci 21: 1617-1625.

Kang MG, Campbell KP (2003) γ Subunit of Voltage-activated Calcium Channels. J Biol Chem 278: 21315-21318.

Kang TC, Kim DS, Yoo KY, Hwang IK, Kwak SE, Kim JE, Jung JY, Won MH, Suh JG, Oh YS (2004) Elevated voltage-gated Ca^{2+} channel immunoreactivities in the hippocampus of seizure-prone gerbil. Brain Res 1029: 168-178.

Kavoussi R (2006) Pregabalin: From molecule to medicine. Eur Neuropsychopharmacol 16 Suppl 2: S128-S133.

Kawasaki K, Eigyo M, Ikeda M, Kihara T, Koike K, Matsushita A, Murata S, Shiomi T, Takada S, Yasui M (1996) A novel benzodiazepine inverse agonist, S-8510, as a cognitive enhancer. Prog Neuropsychopharmacol Biol Psychiatry 20: 1413-1425.

Khosravani H, Altier C, Simms B, Hamming KS, Snutch TP, Mezeyova J, McRory JE, Zamponi GW (2004) Gating effects of mutations in the $Ca_v3.2$ T-type calcium channel associated with childhood absence epilepsy. J Biol Chem 279: 9681-9684.

Khosravani H, Zamponi GW (2006) Voltage-gated calcium channels and idiopathic generalized epilepsies. Physiol Rev 86: 941-966.

Kim D, Song I, Keum S, Lee T, Jeong MJ, Kim SS, McEnery MW, Shin HS (2001) Lack of the burst firing of thalamocortical relay neurons and resistance to absence seizures in mice lacking α_{1G} T-type Ca^{2+} channels. Neuron 31: 35-45.

Kito M, Maehara M, Watanabe K (1996) Mechanisms of T-type calcium channel blockade by zonisamide. Seizure 5: 115-119.

Klöckner U, Lee JH, Cribbs LL, Daud A, Hescheler J, Pereverzev A, Perez-Reyes E, Schneider T (1999) Comparison of the Ca^{2+} currents induced by expression of three cloned α_1 subunits, α_1G, α_1H and α_1I, of low-voltage-activated T- type Ca^{2+} channels. Eur J Neurosci 11: 4171-4178.

Klöckner U, Pereverzev A, Leroy J, Krieger A, Vajna R, Hescheler J, Pfitzer G, Malecot CO, Schneider T (2004) The cytosolic II-III loop of $Ca_v2.3$ provides an essential determinant for the phorbol ester-mediated stimulation of E-type Ca^{2+} channel activity. Eur J Neurosci 19: 2659-2668.

Klotz U (2006) Ziconotide-a novel neuron-specific calcium channel blocker for the intrathecal treatment of severe chronic pain-a short review. Int J Clin Pharmacol Ther 44: 478-483.

Klugbauer N, Marais E, Hofmann F (2003) Calcium channel alpha2delta subunits: differential expression, function, and drug binding. J Bioenerg Biomembr 35: 639-647.

Kohling R, Nischt R, Vasudevan A, Ho M, Weiergraber M, Schneider T, Smyth N (2006) Nidogen and nidogen-associated basement membrane proteins and neuronal plasticity. Neurodegener Dis 3: 56-61.

Koschak A, Reimer D, Huber I, Grabner M, Glossmann H, Engel J, Striessnig J (2001) α_1D (Ca_v1.3) subunits can form L-type Ca^{2+} channels activating at negative voltages. J Biol Chem 276: 22100-22106.

Kubota M, Murakoshi T, Saegusa H, Kazuno A, Zong S, Hu Q, Noda T, Tanabe T (2001) Intact LTP and Fear Memory but Impaired Spatial Memory in Mice Lacking Ca_v2.3 (α_1E) Channel. Biochem Biophys Res Commun 282: 242-248.

Kullmann DM (2002) The neuronal channelopathies. Brain 125: 1177-1195.

Kuzmiski JB, Barr W, Zamponi GW, MacVicar BA (2005) Topiramate inhibits the initiation of plateau potentials in CA1 neurons by depressing R-type calcium channels. Epilepsia 46: 481-489.

Kuzmiski JB, MacVicar BA (2001) Cyclic nucleotide-gated channels contribute to the cholinergic plateau potential in hippocampal CA1 pyramidal neurons. J Neurosci 21: 8707-8714.

Lacinova L (2004) Pharmacology of recombinant low-voltage activated calcium channels. Curr Drug Targets CNS Neurol Disord 3: 105-111.

Lacinova L (2005) Voltage-dependent calcium channels. Gen Physiol Biophys 24 Suppl 1: 1-78.

Lakaye B, Thomas E, Minet A, Grisar T (2002) The genetic absence epilepsy rat from Strasbourg (GAERS), a rat model of absence epilepsy: computer modeling and differential gene expression. Epilepsia 43 Suppl 5: 123-129.

LaRoche SM, Helmers SL (2004) The new antiepileptic drugs: scientific review. JAMA 291: 605-614.

Lee J, Kim D, Shin HS (2004) Lack of delta waves and sleep disturbances during non-rapid eye movement sleep in mice lacking alpha1G-subunit of T-type calcium channels. Proc Natl Acad Sci U S A 101: 18195-18199.

Lee JH, Gomora JC, Cribbs LL, Perez-Reyes E (1999) Nickel block of three cloned T-type calcium channels: Low concentrations selectively block α_1H. Biophys J 77: 3034-3042.

Lee SC, Choi S, Lee T, Kim HL, Chin H, Shin HS (2002) Molecular basis of R-type calcium channels in central amygdala neurons of the mouse. Proc Natl Acad Sci USA 99: 3276-3281.

Leresche N, Parri HR, Erdemli G, Guyon A, Turner JP, Williams SR, Asprodini E, Crunelli V (1998) On the Action of the Anti-Absence Drug Ethosuximide in the Rat and Cat Thalamus. J Neuroscie 18: 4842-4853.

Leroy J, Pereverzev A, Vajna R, Qin N, Pfitzer G, Hescheler J, Malécot CO, Schneider T, Klöckner U (2003) Ca^{2+}-sensitive regulation of E-type Ca^{2+} channel activity depends on an arginine rich region in the cytosolic II-III loop. Eur J Neurosci 18: 841-855.

Levey AI, Edmunds SM, Koliatsos V, Wiley RG, Heilman CJ (1995) Expression of M_1-M_4 muscarinic acetylcholine receptor proteins in rat hippocampus and regulation by cholinergic innervation. J Neurosci 15: 4077-4092.

Li Y, Bennett DJ (2003) Persistent sodium and calcium currents cause plateau potentials in motoneurons of chronic spinal rats. J Neurophysiol 90: 857-869.

Li YV, Hough CJ, Sarvey JM (2003) Do we need zinc to think? Sci STKE 182: 19.

Link TE, Murakami K, Beem-Miller M, Tranmer BI, Wellman GC (2008) Oxyhemoglobin-induced expression of R-type Ca^{2+} channels in cerebral arteries. Stroke 39: 2122-2128.

Lothman EW, Bertram EH, III, Stringer JL (1991) Functional anatomy of hippocampal seizures. Prog Neurobiol 37: 1-82.

Lu Z-L, Pereverzev A, Liu H-L, Weiergraber M, Henry M, Krieger A, Smyth N, Hescheler J, Schneider T (2004) Arrhythmia in isolated prenatal hearts after ablation of the $Ca_v2.3$ (α_1E) subunit of voltage-gated Ca^{2+} channels. Cell Physiol Biochem 14: 11-22.

Lukyanetz EA, Shkryl VM, Kostyuk PG (2002) Selective blockade of N-type calcium channels by levetiracetam. Epilepsia 43: 9-18.

Maneuf YP, Luo ZD, Lee K (2006) Alpha2delta and the mechanism of action of gabapentin in the treatment of pain. Semin Cell Dev Biol 17: 565-570.

Manning JP, Richards DA, Bowery NG (2003) Pharmacology of absence epilepsy. Trends Pharmacol Sci 24: 542-549.

Matar N, Jin W, Wrubel H, Hescheler J, Schneider T, Weiergraber M (2009) Zonisamide block of cloned human T-type voltage-gated calcium channels. Epilepsy Res. in press.

Matsuda Y, Saegusa H, Zong S, Noda T, Tanabe T (2001) Mice Lacking $Ca_v2.3$ (α_1E) Calcium Channel Exhibit Hyperglycemia. Biochem Biophys Res Commun 289: 791-795.

Matsuo F (1999) Lamotrigine. Epilepsia 40 Suppl 5: S30-S36.

Matthews EA, Bee LA, Stephens GJ, Dickenson AH (2007) The $Ca_v2.3$ calcium channel antagonist SNX-482 reduces dorsal horn neuronal responses in a rat model of chronic neuropathic pain. Eur J Neurosci 25: 3561-3569.

McCabe PH (2000) New anti-epileptic drugs for the 21st century. Expert Opin Pharmacother 1: 633-674.

McCarthy RT, TanPiengco PE (1992) Multiple types of high-threshold calcium channels in rabbit sensory neurons: high-affinity block of neuronal L-type by nimodipine. J Neurosci 12: 2225-2234.

McKeown L, Robinson P, Jones OT (2006) Molecular basis of inherited calcium channelopathies: role of mutations in pore-forming subunits. Acta Pharmacol Sin 27: 799-812.

McNamara RK, Wees EA, Lenox RH (1999) Differential subcellular redistribution of protein kinase C isozymes in the rat hippocampus induced by kainic acid. J Neurochem 72: 1735-1743.

McNaughton NC, Davies CH, Randall A (2004) Inhibition of alpha1E Ca^{2+} channels by carbonic anhydrase inhibitors. J Pharmacol Sci 95: 240-247.

Melliti K, Meza U, Adams B (2000) Muscarinic stimulation of α_1E Ca Channels is selectively blocked by the effector antagonist function of RGS2 and phsopholipase C-β1. J Neurosci 20: 7167-7173.

Metz AE, Jarsky T, Martina M, Spruston N (2005) R-type calcium channels contribute to afterdepolarization and bursting in hippocampal CA1 pyramidal neurons. J Neurosci 25: 5763-5773.

Meza U, Bannister R, Melliti K, Adams B (1999) Biphasic, Opposing Modulation of Cloned Neuronal α_1E Ca Channels by Distinct Signaling Pathways Coupled to M_2 Muscarinic Acetylcholine Receptors. J Neurosci 19: 6806-6817.

Michna M, Knirsch M, Hoda JC, Muenkner S, Langer P, Platzer J, Striessnig J, Engel J (2003) $Ca_v1.3$ (alpha1D) Ca^{2+} currents in neonatal outer hair cells of mice. J Physiol 553: 747-758.

Mills JD, Pitman RM (1997) Electrical properties of a cockroach motor neuron soma depend on different characteristics of individual Ca components. J Neurophysiol 78: 2455-2466.

Mingo NS, Cottrell GA, Mendonca A, Gombos Z, Eubanks JH, Burnham WM (1998) Amygdala-kindled and electroconvulsive seizures alter hippocampal expression of the M_1 and M_3 muscarinic cholinergic receptor genes. Brain Res 810: 9-15.

Momiyama T, Ishihara K, Serikawa T, Moritake K, Sasa M (1995) Effect of nicardipine on abnormal excitability of CA3 pyramidal cells in hippocampal slices of spontaneously epileptic rats. Eur J Pharmacol 280: 119-123.

Monnier N, Procaccio V, Stieglitz P, Lunardi J (1997) Malignant-hyperthermia susceptibility is associated with a mutation of the alpha1-subunit of the human dihydropyridine-sensitive L-type voltage-dependent calcium-channel receptor in skeletal muscle. Am J Hum Genet 60: 1316-1325.

Morisset V, Nagy F (1999) Ionic basis for plateau potentials in deep dorsal horn neurons of the rat spinal cord. J Neurosci 19: 7309-7316.

Muller YL, Hanson RL, Zimmerman C, Harper I, Sutherland J, Kobes S, Knowler WC, Bogardus C, Baier LJ (2007) Variants in the $Ca_v2.3$ (alpha 1E) subunit of voltage-activated Ca^{2+} channels are associated with insulin resistance and type 2 diabetes in Pima Indians. Diabetes 56: 3089-3094.

Mulley JC, Scheffer IE, Harkin LA, Berkovic SF, Dibbens LM (2005) Susceptibility genes for complex epilepsy. Human Mol Gen 14: R243-R249.

Newcomb R, Szoke B, Palma A, Wang G, Chen XH, Hopkins W, Cong R, Miller J, Urge L, Tarczy-Hornoch K, Loo JA, Dooley DJ, Nadasdi L, Tsien RW, Lemos J, Miljanich G (1998) Selective peptide antagonist of the class E calcium channel from the venom of the tarantula *Hysterocrates gigas*. Biochemistry 37: 15353-15362.

Nicoll RA, Schmitz D (2005) Synaptic plasticity at hippocampal mossy fibre synapses. Nat Rev Neurosci 6: 863-876.

Ophoff RA, Terwindt GM, Frants RR, Ferrari MD (1998) P/Q-type Ca^{2+} channel defects in migraine, ataxia and epilepsy. TIPS 19: 121-127.

Ophoff RA, Terwindt GM, Vergouwe MN, van Eijk R, Oefner PJ, Hoffmann SMG, Lamerdin JE, Mohrenweiser HW, Bulman DE, Ferrari M, Haan J, Lindhout D, van Ommen G-JB, Hofker MH, Ferrai MD, Frants RR (1996) Familial Hemiplegic Migraine and Episodic Ataxia Type-2 Are Caused by Mutations in the Ca^{2+} Channel Gene CACNL1A4. Cell 87: 543-552.

Osanai M, Saegusa H, Kazuno AA, Nagayama S, Hu Q, Zong S, Murakoshi T, Tanabe T (2006) Altered cerebellar function in mice lacking $Ca_v2.3$ Ca^{2+} channel. Biochem Biophys Res Commun 344: 920-925.

Pereverzev A, Mikhna M, Vajna R, Gissel C, Henry M, Weiergräber M, Hescheler J, Smyth N, Schneider T (2002b) Disturbances in glucose-tolerance, insulin-release and stress-induced hyperglycemia upon disruption of the $Ca_v2.3$ (α_1E) subunit of voltage-gated Ca^{2+} channels. Mol Endocrinol 16: 884-895.

Pereverzev A, Salehi A, Mikhna M, Renstrom E, Hescheler J, Weiergraber M, Smyth N, Schneider T (2005) The ablation of the $Ca_v2.3$/E-type voltage-gated Ca^{2+} channel causes a mild phenotype despite an altered glucose induced glucagon response in isolated islets of Langerhans. Eur J Pharmacol 511: 65-72.

Perez-Reyes E (2003) Molecular Physiology of Low-Voltage-Activated T-type Calcium Channels. Physiol Rev 83: 117-161.

Pierson PM, Liu X, Raggenbass M (2005) Suppression of potassium channels elicits calcium-dependent plateau potentials in suprachiasmatic neurons of the rat. Brain Res 1036: 50-59.

Pietrobon D (2002) Calcium channels and channelopathies of the central nervous system. Mol Neurobiol 25: 31-50.

Pietrobon D (2005) Function and dysfunction of synaptic calcium channels: insights from mouse models. Curr Opinion Neurobiol 15: 257-265.

Pisani A, Bonsi P, Martella G, De Persis C, Costa C, Pisani F, Bernardi G, Calabresi P (2004) Intracellular calcium increase in epileptiform activity: modulation by levetiracetam and lamotrigine. Epilepsia 45: 719-728.

Potier S, Senecal J, Chabot JG, Psarropoulou C, Descarries L (2005) A pentylenetetrazole-induced generalized seizure in early life enhances the efficacy of muscarinic receptor coupling to G-protein in hippocampus and neocortex of adult rat. Eur J Neurosci 21: 1828-1836.

Ptacek LJ, Tawil R, Griggs RC, Engel AG, Layzer RB, Kwiecinski H, McManis PG, Santiago L, Moore M, Fouad G (1994) Dihydropyridine receptor mutations cause hypokalemic periodic paralysis. Cell 77: 863-868.

Randall A, Tsien RW (1995) Pharmacological dissection of multiple types of Ca^{2+} channel currents in rat cerebellar granule neurons. J Neurosci 15: 2995-3012.

Reddy NL, Fan W, Magar SS, Perlman ME, Yost E, Zhang L, Berlove D, Fischer JB, Burke-Howie K, Wolcott T, Durant GJ (1998) Synthesis and pharmacological evaluation of N,N'-diarylguanidines as potent sodium channel blockers and anticonvulsant agents. J Med Chem 41: 3298-3302.

Remy S, Beck H (2006) Molecular and cellular mechanisms of pharmacoresistance in epilepsy. Brain 129: 18-35.

Rogawski MA, Loscher W (2004) The neurobiology of antiepileptic drugs. Nature Reviews Neuroscience 5: 553-564.

Roper P, Callaway J, Shevchenko T, Teruyama R, Armstrong W (2003) AHP's, HAP's and DAP's: how potassium currents regulate the excitability of rat supraoptic neurones. J Comput Neurosci 15: 367-389.

Russo E, Constanti A, Ferreri G, Citraro R, De Sarro G (2004) Nifedipine affects the anticonvulsant activity of topiramate in various animal models of epilepsy. Neuropharmacology 46: 865-878.

Saegusa H, Kurihara T, Zong S, Kazuno A, Matsuda Y, Nonaka T, Han W, Toriyama H, Tanabe T (2001) Suppression of inflammatory and neuropathic pain symptoms in mice lacking the N-type calcium channel. EMBO J 20: 2349-2356.

Saegusa H, Kurihara T, Zong SQ, Minowa O, Kazuno AA, Han WH, Matsuda Y, Yamanaka H, Osanai M, Noda T, Tanabe T (2000) Altered pain responses in mice lacking α_1E subunit of the voltage-dependent Ca^{2+} channel. Proc Natl Acad Sci USA 97: 6132-6137.

Sakata Y, Saegusa H, Zong SQ, Osanai M, Murakoshi T, Shimizu Y, Noda T, Aso T, Tanabe T (2002) $Ca_v2.3$ (α_1E) Ca^{2+} channel participates in the control of sperm function. FEBS Lett 516: 229-233.

Sayer RJ, Brown AM, Schwindt PC, Crill WE (1993) Calcium currents in acutely isolated human neocortical neurons. J Neurophysiol 69: 1596-1606.

Schiller Y (2002) Interictal- and ictal-like epileptic discharges in the dendritic tree of neocortical pyramidal neurons. J Neurophysiol 88: 2954-2962.

Segal MM (1991) Epileptiform activity in microcultures containing one excitatory hippocampal neuron. J Neurophysiol 65: 761-770.

Segal MM (1994) Endogenous bursts underlie seizurelike activity in solitary excitatory hippocampal neurons in microcultures. J Neurophysiol 72: 1874-1884.

Segal MM, Furshpan EJ (1990) Epileptiform activity in microcultures containing small numbers of hippocampal neurons. J Neurophysiol 64: 1390-1399.

Shapiro MS, Gomeza J, Hamilton SE, Hille B, Loose MD, Nathanson NM, Roche JP, Wess J (2001) Identification of subtypes of muscarinic receptors that regulate Ca^{2+} and K^+ channel activity in sympathetic neurons. Life Sci 68: 2481-2487.

Shapiro MS, Loose MD, Hamilton SE, Nathanson NM, Gomeza J, Wess J, Hille B (1999) Assignment of muscarinic receptor subtypes mediating G-protein modulation of Ca^{2+} channels by using knockout mice. Proc Natl Acad Sci USA 96: 10899-10904.

Shin HS (2006) T-type Ca^{2+} channels and absence epilepsy. Cell Calcium 40: 191-196.

Sills GJ (2006) The mechanisms of action of gabapentin and pregabalin. Curr Opin Pharmacol 6: 108-113.

Simon M, Perrier JF, Hounsgaard J (2003) Subcellular distribution of L-type Ca^{2+} channels responsible for plateau potentials in motoneurons from the lumbar spinal cord of the turtle. Eur J Neurosci 18: 258-266.

Sochivko D, Pereverzev A, Smyth N, Gissel C, Schneider T, Beck H (2002) The α_1E calcium channel subunit underlies R-type calcium current in hippocampal and cortical pyramidal neurons. J Physiol 542: 699-710.

Song I, Kim D, Choi S, Sun M, Kim Y, Shin HS (2004) Role of the alpha1G T-type calcium channel in spontaneous absence seizures in mutant mice. J Neurosci 24: 5249-5257.

Soong TW, Stea A, Hodson CD, Dubel SJ, Vincent SR, Snutch TP (1993) Structure and functional expression of a member of the low voltage-activated calcium channel family. Science 260: 1133-1136.

Splawski I, Timothy KW, Decher N, Kumar P, Sachse FB, Beggs AH, Sanguinetti MC, Keating MT (2005) Severe arrhythmia disorder caused by cardiac L-type calcium channel mutations. Proc Natl Acad Sci USA 102: 8089-8096.

Splawski I, Timothy KW, Sharpe LM, Decher N, Kumar P, Bloise R, Napolitano C, Schwartz PJ, Joseph RM, Condouris K, Tager-Flusberg H, Priori SG, Sanguinetti MC, Keating MT (2004) $Ca_v1.2$ calcium channel dysfunction causes a multisystem disorder including arrhythmia and autism. Cell 119: 19-31.

Splawski I, Yoo DS, Stotz sc, Cherry A, Clapham DE, Keating MT (2006) CACNA1H Mutations in Autism Spectrum Disorders. J Biol Chem 281: 22085-22091.

Stefani A, Spadoni F, Bernardi G (1997) Voltage-activated calcium channels: targets of antiepileptic drug therapy? Epilepsia 38: 959-965.

Stefani A, Spadoni F, Siniscalchi A, Bernardi G (1996) Lamotrigine inhibits Ca^{2+} currents in cortical neurons: functional implications. Eur J Pharmacol 307: 113-116.

Stephens GJ, Page KM, Burley JR, Berrow NS, Dolphin AC (1997) Functional expression at rat brain cloned α_1E calcium channels in COS-7 cells. Pflugers Arch 433: 523-532.

Steriade M (2005) Sleep, epilepsy and thalamic reticular inhibitory neurons. Trends Neurosci 28: 317-324.

Steriade M, McCormick DA, Sejnowski TJ (1993) Thalamocortical oscillations in the sleeping and aroused brain. Science 262: 679-685.

Straub H, Speckmann EJ, Bingmann D, Walden J (1990) Paroxysmal depolarization shifts induced by bicuculline in CA3 neurons of hippocampal slices: suppression by the organic calcium antagonist verapamil. Neurosci Lett 111: 99-101.

Striessnig J, Hoda JC, Koschak A, Zaghetto F, Mullner C, Sinnegger-Brauns MJ, Wild C, Watschinger K, Trockenbacher A, Pelster G (2004) L-type Ca^{2+} channels in Ca^{2+} channelopathies. Biochem Biophys Res Commun 322: 1341-1346.

Striessnig J, Koschak A (2008) Exploring the function and pharmacotherapeutic potential of voltage-gated Ca^{2+} channels with gene knockout models. Channels (Austin) 2: 233-251.

Strupp M, Kalla R, Dichgans M, Freilinger T, Glasauer S, Brandt T (2004) Treatment of episodic ataxia type 2 with the potassium channel blocker 4-aminopyridine. Neurology 62: 1623-1625.

Sullivan PG (2005) Interventions with neuroprotective agents: novel targets and opportunities. Epilepsy Behav 7 Suppl 3: S12-S17.

Sun DA, Sombati S, Blair RE, DeLorenzo RJ (2002) Calcium-dependent epileptogenesis in an in vitro model of stroke-induced "epilepsy". Epilepsia 43: 1296-1305.

Sun MK, Alkon DL (2002) Carbonic anhydrase gating of attention: memory therapy and enhancement. Trends Pharmacol Sci 23: 83-89.

Supuran CT, Scozzafava A, Casini A (2003) Carbonic anhydrase inhibitors. Med Res Rev 23: 146-189.

Suzuki S, Kawakami K, Nishimura S, Watanabe Y, Yagi K, Seino M, Miyamoto K (1992) Zonisamide blocks T-type calcium channel in cultured neurons of rat cerebral cortex. Epilepsy Res 12: 21-27.

Suzuki S, Rogawski MA (1989) T-type calcium channels mediate the transition between tonic and phasic firing in thalamic neurons. Proc Natl Acad Sci U S A 86: 7228-7232.

Suzuki T, Delgado-Escueta AV, Aguan K, Alonso ME, Shi J, Hara Y, Nishida M, Numata T, Medina MT, Takeuchi T, Morita R, Bai D, Ganesh S, Sugimoto Y, Inazawa J, Bailey JN, Ochoa A, Jara-Prado A, Rasmussen A, Ramos-Peek J, Cordova S, Rubio-Donnadieu F, Inoue Y, Osawa M, Kaneko S, Oguni H, Mori Y, Yamakawa K (2004) Mutations in EFHC1 cause juvenile myoclonic epilepsy. Nat Genet 36: 842-849.

Tai C, Kuzmiski JB, MacVicar BA (2006) Muscarinic enhancement of R-type calcium currents in hippocampal CA1 pyramidal neurons. J Neurosci 26: 6249-6258.

Talley EM, Solórzano G, Depaulis A, Perez-Reyes E, Bayliss DA (2000) Low-voltage-activated calcium channel subunit expression in a genetic model of absence epilepsy in the rat. Mol Brain Res 75: 159-165.

Tang ZZ, Liang MC, Lu S, Yu D, Yu CY, Yue DT, Soong TW (2004) Transcript scanning reveals novel and extensive splice variations in human L-type voltage-gated calcium channel, $Ca_v1.2$ alpha1 subunit. J Biol Chem 279: 44335-44343.

Tank DW, Sugimori M, Connor JA, Llinas RR (1988) Spatially resolved calcium dynamics of mammalian Purkinje cells in cerebellar slice. Science 242: 773-777.

Todorovic SM, Lingle CJ (1998) Pharmacological properties of T-type Ca^{2+} current in adult rat sensory neurons: Effects of anticonvulsant and anesthetic agents. J Neurophysiol 79: 240-252.

Toriyama H, Wang L, Saegusa H, Zong S, Osanai M, Murakoshi T, Noda T, Ohno K, Tanabe T (2002) Role of $Ca_v2.3$ (alpha1E) Ca^{2+} channel in ischemic neuronal injury. Neuroreport 13: 261-265.

Toselli M, Lang J, Costa T, Lux HD (1989) Direct modulation of voltage-dependent calcium channels by muscarinic activation of a pertussis toxin-sensitive G-protein in hippocampal neurons. Pflugers Arch 415: 255-261.

Toselli M, Lux HD (1989) Opposing effects of acetylcholine on the two classes of voltage-dependent calcium channels in hippocampal neurons. EXS 57: 97-103.

Tottene A, Volsen S, Pietrobon D (2000) Alpha1E Subunits Form the Pore of Three Cerebellar R-Type Calcium Channels with Different Pharmacological and Permeation Properties. J Neuroscie 20: 171-178.

Tsakiridou E, Bertollini L, de Curtis M, Avanzini g, Pape HC (1995) Selective increase in T-type calcium conductance of reticular thalamic neurons in a rat model of absence epilepsy. J Neurosci 15: 3110-3117.

Tsien RW, Nilius B (1987) Cardiac calcium currents at the level of single channels. Experientia 43: 1169-1172.

Turner TJ (1998) Calcium channels coupled to glutamate release. Glutamate Synapse As A Therapeutical Target: Molecular Organization and Pathology of the Glutamate Synapse 116: 3-14.

van de Bovenkamp-Janssen M, Scheenen WJ, Kuijpers-Kwant FJ, Kozicz T, Veening JG, van Luijtelaar EL, McEnery MW, Roubos EW (2004) Differential expression of high voltage-activated Ca^{2+} channel types in the rostral reticular thalamic nucleus of the absence epileptic WAG/Rij rat. J Neurobiol 58: 467-478.

Vitko I, Chen Y, Arias JM, Shen Y, Wu XR, Perez-Reyes E (2005) Functional characterization and neuronal modeling of the effects of childhood absence epilepsy variants of CACNA1H, a T-type calcium channel. J Neurosci 25: 4844-4855.

Voisin DL, Nagy F (2001) Sustained L-type calcium currents in dissociated deep dorsal horn neurons of the rat: characteristics and modulation. Neuroscience 102: 461-472.

Vosu H, Wise RA (1975) Cholinergic seizure kindling in the rat: comparison of caudate, amygdala and hippocampus. Behav Biol 13: 491-495.

Vreugdenhil M, Wadman WJ (1994) Kindling-induced long-lasting enhancement of calcium current in hippocampal CA1 area of the rat: relation to calcium-dependent inactivation. Neuroscience 59: 105-114.

Wakamori M, Niidome T, Rufutama D, Furuichi T, Mikoshiba K, Fujita Y, Tanaka I, Katayama K, Yatani A, Schwartz A, Mori Y (1994) Distinctive Functional Properties of the Neuronal BII (Class E) Calcium Channel. Receptors & Channels 2: 303-314.

Walker D, De Waard M (1998) Subunit interaction sites in voltage-dependent Ca^{2+} channels: role in channel function. Trends Neurosci 21: 148-154.

Wang SJ, Huang CC, Hsu KS, Tsai JJ, Gean PW (1996) Inhibition of N-type calcium currents by lamotrigine in rat amygdalar neurones. Neuroreport 7: 3037-3040.

Wei J, Hemmings GP (2006) A further study of a possible locus for schizophrenia on the X chromosome. Biochem Biophys Res Commun 344: 1241-1245.

Weiergraber M, Henry M, Hescheler J, Smyth N, Schneider T (2005a) Electrocorticographic and deep intracerebral EEG recording in mice using a telemetry system. Brain Res Brain Res Protoc 14: 154-164.

Weiergraber M, Henry M, Ho MS, Struck H, Hescheler J, Schneider T (2008a) Altered thalamocortical rhythmicity in $Ca_v2.3$-deficient mice. Mol Cell Neurosci 39: 605-618.

Weiergraber M, Henry M, Krieger A, Kamp M, Radhakrishnan K, Hescheler J, Schneider T (2006a) Altered seizure susceptibility in mice lacking the $Ca_v2.3$ E-type Ca^{2+} channel. Epilepsia 47: 839-850.

Weiergraber M, Henry M, Radhakrishnan K, Hescheler J, Schneider T (2007) Hippocampal seizure resistance and reduced neuronal excitotoxicity in mice lacking the $Ca_v2.3$ E/R-type voltage-gated calcium channel. J Neurophysiol 97: 3660-3669.

Weiergraber M, Henry M, Sudkamp M, De Vivie ER, Hescheler J, Schneider T (2005b) Ablation of $Ca_v2.3$ / E-type voltage-gated calcium channel results in cardiac arrhythmia and altered autonomic control within the murine cardiovascular system. Basic Res Cardiol 100: 1-13.

Weiergraber M, Hescheler J, Schneider T (2008b) [Human calcium channelopathies. Voltage-gated Ca^{2+} channels in etiology, pathogenesis, and pharmacotherapy of neurologic disorders]. Nervenarzt 79: 426-436.

Weiergraber M, Kamp MA, Radhakrishnan K, Hescheler J, Schneider T (2006b) The $Ca_v2.3$ voltage-gated calcium channel in epileptogenesis--shedding new light on an enigmatic channel. Neurosci Biobehav Rev 30: 1122-1144.

Westenbroek RE, Sakurai T, Elliott EM, Hell JW, Starr TVB, Snutch TP, Catterall WA (1995) Immunochemical identification and subcellular distribution of the α_1A subunits of brain calcium channels. J Neurosci 15: 6403-6418.

Williams ME, Marubio LM, Deal CR, Hans M, Brust PF, Philipson LH, Miller RJ, Johnson EC, Harpold MM, Ellis SB (1994) Structure and functional characterization of neuronal α_1E calcium channel subtypes. J Biol Chem 269: 22347-22357.

Wilson SM, Toth PT, Oh SB, Gillard SE, Volsen S, Ren D, Philipson LH, Lee EC, Fletcher CF, Tessarollo L, Copeland NG, Jenkins NA, Miller RJ (2000) The Status of Voltage-Dependent Calcium Channels in alpha1E Knock-Out Mice. J Neurosci 20: 8566-8571.

Wu LG, Westenbroek RE, Borst JGG, Catterall WA, Sakmann B (1999) Calcium channel types with distinct presynaptic localization couple differentially to transmitter release in single calyx-type synapses. J Neurosci 19: 726-736.

Wycisk KA, Zeitz C, Feil S, Wittmer M, Forster U, Neidhardt J, Wissinger B, Zrenner E, Wilke R, Kohl S, Berger W (2006) Mutation in the Auxiliary Calcium-Channel Subunit CACNA2D4 Causes Autosomal Recessive Cone Dystrophy. Am J Hum Genet 79: 973-977.

Xie X, Hagan RM (1998) Cellular and molecular actions of lamotrigine: Possible mechanisms of efficacy in bipolar disorder. Neuropsychobiology 38: 119-130.

Xu WF, Lipscombe D (2001) Neuronal $Ca_v1.3\alpha_1$ L-type channels activate at relatively hyperpolarized membrane potentials and are incompletely inhibited by dihydropyridines. J Neurosci 21: 5944-5951.

Yang SN, Berggren PO (2005) (beta)-Cell Ca_v channel regulation in physiology and pathophysiology. Am J Physiol Endocrinol Metab 288: E16-E28.

Yeckel MF, Berger TW (1998) Spatial distribution of potentiated synapses in hippocampus: dependence on cellular mechanisms and network properties. J Neurosci 18: 438-450.

Yue C, Remy S, Su H, Beck H, Yaari Y (2005) Proximal persistent Na^+ channels drive spike afterdepolarizations and associated bursting in adult CA1 pyramidal cells. J Neurosci 25: 9704-9720.

Zhang B, Harris-Warrick RM (1995) Calcium-dependent plateau potentials in a crab stomatogastric ganglion motor neuron. I. Calcium current and its modulation by serotonin. J Neurophysiol 74: 1929-1937.

Zhang X, Velumian AA, Jones OT, Carlen PL (2000) Modulation of high-voltage-activated calcium channels in dentate granule cells by topiramate. Epilepsia 41 Suppl 1: S52-S60.

Zhang Y, Mori M, Burgess DL, Noebels JL (2002) Mutations in high-voltage-activated calcium channel genes stimulate low- voltage-activated currents in mouse thalamic relay neurons. J Neurosci 22: 6362-6371.

6. Anhang

Publikationen

1. Pavle M Joksovic, **Marco Weiergräber**, WooYong Lee, Henrik Struck, Toni Schneider and Slobodan M. Todorovic (2009): **ISOFLURANE-SENSITIVE PRESYNAPTIC $CA_V2.3$ CHANNELS CONTRIBUTE TO INHIBITORY SYNAPTIC TRANSMISSION IN THE RAT THALAMUS.** *Journal of Neuroscience*, in press.

2. Nora Matar, Wei Jin, Heiko Wrubel, Jürgen Hescheler, Toni Schneider, **Marco Weiergräber** (2008): **ZONISAMIDE BLOCK OF CLONED HUMAN T-TYPE VOLTAGE-GATED CALCIUM CHANNELS**. *Epilepsy Research,* 83: 224-234.

3. Marco Weiergräber, Margit Henry, Matthew S.P.Ho, Henrik Struck, Jürgen Hescheler, Toni Schneider (2008): **ALTERED THALAMOCORTICAL RHYTHMICITY IN $CA_V2.3$ DEFICIENT MICE.** *Molecular and Cellular Neuroscience,* 2008 Sep 4, in press.

4. Mohammed Banat, Matthias Lüke, Siarhei A. Siapich, Jürgen Hescheler, **Marco Weiergräber**, Toni Schneider (2008): **THE DIHYDROPYRIDINE ISRADIPINE INHIBITS THE MURINE BUT NOT THE BOVINE A-WAVE RESPONSE OF THE ELECTRORETINOGRAM**. *Acta Ophthalmologica Scandinavica, 86(6):676-82.*

5. Marco Weiergräber, Jürgen Hescheler and Toni Schneider (2008): **HUMAN CALCIUM CHANNELOPATHIES – VOLTAGE-GATED CALCIUM CHANNELS IN ETIOLOGY, PATHOGENESIS AND PHARMACOTHERAPY OF NEUROLOGICAL DISORDERS.** *Der Nervenarzt, 79(4):426-436.*

6. Marco Weiergräber, Margit Henry, Kayalvizhi Radhakrishnan, Jürgen Hescheler, Toni Schneider (2007); **HIPPOCAMPAL SEIZURE RESISTANCE AND REDUCED NEURONAL EXCITOTOXICITY IN MICE LACKING THE $CA_V2.3$ E/R-TYPE VOLTAGE-GATED CALCIUM CHANNEL.** *Journal of Neurophysiology, 97(5):3660-9.*

7. Marco Weiergräber, Marcel Kamp, Kayalvizhi Radhakrishnan, Jürgen Hescheler, Toni Schneider (2006): **THE $CA_V2.3$ VOLTAGE-GATED CALCIUM CHANNEL IN EPILEPTOGENESIS - SHEDDING NEW LIGHT ON AN ENIGMATIC CHANNEL**. *Neuroscience & Biobehavioral Reviews*, 30(8):1122-44.

8. Marco Weiergräber, Margit Henry, Andreas Krieger, Marcel Kamp, Kayalvizhi Radhakrishnan, Jürgen Hescheler, Toni Schneider (2006): **ALTERED SEIZURE SUSCEPTIBILITY IN MICE LACKING THE $CA_V2.3$ E-TYPE CA^{2+} CHANNEL**. *Epilepsia*, 47(5):839-850.

9. Rüdiger Köhling, Roswitha Nischt, Neil Smyth, Anju Vasudevan, Matthew Ho, **Marco Weiergräber**, Toni Schneider (2006): **NIDOGEN AND NIDOGEN-ASSOCIATED BASEMENT MEMBRANE PROTEINS AND NEURONAL PLASTICITY**. *Neurodegenerative Diseases*, 3(1-2):56-61.

10. Andreas Krieger, Kayalvizhi Radhakrishnan, Alexey Pereverzev, Siarhei Siapich, Mohammed Banat, Marcel Kamp, Jérôme Leroy, Jürgen Hescheler, Udo Klöckner, **Marco Weiergräber**, Toni Schneider (2006): **THE MOLECULAR CHAPERONE HSP70 INTERACTS WITH THE CYTOSOLIC II-III LOOP OF THE $CA_V2.3$ E-TYPE VOLTAGE-GATED CA^{2+} CHANNEL**. *Cellular Physiology and Biochemistry*, 17(3-4):97-110.

11. Mattthias Lüke, **Marco Weiergräber**, Carl Brand, Siarhei Siapich, Mohammed Banat, Jürgen Hescheler, Christoph Lüke, Toni Schneider (2005): **THE ISOLATED PERFUSED BOVINE RET-**

INA-A SENSITIVE TOOL FOR PHARMACOLOGICAL RESEARCH ON RETINAL FUNCTION. *Brain Research Brain Research Protocols*, 16(1-3):27-36.

12. Matthias Lüke, Margit Henry, Thea Lingohr, Mehran Maghsoodian, Jürgen Hescheler, **Marco Weiergräber**, Werner Sickel, Toni Schneider (2005): **A NI^{2+}-SENSITIVE COMPONENT OF THE ERG-B-WAVE FROM THE ISOLATED BOVINE RETINA IS RELATED TO E-TYPE VOLTAGE-GATED CA^{2+} CHANNELS**. *Graefe's Archive for Clinical and Experimental Ophthalmology*, 243(9):933-41.

13. Marcel Kamp, Andreas Krieger, Margit Henry, Jürgen Hescheler, **Marco Weiergräber**, Toni Schneider (2005): **PRESYNAPTIC $CA_V2.3$ CONTAINING E-TYPE CA^{2+} CHANNELS SHARE DUAL ROLES DURING NEUROTRANSMITTER RELEASE AND LONG TERM POTENTIATION**. *European Journal of Neuroscience*, 21(6):1617-25.

14. Marco Weiergräber, Margit Henry, Jürgen Hescheler, Neil Smyth and Toni Schneider (2005): **ELECTROCORTICOGRAPHIC AND DEEP INTRACEREBRAL EEG RECORDING IN MICE USING A TELEMETRY SYSTEM**. *Brain Research Brain Research Protocols*, 14(3):154-64.

15. Alexey Pereverzev, Albert Salehi, Marina Mikhna, Erik Renstrom, Jürgen Hescheler, **Marco Weiergräber**, Neil Smyth, Toni Schneider (2005): **THE ABLATION OF THE $CA_V2.3$/E-TYPE VOLTAGE-GATED CA^{2+} CHANNEL CAUSES A MILD PHENOTYPE DESPITE AN ALTERED GLUCOSE INDUCED GLUCAGON RESPONSE IN ISOLATED ISLETS OF LANGERHANS**. *European Journal of Pharmacology*, 511(1):65-72.

16. Marco Weiergräber, Margit Henry, Michael Südkamp, Ernst-Rainer de Vivie, Jürgen Hescheler, Toni Schneider (2005): **ABLATION OF THE $CA_V2.3$ VOLATGE-GATED CALCIUM CHANNEL RESULTS IN CARDIAC ARRHYTHMIA AND ALTERED AUTONOMIC CONTROL WITHIN THE MURINE CARDIOVASCULAR SYSTEM**. *Basic Research in Cardiology*, 100(1):1-13.

17. Zhong-Ju Lu, Alexey Pereverzev, Hui-Lin Liu, **Marco Weiergräber**, Margit Henry, Andreas Krieger, Neil Smyth, Jürgen Hescheler, Toni Schneider (2004): **ARRHYTHMIA IN ISOLATED PRENATAL HEARTS AFTER ABLATION OF THE $CA_V2.3$ (α1E) SUBUNIT OF VOLTAGE GATED CALCIUM CHANNEL**. *Cellular Physiology and Biochemistry*, 14(1-2):11-22.

18. Alexey Pereverzev, Marina Mikhna, Rolf Vajna, Cornelia Gissel, Margit Henry, **Marco Weiergräber**, Jürgen Hescheler, Neil Smyth, Toni Schneider (2002): **DISTURBANCE IN GLUCOSE-TOLERANCE, INSULIN-RELEASE AND STRESS-INDUCED HYPER-GLYCEMIA UPON DISRUPTION OF THE $CA_V2.3$ (α1E) SUBUNIT OF VOLTAGE-GATED CA^{2+} CHANNELS**. *Molecular Endocrinology*, 16(4):884-895.

19. Juan-Carlos Gomora, Asif Daud, **Marco Weiergräber**, Edward Perez-Reyes (2001): **BLOCK OF CLONED HUMAN T-TYPE CALCIUM CHANNELS BY SUCCINIMIDE ANTIEPILEPTIC DRUGS**. *Molecular Pharmacology*, 60:1121-1132.

20. Rolf Vajna, Udo Klöckner, Alexey Pereverzev, **Marco Weiergräber**, Xia-hua Chen, George Miljanich, Toni Schneider (2001): **FUNCTIONAL COUPLING BETWEEN R-TYPE CA^{2+} CHANNELS AND INSULIN SECRETION IN THE INSULINOMA CELL LINE INS-1**. *European Journal of Biochemistry,* 268:1066-1075.

21. Marco Weiergräber, Alexey Pereverzev, Rolf Vajna, Margit Henry, Martin Schramm, Wolfgang Nastainczyk, Heike Grabsch, Toni Schneider (2000): **IMMUNODETECTION OF ALPHA1E VOLTAGE-GATED CA^{2+} CHANNEL IN CHROMOGRANIN-POSITIVE MUSCLE CELLS OF RAT HEART, AND IN DISTAL TUBULES OF HUMAN KIDNEY.** *Journal of Histochemistry and Cytochemistry,* 48(6):807-819.

22. Heike Grabsch, Alexey Pereverzev, **Marco Weiergräber**, Martin Schramm, Margit Henry, Rolf Vajna, Ruth Beattie, S.G. Volsen, Udo Klöckner, Jürgen Hescheler, Toni Schneider (1999): **IMMUNOHISTOCHEMICAL DETECTION OF ALPHA1E VOLTAGE-GATED CA^{2+} CHANNEL ISOFORMS IN CEREBELLUM, INS-1 CELLS, AND NEUROENDOCRINE CELLS OF THE DIGESTIVE SYSTEM**. *Journal of Histochemistry and Cytochemistry,* 47(8):981-994.

Buchkapitel

Marco Weiergräber, Matthew S.P. Ho, Jürgen Hescheler, Toni Schneider (2008): **TELEMETRY: RESEARCH, TECHNOLOGY AND APPLICATIONS**, Nova Science Publishers, Inc.NY, in press.

Kongressvorträge

International

1. Weiergräber Marco, Margit Henry, Renate Clemens, Petra Müller, Jürgen Hescheler, Toni Schneider (2005): **CARDIAC ARRHYTHMIA AND ALTERED AUTONOMIC CONTROL IN MICE LACKING THE $CA_V2.3$/E-TYPE VOLTAGE-GATED CALCIUM CHANNEL**. 49th Annual Meeting of the Biophysical Society, 12.2.–16.2.2005, Long Beach, California, USA. Abstract in: *Biophysical Journal*, Suppl. 2005 (P973). **Presentation: Marco Weiergräber**.

2. Weiergräber Marco (2006): **TELEMETRIC ELECTROCORTICOGRAPHIC (ECOG) AND DEEP INTRACEREBRAL EEG RECORDINGS IN MICE – IMPLANTATION, SEIZURE MONITORING AND SUSCEPTIBILITY TESTING IN TRANSGENIC ANIMALS**. European EEG Telemetry User Group Meeting, 10.5.2006, Eli Lilly, UK. **Präsentation: Marco Weiergräber**.

3. Weiergräber Marco (2008): **NOVEL JANUS-LIKE BEHAVIOUR OF $CA_V2.3$ E/R-TYPE VOLTAGE-GATED CALCIUM CHANNELS IN EPILEPTOGENESIS.** 39th Annual Meeting of the Society for Neuroscience (SfN), 15.11.-19.11.2008, Washington. **Präsentation: Marco Weiergräber**.

National

1. Weiergräber Marco, Heike Grabsch, Alexey Pereverzev, Martin Schramm, Edward Perez-Reyes, Jürgen Hescheler, Toni Schneider (1999): **IMMUNHISTOCHEMICAL DETECTION OF VOLTAGE-GATED CA^{2+}-CHANNEL SUBUNITS (α_1E, α_1G). WHICH T-TYPE OF CA^{2+} CHANNEL IS EXPRESSED IN HEART?** 40. Frühjahrstagung der Deutschen Gesellschaft für Experimentelle und Klinische Pharmakologie und Toxikologie, 9.3.-11.3.99, Mainz. Abstract in: *Naunyn-Schmiedeberg's Archive of Pharmacology 359* Suppl. R7. **Präsentation: Marco Weiergräber**.

2. Weiergräber Marco, Margit Henry, Jürgen Hescheler, Toni Schneider (2004): **REGULATION DES HERZSCHLAGES BEI MÄUSEN, IN DENEN DER $CA_V2.3$/E-TYP CA^{2+}-KANAL INAKTIVIERT WURDE**. 45. Frühjahrstagung der Deutschen Gesellschaft für Experimentelle und Klinische Pharmakologie und Toxikologie, 9.3.-11.3.2004, Mainz. Abstract in: *Naunyn-Schmiedeberg's Archive of Pharmacology* 369, Suppl.1. **Präsentation:** krankheitsbedingte Vertretung durch T. Schneider.

3. Weiergräber Marco, Margit Henry, Jürgen Hescheler, Toni Schneider (2005): **STÖRUNGEN DER AUTONOMEN KONTROLLE IM KARDIOVASKULÄREN SYSTEM VON $CA_V2.3$ DEFIZIENTEN MÄUSEN.** 46. Frühjahrstagung der Deutschen Gesellschaft für Experimentelle und Klinische Pharmakologie und Toxikologie, 15.3.-17.3.2005, Mainz. Abstract in: *Naunyn-Schmiedeberg's Archive of Pharmacology*, Vol. 371, Suppl.1**. Präsentation: Marco Weiergräber**.

4. Weiergräber Marco, Andreas Krieger, Margit Henry, Jürgen Hescheler, Toni Schneider (2006): **ALTERED SEIZURE SUSCEPTIBILITY IN MICE LACKING THE $CA_V2.3$ E/R-TYPE CA^{2+} CHANNEL.** 85. Jahrestagung der Deutschen Physiologischen Gesellschaft, 26.3.–29.3.2006, München. Abstract in: *Acta Physiologica*, Vol. 186, Suppl.1. **Präsentation: Marco Weiergräber.**

5. Weiergräber Marco, Nora Matar, Margit Henry, Toni Schneider (2007): **$CA_V2.3$ DEFIZIENTE MÄUSE WEISEN EINE GERINGERE NEUROTOXIZITÄT UND GESTEIGERTE WIDERSTANSFÄHIGKEIT AUF GEGENÜBER HIPPOKAMPALEN EPILEPTISCHEN ANFÄLLEN.** 48. Jahrestagung der Deutschen Gesellschaft für Pharmakologie und Toxikologie, 13.3.-15.3.2007, Mainz. Abstract in: *Naunyn-Schmiedeberg's Archive of Pharmacology*, Vol. 375, Suppl.1. **Präsentation: Marco Weiergräber**.

6. Weiergräber Marco, Jürgen Hescheler, Toni Schneider (2008): **THE $CA_V2.3$ E/R-TYPE VOLTAGE-GATED CALCIUM CHANNEL IS A FUNCTIONAL REGULATOR IN THE THALAMOCORTICAL CIRCUITRY.** 87. Jahrestagung der Deutschen Physiologischen Gesellschaft, 2.3.–5.3.2008, Köln. Abstract in: *Acta Physiologica*, **Präsentation: Marco Weiergräber**.

7. Weiergräber Marco, Nora Matar, Jürgen Hescheler, Toni Schneider (2008): **ZONISAMID-BLOCK SPANNUNGSGESTEUERTER HUMANER T-TYP CA^{2+}-KANÄLE**. 49. Jahrestagung der Deutschen Gesellschaft für Experimentelle und Klinische Pharmakologie und Toxikologie (DGPT), **11.3-13.3.2008, Mainz. Abstract in: *Naunyn-Schmiedeberg's Archive of Pharmacology***. Präsentation: **Marco Weiergräber.**

Weitere Vorträge

Universitätsvorträge (Medizinische Einrichtungen der Universität zu Köln)

1. Weiergräber Marco (1999): **IMMUNHISTOCHEMISCHER NACHWEIS VON E- UND T-TYP KALZIUM-IONENKANÄLEN IN NEUROENDOKRINEN GEWEBEN**. 18.11.99; **Köln-Fortune** (Medizinische Fakultät der Universität zu Köln), Kolloquienreihe Wintersemester 1999/2000, **Präsentation: Marco Weiergräber**.

2. Weiergräber Marco (2003): **DETECTION OF BIOPOTENTIALS IN SMALL LABORATORY ANIMALS.** 26.9.2003, Vortrag im Rahmen der Tagung der Sektion „Molekulare Neurowissenschaften" des Zentrums für Molekulare Medizin Köln (ZMMK), **Präsentation: Marco Weiergräber**.

3. Weiergräber Marco (2004): **FUNCTIONAL ANALYSIS OF THE NEURONAL E-TYPE VOLTAGE-GATED CALCIUM CHANNEL WITHIN THE MURINE CARDIOVASCULAR SYSTEM**. 26.4.2004, Vortrag im Rahmen des Veranstaltungskalenders des Zentrums für Molekulare Medizin Köln (ZMMK), **Präsentation: Marco Weiergräber**.

4. Weiergräber Marco (2004): **FUNCTIONAL CHARACTERISATION OF THE NEURONAL E/R-TYPE VOLTAGE-GATED CALCIUM CHANNEL WITHIN THE MURINE CARDIOVASCULAR SYSTEM**. 5.2.2004, Vortrag in der Klinik III für Innere Medizin (Kardiologie, Pneumologie, Angiologie und internistische Intensivmedizin), Universität zu Köln. **Präsentation: Marco Weiergräber**.

5. Weiergräber Marco (2004): **ABLATION OF THE $CA_V2.3$ VOLATGE-GATED CALCIUM CHANNEL RESULTS IN CARDIAC ARRHYTHMIA AND ALTERED AUTONOMIC CONTROL WITHIN THE MURINE CARDIOVASCULAR SYSTEM** 3.12.-4.12.2004, Vortrag im Rahmen der Klausurtagung des Zentrums für Molekulare Medizin Köln (ZMMK), Wermelskirchen-Dabringhausen, **Präsentation: Marco Weiergräber**.

6. Weiergräber Marco (2007): Molecular mechanisms of rhythm generation and synchronization in electrically coupled cells – Structure & function of voltage-gated Ca^{2+} channels in cardiac and neuronal pacemaker centers and related neuronal circuits, and their role for spontaneous excitability and memory formation - **DISTURBANCES IN RHYTHMOGENESIS FOLLOWING ABLATION OF $CA_V2.3$ E/R-TYPE VOLTAGE-GATED CALCIUM CHANNELS - FUNTIONAL RELEVANCE IN EPILEPTOGENESIS AND EXCITOTOXICITY**. 19.1.-20.1.2007, Vortrag im Rahmen der Klausurtagung des Zentrums für Molekulare Medizin Köln (ZMMK), Wermelskirchen-Dabringhausen, **Präsentation: Marco Weiergräber**.

7. Weiergräber Marco (2008): **FUNCTIONAL RELEVANCE OF VOLTAGE-GATED CA^{2+}-CHANNELS AND CA^{2+}-CHANNEL INTERACTION PARTNERS IN MEDIATING HIPPOCAMPAL EXCITOTOXICITY AND NEURODEGENERATION.** 18.1.-19.1.2008, Vortrag im Rahmen der Klausurtagung des Zentrums für Molekulare Medizin Köln (ZMMK), Wermelskirchen-Dabringhausen, **Präsentation: Marco Weiergräber**.

Universitätsvorträge (Ausland)

1. Weiergräber Marco (2001): **BIOPHYSICAL ANALYSIS OF THE INTERACTION BETWEEN SUCCIMIDE ANTIEPILEPTIC DRUGS AND CLONED HUMAN T-TYPE CALCIUM CHANNELS.** 15.2.2001, Department of Pharmacology, University of Virginia (UVA), School of Medicine, Virginia, USA. **Präsentation: Marco Weiergräber**.

Institutsinterne Vorträge (Neurophysiologie, Universität zu Köln)

1. Weiergräber Marco (2001): **GENERALIZED ABSENCE EPILEPSY: HOW A FUNCTIONAL DISORDER IN THE THALAMOCORTICAL CIRCUITRY CAUSES A NON-CONVULSIVE SEIZURE (I).** 22.1.2001; Institut für Neurophysiologie, Medizinische Einrichtungen der Universität zu Köln. **Präsentation: Marco Weiergräber**.

2. Weiergräber Marco (2001): **GENERALIZED ABSENCE EPILEPSY: HOW A FUNCTIONAL DISORDER IN THE THALAMOCORTICAL CIRCUITRY CAUSES A NON-CONVULSIVE SEIZURE (II) - BLOCK OF CLONED HUMAN T-TYPE CALCIUM CHANNELS BY SUCCINIMIDE ANTIEILEPTIC DRUGS.** 23.04.2001, Institut für Neurophysiologie, Medizinische Einrichtungen der Universität zu Köln. **Präsentation: Marco Weiergräber**.

3. Weiergräber Marco (2004): **FUNCTIONAL CHARACTERISATION OF THE NEURONAL E/R-TYPE VOLTAGE-GATED CALCIUM CHANNEL WITHIN THE MURINE CARDIOVASCULAR SYSTEM**. 24.05.2004, Institut für Neurophysiologie, Medizinische Einrichtungen der Universität zu Köln. **Präsentation: Marco Weiergräber**.

4. Weiergräber Marco (2005): **NEUROLOGICAL CHARACTERIZATION OF MICE LACKING THE $CA_v2.3$ VOLTAGE-GATED CALCIUM CHANNEL - ECOG - DEEP INTRACEREBRAL RECORDINGS, SEIZURE SUSCEPTIBILITY TESTING AND SLEEP ANALYSIS.** 11.07.2005, Institut für Neurophysiologie, Medizinische Einrichtungen der Universität zu Köln. **Präsentation: Marco Weiergräber**.

5. Weiergräber, Marco (2007): **REDUCED NEUROTOXICITY AND INCREASED RESISTANCE TO HIPPOCAMPAL SEIZURE ACTIVITY IN $CA_V2.3$ DEFICIENT MICE**. 23.04.2007, Institut für Neurophysiologie, Medizinische Einrichtungen der Universität zu Köln. **Präsentation: Marco Weiergräber**.

6. Weiergräber, Marco (2007): **ZONISAMIDE BLOCK OF CLONED HUMAN T-TYPE VOLTAGE-GATED CALCIUM CHANNELS**.17.09.2007, Institut für Neurophysiologie, Medizinische Einrichtungen der Universität zu Köln. **Präsentation: Marco Weiergräber**.

Poster-Abstracts

1. Schneider Toni, Alexey Pereverzev, Heike Grabsch, **Marco Weiergräber**, Martin Schramm, Udo Klöckner, Jürgen Hescheler (1999): **EXPRESSION OF α1E VOLTAGE-GATED CA^{2+} CHANNEL ISOFORMS IN BRAIN AND NEUROENDOCRINE CELLS OF THE DIGESTIVE SYSTEM**. 43nd Annual Meeting of the Biophysical Society, 13.2.-17.2.99, Baltimore, USA. Abstract in: *Biophysical Journal* 76, A339.

2. Vajna Rolf, **Marco Weiergräber**, Xiao-hua Chen, George Miljanich, Margit Henry, Jürgen Hescheler, Udo Klöckner Alexey Pereverzev, Toni Schneider (1999): **INSULIN SECRETION AND E-TYPE VOLTAGE-GATED CALCIUM CHANNELS**. Meeting of the International Society of Neurochemistry, 8.8.-l4.8.99, Berlin. Abstract in: *Journal of Neurochemistry* 73, S13OC.

3. Weiergräber Marco, Alexey Pereverzev, Marina Mikhna, Jürgen Hescheler, Edward Perez-Reyes, Toni Schneider (2000): **IMMUNOHISTOCHEMICAL DETECTION OF E- AND T-TYPE VOLTAGE-GATED CALCIUM CHANNELS IN THE NEUROENDOCRINE SYSTEM**. 44th Annual Meeting of the Biophysical Society, 12.2.-16.2.2000, New Orleans, Louisiana, USA. Abstract in: *Biophysical Journal,* Vol. 78, No.1. **Präsentation: Marco Weiergräber**.

4. Weiergräber Marco, Heike Grabsch, Alexey Pereverzev, Toni Schneider (2000): **CHARACTERIZATION AND DETECTION OF E- AND T-TYPE VOLTAGE-GATED CALCIUM CHANNELS IN THE ENDOCRINE SYSTEM.** 4th Maastricht Medical Students Research Conference (MMSRC), 15.3.2000, Maastricht, Niederlande. **Präsentation: Marco Weiergräber**.

5. Schneider Toni, Rolf Vajna, Alexey Pereverzev, **Marco Weiergräber**, Jürgen Hescheler, Udo Klöckner (1999): **EINE VIELZAHL SPANNUNGSABHÄNGIGER CALCIUMKANÄLE STEUERT DIE CA^{2+}-ABHÄNGIGE INSULINFREISETZUNG IN INS-1 ZELLEN (RATTE). FUNKTION EINES α1E R-TYP CA^{2+}-KANALS**. 41. Frühjahrstagung der Deutschen Gesellschaft für Experimentelle und Klinische Pharmakologie und Toxikologie, Mainz. Abstract in: *Naunyn-Schmiedeberg's Archive of Pharmacology, Suppl. Vol. 359, Number 3.*

6. Pereverzev Alexey, Rolf Vajna, **Marco Weiergräber**, Jürgen Hescheler, Toni Schneider (2000): **REDUCTION OF INSULIN SECRETION IN ALPHA1E-DEPLETED INS-1 CELLS**. FENS, 8.7. - 13.7.2000, Brighton.

7. Gomora Juan Carlos, **Marco Weiergräber** y Edward Perez-Reyes (2001): **ANTIEPILEPTICOS DERIVADOS DE SUCCINIMIDA INDUCEN BLOQUEO DEPENDIENTE DEL ESTADO EN TRES CANALES DE CALCIO TIPO T CLONADOS DE HUMANO**. 40. Aniversario: Centro de investigacion y estudios avanzados del IPN, DEPARTAMENTO DE FISIOLOGÍA, BIOFÍSICA Y NEUROCIENCIAS; CINVESTAV, 17 y 18 de Octubre de 2001, MEXICO.

8. Weiergräber Marco, Margit Henry, Zhong-Ju Lu, Hui-Lin Liu, Alexey Pereverzev, Jürgen Hescheler, Toni Schneider (2004): **DISRUPTION OF THE $CA_V2.3$ (α1E) SUBUNIT OF THE VOLT-**

AGE-GATED CA^{2+}-CHANNELS IN NEONATAL MICE INDUCES CARDIAC ARRHYTHMIA. 48th Annual Meeting of the Biophysical Society, 14.2.-18.02.2004, Baltimore, USA. Abstract in: *Biophysical Journal*, Vol. 86, No.1, Suppl.; **Präsentation: Marco Weiergräber**.

9. Krieger Andreas, Marcel Kamp, Margit Henry, Alexey Pereverzev, **Marco Weiergräber**, Jürgen Hescheler, Toni Schneider (2004): **SIGNALLING THROUGH THE E-TYPE VOLTAGE-GATED CALCIUM CHANNEL - IDENTIFICATION OF INTERACTION PARTNERS.** Herbsttagung der GBM, 19.9.-22.9.04, Münster.

10. Radhakrishnan Kayalvizhi, Andreas Krieger, Siarhei Siapich, Alexey Pereverzev, Mohammet Banat, Jürgen Hescheler, Udo Klöckner, **Marco Weiergräber**, Toni Schneider (2006): **NEUE FUNKTIONEN FÜR HSP70 BEI DER FASZILITIERUNG DER PKC-VERMITTELTEN PHOSPHORYLIERUNG DES CA_V2.3 E-TYP CA^{2+}-KANALS**. 47. Frühjahrstagung der Deutschen Gesellschaft für Experimentelle und klinische Pharmakologie und Toxikologie (DGPT), 04.4.-06.04.2006, Mainz. Abstract in: *Naunyn-Schmiedeberg's Archive of Pharmacology* 372, Suppl. 7.

11. **Weiergräber Marco**, Margit Henry, Andreas Krieger, Marcel Kamp, Kayalvizhi Radhakrishnan, Claudia Zynthek, Jürgen Hescheler, Toni Schneider (2006): **FUNKTIONELLE RELEVANZ DES CA_V2.3 KALZIUMKANALS IN IKTOGENESE/EPILEPTOGENESE UND ANFALLSPROPAGATION**. 48. Jahrestagung der Deutschen Gesellschaft für Epileptologie (DGfE), 4.5.-6.5.2006, Strasbourg, Frankreich. Abstract in: *Zeitschrift für Epileptologie*, Band 19, Heft 2. **Präsentation: Marco Weiergräber.**

12. **Weiergräber Marco**, Kayalvizhi Radhakrishnan, Margit Henry, Siarhei Siapich, Andreas Krieger, Marcel Kamp, Mohammed Banat, Nora Matar, Elena Schlapakow, Renate Clemens, Irina Dobrinskaia, Jürgen Hescheler, Toni Schneider (2006): **THE PHARMACORESISTANT CA_V2.3 E/R-TYPE VOLTAGE-GATED CA^{2+}-CHANNEL IN EPILEPTOGENESIS. FUNCTIONAL ROLE OF CYTOSOLIC INTERACTION PARTNERS**. 1. Wissenschaftliches Symposium der Medizinischen Fakultäten der Universitäten Köln und Bonn. 4.10.2006, Bonn. **Präsentation: Marco Weiergräber.**

13. Weiergräber Marco, Margit Henry, Nora Matar, Andreas Krieger, Jürgen Hescheler, Toni Schneider (2006): **THE PHARMACORESISTANT CA_V2.3 E/R-TYPE VOLTAGE-GATED CA^{2+} CHANNEL IN EPILEPTOGENESIS - SHEDDING NEW LIGHT ON AN ENIGMATIC CHANNEL.** Jahrestagung des Kompetenznetzwerks NeuroNRW, Nordrhein-Westfälische Akademie der Wissenschaften, 28. November 2006, Düsseldorf. **Präsentation: Marco Weiergräber.**

14. Weiergräber Marco, Nora Matar, Margit Henry, Jürgen Hescheler, Toni Schneider (2007): **HIPPOCAMPAL SEIZURE RESISTANCE IN CA_V2.3 DEFICIENT MICE UNCOVERS MODULATORY PROPERTIES OF E/R-TYPE VOLTAGE-GATED CA^{2+}-CHANNELS IN NEURONAL EXCITOTOXICITY**. 86. Jahrestagung der Deutschen Physiologischen Gesellschaft; 25.3.–28.3.2007, Hannover.

15. Weiergräber Marco, Margit Henry, Nora Matar, Andreas Krieger, Jürgen Hescheler, Toni Schneider (2007): **THE CA_V2.3 VOLTAGE-GATED CALCIUM CHANNEL – UNMASKING AN ENIGMATIC PLAYER IN EPILEPTOGENESIS.** 7th Meeting of the German Neuroscience Society, 31st Göttingen Neurobiology Conference, 29.3-1.4.2007, Göttingen. **Präsentation: Marco Weiergräber**.

16. Margit Henry, Marcel Kamp, Kayalvizhi Radhakrishnan, Jürgen Hescheler, **Marco Weiergräber**, Toni Schneider (2008): **IDENTIFICATION OF A NOVEL CALMODULIN-2 SPLICE VARIANT IN HUMAN CELL LINES**. 87. Jahrestagung der Deutschen Physiologischen Gesellschaft, 2.3.–5.3.2008, Köln. Abstract in: *Acta Physiologica*.

17. Thomas Galetin, Margit Henry, Jürgen Hescheler, **Marco Weiergräber**, Toni Schneider (2008): **CARDIAC CA_V2.3 E-/R-TYPE VOLTAGE-GATED CALCIUM CHANNELS AT DIFFERENT**

(DEVELOPMENTAL STAGES?), AND ITS GENE INACTIVATION IN DIFFERENT MOUSE STRAINS. 87. Jahrestagung der Deutschen Physiologischen Gesellschaft, 2.3.–5.3.2008, Köln. Abstract in: *Acta Physiologica*.

18. W Albanna, Mohammed Banat, Matthias Lüke, Jürgen Hescheler, **Marco Weiergräber**, Toni Schneider (2008): **ELECTRORETINOGRAMS OF THE ISOLATED AND SUPERFUSED VERTEBRATE RETINA: $NICL_2$ MEDIATED STIMULATION OF B-WAVE AMPLITUDE FROM CA_V2.3-DEFICIENT MICE AND CONTROL ANIMALS.** 87. Jahrestagung der Deutschen Physiologischen Gesellschaft, 2.3.–5.3.2008, Köln. Abstract in: *Acta Physiologica*.

19. Peter Igelmund, Heiko Wrubel, Thomas Galetin, Henrik Stuck, Nora Matar, Jürgen Hescheler, Toni Schneider, **Marco Weiergräber** (2008): **PHARMACORESISTANT CA^{2+} CURRENTS IN HIPPOCAMPAL SLICES FROM CA_V2.3-DEFICIENT AND CONTROL MICE AND IN HETEROLOGOUS EXPRESSION SYSTEMS.** 87. Jahrestagung der Deutschen Physiologischen Gesellschaft, 2.3.–5.3.2008, Köln. Abstract in: *Acta Physiologica*.

20. Theresa Dartsch, R. Fischer, A. Gapelyuk, **Marco Weiergräber**, D. Ladage, H. Reuter, K. Frank, T. Schneider, A. Schirdewan, J. Müller-Ehmsen, C. Zobel (2008): **ALDOSTERONINDUZIERTES ELEKTRISCHES REMODELING UND SPEZIFISCHE (EPLERENON) VERSUS UNSPEZIFISCH (SPIRONOLACTON) BLOCKADE DES MINERALOKORTIKOID-REZEPTORS IN VIVO.** DKG 2008, Mannheim.

21. Theresa Dartsch, R. Fischer, A. Gapelyuk, **Marco Weiergräber**, D. Ladage, H. Reuter, K. Frank, T. Schneider, A. Schirdewan, J. Müller-Ehmsen, C. Zobel (2008): **ALDOSTERONINDUZIERTES ELEKTRISCHES REMODELING UND SPEZIFISCHE (EPLERENON) VERSUS UNSPEZIFISCH (SPIRONOLACTON) BLOCKADE DES MINERALOKORTIKOID-REZEPTORS IN VIVO.** ESC 2008, München.

22. Walid Albanna, Margit Henry, Jürgen Hescheler, Peter Igelmund, **Marco Weiergräber**, Matthias Lüke, Toni Schneider (2008): **STRUCTURE AND FUNCTION OF NI^{2+}-SENSITIVE CA_V2.3 E-TYPE VOLTAGE-GATED CA^{2+} CHANNELS**. FENS Meeting, Genf, 2008.

Lektorat

Lehrbuch „**Aktuelle Proktologie - UNI-MED SCIENCE**", UNI-MED-Verlag (2002).

Lehrbuch „**Prävention des Schlaganfalls - UNI-MED SCIENCE**", UNI-MED-Verlag (2005).

Lehrbuch „**Diagnostik, Differenzialdiagnostik und Therapie der Tagesschläfrigkeit – UNI-MED SCIENCE**", UNI-MED-Verlag (2006).

Lehrbuch **„Das Endocannabinoid-System – Physiologie und klinische Bedeutung – UNI-MED-SCIENCE"**, UNI-MED-Verlag (2006)

Lehrbuch „Reninhemmer in der Therapie der Hypertonie**",** UNI-MED SCIENCE**, UNI-MED-Verlag** (2007)

Reviewer-Tätigkeit

Journal of Neuroscience Methods

Medical Engineering & Physics

Expert Review of Neurotherapeutics

Journal of Neural Regeneration Research

Epilepsia

BMC Neuroscience